



Durham E-Theses

Enhancing the Borylation Experience: Strategies for Heteroaromatic Borylation

SADLER, SCOTT,ALEXANDER

How to cite:

SADLER, SCOTT,ALEXANDER (2015) *Enhancing the Borylation Experience: Strategies for Heteroaromatic Borylation*, Durham theses, Durham University. Available at Durham E-Theses Online: <http://etheses.dur.ac.uk/11288/>

Use policy

The full-text may be used and/or reproduced, and given to third parties in any format or medium, without prior permission or charge, for personal research or study, educational, or not-for-profit purposes provided that:

- a full bibliographic reference is made to the original source
- a [link](#) is made to the metadata record in Durham E-Theses
- the full-text is not changed in any way

The full-text must not be sold in any format or medium without the formal permission of the copyright holders.

Please consult the [full Durham E-Theses policy](#) for further details.

Academic Support Office, Durham University, University Office, Old Elvet, Durham DH1 3HP
e-mail: e-theses.admin@dur.ac.uk Tel: +44 0191 334 6107
<http://etheses.dur.ac.uk>

Statement of Copyright

The copyright of this thesis rests with the author. No quotation from it should be published without prior written consent and information derived from it should be acknowledged.

Declaration

The work described in this thesis was carried out in the Department of Chemistry at Durham University or the Department of Oncology at AstraZeneca, Alderley Park, Alderley Edge between April 2012 and June 2015, under the supervision of Prof. Patrick G. Steel and Mr Bryan Roberts. All the work is my own work, unless otherwise stated, and has not been submitted previously for a degree at this or any other university.

Scott Sadler

Acknowledgements

First and foremost, I would like to thank the continued love and support of my partner Kirsty for taking this journey with me and for tolerating me these three years. I am also extremely thankful to my family for always being there for me and for helping to be where I am now.

On a professional level I would like to thank my supervisor Professor Patrick Steel for his ideas, encouragement and passion for the field, my industrial supervisor Bryan Roberts for helping to make my placement an enjoyable and fulfilling experience, Hazmi Tajuddin for his guidance and support in the early stages of my PhD, Andrew Hones for his effort and hard work towards our research publication, Dr Jonathan Sellars for his support and help towards the compiling of this thesis and masters students Jack Dunleavy and Carys Thomas for their enthusiasm and commitment towards their projects.

Many thanks to Dr Jackie Mosley, Peter Stokes, Dr Alan Kenwright, Juan Aguilar and Catherine Heffernan for providing first class technical support and for their willingness to help and assist me. Thank you to Zhenyang Lin for carrying out computational calculations and assisting in the publications.

Finally, I would like to thank all members of CG001 past and present for making this experience a memorable and fulfilling one.

I can't thank you all enough.

Publications

1. Iridium-Catalyzed C-H Borylation of Pyridines;

Sadler, S.; Tajuddin, H.; Mkhald, I. A. I.; Batsanov, A. S.; Albesa-Jove, D.; Cheung, M/ S.; Maxwell, A. C.; Shukla, L.; Roberts, B.; Blakemore, D.; Lin, Z.; Marder, T. B.; Steel, P. G.; *Org. Biomol. Chem.*, **2014**, *12*, 7318-7327

2. Multidirectional Synthesis of Substituted Indazoles via Iridium-Catalyzed C-H Borylation;

Sadler, S.; Hones, A.; Roberts, B.; Blakemore, D.; Marder, T. B.; Steel, P. G.; *J. Org. Chem.*, **2015**, *80*, 5308-5314

Abstract

Iridium-catalyzed C-H borylation is an attractive method for synthesis of heteroaromatic boronate esters. Disappointingly however the Lewis-basicity of azinyl heterocycles limits their application in this methodology due to coordination to the iridium catalyst. Furthermore, the propensity for certain heteroaromatic boronate esters to undergo protodeborylation limits their application in downstream or one-pot chemistries.

Coordination to the iridium catalyst can be disrupted by substituents *ortho* to the azinyl nitrogen, for example 2-substituted pyridines and protected indazoles undergo reaction efficiently. Following this hypothesis, the direct functionalisation of pyridines, pyrazines, pyrimidines, pyridazines, isoquinolines, indazoles and aza-indazoles has been demonstrated.

When the *ortho*-substituent is sufficiently electron withdrawing it accelerates the formation of *ortho*-azinyl boronate esters which are typically disfavoured due to coulombic repulsion between an emerging negative charge at the site of C-H activation and the *ortho* co-planar azinyl lone pair. Moreover, electron withdrawing *ortho* substituents also sufficiently stabilise *ortho*-azinyl boronate esters to enable their isolation, for example methyl-2-fluoro-6-(Bpin)-isonicotinate and 1-mesyl-3-(Bpin)-indazole were stable to column chromatography. Where isolation is not possible the boronate esters can be used in one-pot Suzuki-Miyaura cross-coupling transformations to enable the synthesis of pharmaceutically interesting biaryls in good yields. Exploiting the functional group tolerance of C-H borylation, the reaction of functionalised starting materials has enabled the multidirectional synthesis of compound libraries following downstream modifications. In alternative downstream sequences reduction of *ortho*-halo substituents provides products arising from functionalisation of an unhindered azinyl heterocycle.

Abbreviations

aq – aqueous

ASAP – atmospheric pressure solid analysis probe

ATR – attenuated total reflectance

bpy – 2,2'-Bipyridine

Boc – *tert*-butoxycarbonyl

ca. – *circa*

Cat – catecholato

cat. – catalytic

COD – 1,5-cyclooctadiene

COE – cyclooctene

COSY – correlation spectroscopy

Cp - cyclopentadienyl

Cp* - pentamethylcyclopentadienyl

cymene – 4-isopropyltoluene

DCM- Dichloromethane

DFT – Density functional theory

Diglyme – diethylene glycol dimethyl ether

DMAP – 4-dimethylaminopyridine

DMAc – *N,N*-Dimethylacetamide

DME – 1,2-dimethoxyethane

dmpe – 1,2-bis(dimethylphosphino)ethane

dmphen – 2,9-dimethyl-1,10-phenanthroline

DoM – directed *ortho* metallation

dppb – 1,4-bis(diphenylphosphino)butane

dppe – 1,2-bis(diphenylphosphino)ethane

dppf – 1,1'-bis(diphenylphosphino)ferrocene

d^tbpy – 4,4'-Di-*tert*-butyl-2,2'-bipyridine

eg – Ethyleneglycolato

EI – electron ionisation

eq. – equivalents

ESI – electrospray ionisation

etc. *et cetera*

FID – flame ionisation detector

GC/MS – Gas chromatography/mass spectrometry

h – hour(s)

HMBC – heteronuclear multiple bonds correlation

HSQC – heteronuclear single quantum coherence

Hz - Hertz

ind – indenyl

IR – infra-red

LC/MS – liquid chromatography/mass spectrometry

m – meta

m/z – mass to charge ratio

min – minutes

Ms - mesyl

MTBE – methyl-*tert*-butylether

μ W – microwave

neo – neopentyl glycolato

NMM- *N*-Methylmorpholine

NMR – nuclear magnetic resonance

NOESY – nuclear Overhauser effect spectroscopy

o – ortho

Oxone® - potassium peroxymonosulfate

p – para

pin – pinacolato

pK_a – Acid dissociation constant

ppm – parts per million

quant. – quantitative

ref. – reference(s)

rt – room temperature

SEM – 2-(Trimethylsilyl)ethoxymethyl

SM – starting material

TC – thiophene-2-carboxylate

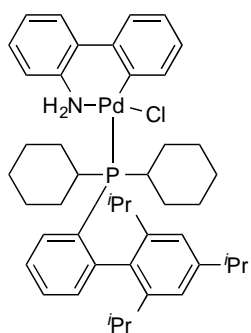
TLC – thin layer chromatography

TSA – toluenesulfonic acid

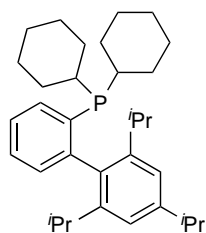
tmphen – 3, 4, 7, 8-tetramethyl-1, 10-phenanthroline

UV – ultraviolet

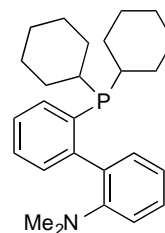
Catalyst and Ligand Glossary



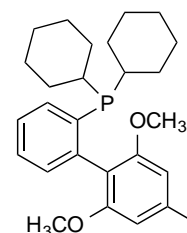
2ndGenPdXPhos



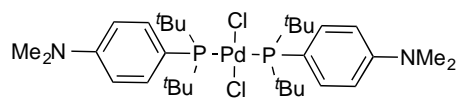
XPhos



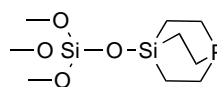
DavePhos



SPhos



Pd(Amphos)Cl₂



Si-SMAP

Table of Contents

1	Introduction.....	16
1.1	General Introduction to Thesis.....	16
1.2	Boronic Acids; Bonding, Physical Properties and Derivatives	16
1.2.1	Boronic Acid Derivatives	18
1.3	Synthetic Routes to Boronic Acids and their Derivatives	19
1.3.1	C-X Borylation Methods	19
1.3.1.1	Trapping of Organometallic Reagents.....	19
1.3.1.2	Transmetallation from Organosilanes.....	23
1.3.1.3	Catalytic C-X Borylation	23
1.3.1.4	Metal-Free C-X Borylation	26
1.3.2	C-H Borylation	28
1.3.2.1	Electrophilic C-H Borylation	28
1.3.2.2	Catalytic C-H Borylation	29
1.3.3	Synthesis of Boronic Acid Derivatives	30
1.4	Synthetic Applications	31
1.4.1	Suzuki-Miyaura Cross-Coupling	32
1.4.1.1	Substrate Scope – Electrophile	32
1.4.1.2	Substrate Scope – Nucleophile	35
1.4.1.2.1	Boronic Acids in Suzuki-Miyaura Cross-Coupling.....	35
1.4.1.2.2	Boronate Esters in Suzuki-Miyaura Cross-Coupling.....	36
1.4.1.2.3	Boronamides in Suzuki-Miyaura Cross-Coupling.....	37

1.4.1.2.4	Trifluoroborate Salts in Suzuki-Miyaura Cross-Coupling	37
1.4.1.2.5	MIDA Boronates in Suzuki-Miyaura Cross-Coupling	38
1.4.1.3	'One-pot' borylation/Suzuki-Miyaura Cross-Coupling Protocols	40
1.4.2	Oxidative Heck Coupling.....	40
1.4.2.1	Variation in Oxidant.....	43
1.4.2.2	Ligand-Assisted Protocols	43
1.4.2.3	Substrate Scope – Boron Component.....	44
1.4.2.4	'One-pot' Borylation/Oxidative Heck Coupling Protocols	44
2	Borylation of Azinyl Heterocycles	45
2.1	Catalytic aromatic C-H borylation	45
2.1.1	History of Catalytic C-H borylation.....	45
2.1.2	Mechanistic Discussion.....	49
2.1.2.1	<i>In-situ</i> active catalyst formation	51
2.1.2.2	Oxidative Addition	52
2.1.2.3	Reductive Elimination	53
2.1.2.4	Catalyst Recycling.....	53
2.1.2.5	The HBpin Cycle	54
2.1.3	Substrate scope	55
2.1.3.1	Borylation of Aromatic Substrates	55
2.1.3.2	Borylation of Heteroaromatic Substrates.....	58
2.1.4	Borylation of Substituents Bearing an Azinyl Nitrogen.....	60
2.1.4.1	Pyridyl-Boron Interactions.....	60

2.1.4.2	Pyridyl-Iridium Interactions.....	62
2.1.4.3	Borylation of 2-Substituted Pyridines.....	63
2.1.4.4	Competition Experiments.....	64
2.1.4.5	<i>ortho</i> -Azinyl Boronate Esters.....	64
2.1.5	Protodeborylation.....	66
2.2	Previous Work and Chapter Goals.....	67
2.3	Results and Discussion.....	73
2.3.1	Borylation of 2-Substituted pyridines.....	73
2.3.2	Borylation of 2,3-Disubstituted pyridines.....	77
2.3.2.1	Tandem Suzuki-Miyaura Cross-Coupling Reactions.....	82
2.3.3	Borylation of 2,4-Disubstituted Pyridines.....	84
2.3.3.1	Tandem Suzuki-Miyaura Cross-Coupling Reactions.....	87
2.3.4	Borylation of 2,5-Disubstituted Pyridines.....	88
2.3.4.1	Tandem Suzuki-Miyaura Cross-Coupling Reactions.....	91
2.3.5	Multi-Directional Synthetic Strategies.....	92
2.3.5.1	2-Chloro Reduction Sequence.....	93
2.3.5.2	S _N Ar Substitution of Aryl-2-Halopyridines.....	94
2.3.6	Borylation of Other Azinyl Heterocycles.....	96
2.3.6.1	Borylation of Pyrazines.....	97
2.3.6.1.1	Tandem Suzuki-Miyaura Cross-Coupling Reactions.....	99
2.3.6.1.2	<i>ipso</i> -Deuteration of (Bpin)-Pyrazine.....	100
2.3.6.2	Borylation of Pyrimidines.....	101

2.3.6.2.1	Solvent Screen	102
2.3.6.2.2	Borylation of 2-Phenylpyrimidine	104
2.3.6.3	Borylation of Indazole	106
2.3.6.4	Borylation of Pyridazines	107
2.3.6.5	Borylation of Isoquinolines	110
2.3.6.6	Borylation of 1,8-Naphthyridine	113
2.3.6.7	Borylation of Pyridine- <i>N</i> -oxides	114
2.4	Conclusions and Future Work	116
3	Multidirectional Synthesis of Functionalised Indazoles	118
3.1	Background and Chapter Aims	118
3.2	Results and Discussion	119
3.2.1	Borylation of 3-Bromoindazole	119
3.2.2	Borylation of Protected Indazoles	121
3.2.2.1	Attempted Traceless Protecting Group Strategies	121
3.2.2.2	Borylation of <i>N</i> -protected Indazoles	124
3.2.2.3	Tandem 'one-pot' Borylation/Suzuki-Miyaura cross-couplings	132
3.2.2.4	Multidirectional Synthesis of Functionalised Indazoles	135
3.2.2.4.1	Borylation of Bromoindazoles	135
3.2.2.4.2	Borylation of 4-Bromoindazole	139
3.2.2.4.3	Suzuki-Miyaura Cross-Coupling of 3-Aryl-Bromoindazoles	141
3.2.2.4.4	Attempts at Directed Borylation of Indazole	143
3.2.2.4.5	Attempted <i>ipso</i> -Deuteration of 3-(Bpin)-Indazole	145

3.2.2.4.6	Selective Protodeborylation of Polyborylated Indazoles	148
3.2.2.4.7	Synthesis of 1,3-bis-Arylindazoles	152
3.2.3	Borylation of Pyrazolo[1,5-a]pyridine	153
3.2.4	Borylation of Pyrazolo[1,2-a]pyridine	156
3.2.5	Borylation of Azaindazoles	159
3.2.5.1	Substrate Synthesis	159
3.2.5.2	Attempted Borylation of 6-Azaindazole	161
3.2.5.3	Borylation of 4-Azaindazole	161
3.2.5.4	Borylation of 7-Azaindazole	163
3.3	Conclusions and Future Work	166
4	Development Towards a 'One-pot' C-H Borylation/Oxidative Heck Coupling Protocol	170
4.1	Aims and objectives	170
4.2	Previous work in the group	170
4.3	Results and Discussion	172
4.3.1	Preliminary Results	172
4.3.2	Optimisation Studies	174
4.3.3	Aromatic Substrate Screening Exercise	179
4.4	Conclusions and future work	182
5	Experimental	183
5.1	General Considerations	183
5.2	General Methods	186

5.3	Experimental Details	192
6	Bibliography	258
7	Appendix	266

1 Introduction

1.1 General Introduction to Thesis

Due to their applicability in a variety of bond-forming reactions and functional group transformations, boronic acids and their derivatives are an extremely desirable class of synthetic intermediate. Reflecting this, efficient routes to these compounds are an important tool for organic chemists. This thesis describes an expedient method, using direct C-H activation, towards (hetero)aromatic boronate esters and their applicability in one-pot reactions. Chapter 2 will explore the application of C-H borylation to stubborn heterocycles that contain a Lewis-basic azinyl nitrogen. Chapter 3 will apply the findings and strategies developed in Chapter 2 to a focussed case study on the borylation of indazoles. Finally, Chapter 4 will discuss work undertaken towards the development of a one-pot single-solvent C-H borylation/oxidative Heck-coupling protocol. The remainder of this chapter will discuss the various routes to boronic acids and their derivatives, as well as their use in functional group transformations and bond forming reactions, with specific focus on their application in the Suzuki-Miyaura cross-coupling reaction and the oxidative Heck coupling.

1.2 Boronic Acids; Bonding, Physical Properties and Derivatives

Boronic acids are trivalent compounds with two bonds to hydroxyl groups and one bond to an organic ('R') group (1). The sp^2 -hybridized boron atom possesses a low energy, non-bonding vacant p orbital orthogonal to the plane of the molecule, which dominates its physical characteristics and reactivity patterns (Figure 1). Its susceptibility to electron donation from Lewis-basic donor groups enables the formation of tetrahedral 'ate' complexes, themselves possessing different patterns of reactivity and chemical properties.

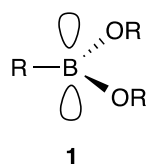
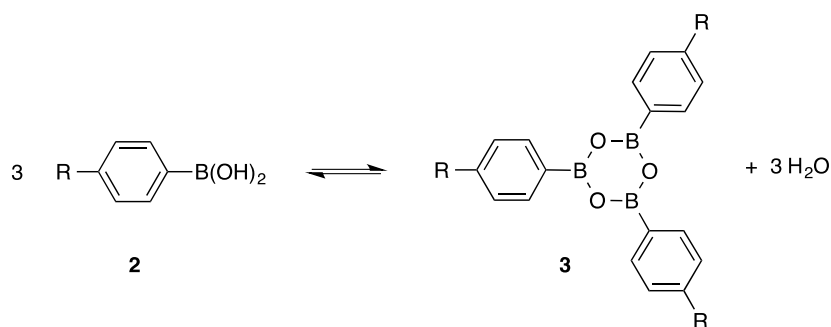


Figure 1: General structure of boronic acids and esters

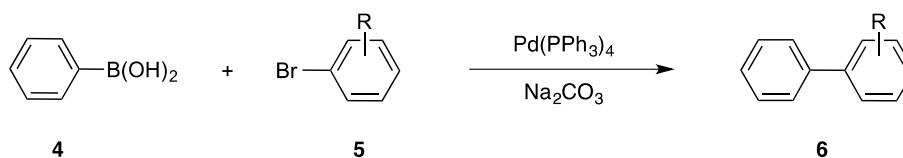
Boronic acids are generally considered chemical and air stable compounds, however over prolonged periods atmospheric oxidation gives rise to boric acids.¹ Moreover, under anhydrous conditions, boronic acids (**2**) have a propensity to form oligomeric anhydrides, such as trimeric boroxines (**3**), which can complicate characterisation and analysis (Scheme 1). In a practical sense this often necessitates the use of excess boronic acid in reactions.



Scheme 1: Dehydrative oligomer formation

In addition, the long-term stability and reactions of some aryl boronic acids are also plagued by potential protolytic pathways, which can cleave C-B bonds despite it being a relatively strong bond (323 kJ mol⁻¹ versus 358 kJ mol⁻¹ for C-C bonds).² These deborylation pathways may occur by acid³, base⁴ or metal-mediated⁵ mechanisms. This phenomena is discussed more fully in Chapter 2.

With the development of the Suzuki-Miyaura cross-coupling process (Scheme 2),⁶ the need for novel, bench-stable reagents prompted an exploration of various boronic acid derivatives that circumvent, at least in part, many of these problems.⁷



Scheme 2: Seminal application of boronic acids in the synthesis of biaryls

1.2.1 Boronic Acid Derivatives

The most commonly employed boronic acid derivatives used in modern cross-coupling chemistry are outlined below (Figure 2).

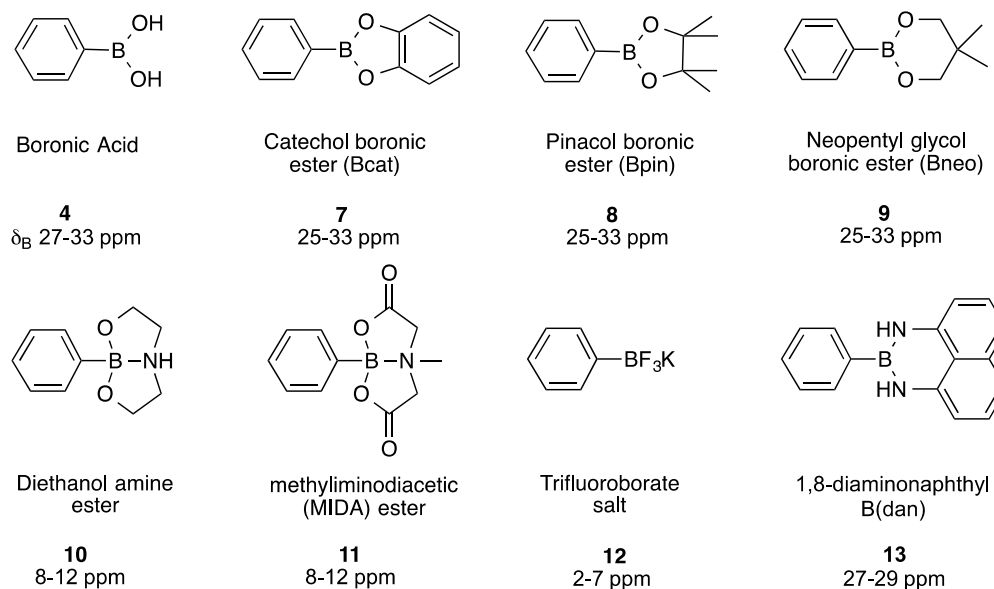


Figure 2: Aryl boronic acid and its derivatives

Due to the varying electronic character of the p orbital, the displayed derivatives often exhibit unique stabilities and reactivity patterns. The relative stability is best exemplified in their varying Suzuki-Miyaura cross-coupling applications, which is discussed later in this chapter (*c.f* Section 1.4.1.2).

1.3 Synthetic Routes to Boronic Acids and their Derivatives

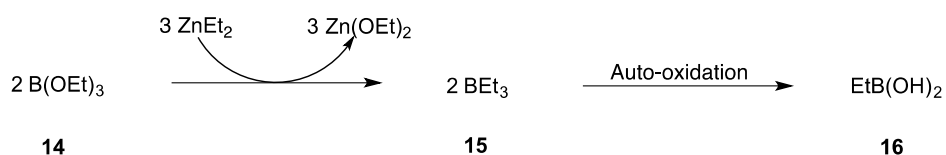
For over a century, the chemistry undertaken to utilise and synthesise arylboronic acids was limited, however, since the development of the groundbreaking cross-coupling reaction by Suzuki and Miyaura (*c.f* Scheme 2), a greater emphasis has been placed on developing robust, economical and efficient routes to these compounds. The following section will discuss their various methods of preparation, emphasising the respective advantages and disadvantages. This section focuses on routes to aryl boronic acids and their derivatives and consequently will not cover methods solely applicable to the synthesis of alkyl, vinyl and alkynyl boronic acids.

1.3.1 C-X Borylation Methods

The following section will explore and discuss the various functional group transformation routes to aryl boronic acids and esters.

1.3.1.1 Trapping of Organometallic Reagents

The seminal report on the synthesis of a boronic acid (**16**) involved the treatment of diethylzinc with triethylborate (**14**) with subsequent auto-oxidation of the borane (**15**) to yield the boronic acid (Scheme 3).⁸



Scheme 3: Seminal synthesis of a boronic acid

This approach has since been developed to provide the classical synthesis of boronic acids, by way of a metallation step, typically to form either a Grignard or organolithium reagent, with subsequent quenching by a boron electrophile. The class of boron electrophile applied may vary, with borates (**18**) (Figure 3a), boronates (**21**) (Figure 3b), boranes, such as pinacol borane (HBpin, **24**), (Figure 3c) and boron halides (**27**) (Figure 3d) all applicable.⁹⁻¹¹ A standard aqueous workup hydrolyses the labile boronate ester substituent, furnishing the desired boronic acid product (**19**, **28**). However, in most cases (reflecting their ease of purification and greater solubility in organic solvent) organic chemists will often isolate the borate or boronate ester (**22**, **25**, **30**) (Figure 3b, c). Several examples are also reported in which (trans)esterification is included within the sequence (Figure 3e).^{12,13}

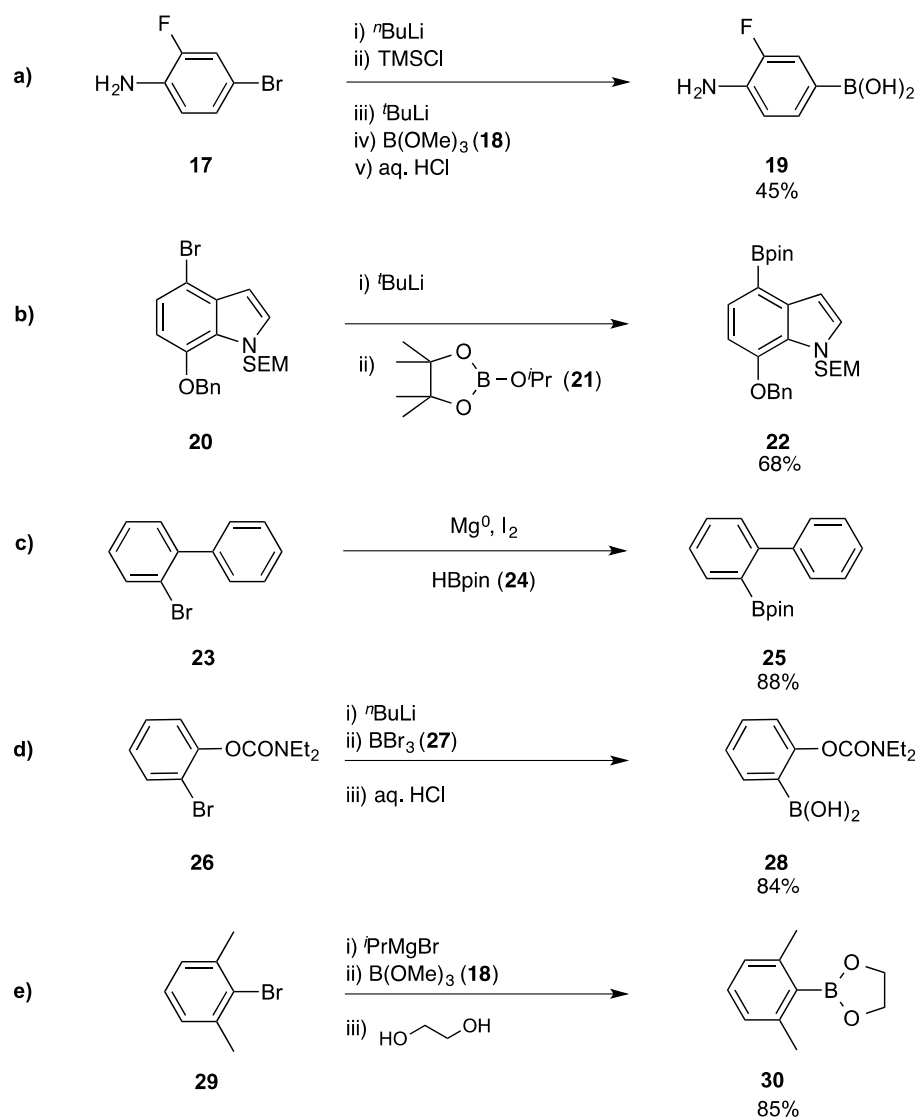
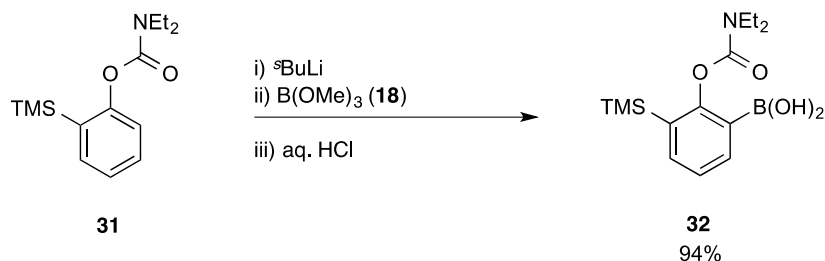


Figure 3: Organoboronic acid/ester synthesis by electrophilic trapping of aryl metal intermediates

Whilst transmetalation occurs most commonly from aryl lithium or magnesium intermediates, within the literature there also exists similar scope for trapping of organocadmium¹⁴, zinc¹⁴ and mercury species.⁹ However, these examples are less common and suffer from the use of toxic metals.

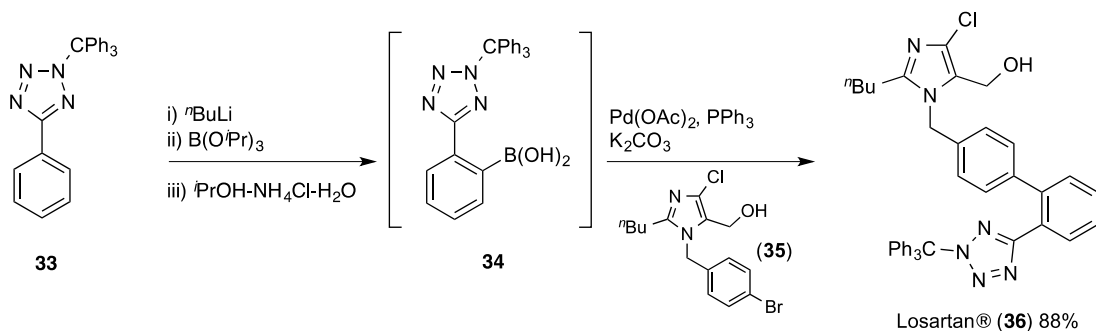
In addition to direct metallation of carbon-halogen bonds, it has been demonstrated that *ortho* directing functional groups, such as ethers¹¹, carbamates (**31**)¹⁵, esters¹⁶ and

amides¹⁷ can direct metallation to neighbouring C-H bonds, in a process known as directed *ortho* metallation (DoM) (Scheme 4).



Scheme 4: Directed *ortho*-metallation approach to aromatic borylation, utilising a carbamate directing group

DoM has found large scale industrial application, for example in the synthesis of the antihypertensive drug Losartan (**36**), in which the initial metallation step is directed by a tetrazole moiety (**33**) (Scheme 5).¹⁸



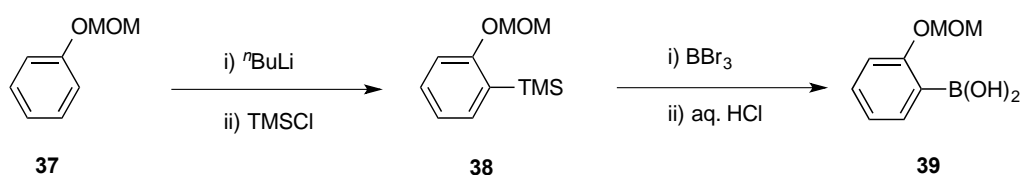
Scheme 5: Application of DoM towards the total synthesis of Losartan®

Despite their having found application on large industrial scale and in target syntheses, direct C-X borylation, via reactive aryl metal intermediates, and DoM methodologies are restrictive in their use. The invoking of strongly nucleophilic and/or basic reagents is not

only a practical hindrance, due to the requirement for low temperatures and stringent anhydrous conditions, it also limits substrate scope as a number of common functional groups such as amides, esters and nitriles, are recalcitrant with this methodology (*c.f.* Figure 3). This means that when applying these reactions in target syntheses, it is usually prudent to incorporate protection steps for potentially sensitive functional groups. With the recent drive towards greener chemistries, organic chemists have attempted to limit the use of protecting groups where possible as each functional group adds two additional steps in linear syntheses. As a consequence, reactions that preclude the use of hard anions or nucleophiles are often invoked.

1.3.1.2 Transmetalation from Organosilanes

The use of an *ipso*-borodesilylation protocol, which proceeds by transmetalation from a soft organosilane (**38**), has also been reported.¹¹ The stability of the newly formed B-C and Si(Sn)-X bonds, relative to the weaker B-X and Si(Sn)-C bonds in the starting materials, provides a thermodynamic driving force for the reaction (Scheme 6).



Scheme 6: *ipso*-borodesilylation of an in-situ generated arylsilane

1.3.1.3 Catalytic C-X Borylation

Reflecting an overall drive towards greener and sustainable processes, synthetic chemists will often use catalytic reactions to reduce steps and enable late-stage

modification of functionalised starting materials. One such direct, expedient approach to aryl boronate esters, which circumvented the need for strongly basic aryl metal intermediates, was proposed by Miyaura and co-workers.^{19,20} In the presence of catalytic palladium, aryl halides (**40**) (or pseudo-halides, **43**) are cross-coupled with diboronate esters, such as bis(pinacolato)diboron (B_2pin_2 , **41**) (Figure 4a). The Masuda group reported an extension of this methodology, utilising metal hydride borylating agents, such as HBpin (**24**) or catechol borane, providing the added advantage of wider reaction scope (due to the more ready availability of dialkoxyborane reagents versus the corresponding diboronate esters) and greater atom economy (Figure 4b).²¹ More recently, the use of bis-boronic acid (**46**) has enabled direct synthesis of boronic acids (**47**),^{22,23} obviating the need for prior synthesis of the corresponding ester with subsequent additional hydrolysis,²⁴ oxidative²⁵ or reductive²⁶ steps (Figure 4c). Direct routes to boronic acids are of great value due to their greater atom economy and reactivity in cross-coupling chemistry compared with the corresponding boronate esters.

Copper-catalysed cross-coupling variations have been investigated by Zhu and Ma, who reported the synthesis of aryl boronates (**49**) catalysed by copper(I)iodide, in the presence of HBpin (**24**) and sodium hydride, from the substituent aryl iodides (**48**) (Figure 4d).²⁷ Substrate scope was expanded to include aryl bromides by Marder and co-workers.²⁸ Complementary iron-catalysed radical transformations of aryldiazonium salts (**50**) were described by Pucheault *et.al* (Figure 4e).²⁹ The resulting aryl aminoboranes act as an intermediary species to boronate esters (**52**) and acids as well as trifluoroborate salts. The use of iron and copper catalysts are an attractive alternative to their palladium counterparts due to their relative abundance, affordability, lower toxicity and environmental innocuousness.

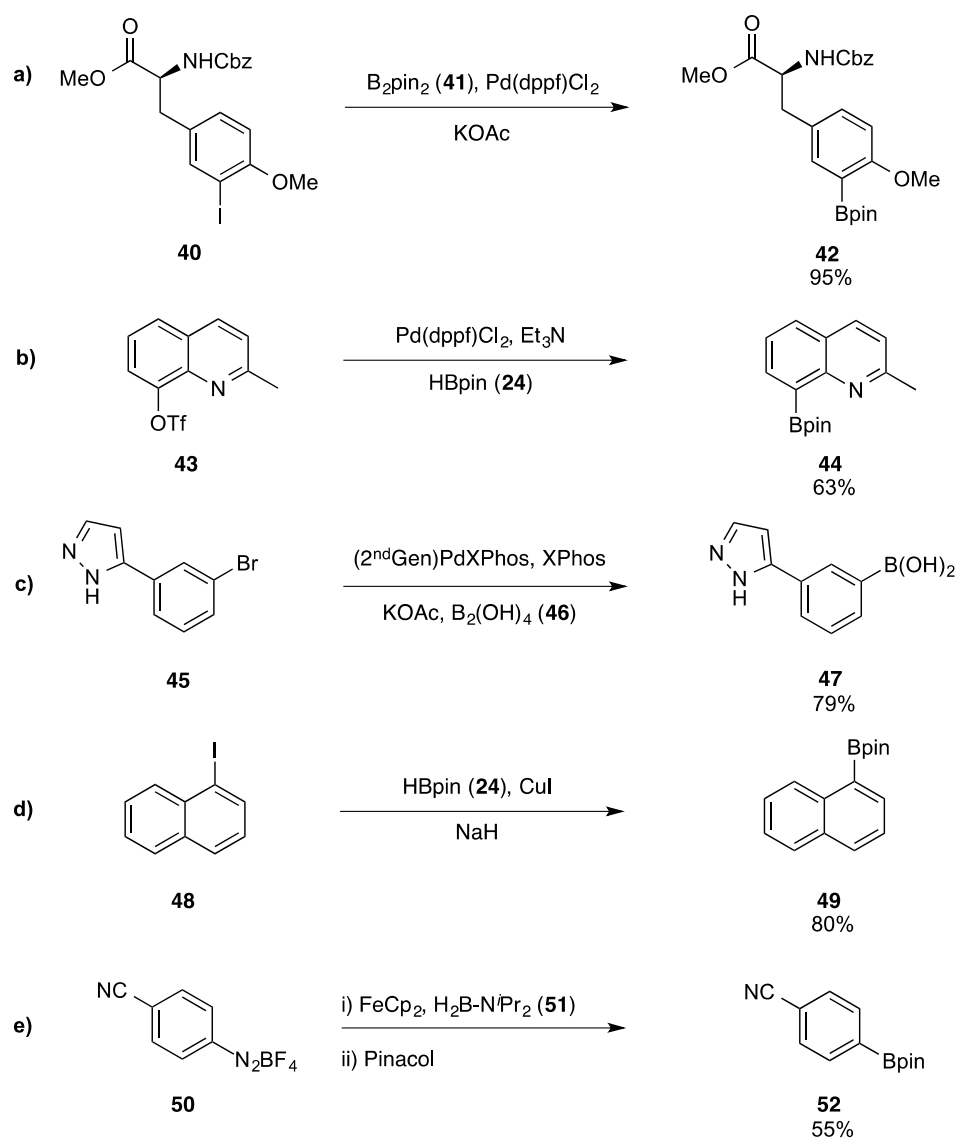


Figure 4: Catalytic C-X borylation strategies

Cross-coupling methods between organic electrophiles and boron-nucleophiles provide a convenient and direct method for the synthesis of boronic acids and their derivatives. Such methods obviate the need for rigorously anhydrous reaction conditions and are, therefore, amenable to a wider substrate scope (due to increased functional group compatibility) arising from low reactivity and stability of the boron reagents as well as the absence of strongly basic reagents (*c.f* Figure 3). This enables access to a range of

structurally diverse functionalised (hetero)aryl boronic acids and esters. Use of potentially costly metal catalysts is, however, a hindrance.

1.3.1.4 Metal-Free C-X Borylation

Due to a declining global supply of heavy transition metals and the costly nature of certain transition-metal catalysts, a greater emphasis is being placed on developing new methodologies that circumvent their use. Recent advances in borylation chemistry reflect this drive, for example Wang and co-workers have developed a modified Sandmeyer process for conversion of aryl amines (**53**) into aryl boronates (**54**) (Figure 5a).³⁰ Aryl amines are an attractive synthon for boronic acid synthesis due to their low cost and abundance (resulting from their ease of synthesis by prior nitration of arenes). This transformation utilises *tert*-butyl nitrite as a diazotisation agent to enable *in-situ* formation of the corresponding diazonium salts (**55**). The presence of catalytic benzoyl peroxide (BPO), as a radical initiator, enables the production of a variety of aryl boronates in short reaction times. The synthetic utility of this process was expounded further in one-pot borylation-Suzuki Miyaura cross-coupling reactions. A modification of this work, reported by Blanchet and co-workers, enabled access to the more reactive boronic acid products (**57**) (Figure 5b).³¹

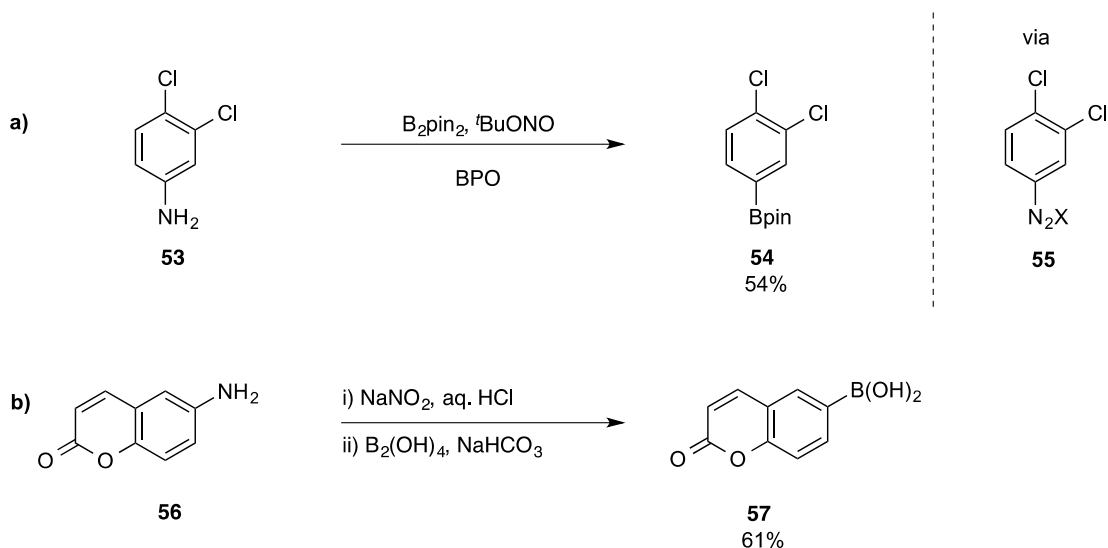


Figure 5: Metal-free borylation of arylamines

Diazotisation routes to boronic acids and esters benefit from experimental simplicity, short reaction times and wide functional group tolerance, however the *in-situ* formation of potentially hazardous diazonium salts is problematic. Furthermore, synthetic routes to these starting reagents are limited by product distribution from the prior aromatic nitration reaction.

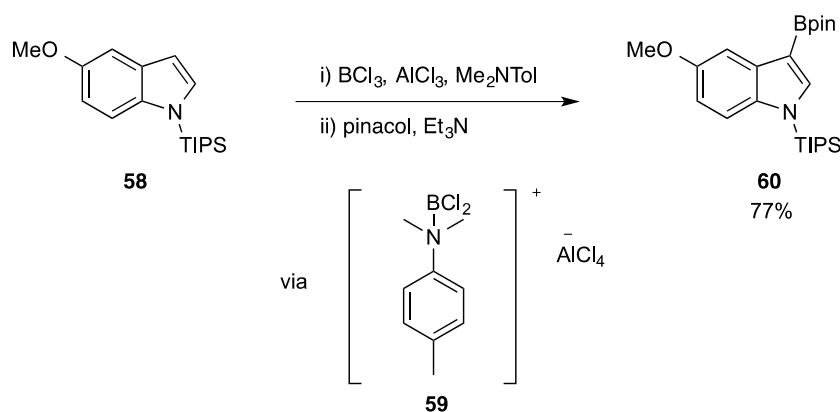
On a more general note, the synthetic utility of C-X borylation itself is limited by the requirement for pre-existing halide or amine functionality. As a result, starting materials often have to be purchased with the required functional group (which may in some cases increase costs), or functionality will need to be incorporated into the molecule, thereby reducing the overall efficiency of any reaction sequence. Consequently, reflecting the drive towards greener and more sustainable processes, there has been a growing focus on C-H activation routes to boron compounds.

1.3.2 C-H Borylation

The following section will consider direct borylation of aromatic C-H bonds. These methods are of particular interest as they circumvent the requirement for pre-existing functionality and are more atom economical.

1.3.2.1 Electrophilic C-H Borylation

Ingleson and co-workers have reported a direct electrophilic borylation protocol.^{32,33} This methodology relies on the *in-situ* formation of highly electrophilic, transient borenium cations (**59**), reacting effectively as $[R_2B]^+$, from commercially available boryl halide starting materials (Scheme 7).³⁴



Scheme 7 Direct electrophilic borylation of an indole substrate

Electrophilic borylations generate catechol or pinacol esters (**60**) in short reaction times, however the requirement for stringent reaction conditions and the limited substrate scope are factors which limit the widespread application of this methodology.³² Moreover, only the borylation of electron-rich aromatics, N-heterocycles (**58**) and thiophenes have been reported to date.³⁵

1.3.2.2 Catalytic C-H Borylation

Catalytic C-H borylation, catalysed by *in-situ* generated iridium tris-boryl complexes, has a varied and diverse substrate scope. Due to the steric bias affecting C-H borylation reactions, regioselectivity is often dictated by steric effects and is, therefore, complementary to electrophilic borylation (Figure 6a).

More recently, the respective groups of Chirik and Darcel have developed C-H borylation catalysed by pincer-ligated cobalt (**64**) and iron bis(diphosphine) complexes (**67**) respectively (Figure 6b, c).^{36,37} Iron and cobalt-catalysed variants represent an attractive future alternative due to the high cost and declining global supply of iridium but are still in their infancy and currently suffer from inconsistent yields and narrow substrate scope.

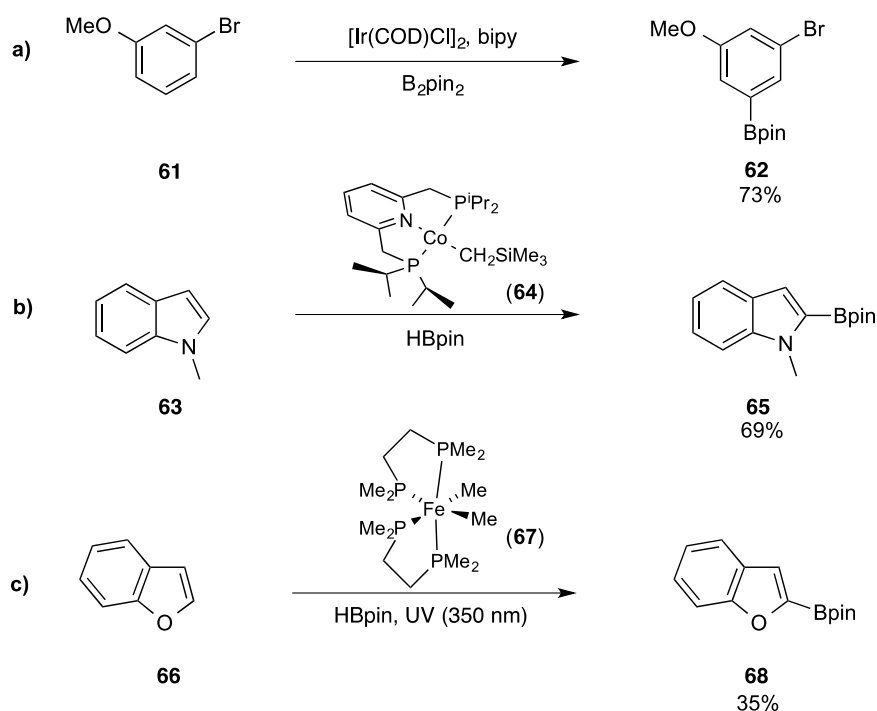


Figure 6: Catalytic C-H borylation

The development of C-H borylation as a catalytic process, its reaction mechanism, substrate scope and regioselectivity are discussed in the next chapter and the work undertaken using this methodology will provide the backbone to this study.

1.3.3 Synthesis of Boronic Acid Derivatives

Whilst there are various direct C-H and C-X borylation protocols towards boronate esters, direct synthesis of the other boronic acid derivatives (by functional group interconversion or C-H activation methods) outlined in Figure 2, is not known. Consequently their synthesis involves reaction of the corresponding boronic acids or esters. For example, aryl trifluoroborate salts (**12**) are prepared from reaction of aryl boronic acids (**4**) or esters with potassium bifluoride (KHF₂), or a combination of potassium fluoride (KF) and tartaric acid (Figure 7a).³⁸⁻⁴⁰ Alternatively, condensation of the boronic acid (**69**, **72**) with diethanolamine ligands, such as *N*-methyiminodiacetic acid (**70**), or with 1,8-diaminonaphthalene (**73**), under Dean-Stark conditions, provide the *N*-coordinated (MIDA) ester (**71**) and B(dan) amide (**74**) respectively (Figure 7b, c).⁴¹

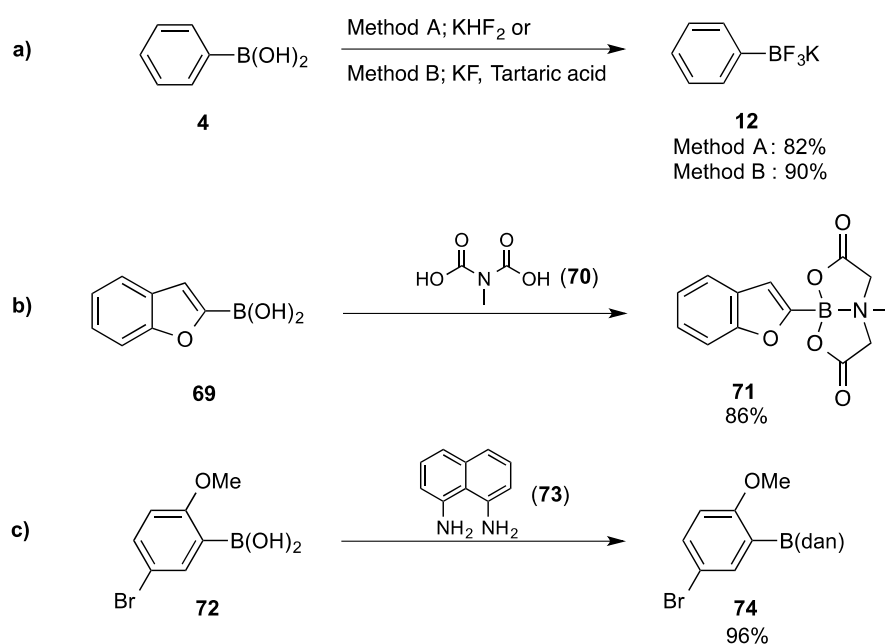


Figure 7: Synthesis of a) trifluoroborate salts; b) MIDA boronates; c) B(dan) amides

1.4 Synthetic Applications

Arylboronic acids and their derivatives are an extremely versatile class of organic intermediate that can act as precursors in a variety of carbon-carbon (C-C) and carbon-heteroatom bond forming processes, as well as functional group transformations including; a. Suzuki-Miyaura cross-couplings; b. oxidative Heck couplings; c. conjugate additions;^{42,43} d. Chan-Lam aminations,⁴⁴⁻⁴⁶ e. Chan-Lam etherifications,^{46,47} f. *ipso*-halogenations;⁴⁸⁻⁵⁴ g. oxidations;^{48,55-58} h. homologations;⁵⁹ i. trifluoromethylations;⁶⁰⁻⁶⁶ j. azidations;⁶⁷⁻⁶⁹ k. nitrations;^{70,71} l. cyanations (Figure 8).⁷²⁻⁷⁵ Given the focus of this thesis and the work undertaken in this study, the following section will only explore the Suzuki-Miyaura cross-coupling, with focus on the scope of organic electrophiles and boron nucleophiles permitted, and the oxidative Heck coupling. A thorough review of the other transformations can be found in the aforementioned references.

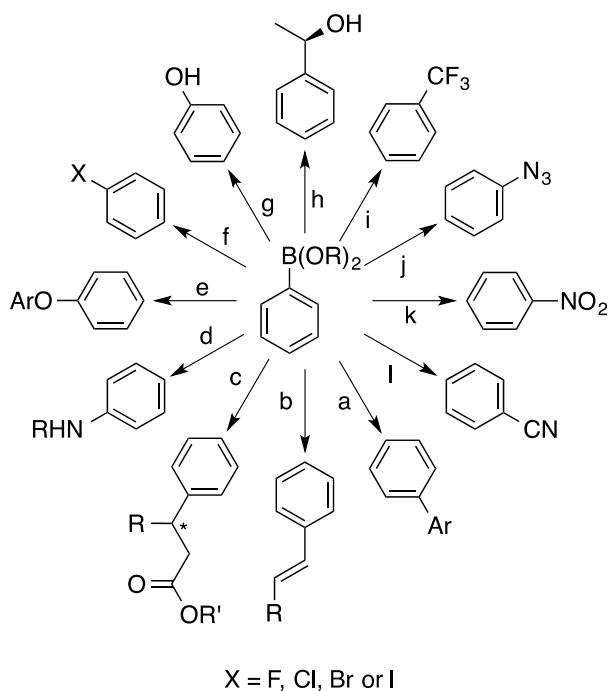


Figure 8 Synthetic applications of boronic acids and their derivatives

1.4.1 Suzuki-Miyaura Cross-Coupling

C-C bond forming reactions are extremely important tools to synthetic chemists as they allow the ‘building up’ of complex molecules from simple substrates and a movement towards more convergent syntheses, whereby complex precursors are prepared separately and subsequently ‘tied together’ at a late stage in the synthesis. Transition metal-catalysed cross-coupling reactions are among the most widely used for C-C bond formation, constituting 25% of all reactions carried out in the pharmaceutical sector (of which, the Suzuki-Miyaura cross coupling reaction makes up the largest proportion).²³

1.4.1.1 Substrate Scope – Electrophile

The Suzuki-Miyaura cross-coupling reaction describes the direct coupling of organoboron nucleophiles (**76**) with halide or pseudohalide electrophiles (**75**) under

palladium or, in some cases, nickel catalysis (Figure 9a). Vast amounts of research has been undertaken, such that a variety of conditions now exist by which an array of aryl and heteroaryl halides, triflates (**78**)⁷⁶ and tosylates (**81**)⁷⁷ can be routinely reacted in good yields even on large industrial scale (Figure 9b, c).⁷⁸

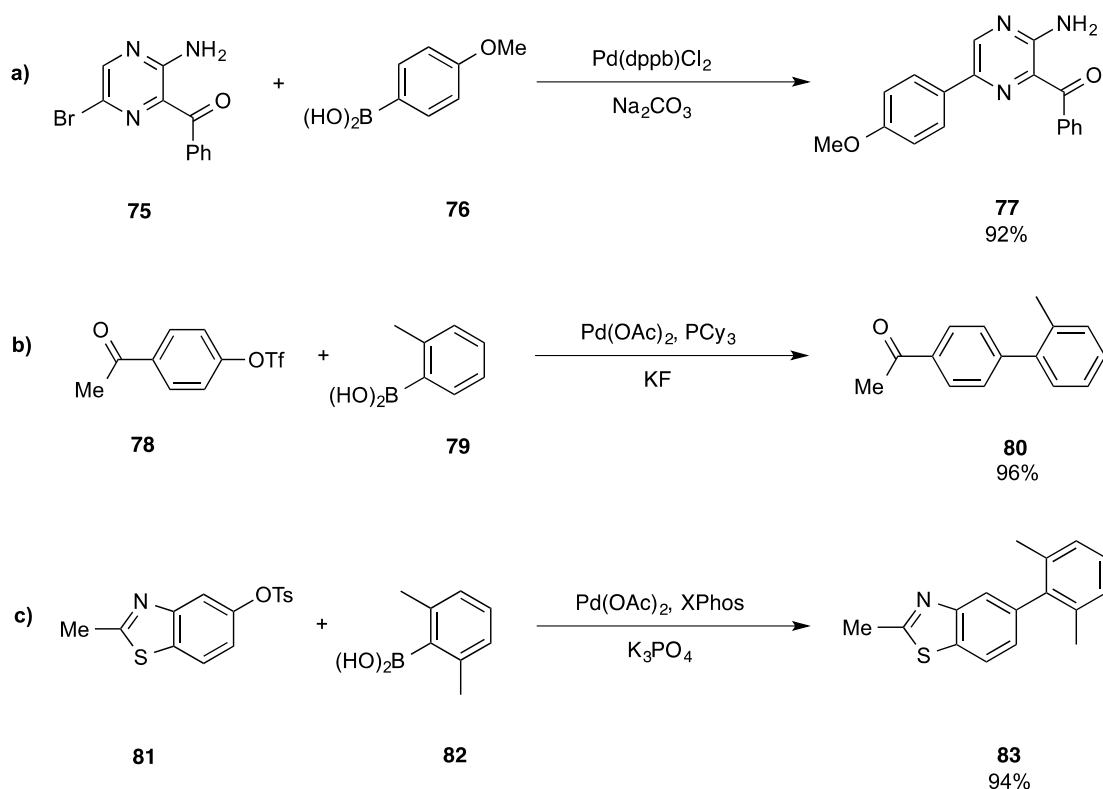


Figure 9: Examples of Suzuki-Miyaura cross-coupling

Although less common, cross-coupling reactions have also been reported with diazonium compounds (**84**),⁷⁹ aryl carbamates (**86**),⁸⁰ aryl carbonates (**88**),⁸¹ thioesters (**90**)⁸² and thioethers (**93**) (Figure 10).⁸³

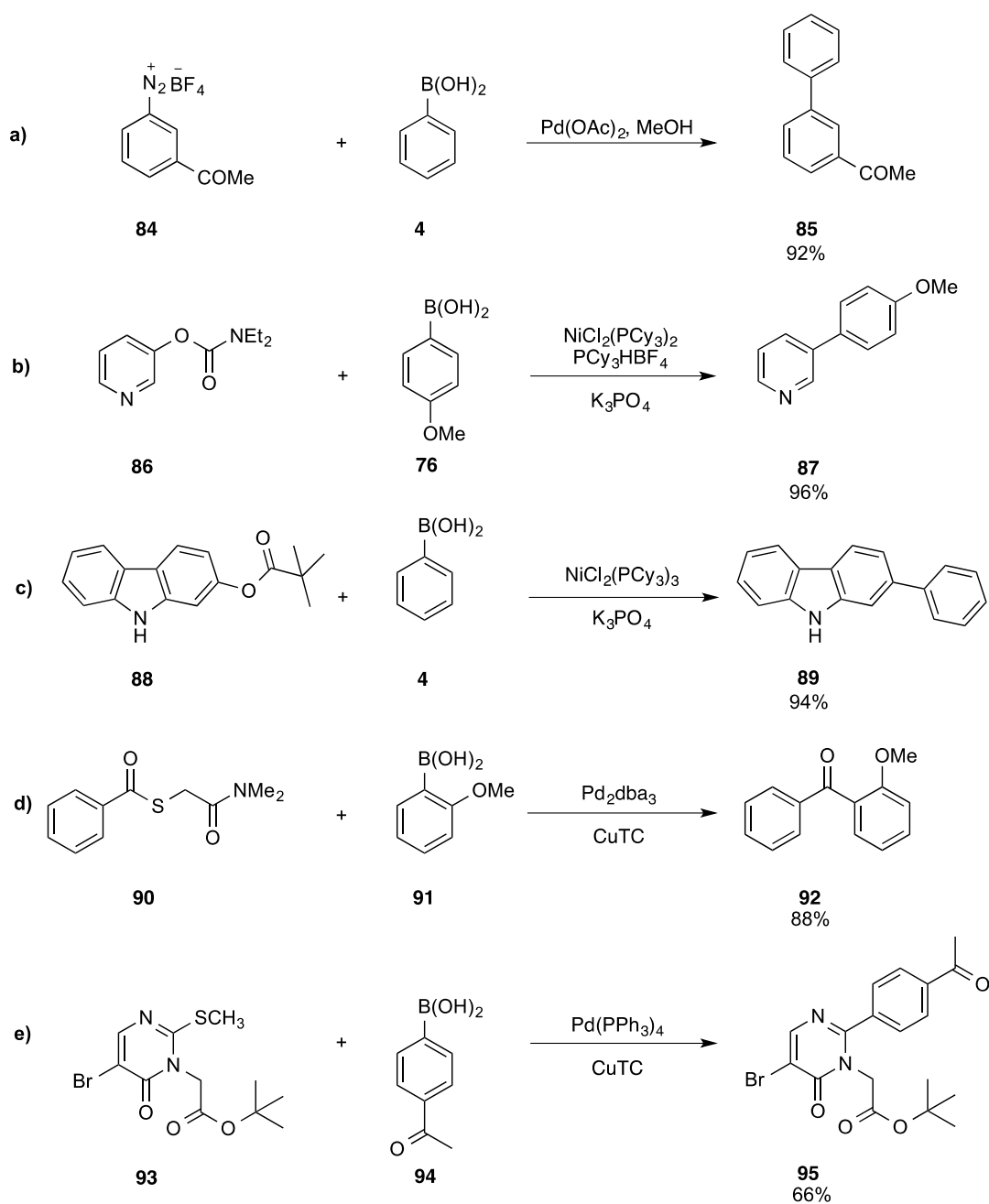


Figure 10: Alternative Suzuki-Miyaura cross-coupling electrophiles

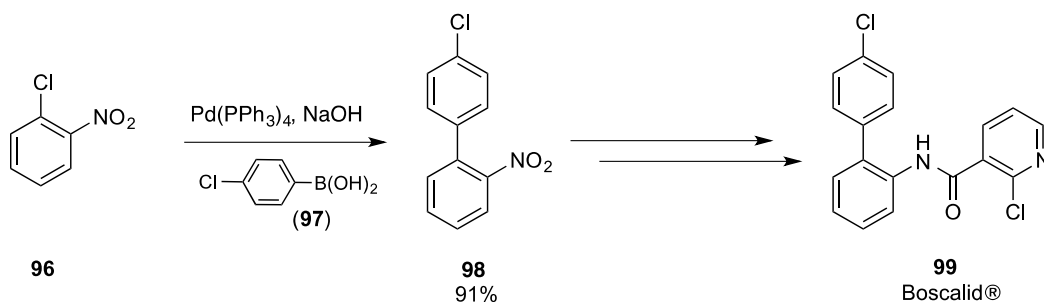
Owing to the functional group tolerance, mild reaction conditions and ease of practical set-up, the Suzuki-Miyaura cross-coupling reaction is used routinely in the pharmaceutical, agricultural and polymer sectors as well as in the synthesis of molecular wires, liquid crystals and natural products.⁸⁴⁻⁸⁷

1.4.1.2 Substrate Scope – Nucleophile

Another key advantage of the Suzuki-Miyaura cross-coupling is the scope of the organoboron component, with organoboranes, boronic acids, boronate esters, trifluoroborate salts, boronamides and MIDA boronates all tolerated. By exploiting their unique stabilities and reactivities, the choice of boron reagent can be tailored to the process or reaction requirements.

1.4.1.2.1 Boronic Acids in Suzuki-Miyaura Cross-Coupling

Given their superior reactivity, ease of synthesis and commercial availability, boronic acids are often the reagent of choice for synthetic chemists. Reflecting this, boronic acids (**97**) are often used in target syntheses, for example in the synthesis of Boscalid® (**99**) (Scheme 8), a multi-purpose fungicide, manufactured on a multi-tonne scale annually, and in the the synthesis of Losartan® (**36**) (*c.f* Scheme 5).⁸⁸



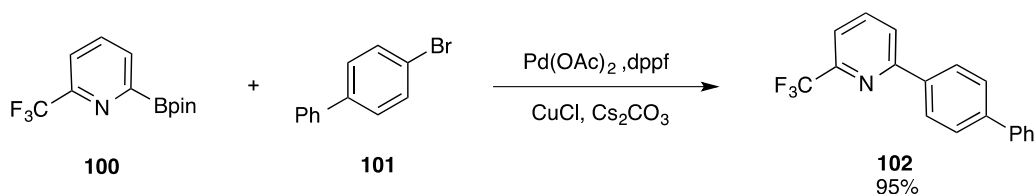
Scheme 8: Application of organoboronic acid cross-coupling towards the total synthesis of Boscalid

However, due to their propensity to undergo side reactions such as homocoupling, oxidation and protodeborylation under aqueous conditions,⁸⁹ as well as their tendency to

form oligomeric boroxines in anhydrous conditions (*c.f.* Scheme 1), excess reagent is often required and yields can often be limited. Reflecting this, it is often prudent to use organoboronic acid derivatives.

1.4.1.2.2 Boronate Esters in Suzuki-Miyaura Cross-Coupling

Boronate esters represent an attractive alternative due to their relative cost, availability, ease of preparation, bench and chromatographic stability. The inductively donating capabilities of the carbon group result in increased conjugation of oxygen into the boron-centre thereby reducing its Lewis acidity and reactivity. Owing to their enhanced stability the cross-coupling of the typically unstable 2-pyridyl moiety (**100**) has been carried out in excellent yields (Scheme 9).⁹⁰ Reactions involving substrates such as these are pertinent to the studies described in Chapters 2 and 3. Reactions of *ortho*-azinyl boronic acids and esters are typically extremely difficult due to their tendency to undergo protodeborylation.



Scheme 9: Application of boronate esters in the cross-coupling of the unstable 2-pyridyl moiety

Modern C-H activation strategies have provided efficient routes to boronic esters and as such they are an attractive reagent for tandem or one-pot reactions. These processes are central to this thesis and will be explored in Chapters 2 and 3.

1.4.1.2.3 Boronamides in Suzuki-Miyaura Cross-Coupling

Boronamides, such as B(dan) amides (**103**), possess complementary reactivity profiles to both boronic esters and acids (**103**), as well as MIDA boronates. The Lewis acidity of the boron atom is tempered by lone pair donation from the amine groups resulting in their stability to column chromatography and aqueous work-ups. Their distinct reactivity is exemplified by the requirement for aqueous acid to affect the hydrolysis to the substituent boronic acid required for cross-coupling. As such, the aqueous basic conditions typically employed for Suzuki reactions leave the B(dan) functionality intact (Figure 11a), enabling orthogonal, iterative cross-coupling strategies as demonstrated by Suginome and co-workers (Figure 11b).⁴¹

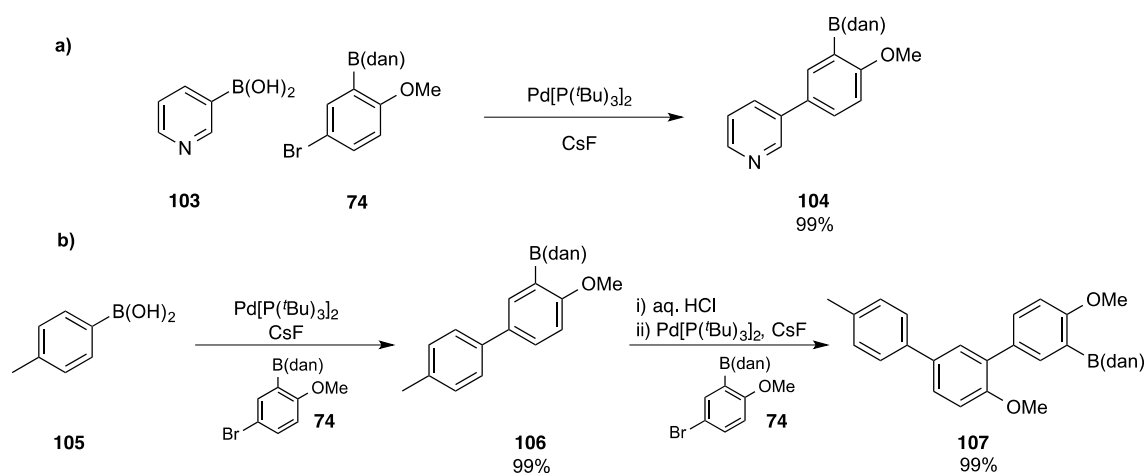
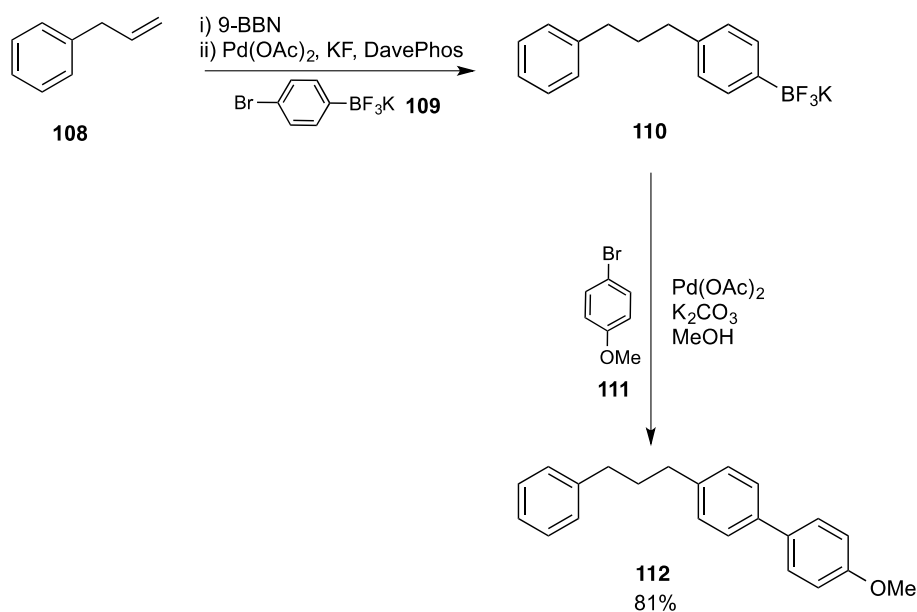


Figure 11: Boron-masking capabilities of the B(dan) functionality

1.4.1.2.4 Trifluoroborate Salts in Suzuki-Miyaura Cross-Coupling

Trifluoroborate salts (**109**) are an ideal boron-masking agent due to their ease of handling and stability to both air and atmospheric moisture. Due to the tetravalency of the boron atom, the usual Lewis acidic properties are attenuated and as a result trifluoroborate

salts can effectively function as a boron protecting group, enabling distal functional group manipulations or iterative cross-coupling strategies.⁹¹⁻⁹³ Their stability in anhydrous media enables site-selective reaction at distal boron functionality, such as boronic acids or boranes, whilst the trifluoroborate group remains intact.⁹⁴ Upon addition of an activating quantity of protic solvent, reaction of the trifluoroborate moiety (**110**) is initiated, proceeding by prior hydrolysis to the free boronic acid (Scheme 10). Reactions involving trifluoroborate salts often proceed in superior yields than with the equivalent boronic acid, due to the suppression of the aforementioned side reactions (*c.f* Section 1.4.1.2.1).⁹⁵



Scheme 10: Iterative cross-coupling application of an aryltrifluoroborate

1.4.1.2.5 MIDA Boronates in Suzuki-Miyaura Cross-Coupling

N-coordinated boronates, such as MIDA boronates (**113**), possess similar properties and reactivity patterns to the aforementioned trifluoroborate salts. The Lewis acidity of boron is masked by a dative bond between boron and a Lewis basic nitrogen atom. As a result

MIDA boronates are stable to column chromatography as well as a variety of reaction conditions, such as oxidation and reduction, and are applicable in similar iterative cross-coupling sequences.^{96,97} In this instance aqueous base is required to trigger the MIDA boronate hydrolysis to the substituent boronic acid, which can then undergo cross-coupling. Exploiting their boron-masking capabilities, Burke has reported their application in the automated flow-synthesis of natural product derivatives and small molecule scaffolds (**118**) (Figure 12a).⁸⁷ MIDA boronates have also found application in the cross-coupling of traditionally unstable 2-pyridyl compounds (**119**), in which a slow-release mechanism keeps the concentration of boronic acid low, minimising competing protodeborylation pathways (Figure 12b).⁹⁸

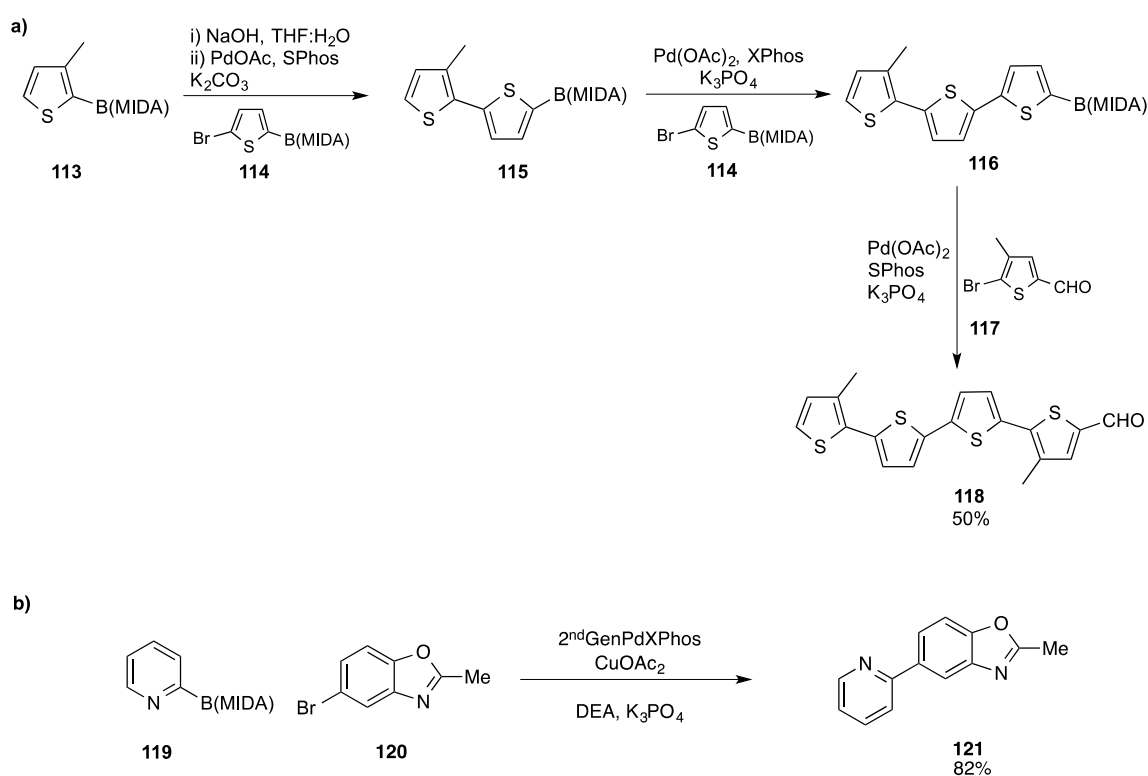


Figure 12: Suzuki-Miyaura cross-coupling applications of MIDA boronates

1.4.1.3 'One-pot' borylation/Suzuki-Miyaura Cross-Coupling Protocols

In order to improve efficiency and remove tedious separation and purifications of intermediates, chemists will often where possible try and combine multiple steps into one reaction vessel. A vast array of examples exist by which the process of C-X or C-H borylation can be combined with Suzuki-Miyaura cross-coupling into tandem one-pot processes (Figure 13).^{23,99-102} Such sequences will be further explored over the course of this thesis.

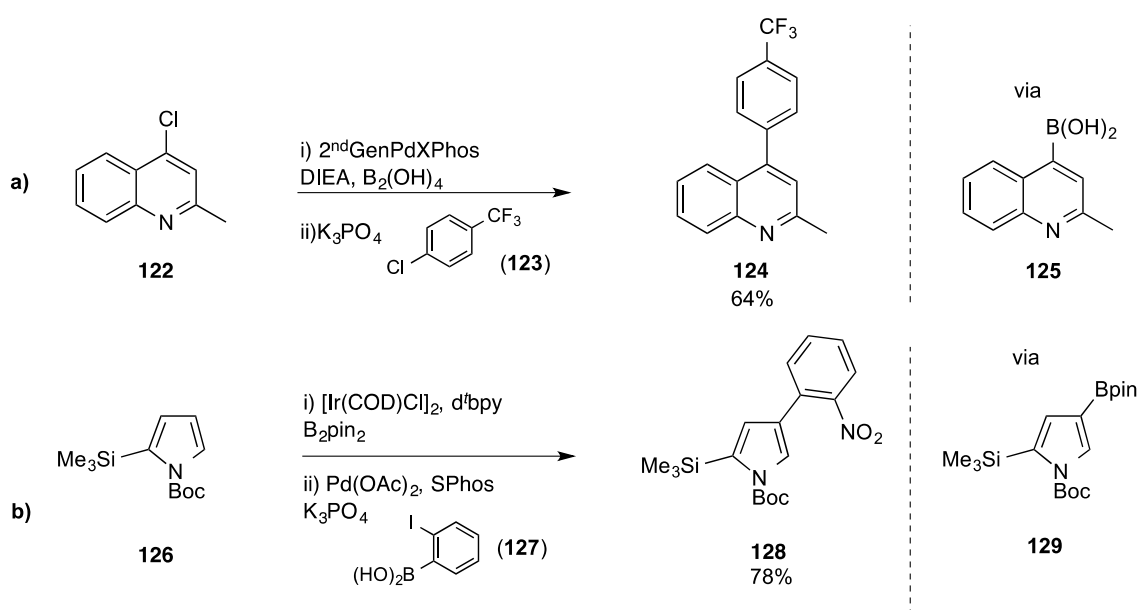
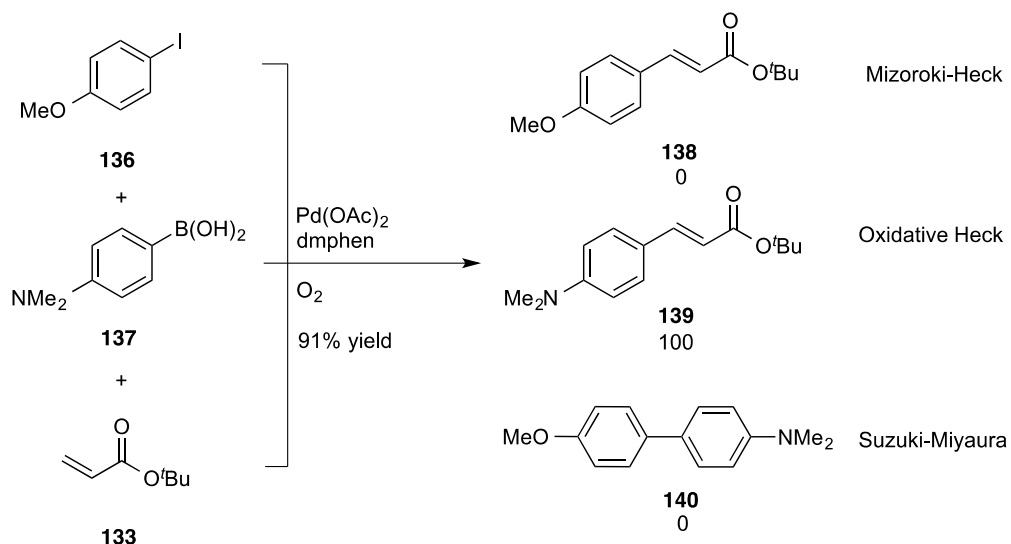


Figure 13: Examples of tandem 'one-pot' borylation/Suzuki-Miyaura cross-coupling reactions

1.4.2 Oxidative Heck Coupling

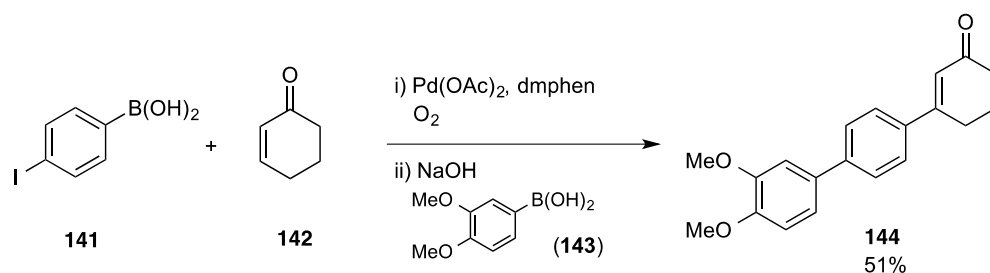
In their separate seminal reports, Mizoroki, Heck and their respective co-workers described the direct coupling of arylation/vinylation of olefins (**131**) with aromatic (or vinylic) electrophiles (**130**), catalysed by palladium salts, now commonly referred to as the Mizoroki-Heck coupling (Scheme 11).^{103,104}

oxidative Heck product (**139**) formation over Heck (**138**) and Suzuki-Miyaura cross-coupling products (**140**) (Scheme 13).



Scheme 13: Suzuki-Miyaura/oxidative Heck competition experiment

Exploiting this distinct mechanistic pathway, Jung and co-workers reported a chemoselective 3-component tandem oxidative Heck/Suzuki-Miyaura cross-coupling reaction (Scheme 14).¹⁰⁸



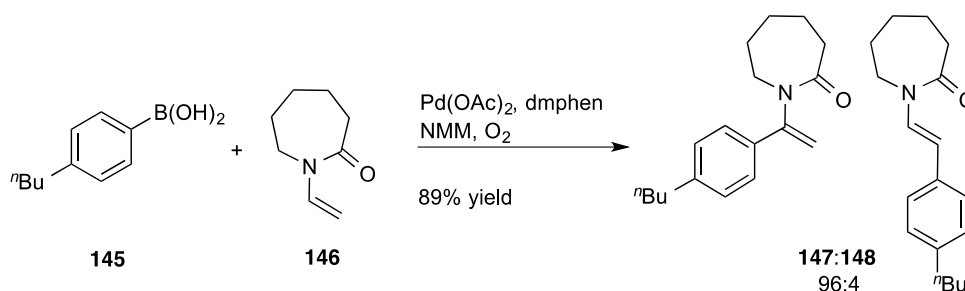
Scheme 14: Multi-component oxidative Heck/Suzuki-Miyaura cross-coupling reaction

1.4.2.1 Variation in Oxidant

Common chemical oxidants employed in oxidative Heck couplings include copper and iron salts or organic oxidants, such as benzoquinone.¹⁰⁹⁻¹¹¹ Alternatively, molecular oxygen or air have also been employed, offering both practical and environmental advantages.^{106,112} Moreover, recent reports have demonstrated that in the absence of a formal oxidant the olefin reagent, present in stoichiometric excess, may also facilitate the reaction by acting as a hydride acceptor after elimination of the cross-coupled product.¹¹³

1.4.2.2 Ligand-Assisted Protocols

Further advances have been reported through ligand-assisted protocols (*c.f.* Scheme 13 and Scheme 14).¹¹⁴ As well as providing improved yields and facilitating the redox processes, chelating dinitrogen ligands have also enabled control of regioselectivity. For example, the arylation of electron-rich olefins, such as vinyl ethers or enamides (**146**), occurs predominantly at the electron-deficient alpha-position (**147**) (Scheme 15).¹¹⁵ Conversely, the corresponding reaction carried out in the absence of 2,9-dimethyl-1,10-phenanthroline (dmphen) gives the opposite regioisomer (**148**).



Scheme 15: Regioselective oxidative Heck coupling example

1.4.2.3 Substrate Scope – Boron Component

The scope for variation within the boron-component is somewhat limited, with substrate scope limited to aryl boronic acids and esters (pinacol (**149**) and neopentyl glycol esters (**151**) (Figure 14).^{106,107} Both electron-rich and electron-poor boronic acids and esters are well tolerated, as well as heteroaryl systems.

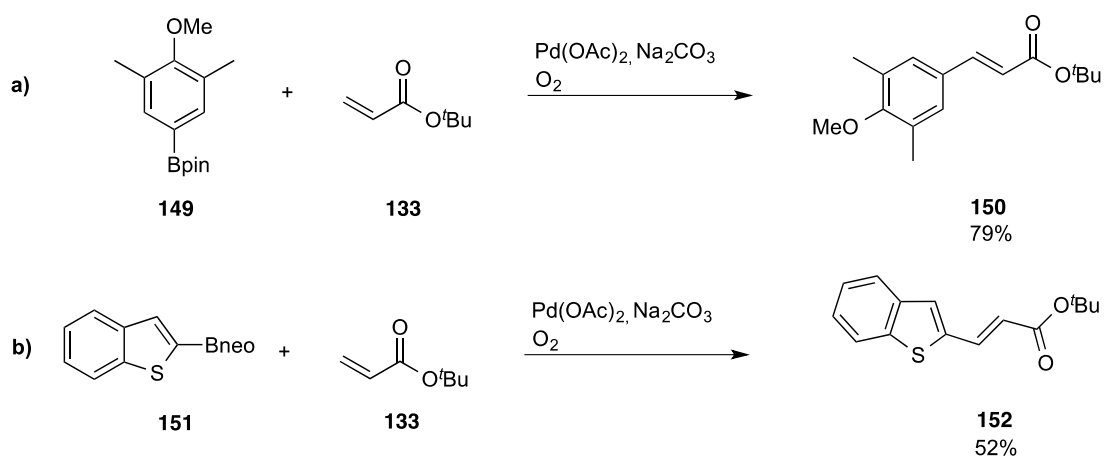


Figure 14: Applications of boronate esters in oxidative Heck couplings

1.4.2.4 ‘One-pot’ Borylation/Oxidative Heck Coupling Protocols

Recent advances in routes to structurally diverse aromatic boronic esters and acids means that there is vast potential for improved reaction and substrate scope. Furthermore, whereas there is a diverse array of literature available detailing one-pot borylation/Suzuki-Miyaura cross-couplings, the analogous one-pot borylation/oxidative Heck couplings have not been reported. Attempts towards their development are described in Chapter 4.

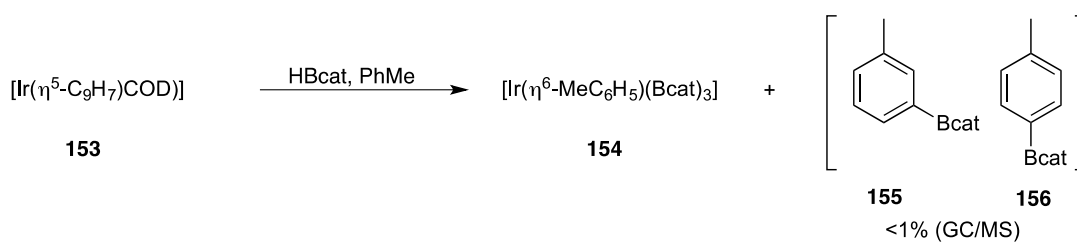
2 Borylation of Azinyl Heterocycles

2.1 Catalytic aromatic C-H borylation

C-H activation has been a longstanding goal in synthetic chemistry and offers an expedient route by which traditionally unreactive C-H bonds can be cleaved and functionalised to yield more desirable and synthetically useful functionalities, avoiding the more classical approach of transforming pre-existing functional groups to achieve the desired functionality (*c.f* Section 1.3.1). This chemistry offers valuable new disconnection strategies for the construction of complex scaffolds as C-H bonds are ubiquitous in all organic molecules. As discussed in the previous chapter, the incorporation of boronic acid-derived functionality allows for a variety of downstream flexibility (*c.f* Figure 8). Building on this theme, this chapter will begin by reviewing the development of aromatic C-H borylation into a mild catalytic reaction, the postulated reaction mechanism and substrate scope of the reaction. From consideration of the reaction mechanism, strategies were gleaned for the borylation of stubborn azinyl heterocycles, which will form the focus of the remainder of the chapter.

2.1.1 History of Catalytic C-H borylation

The first observed C-H borylation product was noted in the supporting information of a paper published in 1993 by Marder and co-workers, in which the target was a trisboryl-iridium complex (**154**).¹¹⁶ The reaction yielded trace amounts (<1% by GC/MS analysis) of two isomers of tolyboronate ester (**155,156**), which arose as a result of borylation of the toluene solvent (Scheme 16). This observation was not eluded to further in the main text and further developments on this work were not pursued at this time.



Scheme 16: First reported C-H borylation products

The first stoichiometric borylations, proceeding by photochemically-induced decay of pre-prepared metal-boryl complexes ($[\text{Mn}(\text{CO})_5\text{Bcat}]$ (**157**), $[\text{Re}(\text{CO})_5\text{Bcat}]$ (**158**) and $[\text{Cp}^*\text{Fe}(\text{CO})_2\text{Bcat}]$ (**159**) in aromatic solvents, were reported by Hartwig *et. al* in 1995 (Figure 15).¹¹⁷

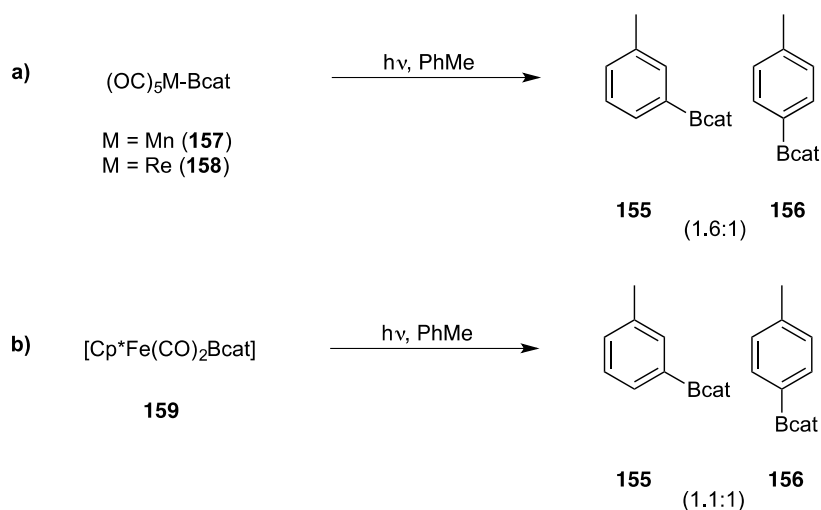


Figure 15: C-H borylation via photochemically-induced decay of metal-boryl complexes

The earliest reported examples of aromatic C-H borylation as a catalytic process used $[\text{Cp}^*\text{Ir}(\text{PMe}_3)(\text{H})(\text{Bpin})]$ (**161**),¹¹⁸ and $[\text{RhCl}(\text{P}^i\text{Pr}_3)_2(\text{N}_2)]$ (**163**) (Figure 16).¹¹⁹ However, these processes generally required high temperatures (in excess of 140 °C), high

catalysts loadings, long reaction times and suffered from chemoselectivity issues (**166**).

Subsequent work was therefore focused towards solving these issues.

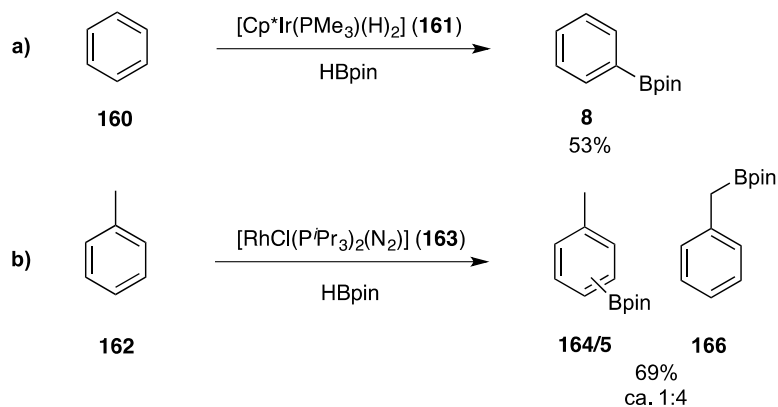


Figure 16: First reported catalytic C-H borylation protocols

In 2002, Smith and co-workers reported that *in-situ* generated phosphine-ligated iridium complexes could catalyse borylation reactions under milder conditions whilst avoiding some of the previously reported selectivity problems (Figure 17a).⁹⁹ This methodology also circumvented the need for expensive or pre-formed boryl complexes, which can be expensive and difficult to synthesise, and improved the practical simplicity by enabling the mixing of simple starting materials in the arene (**167**, **171**) of choice. The synthetic utility of this process was demonstrated in the first reported one-pot borylation/Suzuki-Miyaura cross-coupling protocol (Figure 17b).

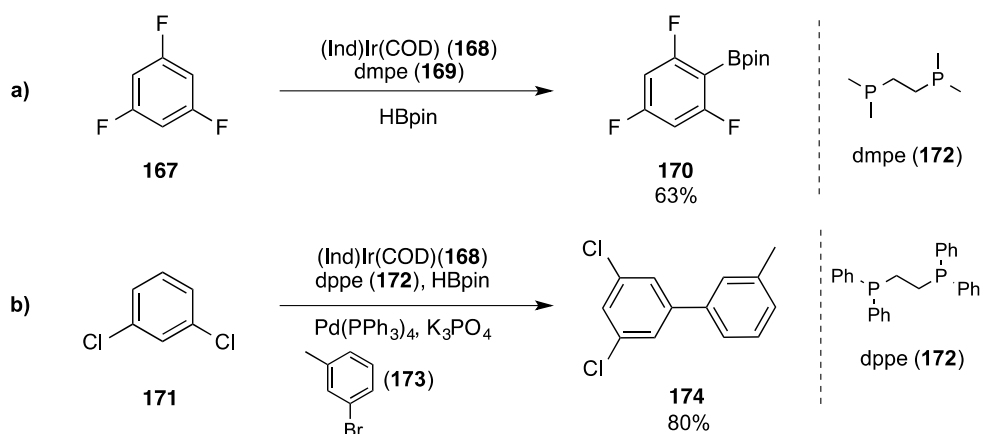


Figure 17: C-H borylation catalysed by phosphine-ligated Iridium complexes

In a report published concurrently with Smith's work, Hartwig, and co-workers reported borylations using *in-situ* generated bipyridine-ligated iridium complexes, which catalysed the reaction in higher turnover numbers than had previously been observed for preceding catalytic borylation protocols (Figure 18a).¹²⁰ This system was also the first reported aromatic C-H borylation to proceed at room temperature (Figure 18b).

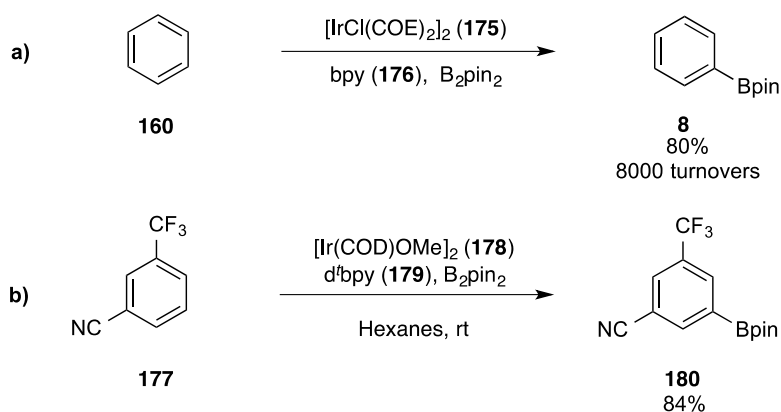
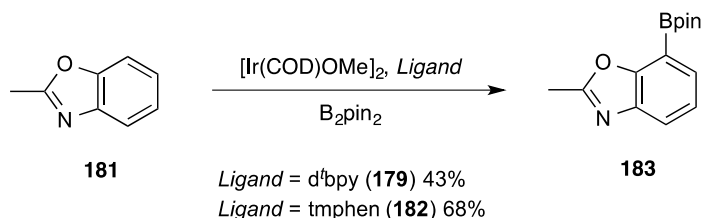


Figure 18: C-H borylation catalysed by bipyridine-ligated iridium

Later work carried out by the same group in 2002 investigated various factors including ligand substituents, iridium precursors, substituent effects and plausible reaction

solvents.¹²¹ It was found that the most effective iridium complexes were comprised from alkoxy-iridium precursors (**178**) with bipyridine ligands (**176**, **179**) containing electron-donating substituents (^tBu, NMe₂ and OMe) at the *para*-position. Whilst most prior reported C-H borylation reactions were carried out in neat arene, the findings of Hartwig and Ishiyama enabled the use of low polarity, non-coordinating solvents such as hexanes (Figure 18b).

One main attraction to iridium-catalysed C-H borylation is the experimental simplicity, with pre-mixing of pre-catalyst, ligand and bis-boryl reagent generating the active catalyst *in-situ*. The combination of [Ir(COD)OMe]₂ (**178**) and d^tbpy (**179**) is still the most widely used catalytic system by synthetic chemists, though recent findings of Smith, Hartwig and their respective groups, suggest improved reactivity may be attained through the use of phenanthroline-based ligands, such as 3,4,7,8-tetramethyl-1,10-phenanthroline (tmphen, **182**) (Scheme 17).^{122,123}



Scheme 17: Comparative performance of Me₄Phen ligand vs d^tbpy

2.1.2 Mechanistic Discussion

C-H borylation catalysed by either phosphine or bipyridine-ligated iridium complexes is believed to follow a similar mechanistic pathway. Since the latter is more commonly used and represents the catalytic system used in this study, this discussion will focus on this particular system.⁹⁹

In light of prior knowledge gleaned from iridium redox chemistry, two mechanistic possibilities were considered; i) an Ir(I)/Ir(III) catalytic cycle or ii) an Ir(III)/Ir(V) catalytic cycle. A computational investigation conducted by Sakaki and co-workers suggested the active catalyst to be Ir(III).¹²⁴ The basis for this was the calculated activation energy of oxidative addition of B₂pin₂ to an Ir(I)boryl complex, which was considerably lower than the calculated activation energy of the oxidative addition of arene. In addition the activation energy barrier to reductive elimination of B₂pin₂ from an Ir(III)trisboryl complex exceeded the experimentally determined energy barrier of C-H bond cleavage during oxidative addition. On these grounds the potential intermediacy of an Ir(I) complex was discounted. These findings have been experimentally supported by Hartwig *et.al*, who have observed an Ir(III)trisboryl complex in catalytic reaction mixtures.¹²⁰ Moreover, reactions involving a pre-formed Ir(III)trisboryl complex showed it to possess excellent catalytic activity.¹²⁵ The overall catalytic cycle as determined by computational calculations and experimental observations is given below (Figure 19);

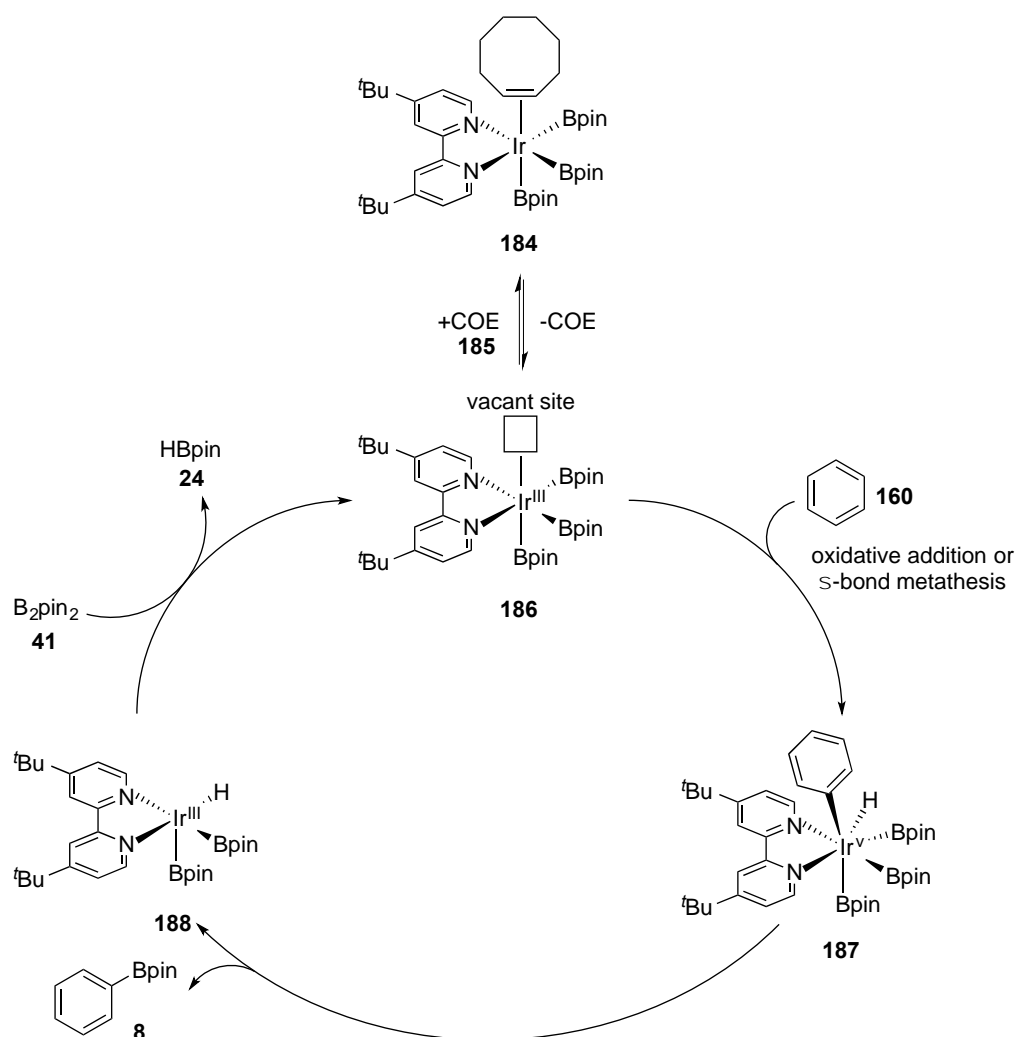


Figure 19: Catalytic cycle

The key steps in the catalytic cycle are summarised in the following sections.

2.1.2.1 *In-situ* active catalyst formation

It was hypothesised that *in-situ* formation of the active catalyst could proceed via initial dissociation of alkene ligand (cyclooctadiene or cyclooctene) (from [Ir(COD)OMe]₂ (**178**) or [Ir(COD)Cl]₂ (**189**)) with subsequent coordination of bipyridine (bipy) ligand (Figure 20). The electron-donating ability of the bipyridine ligand can subsequently supplement

the oxidative addition of bis-boryl reagents. DFT calculations found that reductive elimination of Cl-Beg from IrCl(Beg)₂(bipy) to be highly unfavourable as the reaction was found to be very endothermic. It was calculated that prior oxidative addition of a second molecule of diboron reagent with subsequent Cl-Beg reductive elimination was more energetically favourable, thus reinforcing the intermediacy of Ir(III)trisboryl complexes. Hartwig and co-workers have also noted the observance of an induction period corresponding to required reduction of COD to COE.¹²⁰ This induction period is eliminated with added catalytic quantities of HBPin or with pre-catalysts bearing COE ligands. It was shown that overall the reaction is inverse first order with respect to added COE (**185**), which supported the theory of reversible dissociation of COE prior to oxidative addition.

2.1.2.2 Oxidative Addition

Oxidative addition of arene (**160**) to the active Ir(III)trisboryl complex (**186**) generates the sterically crowded 7-coordinate Ir(V) intermediate (**187**) (Figure 20). DFT calculations supported the formation of the hindered Ir(V) intermediate and attribute its stability to stabilisation by the electron-rich bipyridyl ligand. A primary isotope effect observed in reactions involving the isolated active complex with arenes and deuterated arenes suggests that the C-H activation step is rate-limiting and is in agreement with computational calculations of the activation energy barriers of the individual catalytic cycle steps.

2.1.2.3 Reductive Elimination

Reductive elimination of the arylboronate ester (**8**) from this sterically crowded Ir(V) species proceeds quickly due to the small activation energy barrier to yield an Ir(III)monohydride species (**188**) (Figure 20).

2.1.2.4 Catalyst Recycling

Reformation of the active catalyst is achieved through oxidative addition of a further equivalent of B₂pin₂ (**41**), with subsequent reductive elimination of HBpin (**24**) (Figure 20).

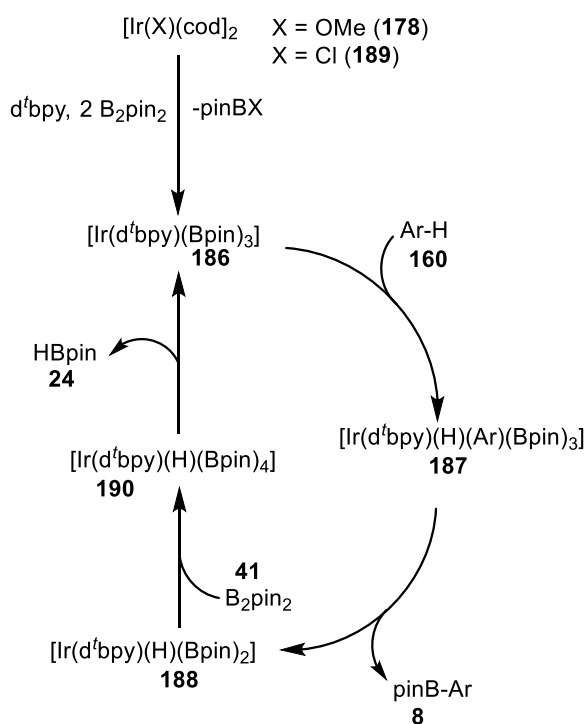


Figure 20: B₂pin₂-mediated catalytic cycle

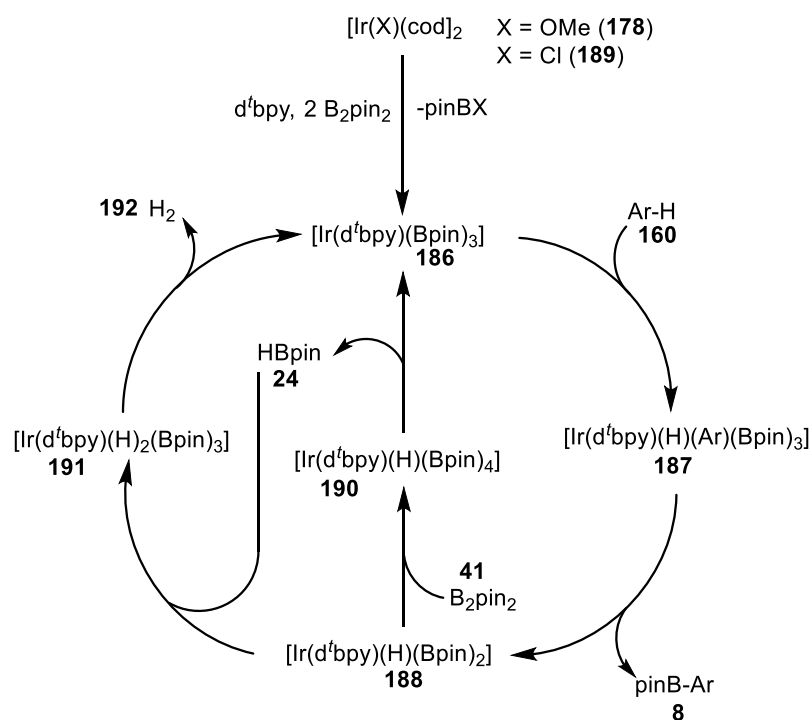


Figure 22: Binary catalytic cycle

2.1.3 Substrate scope

The following section will explore the substrate scope of aromatic C-H borylation, and the relationship between mechanism and regioselectivity.

2.1.3.1 Borylation of Aromatic Substrates

Due to the steric bulk surrounding the active iridium trisboryl complex (**186**), the C-H borylation reaction is highly sensitive to steric effects (*c.f* Figure 19). Reflecting this, borylation *ortho* to substituents is highly disfavoured and as such regioselectivity is, in many cases, predictable.¹²⁰ For example, borylation of 1,3-disubstituted arenes (**193**) yields the 1,3,5-trisubstituted product (**194**) and the borylation of unsymmetrical 1,4-

disubstituted arenes (**195**) yields products favouring borylation *ortho* to the least sterically encumbering substituent (Figure 23).¹²⁶

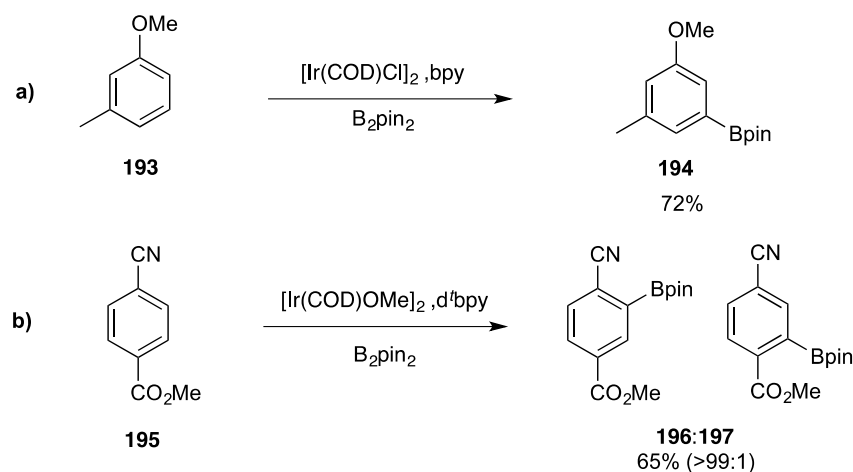
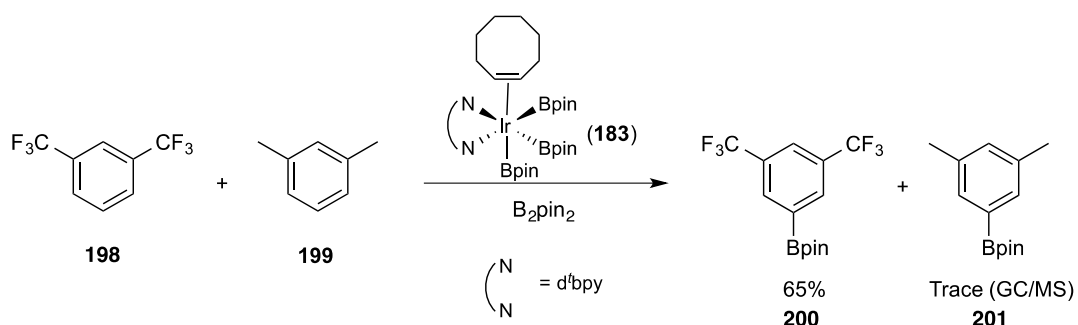


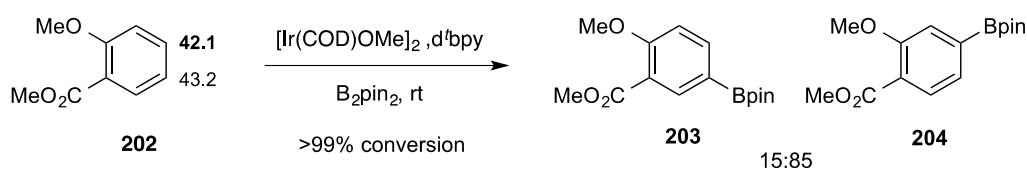
Figure 23: Steric-directed aromatic C-H borylation

In their investigation into the reaction mechanism, Hartwig and co-workers found intermolecular electronic effects, for example electron-deficient arenes, such as 1,3-bis(trifluoromethyl)benzene (**198**) react more efficiently than, and in preference to, electron-rich arenes, such as *m*-xylene (**199**) (Scheme 18).¹²⁵



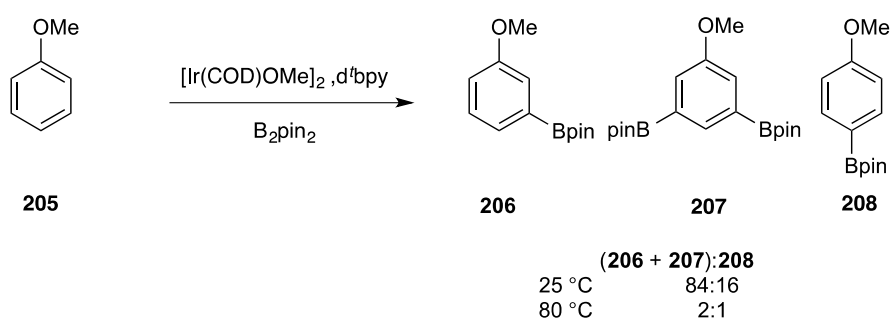
Scheme 18: Intermolecular electronic effects

Our group has demonstrated that intramolecular electronic influences can be observed at lower temperatures. For example, the borylation of unsymmetrical 1,2-disubstituted arenes (**202**) favours borylation *para* to π -electron withdrawing groups (Scheme 19). In many, but not all cases, qualitative selectivity predictions can be made on the basis of relative C-H acidity values.^{127,128} This provides regioselectivity complementary to classical arene functionalisation methods, such as electrophilic aromatic substitution or DoM (*c.f.* Scheme 4).



Scheme 19: C-H acidity as a predictor of regioselectivity

Lower temperatures also lead to enhanced selectivities observed in the borylation of monosubstituted arenes, with borylation of anisole (**205**), for example, showing enhanced ratios in favour of *meta* borylation at room temperature (Scheme 20).¹²⁹



Scheme 20: Electronic effects in the borylation of a monosubstituted arene

2.1.3.2 Borylation of Heteroaromatic Substrates

Electronic effects are more prevalent in the borylation of heteroarenes, with electron-rich heteroaromatics (**209-211**) and their benzofused congeners (**66**, **215**, **216**) undergoing borylation with excellent regiocontrol *ortho* to the heteroatom, consistent with the C-H acidity hypothesis (Figure 24a, b). Steric effects do still dominate, as is evidenced in the borylation of N-TIPS-indole (**219**), which undergoes borylation at C-3 rather than the preferred C-2, due to the presence of the sterically encumbering silyl protecting group, however the absence of borylation of the phenyl ring is noteworthy (Figure 24c).¹³⁰ Smith and co-workers also demonstrated that indole could also undergo borylation at the 7-position through an N-H directing mechanism, in the presence of a C-2 blocking group (**221**) (Figure 24d).

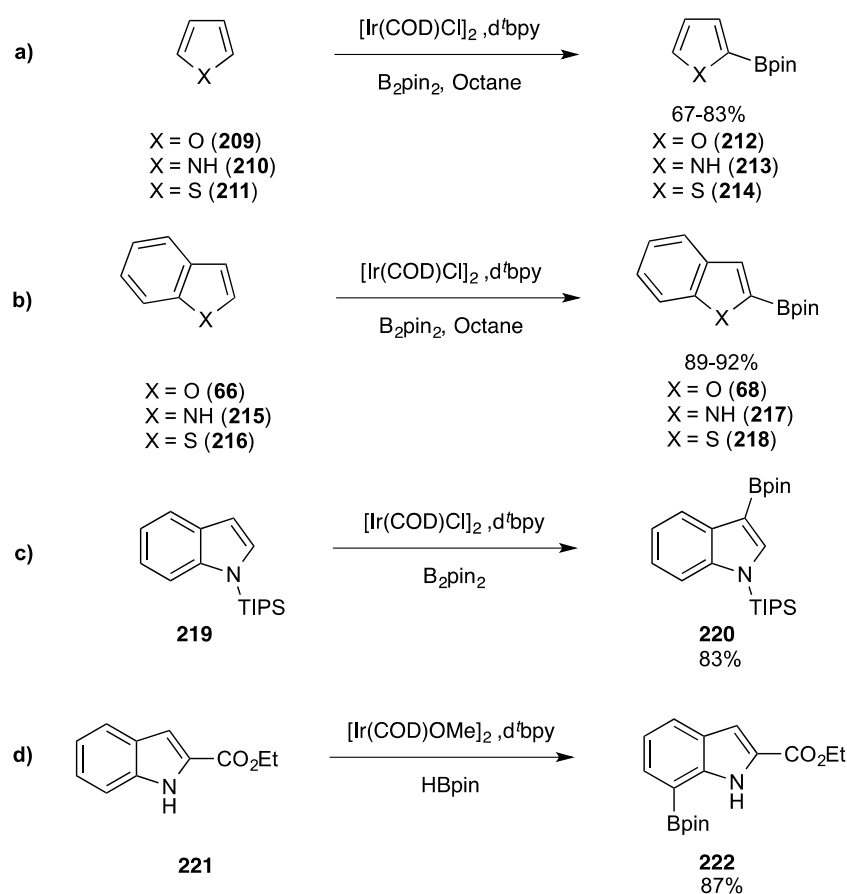
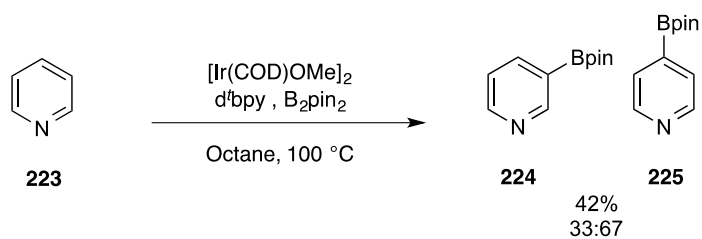


Figure 24: Borylation of electron-rich heteroaromatics

By comparison, the borylation of azinyl heterocycles is less favourable and proceeds with regioselectivity distinct from that observed in reactions involving electron-rich heterocycles. In their seminal study on the borylation of pyridine, Ishiyama and Miyaura found the borylation of pyridine (**223**) to proceed sluggishly, even under forcing conditions, to give a statistical mixture of 3 and 4-boryl products (**224** and **225** respectively) (Scheme 21).¹³¹ This poor reactivity is somewhat surprising given the superior reactivity of electron-deficient arenes vs electron-rich congeners (*c.f* Scheme 18).



Scheme 21: Borylation of pyridine

Reflecting this sluggish reactivity, the scope for borylation of Lewis-basic heterocycles is limited. The following sections will explore the underlying reasons for these observations.

2.1.4 Borylation of Substituents Bearing an Azinyl Nitrogen

Two mechanistic possibilities have been considered to account for the poor reactivity of Lewis-basic substrates; coordination of the azinyl nitrogen lone pair to the Lewis-acidic boron reagent or coordination to the iridium catalyst.

2.1.4.1 Pyridyl-Boron Interactions

The Lewis-acidity of boron and its effect on its chemistry is well established (*c.f.* Section 1.2). Furthermore, Marder and co-workers have reported the formation of Lewis acid-base pyridyl-boron adducts arising due to energetically favourable and fast interactions between bis-catecholodiboron (B_2cat_2 , **226**) and 4-picoline (**227**) (Figure 25).¹³² Lewis acid-base interactions such as these, demonstrable by an upfield shift in the ^{11}B NMR spectroscopic signal, may inhibit the oxidative addition of the bis-boryl species required for active catalyst generation and recovery (*c.f.* Section 2.1.2).

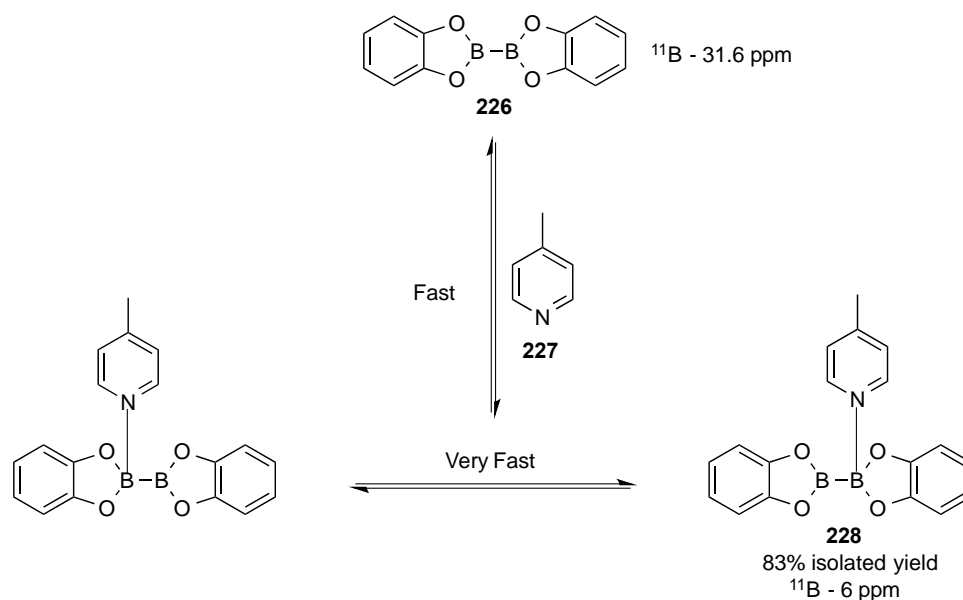
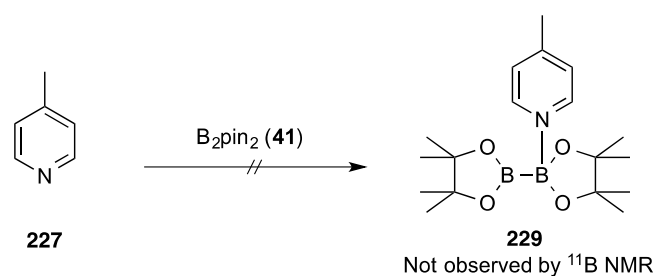


Figure 25: Lewis acid-base pyridyl-boron adduct formation

Our group has investigated such interactions with B_2pin_2 , as this is the standard bisboron reagent used in most borylation reactions. Through ^{11}B NMR studies, Mkhaliid has showed that a solution of 4-picoline (**227**) and B_2pin_2 (**41**) does not lead to formation of a tetravalent boron adduct (**229**), even when independently varying the concentrations of picoline and B_2pin_2 (Scheme 22).¹³³ It was suggested that because the relative electron density at the boron atoms in a molecule of B_2pin_2 is greater than in the catechol derivative (**226**), adduct formation is disrupted. This suggested that azinyl coordination to the iridium centre was solely responsible for the sluggish borylation of pyridyl substrates.



Scheme 22: Attempted reaction between 4-picoline and B_2pin_2

2.1.4.2 Pyridyl-Iridium Interactions

Given that C-H oxidative addition is the rate-determining step of the catalytic cycle, the active Ir(III) trisboryl complex (**186**) will be at greatest concentration at any given point in the reaction (*c.f.* Section 2.1.2.2). The oxidative addition step is contingent upon formation of a vacant coordination site in order to proceed and thus borylation of Lewis-basic substrates bearing coordinating azinyl nitrogen atoms is problematic. It was postulated that Lewis acid-base interactions between coordinating substrates and the Lewis-acidic iridium centre furnishes a coordinatively saturated complex (**230**) which therefore cannot undergo C-H oxidative addition (Figure 26).

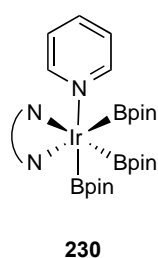


Figure 26: Catalyst poisoning through pyridine coordination

Our group sought to test this hypothesis by reacting of a series of 2-substituted pyridines.

2.1.4.3 Borylation of 2-Substituted Pyridines

Mkhalid demonstrated that the presence of one or two *ortho*-substituents enabled the substrate to undergo borylation efficiently. For example, the borylation of 2-phenylpyridine (**231**) proceeded efficiently, providing good conversion to a 45:55 mixture of 4 and 5-boryl products (**232** and **233** respectively), with complete chemoselectivity for the phenyl ring (Figure 27a). Similarly the borylation of 2-picoline (**234**) provides a 49:51 mixture of isomers (**235**, **236**) (Figure 27b).¹³³

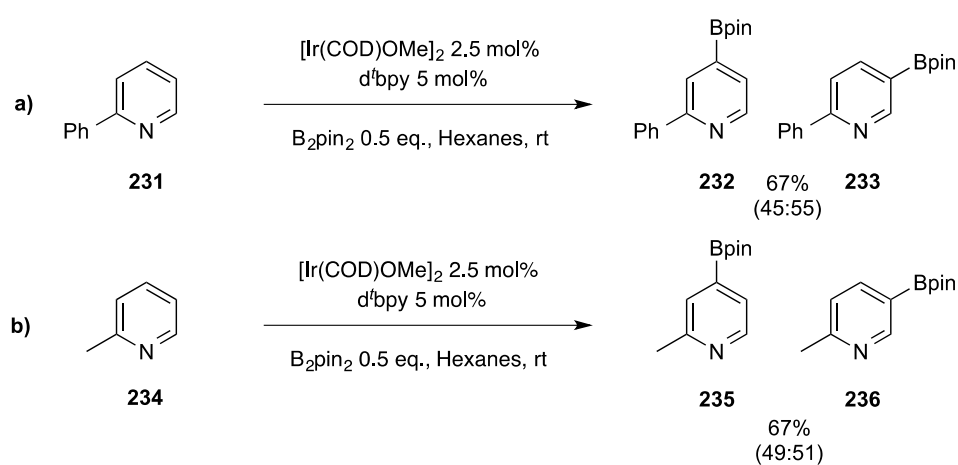
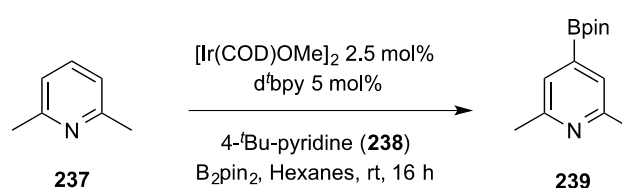


Figure 27: Borylation of 2-substituted pyridines

In light of these results, it was suggested that the presence of *ortho* substituents disrupted the coordination of the azinyl nitrogen. One possible reason for this is that additional steric bulk within the inner coordination sphere is not well tolerated and as a result C-H oxidative addition dominates.

2.1.4.4 Competition Experiments

Confirming this hypothesis, competition experiments entailing the borylation of 2,6-lutidine (**237**) doped with varying quantities of an inhibitor (4-*tert*-butyl-pyridine, **238**) demonstrated the inhibitory nature of azinyl coordination. Near complete shutdown of reactivity was observed even at low levels of inhibitor (Table 1, entry 5). Conversely, control reactions carried out in the absence of **238**, proceeded efficiently, with complete conversion to 4-boryl product (**239**) observed (entry 1).



Entry	4- <i>t</i> Bu-pyridine (equiv.)	B_2pin_2 (equiv.)	Yield ^a (%)
1	N/A	1	100
2	1	0.5	Trace ^b
3	1	1	Trace ^b
4	1	2	Trace ^b
5	0.1	1.1	Trace ^b

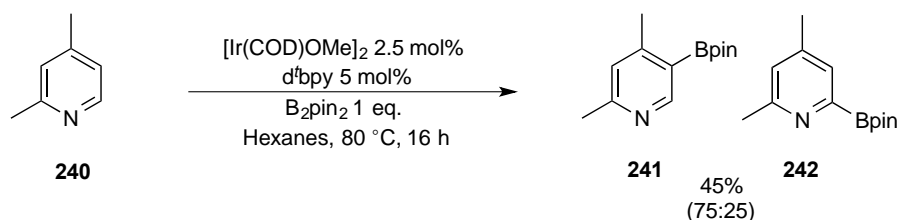
a. Determined by GC/MS; b. Detectable but less than 3%

Table 1: Borylation of 2,6-lutidine doped with varying quantities of 4-*tert*-butyl-pyridine

2.1.4.5 *ortho*-Azinyl Boronate Esters

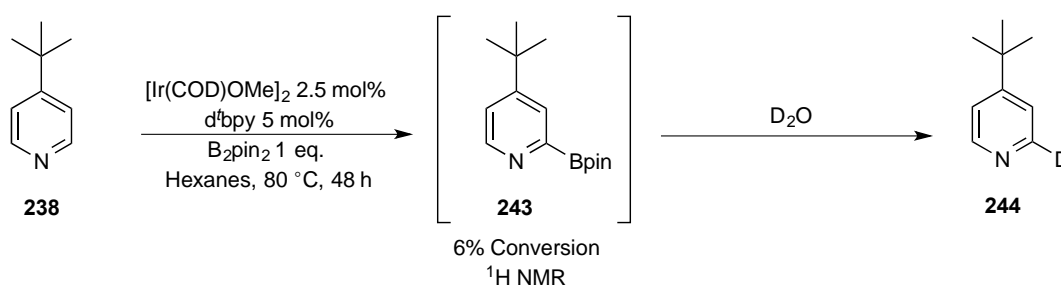
The absence of 6-boryl products in the borylation of 2-substituted pyridines was noteworthy and was initially attributed to steric hindrance imparted by the *ortho* azinyl lone pair, which was postulated to function similarly to a substituent, with the substrate thereby borylating analogously to a 1,2-disubstituted benzene (*c.f.* Scheme 19). However, borylation of 2,4-lutidine (**240**) provided a 75:25 mixture of 5 and 6-boryl

products (**241** and **242** respectively), with borylation occurring preferentially *ortho* to the more sterically encumbering methyl substituent, therefore suggesting an energy barrier to formation of *ortho*-azinyl boronate esters (Scheme 23).



Scheme 23: Borylation of 2,4-lutidine

In addition, *ortho*-azinyl boronate esters have been found to be highly unstable,^{98,122,134,135} for example the borylation of 4-*tert*-butyl pyridine (**238**), whilst unfavourable due to catalyst binding, provided limited formation of *ortho*-azinyl product **243**, which readily underwent C-B bond cleavage upon exposure to D_2O (Scheme 24). The instability of *ortho*-azinyl boronate esters is another key factor limiting their widespread utility and is discussed in the following section.

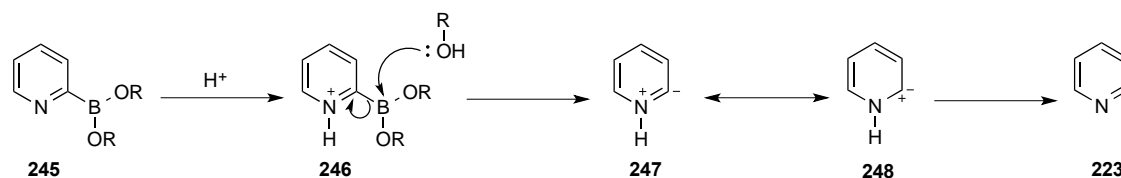


Scheme 24: Attempted borylation of 4-*tert*-butylpyridine, with *in-situ* ipso-deuteration

2.1.5 Protodeborylation

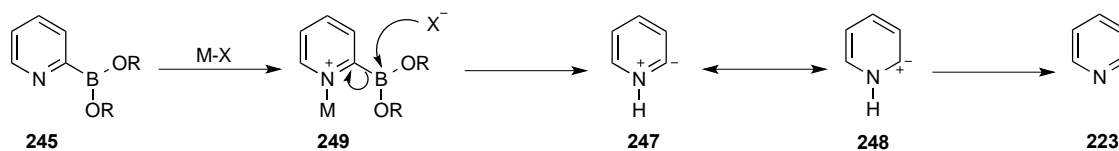
Protodeborylation describes the process by which a boryl group is cleaved and lost from a molecule and replaced with a hydrogen atom. This decomposition pathway represents a long standing limitation on the handling and reactions of 2-heteroaryl boronic acids and esters.

Although widely reported, the mechanism is not well understood. Nonetheless, work carried out to date has enabled pathways to be postulated. Seminal work carried out by Kuivila and co-workers demonstrated that protodeborylation may proceed via acid, base or metal-mediated catalysis.³⁻⁵ Stevens later proposed that acid-mediated protodeborylation of 2-pyridine boronic acids or esters (**245**) proceeds via initial protonation of the azinyl nitrogen (**246**), with nucleophilic displacement of the boronic acid or ester forming a ylide intermediate (**247**) which could then rearrange to restore aromaticity (**223**) (Scheme 25).¹³⁵



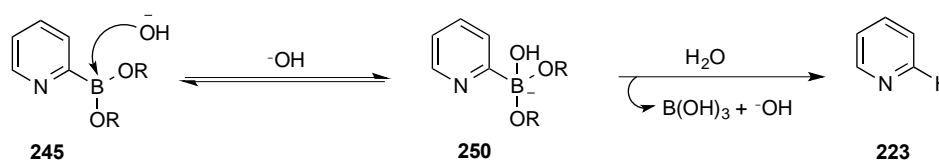
Scheme 25: Mechanism of acid-mediated protodeborylation

Stevens also postulated that due to the Lewis-basicity of the azinyl nitrogen, similar pre-coordination to Lewis-acidic metal salts (**249**) could initiate a similar mechanistic pathway (Scheme 26). Due to the requirement for metal salts in downstream cross-coupling pathways this pathway is particularly problematic and limits the application 2-pyridyl boronic acids and esters in synthesis.



Scheme 26: Mechanism of metal-mediated protodeborylation

Similarly, due to the requirement for base in Suzuki-Miyaura cross-couplings, the base-catalysed pathway is also pertinent. Boronate (**250**) generation arising from nucleophilic attack of base or *in-situ* generated hydroxide ion and subsequent B-C cleavage by protonolysis is accepted as the general base-catalysed mechanism, however the role of the azinyl nitrogen or *ortho*-heteroatom is unclear (Scheme 27).⁸⁹



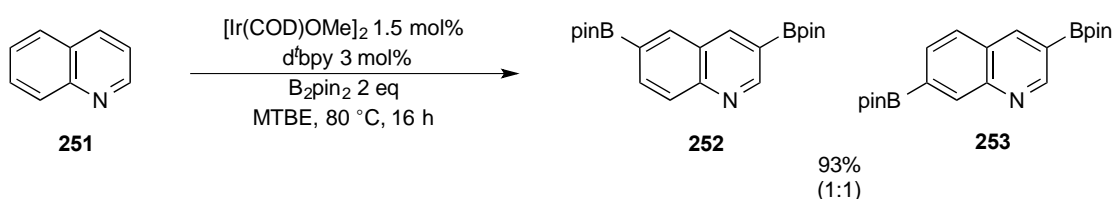
Scheme 27: Mechanism of base-mediated mechanism

Reflecting the instability of *ortho*-azinyl boronic acids and esters, several groups have reported the use of boronic acid derivatives, such as MIDA boronates or triol borates, as surrogates, with slow release cross-coupling mechanisms minimising the *in-situ* concentrations of the unstable boronic acid or ester species (*c.f* Figure 12).^{98,134,136,137}

2.2 Previous Work and Chapter Goals

As described in section 2.1.4, whilst borylation of pyridine is difficult, the presence of a 2-substituent enables pyridyl substrates to react efficiently. This was attributed to inhibition of coordination to the catalyst. Similarly, other work in the group has

demonstrated the surprising reactivity of quinoline substrates (**251**), which built on previous work by Miyaura and Ishiyama (Scheme 28).¹³¹ This was attributed to the inhibitory effect of the *peri* C-H bond which prevents coordination of the azinyl nitrogen.^{127,129}



Scheme 28: Borylation of quinoline

Consistent with previous observations (*c.f.* Figure 27), was the lack of formation of 2-boryl products, for example borylation of 4-chloro-7-(trifluoromethyl)quinoline (**254**) gave full conversion to the 3-boryl product (**256**), with the 2-boryl product (**255**) not observed even at trace levels by GC/MS analysis (Figure 28a). Similarly borylation of 4-methyl-7-(trifluoromethyl)quinoline (**257**) was recalcitrant to borylation due to steric inhibition of C-3 (Figure 28b).

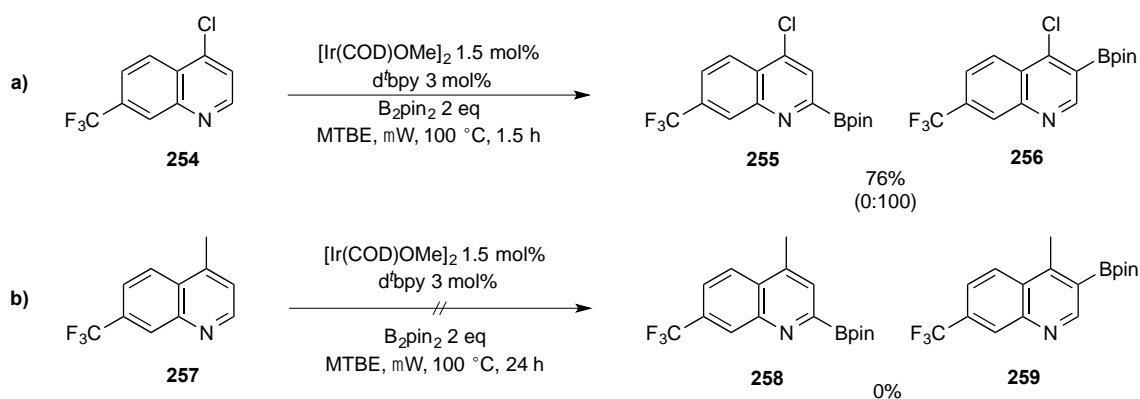


Figure 28: Borylation of 4,7-disubstituted quinolines

Moreover, work carried out by Mkhaldid studying the borylation of bipyridines found that there was a similar reluctance to borylation *ortho* to the azinyl nitrogen. For example borylation of 4,4'-dimethoxy-2,2'-bipyridine (**260**) gives 5,5'-bisboryl product (**261**) as the solitary product despite the presence of substituents *ortho* to the site of functionalisation (Figure 29a). However, the presence of a sufficiently bulky 4-substituent enables borylation *ortho* to the azinyl nitrogen, as is evident by the borylation of d^tbpy (**179**) which provided sole access to the 6,6'-diboryl product (**262**) (Figure 29b).¹³⁸

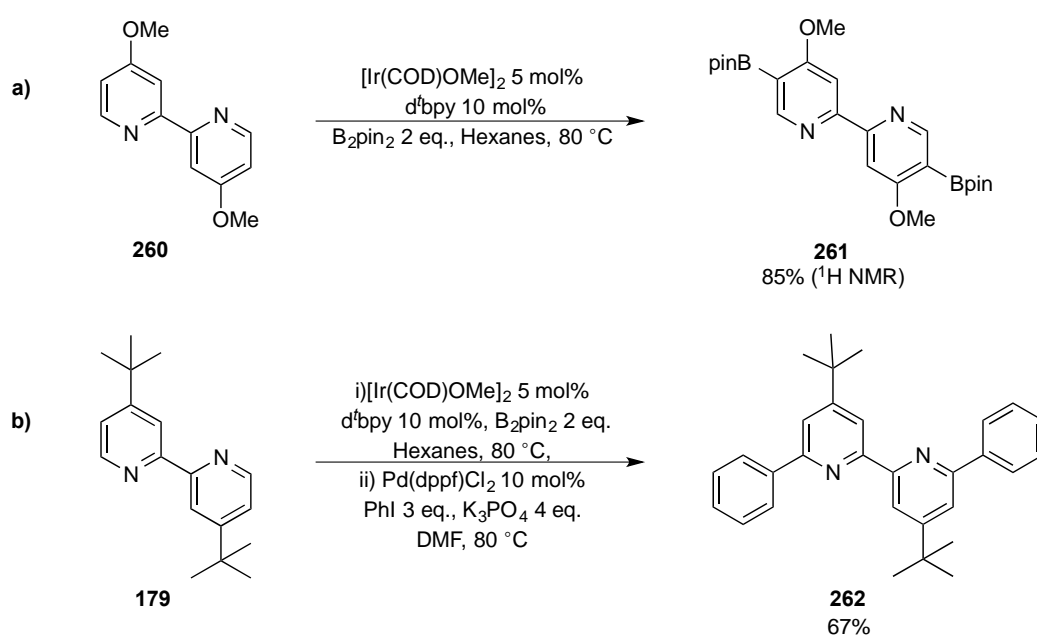


Figure 29: Borylation of 2,2'-bipyridines

This surprising result contrasted the result described previously, in which 4-tert-butylpyridine (**238**) borylated sluggishly (*c.f.* Scheme 24). This was attributed to both disruption of coordination to the iridium and the inductive withdrawing effect of the 2-pyridyl substituent, which reduces the relative basicity of the azinyl lone pair and stabilises a key transition-state structure in which oxidative addition forms a partial negative charge on the *ortho*-carbon (Figure 30).

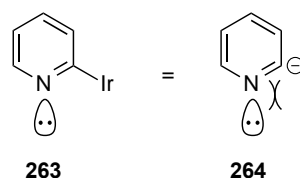
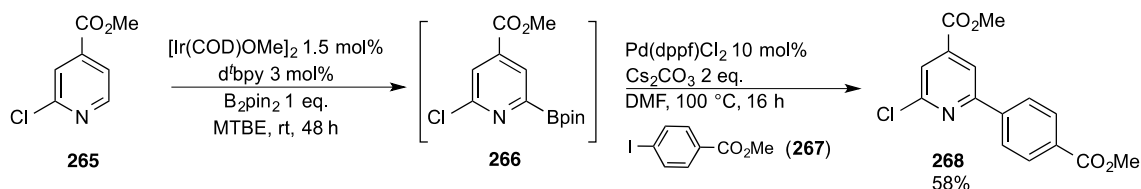


Figure 30: Disfavoured repulsive interactions arising from *ortho* oxidative addition of pyridine

The resistance to borylation *ortho* to Lewis-basic nitrogens was, therefore, rationalised on the basis of disfavoured coulombic repulsions between an emerging negative charge at the site of C-H activation and the lone pair on the aziridyl nitrogen (**264**), which provides an energy barrier to oxidative addition at these sites. Early work by Tajuddin has demonstrated that by increasing the inductive withdrawing capabilities of the 2-substituent, formation of *ortho*-aziridyl products occurs more readily, for example borylation of methyl-2-chloroisonicotinate (**265**) undergoes conversion to *ortho*-aziridyl product **266** efficiently, at room temperature. Whilst to date the instability of the resulting boronate esters has precluded their purification by column chromatography, their solution lifetime was sufficient to enable *in-situ* trapping by Suzuki-Miyaura cross-coupling reactions, which circumvented their isolation and provided access to potentially pharmaceutically interesting privileged biaryl structures (**268**) (Scheme 29). Work in this chapter will seek to build on this observation.



Scheme 29: Tandem 'one-pot' borylation/Suzuki-Miyaura cross-coupling reaction of methyl-2-chloroisonicotinate

Given that electronic repulsion between the azinyl lone pair and the developing negative charge on the α -carbon atom is likely to be related to the relative availability of the *N*-lone pair, the reactivity of a series of 2-substituted pyridines (**274-277**) will be considered to test this hypothesis (Figure 31).¹³⁹

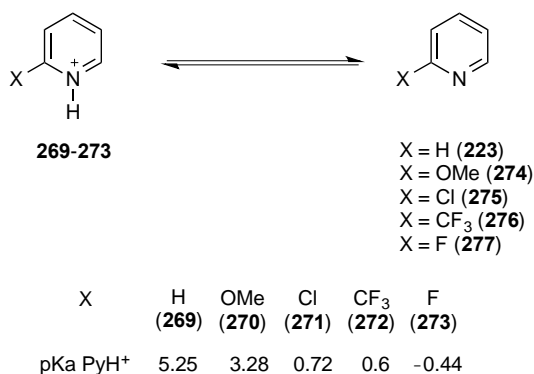


Figure 31: pKa of various 2-substituted pyridinium salts

There is also evidence to suggest that protodeborylation may also be sensitive to azinyl basicity. Analysis of the acid-mediated mechanism shows that it proceeds via an initial protonation of the azinyl-nitrogen (*c.f* Scheme 25). Brown has demonstrated the effects of *ortho* substituents on pyridine basicity, for example 2,6-dichloropyridine is completely resistant to protonation.¹³⁹ Moreover, work by Raoult and co-workers has shown that halopyridyl boronate derivatives (**281**, **282**) exhibit greater stability by comparison with pyridines bearing electron-donating substituents. This was illustrated in the attempted synthesis of 2-methoxy-6-(Bpin)-pyridine (**284**), whereby the instability precluded its isolation (Figure 32).¹⁴⁰

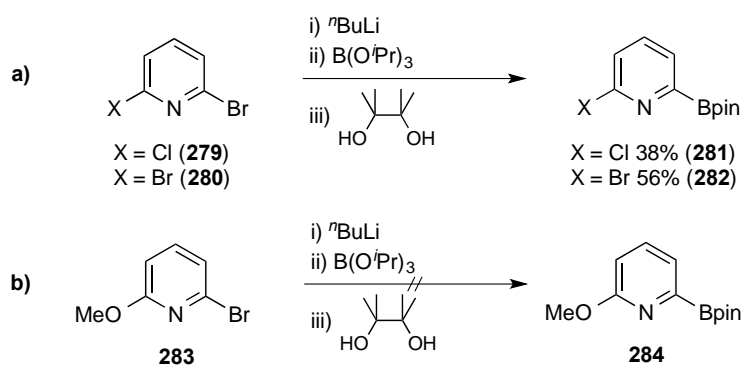


Figure 32: Literature synthesis of 2-substituted *ortho*-pyridyl boronate esters

The remainder of this chapter will explore the issue of boronate stability and find strategies to enable efficient synthesis and isolation of *ortho*-azinyll boronate esters. The rate of borylation and stability of the boronate esters will be explored in relation to their relative azinyll basicity. Where instability on silica precludes chromatographic purification, regioselectivity will be confirmed by trapping the boronate adduct *in-situ* via a Suzuki-Miyaura cross-coupling reaction. Furthermore, the functional group tolerance of C-H borylation will be exploited to enable multi-directional synthesis of privileged structures, combining a one-pot C-H borylation/Suzuki-Miyaura cross-coupling with downstream reactions with a view to small compound library synthesis.

2.3 Results and Discussion

2.3.1 Borylation of 2-Substituted pyridines

Initial work focussed on borylation of the aforementioned series of 2-substituted pyridines (*c.f* Figure 31). Exploiting the homogeneity of the C-H borylation reaction and the *in-situ* formation of active catalyst, catalyst stock solutions containing the iridium pre-catalyst, d⁴bpy and B₂pin₂ were prepared (see Experimental Section). This allowed long term storage of bulk mixtures, improved the simplicity of the experimental set-up and enabled consistent reproducibility.

Preliminary experiments explored the borylation of 2-methoxypyridine (**274**). An aliquot of catalyst stock solution was added to a sealed vial containing the substrate. Given the propensity for products containing an *ortho*-azinyl boronate ester functionality to undergo fast protodeboration, reaction ratios were monitored by *in-situ* ¹H NMR spectroscopy. A 0.5 mL aliquot of the reaction solution was transferred to a Young's tap sealed NMR tube. NMR spectra were referenced against a coaxial acetone-d₆ solvent stick, exploiting the high deuterium loading of the solvent to enable efficient referencing. In order to gauge the relative rates of reaction of the individual substrates, reactions were monitored up to 24 h, at which point the reaction mixture was concentrated *in vacuo*. GC/MS and ¹H NMR spectroscopic analyses were carried out on the crude reaction mixture and ratios compared to this acquired by *in-situ* measurements for validation. As bis-borylated products represented a significant outcome of the reaction, the reaction was also carried out with sub-stoichiometric (0.5 eq.) B₂pin₂.

Identification of product regioselectivity was achieved by observation of an approximate 0.3 - 0.5 ppm shift to higher frequency of signals (relative to their chemical shift in the ¹H spectrum of the starting material) corresponding to protons *ortho* to the inductively withdrawing C-B bond coupled with a change in multiplicity (Figure 33).

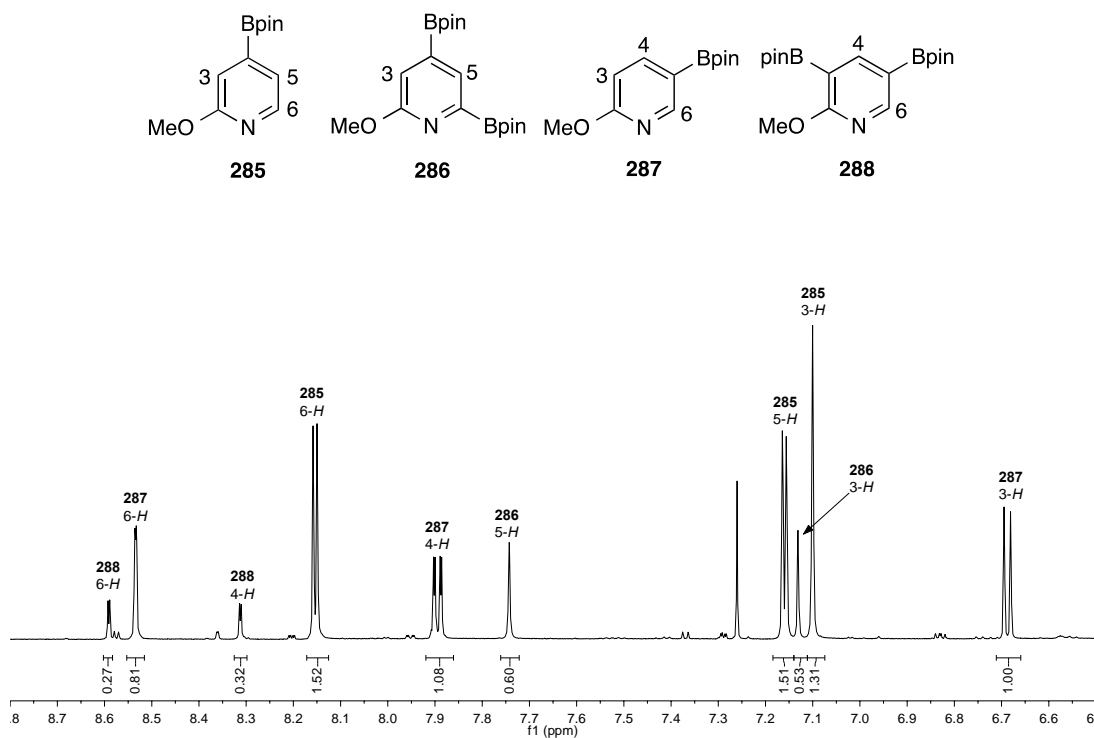
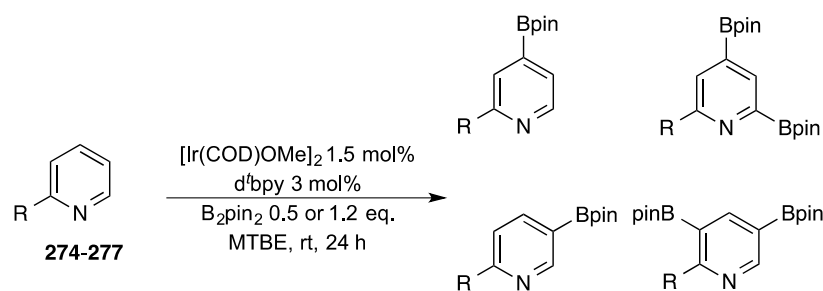


Figure 33: Borylation of 2-methoxypyridine (**274**) (^1H NMR spectrum of crude product mixture)

Product **285** is identifiable by a shift in the 3 and 5-*H* signals, with a further downfield shift of 5-*H* observed upon conversion to bis-boryl product **286**. Similarly, product **287** was identified by a shift in both 4 and 6-*H* signals with a similar downfield shift of the 4-*H* signal again occurring upon conversion to bis-boryl product **288**.

Following this same procedure of experimentation and assignment, the series of 2-substituted pyridines was completed, and the results are summarised in the table below (Table 2);



Entry	274-277	B ₂ pin ₂ (eq.)	Conversion (%) ^a	Product ratios ^a
1	R = OMe (274)	1.2	100	43:17:31:9
	R = OMe	0.5	42	73:0:27:0
2	R = Cl (275)	1.2	100	28:38:27:7
	R = Cl	0.5	55	75:0:25:0
3	R = CF ₃ (276)	1.2	100	25:36:39:0
	R = CF ₃	0.5	83	65:0:65:0
4	R = F (277)	1.2	100	45:15:10:19 ^b
	R = F	0.5	89	57:2:19:5 ^c

a. Determined by ¹H NMR spectroscopy; b. 11% of 2-fluoro-3-(Bpin)pyridine (**301**) obtained; c. 17% of **301** obtained.

Table 2: Borylation of 2-substituted pyridines (**274-277**)

Bis-borylation represented a significant outcome with substantial quantities of the 4,6-bisborylated products observed. The degree of 6-borylation correlated well with azinyl nitrogen basicity, with greater degrees of 4,6-bis(Bpin) formation observed for 2-chloro (entry 2) and 2-trifluoromethyl pyridine (entry 3) than for the more basic 2-

methoxypyridine (entry 1), whereby the ratio of 4-Bpin to 4,6-bis(Bpin) products demonstrated a reluctance to *ortho*-azinyl boronate ester formation. Unfortunately, due to the low steric demands of the fluorine atom, *ortho*-borylation became competitive, thus complicating the reaction (entry 4). This was demonstrable from the observed 2-fluoro-3-(Bpin) product (**301**) in both reactions of 2-fluoropyridine.

Experiments conducted with sub-stoichiometric B₂pin₂ clearly demonstrated that 6-substitution arose as a result of prior reaction at the 4-position (which rendered C-5 sterically hindered). Similarly 3,5-bisboryl products required initial borylation at the 5-position as C-3 is sterically inhibited by the 2-substituent. In all cases, product ratios favoured products arising from initial borylation at C-4 over C-5 which is consistent with the C-H acidity hypothesis (Figure 34).¹²⁸ These ratios differed from the 1:1 mixtures observed previously by Mkhaliid in the borylation of 2-phenylpyridine and 2-picoline (*c.f.* Figure 27). The lack of borylation at the most deshielded C-6 (in the absence of steric effects) reinforced the proposed energy barrier, which prevents C-H activation at this site even when the relative Lewis basicity is low.

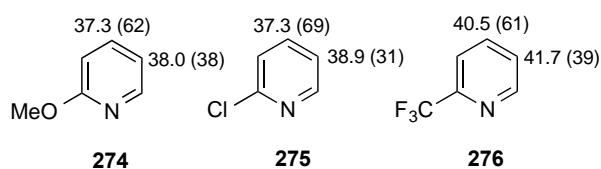


Figure 34: C-H acidity values of 2-substituted pyridines

Relatively speaking, the rates of reaction and extent of the reaction mirrored the previously described pK_a series (*c.f.* Figure 31) with faster rates and better conversions observed in the presence of more inductively withdrawing 2-substituents. This was unsurprising given the propensity for electron-deficient substrates to undergo faster reactions.¹²⁵

Encouraged by these preliminary results a series of bis-functionalised pyridines were then subjected to these borylation conditions in order to further gauge the relative stability of *ortho*-azinyl boronate esters and in order to provide single products for isolation or one-pot elaboration.

2.3.2 Borylation of 2,3-Disubstituted pyridines

In order to gauge the extent of the influence of the 2-substituent on reaction rates and boronate stability, a series of nicotinate esters were chosen as test substrates. Whereas the 2-chloro and 2-(trifluoromethyl) derivatives are commercially affordable, the high cost of the 2-methoxy and 2-fluoroderivatives meant synthesis from their substituent carboxylic acids was required (Figure 35).

Methylation of 2-methoxynicotinic acid (**302**) with methanol using a substoichiometric of concentrated sulfuric acid generated the methyl ester in excellent yield without the need for further purification after neutralisation with saturated NaHCO₃ solution and extraction. The product (**304**) was characterised by observation of a strong carbonyl stretch in the IR spectrum at 1731 cm⁻¹ and a singlet at 3.90 ppm, in the ¹H NMR spectrum

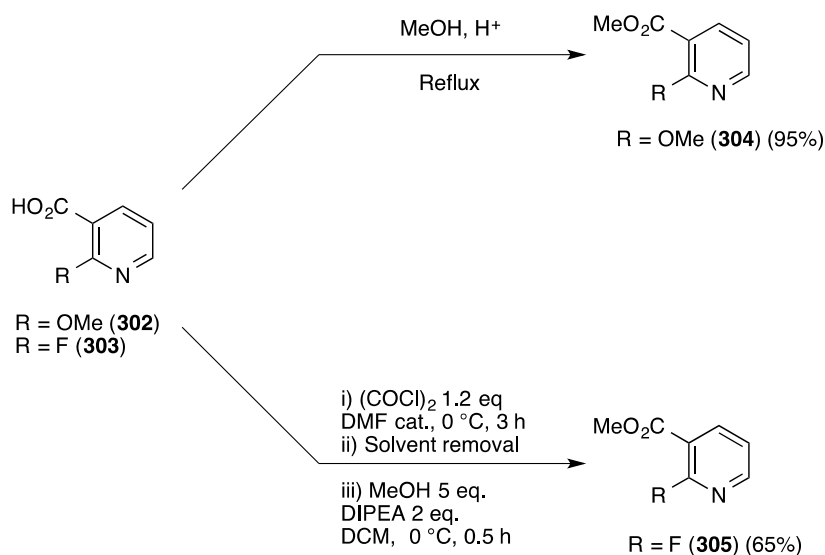


Figure 35: Synthesis of 2-substituted nicotinate esters

Given the potential lability of the C-F bond in 2-fluoropyridyl substrates, a milder method of esterification was sought for the esterification of 2-fluoronicotinic acid (**303**). Reaction with oxalyl chloride ($(\text{COCl})_2$) in the presence of catalytic DMF enabled formation of the acyl chloride as confirmed by IR analysis, which displayed a carbonyl stretch at 1758 cm^{-1} , in conjunction with the absence of the broad OH stretch. Methylation of the acid chloride provided methyl ester (**305**), as confirmed by an observed resonance at 3.94 ppm in the ^1H NMR spectrum.

With the nicotinate series in hand, the substrates were then tested in the C-H borylation process. Preliminary experiments explored the borylation of 2-methoxynicotinate (**304**) using the previously described method (*c.f* Section 2.3.1). Consistent with previous observations, the preferred regioselectivity was confirmed by disappearance of the 5-*H* resonance and corresponding downfield shifts in 4 and 6-*H* resonances. Similarly minor product (**307**) assignment was obtained by observed loss in the 6-*H* resonance and a shift to higher frequency in the neighbouring 5-*H* resonance (Figure 36).

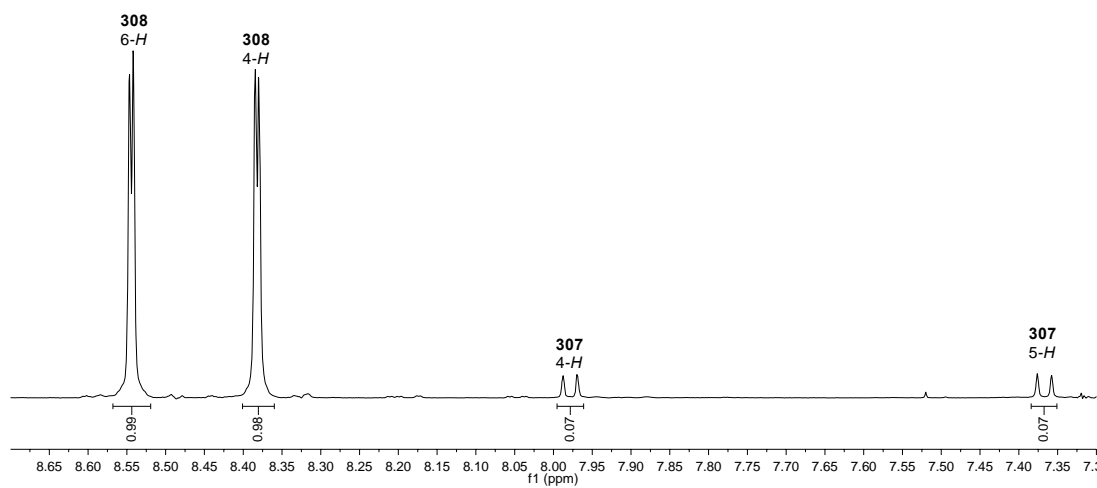
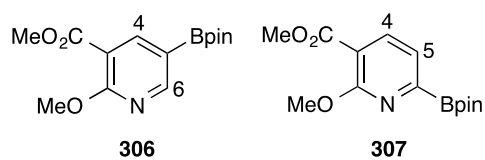
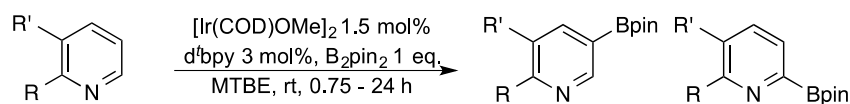


Figure 36: Borylation of methyl-2-methoxynicotinate (**304**) (^1H NMR spectrum of crude product mixture)

Following this method of characterisation, the data was collected and tabulated for the remaining compounds within the series (Table 3).



Entry	SM	Time(h)	Conversion (%) ^a	Products and Ratios ^a
1	R = OMe, R' = CO ₂ Me (304)	24	100	 306 307 93:7 (76%) ^b
2	R = F, R' = CO ₂ Me (305)	0.75	100	 308 309 91:9 (62%) ^b
3	R = Cl, R' = CO ₂ Me (310)	24	75	 311 312 94:6 (52%) ^c
4	R = CF ₃ , R' = CO ₂ Me (313)	1	100	 314 315 100:0 (75%) ^b
5	R = Cl, R' = Cl (316)	5	100	 317 318 100:0 (44%) ^d

a. Determined by ¹H NMR spectroscopy; b. Isolated yield of major product after tandem Suzuki-Miyaura cross-coupling (see experimental); c. Isolated yield of major product as Bpin ester.

Table 3: Borylation of 2,3-disubstituted pyridines

Consistent with the previously noted observations, borylation proceeded with excellent selectivity at the 5-position. This selectivity mirrors the greater C-H acidity of 5-*H* with respect to 6-*H*, however selectivity is likely influenced by the energetic barrier to 6-borylation and steric inhibition of the 4-position (Figure 37). In line with the relative azinyl-basicity, the greatest degree of 6-borylation is observed in the borylation of the 2-fluoroderivative (entry 2), however the lack of 6-borylation observed in the borylation of the trifluoromethyl derivative (entry 4) is surprising (*c.f.* Figure 31).

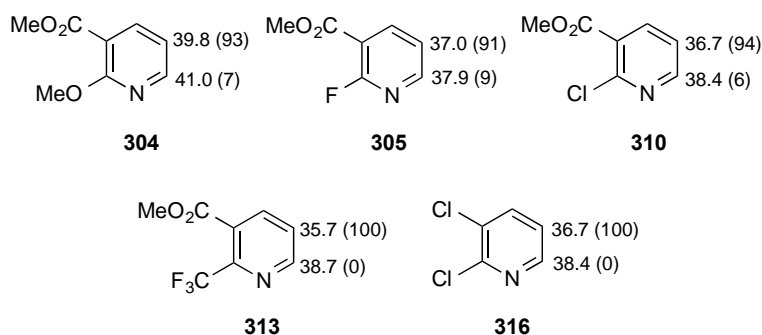
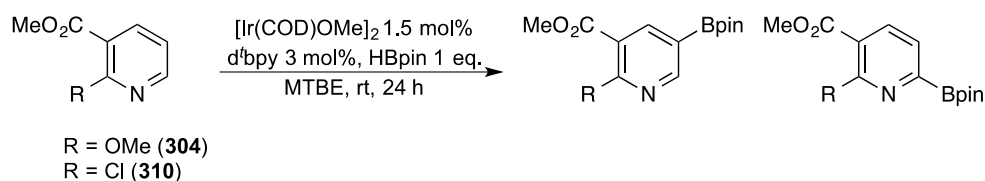


Figure 37: C-H acidity values of 2,3-disubstituted pyridines

Disappointingly, the borylation of methyl-2-chloronicotinate (**310**) did not proceed to completion even when left over an extended period of time (entry 3). This was somewhat surprising given the relative electron-deficiency of the ring relative to the 2-methoxy derivative (**304**), which reacted efficiently (entry 1). The catalysed reduction of 2-halo pyridines is known within the literature and potential for reduction with *in-situ* generated HBpin or H₂ was considered. Reflecting this, reactions of both substrates were carried out with a stoichiometric equivalent of HBpin using a method analogous to that which was previously described (*c.f* Section 2.3.1) (Table 4).



Entry	SM	Conversion (%) ^a	Products and Ratios ^a
1	304	48	306 + 307 (54:46)
2	310	15	311 + 312 (76:24)

a. Determined by ¹H NMR spectroscopy

Table 4: Borylation of 2,3-disubstituted pyridines with HBpin

The regioselectivity ratios obtained were surprising, with increased formation of the 6-boryl products (**307**, **312**) observed. At the time of publishing, this remained an unexplained result and has not since been embellished upon. Whilst relative conversions followed a similar pattern to reactions conducted with B₂pin₂, analysis of both crude GC and LC/MS traces found no evidence of chlorine reduction ($m/z = 137$) even at trace levels. In addition, the reaction of 2,3-dichloropyridine (**316**) with B₂pin₂ was also carried out and proceeded efficiently and with full conversion to product, demonstrating that C-Cl bond reduction was not a limiting factor (Table 3, entry 5).

Due to the low observed levels of minor products, direct chromatographic purification of the crude mixtures enabled isolation of boronate esters **311** and **317**. The pure boronate esters were characterised by NMR spectroscopy, for example compound **317** was identified by a characteristically broad ¹¹B NMR resonance at 30.0 ppm in conjunction with a small (1.5 Hz) ⁴J_{H-H} coupling, observed between 4 and 6-*H* resonances (thereby confirming the previously assigned regioselectivity).

2.3.2.1 Tandem Suzuki-Miyaura Cross-Coupling Reactions

Disappointingly, attempted column chromatographic purification of **306**, **308** and **314** failed to yield a pure product sample. Post TLC development with phosphomolybdic acid (PMA) solution demonstrated the tendency of the boryl products to streak. This often meant pinacol was observed in large quantities in the post-chromatographic ¹H NMR spectrum. Where chromatographic purification of the boronate ester was not possible, the borylation reaction was monitored to optimum conversion then concentrated *in vacuo*. To the crude boronate ester was added Pd(dppf)Cl₂, Cs₂CO₃, iodoanisole and DMF. Given that C-H borylation is an ideal strategy for late-stage functionalisation, the starting pyridine was used as the limiting reagent and a standard reaction stoichiometry was employed. Subsequent microwave irradiation enabled trapping of the boronate

esters as Suzuki-Miyaura cross-coupling products. The cross-coupling conditions used were not optimised for any one substrate as final products were only required for analytical purposes and to confirm the regioselectivity of the borylation reaction. (Figure 38). The reported cross-coupling yields are based on the starting heteroarene.

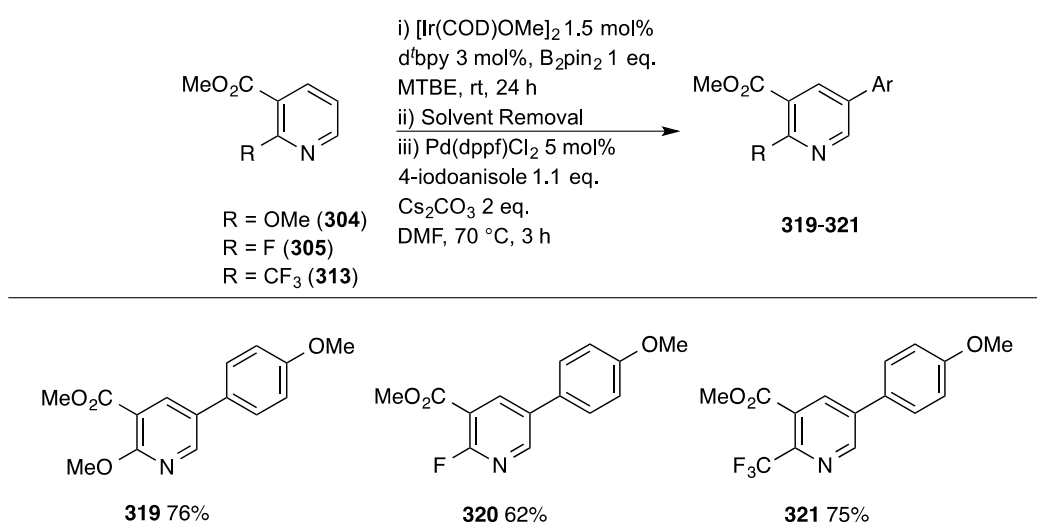


Figure 38: Tandem ‘one-pot’ borylation/Suzuki-Miyaura cross-couplings of 2,3-disubstituted pyridines

GC/MS analyses after 3 h heating showed full consumption of the intermediate boronate ester in all cases. Cross-coupled products **319**, **320** and **321** were identified by diagnostic molecular ion peaks of $m/z = 274$, 261 and 311 respectively.

Due to the lack of observed formation of *ortho*-azinyl boronate esters in isolable quantities to this point, it was then of interest to investigate 2,4-disubstituted pyridines, in which all other C-H bonds were sterically encumbered.

2.3.3 Borylation of 2,4-Disubstituted Pyridines

Due to high commercial costs, the methyl esters of 2-methoxy (**322**), 2-(trifluoromethyl) (**323**) and 2-fluoroisonicotinic acids (**324**) were synthesised using the prior discussed methods (*c.f* Figure 35). Methylation was confirmed by observation of ¹H NMR singlet resonances at 3.96, 4.00 and 3.97 ppm for 2-methoxy (**325**), 2-(trifluoromethyl) (**326**) and 2-fluoroisonicotinate (**327**) esters respectively.

Preliminary C-H borylation reactions were carried out with 2-chloro-4-(trifluoromethyl)pyridine (**328**) using the method discussed previously (*c.f* Section 2.3.1). Due to steric hindrance imparted by the 4-trifluoromethyl moiety, borylation at C-5 was disfavoured and consequently no 5-(Bpin) product (**329**) was observed. Consistent with selective borylation at C-6, the *in-situ* borylation product (**330**) possessed a ¹H NMR trace lacking the 6-*H* resonance in conjunction with a neighbouring 5-*H* resonance shifted to higher frequency (Figure 39).

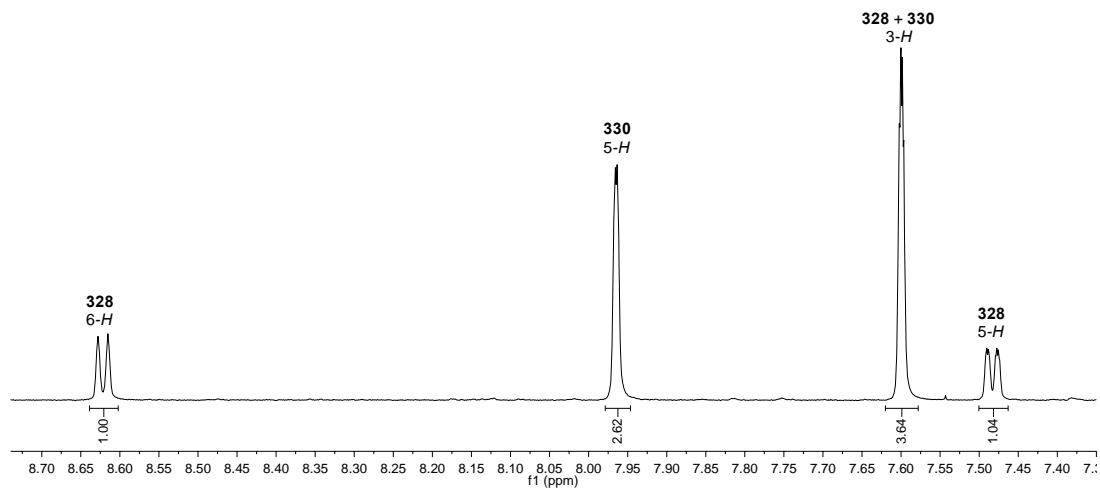
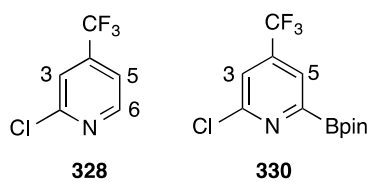


Figure 39: Borylation of 2-chloro-4-(trifluoromethyl)pyridine (**328**) (^1H NMR spectrum of crude reaction mixture)

Encouraged by this preliminary result, a series of 2,4-disubstituted pyridines were borylated and the results are summarised in the table below (Table 5);

Entry	SM	Time(h)	Conversion (%) ^a	Products and Ratios ^a
1	R = Cl, R' = CF ₃ (328)	24	72	 329 330 (0:100) (51%) ^b
2 ^c	R = Cl, R' = Cl (331)	24	95	 332 333 (50:50) (68%) ^{b, d}
3	R = OMe R' = CO ₂ Me (325)	24	57	 334 335 (0:100) (41%) ^b
4	R = CF ₃ R' = CO ₂ Me (326)	24	93	 336 337 (0:100) (66%) ^b
5	R = F R' = CO ₂ Me (327)	18	100	 338 339 (0:100) (29%) ^e

a. Determined by ¹H NMR spectroscopy; b . Isolated yield after tandem Suzuki Miyaura cross-coupling (see experimental); c. Reaction performed by Hazmi Tajuddin; d. Gross yield of two isomeric cross-coupled products obtained in 40% and 28% yield respectively; e. Isolated yield of boronate ester

Table 5: Borylation of 2,4-disubstituted pyridines

Despite the prevalence of steric effects in borylation, 5-boryl products were still observed in instances whereby the 4-substituent was sterically smaller. For example borylation of 2,4-dichloropyridine (**331**) gave a 1:1 mixture of 5 and 6-boryl products (**332** and **333**

respectively) (entry 2). Similarly, the previously described borylation of 2,4-lutidine (**240**) gave a 3:1 ratio of 6:5-boryl products (*c.f* Scheme 23).

Analysis of the borylation products of the isonicotinate series, whereby the 4-methoxycarbonyl moiety is sufficiently sterically encumbering to force borylation to C-6, demonstrates that enhanced conversions and reaction rates were obtained in substrates containing less-basic azinyl nitrogens. For example, borylation of methyl-2-fluoroisonicotinate (**327**) proceeds to completion (entry 5) whereas borylation of the analogous 2-methoxy derivative (**325**) proceeds only sluggishly to 57% conversion (entry 3). This is representative of a sufficiently decreased energy barrier to 6-borylation provided by inductively withdrawing *ortho* substituents.

Attempts to purify the boronate esters were largely unsuccessful, with complete reversion to the starting material observed after column chromatography in most cases. However, in line with previous observations made by Raoult and co-workers (*c.f* Figure 32), the 2-fluoro derivative was amenable to chromatographic purification enabling isolation of the 6-(Bpin) product (**339**), as confirmed by post-purification GC/MS analysis ($m/z = 281$, $[M]^+$), in modest yield. This confirmed that not only do inductively withdrawing 2-substituents reduce the barrier to formation of *ortho*-boryl compounds, they stabilise the products and sufficiently slow the rate of protodeborylation.

2.3.3.1 Tandem Suzuki-Miyaura Cross-Coupling Reactions

Owing to the instability of the majority of the 6-boryl products, the crude boronate esters were subjected to the previously described Suzuki-Miyaura cross-coupling conditions (*c.f* Section 2.3.2.1) with iodoanisole to give the biaryl products (**341-344**) in good yields across the two steps (Figure 40).

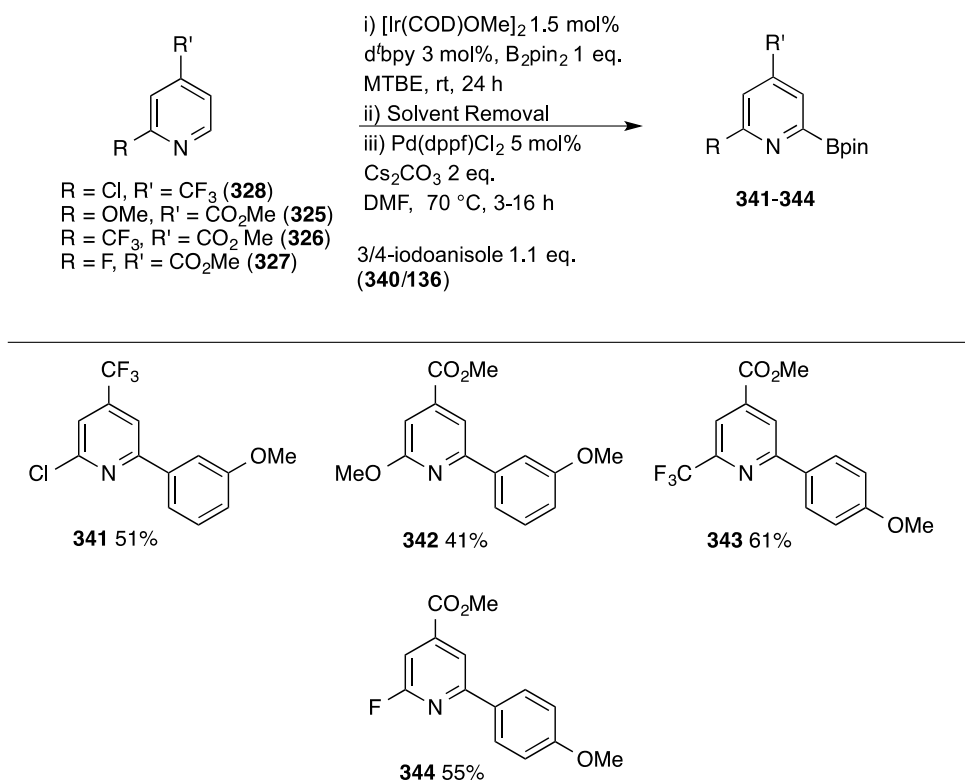


Figure 40: Tandem ‘one-pot’ borylation/Suzuki-Miyaura cross-couplings of 2,4-disubstituted pyridines

The cross-coupled products bore a characteristic singlet at ca. 3.9 ppm in the ¹H NMR spectrum corresponding to the incorporated anisole OCH₃ functionality. The observed reduction in overall yield of the one-pot reactions relative to those described in Section 2.3.2.1 was attributed to the reduction in stability of the intermediate boronate esters (*c.f.* Table 3).

2.3.4 Borylation of 2,5-Disubstituted Pyridines

Application of the previously described esterification method to 6-fluoronicotinic acid (**345**) enabled the synthesis of methyl-6-fluoronicotinate (**346**) (*c.f.* Figure 35). Methylation was confirmed through observation of a ¹H NMR singlet at 3.95 ppm.

Preliminary borylation experiments explored the reactivity of 2,5-dichloropyridine (**347**) using the previously described procedure (*c.f* Section 2.3.1). Regioselectivity was assigned based on a downfield shift of the neighbouring 3 or 4-*H* resonances upon incorporation of the boryl group (Figure 41).

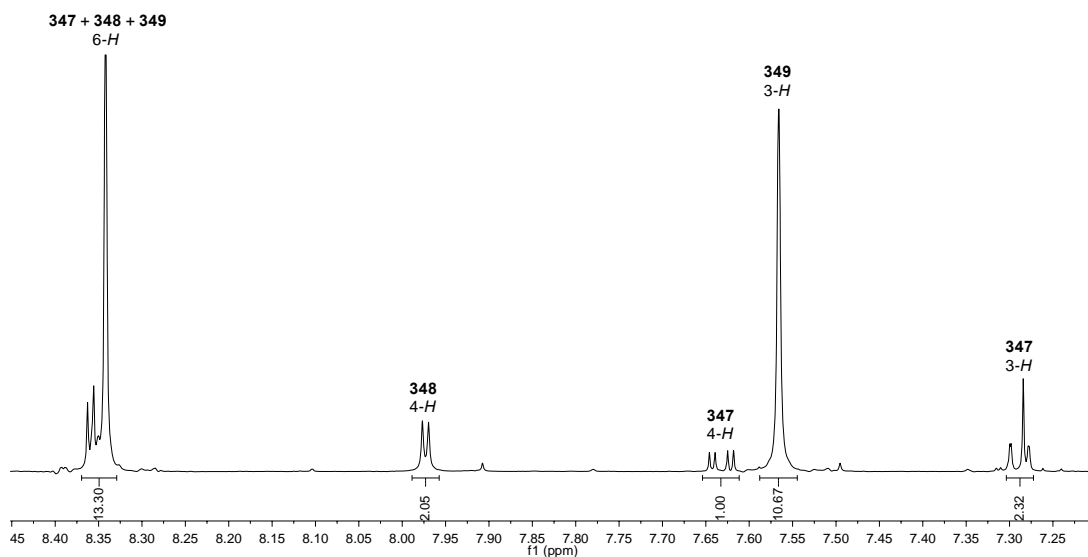
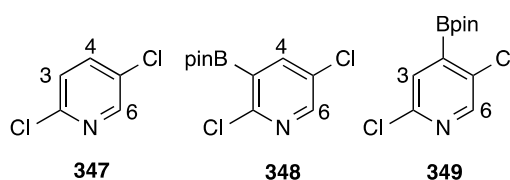
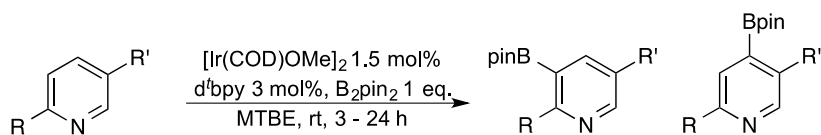


Figure 41: Borylation of 2,5-dichloropyridine (**347**) (^1H NMR spectrum of crude product mixture)

Following this method of characterisation, the data was collected and tabulated for a series of 2,5-disubstituted pyridines (Table 6).



Entry	SM	Time(h)	Conversion (%) ^a	Products and Ratios ^a
1	R = Cl, R' = Cl (347)	24	93	 348 349 (16:84) ^b
2	R = Me, R' = Me (350)	24	10	 351 352 (0:100)
3	R = Cl, R' = CO ₂ Me (353)	24	46	 354 355 (100:0) (32%) ^c
4	R = F, R' = F (356)	8	100	 357 358 (20:80) ^d
5	R = F, R' = CO ₂ Me (346)	3	100	 359 360 (100:0) (77%) ^e

a. Determined by ¹H NMR spectroscopy; b . Trace bis-borylated products (GC/MS); c. Isolated yield after tandem Suzuki Miyaura cross-coupling; d. 9% bis products observed (**361**, **362**) (see experimental); e. Isolated yield of boronate ester.

Table 6: Borylation of 2,5-disubstituted pyridines

The reaction of 2,5-disubstituted pyridines generally proceeded sluggishly due to the requirement for unfavourable borylation *ortho* to functional groups. For example, 2,5-lutidine (**350**) borylated with a 10% conversion and failed to provide improved consumption even when reacted over longer time periods of up to 96 h (entry 2). Conversely, owing to the small steric size of the fluorine atom and the electron-withdrawing capability of the fluoro substituents, the borylation of difluoro derivative **356**

proceeded efficiently with bis-borylated products observed by ^1H NMR spectroscopy (entry 4).

Consistent with calculated C-H acidity values, symmetrically disubstituted substrates gave product ratios favouring borylation at the more deshielded C-4 (Figure 42). Whilst the observed regioselectivity of reactions involving unsymmetrical substrates also favoured the more acidic C-H bonds, it is more likely that this is reflective of the steric bias of the reaction.

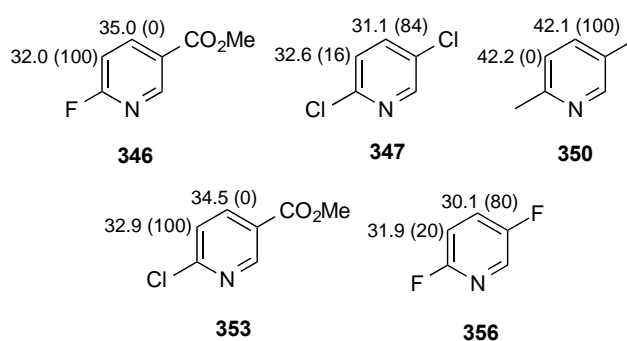


Figure 42 C-H acidity values of 2,5-disubstituted pyridines

Isolation of single product **359**, characterised by a shift in ^{19}F NMR signal to -52.2 ppm and a broad ^{11}B singlet at 29.7 ppm, was possible after column chromatography. This boronate ester could also be elaborated by *in-situ* Suzuki-Miyaura cross-coupling with 4-iodoanisole providing the bis-aryl product (**364**) in good yield (Figure 43).

2.3.4.1 Tandem Suzuki-Miyaura Cross-Coupling Reactions

Attempted column chromatographic purification of single product **353** was unsuccessful due to co-elution with B_2pin_2 . Application of the standard Suzuki-Miyaura cross-coupling conditions enabled synthesis of the biaryl (**363**) as demonstrated by *in-situ* LC/MS, with

the diagnostic chlorine isotopic pattern evident in the observed molecular ion peaks ($m/z = 279$ (^{37}Cl , $[\text{M}+\text{H}]^+$), 277 (^{35}Cl , $[\text{M}+\text{H}]^+$)) (Figure 43) (c.f Figure 38).

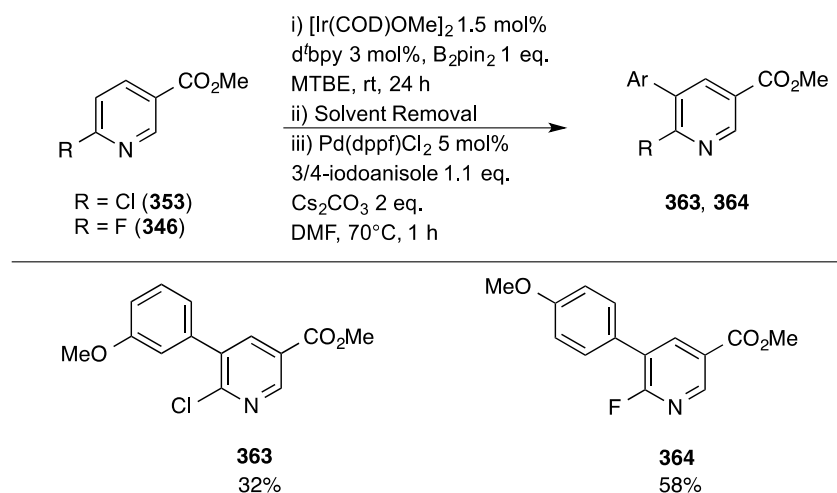


Figure 43: Tandem ‘one-pot’ borylation/Suzuki-Miyaura cross-couplings of 2,5-disubstituted pyridines

2.3.5 Multi-Directional Synthetic Strategies

Thus far, it has been demonstrated that by judicious choice of substitution pattern, pyridines are a viable substrate for C-H borylation, with boronate esters isolable in good yields after column chromatography or tandem ‘one-pot’ Suzuki-Miyaura cross-couplings. Moreover, in the presence of sufficiently electronegative *ortho* substituents, it provides sufficient stability to the resulting boronate ester that the yields and reaction rates are enhanced. It was also envisaged that a range of downstream chemistries, which exploit the reactivity of 2-halopyridines, would become viable to enable multi-directional synthesis of small compound libraries.

2.3.5.1 2-Chloro Reduction Sequence

Initial focus centred upon the desire for substitution with a hydrogen atom, as this provides a formal protecting group approach to the 2-pyridyl boronate problem. A survey of the literature suggested direct S_NAr substitution of a 2-halo substituent with hydride is not known, however, scope exists for chloroarenes to undergo reduction under transfer hydrogenation conditions.¹⁴¹⁻¹⁴⁴

Using the previously described method of tandem borylation/Suzuki-Miyaura cross coupling (*c.f* Section 2.3.2.1), reaction of methyl-2-chloroisonicotinate (**266**) with 4-iodoanisole provided the desired cross-coupled intermediate (**365**) as observed by *in-situ* GC/MS ($m/z = 279$ (^{37}Cl , $[M]^+$), 277 (^{35}Cl , $[M]^+$)). The ratio of desired product to starting material was observed as 55:45 as a result of incomplete (73%) conversion to boronate ester (**267**) and losses incurred during the cross-coupling step. TLC analysis after the cross-coupling step showed a complex mixture and as a consequence a work-up was carried out prior to reduction. Under a stream of nitrogen, Pd/C was added to an ethanolic solution of the crude mixture and ammonium formate. Celite filtration enabled separation of the catalyst and GC/MS analysis showed full consumption within 2 h at room temperature ($m/z = 243$ $[M]^+$), with the notable absence of the chlorine isotopic pattern confirming conversion to the reduced product (**366**) (Figure 44).

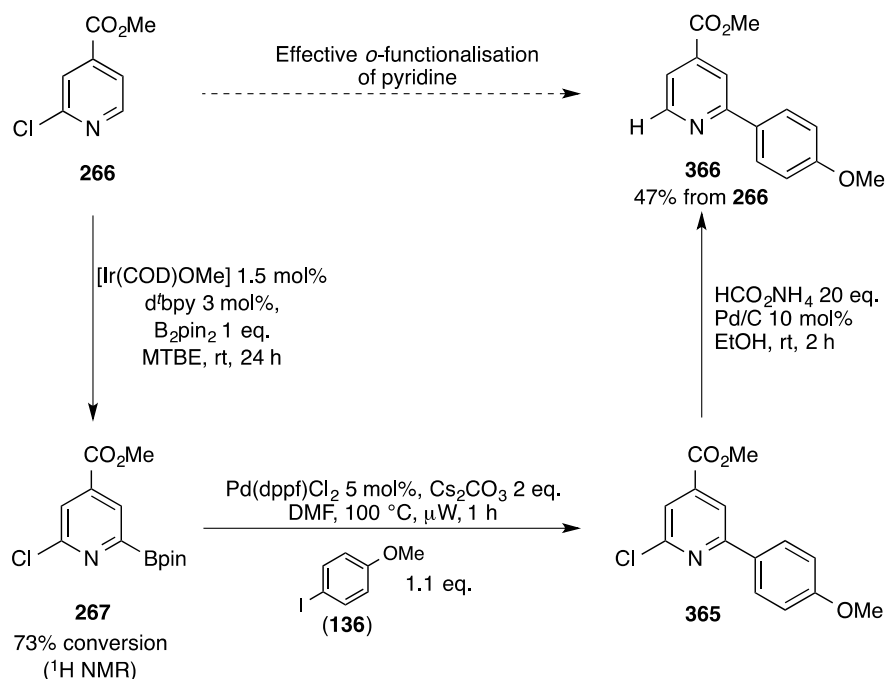


Figure 44: ‘Protecting group’ approach to 2-pyridyl borylation

2.3.5.2 $\text{S}_{\text{N}}\text{Ar}$ Substitution of Aryl-2-Halopyridines

In addition, both 2-chloro and fluoro products were also subjected to $\text{S}_{\text{N}}\text{Ar}$ conditions to enable a second mode of variation in multi-directional synthesis. Due to the potential for nucleophilic cleavage of the 2-halo bond, reactions were carried out neat (with respect to the nucleophile) or in polar aprotic solvents. Simple reaction of the 2-fluoro starting material with the desired nucleophile in refluxing dioxane gave products lacking the ^{19}F signal by NMR spectroscopy. Confirmation of product formation was provided by LC/MS analysis with the characteristic molecular ion peaks $m/z = 273$ ($[\text{M}]^+$), 329 ($[\text{M}+\text{H}]^+$) and 328 ($[\text{M}+\text{H}]^+$) observed for compounds **319**, **369** and **371** respectively. $\text{S}_{\text{N}}\text{Ar}$ of the chloro derivatives was carried out using a literature protocol.¹⁴⁵ The results are presented in the below (Table 7).



Entry	SM	Conditions ^a	Nucleophile	Product	Yield (%) ^b
1	320	A	-OMe	 319	81
2	320	B	 367 368	 369	93
3	320	B	 370	 371	89
4 ^c	 372^d	C	 368	 373	43
5 ^c	372	C	 374	 375	50
6 ^c	 376^d	C	 377	 378	61

a. Conditions- A) NaOMe (5 eq.), MeOH, reflux, 16h; B) Nucleophile (1.2 eq.), K₂CO₃ (1.2 eq.), Dioxane, 100 °C, 6 h; C) Nucleophile (2.5 eq.), MeOH, μ W, 130 °C, 30 min; b. Isolated yield; c. Experiment carried out by Carys Thomas; d. Synthesised by Carys Thomas.

Table 7: S_NAr substitution of 2-halo-arylpyridines

Reflecting the greater electronegativity of the fluorine atom, reactions involving the displacement of fluoride proceeded in superior yields (entries 1-3). This is exemplified in the respective yields of entries 2 and 4. Displacement was demonstrated with both oxygen and nitrogen nucleophiles in excellent yields. The use of 1,2-diamines (**377**) as

nucleophile provides a facile route to substituted pyridodiazepine (**378**) scaffolds of potential biological interest (entry 6).

With scope for variation in both the Suzuki-Miyaura cross-coupling partner as well as the nucleophilic component, there is promising potential for small molecule library building. Research in this area is ongoing within the group with both variation in Suzuki-Miyaura cross-coupling partner and a variety of downstream chemistries, including decarboxylative couplings which seek to functionalise at the ester carbons, currently under investigation.

2.3.6 Borylation of Other Azinyl Heterocycles

Having established that the inhibition of azinyl nitrogen coordination was key to overcoming the poor reactivity of pyridine, it was then of interest to apply this strategy to other Lewis-basic heterocycles. Reflecting this, the basicity of a series of other such heterocycles was considered (Figure 45).

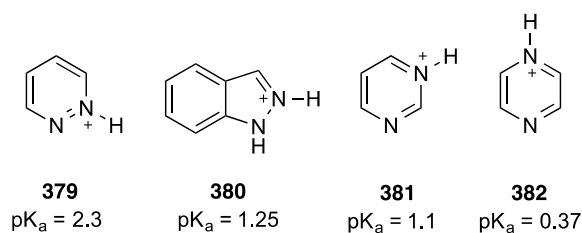
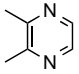
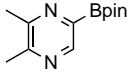
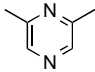
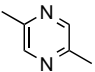
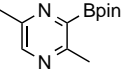
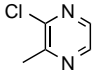
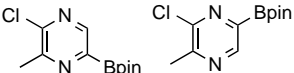


Figure 45: pKa of other azinyl heterocycles

The remainder of this chapter will explore the borylation of these substrates, with a focussed case study on indazoles forming the basis of the following chapter.

2.3.6.1 Borylation of Pyrazines

Work in this area began with a study of the borylation of pyrazine, due to its markedly lower basicity. Preliminary work explored the attempted borylation of 2,3-dimethylpyrazine (**383**) with an aliquot of borylation stock solution at room temperature as previously described (*c.f.* Section 2.3.1). Pleasingly, and consistent with the earlier hypothesis, the substrate underwent efficient borylation at room temperature, as evident by a downfield shift in the solitary aromatic resonance in the ^1H NMR spectrum. Encouraged by this, a series of pyrazine substrates were subjected to analogous conditions, the results of which are summarised in the table below (Table 8). In the absence of reactivity at room temperature, the reaction was repeated at 80 °C.

Entry	Substrate	Conditions ^{a,b}	Product(s)
1	 383	A	 384 (90%) ^c (44%) ^d
2	 385	B	No products observed
3	 386	B	 387 (56%) ^c (28%) ^d
4	 388	A	 389 390 (23%) ^d (91%) ^c (1:3)

a. $[\text{Ir}(\text{COD})\text{OMe}]_2$ 2.5 mol%, $d^f\text{bpy}$ 5 mol%, B_2pin_2 1 eq. b. Conditions A) rt, 24 h; B) 80 °C, 16 h; c. ^1H NMR conversion; d. Yield after Suzuki-Miyaura cross-coupling (see experimental section for details)

Table 8: Borylation of substituted pyrazines

Despite its lower basicity, borylation of pyrazine heterocycles also required judicious choice of substitution pattern in order to enable boronate ester formation. Steric inhibition of azinyl nitrogen coordination remained a prerequisite for borylation of these substrates, for example 2,6-dimethylpyrazine (**385**) was recalcitrant to borylation, even under forcing reaction conditions, (entry 2) whereas 2,3-dimethylpyrazine (**383**) borylated readily (90% conversion by ^1H NMR) at room temperature (entry 1). Despite the steric hindrance imposed by neighbouring methyl groups, 2,5-dimethylpyrazine (**386**) also underwent successful reaction (entry 3), however, higher temperatures were required relative to the borylation of **383**.

Reflecting the preference for borylation *ortho* to the less basic azinyl nitrogen, borylation of 2-chloro-3-methylpyrazine (**388**) occurred preferentially at C-6. The inductively donating effect of the methyl group renders the *ortho* azinyl nitrogen more electron rich and as such borylation at C-5 is more disfavoured. This regioselectivity mirrors calculated C-H acidities (Figure 46). Regioselectivity was again assigned based on downfield shifts, relative to starting material **388**, of neighbouring ^1H resonances upon incorporation of neighbouring Bpin ester groups. High field NMR analysis enabled characterisation of the starting material on the basis of a small but detectable $^5\text{J}_{\text{H-H}}$ coupling (0.76 Hz) between 5-*H* and CH_3 resonances.

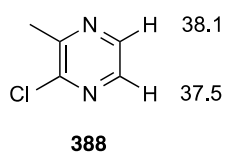


Figure 46: C-H acidity values of 2-chloro-3-methylpyrazine

2.3.6.1.1 Tandem Suzuki-Miyaura Cross-Coupling Reactions

Purification of the resulting boronate esters remained problematic, with products **384** and **387** undergoing full reversal to starting material by protodeborylation during flash column chromatography. Reflecting this, tandem 'one-pot' cross-coupling reactions using the previously described procedure were carried out (Figure 47) (c.f Section 2.3.2.1). Compound identification was enabled by both ^1H NMR spectroscopy and mass spectrometry analysis, for example compound **391** displayed characteristic ^1H NMR singlet resonances at 8.65 and 3.86 ppm, corresponding to 6-*H* and OCH_3 resonances respectively, as well as the diagnostic molecular ion signal by ASAP accurate mass analysis ($m/z = 215.1187$ $[\text{M}+\text{H}]^+$)

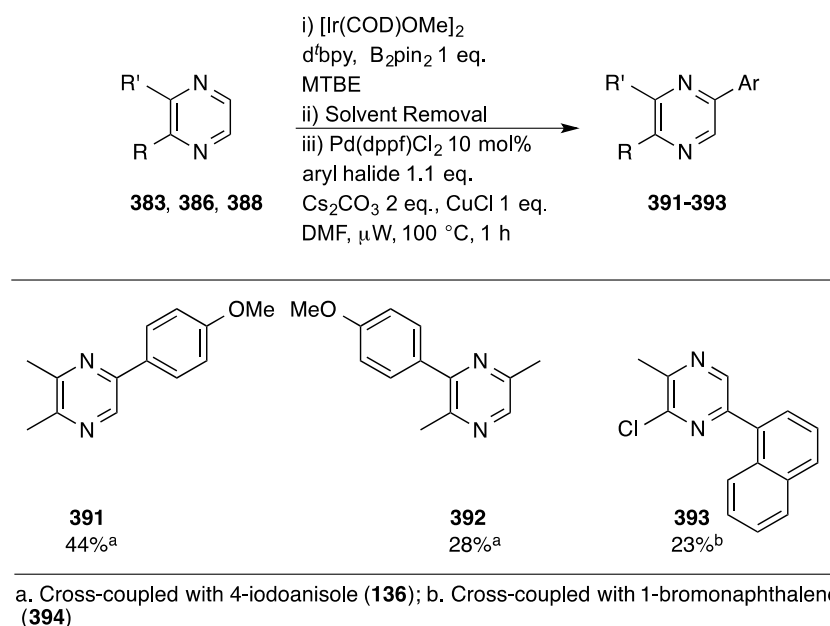
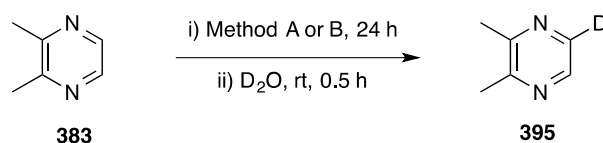


Figure 47: Tandem 'one-pot' borylation/Suzuki-Miyaura cross-couplings of pyrazine substrates

2.3.6.1.2 *ipso*-Deuteration of (Bpin)-Pyrazine

As has been previously noted the isolation of *ortho*-azinyl boronate esters and their Suzuki-Miyaura products is challenging due to their propensity to undergo rapid protodeborylation, catalysed by acids, bases and various metal ions.³⁻⁵ In light of the previously discussed acid-mediated mechanism and observations made by Mkhaliid,¹³³ it was suggested that use of mild deuterated acid surrogates could facilitate efficient *ipso*-deuteration of heterocycles (*c.f* Scheme 25 and Scheme 24).

To build on this earlier observation, 2,3-dimethylpyrazine was treated with an aliquot of stock solution to provide efficient conversion to 2,3-dimethyl-5(Bpin)-pyrazine (**384**) as described above. Disappointingly, direct addition of D₂O to the reaction mixture gave only limited conversion to the *ipso*-deuterated product (**395**) (Table 9, entry 1). Interestingly, and somewhat surprisingly, when the order of addition of C-H borylation reagents was changed so that an MTBE solution of B₂pin₂ and **383** was added to a solution of [Ir(COD)OMe]₂ and d'bpy, D₂O quenching gave full conversion of the intermediate boronate ester to the desired *ipso*-deuterated product (entry 2). The current reasons for this observed order of addition effect are unknown and this remains an anecdotal observation.



Entry	A or B	¹ H NMR Conversion (%)	² H Incorporation (%)
1	A	90	4
2	B	76	100

Method A - Pre-prepared stock solution added to substrate
Method B - Solution of substrate and B₂pin₂ added to solution containing catalyst plus ligand

Table 9: *ipso*-deuteration of in-situ generated 2,3-dimethyl-5-(Bpin)pyrazine (**384**)

The degree of ^2H incorporation was calculated based on the degree of depletion of the 6-*H* resonance of 2,3-dimethyl-5(Bpin)-pyrazine (**384**) as judged by comparisons between crude ^1H NMR taken before and after deuteration (Figure 48). In this instance a disappearance of the 6-*H* resonance equated to complete deuteration. ^2H NMR spectroscopy, using the previously reported W5 solvent suppression technique,¹⁴⁶ run in protiated solvent enabled observation of the ^2H resonance at 8.30 ppm.

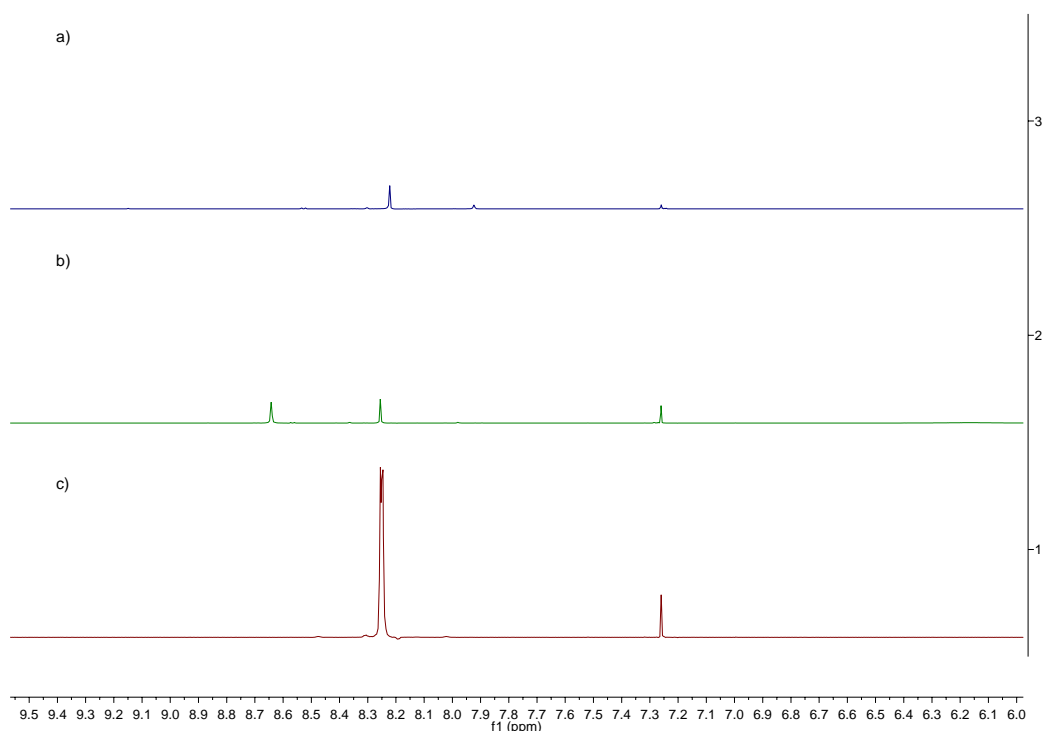
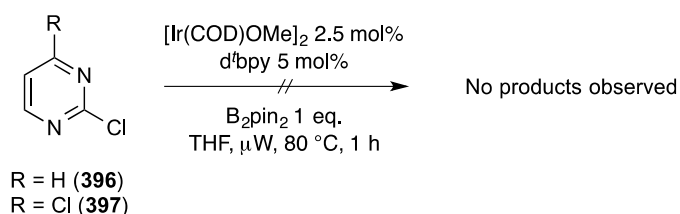


Figure 48: ^1H NMR spectrum; a. after deuteration; b. before deuteration; c. reference of 2,3-dimethylpyrazine starting material.

2.3.6.2 Borylation of Pyrimidines

Despite the markedly reduced basicity of pyrazinyl heterocycles with respect to pyridinyl substrates, disruption of azinyl coordination remained a pre-requisite for the borylation of pyrazine substrates. In light of observations made up to this point, initial focus of

pyrimidine borylation centred upon 2-substituted pyrimidines, as it was hypothesised that this would disrupt potential coordination of both azinyl nitrogens. Reflecting this, 2-chloropyrimidine (**396**) was chosen as a test substrate. In addition to disrupting azinyl coordination, the chlorine substituent would enable flexibility in downstream chemistries. On the basis of poor solubility at both room temperature and 80 °C with microwave irradiation, the attempted borylation of the starting material with a THF stock solution was unsuccessful. Frustratingly, poor solubility also accounted for the unsuccessful attempted borylation of 2,4-dichloropyrimidine (**397**) under analogous conditions (Scheme 30).



Scheme 30: Attempted borylation of 2-chloropyrimidines

Reflecting this, a solvent screen was embarked upon in an attempt to broaden the potential substrate scope.

2.3.6.2.1 Solvent Screen

Due to its predictable regioselectivity and reliable reactivity, *m*-xylene (**198**) was chosen as the test substrate. Initially a control reaction was run in MTBE as this is the standard solvent used for most borylations within the group and in literature protocols (Table 10, entry 1). To a vial containing the iridium catalyst, d'fpy and B₂pin₂ was added 2 mL of MTBE. At the point of full solubilisation of all solid, *m*-xylene (1 mmol) was added and

the reaction mixture subjected to microwave irradiation for 1 h. Given that many of the screened solvents were less volatile than the substrate itself, the NMR conversions was calculated *in-situ* without prior solvent removal, using the previously described method (*c.f* Section 2.3.1). Based on a downfield shift in the neighbouring 4/6-*H* resonance, the ¹H NMR conversion was calculated as 93%. Following this general protocol, a range of solvents were tested. The results of the solvent screen are summarised in the table below (Table 10);

Reaction scheme: 1,3-dimethylbenzene (**198**) reacts with $[\text{Ir}(\text{COD})\text{OMe}]$ (2.5 mol%), d/bpy (5 mol%), and B_2pin_2 (1 eq.) in a solvent at 80 °C for 1 h under microwave irradiation (μW) to yield 1,3-dimethyl-4-borylbenzene (**200**).

Entry	Solvent	Conversion (%)	
		¹ H NMR ^a	GC-MS
1	MTBE	87	93
2	Hexanes	51	70
3	THF	78	87
4	1,2-DME	77	85
5	Diglyme	75	86
6	Triglyme	0	0
7	DMAc	16	21
8	NMP	64	85

a. Run *in-situ*

Table 10: Borylation solvent screen

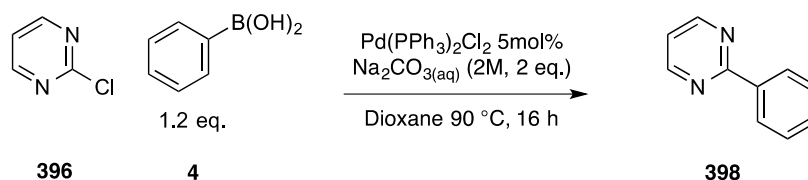
Predictably, due to their relatively low coordinating capabilities, ethereal solvents were well tolerated, with both 1,2-DME and diglyme (entries 4 and 5 respectively) performing

comparably to the more commonly used THF (entry 3), however, employment of triglyme resulted in complete loss of reactivity (entry 6). The poor performance of hexanes was surprising given its lack of coordinating ability. The relative activity of NMP (entry 8) was surprising due to its structural similarities to DMAc (entry 7), in which reactions proceeded sluggishly.

With the results of the solvent screen in hand, it was then of interest to test both the solubility and reactivity of both 2-chloro (**396**) and 2,4-dichloropyrimidine (**397**) in a more polar solvent. Subsequent solubility tests carried out with both diglyme and 1,2-DME showed that both substrates were readily soluble in both solvents and as such borylations were attempted in these solvents using the procedure described above (*c.f.* Scheme 30). Disappointingly however, both substrates were recalcitrant to borylation even at high temperatures and with microwave irradiation with only starting material observed by *in-situ* ^1H NMR spectroscopy. This pointed to a more fundamental problem specific to these substrates.

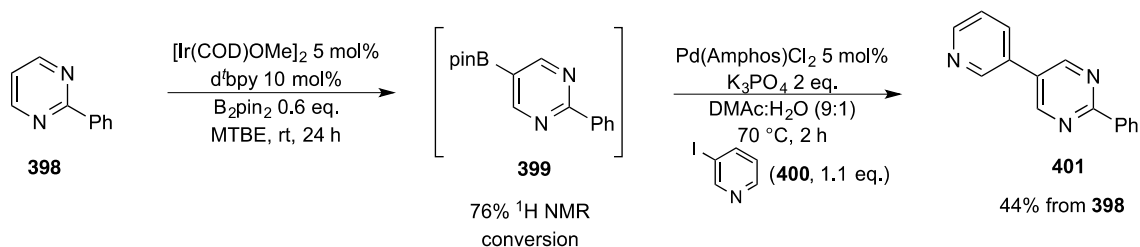
2.3.6.2.2 Borylation of 2-Phenylpyrimidine

As a consequence, and reflecting the difficulties also encountered with some 2-chloro substrates (*c.f.* Table 3 and Table 4), pre-functionalisation of the C-Cl bond was attempted. 2-Phenylpyrimidine (**398**) was synthesised by a literature reported Suzuki-Miyaura cross-coupling reaction of 2-chloropyrimidine (**396**) with phenylboronic (**4**) (Scheme 31).¹⁴⁷ Upon cooling a white precipitate was observed amongst a yellow supernatant solution. After work-up and chromatographic purification, **398** was isolated as a white amorphous solid and bore the characteristic molecular ion peak ($m/z = 156$, $[\text{M}]^+$) by GC/MS analysis, with a notable absence of the chlorine isotopic pattern.



Scheme 31: Synthesis of 2-phenylpyrimidine

With 2-phenylpyrimidine in hand, the substrate was then tested in the C-H borylation process. In order to prevent competing borylation on the phenyl ring, a substoichiometric (0.6 equivalents) quantity of diboryl reagent was used at room temperature. Pleasingly, the borylation proceeded efficiently with good regioselectivity and chemoselectivity for the more electron-deficient pyrimidine ring, thereby mirroring the selectivity of previously discussed reactions involving 2-phenylpyridine (*c.f.* Figure 27). Borylation was selective for the 5-position (**399**) as evident by the shift in the 4/6-*H* resonance to higher frequency in the ^1H NMR spectrum. *In-situ* trapping by Suzuki-Miyaura cross-coupling with 3-iodopyridine (**400**) using the method detailed previously (*c.f.* Section 2.3.2.1), was monitored by LC/MS, with full consumption of the intermediate boronate ester observed within 1 h. The desired molecular ion peak ($m/z = 234$ $[\text{M}+\text{H}]^+$) was observed, thereby confirming the presence of product **401** (Scheme 32).



Scheme 32: Tandem 'one-pot' borylation/Suzuki-Miyaura cross-coupling of 2-phenylpyrimidine

The requirement for a 2-phenyl substituent limits the potential substrate scope of pyrimidines, however, the chemoselective preference for borylation of the heteroaromatic ring is promising and allows for late-stage functionalisation of these scaffolds.

2.3.6.3 Borylation of Indazole

The application of indazole in the C-H borylation process was attractive due to its isosterism with indole. It was hypothesised, however, that due to the presence of an additional azinyl nitrogen, that its reactivity pattern would be distinct to that of indole (*c.f* Figure 24b).

To explore this hypothesis, the parent indazole (**402**) was reacted with an aliquot of stock solution in a microwave reactor at 120 °C. Consistent with the above hypothesis, borylation products were not observed, as evident by ¹H NMR spectroscopic analysis of the crude reaction mixture (Figure 49a). GC/MS and LC/MS analyses also failed to detect products even at trace levels. However, consistent with disruption of azinyl coordination to the iridium catalyst, an *ortho* *N*-methyl protecting group is sufficient to enable efficient reaction. This is consistent with results obtained previously in the borylation of 2-picoline (Figure 49b) (*c.f* Figure 27b). Strategies for indazole borylation are discussed more fully in Chapter 3.

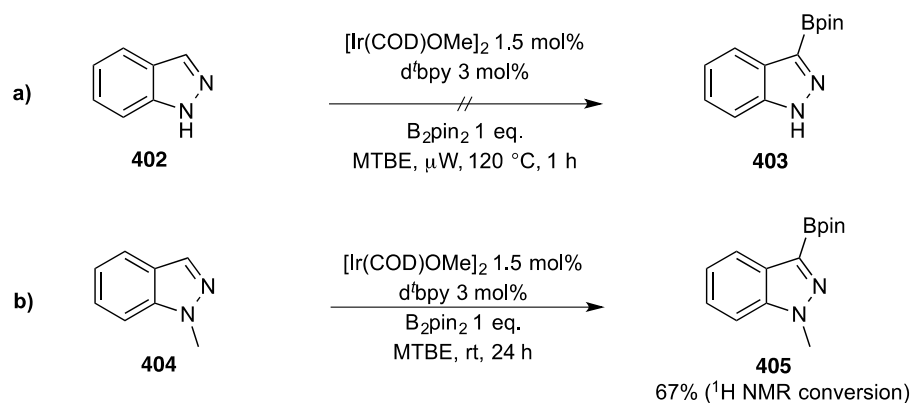
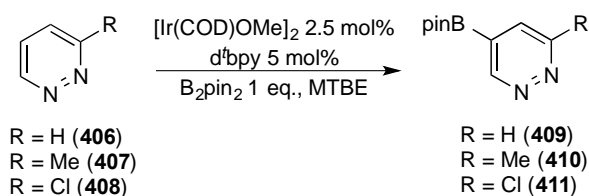


Figure 49: Borylation of indazoles

2.3.6.4 Borylation of Pyridazines

Pyridazine was a substrate of potential interest due to the neighbouring azinyl nitrogens and their potential effect on reactivity. Preliminary investigation involved the reaction of the parent heterocycle with an aliquot of stock solution. Unsurprisingly, given the presence of two unencumbered azinyl nitrogens, the borylation of the parent pyridazine heterocycle (**406**) proceeded sluggishly even with high temperature microwave irradiation. Conversion was tentatively assigned as 57% based on C-4 borylation (**409**) and a subsequent downfield shift of neighbouring 3 and 5-*H* resonances, however, significant quantities of decomposition products were observed by ¹H NMR and as such an accurate measure was not possible. GC/MS analysis failed to confirm the conversion ratio and to identify the decomposition products. Reflecting this, subsequent reactions were carried out on 3-substituted substrates and the results are summarised in the table below (Table 11);



Entry	R	Temp (°C)	Time (h)	Conversion (¹ H NMR)	Yield
1 ^a	H	80	1	57%	N/A
2	Me	rt	24	100%	63% ^b
3 ^{a,c}	Cl	80	1	0%	N/A

a. Run in microwave reactor; b. Contains minor impurities;
c. Reaction attempted in THF, NMP and diglyme

Table 11: Borylation of pyridazines

The corresponding borylation of 3-methylpyridazine (**407**) proceeded smoothly with a serendipitous crystallisation of the 5-boryl product (**410**) enabling easy identification of regioselectivity with 4 and 6-*H* singlet resonances observed at 7.64 and 9.22 ppm respectively in the ¹H NMR spectrum (Table 11, entry 2) (Figure 50). Copious washings with cold MTBE and attempted recrystallisations failed to remove co-crystallised boron-impurities observed at 22.5 ppm in the ¹¹B NMR spectrum and as such an analytically pure sample was not obtained. The filtration liquors were concentrated *in vacuo* and analysed by ¹H NMR to confirm the absence of any minor borylation products and starting pyridazine, thereby confirming the full clean conversion to product. Disappointingly, 3-chloropyridazine (**408**) was recalcitrant to borylation due to its poor solubility in both THF and the more polar diglyme and NMP (entry 3).

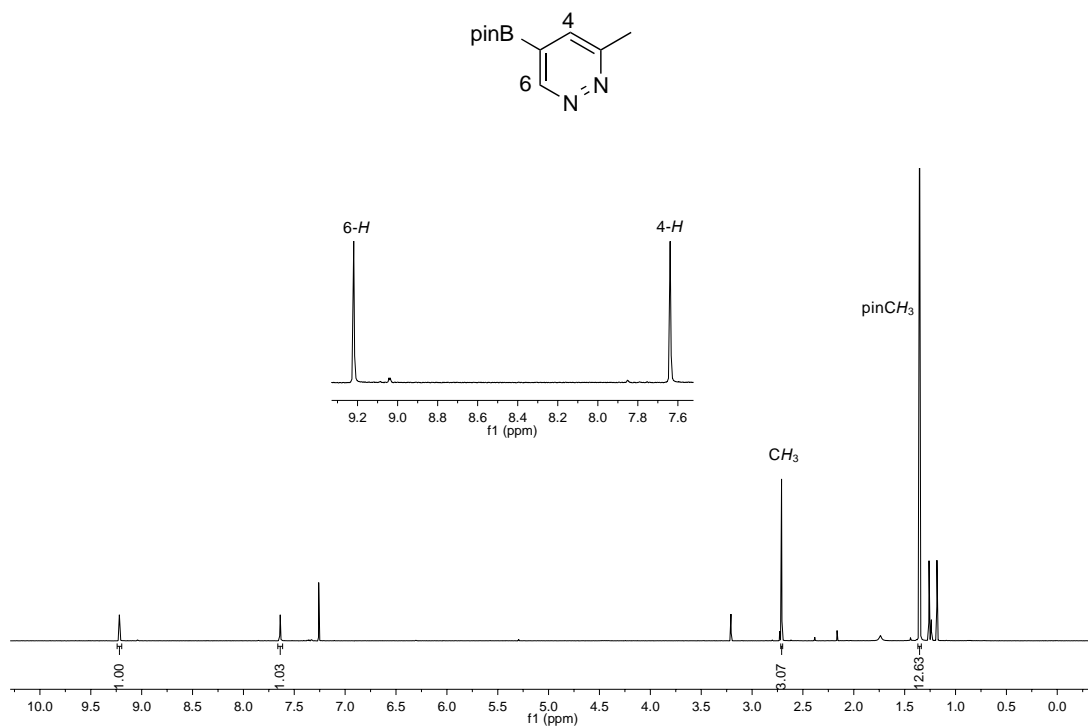
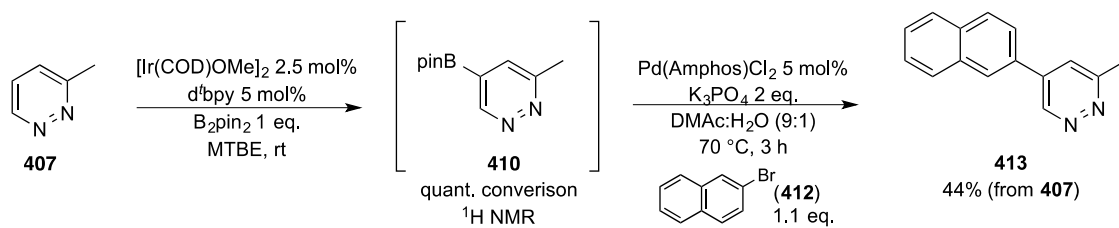


Figure 50: ¹H NMR spectrum of 3-methyl-5-(Bpin)-pyridazine

Reflecting the difficulties in purification, 3-methyl-5-(Bpin)pyridazine (**410**) was trapped by a tandem 'one-pot' Suzuki-Miyaura cross-coupling with 2-bromonaphthalene (**412**) using the method previously described (Scheme 33) (c.f Section 2.3.2.1).



Scheme 33: Tandem 'one-pot' borylation/Suzuki-Miyaura cross-coupling of 3-methylpyridazine

Product **413** was characterised by a shift in the 4 and 6-*H* resonances to 7.63 and 9.43 ppm respectively, as well as the diagnostic molecular ion found by ASAP accurate mass ($m/z = 220.1000$, $[M]^+$).

2.3.6.5 Borylation of Isoquinolines

The borylation of quinoline scaffolds is well established both in literature and within the research group (*c.f* Section 2.2). The borylation of isoquinoline and its derivatives has remained a somewhat neglected area but with the wide range of reported biological activities exhibited by isoquinoline derivatives, direct functionalisation of the isoquinoline core is an attractive tool for synthetic chemists.¹⁴⁸ Reflecting this, a series of simple isoquinoline substrates were screened. Preliminary experiments studied the direct functionalisation of the parent heterocycle by reaction with an aliquot of catalyst stock solution (**414**). GC/MS analysis of the crude concentrated product displayed no borylation products and full conversion of the starting material to an unknown product bearing the molecular ion peak $m/z = 102$. The mass loss corresponds to loss of HCN ($m/z = 27$), likely initiated by coordination of the azinyl nitrogen to the iridium catalyst. Reflecting this observation, and in light of knowledge gained previously in the study, a series of 1 and 3-substituted isoquinolines were subjected to C-H borylation (Table 12).

Entry	SM		Time (h)	Products
	R	R'		
1 ^a	H	H	24	No borylation products observed ^b
	414			
2	Cl	H	72	No borylation products observed
	415			
3	Me	H	72	<div style="display: flex; justify-content: space-around; align-items: center;"> <div style="text-align: center;"> 417 </div> <div style="text-align: center;"> 418 </div> </div> 1:1 ^c
	416			
4	H	Me	24	<div style="display: flex; justify-content: space-around; align-items: center;"> <div style="text-align: center;"> 420 </div> <div style="text-align: center;"> 421 </div> </div> 63% ^e (53:47)
	419			

a. Reaction run at 80 °C; b. Decomposition of substrate observed by GC/MS; c. Minor isomer detected ca. 10%; d. Isolated yield as compound mixture after tandem Suzuki-Miyaura cross-coupling reaction - Conditions: 2ndGenPdXPhos (5 mol%), K₃PO₄ (2 eq.), 3-iodo-fluorobenzene (1.1 eq.), Dioxane:H₂O (5:1), 70 °C, 1 h

Table 12: Borylation of isoquinolines

Disappointingly, 1-chloroisoquinoline (**415**) was recalcitrant to the borylation conditions showing no conversion to borylation products by *in-situ* ¹H NMR spectroscopy (entry 2). 1-methylisoquinoline (**416**) borylated readily at room temperature displaying a 94% GC/MS conversion to borylated products. The complex mixture observed by ¹H NMR spectroscopy precluded the calculation of a regioisomeric ratio. GC/MS ratios showed a 96:4 ratio of monoborylated ($m/z = 269$, [H]⁺) to bis-borylated ($m/z = 395$, [M]⁺) products (entry 3). Analysis of *in-situ* ¹H spectra taken early in the reaction enabled tentative assignment of 6 and 7-boronate esters (**417**, **418**) as the major products on the grounds of downfield shifts of 5 and 8-*H* resonances with accompanying change in multiplicity. The 4-boryl product was discounted on the grounds of no observed change in the *peri* 5-H resonance (Figure 51).

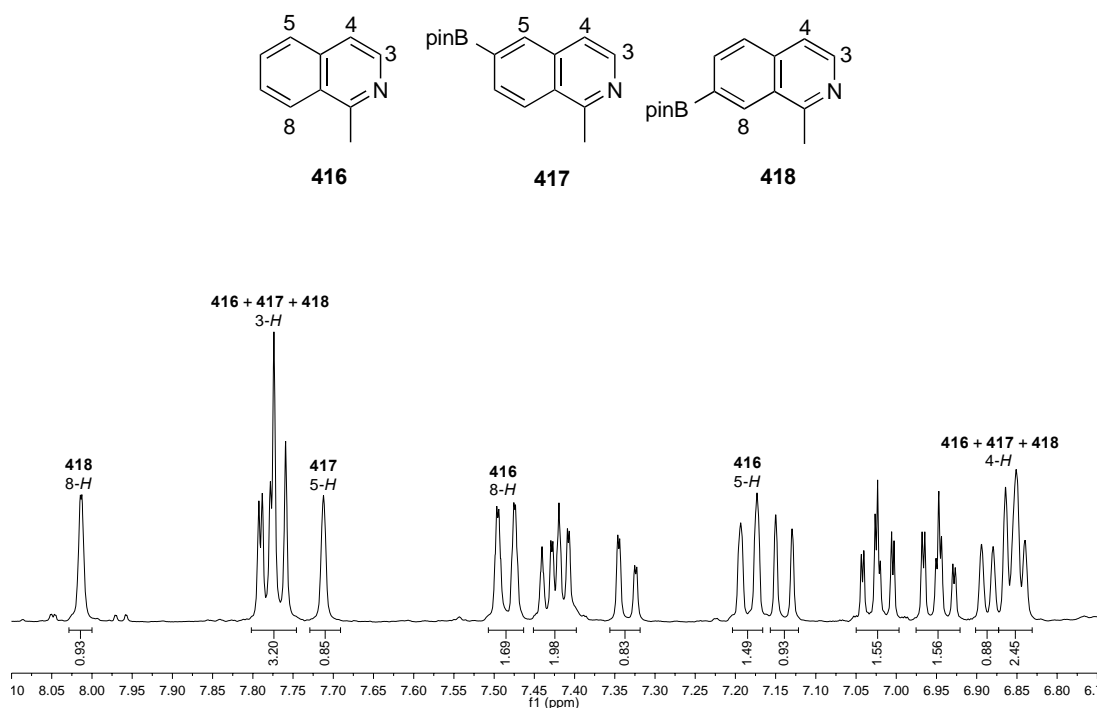
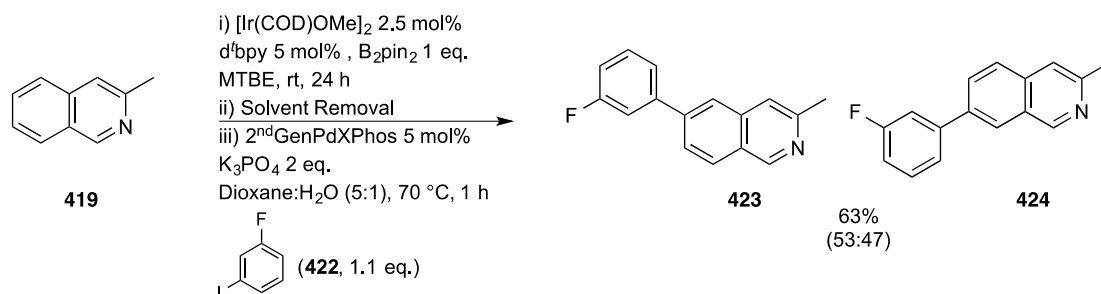


Figure 51: Borylation of 1-methylisoquinoline (*In-situ* ^1H NMR spectrum)

Borylation of the 3-methyl derivative (**419**) gave a 75% conversion to a 53:47 mixture of two monoborylated products (**420**, **421**) by GC/MS. After concentration and reaction with 3-fluoro-iodobenzene (**422**) catalysed by the 2ndGenPdXPhos pre-catalyst using the previously discussed method (c.f Section 2.3.2.1), products **423** and **424** were isolated as an inseparable mixture in a roughly 1:1 ratio (Scheme 34).

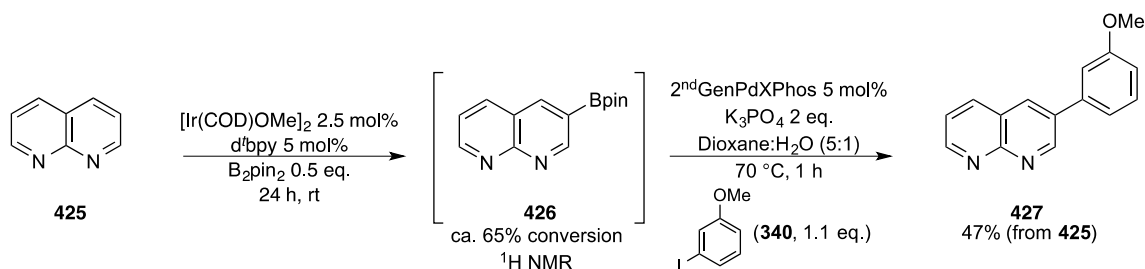


Scheme 34: Tandem 'one-pot' borylation/Suzuki-Miyaura cross-coupling of 3-methylisoquinoline

The final products after Suzuki-Miyaura cross-coupling were confirmed by two merged, indistinguishable ^{19}F signals at -112.6 ppm as well as two closely eluting LC/MS peaks exhibiting the desired molecular ion peak ($m/z = 238$, $[\text{M}+\text{H}]^+$). The regioselectivity and compound mixture obtained was unsurprising given the steric and electronic similarities of 6 and 7-*H*.

2.3.6.6 Borylation of 1,8-Naphthyridine

Due to their potential use in medicinal chemistry as quinoline isosteres, there has been increased interest towards synthesis of naphthyridine derivatives. Substituted naphthyridine cores have often been prepared *via de novo* synthesis.^{149,150} Development of strategies which permit late stage functionalisation is more synthetically desirable and as such work was focussed on direct borylation of the 1,8-naphthyridine core (**425**). In order to prevent excessive formation of bis-borylated products, reactions were conducted at room temperature with sub-stoichiometric B_2pin_2 (Scheme 35).



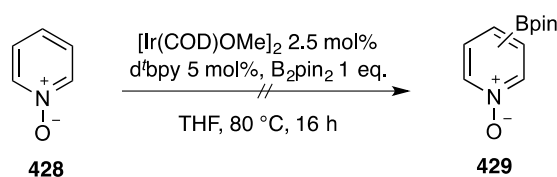
Scheme 35: Tandem 'one-pot' borylation/Suzuki-Miyaura cross-coupling of 1,8-naphthyridine

Consistent with desymmetrisation of the molecule, the 3-boryl product (**426**) was observed by shifts to higher frequency of 2-*H* and 4-*H* resonances. Conversion was tentatively assigned as 65%. Attempted purification of the boronate ester was

problematic due to the streaky nature of the product on both silica and alumina matrices. As such the 3-boryl product and regioselectivity was confirmed after tandem Suzuki-Miyaura cross-coupling reaction of the crude boronate ester with 3-iodoanisole (**340**). Product **427** was confirmed by observation of a 2.6 Hz $^4J_{\text{H-H}}$ coupling between 2 and 6-*H* resonances and a singlet at 3.92 ppm, corresponding to the newly incorporated OCH_3 functionality.

2.3.6.7 Borylation of Pyridine-*N*-oxides

Direct borylation of pyridine *N*-oxides was also of interest due to their distinct electronic character, with respect to azinyl heterocycles, and their pre-existing capped azinyl nitrogen. Reflecting this, borylation of pyridine-*N*-oxide (**428**) was attempted with a THF stock solution for solubility reasons. Consistent with previous findings, the attempted direct borylation of pyridine-*N*-oxide was unsuccessful, with only starting material observed by ^1H NMR after concentration of the reaction mixture. Significant quantities of oxidised B_2pin_2 were observed by GC/MS ($m/z = 270$), likely a by-product of the oxidative nature of the substrate (Scheme 36).



Scheme 36: Attempted borylation of pyridine-*N*-oxide

In light of this finding, the *N*-oxide was alkylated in order to suppress the formation of oxidised B_2pin_2 and prevent coordination to the iridium catalyst. Consideration was given to ensure the product counter ion facilitated solubility of the product in low polarity

borylation reaction media and was itself non-coordinating. Reflecting this, a solution of Meerwein's salt (**430**) was slowly added to a DCM solution of **428**. Concentration *in vacuo* gave the crude product as a pink solid. Recrystallisation from hot EtOAc with copious washings with cold Et₂O gave the product (**431**) as a white solid, characterised by a quartet and triplet ($J = 7.0$ Hz) at 4.70 and 1.39 ppm respectively, corresponding to the newly incorporated alkyl resonances, in the ¹H NMR spectrum (Figure 52a).

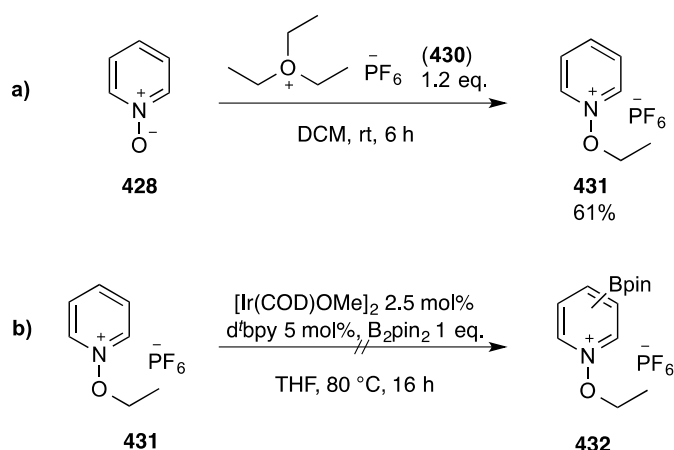


Figure 52: a. Alkylation of pyridine-N-oxide; b. Attempted borylation of alkylated pyridine-N-oxide

Disappointingly, despite good solubility in THF and the conversion of the oxide functionality into an ethereal oxygen, the attempted borylation of **431** with a THF stock solution gave no observable C-H borylation products after overnight heating, as evident by ¹H NMR and LC/MS analysis of the crude reaction mixture (Figure 52b).

2.4 Conclusions and Future Work

Through judicious choice of substrates, iridium-catalysed C-H borylation can be conducted with Lewis-basic heterocycles. Borylation is contingent upon the presence of an *ortho*-substituent to disrupt azinyl coordination to the iridium catalyst.

The borylation of 2-substituted pyridines gives product mixtures, with the preferred regioselectivity correlating well with the relative acidity of C-H bonds. The reaction of difunctionalised pyridines enables synthesis of single products, which are isolable by column chromatography (stability permitting) or applicable in tandem 'one-pot' Suzuki-Miyaura cross-coupling reactions in good yields.

The borylation of C-H bonds *ortho* to azinyl nitrogen atoms is disfavoured on the grounds of unfavourable repulsive interactions between the lone pair and a partial negative charge during oxidative addition. However, the presence of a suitably sterically encumbering group at C-4 is sufficient to overcome this energy barrier. In addition, electron-withdrawing groups at C-2 accelerate the reaction by sequestering the Lewis basicity of the lone pair. Moreover, this also stabilises them to chromatographic purification by sufficiently slowing the rate of protodeborylation. These findings somewhat contradict a concurrent report published by Hartwig *et al.*, in which it was suggested that the lack of *ortho* azinyl borylation was attributable to rapid *in-situ* protodeborylation rather than an intrinsic barrier to C-H activation.¹²²

Where the instability of the boronate esters precludes their purification by chromatographic methods, they have been trapped by Suzuki-Miyaura cross-coupling reactions. Whilst Burke and co-workers have reported strategies for the cross-coupling of 2-pyridyl boronic species (*c.f* Scheme 9), these strategies often require the use of a large excess of boron compound or proceed from the MIDA boronate (synthesised in multiple steps via the boronic acid) (*c.f* Figure 12).

Whilst their basicity is markedly lower than pyridine, the borylation of pyrazines, pyrimidines, pyridazines and isoquinolines also required an *ortho*-substituent to improve efficiency. The activity of 3-methylpyridazine was somewhat surprising, because despite the steric bulk present at C-3 to disrupt the coordinating effects of N-2, the N-1 azinyl lone pair remained unencumbered and was expected to partially suppress the reaction. It was postulated that the repulsion caused by the co-planar azinyl lone pair of N-2 restricted the coordination of the N-1 lone pair to the iridium catalyst thereby enabling borylation to occur. Also surprising, was that 1,8-naphthyridine also borylated without the requirement for pre-functionalisation. This was rationalised on the basis that the co-planar *peri* lone pairs effectively cancel out one another and prevent the docking onto the iridium on the basis of repulsion.

Current work in the group is seeking to expand upon the multi-directional synthetic strategies expounded upon in this chapter. Exploiting the functional group tolerance of C-H borylation, the synthesis of functionalised biaryls has been demonstrated. The pre-existing functionality was then reacted in downstream chemistry to allow small library synthesis.

3 Multidirectional Synthesis of Functionalised Indazoles

3.1 Background and Chapter Aims

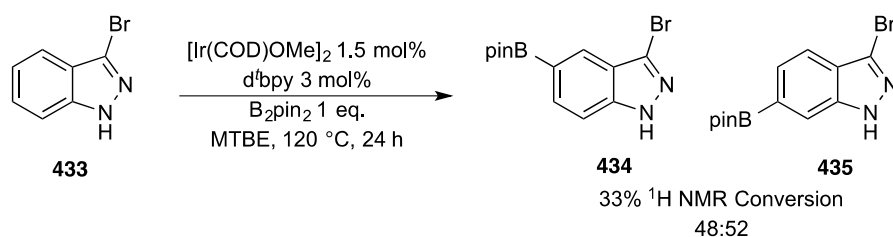
The C-H borylation of indole substrates is well established in the literature (*c.f* Figure 24). Due to its isosterism with indoles, indazoles are an important class of heterocycle in medicinal chemistry and agrochemical programs.¹⁵¹ Amongst other applications, indazole derivatives have been found to possess antifertility,¹⁵² anticancer,¹⁵³ antispermatogenic^{154,155} and HIV protease inhibitory activity.¹⁵⁶ Therefore, protocols by which substituted and functionalised indazole derivatives can be synthesised in good yields and with good atom efficiency would have widespread synthetic utility in the pharmaceutical sector and in drug discovery programs.

Direct C-H borylation is particularly attractive for a drug or agrochemical discovery program as it allows for efficient library synthesis from known and readily available starting materials, or for later stage functionalisation of common precursors. Therefore, in order to investigate the potential utility of the indazole moiety in these programs, work was first carried out to probe the reactivity of the unmodified parent heterocycle. As previously discussed, the parent heterocycle was recalcitrant to borylation even at high temperatures and with microwave irradiation (*c.f* Figure 49). This chapter addresses the steps taken to address the limited reactivity of indazole, in light of the strategies gleaned from the previous chapter, in order to enable its application in multidirectional synthetic strategies towards privileged multiaryl units.

3.2 Results and Discussion

3.2.1 Borylation of 3-Bromoindazole

Given the propensity for unmodified indole to undergo fast and selective borylation, it was hypothesised that the additional azinyl nitrogen present in indazole (relative to indole) was inhibiting borylation through coordination to the Ir-centre at the vacant coordination site. This effect is similar to that previously observed in the borylation of pyridyl substrates (*c.f* Section 2.1.4.2). In order to circumvent this issue, coordination of the azinyl nitrogen to the iridium catalyst would need to be disrupted. In light of previous observations (*c.f* Section 2.1.4.3), two solutions were suggested; incorporation of a formal substituent *C*-3 ortho to the coordinating azinyl nitrogen, or incorporation of an *N*-protecting group. Given the commercial availability of 3-haloindazoles and the drive towards green chemistry that avoids the use of protecting groups (where possible) in drug discovery programs, the former strategy was investigated. It was also postulated that nitrogen protection could induce regioselectivity issues and prevent potential *N*-directed borylation as previously observed in the borylation of 2-substituted indole substrates (*c.f* Figure 24d). Moreover, the presence of 3-halosubstitution could allow for downstream modification, enabling multidirectional synthesis and the efficient synthesis of small compound libraries. On this basis, the commercially available 3-bromoindazole (**433**) was selected as a substrate to explore (Scheme 37).



Scheme 37: Borylation of 3-bromoindazole

The reaction of **433** with an equivalent of B₂pin₂ in the presence of 3 mol% iridium was sluggish even with heating at 120 °C over extended periods. However, the fact that borylation products (**434**, **435**) were observed confirmed inhibition of coordination was key to enabling indazoles to undergo borylation. ¹H NMR spectroscopic analysis enabled characterisation of a roughly 1:1 mixture of products arising from borylation at C-5 and C-6, which could be distinguished using the previously outlined method (*c.f* Figure 36), through observation of downfield shifts in neighbouring ¹H resonances (Figure 53).

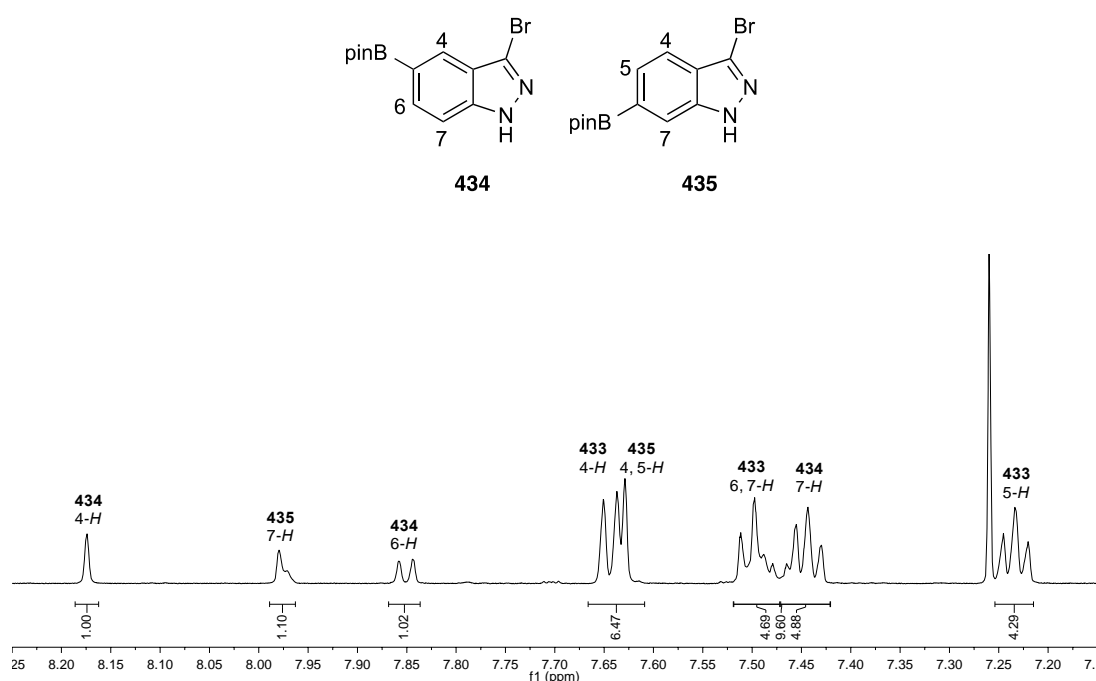


Figure 53: Borylation of 3-bromoindazole (**433**) (¹H NMR spectrum of the crude product mixture)

Whilst an *ortho* substituent was sufficient to enable pyridyl substrates to undergo efficient borylation at room temperature, it was insufficient to suppress sufficiently azinyl coordination in this instance. It was hypothesised that the suppressive effect of the *ortho*-substituent on azinyl nitrogen coordination was less significant on 5-membered motifs,

due to their expanded H-C-C bond angles, relative to 6-membered systems. It was also envisaged that, like the parent heterocycle, 3-bromoindazole could exist in 2-tautomeric forms in solution (Figure 54). Given the low catalyst loadings employed in this reaction, only a small concentration of the minor tautomer (**433b**), bearing the unhindered azinyl nitrogen, would be required to inhibit reactivity.

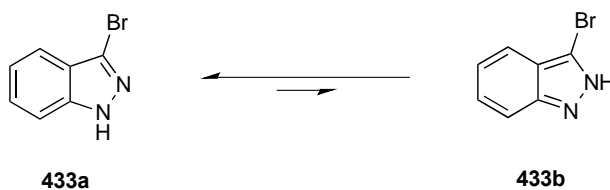


Figure 54: Tauomerisation of 3-bromoindazole

With the low selectivity and sluggish reactivity observed, focus was therefore turned to borylation of protected indazoles.

3.2.2 Borylation of Protected Indazoles

3.2.2.1 Attempted Traceless Protecting Group Strategies

Initially the possibility of traceless protecting groups was explored, as this offers the added advantage of not requiring formal protection and deprotection steps in a synthetic pathway. A survey of the literature found two potential protocols of interest.

Smith and co-workers had demonstrated that Bpin could function as a Boc group surrogate in the borylation of nitrogen heterocycles (Figure 55, Route B)¹⁵⁷ Pre-exposure to HBpin was shown to form a *N*-boryl adduct (**439**) which functioned as a formal protecting group subsequently enabling regioselective borylation of the heterocycle and thereby circumventing the need for protection and deprotection steps.

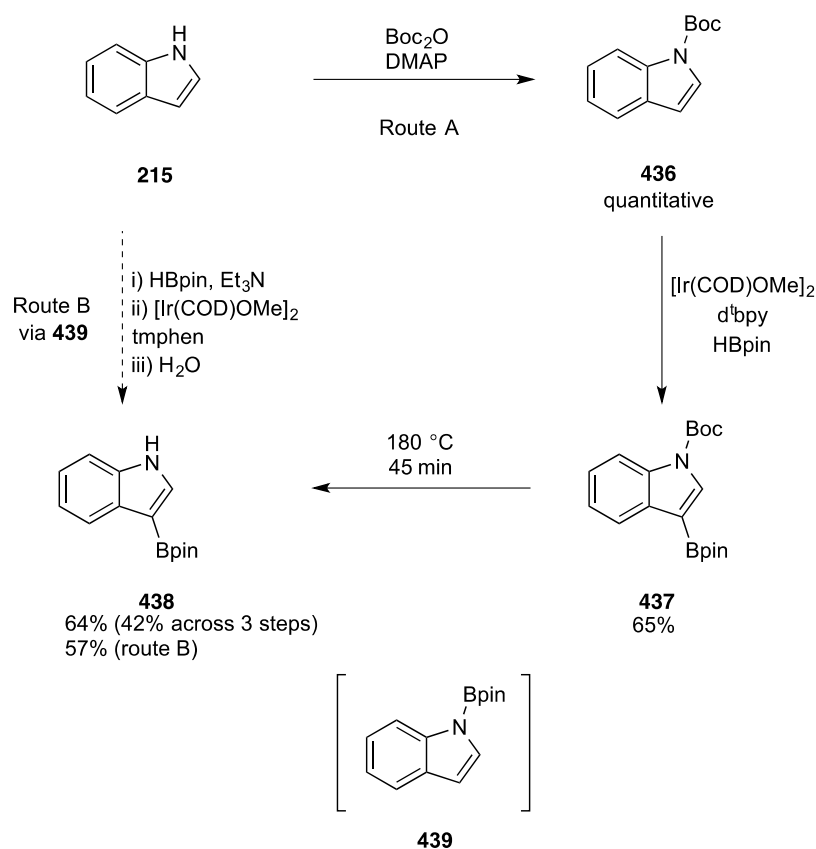
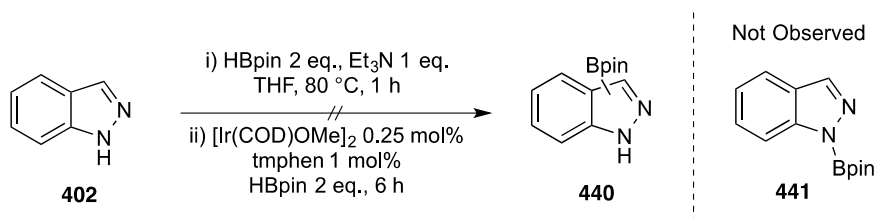


Figure 55: Bpin as a traceless protecting group for indole borylation

Attempts were then made to apply this protocol to the borylation of indazole (Scheme 38). Prior to the addition of an aliquot of catalyst stock solution, indazole (**402**) was reacted with excess HBpin in the presence of triethylamine (Et_3N). No change in ^{11}B NMR shift was observed after stage 1, which suggested formation of the *N*-boryl adduct (**441**) was unsuccessful, however given the potential instability of the adduct, the stock solution was added to the crude reaction mixture and the reaction continued as planned.



Scheme 38: Attempted borylation of indazole with traceless Bpin protecting group

Analysis of the crude reaction mixture by ^1H NMR spectroscopy and GC/MS found only unreacted starting indazole. Reflecting this unfortunate result, an alternative protocol was considered.

Given that the Lewis-basicity of the azinyl nitrogen had to this point been a practical hindrance to the direct borylation of indazole, it was hypothesized that the substrate could be activated by coordination of a supplementary metal species present in the reaction media. Gorelsky had previously showed that the Palladium-catalysed direct C-H arylation of azoles could be accomplished in the presence of a non-reactive copper source, whose primary role was coordination to the azinyl nitrogen (Figure 56).¹⁵⁸

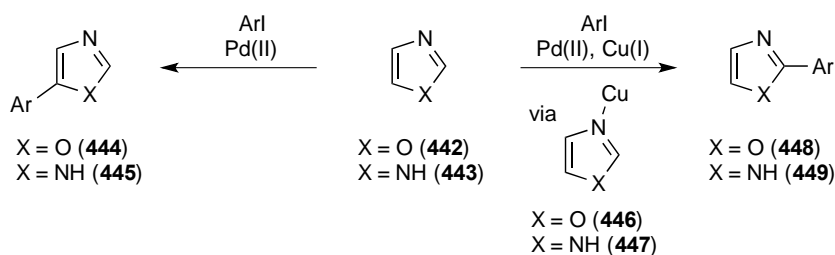
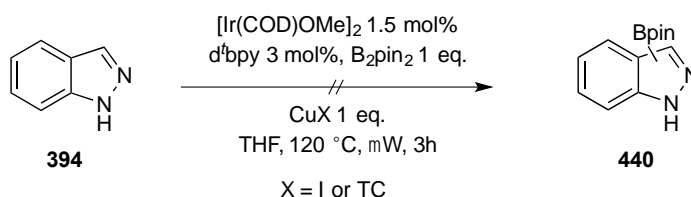


Figure 56: Regioselectivity tuning with Cu(I) salts

It was also observed that copper binding enhanced C-H acidities of proximal protons, thereby adjusting the preferred regioselectivity. C-H acidity has been found to have an important role in predicting preferred regioselectivity of C-H borylation and thus this

method was pursued and applied to indazole. It was postulated that the azinyl nitrogen would bind to copper in preference to the iridium catalyst, thereby allowing C-H oxidative addition by transmetalation onto the iridium catalyst. Following this hypothesis, one equivalent of CuX was added to the substrate prior to the addition of catalyst stock solution (Scheme 39).

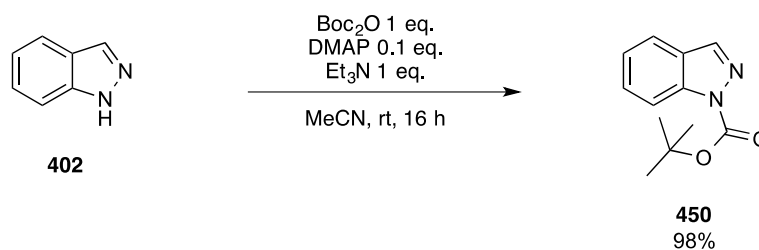


Scheme 39: Attempted borylation of indazole, with Cu(I) salts as traceless protecting groups

Disappointingly, the reaction was unsuccessful both with suspended Cu(I)I and with soluble Cu(I)TC (copper (I) thiophene-2-carboxylate). Concentration of the reaction mixture after celite filtration (to remove copper species) gave a crude mixture bearing only unreacted starting material. Protodeborylation prior to analysis was possible, but unlikely given the mild work-up conditions.

3.2.2.2 Borylation of *N*-protected Indazoles

The unsuccessful investigation into traceless protecting strategies suggested formal protecting groups would be required to facilitate C-H borylation. Various literature precedents have been reported for the protection of indazole substrates with a variety of protecting groups.¹⁵⁹⁻¹⁶¹ Given that its synthesis avoids the use of strong bases, attention first focused on the use of *N*-Boc-1H-indazole (**450**) (Scheme 40).



Scheme 40: Boc-protection of indazole

Simple reaction with di-*tert*-butyl-dicarbonate (Boc_2O) in MeCN afforded **450**, which lacked the characteristic N-H stretch of the parent indazole. Confirmation of Boc-protection was provided by a strong CO stretch at 1732 cm^{-1} in the IR spectrum and a singlet at 1.66 ppm in the ^1H NMR spectrum, corresponding to the methyl (CCH_3) resonance of the *tert*-butyl moiety. The regioselectivity was confirmed by comparison to literature data. With the protected indazole in hand, work focused on testing the substrate in the borylation process.

Using pre-prepared catalyst stock solutions, full clean conversion to the 3-borylated product (**451**) was observed within two hours by *in-situ* ^1H NMR spectroscopy (Scheme 41). *In-situ* NMR analysis was facilitated using the previously described method (*c.f.* Section 2.3.1).



Scheme 41: Borylation of Boc-1H-indazole

Confirmation of 3-borylation was obtained from the ^1H NMR spectrum, in which loss of the 3-*H* singlet was observed to leave a single four-spin system as observed by correlation spectroscopy (COSY). Moreover, consistent with 3-borylation was an observed upfield (ca. 0.4 ppm) shift of the *peri* 4-*H* proton (Figure 57).

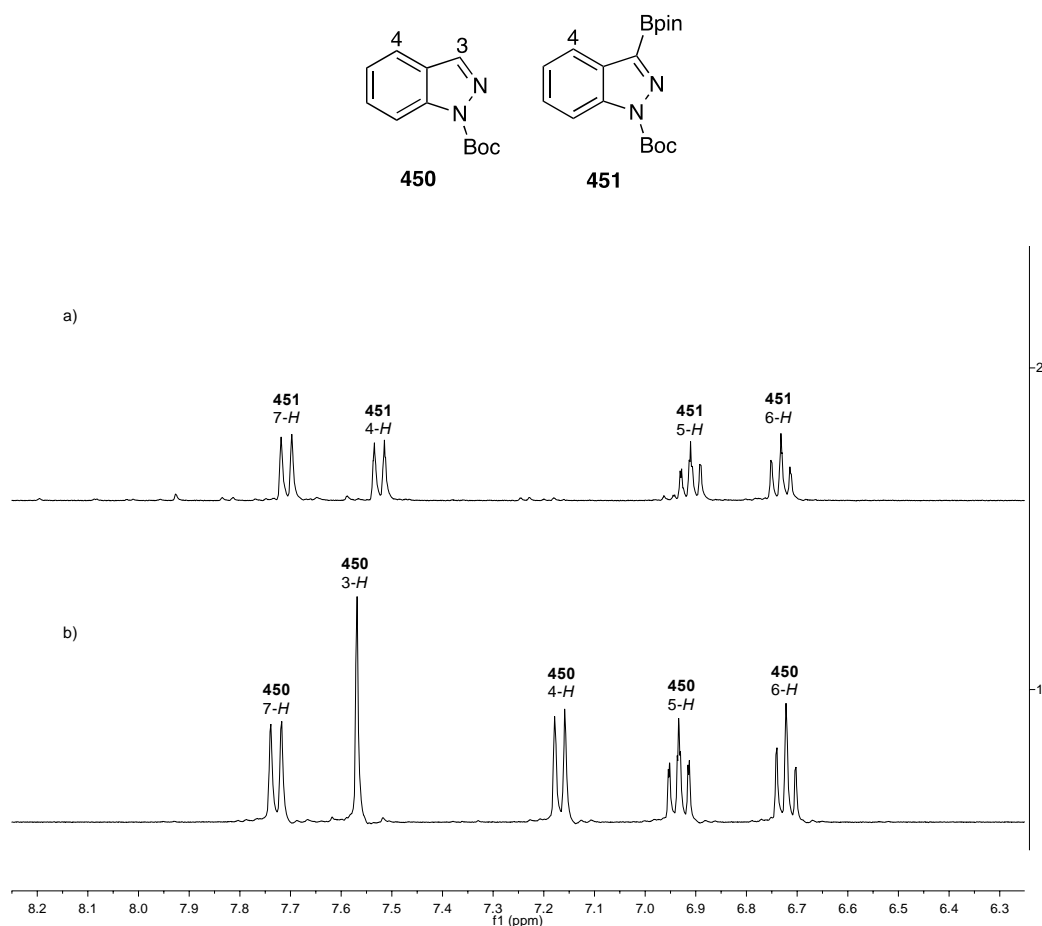


Figure 57: a. *in-situ* ^1H NMR spectrum of borylation of Boc-indazole; b. Reference spectra of **450** (enhanced aromatic region).

Regioselectivity in this instance is chemoselective for the heteroaromatic ring with preferential reactivity at the most acidic C-H bond.¹⁶⁰ This is in keeping with many previously recorded observations within the group.¹²⁹ Frustratingly, attempts to purify the

mono-borylated product were unsuccessful, with flash column chromatography leading to significant protodeborylation back to starting material.

Having established that *ortho*-azinyl boronate ester stability was sensitive to the electronic effects of *ortho* functionality (*c.f.* Table 5), it was envisaged that indazoles bearing more electron-withdrawing protecting groups would enable chromatographic purification. Removal of electron density from the azinyl nitrogen would reduce the prominence of hydrolytic degradation pathways. It was also of interest to study the relative rates of formation of *ortho*-azinyl boronate esters as a function of protecting group electronics. Consequently, a series of protected indazoles were prepared (Table 13). Given the propensity for kinetic control in indazole protection to provide 2-protected indazoles, it was also suggested that access to these alternative substrates may enable a redirection in regioselectivity by steric effects.

Entry	R-X	Conditions ^a	Products and Yields ^b	
1	 452	A	 404 48%	 453 30%
2	 454	A	 455 35%	 456 52%
3	 457	A	 458 66%	
4	457	B	 459 74% ^c	
5	 460	C	 461 54%	 462 0% ^d
6	 463	D	 464 25%	 465 25%

a: Conditions A: i) NaH (1 eq.), 0 °C, 0.5 h ii) Alkyl-X (1.1 eq.) iii) rt, 3 h; B: Alkyl-X (1.2 eq.), Cy₂NMe (1.2 eq.), THF, rt, 3 h; C: Ms-Cl (1.2 eq.), Et₃N (1.2 eq.), DCM, rt, 18 h; D: 3,4-dihydro-2H-pyran (1.2 eq.), pTSA.H₂O (0.1 eq.), DCM, rt, 24 h; b: Isolated yields after column chromatography; c: Synthesised with conditions B; d: Product not observed in crude NMR

Table 13: Preparation of a series of protected indazoles

Slow addition of a solution of indazole (**402**) in THF to a NaH suspension in THF at 0 °C gave a homogeneous grey solution. Addition of MeI (**452**) enabled the synthesis of both *N*-methyl isomers (**404** and **453**) (entry 1). Repetition of this procedure with electrophiles

454 and **457** enabled synthesis of **455**, **456** and **458**. Regioselective synthesis of 2-[[2-(trimethylsilyl)ethoxy]methyl]-2H-indazole (2-SEM-2H-indazole, **459**) and synthesis of the *N*-mesyl species (**461**), were carried out in accordance with literature procedures (entries 4 and 5).^{160,162} Addition of a catalytic quantity of solid *p*TSA.H₂O to indazole and dihydropyran in DCM, accompanied by a loss in turbidity and a gradual colour change from grey to faint pink, enabled synthesis of THP (tetrahydropyran-2-yl) derivatives (**464** and **465**) (entry 6).

Characterisation was achieved through mass spectrometry in conjunction with ¹H NMR spectroscopy, for example *N*-methyl-1H-indazole (**404**) and *N*-methyl-2H-indazole (**453**) were identified by their characteristic LC/MS molecular ion peaks 133 ([M]⁺) and 134 ([M+H]⁺) respectively, as well as their respective CH₃ resonances in the ¹H NMR spectrum at 4.08 and 4.21 ppm.

Differentiation between the regioisomers was accomplished by observation of long range coupling in the HMBC spectrum between the NCH₃ carbon and 3-*H* proton and also between the corresponding NCH₃ protons and C-3 carbon. This far range correlation was present in the 2-protected isomers but absent in the 1-protected isomers (Figure 58). This pattern was observed in all cases where the protecting groups bore (pseudo)benzylic proton resonances (entries 1, 2, 3, 4 and 6).

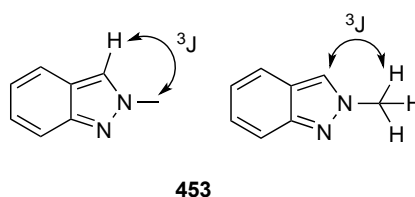
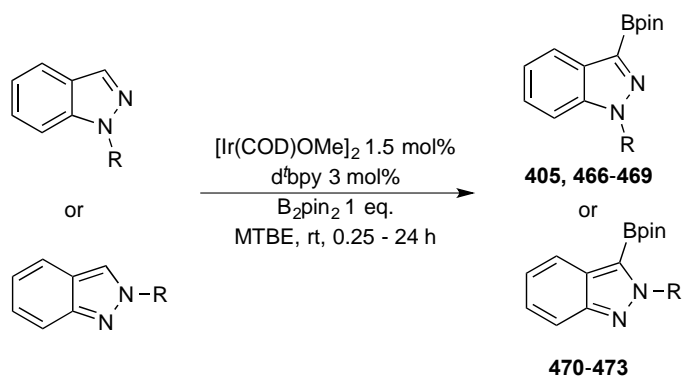


Figure 58: Regioselectivity assignment by HMBC correlations

To test their applicability to C-H borylation, the protected indazoles were treated with an aliquot of stock solution and the results are tabulated below (Table 14). Reactions were monitored by *in-situ* ^1H NMR up to 24 h to enable analysis of relative reaction rates and product regioselectivity was assigned using the previously described method (*c.f* Figure 57).



Entry	SM	R	Time (h)	Conversion (%) ^a	Product
1	404	Me	24	67	405
2	455	Bn ^b	24	61	466
3	458	SEM	24	63	467
4	461	Ms	1	100 (62) ^c	468
5	464	THP	24	83	469
6	453	Me	1	100	470
7	456	Bn ^b	0.25	100	471
8	459	SEM	6	100	472
9	465	THP	20	100	473

a. Determined by ^1H NMR; b. 3,5-dimethylbenzyl c. Isolated yield

Table 14: Borylation of a series of 1 and 2-protected indazoles

Significantly, and consistent with the previously observed results obtained for 2-substituted pyridine borylation (*c.f* Table 2), more strongly electron-withdrawing protecting groups led to faster reactions and higher conversions. This was evident by the

superior reactivity of both the mesyl-derivative (**461**) (entry 4) and the previously described Boc-derivative (**450**) (c.f Scheme 41). Surprisingly, borylation of 2-protected indazoles occurred more rapidly and in higher conversions than the corresponding 1-protected isomers, with no change in regioselectivity observed (entries 6-9). This occurred in spite of the presence of bulky THP or benzyl protecting groups *ortho* to the preferred site of functionalisation. The higher reactivity of these isomers was most notably observed with complete borylation of the bulky 3,5-dimethylbenzyl derivative (**456**) being observed in minutes (entry 7), in contrast to the many hours required for the analogous 1-*N*-protected isomer (**455**) (entry 2). This pattern was attributed to Coulombic repulsive interactions between the emerging negative charge at C-2 and the 2-*N* azinyl lone pair (**475**) (Figure 59a). These interactions are notably absent in the borylation of 2-*N*-protected isomers, in which oxidative addition occurs distal to the azinyl lone pair (**476**, **477**) (Figure 59b). This may also explain the enhanced reaction rates observed for borylation of indazoles bearing electron withdrawing protecting groups. The increased electron-withdrawal by the Boc and mesyl protecting groups diminishes the destabilising repulsive effect of the azinyl lone pair, thus accelerating the rate of borylation *ortho* to the azinyl nitrogen.

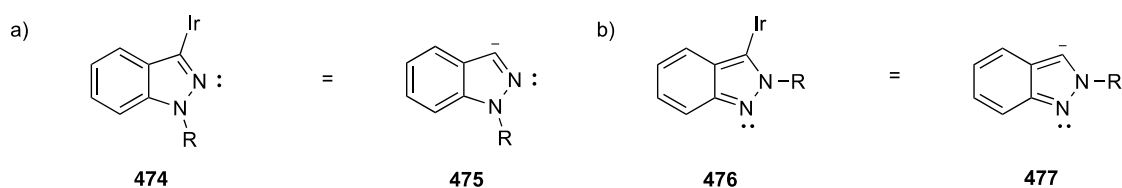


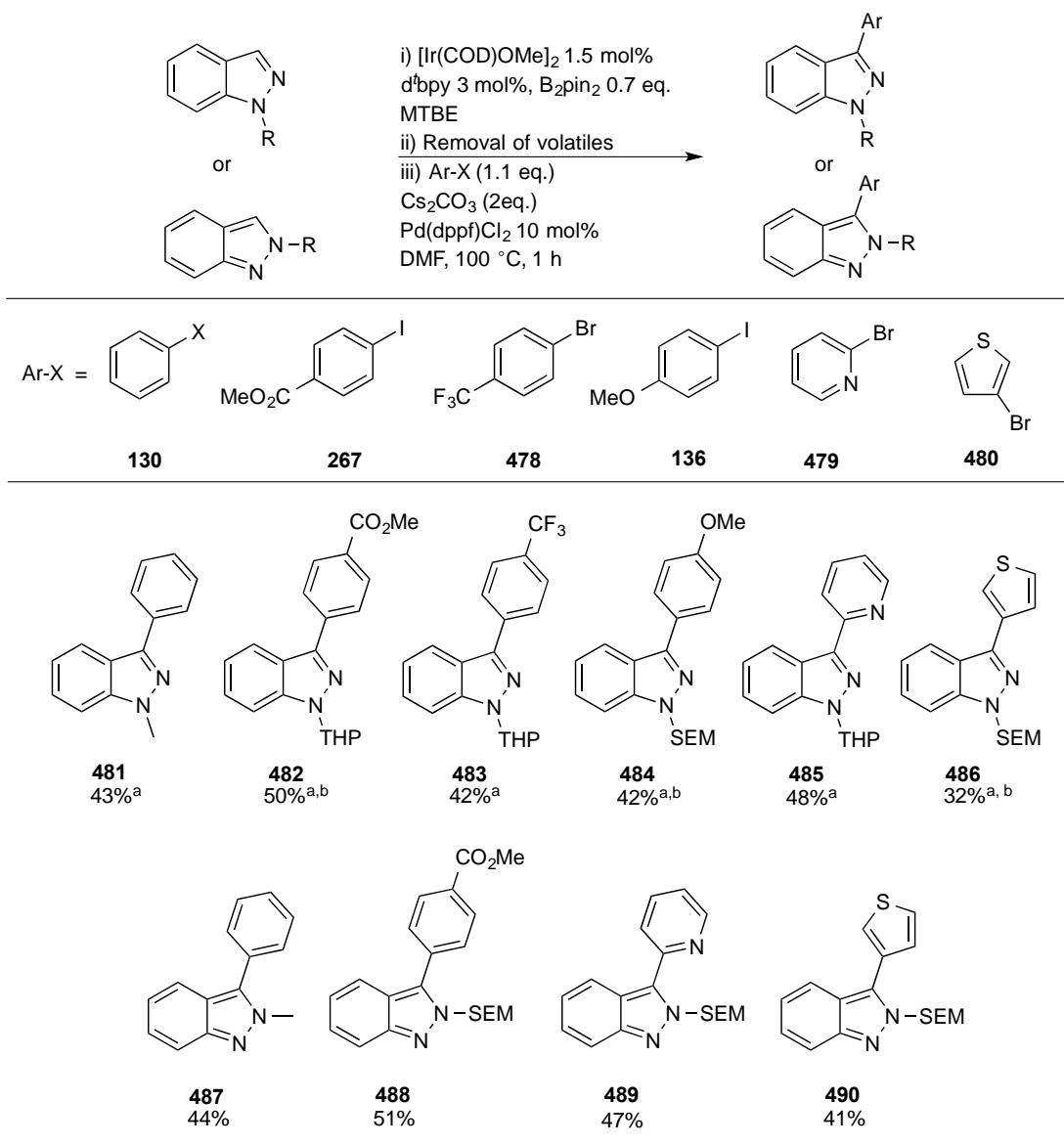
Figure 59: a. Disfavoured repulsive interactions from *ortho* oxidative addition of indazole; b. Favoured oxidative addition distal from the azinyl lone pair

A second observation arose from these studies. Unlike borylation products **405** and **451** which underwent significant protodeborylation on both silica and alumina column

matrices, product **468** (entry 4) was stable towards column chromatography. Isolation of **468** was confirmed by observation of a characteristically broad singlet at 28.9 ppm in the ^{11}B NMR spectrum as well as the diagnostic molecular ion peak $m/z = 321.1195$ ($[\text{M}]^+$) by ASAP accurate mass measurement. The electron-withdrawing capabilities of the mesyl group render the azinyl lone pair less basic and thus sufficiently slows the rate of protodeborylation to enable chromatographic purification.¹³⁵ This is consistent with the observed stability of methyl-2-fluoro-6-(Bpin)-nicotinate (**339**) described previously (*c.f.* Table 5).

3.2.2.3 Tandem 'one-pot' Borylation/Suzuki-Miyaura cross-couplings

Although the isolation of this typically unstable boronate ester was pleasing, the instability of the other boronate esters was so far a limiting factor in the application of C-H borylation methodology to indazole substrates. Furthermore, whilst the stability of many of these boronate esters was insufficient for them to be purified by column chromatography, it was envisaged that their solution lifetime might be sufficient enough to trap them *in-situ* by Suzuki-Miyaura cross-coupling (Figure 60). Consequently a series of 1 and 2-protected indazoles were borylated and then reacted with a selection of aryl halides, the results of which are shown below.



a. Suzuki-Miyaura step run in presence of CuCl (1 eq.); b. Reaction carried out by Andrew Hones.

Figure 60: Tandem ‘one-pot’ borylation/Suzuki-Miyaura cross-coupling of protected indazoles

Given that borylation of certain *N*-1 protected indazoles had previously failed to reach full conversion and in some cases lead to minor product formation (*c.f* Table 14), sub-stoichiometric B₂pin₂ and higher borylation reaction temperatures were employed to ensure single product formation. Borylation reactions were monitored by GC/MS until optimum conversion was reached, at which point the reaction was concentrated *in vacuo* and the Suzuki-Miyaura reagents and degassed DMF were added to the reaction

mixture. CuCl was added in order to increase the rate of transmetallation onto the Pd-catalyst in step iii and thus reduce the prominence of protodeborylation.⁹⁰ The absence of CuCl lead to greatly reduced yields for reactions involving 1-protected indazoles, for example the equivalent reaction involving 1-methyl-1H-indazole (**404**) with iodobenzene (**130**) carried out in the absence of CuCl gave only an 11% yield. Confirmation of cross-coupled product formation was confirmed by mass spectrometry, for example **481** possessed the diagnostic molecular ion peak by ASAP accurate mass measurement; $m/z = 208.0995$, $[M]^+$.

N-2 protected indazoles proceeded cleanly to 3-boryl intermediates. The Suzuki-Miyaura cross-coupling step was set up in an analogous fashion in the absence of CuCl as this was observed to have no beneficial effect on the isolated yields, for example, the equivalent reaction involving 2-methyl-2H-indazole (**453**) with iodobenzene (**130**) carried out in the presence of CuCl gave only a slightly diminished yield (41%). This was attributed to the fact that the 2-protected-3-(Bpin)-indazole intermediates are not *ortho*-azinyl boronates and are therefore less prone to protodeborylation pathways. The *N*-2 protected Suzuki-Miyaura products were characterised in an analogous fashion.

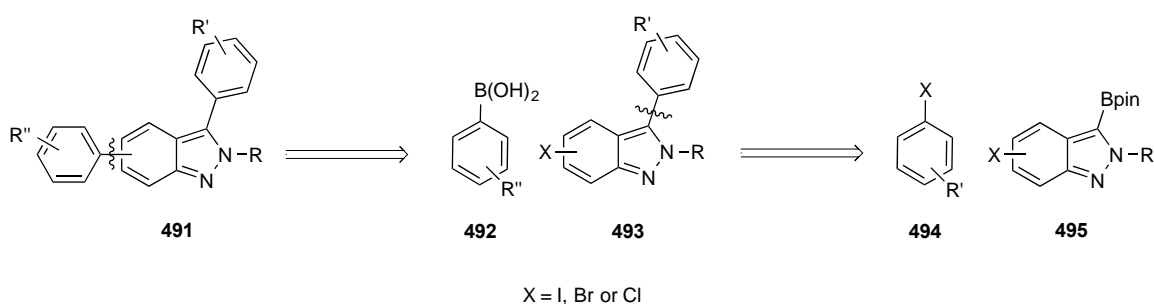
The isolated yields obtained clearly demonstrated that competitive protodeborylation was yield-limiting. Borylation conditions were sufficiently forcing to enable 100% conversion to boronate ester in many cases as evident by GC/MS after stage 1. This, therefore, showed that yield losses were incurred during the Suzuki-Miyaura cross-coupling step. This observation was attributed to potential metal or base-mediated protodeborylation pathways, both of which are potentially prevalent in cross-coupling reactions.^{4,5}

Overall, the method is general for a range of electron-rich and electron-poor aryl and heteroaryl iodides and bromides. Frustratingly, the cross-coupling of aryl chlorides proved not to be viable under these standard cross-coupling conditions even when

reactive 2-heteroaryl chlorides, such as 2-chloropyridine (**275**), were used as coupling partners. Moreover, the attempted reaction with the even more reactive 2-chloropyrimidine (**396**) was also unsuccessful.

3.2.2.4 Multidirectional Synthesis of Functionalised Indazoles

Having successfully demonstrated the regioselective borylation, and subsequent arylation, of protected indazoles, it was then of interest to apply this strategy in multidirectional syntheses of privileged multiaryl scaffolds. The functional group tolerance of C-H borylation enables borylation of functionalised starting materials, which would be otherwise recalcitrant to classical synthetic routes to boronate esters (*c.f.* Section 1.3.1.1). A retrosynthetic analysis of a multiaryl indazole suggested protected-bromoindazoles as suitable starting materials due to their availability, synthetic utility and the stability of the bromo functionality to C-H borylation (Scheme 42).

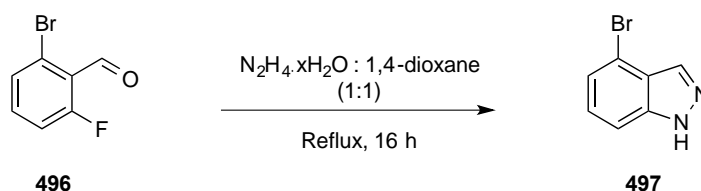


Scheme 42: Retrosynthetic analysis of bis-arylandazoles

3.2.2.4.1 Borylation of Bromoindazoles

With this objective in mind, initial work focussed on assembly of the required precursors. Due to their low cost, 5, 6 and 7-bromo-1H-indazoles could be purchased from

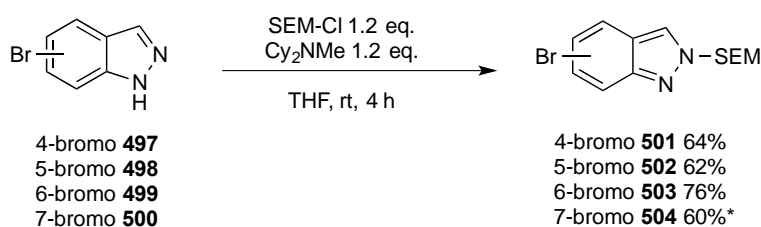
commercial suppliers whereas the 4-substituted isomer would require pre-formation of the indazole framework. This was accomplished by reaction of the substituent bromo-fluorobenzaldehydes with hydrazine (Scheme 43).



Scheme 43: Synthesis of 4-bromoindazole

Simple reflux of the required bromo-fluorobenzaldehyde (**496**) in a 1:1 mixture of dioxane:hydrazine hydrate gave the desired product (**497**), lacking the ^{19}F and aldehyde *CHO* resonances. Confirmation of indazole formation was provided by a broad N-*H* resonance at 10.67 ppm, in conjunction with a 3-*H* singlet at 8.13 ppm.

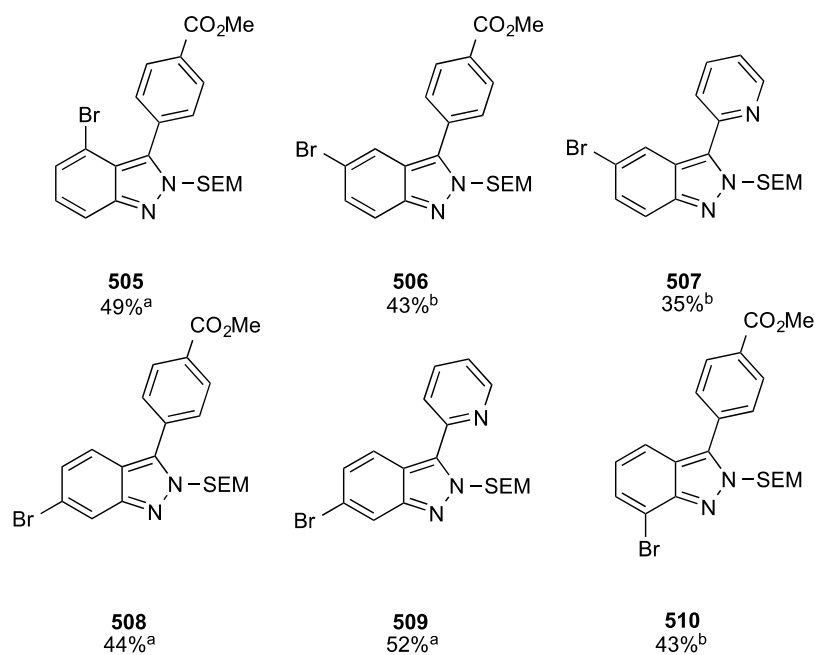
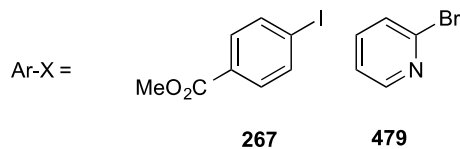
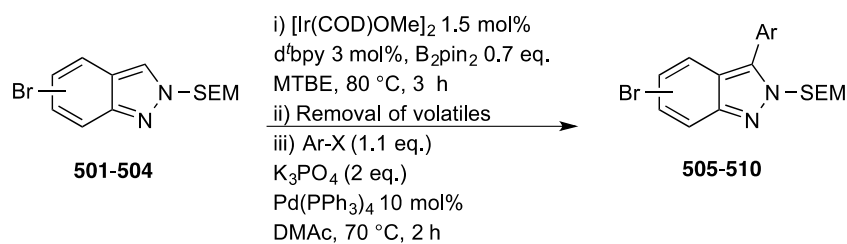
In order to enable borylation, prior protection was required. 2-SEM protected indazoles were chosen due to their selective synthesis and superior reactivity in the borylation reaction relative to the 1-protected congeners (*c.f.* Table 14). As such, the protection of bromo-indazoles was undertaken using the previously outlined method (Scheme 44) (*c.f.* Table 13).



* 504 synthesised by Andrew Hones

Scheme 44: Regioselective 2-SEM protection of bromoindazoles

Initial attempts to apply the previously described tandem 'one-pot' borylation/Suzuki-Miyaura cross-coupling protocol were undertaken with the 6-bromo derivative (**503**) (c.f. Figure 60). Predictably, *in-situ* ^1H NMR spectroscopy showed full clean conversion to monoborylated product, the regioselectivity of which was confirmed using the previously stated method of characterisation (c.f. Section 3.2.2.2). Attempts at cross-coupling with methyl-4-iodobenzoate (**267**) catalysed by $\text{Pd}(\text{dppf})\text{Cl}_2$, led to small but detectable amounts of homocoupled indazole products by LC/MS ($m/z = 574$ (^{81}Br , $[\text{M}]^+$), 572 (^{79}Br , $[\text{M}]^+$)). In order to suppress competing pathways, milder cross-coupling conditions were sought. It was hypothesised that the milder $\text{Pd}(\text{PPh}_3)_4$ catalyst would effect a more clean reaction and avoid unwanted by-products. Gratifyingly, this catalyst swap meant no such homocoupling products were observed. With the modified one-pot method in hand, the bromoindazoles were reacted with **267** or 2-bromopyridine (**479**) and the results are shown below (Figure 61).



a. Isolated as part of 31:69 mixture with 6-arylated isomer (**511**); b. Reaction carried out by Andrew Hones.

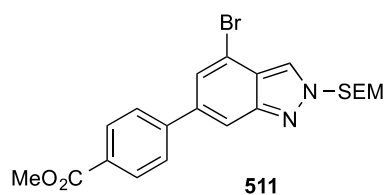


Figure 61: Tandem 'one-pot' borylation/Suzuki-Miyaura cross-couplings of bromo-indazoles

Confirmation of cross-coupled product formation was provided by ¹H NMR spectroscopy supported by mass spectrometry, for example compound **508** displayed a diagnostic

singlet at 3.98 ppm of the ^1H NMR spectrum, characteristic of the incorporated CO_2CH_3 functionality. Mass spectrometry analysis provided the diagnostic molecular ion peaks with the characteristic 1:1 bromine isotopic ratio; $m/z = 462$ (^{81}Br , $[\text{M}]^+$) and 460 (^{79}Br , $[\text{M}]^+$).

The yields observed were consistent with previous tandem 'one-pot' reactions of indazoles (*c.f* Figure 60).

3.2.2.4.2 Borylation of 4-Bromoindazole

An interesting observation arose from the borylation of bromoindazoles. Reaction of the 4-bromo derivative **501** was not regioselective for C-3, as evident by the regioisomeric mixture of 3 and 6-arylated products (**505**, **511**) observed after cross-coupling. This was attributed to the increased steric hindrance imparted by a 4-bromo substituent relative to a 4-hydrogen. As a consequence oxidative addition at C-3 is disfavoured (Figure 62). Consequently, this rendered C-H activation disfavoured at C-3 and partially redirected reaction to the more sterically accessible C-6. It was hypothesised that borylation was favoured at C-6 over the equally sterically accessible C-7 due to the fact that an developing negative charge at C-7 in the oxidative addition step would be located *peri* to the lone pair of the 1-N azinyl nitrogen. In light of this observation, attempts were made to develop a protocol for regioselective borylation at C-6.

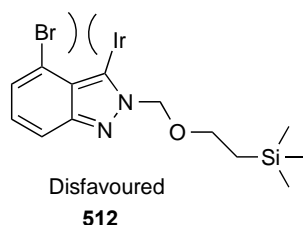


Figure 62: Disfavoured C-3 oxidative addition of 4-bromoindazole

Previously within the group, Tajuddin had observed enhanced regioselectivities upon running reactions at room temperatures (*c.f* Scheme 20). Reflecting this, a room temperature borylation experiment was run to attempt selective borylation at C-6 of **501** (Figure 63). Initial experiments utilising 3 mol% iridium proceeded slowly therefore subsequent reactions were run with a higher catalyst loading in order to accelerate the reaction rate.

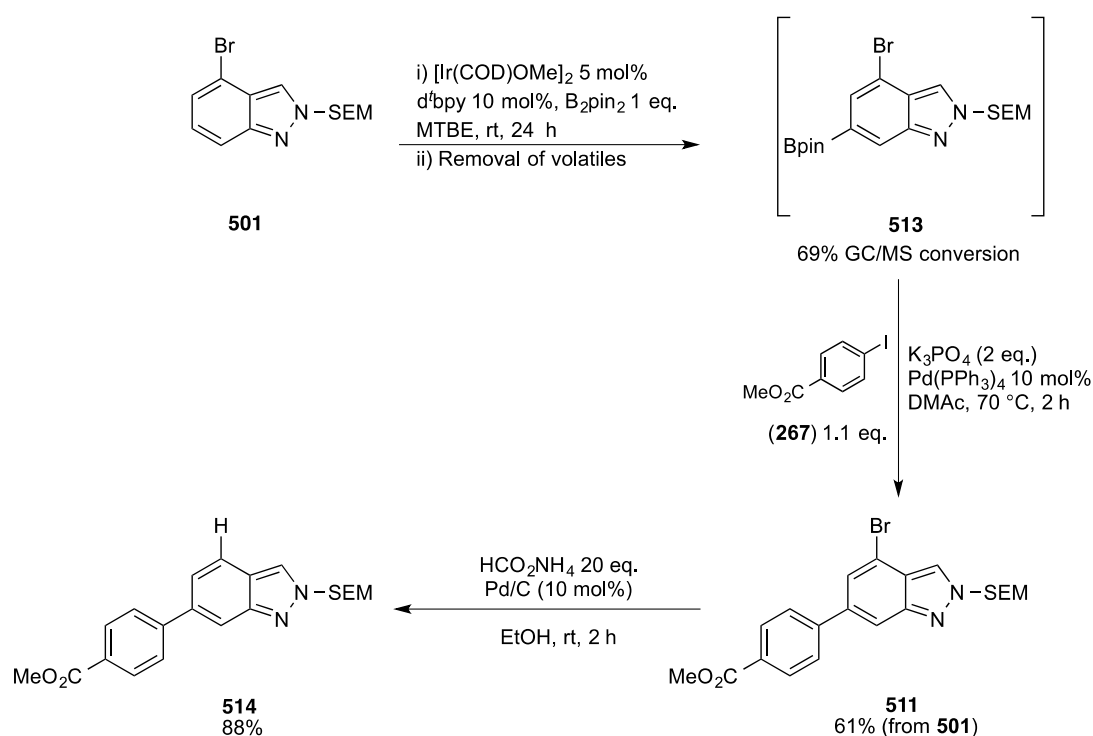


Figure 63: Regioselective borylation/cross-coupling/reduction sequence of 4-bromoindazole

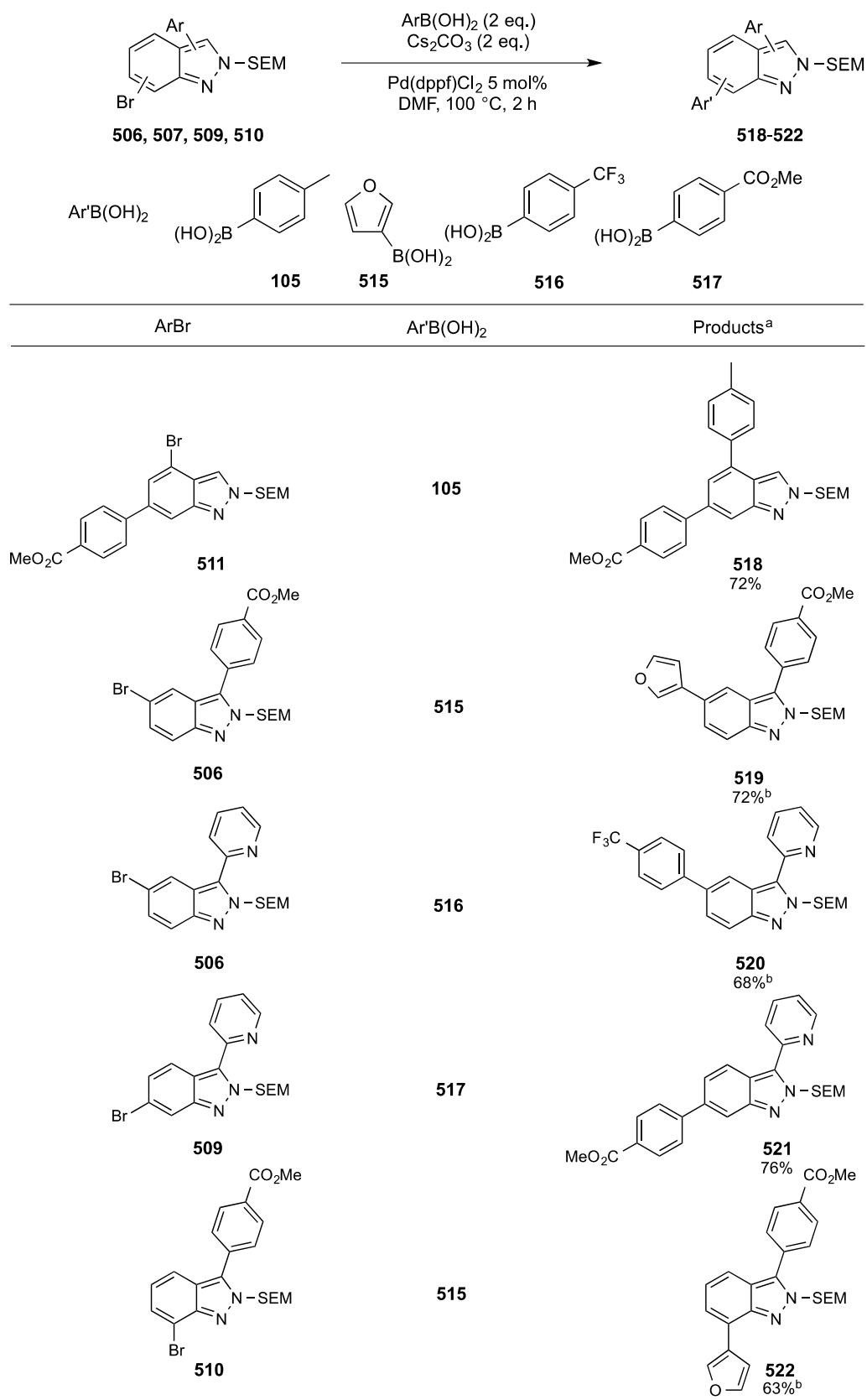
Using a stoichiometric quantity of B₂pin₂ and 10 mol% iridium, selective borylation at C-6 was observed as evidenced by a single product peak, displaying the characteristic molecular ion peak in the crude GC/MS trace after borylation; *m/z* = 454 (⁸¹Br, [M]⁺), 452 (⁷⁹Br, [M]⁺). Regioselectivity was confirmed by disappearance of the 6-*H* signal in conjunction with a corresponding shift to higher frequency of the neighbouring 5 and 7-*H* resonances in the ¹H NMR spectrum. Using the tandem method described previously

(*c.f.* Figure 61), **511** was isolated and characterised by a strong IR stretch at 1723 cm⁻¹, coupled with the observation of the characteristic CO₂CH₃ resonance at 167 ppm of the ¹³C NMR spectrum. Given the stability of the intermediate boronate ester relative to the previously observed 3-boronate intermediates, fewer material losses were incurred in the cross-coupling step and as such an improved cross-coupling yield was obtained.

As observed previously in Chapter 2, halide substituents may undergo reduction under transfer hydrogenation conditions (*c.f.* Figure 44). It was suggested that this method could be applied as an alternative second stage of a multi-directional sequence, whereby the 4-bromo substituent acts as a blocking/directing group for borylation and cross-coupling, with subsequent reduction enabling a net protecting group strategy for adjusting regioselectivity. Applying the conditions utilised previously, reductive debromination gave product **514**, which lacked the characteristic 1:1 bromine isotopic ratio by crude GC/MS ($m/z = 382$, [M]⁺).

3.2.2.4.3 Suzuki-Miyaura Cross-Coupling of 3-Aryl-Bromoindazoles

Having successfully demonstrated that protected bromoindazoles could undergo tandem borylation/Suzuki-Miyaura cross-coupling sequences without competitive homocoupling, the next step focused on cross-coupling of the bromine functionality with a series of boronic acids in order to complete the multidirectional sequence (Figure 64).



a. Yields are for purified isolated products; b. Reaction carried out by Andrew Hones

Figure 64: Suzuki-Miyaura cross-coupling of aryl-bromoindazoles

Reacting the bromoindazoles with an excess of boronic acid in the presence of Cs_2CO_3 and 5 mol% catalyst gave efficient conversion to tris-aromatic products. Reactions were monitored by TLC (9:1 Hexanes:Ethyl Acetate) and showed full, clean starting material consumption within two hours of reaction time. ^1H NMR spectroscopy supported by LC or GC/MS analysis enabled product characterisation, for example, observation of the tolyl CH_3 resonance at 2.45 ppm and ester CO_2CH_3 resonance 3.95 ppm, in conjunction with the absence of the 1:1 bromine isotopic ratio, confirmed the synthesis of products **518** and **521** respectively.

3.2.2.4.4 Attempts at Directed Borylation of Indazole

To this point, it has been observed that borylation of protected indazoles proceeds rapidly and selectively at the 3-position. Subsequent borylation of the phenyl ring proceeds unselectively in the absence of steric effects. In order to circumvent the requirement for pre-existing functionality, the directed C-H borylation protocols described by Hartwig, Ishiyama and their respective co-workers were considered (Figure 65)^{163,164} Mechanistically, these reactions proceed via pre-coordination of the nitrogen atom to a directing ligand group, such as a hydrosilyl moiety. Immobilisation of the substrate enables directed borylation via a stable iridacycle (**524**) after C-H activation. Given the Lewis-basicity of the indazole heterocycle, it was speculated that application of these methodologies to indazole may enable a change in regioselectivity, with the azinyl nitrogen directing functionalisation to C-7 as opposed to the more favoured C-3 position.

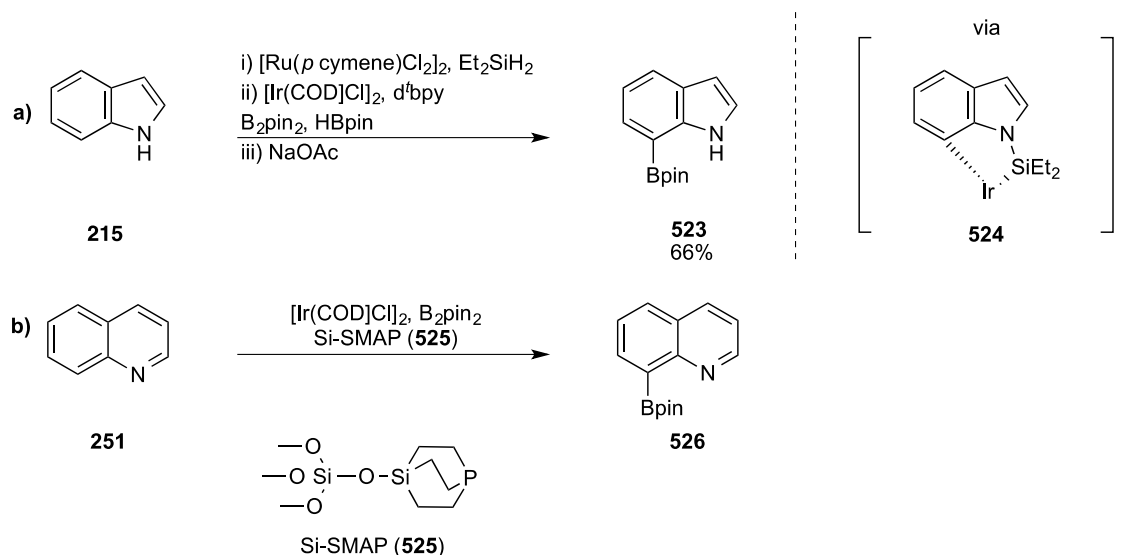
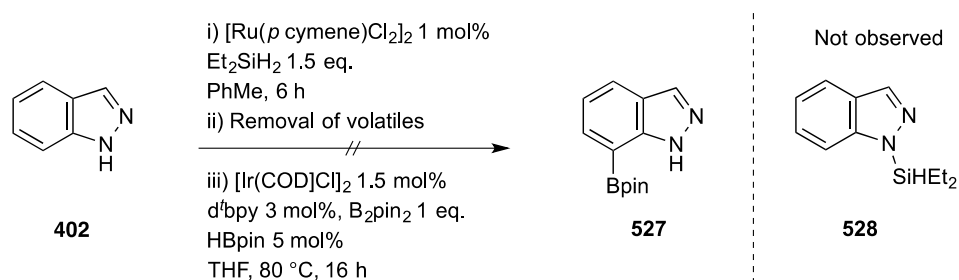


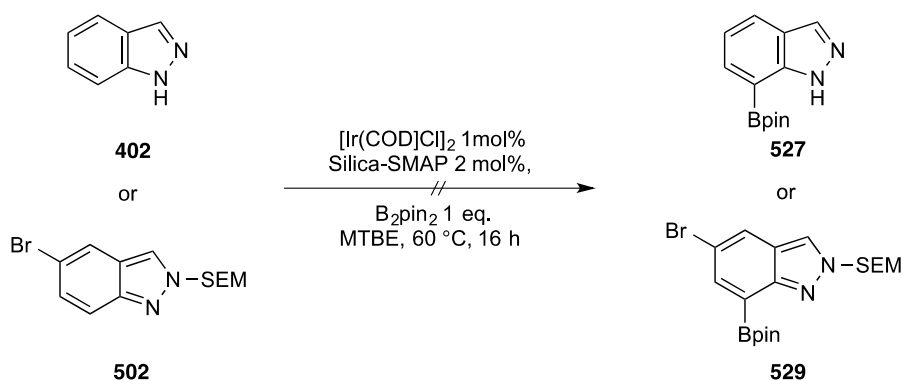
Figure 65: Literature protocols for the directed borylation of azinyl heterocycles

Addition of diethylsilane and toluene to a vial containing indazole (**402**) and $[\text{Ru}(p\text{-cymene})\text{Cl}_2]$ gave a deep-red solution. The required indazole-silyl intermediate (**528**) was not observed by GC/MS analysis (Scheme 45). Speculating that the intermediate may be unstable to the GC/MS method, the reaction was continued with the removal of volatiles and subsequent addition of an aliquot of borylation catalyst stock solution. Disappointingly, ^1H NMR spectroscopy and GC/MS analysis of the crude reaction mixture showed only unreacted starting indazole.



Scheme 45: Attempted silyl-directed borylation of indazole

As a consequence, attempts were made to apply Ishiyama's directed protocol. Indazole (**402**) was reacted with a stoichiometric equivalent of B_2pin_2 in the presence of 2 mol% iridium and Silica-SMAP ligand (**525**) at 60 °C. The suspended silica supported ligand was removed by celite filtration prior to removal of volatiles. Only the starting material was observed by 1H NMR spectroscopy and GC/MS analysis of the crude reaction mixture. Attempts with both protected and unprotected indazole were tried so as to ensure purported docking of indazole onto the iridium was ruled out as a limiting factor, however this returned neither the intended 7-(Bpin) product or (more surprisingly) the previously observed 3-Bpin product (Scheme 46).



Scheme 46: Attempted Silica-SMAP directed borylation of indazoles

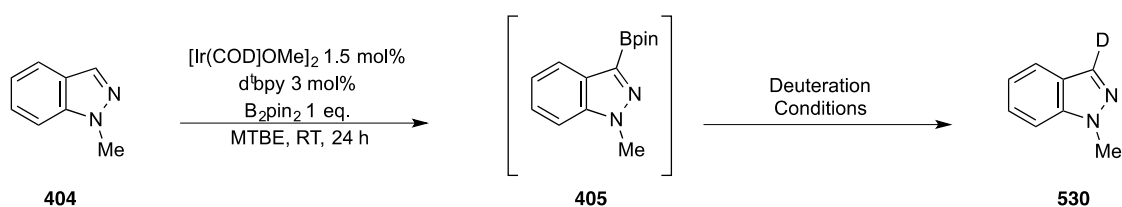
Given that to this point selective borylation of the phenyl ring of the indazole framework had proved elusive without the use of steric directing groups, a new procedure was sought which exploited this.

3.2.2.4.5 Attempted *ipso*-Deuteration of 3-(Bpin)-Indazole

Whilst borylation at C-3 of the indazole occurred with good efficiency (in the absence of steric effects), the instability of the obtained boronate esters were notable. This was best

exemplified by the relative cross-coupling yields of 3-Bpin products *versus* the 6-Bpin product (**511**) obtained from borylation of the 4-bromo derivative (**513**) (*c.f* Figure 61 and Figure 63). It was speculated that due to the relative stability of the two Bpin ester moieties, strategies could be developed whereby selective hydrolytic cleavage of the unstable 3-Bpin of a polyborylated indazole would leave the more stable phenyl-Bpin functionality, which could then undergo cross-coupling. The net effect of this would be to enable access to alternate multiaryl scaffolds and substitution patterns. In order to devise the synthetic sequence, it was first of interest to develop conditions for controlled, facile protodeborylation of a 3-(Bpin)-indazole product.

The propensity for *ortho*-boryl products to undergo fast, acid-mediated protodeborylation under mild conditions had been demonstrated previously with the synthesis of an *ortho*-deuterated pyrazine (**395**), using D₂O as a mild acid surrogate to mediate C-B bond cleavage (*c.f* Table 9). Speculating that this sequence may be applicable to 3-(Bpin)-indazole products, an *in-situ* boronate ester was subjected to a variety of deuteration conditions based on the previously described procedure and the results are tabulated below (Table 15).



Deuteration Conditions ^a			
Entry	'D' Source	Temperature	Product
1	D ₂ O	rt	No deuterium incorporation
2	D ₂ O	80 °C	No deuterium incorporation
3	CD ₃ COOD	rt	No deuterium incorporation
4	CD ₃ COOD	80 °C	No deuterium incorporation
5	n/a ^b	RT	No protodeborylation observed

a. Deuterating agent added directly to borylation reaction mixture and stirred at stated temperature for 3 h; b. Loose silica added

Table 15: Attempted *ipso*-deuteration of 3-(Bpin)-indazole

Disappointingly, implementation of the previously described deuteration conditions failed to yield any deuterated product (**530**) by ¹H or ²H NMR spectroscopy, which showed only unreacted boronate ester (**405**). Protodeborylated product was not even observed at trace levels by GC/MS (entry 1). Addition of D₂O with subsequent heating to 80 °C was also unsuccessful (entry 2). Substituting in the stronger CD₃COOD (acetic acid – d₄) in place of D₂O also failed to furnish the desired deuterated products (entries 3 and 4). Given the propensity of the protected indazoles to undergo protodeborylation during attempted purification of silica gel chromatography, addition of loose silica (with stirring) was added to attempt to induce protodeborylation (entry 5). Frustratingly, this was also unsuccessful with 3-borylated products remaining intact over several hours with stirring. Given that part of the attraction of C-H borylation is the potential for late-stage functionalisation of functionalised substrates, stronger acids were resisted as the

sensitivity of certain functional groups to acidic media may hinder applicability of such a method. Consequently, an alternative method of protodeborylation was sought.

Having observed significant amounts of starting indazole in crude reaction mixtures after one-pot borylation/Suzuki-Miyaura cross-coupling reactions (speculated to be as a result of either metal or base-mediated protodeborylation during the Suzuki-Miyaura step), it was hypothesised that controlled exposure to base could facilitate protodeborylation of a 3-(Bpin) ester.

3.2.2.4.6 Selective Protodeborylation of Polyborylated Indazoles

Given the requirement for base in Suzuki-Miyaura cross-couplings, it was postulated that exposure of a polyborylated indazole (whereby one boryl group is situated at C-3) to base prior to addition of the metal catalyst and cross-coupling partner would therefore enable selective access to cross-coupled products arising from reaction with the more stable boronate ester.

In order to test this hypothesis, 5-bromo-2-SEM-indazole (**502**) was initially reacted with an aliquot of catalyst stock solution containing an extra equivalent of B₂pin₂. Confirmation of bis-borylation was provided by ¹H NMR spectroscopy. Consistent with conversion to a tris-functionalised indazole, two ⁴J_{H-H} doublets (*J* = 1.9 Hz), corresponding to the 4-H and 6-H resonances, were observed in the crude ¹H NMR spectrum of 5-bromo-3,7-bisborylindazole (**531**) (Figure 66).

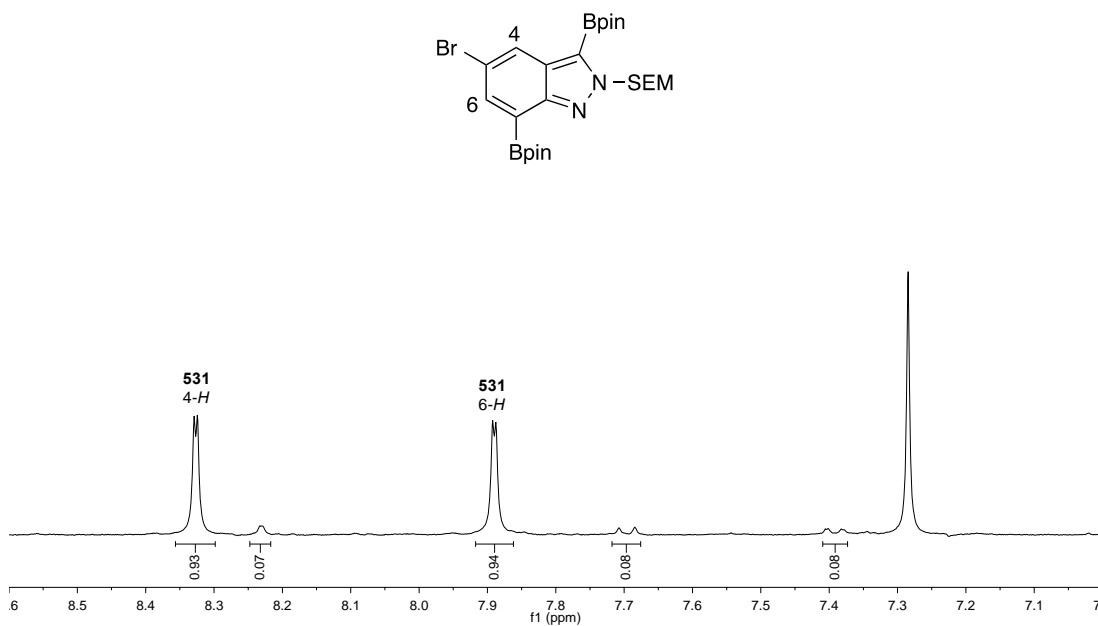
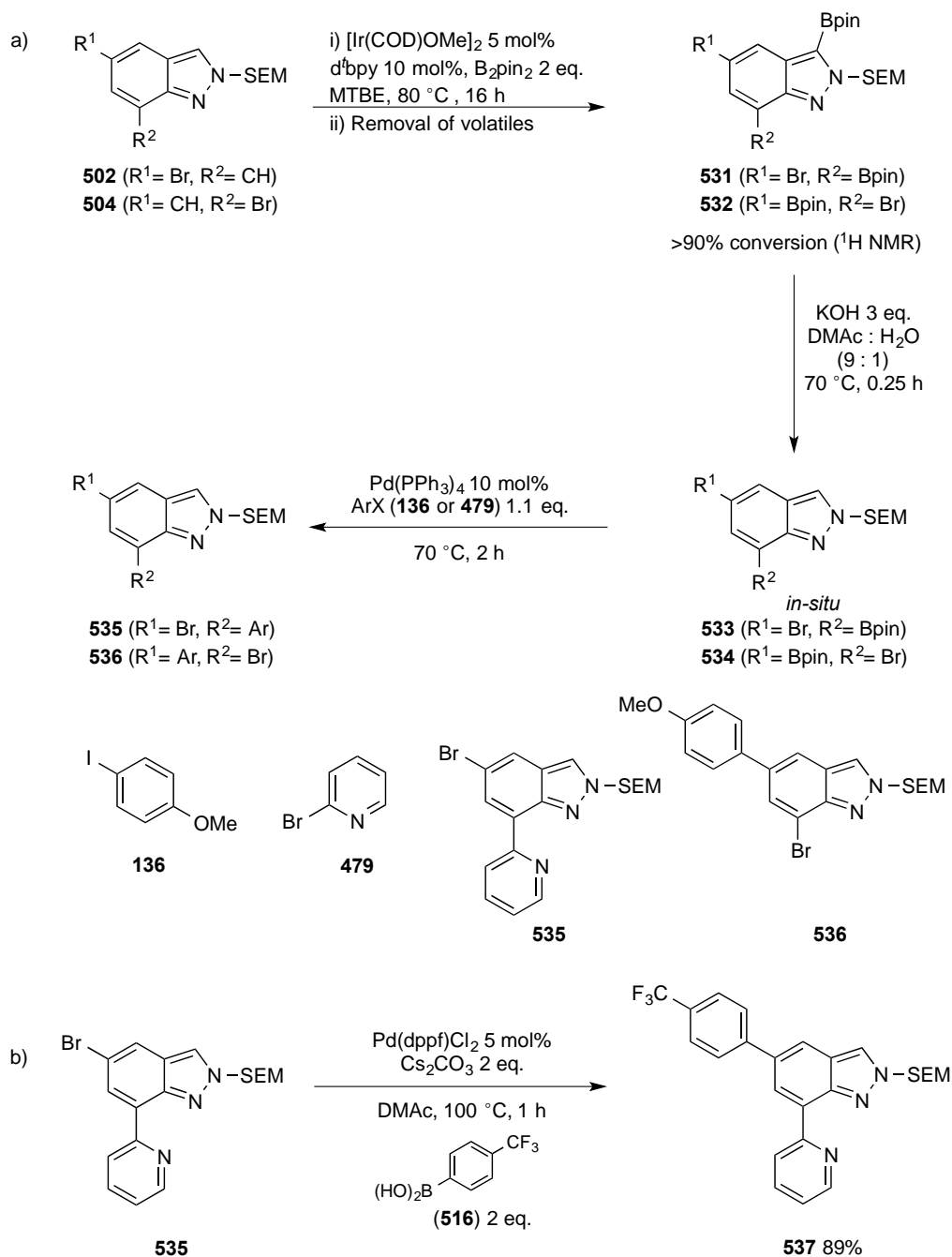


Figure 66: Crude ¹H NMR spectrum of borylation of 5-bromo-indazole with excess B₂pin₂

To the crude borylation reaction mixture was added a mixture of KOH (3 eq.) in DMAc:H₂O (9:1). Subsequent heating led to full conversion to mono-boryl product (**533**) as confirmed by GC/MS analysis ($m/z = 454$). To complete the sequence, palladium catalyst and 2-bromopyridine (**479**) were added to the reaction mixture affording the 7-aryl product **535**, characterised by the diagnostic molecular ion peak ($m/z = 404$, [⁷⁹Br)M+H]⁺). The 3-*H* singlet resonance at 8.15 ppm in the ¹H NMR spectrum confirmed selective protodeborylation at C-3. This protocol was also successfully applied to the 7-bromo derivative (**504**) to afford the 5-aryl product (**536**) (Figure 67).



a. Reaction carried out by Andrew Hones

Figure 67: Selective protodeborylation of polyborylated indazoles

Subsequent Suzuki-Miyaura cross-coupling of **535** with 4-(trifluoromethyl)benzeneboronic acid (**516**), using the previously described method (*c.f*

Figure 64), afforded the 5,7-bisarylated indazole (**537**) in excellent yield, identified by a singlet resonance at -62.3 ppm in the ^{19}F NMR spectrum.

Attempts to apply this procedure to protected 6-bromoindazole (**503**), to allow direct functionalisation at C-4 was unsuccessful. Borylation with excess diboryl reagent afforded only the monoborylated 3-functionalised product (**538**). It was suggested that this initial borylation prevented subsequent borylation at C-4 due to steric inhibition (Figure 68).

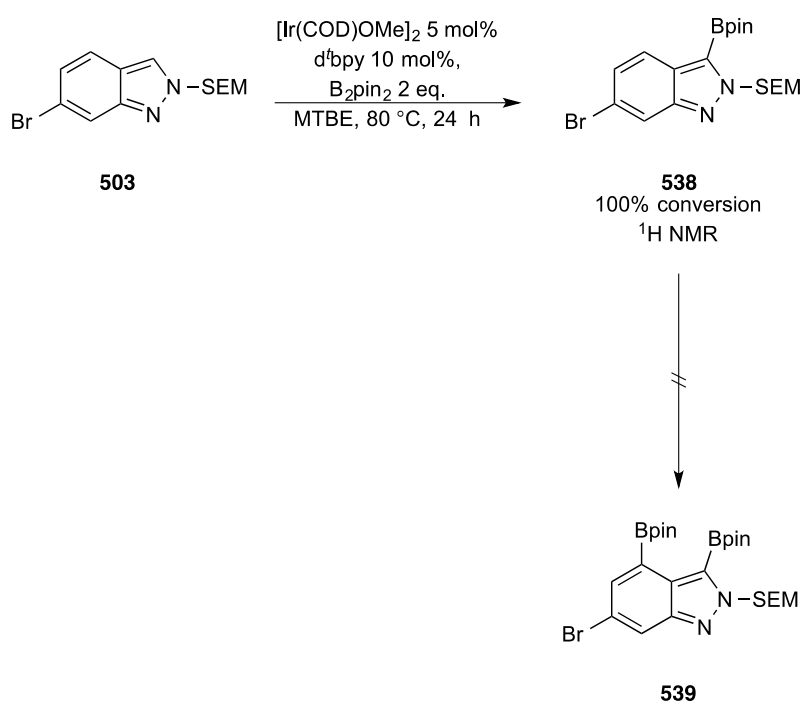


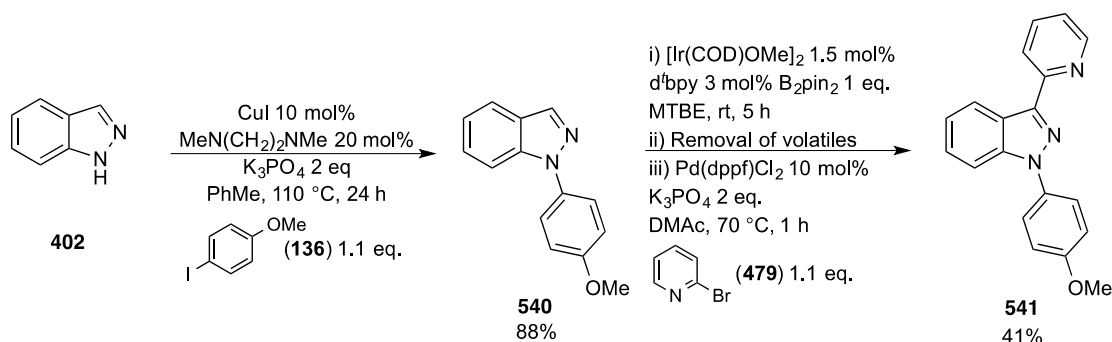
Figure 68: Attempted polyborylation of 6-bromoindazole

Overall, a strategy for synthesis of mono and bis-arylated indazoles via a one-pot C-H borylation/Suzuki-Miyaura cross-coupling protocol has been developed. By exploiting the lability of *ortho*-azinyl boronate esters and the influence of steric effects in C-H borylation, products arising from direct functionalisation at C-3, 5, 6, and 7 may be obtained.

3.2.2.4.7 Synthesis of 1,3-bis-Arylindazoles

Thus far, the multidirectional strategies discussed have focussed on tandem borylation/Suzuki-Miyaura cross-coupling reactions of functionalised starting materials. Subsequent elaboration of the pre-existing bromide functionality enabled the construction of privileged tris(hetero)aryl scaffolds. Given the recalcitrance of the parent indazole to the borylation procedure, protecting groups have been employed to activate the substrate allowing borylation. Several groups have reported the *N*-arylation of nitrogenated heterocycles, using both Chan-Lam and Ullmann methodologies.^{44,165,166} *N*-(hetero)aryl scaffolds are subunits in numerous biological and medicinal targets.¹⁶⁷ Reflecting this an alternative multi-directional strategy was proposed, whereby the *N*-H was capped with an aryl unit to facilitate borylation, with subsequent borylation providing expedient access to privileged 1,3-disubstituted products.

Sequential addition of 4-iodoanisole (**136**) and amine ligand to a suspension of indazole (**402**), K₃PO₄ and CuI in toluene gave, after heating, the *N*-arylated product lacking the N-H stretch of the parent indazole (Scheme 47). Confirmation of arylation was provided by the observed singlet at 3.88 ppm of the ¹H NMR spectrum, corresponding to the OCH₃ functionality.



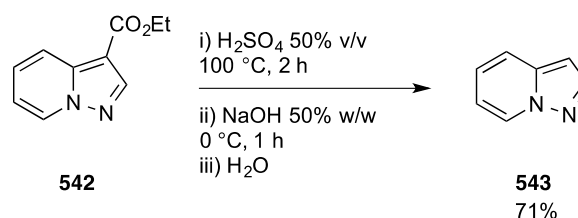
Scheme 47: N-H arylation/3-borylation and cross-coupling sequence

In order to complete the multidirectional sequence, compound **540** was reacted with an aliquot of borylation stock solution. Conversion was not clear by *in-situ* ^1H NMR spectroscopy due to partial precipitation within the NMR tube. At this point, volatile material was removed *in vacuo* and the Suzuki-Miyaura reaction with 2-bromopyridine was carried out as previously described (*c.f* Figure 60). Two separate 4-spin systems (corresponding to the pyridyl and indazole rings), observed in the COSY spectrum of the product, and the loss of the 3-*H* singlet confirmed the product structure and the regioselectivity.

3.2.3 Borylation of Pyrazolo[1,5-*a*]pyridine

Having established strategies for direct indazole borylation, it was of interest to explore the reactivity of indazole isomers, such as pyrazolopyridines. Pyrazolopyridines are an important scaffold, due to its wide applications in medicinal chemistry^{168,169} and, therefore, methods for their late-stage functionalisation are of great value to organic chemists.

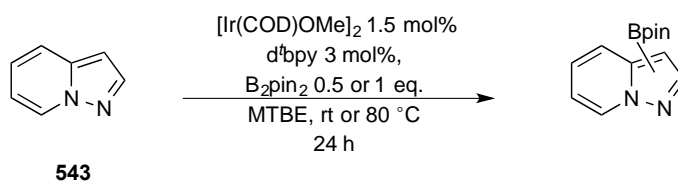
Attention was first focussed on the borylation of pyrazolo[1,5-*a*]pyridine (**543**). Given the high cost of the parent heterocycle from commercial suppliers, the ring was synthesised from the more affordable 3-ethyl ester (**542**) by a decarboxylation reaction (Scheme 48)¹⁶⁹



Scheme 48: Synthesis of pyrazolo[1,5-*a*]pyridine

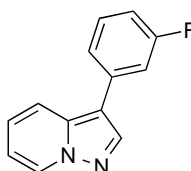
542 was heated in aqueous acid for 2 h as per the literature method. Slow addition of sodium hydroxide solution over a 1 h time frame, required in order to maintain the temperature below 10 °C, resulted in a vigorous exotherm. GC/MS analysis carried out prior to work-up showed full consumption of starting material and provided confirmation of decarboxylation ($m/z = 118$, $[M]^+$). ^1H NMR spectroscopy carried out after purification showed a surprisingly small ($J = 1.8$ Hz) coupling between protons 2-H and 3-H (nuclear Overhauser effect spectroscopy (NOESY) experiments confirmed the protons were neighbouring despite the low coupling by observation of a through-space correlation).

With compound **543** in hand, work focussed on screening conditions for C-H borylation of the substrate (Table 16). Reaction with a stoichiometric quantity of B_2pin_2 led to complex mixtures (as shown by ^1H NMR spectroscopy) at both room temperature and 80 °C (entries 1 and 2). Consequently, subsequent reactions used sub-stoichiometric B_2pin_2 in order to gauge the preferred regioselectivity and suppress competitive or bis-borylation. The corresponding reaction with 0.5 equivalents of B_2pin_2 resulted in a fortuitous crystallisation of the 3-boryl product (**544**), observed after 16 h at room temperature. Filtration of the precipitate and subsequent recrystallisation from hot MTBE gave pure **544** in modest yield (entry 3). Observation of a downfield shift in the 2-*H* resonance, from 7.93 ppm in the starting material to 8.23 ppm in **544**, is consistent with borylation at C-3. The broad singlet observed at 29.7 ppm in the ^{11}B NMR spectrum was consistent with an aromatic boronate ester. The modest yields observed were attributed to the sluggish nature of the HBpin-mediated catalytic cycle (*c.f* Section 2.1.2.5) (prominent at low concentrations of B_2pin_2) and to possible losses incurred during the recrystallisation process.



Entry	B_2pin_2 (eq.) ^a	Temperature (°C)	Product(s) ^b
1	1	80	Complex mixture ^c
2	1	rt	Complex mixture ^c
3	0.5	rt	 544 24% ^d
4	0.5	rt	 544 31% ^e

a. Relative to starting heterocycle; b. As determined by ¹H NMR spectroscopy; c. Structural elucidation of products not possible; d. Isolated after recrystallisation; e. Isolated after tandem Suzuki-Miyaura cross coupling: Conditions - $\text{Pd}(\text{Amphos})\text{Cl}_2$ (6 mol%), Na_2CO_3 (2M, 2 eq.), 3-iodo-fluorobenzene (422) (1.2 eq.), DME, 80 °C, 3h (see experimental section) (**545**)



545

Table 16: Borylation of pyrazolo[1,5-a]pyridine

In order to correct for possible losses incurred in the filtration and recrystallisation steps, an *in-situ* trapping of the boronate adduct by Suzuki-Miyaura cross-coupling with 3-iodo-fluorobenzene was carried out (**422**) (entry 4). Attempts to monitor the cross-coupling by LC/MS were complicated due to the intermediate boronate ester and desired product bearing the same retention time. Therefore, TLC analysis (1:1 hexanes:ethyl acetate), exploiting the superior longwave ultraviolet (UV) absorption of product **545**, was chosen

as an alternative analytical method. Cross-coupled product **545** was characterised by a multiplet at -112.8 ppm in the ^{19}F NMR spectrum and the observation of the desired molecular ion peak by electrospray ionisation (ESI) fragmentation ($m/z = 212$, $[\text{M}]^+$)

The surprising activity of heterocycle **543** towards C-H borylation was attributed to two possible factors; firstly it was considered that the inductive withdrawing effect of the neighbouring bridgehead nitrogen significantly lowers the Lewis-basicity of the azinyl nitrogen disrupting inhibitory coordination to the iridium catalyst. Alternatively, it was postulated that the *peri* 7-*H* proton prevents coordination of the azinyl nitrogen to the iridium catalyst.

3.2.4 Borylation of Pyrazolo[1,2-*a*]pyridine

Reaction of the parent heterocycle pyrazolo[1,2-*a*]pyridine (**546**) with an aliquot of catalyst stock solution gave borylation products arising from preferential reaction at C-3 (Figure 69). The preferred regioselectivity of the borylation was confirmed by ^1H NMR spectroscopy, through observation of a downfield shift to higher frequency of the *ortho* 2-*H* and *peri* 4-*H* resonances. A minor unidentifiable product was observed by both GC/MS ($m/z = 244$) and ^1H NMR spectroscopy. Integration of the respective signals gives the approximate ratio 15:1 of major to minor borylation products.

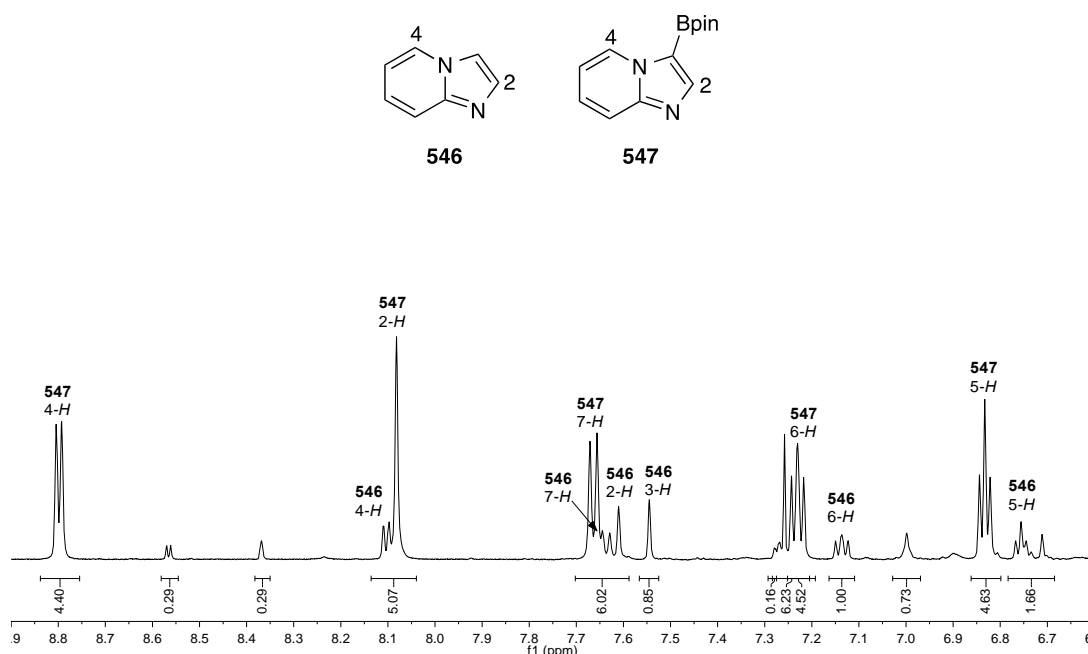
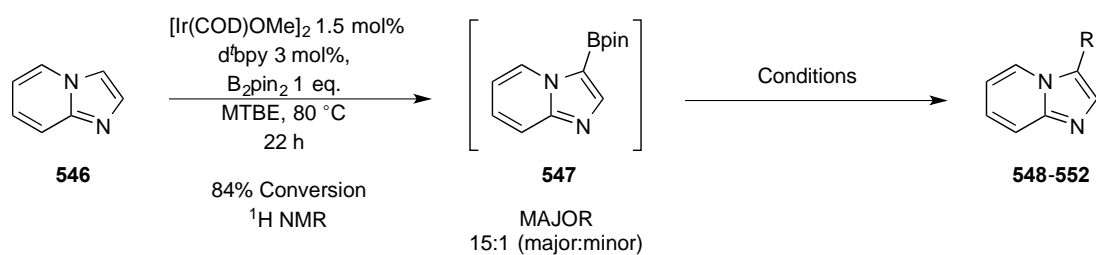


Figure 69: Crude ¹H NMR spectrum of borylation of pyrazolo[1,2-a]pyridine

Attempts to purify the crude borylation mixture by flash column chromatography were unsuccessful, with full reversal by protodeborylation meaning only starting heterocycle was isolated after attempted column chromatography. Reflecting this, *in-situ* transformations of the boronate ester were sought (Table 17). After *in-situ* analysis confirmed the conversion to borylated products, the reaction media was concentrated and the crude residue subjected to a variety of conditions. Reaction of the crude boronate ester with aqueous oxone, CuCl₂ and KHF₂ as per the literature procedures,^{40,51,56} failed to yield the hydroxyl (**548**), chloro (**549**) or trifluoroborate species (**560**) respectively (entries 1-3). Analysis of the crude residues by LC/MS showed no desired product in any case with only the starting heterocycle ($m/z = 119$, $[M+H]^+$) observed. This was attributed to the aqueous reaction media employed in each reaction, which may have mediated protodeborylation pathways.



Entry	Conditions ^a	Desired product	Yield ^b
1	A	548	N/A
2	B	549	N/A
3	C	550	N/A
4	D	551	N/A
5	E	552	41%

a. Conditions: A - Oxone® 1 eq., Acetone:H₂O (1:1), RT, 16 h; B - CuCl₂ 3 eq., MeOH:H₂O (1:1), 90 °C, 72 h; C - KHF₂ 10 eq., THF:H₂O (4:1), RT, 16 h; D - Pd(dppf)Cl₂ 10 mol%, Cs₂CO₃ 2 eq., Methyl-4-iodobenzoate 2 eq., CuCl 1 eq., DMF, 100 °C, 1 h; E - 2nd Gen PdXPhos pre-cat 5 mol%, K₃PO₄ 2eq., 3-iodoanisole 1.1 eq., DMAc, 50 °C, 2 h; b. Based on starting material **546**

Table 17: Attempted in-situ trapping of 3-(Bpin)-pyrazolo[1,2-a]pyridine

Disappointingly, the previously described Suzuki-Miyaura conditions (*c.f.* Figure 60 and Figure 61) were unsuccessful with both *in-situ* LC/MS and GC/MS analyses showing no conversion to the desired product (**551**) (entry 4). The use of a more active pre-catalyst

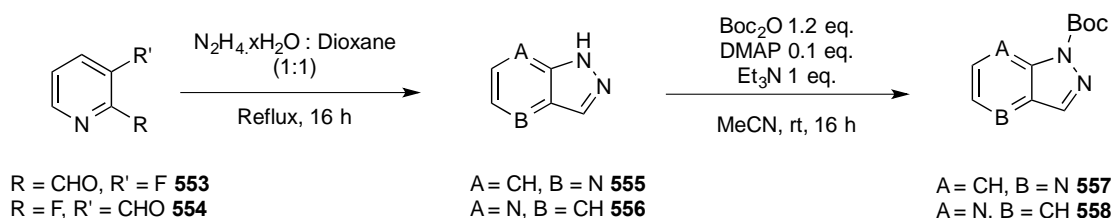
in conjunction with a milder base and lower temperatures helped to furnish the desired product (**552**) in moderate yields across the two-steps (entry 5). In process LC/MS analysis confirmed the presence of the desired molecular ion peak ($m/z = 225 [M+H]^+$). The pure isolated product was characterised by the diagnostic OCH_3 singlet resonance at 3.87 ppm in the 1H NMR spectrum. The promising conversion observed during stage 1 borylation suggested the yield losses were incurred by protodeborylation during the Suzuki-Miyaura cross-coupling step.

3.2.5 Borylation of Azaindazoles

Having carried out in depth studies of the borylation of pyridine and indazole scaffolds, it was of interest to investigate the selectivity of various aza-indazole derivatives. This would enable application of methodologies developed for both pyridine and indazole borylation to a novel borylation substrate.

3.2.5.1 Substrate Synthesis

Given the high cost of azaindazoles from commercial suppliers, the heterocycles (**555**, **556**) were synthesised based on literature protocols from fluoropyridine carboxaldehyde starting materials (**553**, **554**), as carried out previously (Scheme 49) (*c.f* Scheme 43)¹⁷⁰

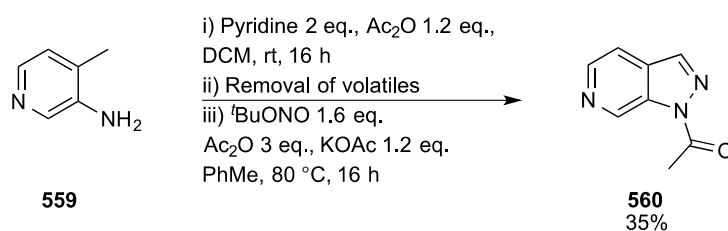


Scheme 49: Synthesis of Boc-protected 4 and 7-azaindazoles

Removal of dioxane *in vacuo* and extraction into ethyl acetate gave crude products that were clean by ^1H NMR spectroscopy and suitable to carry through without further purification. The N-H protons were not observed by ^1H NMR, however IR spectroscopy confirmed the presence of the functionality with broad peaks observed at 3141 and 3147 cm^{-1} for compounds **555** and **556** respectively. The 3-H resonances observed at 8.14 (**555**) and 8.36 ppm (**556**) were distinct from the usual chemical shift (ca. 10 ppm) of aldehyde CHO signals (thereby confirming conversion of the starting materials). Surprisingly, a small ($J = 0.9$ Hz) $^5\text{J}_{\text{H-H}}$ coupling was observed in compound **555** between protons 3-H and 7-H.

Control reactions of azaindazoles **555** and **556** with an aliquot of borylation stock solution unsurprisingly failed to generate any borylation products even at trace levels. Reflecting this, in order to disrupt the coordinating capability of the azinyl nitrogens, both substrates were Boc-protected using the procedure described previously (*c.f.* Scheme 40). IR spectroscopic analyses of Boc-protected compounds **557** and **558** confirmed the presence of the newly incorporated protecting group through the observation of strong carbonyl stretches at 1739 and 1751 cm^{-1} respectively (with a corresponding absence of the broad N-H stretch signals).

Due to the high commercial cost of 3-fluoropyridine-4-carboxaldehyde, a different synthetic method was sought for the synthesis of the 6-azaindazole core. Acetylation of 3-amino-4-methylpyridine with acetic anhydride gave full conversion to the monoacetylated intermediate by crude GC/MS ($m/z = 150$ $[\text{M}]^+$). Reaction of this crude residue with *tert*-butyl nitrite and KOAc gave product **560**, lacking the (pseudo)tolyl resonances at ca. 2-3 ppm by ^1H NMR spectroscopy (Scheme 50). Observation of the 3-H resonance at 8.19 ppm confirmed formation of the indazole motif. Given the outcome of the reaction was an N-protected indazole, no further elaborations were made prior to borylation.



Scheme 50: Synthesis of protected 6-azaindazole

3.2.5.2 Attempted Borylation of 6-Azaindazole

With the various protected aza-indazoles in hand, the substrates were then tested under standard C-H borylation conditions with an aliquot of stock solution. Consistent with previous observations, 6-azaindazole (**560**) was recalcitrant to the borylation conditions due to the presence of an encumbered azinyl nitrogen (Scheme 51).



Scheme 51: Attempted borylation of protected 6-azaindazole

3.2.5.3 Borylation of 4-Azaindazole

Despite lacking an *ortho*-substituent (to disrupt azinyl coordination), the protected 4-azaindazole substrate underwent borylation efficiently. It was postulated that the *peri* C-H bond at C-3 prevented any inhibitory binding of the substrate to the iridium catalyst. *In-situ* ¹H NMR spectroscopic analysis of the borylation of **562** showed similar relative rates for borylation at C-3 and C-6 (as evident by downfield shifts in 5 and 7-*H* resonances, as well as a small but noticeable 1.4 Hz ⁴J_{H-H} coupling by ¹H NMR

spectroscopy). Attempts at selective cross-coupling of the more reactive 3-Bpin was unsuccessful with no desired product (**563**) observed by in process GC/MS analysis using the previously described methods (Figure 70) (c.f Figure 60 and Figure 61).

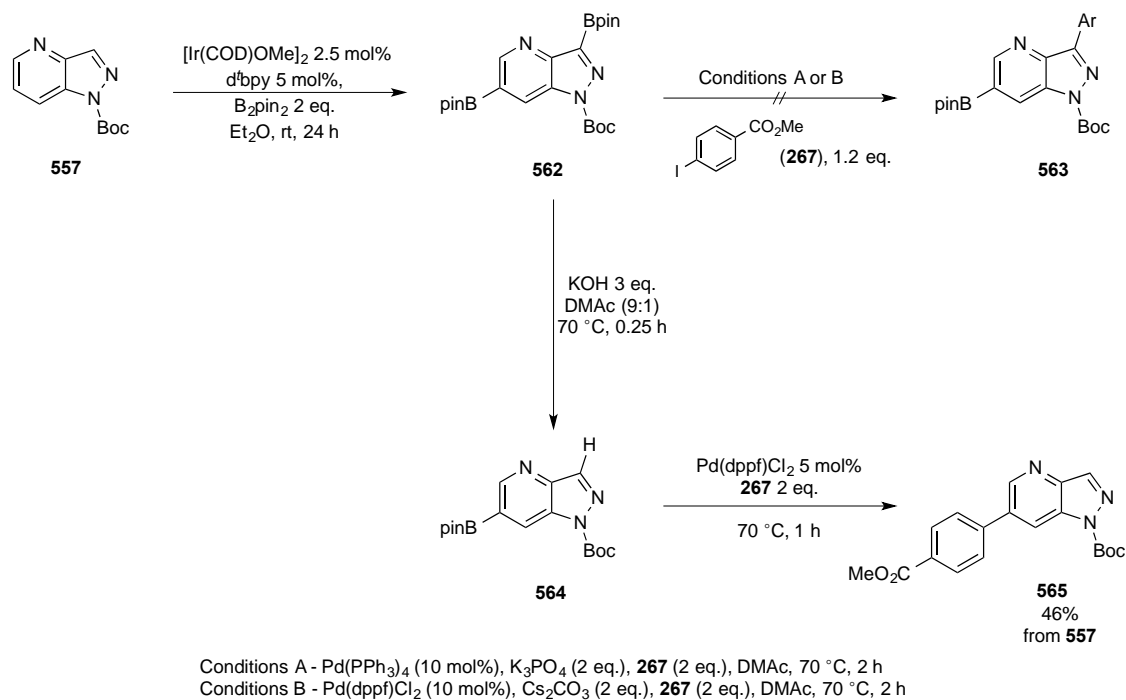


Figure 70: Selective protodeborylation of polyborylated 4-azaindazole

Reflecting this, compound **557** was reacted with an excess of B₂pin₂ which effected full conversion to the 3,6-bisboryl product (**562**). Using the previously described method (c.f Figure 67), reaction of the crude bis-boryl product with KOH afforded the monoboryl product **564** *in-situ* as evidenced by GC/MS (*m/z* = 325). Subsequent cross-coupling with methyl-4-iodobenzoate (**267**) afforded product **565**, characterised by the observed CO₂CH₃ resonance at 3.96 ppm in the ¹H NMR spectrum.

3.2.5.4 Borylation of 7-Azaindazole

The reaction of 7-azaindazole (**558**) with a stoichiometric quantity of B₂pin₂ proceeded rapidly to give a complex mixture of products by ¹H NMR spectroscopy. The efficient reaction was attributed to inhibition of azinyl coordination by the sterically large *peri* Boc-protecting group. Regioselectivity of the major products (**566** and **567**) was assigned on the basis of downfield shifts in the respective *peri* resonances. In order to suppress the formation of minor products, the substrate was instead reacted with 0.7 equivalents of B₂pin₂, which provided the 3 and 4-boryl products exclusively in a 57:43 ratio by ¹H NMR spectroscopy (Figure 71 and Figure 72). Disappointingly, application of the aforementioned cross-coupling strategies were unsuccessful and resulted in no-product formation by *in-situ* LC/MS or GC/MS analyses (*c.f* Figure 60, Figure 61 and Figure 67). Attempts to complete one-pot borylation/cross-coupling sequences of 7-azaindazole are ongoing within the group.

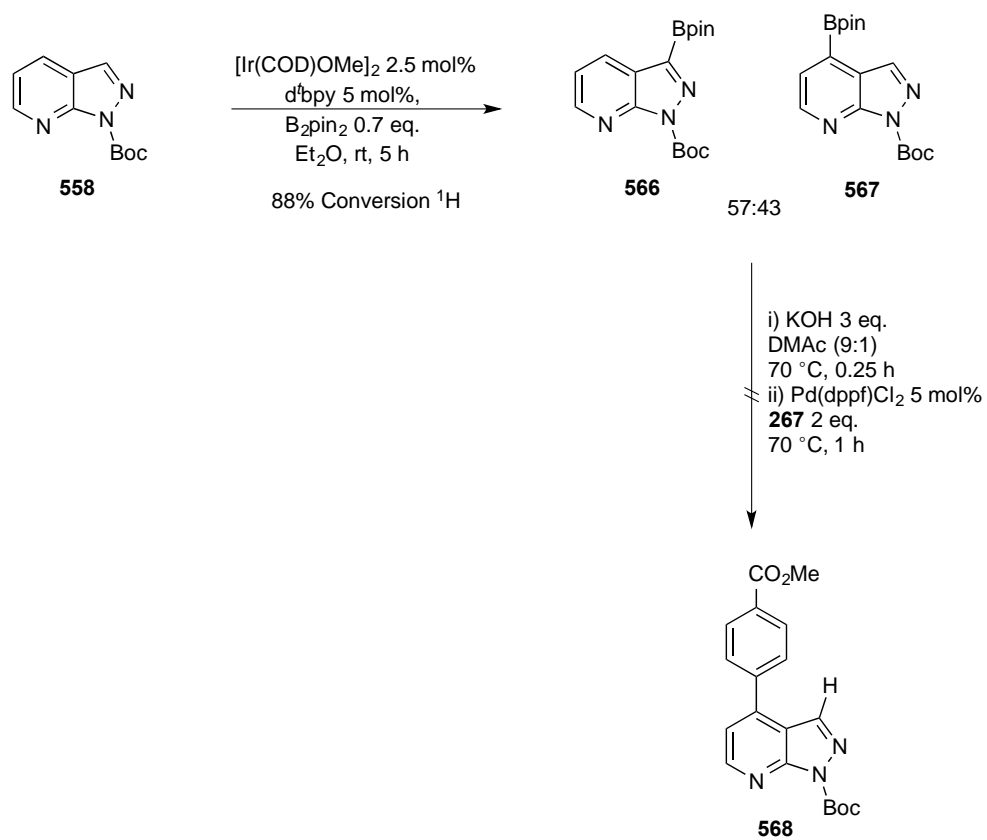


Figure 71: Borylation of 7-azaindazole

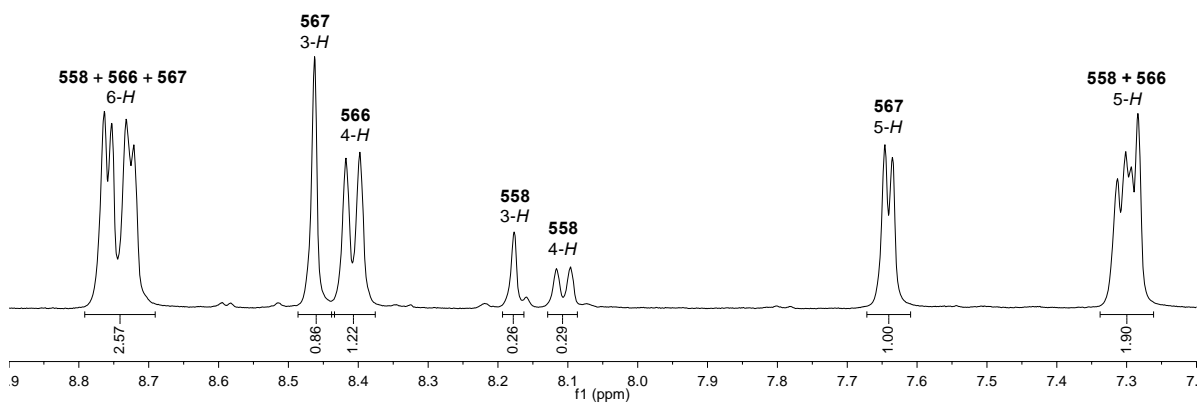
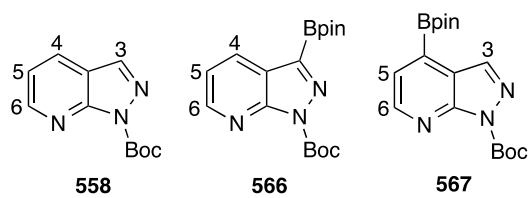


Figure 72: ^1H NMR spectrum of borylation of 7-azaindazole

3.3 Conclusions and Future Work

The borylation of protected-indazoles occurs efficiently and with good regioselectivity at the 3-position. Although the application of protecting groups is undesirable from a green chemistry perspective, this strategy avoids the requirement for pre-existing functionality within starting materials. Despite the presence of steric bulk *ortho* to the preferred site of activation, protected *2H*-indazoles react faster and more completely than their 1-protected counterparts. This is attributed to unfavourable interactions between a proximal emerging negative charge at C-3 and the neighbouring azinyl nitrogen lone-pair in protected *1H*-indazoles. Protodeborylation on silica prevents chromatographic purification of most Bpin esters. However, the presence of a strongly electron-withdrawing mesylate protecting group stabilises the 3-boryl product to allow its isolation in good yield. Alternatively, the boronate products may be elaborated *in-situ* by tandem Suzuki-Miyaura cross-coupling reactions with a variety of (hetero)aryl bromides and iodides.

Published concurrently with these findings, was the work of Burton and co-workers, who reported similar one-pot borylation/cross-coupling reactions.¹⁷¹ Whilst the cross-coupling of 1-methyl-3-boryl indazole was favoured with a variety of (hetero)aryl iodides bromides and chlorides, the cross-coupling of the more reactive protected *2H*-indazoles (**453**) was precluded due to dominating protodeborylation and fragmentation pathways. In addition, the cross-coupling stoichiometry used is not conducive to late stage functionalisation due to the requirement for a large excess of boronate ester (relative to aryl halide) (Figure 73).

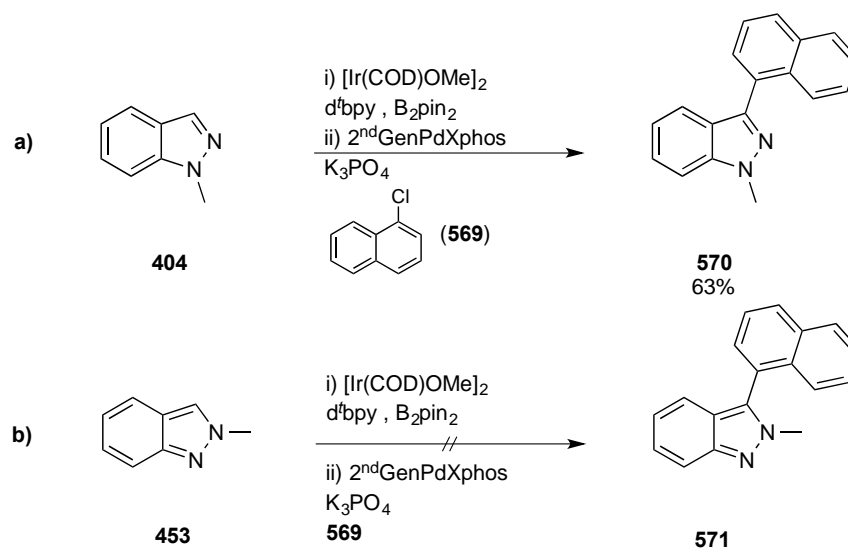


Figure 73: ‘One-pot’ borylation/Suzuki-Miyaura cross-coupling of indazoles by Burton and co-workers

Previously reported approaches to 3-arylidazoles, a structure of interest to the pharmaceutical industry (Figure 74), have required the use of toxic or explosive reagents, such as the condensation of hydrazines with fluorobenzophenones,^{172,173} or the cycloaddition of arynes with diazomethanes.^{174,175} In addition, direct metallation of C-3 of the indazole core has often been problematic, with several groups reporting fragmentation of the indazole framework due to the instability of the N-N bond, resulting in aminonitriles.^{176,177} Measures taken to circumvent this issue have relied on the use of toxic Negishi reagents,¹⁶¹ or direct C-H arylation,¹⁷⁸⁻¹⁸⁰ with widespread scope of the latter limited by the requirement for the more expensive aryl iodides and harsh reaction conditions. Arylation via boronate intermediates provides an elegant solution for these problems due to the lower toxicity, air stability and inert by-products associated with boron reagents as well as the milder conditions required to effect their coupling.

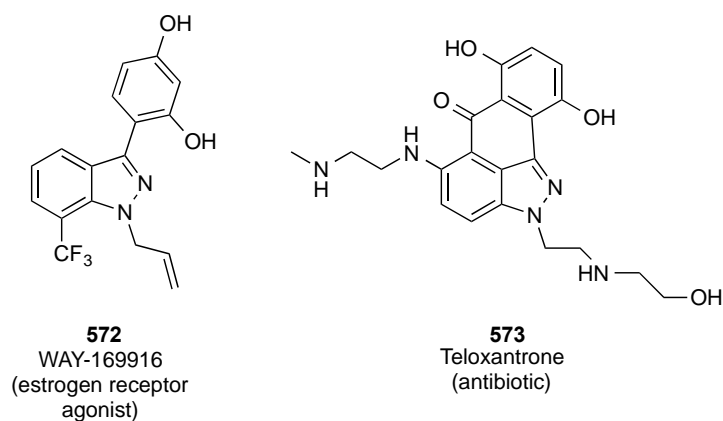


Figure 74: Biologically active 3-aryl indazoles

Exploiting the functional group tolerance of C-H borylation the borylation of functionalised indazole reagents enabled the multi-directional synthesis of small libraries of multisubstituted indazoles. The steric bias and lability of ortho-aziny boronate esters was exploited to enable a change in the regioselectivity of borylation and subsequent cross-couplings. The net effect is that direct C-H functionalisation is possible at all positions on the indazole core with the exception of C-4.

The C-H borylation of isomeric pyrazolo[1,5-a]pyridine and pyrazolo[1,2-a]pyridine was also achieved. The former affords the 3-boryl product in the presence of sub-stoichiometric B_2pin_2 however the competitive side reactions precludes its isolation in high yields. Whilst the latter borylated more selectively, the instability of the resultant boronate ester limited the scope for one-pot transformations, with only the Suzuki-Miyaura product obtainable in modest yield.

Application of these strategies to the borylation of aza-indazoles enabled similar observations, with 6-azaindazole recalcitrant to borylation due to inhibitory binding to the iridium catalyst. Protected 4 and 7-azaindazoles provided product mixtures arising due to competitive borylation on the pyridyl ring. Selective Suzuki-Miyaura cross-coupling was unsuccessful, however, exploiting the relative lability of the 3-boryl product enabled

selective formation of products arising from arylation of the pyridyl ring. One-pot arylation/cross-coupling sequences of aza-indazoles are the subject of ongoing work within the group.

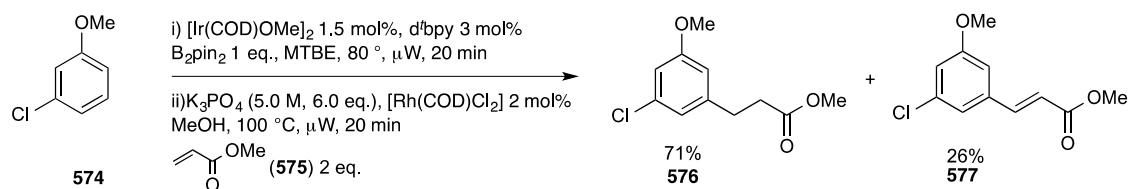
4 Development Towards a ‘One-pot’ C-H Borylation/Oxidative Heck Coupling Protocol

4.1 Aims and objectives

The development of robust, efficient and general combinatorial or array strategies for the formation of C-C bonds is an important strategy for the synthesis of compound libraries. Iridium-catalysed borylation is ideally suited to combinatorial chemistry as it circumvents the need for pre-existing functionality and is tolerant of a wide range of functional groups (*c.f* Sections 1.3.2.2 and 2.1.3). Moreover recent advances have enabled C-H borylation of both arenes and heteroarenes in good, reliable regioselectivity (*c.f* Section 2.3 and 3.2.2.2). Exploiting the synthetic utility of the resulting boronate ester, a variety of one-pot protocols have been reported, whereby in-situ elaboration enables access to a variety of functionalised (hetero)arenes.^{51,53,54,56,73,101,102,181-186} Furthermore the efficiency of any “one-pot” protocol may be improved by minimising the manipulation required, for example by using a single solvent. In addition, consistent with the recent drive towards sustainable chemistry and processes, there is an increased focus on greener processes, with fewer steps and reduced waste. Herein this chapter describes efforts undertaken towards the development of a one-pot single solvent C-H borylation/oxidative Heck cross-coupling protocol.

4.2 Previous work in the group

In early work undertaken towards the optimisation of a one-pot C-H borylation/Rh-catalysed 1,4-conjugate addition sequence, Tajuddin noted that oxidative Heck coupled products (**577**) were commonly observed by-products (Scheme 52).^{129,181}



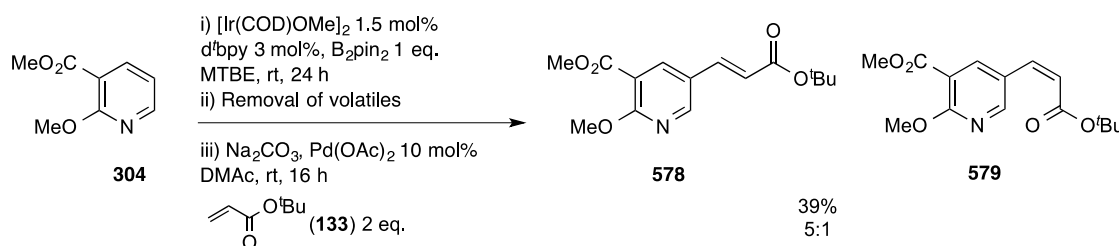
Scheme 52: Oxidative Heck coupling by-product in Rh(I)-catalysed conjugate addition

This was attributed to incomplete degassing of the solvent used in step 2. A subsequent literature review into the reported oxidative Heck couplings to date showed that no such one-pot C-H borylation/oxidative Heck-coupling protocol had been reported to date (*c.f.* Section 1.4.2.4). Reflecting this, an investigation was embarked upon to enable selective formation of the complementary vinylation products.

4.3 Results and Discussion

4.3.1 Preliminary Results

Initial work in this area began by applying a crude boronate ester, synthesised by iridium-catalysed C-H borylation, in Jung's oxidative Heck protocol (*c.f* Figure 14).¹⁰⁶ This method was chosen as it was found to be general and applicable to a variety of boron nucleophiles, including pinacol boronate esters. Addition of an aliquot of borylation stock solution to methyl-2-methoxynicotinate (**304**) gave, after 24 h stirring at room temperature, full conversion (¹H NMR) to 5-borylated product (**306**). Consistent with previous observations, trace amounts of the minor 6-borylated product (**307**) were also observed (*c.f* Table 3) Concentration *in vacuo* and subsequent addition of Pd(OAc)₂, Na₂CO₃, and DMAc gave, after evacuation/O₂ backfill cycles (3 x) and subsequent addition of *tert*-butylacrylate (**133**), the desired product in 39% overall yield, as a 5:1 mixture of *E:Z* isomers (**578:579**), based on the starting arene (Scheme 53) (N.B evacuation backfill cycles were performed without a cold trap to avoid condensation of liquid O₂).



Scheme 53: Initial attempts at a tandem 'one-pot' borylation/oxidative Heck coupling

Isomers were differentiated based off of their respective vinylic ³J H-H coupling constants; 16.0 and 12.2 Hz for *E*-(**578**) and *Z*-isomers (**579**) respectively. In addition

each isomer possessed distinct singlets for $C(CH_3)_3$ resonances at 1.52 (**578**) and 1.47 ppm (**579**). No evidence of α -arylation products were observed by 1H NMR (Figure 75).

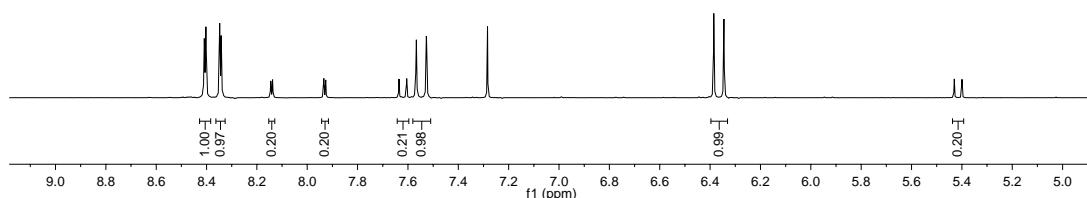
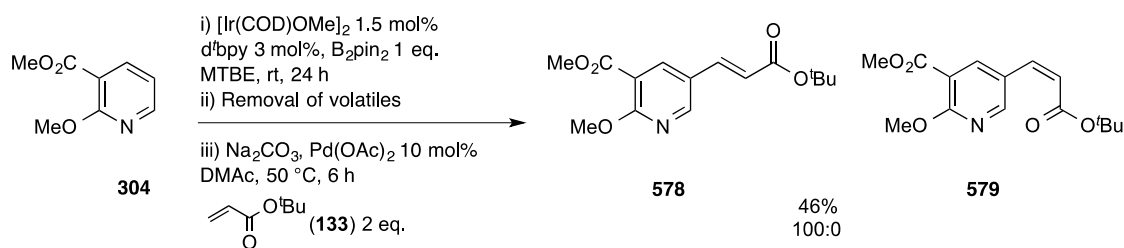


Figure 75: 1H NMR spectrum of E/Z isomeric mixture (aromatic enhancement)

Mass spectrometry analysis was complicated due to the equivalence of the product and intermediate boronate ester molecular ion peaks ($m/z = 293$), however distinctions could be made upon analysis of the fragmentation patterns, for example the desired product spectrum possessed an ion peak arising from loss of the diagnostic *tert*-butyl cation ($m/z = 237$ $[M-C(CH_3)_3]^+$). Conversely the boronate ester commonly fragments with initial loss of a methyl group ($m/z = 278$, $[M-CH_3]^+$).

Whilst the early result was promising, yield losses accrued in the oxidative Heck-coupling step were problematic. Analysis of the crude product ratio by GC/MS, taken prior to chromatographic purification, showed ca. 22% starting arene, as a result of reversal by protodeborylation. Reflecting this the procedure was repeated with heating during the oxidative Heck coupling step in order to attempt to increase the rate of product formation relative to the rate of protodeborylation.

Following the previously described procedure, with heating to 50 °C during step iii, the desired product (**578**) was produced in 46% yield as a single isomer (Scheme 54).

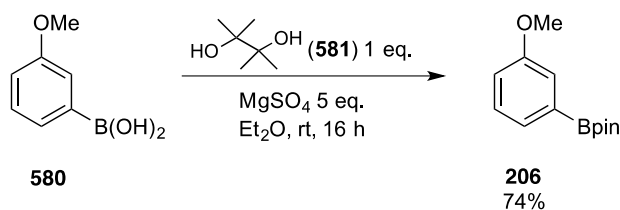


Scheme 54: Selective synthesis of *E*-isomer

4.3.2 Optimisation Studies

Whilst the isolation of the desired product as a single product was an improvement, the failure to observe a substantial improvement in yield remained problematic. In light of this, attempts were made to optimise the oxidative Heck reaction in isolation. In order to carry out optimisation studies, the simple boronate ester 3-(Bpin)-anisole (**206**) was chosen as a test substrate due to its ease of synthesis, in bulk, from the substituent boronic acid (Scheme 55).

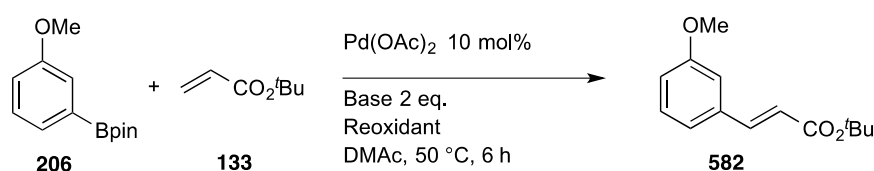
Under an argon atmosphere, a suspension of the substituent boronic acid (**580**), pinacol (**581**) and magnesium sulphate in Et_2O was stirred at room temperature. Filtration through a silica pad with copious Et_2O washings gave **206** in good yield.



Scheme 55: Synthesis of 3-(Bpin)-anisole

The boronate ester (**206**) could be clearly ascertained by observation of a diagnostic singlet at 1.35 ppm, corresponding to the newly incorporated pinCH₃ resonances, in the ¹H NMR spectrum.

With the test substrate in hand, focus was turned to the oxidative Heck coupling optimisation study. To a DMAc solution of boronate ester (**206**) and base under an oxygen atmosphere was added *tert*-butylacrylate (**133**). All experiments were run at 50 °C over 6 h at the same concentration in order to minimise yield discrepancies. Work-ups were carried out by celite filtration, to remove suspended base or metal salts, followed by direct loading onto silica in order to minimise yield losses and inconsistencies by aqueous work-up (Table 18).



Entry	Base	Reoxidant	Yield ^a
1	Na ₂ CO ₃	O ₂	42
2	N/A	O ₂	44
3	Cs ₂ CO ₃	O ₂	83
4	Na ₂ CO ₃	Cu(OAc) ₂	31
5 ^b	Na ₂ CO ₃	O ₂	Trace ^c
6 ^b	N/A	O ₂	Trace ^c

a. Isolated yield; b. 10 mol% bpy used;
c. Trace conversion to product observed by crude GC/MS

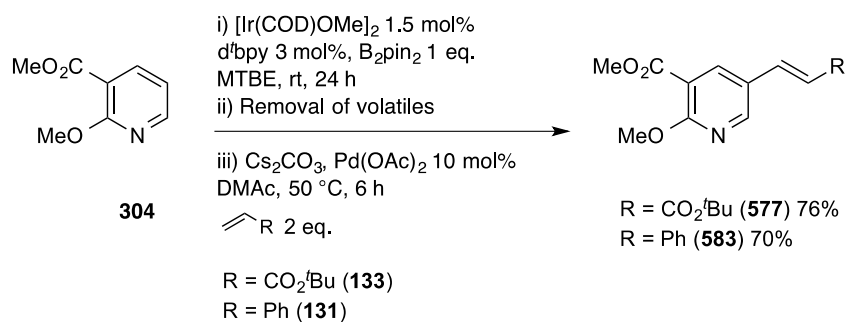
Table 18: Condition screening for oxidative Heck coupling

A common limiting factor observed across most reactions was the gradual darkening of the reaction solution from light orange, reflecting the starting colour of the Pd(OAc)₂, to black, coinciding with precipitation of the palladium catalyst as 'palladium black' (entries

1-4). This was avoided with the use of bipyridine (bpy) ligated catalysts, however, these reactions only furnished trace quantities of product(entries 5 and 6).

Consistent with previous results, the Na₂CO₃ mediated reaction of the boronate ester produced the desired products in only modest yields (entry 1). Whilst base-free coupling protocols are well established,^{113,187} the absence of base in this case failed to generate any significant improvements in yield (entry 2). Conversely, changing the base to Cs₂CO₃ resulted in a vast improvement in yield (entry 3). This was rationalised by the increased solubility of heavy metal bases, such as Cs₂CO₃, in organic solvents. Frustratingly a change in oxidant resulted in further yield reductions, in spite of use of copper and iron salts being well established in the literature (entry 4).^{109,110} Furthermore the use of ligating bipyridine ligands, reported to enhance both reaction rates and yields, failed to generate any isolable products (entries 5 and 6).¹⁰⁷ GC/MS analysis of the crude reaction mixtures found only trace (<10%) conversion to desired product (*m/z* = 234, [M]⁺), with remaining mass balance satisfied by sole observation of unreacted starting material (*m/z* = 234, [M]⁺). Starting material and product mass spectrometry traces were distinguished as previously described (*c.f* Section 4.3.1).

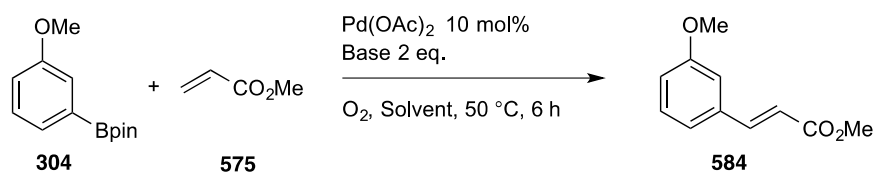
In light of the observed improved yields observed from simple substitution of Cs₂CO₃ into the reaction for Na₂CO₃, the previously described reaction involving methyl-2-methoxynicotinate (**304**) was re-run, as previously described, invoking this base change (*c.f* Scheme 54). In order to eliminate the possibility of substrate specificity, a separate reaction was also run with styrene (**131**) as an alternative coupling partner (Scheme 56).



Scheme 56: Tandem 'one-pot' borylation/oxidative Heck coupling run with Cs_2CO_3

Product **577** was characterised as previously described (*c.f* Section 4.3.1). Styrylation product **583** was confirmed by the observed characteristic molecular ion peak in GC/MS analysis ($m/z = 269$, $[\text{M}]^+$).

The improved yields obtained provided a good starting point for further development and movement towards a more efficient single solvent process. DMAc is not a suitable one-pot solvent due to its poor performance in borylation chemistry (*c.f* Table 10). Solvents which perform well in C-H borylation have tended to be low polarity and non-coordinating, although the comparable performance of reactions run in NMP with reactions run in ethereal solvents was surprising. Reflecting this Dunleavy ran a solvent screening exercise of the oxidative Heck step in isolation using the preprepared 3-(Bpin)-anisole (**304**) (Table 19).



Entry	Base	Solvent ^a	Isolated Yield (%)
1	Cs ₂ CO ₃	THF	0
2	Cs ₂ CO ₃	THF:H ₂ O (3:1)	29
3	Cs ₂ CO ₃	1,4-dioxane	40
4	Cs ₂ CO ₃	Diglyme	45
5	Cs ₂ CO ₃	NMP	55 ^b
6	Cs ₂ CO ₃	NMP ^c	0
7	KF	Diglyme	25 ^b
8	CsF	Diglyme	75 ^b

a. Anhydrous unless otherwise stated; b. ¹H NMR conversion; c. Solvent contained trace amounts of water

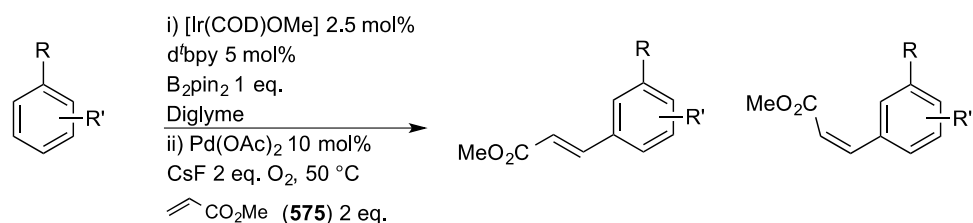
Table 19: Oxidative Heck solvent screen

Disappointingly THF, despite being a suitable borylation solvent, is not applicable to one-pot chemistry because of the poor performance observed in oxidative Heck coupling (entry 1). Addition of an aliquot of water to the reaction improved the yield but insufficiently to make for a viable one-pot process. Reactions utilising anhydrous ethereal solvents 1,4-dioxane and diglyme showed better performance (entries 3 and 4), with the best yields obtained with the more polar NMP (entry 5). Overall the role of water in the reaction was inconclusive from these results, for example whilst addition of water improved reactions utilising THF as solvent (entry 2), the presence of trace water in commercially purchased NMP completely shutdown any reactivity (entry 6). Due to these inconsistencies, and reflecting the intolerance of C-H borylation to even trace quantities of water, ensuing studies used only anhydrous reaction conditions.¹²³ The role of base within cross-coupling reactions remains a topic of debate, with conflicting reports on the mechanism of transmetallation.^{7,188} Moreover the potential for mechanistic variability

between boron reagents is also problematic.¹⁸⁹ It has also been shown that in certain cases the use of fluoride bases is permitted, whereby fluoride acts as a mechanistic substitute for the role of oxo-bases.^{190,191} In addition their ability to mediate reactions in anhydrous conditions is an added bonus. Reflecting this the test reaction was also conducted utilising both KF and CsF, with use of CsF in anhydrous diglyme giving the best result thus far (entries 7 and 8).

4.3.3 Aromatic Substrate Screening Exercise

Given the time constraints, further optimisation studies were postponed and focus was turned to exploring substrate scope. Given its appreciable performance in both the borylation and oxidative Heck screening experiments, diglyme was chosen as the one-pot solvent. An aliquot of borylation stock solution was added to a thick walled microwave vessel containing the appropriate substrates. The borylation was monitored up to optimum conversion by a combination of ¹H NMR spectroscopy (as per previously described method (*c.f* Section 2.3.1) and GC/MS. At this point both CsF and Pd(OAc)₂ were added and the atmosphere oxygenated prior to addition of methyl acrylate (**575**) (Table 20). Reactions were carried out with Dunleavy.



Entry	SM	Products ^{a, b}	
1			
	316	585	586
		67%	100:0
2 ^c			
	171	587	588
		36%(41)	97:3
3 ^c			
	589	590	591
		45%(48)	91:9
4 ^c			
	592	593	594
		0%	
5 ^c			
	193	595	596
		19%(29)	94:6
6 ^c			
	597	598	599
		40%(50)	83:17

a. Isolated yield; b. Corrected yields based on unreacted arene after borylation can be found in parentheses; c. Reaction carried out by J. Dunleavy

Table 20: Screening of aromatic substrates for 'one-pot' borylation/oxidative Heck reaction

Products were characterised by GC/MS and observation of CO_2CH_3 resonances in the ¹H NMR spectrum, for example compound **585** possessed the characteristic resonance at 3.83 ppm and the diagnostic chlorine isotope ratio by mass spectrometry analysis (m/z

= 233 (^{37}Cl , $[\text{M}]^+$), 231 (^{35}Cl , $[\text{M}]^+$). *E/Z* isomer differentiation was achieved as per the previously described method (*c.f* Section 4.3.1).

The inconsistent yields observed thus far are a limiting factor. In all cases yield losses are mostly accrued in step 2, with only minor improvements in yields corrected for incomplete stage 1 conversion. The formation of “palladium black”, observed by a darkening of the reaction solution and the formation of a black precipitate is also a hindrance that will have to be addressed in future modifications to this work.

4.4 Conclusions and future work

The one-pot C-H borylation/oxidative Heck coupling has been demonstrated in a single solvent and reaction vessel with varying success. Non-coordinating solvents such as diglyme are required as these performed well both in C-H borylation and oxidative Heck couplings in isolation. Whilst the role of water in the cross-coupling step of the reaction is not yet well understood, the use of fluoride bases enabled the use of completely anhydrous solvents, a pre-requisite for C-H borylation. The visible formation of “palladium black” is a factor limiting widespread application and although this is prevented through the use of bipyridine ligands, the loss of reactivity observed is surprising. Further screening of ligands is required at this stage. Whilst solvents, bases and ligands have been explored in isolation, a high throughput statistical design of experiments (DoE) would enable a more thorough optimisation of this multi-factorial reaction. This would allow for an improvement in yields and substrate scope of the reaction. Due to time constraints variation in the olefinic component has not been explored and will be conducted in future investigations.

5 Experimental

5.1 General Considerations

All borylation reactions were carried out under a dry nitrogen atmosphere using standard Schlenk techniques or in an Innovative Technology Inc. System 1 double-length glove box. Glassware was oven dried before all borylation reactions. Solvents used for borylation reactions were anhydrous and degassed by multiple freeze-pump-thaw cycles. Solvents used for Suzuki-Miyaura reactions were used without drying but with multiple freeze-pump-thaw degassing cycles.

Solvents

Methyl-tert-butyl-ether (MTBE) was purchased anhydrous from Sigma Aldrich. DMF and DMAc were purchased from Sigma-Aldrich. All other reaction solvents were dried using an Innovative Technology Solvent Purification System (SPS) and stored under argon. Deuterated solvents were purchased from Apollo Scientific, dried over 4 Å molecular sieves and used without further treatment.

Reagents

$[\text{Ir}(\text{COD})\text{OMe}]_2$ was synthesised, as previously described,¹⁹² from $\text{IrCl}_3 \cdot 3\text{H}_2\text{O}$, obtained from Precious Metals Online. B_2pin_2 was supplied as a generous gift by AllyChem Co. Ltd. (P.R.China) and was used without further purification. All other compounds were obtained from Sigma-Aldrich, Alfa Aesar, Fluorochem, Acros, Apollo Scientific or Lancaster and used without further purification.

NMR Spectroscopy

NMR spectra were recorded at ambient temperature on Bruker Avance-400 (^1H , ^{11}B , ^{19}F), Varian Inova-600 (^1H , ^{13}C [^1H], HSQC, HMBC, COSY) or Varian VNMRS-700 (^1H , ^{13}C [^1H], HSQC, HMBC, COSY) spectrometers. The ^1H and ^{13}C chemical shifts are

reported in ppm using the residual solvent signal of the deuterated solvents (CDCl_3 : $\delta_{\text{H}} = 7.26$ ppm, $\delta_{\text{C}} = 77.16$ ppm; Acetone d_6 : $\delta_{\text{H}} = 2.05$ ppm, $\delta_{\text{C}} = 206.26/29.84$ ppm; DMSO d_6 : $\delta_{\text{H}} = 2.50$ ppm, $\delta_{\text{C}} = 39.51$ ppm). All chemical shifts are reported in parts per million relative to tetramethylsilane ($\delta_{\text{H}} = 0.00$ ppm). All coupling constants are reported in Hz. ^{11}B NMR chemical shifts are referenced to external $\text{BF}_3 \cdot \text{Et}_2\text{O}$ ($\delta_{\text{B}} = 0.0$ ppm). Multiplicities are reported using the following abbreviations; s (singlet), d (doublet), t (triplet), q (quartet), m (unresolved multiplet) and br (broad). Assignment of spectra was carried out using 2D COSY, HMBC, HSQC and NOESY techniques.

Mass Spectrometry

GC/MS analyses were performed on an Agilent 6890N gas chromatograph (column: HP-5MS, 10 m, Ø 0.25 mm, film 0.25 μm ; injector: 250 $^{\circ}\text{C}$; oven: 70 $^{\circ}\text{C}$ (2 min), 70 $^{\circ}\text{C}$ to 250 $^{\circ}\text{C}$ (20 $^{\circ}\text{C min}^{-1}$), 250 $^{\circ}\text{C}$ (5 min); carrier gas: helium (1.6 mL min^{-1}) equipped with an Agilent 5973 inert mass selective detector operating in EI mode and a custom built Anatune liquid handling system functioning as autosampler/injector. Electrospray (ES) mass spectra were obtained on a Micromass LCT Mass Spectrometer. High Resolution mass spectra were obtained using a Thermo Finnigan LTQFT mass spectrometer or Xevo QToF mass spectrometer (Waters UK, Ltd) by the Durham University Mass Spectrometry Service.

IR Spectroscopy

Infrared spectra were measured on a Perkin-Elmer Paragon 1000 FT-IR spectrometer *via* the use of a Diamond ATR (attenuated total reflection) accessory (Golden Gate). Assigned peaks are reported in wavenumbers (cm^{-1}).

Thin-Layer Chromatography (TLC)

TLC was performed on 'Polygram Sil G/UV' plastic-backed silica plates with a 0.2 mm silica gel layer doped with a fluorescent indicator. Plates were purchased from VWR International.

Flash Column Chromatography

Flash column chromatography refers to purification by automated operation using a Teledyne Isco CombiFlash Rf machine on pre-packed silica Redisep® Rf cartridges with the stated solvent gradient and at a constant flow rate of 35 mL/min. Reverse phase chromatography used pre-packed C₁₈ silica Redisep® Rf cartridges and a 0-100% MeOH in H₂O (containing 0.1% HCOOH) gradient elution.

Microwave Reactor

Microwave reactions were carried out in septum-containing, crimp-capped, sealed vials in a monomodal Emrys™ Optimizer reactor from Personal Chemistry. The wattage was automatically adjusted to maintain the desired temperature for the desired period of time.

5.2 General Methods

General Procedure for the Preparation of a Catalyst Stock Solution for C-H Borylation

In a glovebox, a catalyst stock solution was prepared by weighing $[\text{Ir}(\text{COD})\text{OMe}]_2$, dtbpy and B_2pin_2 into a volumetric flask followed by the addition of MTBE to make up the volume to 25 mL of solution. Stock solutions of varying concentrations with respect to iridium were prepared;

Solution A; $[\text{Ir}(\text{COD})\text{OMe}]_2$ (100 mg, 0.15 mmol), d⁴bpy (80 mg, 0.30 mmol) and B_2pin_2 (2.54 g, 10.0 mmol)

Solution B; $[\text{Ir}(\text{COD})\text{OMe}]_2$ (167 mg, 0.25 mmol), d⁴bpy (134 mg, 0.50 mmol) and B_2pin_2 (2.54 g, 10.0 mmol)

Solution C; $[\text{Ir}(\text{COD})\text{OMe}]_2$ (331 mg, 0.50 mmol), d⁴bpy (268 mg, 1.00 mmol) and B_2pin_2 (2.54 g, 10.0 mmol)

The flask was vigorously shaken until the solution developed a deep red colour and no more solid was visible. The solution was transferred to and stored in, a crimp-cap septum-sealed tube in a freezer and used within 2 weeks.

General procedure for *in-situ* NMR Reaction Monitoring

For all room temperature borylation reactions, an aliquot (0.5 mL) of the reaction mixture was removed and transferred (in a glovebox or by Schlenk techniques) to a Young's Tap-sealed NMR tube containing a coaxial tube filled with acetone-d₆. The reactions were monitored for 24 h or until full consumption of starting material was observed by NMR spectroscopy.

General Procedure A: C-H Borylation using pre-prepared stock-solution

In a glovebox, a thick-walled microwave synthesis vial was charged with the stated heterocycle followed by the addition of an aliquot of the stated catalyst stock solution. The vessel was sealed with a crimp top septum cap and shaken until all of the substrate was dissolved. The reaction mixture was stirred on a magnetic stirring block for the time stated at the stated temperature or irradiated in a microwave reactor for the stated time. *In-situ* reaction monitoring by ^1H NMR spectroscopy was carried out as previously described. Upon completion, the volatiles were removed *in vacuo* to afford the crude product. Where stated, the crude product was dry-loaded onto silica gel and purified by silica gel flash column chromatography using the stated conditions to afford the purified product.

General Procedure B: C-H Borylation using sub-stoichiometric B_2pin_2

In a glovebox, a premixed solution of $[\text{Ir}(\text{COD})\text{OMe}]_2$ (1.5 mol%), $d^4\text{bpy}$ (3 mol%) and B_2pin_2 (0.5 eq.) (or HBpin (1.0 eq) where stated) in MTBE (2.5 mL) was added to a thick-walled microwave synthesis vial containing the stated heterocycle (1 eq.). The mixture was shaken vigorously to ensure complete mixing, and then the mixture was stirred at room temperature or heated at $80\text{ }^\circ\text{C}$ for the stated time. *In-situ* NMR reaction monitoring was carried out as previously described.

General Procedure C: Esterification under general acid catalysis

A substoichiometric quantity (*ca.* 0.1 mL) of concentrated sulphuric acid was added to a solution of carboxylic acid in methanol (10 mL). The solution was heated at reflux for the time stated. The solution was cooled to room temperature and charged with saturated $\text{NaHCO}_3(\text{aq})$ solution until pH 7. The mixture was concentrated *in vacuo* to remove methanol. The aqueous mixture was extracted with DCM (2 x 10 mL). The combined organic extracts were washed with brine (5 mL), dried over anhydrous magnesium

sulfate and filtered through celite. Concentration *in vacuo* gave the methyl ester which was carried through without further purification.

General Procedure D: Esterification via in-situ acid chloride formation

Procedure carried out under an argon atmosphere. At 0 °C, oxalyl chloride (1.2 eq.) was added dropwise to a DCM (5 mL) solution of carboxylic acid (1 eq.) and DMF (10 drops). The water bath was then removed and the reaction was stirred at room temperature for 3 h. Toluene (5 mL) was charged and the reaction concentrated to dryness *in vacuo*. The crude residue was redissolved in DCM (5 mL) and added dropwise to a DCM (5 mL) solution of MeOH (5 eq.) and DIPEA (2 eq.) at 0 °C. The reaction was stirred at room temperature for 0.5 h then quenched with saturated NaHCO_{3(aq)} (5 mL). The layers were separated and the aqueous layer re-extracted with DCM (5 mL). The combined organics were washed with brine (10 mL), dried over MgSO₄, filtered and concentrated *in vacuo*. The crude residue was purified by flash column chromatography using the stated solvent system.

General Procedure E for the tandem “one-pot” C-H Borylation/Suzuki-Miyaura Cross-Coupling

The borylation step was carried out as per General Procedure A. Upon completion, volatiles were removed *in vacuo*. To the crude mixture under N₂, was added palladium catalyst (5 or 10 mol%), base (2 eq.), aryl halide (1.1 - 2 eq.) and the stated solvent. The reaction was heated at the stated temperature for the stated time. The reaction mixture was diluted with water and extracted into EtOAc. The organic phase was dried over MgSO₄, filtered and concentrated *in vacuo* to give the crude product. This was dry-loaded onto silica gel and purified by silica gel flash column chromatography using the stated solvent system.

General Method F S_NAr substitution of 2-fluorinated pyridines

A mixture of the 2-fluorinated pyridine (1 eq.), K₂CO₃ (2 eq.) and amine (2 eq.) were refluxed in dioxane for 6 h. The reaction was cooled to room temperature and filtered through celite. The organic residue was then dry loaded onto silica and purified by flash column chromatograph using the stated solvent system.

General Method G for the Boc-protection of N-heterocycles

Under an argon atmosphere, heterocycle (1 eq.), DMAP (5 mol%), Boc₂O (1.1 eq.) and Et₃N (1 eq.) were stirred in MeCN (10 mL) for 16 h. The reaction was then dry loaded onto silica and purified by flash column chromatography using the stated solvent system.

General Method H for the protection of indazole by deprotonation and alkylation

Procedure performed under a nitrogen atmosphere. A solution of indazole (1 eq.) in anhydrous THF (10 mL) was added dropwise, to a suspension of sodium hydride (60% oil dispersion, 1 eq.) in anhydrous THF (10 mL). The reaction was cooled to 0 °C in an ice bath and the appropriate halide (1.1 eq.) was added dropwise. The reaction was allowed to warm to room temperature and stirred for 3 hours. The reaction was quenched with an IPA:H₂O mixture (1:1, 10 mL) and concentrated *in vacuo* to remove the THF. The aqueous residues were extracted with DCM (2 x 15 mL). The combined organic extracts were washed with brine (10 mL), dried, filtered and concentrated *in vacuo* to yield the crude product. Purified by flash column chromatography using the stated solvent system.

General Method I for the regioselective SEM protection of 2H-indazole

Procedure carried out in oven-dried glassware under an argon atmosphere. Dicyclohexylamine (1.2 eq.) followed by 2-(trimethylsilyl)ethoxymethyl chloride (1.2 eq.) were added slowly to a solution of the indazole (1 eq.) in anhydrous THF (5 mL). The reaction was stirred at room temperature for 3 h before being quenched with aqueous sodium hydroxide solution (0.5 M, 5 mL). The aqueous mixture was concentrated *in vacuo* to remove the THF then extracted with ethyl acetate (2 x 10 mL). The combined

organic extracts were washed with brine (10 mL), dried over anhydrous magnesium sulphate and filtered through celite to yield the crude product. Purification was carried out by flash column chromatography using the stated solvent system.

General Procedure J for the one-pot C-H Borylation/Suzuki-Miyaura Cross-Coupling of protected indazoles

The borylation step was carried out as per General Procedure B with additional B_2pin_2 (0.2 eq.) and heating at 80 °C for 3 h. Upon completion, volatiles were removed *in vacuo*. To the crude mixture under N_2 , was added $Pd(dppf)Cl_2$ (10 mol%), Cs_2CO_3 (2 eq.) and aryl halide (1.1 eq.). Where stated, the reaction was carried out with $CuCl$ (1 eq.). The vessel was sealed and DMF (3 mL) was added. The reaction was irradiated at 100 °C for 1 h in a microwave reactor. The reaction mixture was worked up and purified as per General Method E.

General Method K for the formation of the (aza)indazole core

The starting 2-fluorobenzaldehyde (or 2-fluoronicotinaldehyde) was refluxed (24 h) in hydrazine hydrate:DME (1:1) (20 mL). The reaction mixture was left to cool, diluted with water (5 mL) before removal of DME was carried out *in vacuo*. The aqueous residue was extracted with DCM (2 x 5 mL). The combined organic extracts were washed with brine (10 mL), dried over anhydrous magnesium sulphate and filtered through celite to yield the crude product carried through without further purification.

General Procedure L for the one-pot C-H Borylation/Suzuki-Miyaura Cross-Coupling of protected bromo-2H-indazoles

The borylation step was carried out as per General Procedure B with additional B_2pin_2 (0.2 eq.) and heating at 80 °C for 3 h. Upon completion, volatiles were removed *in vacuo*. To the crude mixture under N_2 , was added $Pd(PPh_3)_4$ (10 mol%), K_3PO_4 (2 eq.) and aryl halide (1.1 eq.) and DMAc (3 mL). The reaction was heated at 70 °C for 2 h. The reaction mixture was worked up and purified as per General Method E.

General Method M for the Suzuki-Miyaura cross-coupling of n-bromo-3-arylindazoles

Under an argon atmosphere, the bromo-arylindazole (1 eq.), Pd(dppf)Cl₂ (5 mol%), Cs₂CO₃ (2 eq.) and arylboronic acid (2 eq.) were reacted at 100 °C in DMAc for 2 h. The reaction was worked up as per General Method E and purified by flash column chromatography using the stated solvent system.

General Method N for the deborylation and Suzuki-Miyaura cross coupling of bis-borylated heterocycles

As per General Method A, the starting heterocycle (1 eq.) was reacted with an aliquot of the stated stock solution and additional B₂pin₂ (1 eq.) at 80 °C for 16 h. The reaction was concentrated *in vacuo* to yield the crude boronate ester which was then reacted with KOH (3 eq.) at 70 °C for 15 min in DMAc:H₂O (9:1). Pd(dppf)Cl₂ (5 mol%) and aryl halide (2 eq.) were then added and reaction continued for a further 1 h. The reaction was worked up as per General Method E and purified by flash column chromatography using the stated solvent system.

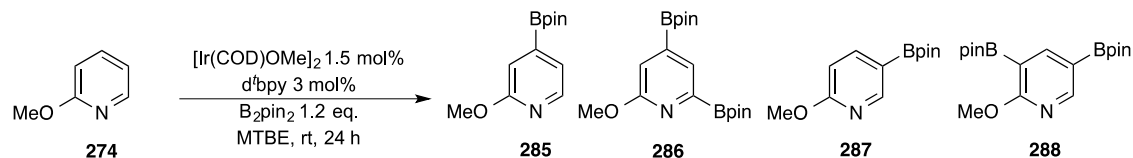
General Procedure O for the tandem “one-pot” C-H Borylation/Oxidative Heck coupling

The borylation step was carried out as per General Procedure A. Upon completion, volatiles were removed *in vacuo*. To the crude mixture was added Pd(OAc)₂ (10 mol%), Na₂CO₃ or Cs₂CO₃ (2 eq.) and alkene (2 eq.) in DMAc. The vessel was sealed and evacuated/backfilled with O₂ (x 3 cycles). The reaction was heated at 50 °C for the stated time. The reaction mixture was cooled to room temperature then diluted with water and extracted into ether (2 x 10 mL). The combined organic extracts were washed with brine (10 mL), dried over MgSO₄, filtered and concentrated *in vacuo* to give the crude product. This was dry-loaded onto silica gel and purified by silica gel flash column chromatography using the stated solvent system.

5.3 Experimental Details

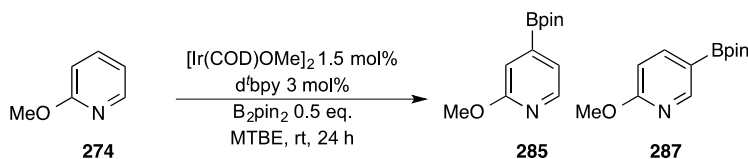
Borylation of Azinyl Heterocycles

Borylation of 2-methoxypyridine (274)



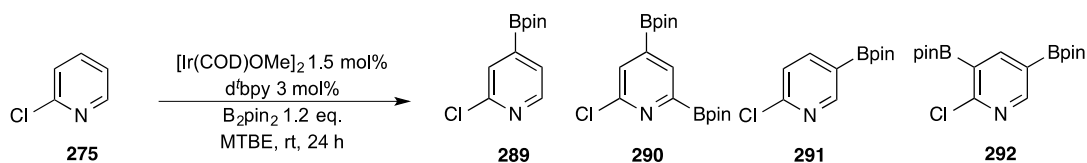
General procedure A was applied to **274** (109 mg, 1 mmol) using Stock Solution A with additional B_2pin_2 (51 mg, 0.2 mmol). The reaction mixture was stirred at room temperature for 24 h giving full conversion (^1H NMR) to **285**, **286**, **287** and **288** in a 43:17:31:9 ratio.

Borylation of 2-methoxypyridine (274) under boron-limiting conditions



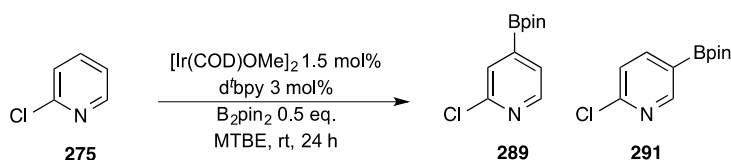
General procedure B was applied to **274** (109 mg, 1 mmol). The reaction mixture was stirred at room temperature for 24 h giving 42% conversion (^1H NMR) to afford **285** and **287** in a 73:27 ratio.

Borylation of 2-chloropyridine (**275**)



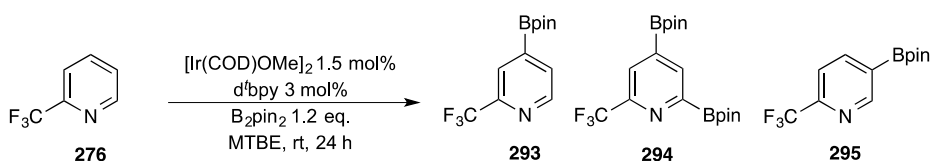
General procedure A was applied to **275** (114 mg, 1 mmol) using Stock Solution A with additional B_2pin_2 (51 mg, 0.2 mmol). The reaction mixture was stirred at room temperature for 24 h giving full conversion (^1H NMR) to **289**, **290**, **291** and **292** in a 28:38:27:7 ratio.

Borylation of 2-chloropyridine (**275**) under boron-limiting conditions



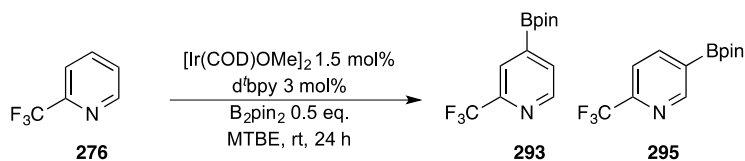
General procedure B was applied to **275** (114 mg, 1 mmol). The reaction mixture was stirred at room temperature for 24h giving 55% conversion (^1H NMR) to afford **289** and **291** in a 75:25 ratio.

Borylation of 2-(trifluoromethyl)pyridine (**276**)



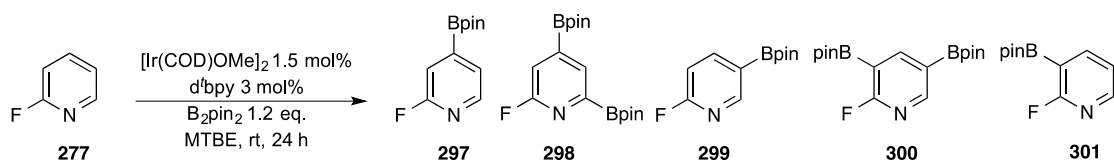
General procedure A was applied to **276** (147 mg, 1 mmol) using Stock Solution A with additional B_2pin_2 (51 mg, 0.2 mmol). The reaction mixture was stirred at room temperature for 24 h giving full conversion (^1H NMR) to **293**, **294** and **295** in a 25:36:39 ratio.

Borylation of 2-(trifluoromethyl)pyridine (**276**) under boron-limiting conditions



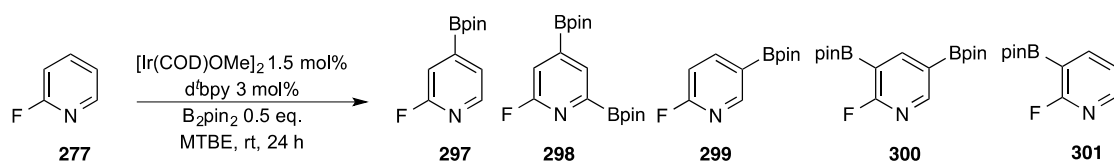
General procedure B was applied to (**276**) (147 mg, 1 mmol). The reaction mixture was stirred at room temperature for 24 h giving 83% conversion (^1H NMR) to afford **293** and **295** in a 65:35 ratio.

Borylation of 2-fluoropyridine (**277**)



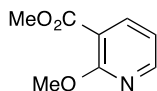
General procedure A was applied to **277** (97 mg, 1 mmol) using Stock Solution A with additional B_2pin_2 (51 mg, 0.2 mmol). The reaction mixture was stirred at room temperature for 24 h giving full conversion (^1H NMR) to afford **297**, **298**, **299**, **300** and **301** in a 45:15:10:19:11 ratio.

Borylation of 2-fluoropyridine (**277**) under boron-limiting conditions



General procedure B was applied to **277** (97 mg, 1 mmol). The reaction mixture was stirred at room temperature for 24 h giving 89% conversion (^1H NMR) to afford **297**, **298**, **299**, **300** and **301** in a 57:2:19:5:17 ratio.

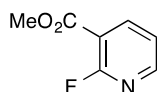
Methyl-2-methoxynicotinate (304)



General method C applied to 2-methoxynicotinic acid (**302**) (1.53 g, 10 mmol). **304** isolated as pale yellow oil (1.58 g, 95%)

δ_{H} (700 MHz, CDCl_3) 8.31 (1H, dd, $J = 4.9, 1.9$, 6-*H*), 8.16 (1H, dd, $J = 7.5, 1.9$, 4-*H*), 6.95 (1H, dd, $J = 7.5, 4.9$, 5-*H*), 4.05 (3H, s, OCH_3), 3.90 (3H, s, CO_2CH_3); δ_{C} (176 MHz, CDCl_3) 165.6 (CO_2CH_3), 162.5 (C-2), 150.8 (C-6), 141.4 (C-4), 116.5 (C-5), 141.2 (C-3), 54.4 (OCH_3), 52.4 (CO_2CH_3); ν_{max} (ATR) 1731, 1577, 1469, 1406, 1318, 1268, 1129, 1084, 1012 cm^{-1} ; Accurate Mass (ESI) m/z found $[\text{M}+\text{H}]^+$ 168.0640; $\text{C}_8\text{H}_{10}\text{NO}_3$ requires M , 168.0661.

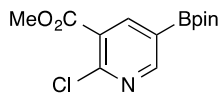
Methyl-2-fluoronicotinate (305)



General procedure D was applied to 2-fluoronicotinic acid (**303**) (1.1 g, 7.8 mmol). Column eluent 0-50% Et_2O in hexanes. **305** (0.79 g, 65%) isolated as a white amorphous solid.

δ_{H} (600 MHz, CDCl_3) 8.38 (2H, m, 4, 6-*H*), 7.29 (1H, m, 5-*H*), 3.94 (3H, s, CO_2CH_3); δ_{C} (151 MHz, CDCl_3) 163.8 (d, $J = 8.1$, CO_2CH_3), 161.7 (d, $J = 249.7$, C-2), 151.8 (d, $J = 15.4$, ArC), 143.3 (d, $J = 1.6$, ArC), 121.5 (d, $J = 4.9$, C-5); 113.9 (d, $J = 25.0$, C-3), 52.9 (CO_2CH_3); δ_{F} (376 MHz, CDCl_3), -61.8 (s); ν_{max} 1723, 1600, 1430, 1312, 1294, 1277, 1134, 1088, 1059 cm^{-1} ; Accurate Mass (ESI) m/z found $[\text{M}+\text{H}]^+$ 156.0460; $\text{C}_7\text{H}_7\text{FNO}_3$ requires M , 156.0461.

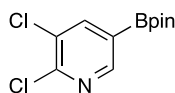
Methyl-2-chloro-5-(Bpin)nicotinate (311)



General procedure A was applied to methyl-2-chloronicotinate (**310**) (172 mg, 1 mmol) using Stock Solution A. The reaction mixture was stirred at room temperature for 24 h giving 75% conversion (¹H NMR) to 5-(Bpin) (**311**) and 6-(Bpin) products (**312**) in a 94:6 ratio. The crude product was purified by reverse phase column chromatography to give pure **311** (155 mg, 52%) as a white amorphous solid.

δ_{H} (400 MHz, CDCl₃) 8.80 (1H, d, $J = 1.9$, 6-*H*), 8.49 (1H, d, $J = 1.9$, 4-*H*), 3.95 (3H, s, CO₂CH₃), 1.36 (12H, s, pinCH₃); δ_{C} (101 MHz, CDCl₃) 165.1 (CO₂CH₃), 157.4 (C-6), 152.6 (C-2), 146.3 (C-4), 126.2 (C-3), 84.8 (C(CH₃)₂), 52.8 (CO₂CH₃), 24.9 (pinCH₃); ¹¹B NMR (128 MHz, CDCl₃) δ 30.4 (s(br)); ν_{max} (neat) 1738, 1694, 1588, 1548, 1426, 1359, 1255, 1138, 1108, 1062, 971 cm⁻¹; Accurate Mass (ESI) m/z found [M]⁺ 297.1047; C₁₃H₁₈¹⁰B³⁵ClNO₄ requires M , 297.1054.

2,3-Dichloro-5-(Bpin)-pyridine (317)

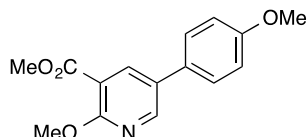


General procedure A was applied to 2,3-dichloropyridine (**316**) (148 mg, 1 mmol) using Stock Solution A. The reaction mixture was stirred at room temperature for 5 h giving full conversion (¹H NMR) to **317**. The crude product was purified by flash column chromatography (eluent; 0-5% MeOH in DCM) to give pure **317** (0.12 g, 44%) as a white amorphous solid.

δ_{H} (700 MHz, CDCl₃) 8.57 (1H, d, $J = 1.5$, 6-*H*), 8.09 (1H, d, $J = 1.5$, 4-*H*), 1.33 (12H, s, pinCH₃); δ_{C} (176 MHz, CDCl₃) 152.9 (C-6), 151.8 (C-2), 144.6 (C-4), 130.5 (C-3), 84.9

(C(CH₃)₂), 25.0 (pinCH₃); δ_B (128 MHz, CDCl₃) 30.0 (s (br)); GC/MS (EI) *m/z* 277 ([M]⁺, ³⁷Cl₂), (275 ([M]⁺, ³⁷Cl³⁵Cl), 273 ([M]⁺, ³⁵Cl₂), 262 ([M-CH₃]⁺, ³⁷Cl₂), 260 ([M-CH₃]⁺, ³⁷Cl³⁵Cl), 258 ([M-CH₃]⁺, (³⁵Cl₂)); Accurate Mass (ASAP) *m/z* found [M+H]⁺ 273.0625; C₁₁H₁₅¹⁰BNO₂³⁵Cl₂ requires *M*, 273.0609.

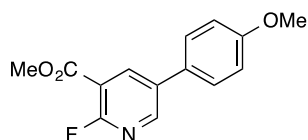
Methyl-2-methoxy-5-(4'-methoxyphenyl)nicotinate (319)



General procedure E was applied to methyl-2-methoxynicotinate (**304**) (184 mg, 1.1 mmol). Borylation with Stock Solution A for 24 h at room temperature gave full conversion (¹H NMR) to 5-(Bpin) (**306**) and 6-(Bpin) (**307**) products in a 93:7 ratio. Suzuki-Miyaura step was carried out for 2 h with Pd(dppf)Cl₂ (40 mg, 0.06 mmol, 5 mol%), Cs₂CO₃ (720 mg, 2.2 mmol) and 4-iodoanisole (280 mg, 1.2 mmol) in DMF (3 mL) at 70 °C. Column eluent 0-15% EtOAc in heptane. **319** (229 mg, 76%) isolated as a white amorphous solid.

δ_H (700 MHz, CDCl₃) 8.49 (1H, d, *J* = 2.2, 6-*H*), 8.34 (1H, d, *J* = 2.2, 4-*H*), 7.48 (2H, m, 2', 6'-*H*), 7.00 (2H, m, 3', 5'-*H*), 4.10 (3H, s, 2-COCH₃), 3.93 (3H, s, CO₂CH₃), 3.86 (3H, s, 4'-COCH₃); δ_C (176 MHz, CDCl₃) 165.7 (CO₂CH₃), 161.4 (C-2), 159.7 (C-4'), 148.2 (C-6), 139.7 (C-4), 129.8 (C-5), 129.3 (C-1'), 128.0 (C-2', 6'), 114.7 (C-3', 5'), 113.9 (C-3), 55.5 (4'-COCH₃), 54.6 (2-COCH₃), 52.5 (CO₂CH₃); ν_{max} (ATR) 1732, 1606, 1563, 1519, 1474, 1417, 1327, 1285, 1245, 1181, 1087, 1060, 1014 cm⁻¹; Accurate Mass (ASAP) *m/z* found [M+H]⁺ 274.1075; C₁₅H₁₆NO₄ requires *M*, 274.1079.

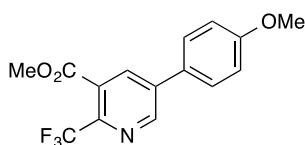
Methyl-2-fluoro-5-(4'-methoxyphenyl)nicotinate (320)



General procedure E was applied to methyl-2-fluoronicotinate (**305**) (682 mg, 4.4 mmol). Borylation with Stock Solution A for 45 min at room temperature gave full conversion (¹H NMR) to 5-(Bpin) (**308**) and 6-(Bpin) (**309**) products in a 91:9 ratio. The Suzuki-Miyaura step was carried out for 2 h with Pd(dppf)Cl₂ (161 mg, 0.22 mmol), Cs₂CO₃ (2.87 g, 8.8 mmol) and 4-iodoanisole (1.13 g, 4.8 mmol) in DMF (10 mL) at 70 °C. Column eluent 0-20% EtOAc in heptane. **320** (715 mg, 62%) isolated as an off-white amorphous solid.

δ_{H} (700 MHz, CDCl₃) 8.51 (2H, m, 4, 6-*H*), 7.50 (2H, m, 2', 6'-*H*), 7.01 (2H, m, 3', 5'-*H*), 3.98 (3H, s, CO₂CH₃), 3.86 (OCH₃); δ_{C} (176 MHz, CDCl₃) 164.0 (d, *J* = 8.1, CO₂CH₃), 160.5 (d, *J* = 249.8, C-2), 160.3 (C-4'), 149.1 (d, *J* = 15.4, ArC), 141.7 (d, *J* = 1.6, ArC), 135.0 (C-5), 128.3 (C-2', 6'), 128.0 (C-1'), 114.9 (C-3, 5'), 113.4 (d, *J* = 25.6, C-3), 55.6 (OCH₃), 53.0 (CO₂CH₃); δ_{F} (376 MHz, CDCl₃) -66.3 (s); ν_{max} (neat) 1722, 1603, 1459, 1446, 1327, 1292, 1249, 1179, 1089, 1042, 977 cm⁻¹; Accurate Mass (ASAP) *m/z* found [M]⁺ 261.0824; C₁₄H₁₂FNO₃ requires *M*, 261.0801

Methyl-2-(trifluoromethyl)-5-(4'-methoxyphenyl)nicotinate (321)

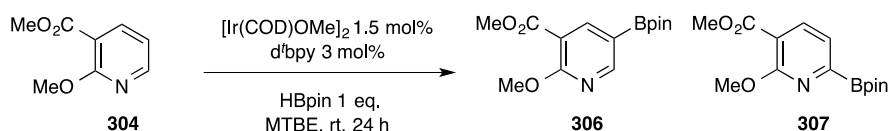


General procedure E was applied to methyl-2-(trifluoromethyl)nicotinate (**313**) (287 mg, 1.4 mmol). Borylation with Stock Solution A for 1 h at room temperature gave full conversion (¹H NMR) to the 5-(Bpin) (**314**) product. Suzuki-Miyaura step carried out for 3 h using Pd(dppf)Cl₂ (51 mg, 0.07 mmol), Cs₂CO₃ (910 mg, 2.8 mmol) and 4-iodoanisole

(360 mg, 1.5 mmol) in DMF (5 mL) at 70 °C. Crude product purified by reverse phase column chromatography. **321** (332 mg, 75%) isolated as a white amorphous solid.

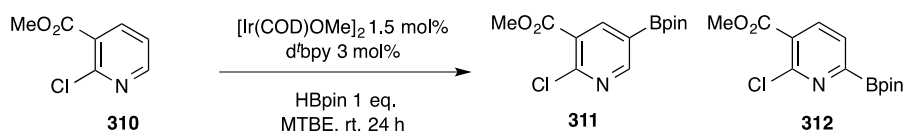
δ_{H} (700 MHz, CDCl_3) 8.96 (1H, d, $J = 2.1$, 6-*H*), 8.22 (1H, d, $J = 2.1$, 4-*H*), 7.58 (2H, m, 2', 6'-*H*), 7.05 (2H, m, 3', 5'-*H*), 3.99 (3H, s, CO_2CH_3), 3.88 (3H, s, COCH_3); δ_{C} (176 MHz, CDCl_3) 166.2 (CO_2CH_3), 161.0 (C-4'), 148.6 (C-6), 143.4 (m, C-2), 138.9 (C-5), 135.7 (C-4), 128.7 (C-2', 6'), 127.8 (C-3), 127.6 (C-1'), 121.4 (q, $J = 274.6$, CF_3), 115.1 (C-3', 5'), 55.6 (OCH_3), 53.4 (CO_2CH_3); δ_{F} (376 MHz, CDCl_3) -64.3 (s); ν_{max} (neat) 1738, 1609, 1519, 1440, 1324, 1252, 1142, 1065, 1049 cm^{-1} ; Accurate Mass (ASAP) m/z found $[\text{M}]^+$ 311.0768; $\text{C}_{15}\text{H}_{12}\text{F}_3\text{NO}_3$ requires M , 311.0769.

Borylation of methyl-2-methoxynicotinate (**304**) with HBpin



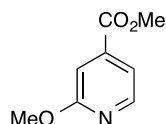
General Procedure B was applied to **304** (1 mmol) using HBpin. The reaction mixture was stirred at room temperature for 24 h giving 48% conversion (^1H NMR) to afford **306** and **307** in a 54:46 ratio.

Borylation of methyl-2-chloronicotinate (**310**) with HBpin



General Procedure B was applied to **310** (1 mmol) using HBpin. The reaction mixture was stirred at room temperature for 24 h giving 15% conversion (^1H NMR) to afford **311** and **312** in a 76:24 ratio.

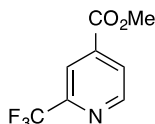
Methyl-2-methoxyisonicotinate (325)



General procedure C applied to 2-methoxyisonicotinic acid (**322**) (500 mg, 3.3 mmol). **325** (518 mg, 95%) isolated as a pale yellow oil.

δ_{H} (700 MHz, CDCl_3) 8.27 (1H, d, $J = 5.1$, 6-*H*), 7.39 (1H, d, $J = 5.1$, 5-*H*), 7.30 (1H, s, 3-*H*), 3.96 (3H, s, OCH_3), 3.93 (3H, s, CO_2CH_3); δ_{C} (176 MHz, CDCl_3) 165.7 (CO_2CH_3), 165.0 (C-2), 147.8 (C-6), 140.2 (C-4), 115.8 (C-5), 111.4 (C-3), 54.0 (OCH_3), 52.8 (CO_2CH_3); ν_{max} (ATR) 1732, 1708, 1588, 1576, 1467, 1404, 1308, 1258, 1237, 1126, 1082, 1011 cm^{-1} ; Accurate Mass (ESI) m/z found $[\text{M}+\text{H}]^+$ 168.0660; $\text{C}_8\text{H}_{10}\text{NO}_3$ requires M , 168.0661.

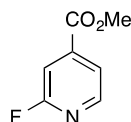
Methyl-2-(trifluoromethyl)isonicotinate (326)



General procedure C applied to 2-(trifluoromethyl)isonicotinic acid (**323**) (400 mg, 2.1 mmol). **326** (380 mg, 88%) isolated as a colourless oil.

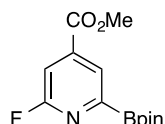
δ_{H} (700 MHz, CDCl_3) 8.90 (1H, d, $J = 4.9$, 6-*H*), 8.23 (1H, m, 3-*H*), 8.06 (1H, m, 5-*H*), 4.00 (3H, s, CO_2CH_3); δ_{C} (176 MHz, CDCl_3) 164.4 (CO_2CH_3), 151.1 (C-6), 149.5 (q, $J = 35.4$, C-2), 139.2 (C-4), 125.9 (C-5), 121.4 (q, $J = 247.3$, CF_3), 120.1 (q, $J = 3.5$, C-3), 53.3 (CO_2CH_3); δ_{F} (376 MHz, CDCl_3) -68.1 (s); ν_{max} (ATR) 1734, 1442, 1334, 1295, 1256, 1179, 1130, 1082, 970 cm^{-1} ; Accurate Mass (ASAP) m/z found $[\text{M}+\text{H}]^+$ 206.0426; $\text{C}_8\text{H}_7\text{F}_3\text{NO}_2$ requires M , 206.0429.

Methyl-2-fluoroisonicotinate (327)



General procedure D was applied to 2-fluoroisonicotinic acid (**324**) (0.99 g, 7.0 mmol). Column eluent 0-10% EtOAc in hexanes. **327** (0.68 g, 65%) isolated as a colourless oil. δ_{H} (600 MHz, CDCl_3) 8.37 (1H, d, $J = 5.1$, 6-*H*), 7.74 (1H, dt, $J = 5.1$, 1.5, 5-*H*), 7.49 (1H, m, 3-*H*), 3.97 (3H, s, CO_2CH_3); δ_{C} (151 MHz, CDCl_3) 164.4 (d, $J = 4.1$, CO_2CH_3), 164.3 (d, $J = 240.1$, C-2), 148.8 (d, $J = 14.5$, C-6), 142.9 (d, $J = 7.8$, C-4), 120.9 (d, $J = 4.7$ Hz, C-5), 110.0 (d, $J = 39.2$, C-3), 53.2 (CO_2CH_3); δ_{F} (376 MHz, CDCl_3) -66.3 (s); ν_{max} (ATR) 1733, 1573, 1438, 1399, 1288, 1214, 1095, 985, 900 cm^{-1} ; Accurate Mass (ESI) m/z found $[\text{M}+\text{H}]^+$ 156.0456; $\text{C}_7\text{H}_7\text{FNO}_3$ requires M , 156.0461.

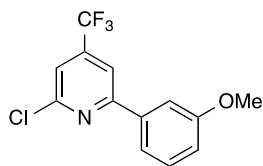
Methyl-2-fluoro-6-(Bpin)isonicotinate (339)



General procedure A was applied to methyl 2-fluoroisonicotinate (**327**) (170 mg, 1.1 mmol) using Stock Solution A. The reaction mixture was stirred at room temperature for 18 h giving full conversion (^1H NMR) to **339**. Column eluent (0-10% MeOH in DCM) afforded **339** (89 mg) as an off white solid containing minor impurities.

δ_{H} (700 MHz, CDCl_3) 8.23 (1H, s, 5-*H*), 7.52 (1H, m, 3-*H*), 3.96 (3H, s, CO_2CH_3), 1.38 (12H, s, pin CH_3); δ_{C} (176 MHz, CDCl_3) 164.7 (d, $J = 4.0$, CO_2CH_3), 164.3 (d, $J = 241.1$, C-2); 141.9 (d, $J = 7.0$, C-4), 127.7 (d, $J = 3.5$, C-5), 111.9 (d, $J = 40.5$, C-3), 85.3 ($\text{C}(\text{CH}_3)_2$), 53.1, (CO_2CH_3), 25.0 (pin CH_3).

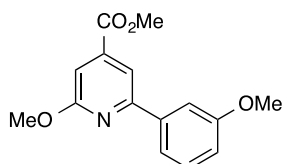
2-Chloro-4-(trifluoromethyl)-6-(3'-methoxyphenyl)pyridine (341)



General procedure E was applied to 2-chloro-4-(trifluoromethyl)pyridine (**328**) (182 mg, 1 mmol). Borylation with Stock Solution A for 24 h at room temperature gave 72% conversion (¹H NMR) to 6-(Bpin) product **330**. The Suzuki-Miyaura step was carried out for 3 h using Pd(dppf)Cl₂ (37 mg, 0.05 mmol), Cs₂CO₃ (650 mg, 2 mmol) and 3-iodoanisole (260 mg, 1.1 mmol) in DMF (3 mL) at 70 °C. Column eluent 0-3% Et₂O in heptane. **341** (147 mg, 51%) isolated as an off-white amorphous solid.

δ_{H} (700 MHz, CDCl₃) 7.83 (1H, s, 5-*H*), 7.59 (1H, t, *J* = 2.3, 2'-*H*), 7.58 (1H, d, *J* = 7.9, 6'-*H*), 7.48 (1H, s, 3-*H*), 7.41 (1H, t, *J* = 7.9, 5'-*H*), 7.03 (1H, dd, *J* = 7.9, 2.3, 4'-*H*), 3.91 (3H, s, OCH₃); δ_{C} (176 MHz, CDCl₃) 160.4 (C-3'), 159.4 (C-6), 152.4 (C-2), 141.8 (q, *J* = 34.3, C-4), 138.0 (C-1'), 130.2 (C-5'), 122.3 (q, *J* = 274.0, CF₃), 119.6 (C-6'), 118.7 (q, *J* = 3.7, C-3), 116.6 (C-4'), 114.8 (q, *J* = 3.5, C-5), 112.6 (C-2'), 55.6 (OCH₃); δ_{F} (376 MHz, CDCl₃) -64.7 (s); ν_{max} (ATR) 1600, 1561, 1459, 1400, 1333, 1274, 1221, 1177, 1142, 1102 cm⁻¹; Accurate Mass (ASAP) *m/z* found [M]⁺ 287.0330; C₁₃H₉³⁵ClF₃NO requires *M*, 287.0325.

Methyl-2-methoxy-6-(3'-methoxyphenyl)isonicotinate (342)

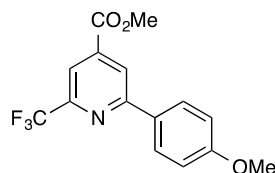


General procedure E applied to methyl-2-methoxyisonicotinate (**325**) (167 mg, 1 mmol). Borylation with Stock Solution A for 24 h at room temperature gave 57% conversion (¹H

NMR) to 6-(Bpin) product **335**. The Suzuki-Miyaura step was carried out for 16 h using Pd(dppf)Cl₂ (37 mg, 0.05 mmol), Cs₂CO₃ (650 mg, 2 mmol) and 3-iodoanisole (260 mg, 1.1 mmol) in DMF (3 mL) at 70 °C. Column eluent 7% EtOAc in heptane. **342** (112 mg, 41%) isolated as an off-white amorphous solid.

δ_{H} (700 MHz, CDCl₃) 7.88 (1H, s, 5-*H*), 7.67 (2H, m, 2', 6'-*H*), 7.38 (1H, t, *J* = 8.0, 5'-*H*), 7.25 (1H, s, 3-*H*), 6.97 (1H, dd, *J* = 8.0, 2.4, 4'-*H*), 4.07 (3H, s, 2-COCH₃), 3.96 (3H, s, CO₂CH₃), 3.89 (3H, s, 3'-COCH₃); δ_{C} (176 MHz, CDCl₃) 165.9 (CO₂CH₃), 164.5 (C-2), 160.1 (C-3'), 155.5 (C-6), 141.0 (C-4), 139.9 (C-1'), 129.8 (C-5'), 119.4 (C-6'), 115.0 (C-4'), 112.6 (C-2'), 112.3 (C-5), 109.8 (C-3), 55.5 (2-COCH₃), 53.9 (3'-COCH₃), 52.8 (CO₂CH₃); ν_{max} (ATR) 1731, 1568, 1452, 1386, 1354, 1258, 1225, 1208, 1108, 1045 cm⁻¹; Accurate Mass (ASAP) *m/z* found [M]⁺ 273.1008; (C₁₅H₅NO₄) requires *M*, 273.1001.

Methyl-2-(trifluoromethyl)-6-(4'-methoxyphenyl)isonicotinate (343)

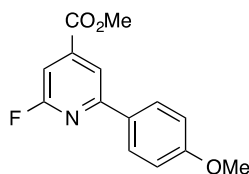


General procedure E was applied to methyl-2-(trifluoromethyl)isonicotinate (**326**) (83 mg, 0.4 mmol). Borylation with Stock Solution A for 24 h at room temperature gave 93% conversion (¹H NMR) to 6-(Bpin) product **337**. The Suzuki-Miyaura step was carried out for 16 h with Pd(dppf)Cl₂ (37 mg, 0.05 mmol), K₃PO₄ (170 mg, 0.8 mmol), 4-iodoanisole (100 mg, 0.44 mmol) in DMAc (2 mL) at 70 °C. Column eluent 3% EtOAc in heptane. **343** (82 mg, 66%) isolated as a white amorphous solid.

δ_{H} (600 MHz, CDCl₃) 8.42 (1H, s, 5-*H*), 8.10 (2H, m, 2', 6'-*H*), 8.05 (1H, d, *J* = 0.9, 3-*H*), 7.02 (2H, m, 3', 5'-*H*), 4.02 (3H, s, CO₂CH₃), 3.88 (3H, s, OCH₃); δ_{C} (151 MHz, CDCl₃)

164.9 (CO₂CH₃), 161.7 (C-4'), 158.8 (C-6), 149.1 (q, *J* = 35, C-2), 139.8 (C-4), 129.7 (C-1'), 128.8 (C-2', 6'), 121.6 (C-5), 121.5 (m, CF₃), 117.1 (q, *J* = 2.7, C-3), 114.5 (C-3', 5'), 55.6 (OCH₃), 53.2 (CO₂CH₃); δ_F (376 MHz, CDCl₃) -68.2 (s); ν_{max} (ATR) 1735, 1609, 1565, 1519, 1429, 1373, 1257, 1187, 1144, 1072, 1032, 979, 914 cm⁻¹; Accurate Mass (ASAP) *m/z* found [M]⁺ 311.0784; C₁₅H₁₂F₃NO₃ requires *M*, 311.0769.

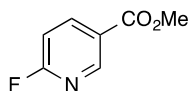
Methyl-2-fluoro-6-[4'-(methoxycarbonyl)phenyl]isonicotinate (344)



General procedure E was applied to methyl 2-fluoroisonicotinate (**327**) (170 mg, 1.1 mmol). Borylation with Stock Solution A for 18 h at room temperature gave full conversion (¹H NMR) to 6-(Bpin) product **339**. Suzuki-Miyaura cross-coupling was carried out for 1 h using Pd(dppf)Cl₂ (40 mg, 0.06 mmol), Cs₂CO₃ (717 mg, 2.2 mmol), 4-iodoanisole (510 mg, 2.2 mmol) in DMF (5 mL) at 100 °C in a microwave reactor. Column eluent 0-20% EtOAc in hexanes. **344** (157 mg, 55%) isolated as a colourless oil.

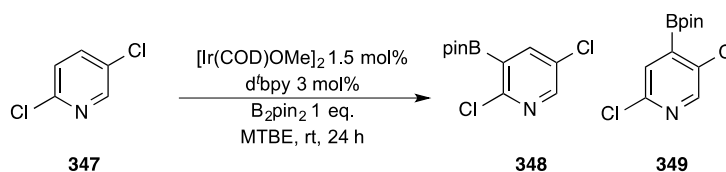
δ_H (700 MHz, CDCl₃) 8.13 (1H, m, 5-*H*), 8.03 (2H, m, 2', 6'-*H*), 7.32 (1H, m, 3-*H*), 7.00 (2H, m, 3', 5'-*H*), 4.00 (3H, s, CO₂CH₃), 3.88 (3H, s, COCH₃); δ_C (176 MHz, CDCl₃) 164.8 (d, *J* = 4.2, CO₂CH₃), 162.3 (d, *J* = 247.0, C-2), 161.5 (C-4'), 157.2 (d, *J* = 14.0, C-6), 143.4 (d, *J* = 8.0, C-4), 129.5 (C-1'), 128.6 (C-2', 6'), 116.3 (d, *J* = 5.0, C-5), 114.4 (C-3', 5'), 106.7 (d, *J* = 40.0 Hz, C-3), 55.6 (CO₂CH₃), 53.1 (OCH₃); δ_F (376 MHz, CDCl₃) -66.2 (s); ν_{max} (ATR) 1733, 1608, 1568, 1520, 1420, 1396, 1352, 1252, 1206 1177 cm⁻¹; GC/MS (EI) *m/z* 261 [M]⁺, 246 [M-CH₃]⁺, 230 [M-OCH₃], 218, 203, 187, 159; Accurate Mass (ASAP) *m/z* found [M]⁺ 261.0811; C₁₄H₁₂FNO₃ requires *M*, 261.0801

Methyl-6-fluoronicotinate (**346**)



General procedure D was applied to 6-fluoronicotinic acid (**345**) (0.99 g, 7.0 mmol). Column eluent 0-10% EtOAc in hexanes. **346** (0.65 g, 60%) isolated as a colourless oil. δ_{H} (600 MHz, CDCl_3) 8.88 (1H, d, $J = 2.4$, 2-*H*), 7.40 (1H, ddd, $J = 8.5$, 7.7, 2.4, 4-*H*), 7.00 (1H, dd, $J = 8.5$, 2.9, 5-*H*) 3.95 (3H, s, CO_2CH_3); δ_{C} (151 MHz, CDCl_3) 165.8 (d, $J = 246$, C-6), 164.7 (CO_2CH_3), 150.3 (d, $J = 16.5$, C-2), 142.5 (d, $J = 9.3$, C-4), 124.4 (d, $J = 4.5$, C-3); 109.5 (d, $J = 37.5$, C-5), 52.5 (CO_2CH_3); ν_{max} (ATR) 1721, 1601, 1430, 1311, 1277, 1220, 1134, 1058 cm^{-1} ; Accurate Mass (ESI) m/z found $[\text{M}+\text{H}]^+$ 156.0458; $\text{C}_7\text{H}_7\text{FNO}_3$ requires M , 156.0461.

Borylation of 2,5-dichloropyridine (**347**)



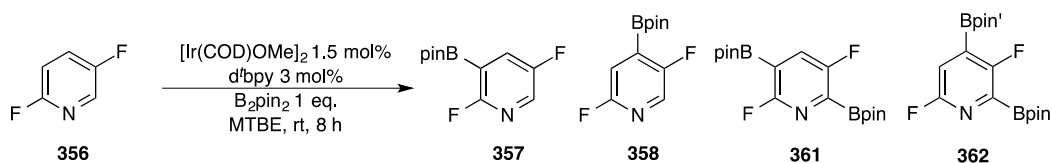
General procedure A was applied to **347** (148 mg, 1 mmol) using Stock Solution A. The reaction mixture was stirred at room temperature for 24 h giving 93% conversion (^1H NMR) to **348** and **349** in a 16:84 ratio. GC/MS analysis showed trace amounts of bis-borylated products.

Borylation of 2,5-lutidine (**350**)



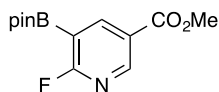
General procedure A was applied to **350** (107 mg, 1 mmol) using Stock Solution A. The reaction mixture was stirred at room temperature for 24 h giving 10% conversion (^1H NMR) to **352**.

Borylation of 2,5-difluoropyridine (**356**)



General procedure A was applied to 2,5-difluoropyridine (**356**) (115 mg, 1 mmol) using Stock Solution A. The reaction mixture was stirred at room temperature for 8 h giving full conversion (^1H NMR) to **357**, **358**, **361** and **362** in a 19:72:6:3 ratio.

Methyl-6-fluoro-5-(Bpin)nicotinate (**359**)

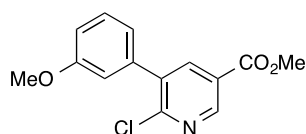


General procedure A was applied to methyl 6-fluoronicotinate (**346**) (109 mg, 0.7 mmol) using Stock Solution A. The reaction mixture was stirred at room temperature for 3 h giving full conversion (^1H NMR) to **359**. Column eluent 0-10% MeOH in DCM afforded **359** (141 mg, 77%) as a white amorphous solid.

δ_{H} (600 MHz, CDCl_3) 8.91 (1H, d, $J = 2.5$, 6-*H*), 8.74 (1H, dd, $J = 7.9$, 2.5, 4-*H*), 3.93 (3H, s, CO_2CH_3), 1.36 (12H, s, pin CH_3); δ_{C} (151 MHz, CDCl_3) 169.1 (d, $J = 251.0$, C-6), 164.9

(CO₂CH₃), 153.1 (d, *J* = 17.0, C-2), 150.0 (d, *J* = 9.0, C-4), 124.2 (d, *J* = 5.0, C-3), 84.9 (C(CH₃)₂), 52.5, (CO₂CH₃), 24.9 (pinCH₃); δ_B (128 MHz, CDCl₃) 29.7 (s(br)); δ_F (564 MHz, CDCl₃) -52.2 (m); ν_{max} (ATR) 1722, 1604, 1578, 1444, 1421, 1393, 1392, 1390, 1349, 1336, 1260, 1215, 1188, 1171, 1145, 1123, 1079 cm⁻¹. GC/MS (EI) *m/z* 281 [MH]⁺, 266 [M-CH₃], 250 [M-OCH₃]⁺, 238, 222 [M-CO₂CH₃]⁺, 208, 197, 182, 150; Accurate Mass (ASAP) *m/z* found [M+H]⁺ 281.1340; C₁₃H₁₈¹⁰BNO₄F requires *M*, 281.1349.

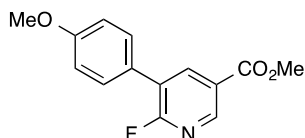
Methyl-6-chloro-5-(3'-methoxyphenyl)nicotinate (363)



General procedure E was applied to methyl-6-chloronicotinate (**353**) (172 mg, 1 mmol). Borylation with Stock Solution A for 24 h at room temperature gave 46% conversion (¹H NMR) to 5-(Bpin) product **354**. The Suzuki-Miyaura step was carried out for 1 h using Pd(dppf)Cl₂ (37 mg, 0.05 mmol), Cs₂CO₃ (652 mg, 2 mmol) and 3-iodoanisole (257 mg, 1.1 mmol) in DMF (3 mL) at 70 °C. Column eluent 0-15% EtOAc in heptane. **363** (89 mg, 32%) isolated as a white amorphous solid.

δ_H (700 MHz, CDCl₃) 8.98 (1H, d, *J* = 2.2, 2-*H*), 8.27 (1H, d, *J* = 2.2, 4-*H*), 7.39 (1H, m, 5'-*H*), 7.03 (1H, m, 6'-*H*), 6.99 (2H, m, 2', 4'-*H*), 3.97 (3H, s, CO₂CH₃), 3.86 (3H, s, COCH₃); δ_C (176 MHz, CDCl₃) 165.2 (CO₂CH₃), 159.7 (C-3'), 153.9 (C-6), 149.6 (C-2), 140.5 (C-4), 137.9 (C-1'), 136.9 (C-5), 129.8 (C-5'), 125.4 (C-3), 121.7 (C-6'), 115.1 (ArC), 114.4 (ArC), 55.5 (OCH₃), 52.8 (CO₂CH₃); ν_{max} (ATR) 1728, 1590, 1394, 1316, 1265, 1228, 1129, 1036, 907 cm⁻¹; Accurate Mass (ASAP) *m/z* found [M+H]⁺ 277.0497; C₁₄H₁₂³⁵CINO₃ requires *M*, 277.0506.

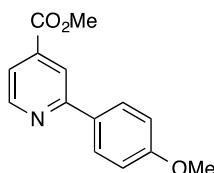
Methyl-6-fluoro-5-(4'-methoxyphenyl)nicotinate (364)



General procedure E was applied to methyl 6-fluoroisonicotinate (**346**) (109 mg, 0.7 mmol). Borylation with Stock Solution A for 3 h at room temperature gave full conversion (^1H NMR) to **359**. The Suzuki-Miyaura step was carried out for 1 h using $\text{Pd}(\text{dppf})\text{Cl}_2$ (26 mg, 0.04 mmol), Cs_2CO_3 (460 mg, 1.4 mmol), 4-iodoanisole (330 mg, 1.4 mmol) in DMF (3 mL) in DMF (3 mL) at 70 °C. Column eluent 0-50% EtOAc in hexanes. **364** (107 mg, 58%) isolated as a pale yellow amorphous solid.

δ_{H} (600 MHz, CDCl_3) 8.77 (1H, m, 6-*H*), 8.45 (1H, m, 4-*H*), 7.54 (2H, d, $J = 8.6$, 2', 5'-*H*), 7.01 (2H, d, $J = 8.6$, 3', 5'-*H*), 3.96 (3H, s, CO_2CH_3), 3.86 (3H, s, OCH_3); δ_{C} (151 MHz, CDCl_3) 165.0 (CO_2CH_3), 162.6 (d, $J = 246.2$, C-6), 160.3 (C-4'), 147.8 (dd, $J = 16.7, 5.1$, C-6), 141.5 (d, $J = 6.4$, C-4), 130.2 (d, $J = 6.4$, C-2', 6'), 125.1 (m, C-1'), 123.7 (d, $J = 28.6$, C-3), 114.5 (C-3', 5'), 55.5 (OCH_3), 52.7 (CO_2CH_3); δ_{F} (376 MHz, CDCl_3) -65.4 (s); ν_{max} (ATR) 1725, 1609, 1518, 1434, 1411, 1313, 1250, 1200, 1181, 1120, 1047, 1029 cm^{-1} ; Accurate Mass (ASAP) m/z found $[\text{M}]^+$ 261.0819; $\text{C}_{14}\text{H}_{12}\text{FNO}_3$ requires M , 261.0801

Methyl 2-(4'-methoxyphenyl)isonicotinate (366)

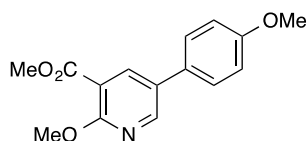


General procedure E was applied to methyl-2-chloroisonicotinate (**266**) (344 mg, 2 mmol). Borylation with Stock Solution A for 24 h at room temperature gave 73% conversion (^1H NMR) to 6-(Bpin) product **267**. The Suzuki-Miyaura step was carried out

for 1 h using Pd(dppf)Cl₂ (73 mg, 0.1 mmol), Cs₂CO₃ (1.3 g, 4 mmol) 4-iodoanisole (940 mg, 4 mmol) in DMF (5 mL) at 100 °C in a microwave reactor. Without purification, the crude cross-coupling reaction product was dissolved in ethanol (20 mL) and ammonium formate (2.5 g, 40 mmol) was added. The reaction vessel was evacuated and backfilled with nitrogen (x 3 cycles) before 10% Pd/C (106 mg, 0.1 mmol) was slowly added under a positive pressure of nitrogen. The reaction was stirred at room temperature for 2 h then filtered through a plug of celite and absorbed onto silica. Purification by flash column chromatography (0-20 % ethyl acetate in hexanes) afforded **366** as a white amorphous solid (0.23 g, 47%).

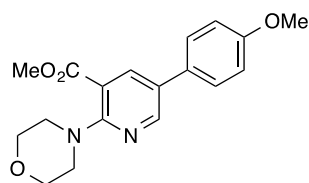
δ_{H} (700 MHz, CDCl₃) 8.77 (1H, d, $J = 5.0$ 6-*H*), 8.22 (1H, s, 3-*H*), 8.01 (2H, m, 2', 6'-*H*), 7.69 (1H, d, $J = 5.0$, 5-*H*), 7.00 (2H, m, 3', 5'-*H*), 3.97 (3H, s, CO₂CH₃), 3.86 (3H, s, OCH₃); δ_{C} (176 MHz, CDCl₃) 166.0 (CO₂CH₃), 161.0 (C-4'), 158.2 (C-2), 150.4 (C-6), 138.1 (C-4), 131.2 (C-1'), 128.4 (C-2', 6'), 120.4 (C-5), 119.0 (C-3), 114.3 (C-3', 5'), 55.5 (OCH₃), 52.8 (CO₂CH₃); ν_{max} (ATR) 1730, 1607, 1580, 1557, 1516, 1467, 1436, 1421, 1390, 1301, 1274, 1249, 1176, 1111, 1060, 1031 cm⁻¹; Accurate Mass (ASAP) m/z found [M+H]⁺ 244.0957; C₁₄H₁₄NO₃ requires M , 244.0974.

Methyl-2-methoxy-5-(4'-methoxyphenyl)nicotinate (319)



320 (115 mg, 0.44 mmol), and NaOMe (119 mg, 2.20 mmol) were refluxed in MeOH (5 mL) for 16 h. The reaction mixture was dry loaded onto silica and purified by flash column chromatography 0-15% EtOAc in heptane. **319** (229 mg, 81%) isolated as a white amorphous solid. *Data as previously stated.*

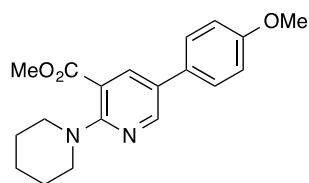
Methyl-2-(N-morpholinyl)-5-(4''-methoxyphenyl)nicotinate (369)



General Method F applied to **320** (120 mg, 0.46 mmol) with morpholine (**368**). Column eluent 20-30% EtOAc in heptane. **369** (141 mg, 93%) isolated as a white amorphous solid.

δ_{H} (700 MHz, CDCl_3) 8.51 (1H, s, 6-*H*), 8.20 (1H, s, 4-*H*), 7.47 (2H, d, $J = 8.0$, 2'', 6''-*H*), 6.98 (2H, d, $J = 8.0$, 3'', 5''-*H*), 3.91 (3H, s, CO_2CH_3), 3.85 (7H, m, OCH_3 , 3', 5'-*H*), 3.44 (4H, m, 2', 6'-*H*); δ_{C} (176 MHz, CDCl_3) 167.5 (CO_2CH_3), 159.3 (C-4''), 158.2 (C-2), 148.4 (C-6), 138.8 (C-4), 129.5 (C-1''), 127.6 (C-5), 127.4 (C-2'', 6''), 114.5 (C-3'', 5''), 113.6 (C-3), 66.9 (C-3', 5'), 55.4 (OCH_3), 52.2 (CO_2CH_3), 49.9 (C-2'', 6''); ν_{max} (ATR) 1717, 1601, 1472, 1440, 1246, 1212, 1182, 1114, 1087 cm^{-1} ; Accurate Mass (ESI) m/z found $[\text{M}+\text{H}]^+$ 329.1510; $\text{C}_{18}\text{H}_{21}\text{N}_2\text{O}_4$ requires M , 329.1501.

Methyl-2-(N-piperazinyl)-5-(4''-methoxyphenyl)nicotinate (371)

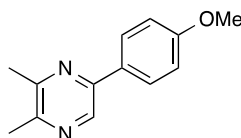


General Method F applied to **320** (51 mg, 0.20 mmol) with piperazine (**370**). Column eluent 0-15% EtOAc in heptane. **371** (57 mg, 89%) isolated as a yellow amorphous solid.

δ_{H} (700 MHz, CDCl_3) 8.47 (1H, d, $J = 2.4$, 6-*H*), 8.11 (1H, d, $J = 2.4$, 4-*H*), 7.45 (2H, d, $J = 8.6$, 2'', 6''-*H*), 6.97 (2H, d, $J = 8.6$, 3'', 5''-*H*), 3.91 (3H, s, CO_2CH_3), 3.84 (3H, s, OCH_3), 3.39 (4H, m, 2', 6'-*H*), 1.68 (6H, m, 3', 4', 5'-*H*); δ_{C} (176 MHz, CDCl_3) 168.4 (CO_2CH_3), 159.2 (C-4''), 158.6 (C-2), 148.3 (C-6), 138.7 (C-4), 130.0 (C-1''), 127.5 (C-2'', 6''), 126.4

(C-5) 114.6 (C-3', 5'), 113.4 (C-3), 55.5 (OCH₃), 52.3 (CO₂CH₃), 50.7 (C-2', 6'), 26.1 (AlkC), 24.7 (AlkC); ν_{\max} (ATR) 1716, 1694, 1608, 1441, 1247, 1180 cm⁻¹; Accurate Mass (ESI) m/z found [M+H]⁺ 327.1701; C₁₉H₂₃N₂O₃ requires M , 327.1709.

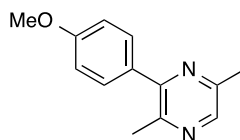
2,3-Dimethyl-5-(4'-methoxyphenyl)pyrazine (391)



General procedure E was applied to 2,3-dimethylpyrazine (**383**) (108 mg, 1 mmol). Borylation with Stock Solution B for 24 h at room temperature gave 90% conversion (¹H NMR) to 5-(Bpin) product **384**. The Suzuki-Miyaura step was carried out for 1 h using Pd(dppf)Cl₂ (73 mg, 0.1 mmol), K₃PO₄ (420 mg, 2 mmol), 4-iodoanisole (260 mg, 1.1 mmol) and CuCl (99 mg, 1 mmol) in DMAc (2.5 mL) at 70 °C. Column eluent 15% EtOAc in hexanes. **391** (94 mg, 44%) isolated as a grey amorphous solid.

δ_{H} (600 MHz, CDCl₃) 8.65 (1H, s, 6-*H*), 7.94 (2H, d, $J = 8.8$, 2', 6'-*H*), 7.00 (2H, d, $J = 8.8$, 3', 5'-*H*), 3.86 (3H, s, OCH₃), 2.58 (3H, s, CH₃), 2.55 (3H, s, CH₃); δ_{C} (151 MHz, CDCl₃) 160.8 (C-4'), 151.6 (C-3), 149.7 (C-2), 149.3 (C-5), 137.8 (C-6), 129.6 (C-1'), 128.1 (C-2', 6'), 114.5 (C-3', 5'), 55.5 (OCH₃), 22.4 (CH₃), 21.8 (CH₃); ν_{\max} (ATR) 1609, 1514, 1456, 1290, 1251, 1177, 1033, 906 cm⁻¹; Accurate Mass (ASAP) m/z found [M+H]⁺ 215.1187; C₁₃H₁₅N₂O requires M , 215.1184.

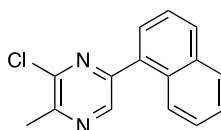
2,5-Dimethyl-3-(4'-methoxyphenyl)pyrazine (**392**)



General procedure E was applied to 2,5-dimethylpyrazine (**386**) (108 mg, 1 mmol). Borylation with Stock Solution B for 16 h at 80 °C gave 56% conversion (¹H NMR) to 3-(Bpin) product **387**. The Suzuki-Miyaura step was carried out for 16 h with Pd(dppf)Cl₂ (37 mg, 0.05 mmol), K₃PO₄ (420 mg, 2 mmol), 4-iodoanisole (260 mg, 1.1 mmol) in DMAc:H₂O (9:1) (2.5 mL) at 70 °C. Column eluent 10-25% EtOAc in heptane. **392** (59 mg, 28%) isolated as a pale yellow oil.

δ_{H} (600 MHz, CDCl₃) 8.28 (1H, s, 6-*H*), 7.52 (2H, m, 2', 6'-*H*), 7.00 (2H, m, 3', 5'-*H*), 3.86 (3H, s, OCH₃), 2.58 (3H, s, CH₃), 2.56 (3H, s, CH₃); δ_{C} (151 MHz, CDCl₃) 160.1 (C-4'), 152.6 (C-3), 150.4 (ArC), 148.2 (ArC), 141.5 (C-6), 131.5 (C-1'), 130.5 (C-2', 6'), 114.0 (C-3', 5'), 55.5 (OCH₃), 22.9 (2-CCH₃), 21.3 (5-CCH₃); ν_{max} (ATR) 1610, 1513, 1448, 1407, 1372, 1290, 1249, 1176, 1161, 1068, 1033, 968, 908 cm⁻¹; Accurate Mass (ASAP) m/z found [M+H]⁺ 215.1183; C₁₃H₁₅N₂O requires M , 215.1184.

2-Chloro-3-methyl-6-naphthalen-1'-yl-pyrazine (**393**)



General procedure E was applied to 2-chloro-3-methylpyrazine (**388**) (185 mg, 1.44 mmol). Borylation with Stock Solution C for 24 h at room temperature gave 91% conversion (¹H NMR) to 5-(Bpin) (**389**) and 6-(Bpin) (**390**) products in a 1:3 ratio. The Suzuki-Miyaura step was carried out for 1 h with Pd(dppf)Cl₂ (110 mg, 0.14 mmol), K₃PO₄ (611 mg, 2.88 mmol), 1-bromonaphthalene (600 mg, 2.88 mmol) and CuCl (143 mg, 1.44

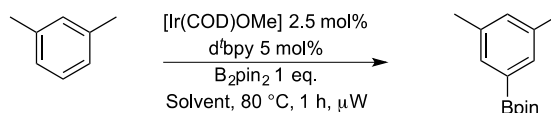
mmol) in DMAc (3 mL) at 70 °C. Column eluent 0-20% Et₂O in hexanes. **393** (85 mg, 23%) isolated as a white amorphous solid. Product tentatively assigned as 6-naphthalenyl isomer.

δ_{H} (700 MHz, CDCl₃) 8.69 (1H, s, 5-*H*), 8.10 (1H, m, *ArH*), 7.96 (1H, d, *J* = 8.2, *ArH*), 7.93 (1H, m, *ArH*), 7.64 (1H, d, *J* = 8.2 Hz, *ArH*), 7.57 (1H, m, 3'-*H*), 7.53 (2H, m, *ArH*) 2.78 (3H, s, CH₃); δ_{C} (176 MHz, CDCl₃) 152.0 (*ArC*), 151.1 (*ArC*), 148.3 (*ArC*), 142.7 (*C*-5), 134.1 (*ArC*), 133.4 (*ArC*), 131.03 (*ArC*), 130.3 (*ArC*), 128.7 (*ArC*), 128.4 (*ArC*), 127.3 (*ArC*), 126.4 (*ArC*), 125.4 (*C*-3'), 124.9 (*ArC*), 22.2 (CH₃); GC/MS (EI) *m/z* 256 [M(³⁷Cl)]⁺, 254 [M(³⁵Cl)]⁺, 219 [M-Cl]⁺, 127 [C₁₀H₈]⁺; Accurate Mass (ASAP) *m/z* found [M+H]⁺ 255.0676; C₁₅H₁₂³⁵ClN₂ requires *M*, 255.0689.

Borylation of 2,3-dimethylpyrazine (383): Synthesis of 2,3-dimethyl-5-(Bpin)-pyrazine (384)

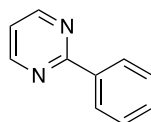
A solution of [Ir(COD)OMe]₂ (17 mg, 0.025 x 10 mmol) and dtbpy (13 mg, 0.05 mmol) in MTBE (2 mL) was added to a solution of B₂pin₂ (254 mg, 1 mmol) and **383** (108 mg, 1 mmol) in MTBE (3 mL). After stirring at room temperature for 24 h ¹H NMR spectroscopic analysis revealed 76% conversion to **384**. The reaction was quenched with D₂O (2 drops) before being concentrated and analysed by both ¹H and ²H NMR spectroscopy; δ_{D} (Acetone d₆, 92.1 MHz): 8.30 ppm (s, 1D).

Solvent Screen using *m*-xylene (**198**)



General Method A was applied to **198** (106 mg, 1 mmol) using Stock Solution B prepared in a series of solvents. The reactions were irradiated at 80 °C for 1 h in a microwave reactor and analysed by *in-situ* ¹H NMR analysis.

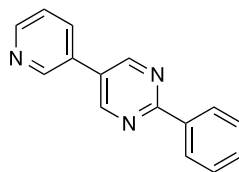
2-Phenylpyrimidine (**398**)



A mixture of 2-chloropyrimidine (**396**) (1g, 8.7 mmol), phenylboronic acid (**4**) (1.3 g, 10.4 mmol) Na₂CO_{3(aq)} (2M, 1.84 g, 17.4 mmol) and PdCl₂(PPh₃)₂ (310 mg, 0.44 mmol) in dioxane (8.7 mL) was heated at 90 °C for 16 h. The reaction was then cooled to room temperature and the volume was then reduced *in vacuo*. The aqueous residue was diluted with water (10 mL) and extracted with EtOAc (2 x 10 mL). The combined organics were washed with brine (10 mL), dried over MgSO₄, filtered and concentrated *in vacuo*. The crude product was purified by flash column chromatography (10% EtOAc in hexanes) to give **398** (0.99g, 73%) as a white amorphous solid.

δ_{H} (700 MHz, CDCl₃) 8.79 (2H, d, $J = 4.8, 4, 6\text{-H}$), 8.45 (2H, m, 2', 6'-H), 7.49 (3H, m, 3', 4', 5'-H), 7.15 (1H, t, $J = 4.8, 5\text{-H}$); δ_{C} (176 MHz, CDCl₃) 164.8 (C-2), 157.3 (C-4, 6), 137.7 (C-1'), 130.9 (ArC), 128.7 (ArC), 128.2 (C-2', 6'), 119.2 (C-5); ν_{max} (ATR) 1566, 1553, 1414, 1407, 1317, 1173, 1026 cm⁻¹; Accurate Mass (ESI) m/z found [M+H]⁺ 157.0765; C₁₀H₉N₂ requires M , 157.0766.

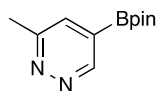
2-Phenyl-5-pyridin-3''-yl-pyrimidine (**401**)



General procedure B was applied to 2-phenylpyrimidine (**398**) (94 mg, 0.6 mmol) using additional B₂pin₂ (15 mg, 0.06 mmol). The reaction was stirred at room temperature for 24 h. NMR spectroscopic analysis of the crude mixture showed 76% conversion to 5-(Bpin) product **399**. As per General Method E, Pd(amphos)Cl₂ (21 mg, 0.03 mmol), K₃PO₄ (254 mg, 1.2 mmol), 3-iodopyridine (135 mg, 0.66 mmol) and DMAc:H₂O (9:1) (5 mL) were added to the crude mixture and the reaction was heated to 70 °C for 2 h. Flash column chromatography heptane:EtOAc (1:1) provided **401** as an orange amorphous solid (110 mg, 47%).

δ_{H} (700 MHz, CDCl₃) 9.03 (2H, s, 4, 6-*H*), 8.92 (1H, s, 2''-*H*), 8.72 (1H, d, *J* = 4.6, 6''-*H*), 8.50 (2H, m, 2', 6'-*H*), 7.95 (1H, d, *J* = 7.8, 4''-*H*), 7.53 (3H, m, 3', 5', 4'-*H*), 7.48 (1H, dd, *J* = 7.8, 4.6, 5''-*H*); δ_{C} (176 MHz, CDCl₃) 164.4 (C-2), 155.4 (C-4, 6), 150.0 (C-6''), 147.9 (C-2''), 137.1 (C-1'), 134.3 (C-4''), 131.2 (C-4'), 130.7 (C-5), 128.9 (C-3', 5', 3''), 128.4 (C-2', 6'), 124.2 (C-5''); ν_{max} (ATR) 1534, 1442, 1425, 1374, 1334 cm⁻¹; Accurate Mass (ASAP) *m/z* found [M]⁺ 233.0954; (C₁₅H₁₁N₃) requires *M*, 233.0953.

3-Methyl-5-(Bpin)-pyridazine (**410**)

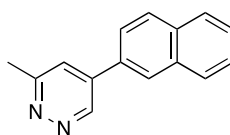


General procedure A was applied to 3-methylpyridazine (**407**) (94 mg, 1.0 mmol) using Stock Solution B. The reaction mixture was stirred at room temperature for 24 h at which point the observed precipitate was filtered and washed copiously with cold MTBE. The

crude solid was recrystallized from hot MTBE, then filtered and washed copiously again with cold MTBE. **410** (139 mg, 63%) was isolated as a powdered beige solid containing minor impurities.

δ_{H} (700 MHz, CDCl_3) 9.22 (1H, s, 6-*H*), 7.64 (1H, s, 4-*H*), 2.71 (3H, s, CH_3), 1.35 (12H, s, pin CH_3); δ_{C} (176 MHz, CDCl_3) 159.8 (C-3), 152.7 (C-6), 132.5 (C-4), 85.2 (C(CH_3)₂), 25.0 (pin CH_3), 22.4 (CH_3); δ_{B} (128 MHz, CDCl_3) 30.2 (s(br)).

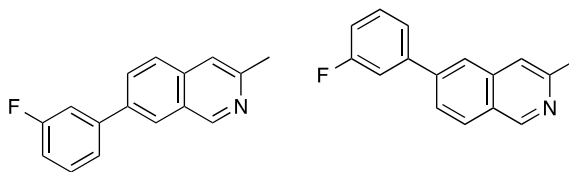
3-Methyl-5-naphthalen-2'-ylpyridazine (**413**)



General procedure E was applied to 3-methylpyridazine (**407**) (94 mg, 1 mmol). Borylation with Stock Solution B for 24 h at room temperature gave full conversion to 5-(Bpin) product **410**. The Suzuki-Miyaura step was carried out for 3 h with Pd(amphos) Cl_2 (35 mg, 0.05 mmol), K_3PO_4 (420 mg, 2 mmol), 2-bromonaphthalene (230 mg, 1.1 mmol) in DMAc:H₂O (9:1) (2.5 mL). Column eluent 60% EtOAc in heptane. **413** (96 mg, 44%) was isolated as an orange amorphous solid.

δ_{H} (700 MHz, CDCl_3) 9.43 (1H, d, $J = 2.0$, 6-*H*), 8.16 (1H, s, 1'-*H*), 8.00 (1H, d, $J = 8.5$, 4'-*H*), 7.93 (2H, m, 5', 8'-*H*), 7.75 (1H, dd, $J = 8.5$, 1.7, 3'-*H*), 7.63 (1H, d, $J = 2.0$, 4-*H*), 7.58 (2H, m, 6', 7'-*H*), 2.83 (3H, s, CH_3); δ_{C} (176 MHz, CDCl_3) 160.0 (C-3), 148.0 (C-6), 138.5 (C-5), 133.7 (C-4a), 133.4 (C-1a), 132.0 (C-2'), 129.4 (C-4'), 128.5 (ArC), 127.8 (ArC), 127.4 (ArC), 127.0 (ArC), 126.9 (C-1'), 124.0 (C-3'), 123.8 (C-4), 22.4 (CH_3); ν_{max} (ATR) 1590 cm^{-1} ; Accurate Mass (ASAP) m/z found $[\text{M}]^+$ 220.0999; $\text{C}_{15}\text{H}_{12}\text{N}_2$ requires M , 220.1000.

3-Methyl-6-(3'-fluorophenyl)isoquinoline (**423**) and *3-Methyl-7-(3'-fluorophenyl)isoquinoline* (**424**)

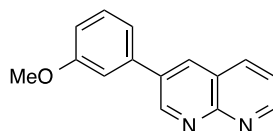


General procedure E was applied to 3-methylisoquinoline (**419**) (143 mg, 1 mmol). Borylation with Stock Solution B for 24 h at room temperature gave a 75% conversion to 6-(Bpin) (**420**) and 7-(Bpin) (**421**) products in 53:47 ratio. The Suzuki-Miyaura step was carried out for 1 h with 2nd Generation PdXPhos (39 mg, 0.05 mmol), K₃PO₄ (420 mg, 2 mmol), 3-fluoro-iodobenzene (244 mg, 1.1 mmol) in dioxane:H₂O (5:1) (2.5 mL) at 70 °C. Reverse phase column chromatography gave **423** and **424** as an inseparable mixture (150 mg, 63%).

δ_{H} (600 MHz, CDCl₃) 9.23 (1H, s, **424**, 1-*H*), 9.20 (1H, s, **423**, 1-*H*), 8.09 (1H, s, **424**, 8-*H*), 7.99 (1H, m, **423**, 8-*H*), 7.86 (2H, m, **423**, 5-*H* and **424**, 6-*H*), 7.80 (1H, m, **424**, 5-*H*), 7.73 (1H, m, **423**, 7-*H*), 7.51 (1H, s, **423**, 4-*H*), 7.50 (1H, s, **424**, 4-*H*), 7.47 (4H, m, **423**, 5', 6'-*H* and **424**, 5', 6'-*H*), 7.40 (1H, s, 2'-*H*), 7.38 (1H, s, 2'-*H*), 7.10 (2H, m, **423**, 4'-*H* and **424**, 4'-*H*), 2.72 (6H, s, **423**, CH₃ and **424**, CH₃); δ_{C} (151 MHz, CDCl₃) 163.3 (d, $J = 247.6$, C-3'), 163.2 (d, $J = 247.6$, C-3'), 152.3 (**423**, C-3), 152.3 (**424**, C-1), 152.1 (**424**, C-3), 151.7 (**423**, C-1), 142.6 (d, $J = 13.6$, **423**, C-1'), 142.6 (d, $J = 13.6$, **424**, C-1'), 141.6 (d, $J = 3.0$, **423**, C-6), 137.7 (d, $J = 3.0$, **424**, C-7), 136.8 (**423**, C-4a), 135.9 (**424**, C-4a), 130.5 (ArC), 130.4 (ArC), 129.6 (**424**, C-6), 128.2 (**423**, C-8), 127.00 (**424**, C-1a), 126.7 (**424**, C-5), 126.1 (**423**, C-1a), 125.8 (**423**, C-7), 125.4 (**424**, C-8), 123.9 (**423**, C-5), 123.2 (d, $J = 3.0$, ArC), 122.9 (d, $J = 3.0$, ArC), 118.6 (**423**, C-4), 118.2 (**424**, C-4), 114.9 (d, $J = 21.1$, C-4'), 114.5 (d, $J = 21.1$, C-4'), 114.4 (d, $J = 21.1$, C-2'), 114.1 (d, $J = 22.7$, C-2'), 24.3 (CH₃), 24.2 (CH₃); δ_{F} (376 MHz, CDCl₃): -112.6 (m, **423**, C-F and **424**, C-F); ν_{max}

(ATR) 1630, 1587, 1479, 1447, 1262, 1173, 1159, 904 cm^{-1} ; Accurate Mass (ESI) m/z found $[\text{M}+\text{H}]^+$ 238.1032; $\text{C}_{16}\text{H}_{13}\text{NF}$ requires M , 238.1034.

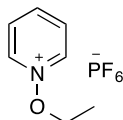
3-(3'-Methoxyphenyl)-1,8-naphthyridine (427)



General procedure E was applied to 1,8-naphthyridine (**425**) (130 mg, 1 mmol). Borylation with Stock Solution C (in THF) for 24 h at room temperature gave an approximate 65% conversion to 3-(Bpin) product **426**. The Suzuki-Miyaura step was carried out for 1 h with 2nd Generation PdXPhos (39 mg, 0.05 mmol), K_3PO_4 (420 mg, 2 mmol), 3-iodoanisole (257 mg, 1.1 mmol) in dioxane: H_2O (5:1) (2.5 mL) at 70 °C. Column eluent 0-3% MeOH in DCM. **427** (110 mg, 47%) isolated as an orange amorphous solid.

δ_{H} (700 MHz, $(\text{CD}_3)_2\text{CO}$): 9.41 (1H, d, $J = 2.6$, 2-*H*), 9.10 (1H, dd, $J = 4.1$, 2.0, 7-*H*), 8.65 (1H, d, $J = 2.6$, 4-*H*), 8.49 (1H, dd, $J = 8.1$, 2.0, 5-*H*), 7.64 (1H, dd, $J = 8.1$, 4.1, 6-*H*), 7.49 (1H, m, 5'-*H*), 7.44 (2H, m, 2', 6'-*H*), 7.05 (1H, m, 4'-*H*), 3.92 (3H, s, OCH_3); δ_{C} (176 MHz, $(\text{CD}_3)_2\text{CO}$) 161.5 (C-3'), 156.6 (C-1a), 154.2 (C-7), 153.4 (C-2), 139.4 (C-1'), 138.4 (C-5), 135.2 (C-3), 135.1 (C-4), 131.2 (C-5'), 123.5 (C-4a), 123.5 (C-6), 120.5 (ArC), 114.9 (C-4'), 113.8 (ArC), 55.8 (OCH_3); ν_{max} (ATR) 1599, 1581, 1479, 1469, 1358, 1326, 1285, 1208, 1171, 1043, 1031 cm^{-1} ; Accurate Mass (ESI) m/z found $[\text{M}+\text{H}]^+$ 237.1028; $\text{C}_{15}\text{H}_{13}\text{N}_2\text{O}$ requires M , 237.1025.

N-Ethoxy-pyridinium hexafluorophosphate (**431**)

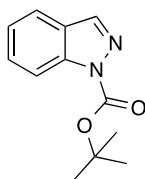


Under N₂, a solution of pyridine-N-oxide (**428**) (1 g, 10.5 mmol) and triethyloxonium hexafluorophosphate (**430**) (3.13 g, 12.6 mmol) in DCM (10 mL) was stirred at room temperature for 6 h. The reaction was then concentrated *in vacuo*. The resulting pink solid was crystallised at room temperature overnight from EtOAc (10 mL). The crystals were filtered and washed with cold EtOAc (3 x 15 mL) to give **431** as a white amorphous solid (1.72 g, 61%).

δ_{H} (600 MHz, CDCl₃) 9.44 (2H, m, 2, 6-*H*), 8.63 (1H, m, 4-*H*), 8.26 (2H, m, 3, 5-*H*), 4.71 (2H, q, $J = 7.0$, OCH₂CH₃), 1.39 (3H, t, $J = 7.0$, OCH₂CH₃); δ_{C} (151 MHz, CDCl₃) 145.6 (C-4), 142.1 (C-2, 6), 129.7 (C-3, 5), 79.5 (OCH₂CH₃), 13.3 (OCH₂CH₃); δ_{F} (376 MHz, CDCl₃) -70.6 (d, $J = 713.6$ Hz); δ_{P} (162 MHz, CDCl₃) 164.6 (hept, $J = 713.6$) ; Accurate Mass (ESI) m/z found [M-PF₆]⁺ 124.0754; C₇H₁₀NO requires M , 124.0762.

Borylation of Indazoles

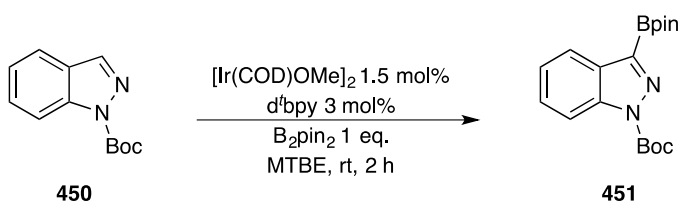
*t*Butyl-1H-indazole-1-carboxylate (**450**)



General Method G applied to indazole (**402**) (500 mg, 4.0 mmol). Column eluent 0-20% Et₂O in hexanes. **450** (850 mg, 98%) isolated as a colourless oil.

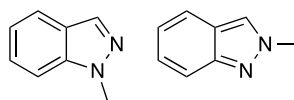
δ_{H} (600 MHz, CDCl₃) 8.12 (1H, d, $J = 7.9$, 7-*H*), 8.09 (1H, s, 3-*H*), 7.63 (1H, d, $J = 7.9$, 4-*H*), 7.43 (1H, t, $J = 7.9$, 6-*H*), 7.21 (1H, t, $J = 7.9$, 5-*H*), 1.66 (9H, s, C(CH₃)₃); δ_{C} (151 MHz, CDCl₃) 149.1 (CO₂^tBu), 139.6 (C-1a), 139.4 (C-3), 128.7 (C-6), 125.7 (C-3a), 123.5 (C-5), 120.9 (C-4), 114.5 (C-7), 84.6 (C(CH₃)₃), 28.1 (C(CH₃)₃); LC/MS (ES⁺) m/z 460[M₂Na]⁺, 241 [MNa]⁺, 219 [M]⁺, 164 [M-C₄H₉]⁺, 119 [M-COC₄H₉]⁺; Accurate Mass (ESI) m/z found [M+Na]⁺ 241.0974; C₁₂H₁₄N₂O₂Na requires M , 241.0953.

Borylation of *t*butyl-1H-indazole-1-carboxylate (**450**)



General procedure A was applied to **450** (97 mg, 0.4 mmol) using Stock Solution A. *In-situ* ¹H NMR monitoring showed full conversion to **451** after 2 h.

1-Methyl-1H-indazole (**404**) and 2-Methyl-2H-indazole (**453**)^{193,194}

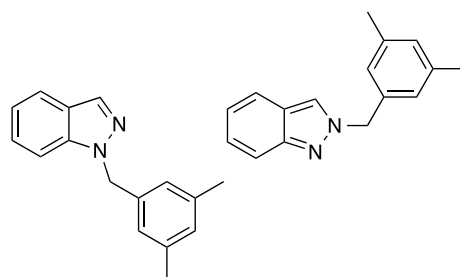


General Method H applied to indazole (**402**) (1 g, 8.5 mmol) with methyl iodide (**452**). Column eluent 20% EtOAc in hexanes. **404** (0.54 g) and **453** (0.34 g) (total yield 0.88 g, 78%) isolated as white amorphous solids.

404: δ_{H} (700 MHz, CDCl_3) 7.99 (1H, s, 3-*H*), 7.73 (1H, d, $J = 8.0$, 4-*H*), 7.39 (2H, m, 6, 7-*H*), 7.15 (1H, ddd, $J = 8.0, 5.0, 2.6$, 5-*H*), 4.08 (3H, s, NCH_3); δ_{C} (176 MHz, CDCl_3) 140.0 (C-1a), 132.8 (C-3), 126.3 (C-6), 124.1 (C-3a), 121.2 (C-4), 120.5 (C-5), 109.0 (C-7), 35.6 (NCH_3); LC/MS (ES^+) m/z 133 [M]⁺.

453: δ_{H} (700 MHz, CDCl_3): 7.87 (1H, s, 3-*H*), 7.69 (1H, d, $J = 8.9$, 7-*H*), 7.63 (1H, d, $J = 8.2$, 4-*H*), 7.27 (1H, m, 6-*H*), 7.07 (1H, m, 5-*H*), 4.21 (3H, s, NCH_3); δ_{C} (176 MHz, CDCl_3): 149.2 (C-1a), 126.0 (C-6), 123.6 (C-3), 122.3 (C-3a), 121.8 (C-5), 120.1 (C-4), 117.4 (C-7), 40.5 (NCH_3); LC/MS (ES^+) m/z 134 [$\text{M}+\text{H}$]⁺.

1-(3', 5'-Dimethylbenzyl)-1H-indazole (**455**) and 2-(3', 5'-Dimethylbenzyl)-2H-indazole (**456**)

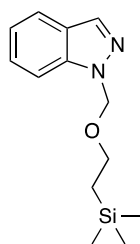


General procedure H was applied to indazole (**402**) (1 g, 8.5 mmol) with 3,5-dimethylbenzyl bromide (**454**). Column eluent 10% EtOAc in hexanes. **455** (0.70 g) and **456** (1.05 g) (total yield 1.75 g, 87%) isolated as colourless oils.

455: δ_{H} (700 MHz, CDCl_3) 8.04 (1H, s, 3-*H*), 7.74 (1H, m, 4-*H*), 7.38 (1H, m, 7-*H*), 7.34 (1H, m, 6-*H*), 7.14 (1H, m, 5-*H*), 6.89 (1H, s, 4'-*H*), 6.84 (2H, s, 2', 6'-*H*), 5.52 (2H, s, NCH_2Ar), 2.25 (6H, s, CH_3); δ_{C} (176 MHz, CDCl_3) 139.7 (C-1a), 138.5 (C-3', 5'), 136.9 (C-1'), 133.4 (C-3), 129.6 (C-4'), 126.5 (C-6), 125.3 (C-2', 6'), 124.50 (C-3a), 121.3 (C-4), 120.7 (C-5), 109.5 (C-7), 53.1 (NCH_2Ar), 21.5 (CH_3); GC/MS (EI) m/z 236 $[\text{M}]^+$, 119 $[\text{M}-\text{CH}_2\text{C}_6\text{H}_3(\text{CH}_3)_2]^+$, 91 $[\text{CH}_2\text{C}_6\text{H}_5]^+$, 77 $[\text{C}_6\text{H}_5]^+$; Accurate Mass (ESI) found $[\text{M}]^+$ 236.1321; $\text{C}_{16}\text{H}_{16}\text{N}_2$ requires M , 236.1313.

456: δ_{H} (700 MHz, CDCl_3) 7.88 (1H, s, 3-*H*), 7.73 (1H, m, 7-*H*), 7.63 (1H, m, 4-*H*), 7.28 (1H, m, 6-*H*), 7.07 (1H, m, 5-*H*), 6.96 (1H, s, 4'-*H*), 6.92 (2H, s, 2', 6'-*H*), 5.52 (2H, s, NCH_2Ar), 2.29 (6H, s, CH_3); δ_{C} (176 MHz, CDCl_3): 149.1 (C-1a), 138.8 (C-3', 5'), 135.7 (C-1'), 130.2 (C-4'), 126.1 (C-2', 6'), 126.0 (C-6), 122.9 (C-3), 122.3 (C-3a), 121.8 (C-5), 120.3 (C-4), 117.8 (C-7), 57.8 (NCH_2Ar), 21.4 (CH_3); GC/MS (EI) m/z 236 $[\text{M}]^+$, 119 $[\text{M}-\text{CH}_2\text{C}_6\text{H}_3(\text{CH}_3)_2]^+$, 91 $[\text{CH}_2\text{C}_6\text{H}_5]^+$, 77 $[\text{C}_6\text{H}_5]^+$; Accurate Mass (ESI) found $[\text{M}]^+$ 236.1318; $\text{C}_{16}\text{H}_{16}\text{N}_2$ requires M , 236.1313.

1- $[\text{2}-(\text{Trimethylsilyl})\text{ethoxy}]\text{methyl}$ -1*H*-indazole (**458**)

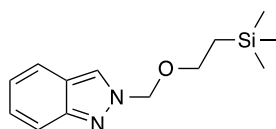


General Method H was applied to indazole (**402**) (0.5 g, 4.2 mmol) with 2-(trimethylsilyl)ethoxymethyl chloride (**457**). Column eluent 0-50% EtOAc in hexanes. **458** (0.69 g, 66%) isolated as a colourless oil.

δ_{H} (700 MHz, CDCl_3) 8.02 (1H, s, 3-*H*), 7.75 (1H, d, $J = 7.9$, 4-*H*), 7.59 (1H, d, $J = 7.9$, 7-*H*), 7.42 (1H, t, $J = 7.9$, 6-*H*), 7.20 (1H, t, $J = 7.9$, 5-*H*), 5.75 (2H, s, NCH_2O), 3.55 (2H, t,

$J = 8.2$, OCH_2CH_2), 0.88 (2H, t, $J = 8.2$, $\text{CH}_2\text{Si}(\text{CH}_3)_3$), -0.07 (9H, s, $\text{Si}(\text{CH}_3)_3$); δ_{C} (176 MHz, CDCl_3) 139.9 (C-1a), 134.2 (C-3), 126.9 (C-6), 125.0 (C-3a), 121.5 (C-5), 121.2 (C-4), 109.8 (C-7), 77.9 (NCH_2O), 66.6 (OCH_2CH_2), 18.0 ($\text{CH}_2\text{Si}(\text{CH}_3)_3$), -1.3 ($\text{Si}(\text{CH}_3)_3$); GC/MS (EI) m/z 248 $[\text{M}]^+$, 175 $[\text{M}-\text{SiMe}_3]^+$, 148 $[\text{M}-\text{CH}_2\text{CH}_2\text{SiMe}_3]^+$, 132 $[\text{M}-\text{OCH}_2\text{CH}_2\text{SiMe}_3]^+$, 118 $[\text{M}-\text{CH}_2\text{OCH}_2\text{CH}_2\text{SiMe}_3]^+$; Accurate Mass (ESI) m/z found $[\text{M}+\text{H}]^+$ 249.1470 ; $\text{C}_{13}\text{H}_{21}\text{N}_2\text{OSi}$ requires M , 249.1423 .

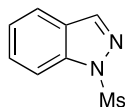
2-[[2-(Trimethylsilyl)ethoxy]methyl]-2H-indazole (**459**)



General procedure I was applied to indazole (**402**) (0.5 g, 4.2 mmol). Column eluent 0-10% EtOAc in hexanes. **459** (0.77 g, 74%) isolated as a colourless oil.

δ_{H} (700 MHz, CDCl_3) 8.10 (1H, s, 3- H), 7.73 (1H, d, $J = 8.1$, 7- H), 7.68 (1H, d, $J = 8.1$, 4- H), 7.30 (1H, t, $J = 8.1$, 6- H), 7.10 (1H, t, $J = 8.1$, 5- H), 5.73 (2H, s, NCH_2O), 3.63 (2H, t, $J = 8.3$, OCH_2CH_2), 0.94 (2H, t, $J = 8.3$, $\text{CH}_2\text{Si}(\text{CH}_3)_3$), -0.03 (9H, s, $\text{Si}(\text{CH}_3)_3$); δ_{C} (176 MHz, CDCl_3) 149.0 (C-1a), 126.5 (C-6), 122.7 (C-3), 122.4 (C-3a), 122.3 (C-5), 120.6 (C-4), 118.1 (C-7), 82.0 (NCH_2O), 67.6 (OCH_2CH_2), 18.0 ($\text{CH}_2\text{Si}(\text{CH}_3)_3$), -1.3 ($\text{Si}(\text{CH}_3)_3$); GC/MS (EI) m/z 248 $[\text{M}]^+$, 175 $[\text{M}-\text{SiMe}_3]^+$, 148 $[\text{M}-\text{CH}_2\text{CH}_2\text{SiMe}_3]^+$, 132 $[\text{M}-\text{OCH}_2\text{CH}_2\text{SiMe}_3]^+$, 118 $[\text{M}-\text{CH}_2\text{OCH}_2\text{CH}_2\text{SiMe}_3]^+$; Accurate Mass (ESI) m/z found $[\text{M}+\text{H}]^+$ 249.1390 ; $\text{C}_{13}\text{H}_{21}\text{N}_2\text{OSi}$ requires M , 249.1423 .

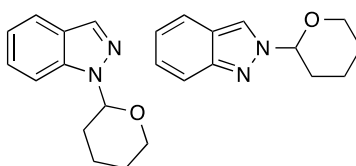
1-(Methanesulfonyl)-1H-indazole (**461**)



Methanesulfonyl chloride (**460**) (0.23 g, 0.15 mL, 2 mmol) was added to dropwise to a solution of indazole (**402**) (0.24 g, 2 mmol) and anhydrous triethylamine (0.2 g, 0.28 mL, 2 mmol) in anhydrous DCM (5 mL). The reaction was stirred for 18 h at room temperature before the mixture was dry loaded onto silica and purified by flash column chromatography (0-20% Et₂O in Hexanes). **461** (0.21g, 54%) was isolated as a pink oil.

δ_{H} (700 MHz, CDCl₃) 8.28 (1H, d, $J = 0.9$, 3-*H*), 8.06 (1H, dd, $J = 8.2$, 0.9, 7-*H*), 7.76 (1H, dd, $J = 8.2$, 0.9, 4-*H*), 7.54 (1H, ddd, $J = 8.2$, 7.1, 0.9, 6-*H*), 7.36 (1H, ddd, $J = 8.2$, 7.1, 0.9, 5-*H*), 3.23 (3H, s, SO₂CH₃); δ_{C} (176 MHz, CDCl₃) 141.3 (C-3), 140.2 (C-1a), 129.5 (C-6), 125.6 (C-3a), 124.4 (C-5), 121.5 (C-4), 113.0 (C-7), 41.0 (SO₂CH₃); ν_{max} (ATR) 1606, 1498, 1362, 1282, 1247, 1144, 1122, 1064, 958, 901 cm⁻¹; GC/MS (EI) m/z 196 [M]⁺, 118 [M-SO₂CH₃]⁺; Accurate Mass (ESI) m/z found [M+H]⁺ 197.0378; C₈H₉N₂O₂S requires M , 197.0385.

1-(Tetrahydro-2H-pyran-2'-yl)-1H-indazole (**464**) and 2-(Tetrahydro-2H-pyran-2'-yl)-2H-indazole (**465**)



p-toluenesulfonic acid hydrate (p.TSA) (0.25 g, 1.3 mmol) was added to a solution of indazole (**402**) (1.53 g, 13 mmol) and 3,4-dihydro-2H-pyran (**463**) (1.31 g, 15.6 mmol) in DCM (10 mL). Reaction was stirred at room temperature for 24 hours at which point additional pTSA (0.25 g, 1.3 mmol) was added. The reaction was stirred for a further 6

hours at which point TLC analysis (eluent 7:3 Hexanes:Et₂O) showed full consumption of the parent indazole. The reaction was then quenched with aqueous sodium hydroxide (0.5 M, 10 mL). The layers were separated and the aqueous layer was re-extracted with DCM (15 ml). The combined organic extracts were washed with brine (10 mL), dried, filtered and concentrated in vacuo to yield crude product as orange oil. Purification by column chromatography (gradient elution 0-15% Et₂O in Hexane) afforded **464** (0.67 g) and **465** (0.65 g) (total yield 1.32 g, 50 %).

464: δ_{H} (700 MHz, CDCl₃) 8.03 (1H, s, 3-*H*), 7.73 (1H, d, *J* = 8.0, 4-*H*), 7.60 (1H, d, *J* = 8.0, 7-*H*), 7.39 (1H, t, *J* = 8.0, 6-*H*), 7.16 (1H, t, *J* = 8.0, 5-*H*), 5.73 (1H, dd, *J* = 9.4, 2.7, 2'-*H*), 4.04 (1H, m, 6'-*H*_A), 3.75 (1H, m, 6'-*H*_B), 2.59 (1H, m, 3'-*H*_A), 2.17 (1H, m, 4'-*H*_A), 2.09 (1H, m, 3'-*H*_B), 1.76 (3H, m, 4'-*H*_B, 5'-*H*₂); δ_{C} (176 MHz, CDCl₃) 139.6 (C-1a), 134.1 (C-3), 126.6 (C-6), 124.9 (C-3a), 121.3 (C-5), 121.2 (C-4), 110.2 (C-7), 85.4 (C-2'), 67.7 (C-6'), 29.6 (C-3'), 25.3 (C-5'), 22.8 (C-4'); GC/MS (EI) *m/z* 202 [M]⁺, 118 [M-THP]⁺; Accurate Mass (ESI) *m/z* found [M+H]⁺ 203.1213; C₁₂H₁₅N₂O₂ requires *M*, 203.1184.

465: δ_{H} (700 MHz, CDCl₃) 8.16 (1H, s, 3-*H*), 7.73 (1H, d, *J* = 8.6 Hz, 7-*H*), 7.66 (1H, d, *J* = 8.6 Hz, 4-*H*), 7.28 (1H, m, 6-*H*), 7.07 (1H, m, 5-*H*), 5.69 (1H, dd, *J* = 7.5, 4.8 Hz, 2'-*H*), 4.14 (1H, m, 6'-*H*_A), 3.79 (1H, m, 6'-*H*_B), 2.23 (2H, m, 3'-*H*₂), 2.06 (1H, m, 4'-*H*_A), 1.76 (2H, m, 4'-*H*_B, 5'-*H*_A), 1.67 (1H, m, 5'-*H*_B); δ_{C} (176 MHz, CDCl₃): 148.7 (C-1a), 126.4 (C-6), 122.1 (C-5), 121.7 (C-3a), 121.1 (C-3), 120.7 (C-4), 118.1 (C-7), 89.2 (C-2'), 68.2 (C-6'), 31.6 (C-3'), 25.2 (C-5'), 22.4 (C-4'); GC/MS (EI) *m/z* 202 [M]⁺, 118 [M-THP]⁺; Accurate Mass (ESI) *m/z* found [M+H]⁺ 203.1208; C₁₂H₁₅N₂O₂ requires *M*, 203.1184.

Borylation of 1-methyl-1H-indazole (**404**)



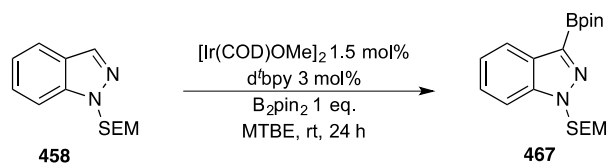
General procedure A was applied to **404** (135 mg, 1 mmol) using Stock Solution A. *In-situ* ^1H NMR monitoring showed 67% to **405** conversion after 24 h.

Borylation of 1-(3', 5'-dimethylbenzyl)-1H-indazole (**455**)



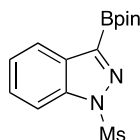
General procedure A was applied to **455** (185 mg, 0.8 mmol) using Stock Solution A. *In-situ* ^1H NMR monitoring showed 61% conversion to **466** after 24 h.

Borylation of 1-[[2-(trimethylsilyl)ethoxy]methyl]-1H-indazole (**458**)



General procedure A was applied to **458** (250 mg, 1 mmol) using Stock Solution A. *In-situ* ^1H NMR monitoring showed 63% conversion to **467** after 24 h.

1-(Methanesulfonyl)-3-(Bpin)-1H-indazole (**468**)



General procedure A was applied to 1-(methanesulfonyl)-1H-indazole (**461**) (185 mg, 0.8 mmol) using Stock Solution A. *In-situ* ^1H NMR spectroscopy showed full conversion to **468** in 1 h at room temperature. Column eluent 0-5% MeOH in CHCl_3 . **468** (154 mg, 62%) isolated as an off-white amorphous solid.

δ_{H} (400 MHz, CDCl_3) 8.13 (1H, d, $J = 8.0$, 4-*H*), 8.08 (1H, d, $J = 8.5$, 7-*H*), 7.53 (1H, m, 6-*H*), 7.38 (1H, m, 5-*H*), 3.33 (3H, s, SO_2CH_3), 1.42 (12H, s, pin CH_3); δ_{C} (176 MHz, CDCl_3) 140.2 (C-1a), 130.5 (C-3a), 129.0 (C-6), 124.3 (C-5), 123.2 (C-4), 112.8 (C-7), 85.0 (C(CH $_3$) $_2$), 41.5 (SO_2CH_3), 25.0 (CH $_3$); δ_{B} (128 MHz, CDCl_3): 28.9 (s(br)); ν_{max} (ATR) 1503, 1373, 1325, 1266, 1176, 1142, 1078, 956, 907 cm^{-1} ; Accurate Mass (ASAP) m/z found $[\text{M}]^+$ 321.1177; $\text{C}_{14}\text{H}_{19}^{10}\text{BN}_2\text{O}_4\text{S}$ requires M , 321.1195.

Borylation of 1-(tetrahydro-2H-pyran-2'-yl)-1H-indazole (**464**)



General procedure A was applied to **464** (138 mg, 0.7 mmol) using Stock Solution A. *In-situ* ^1H NMR monitoring showed 83% conversion to **469** after 24 h.

Borylation of 2-(methyl)-2H-indazole (453)



General procedure A was applied to **453** (114 mg, 0.9 mmol) using Stock Solution A. *In-situ* ^1H NMR monitoring showed full conversion to **470** after 1 h.

Borylation of 2-(3', 5'-dimethylbenzyl)-2H-indazole (456)



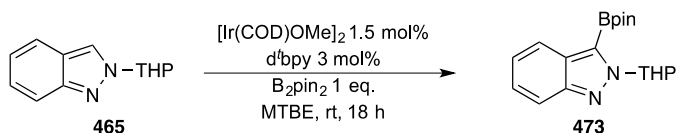
General procedure A was applied to **445** (209 mg, 0.9 mmol) using Stock Solution A. *In-situ* ^1H NMR monitoring showed full conversion to **471** after 0.25 h.

Borylation of 2-[[2-(trimethylsilyl)ethoxy]methyl]-2H-indazole (459)



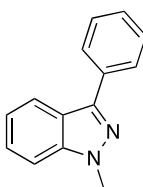
General procedure A was applied to **459** (93 mg, 0.4 mmol) using Stock Solution A. *In-situ* ^1H NMR monitoring showed full conversion to **472** after 6 h.

Borylation of 2-(tetrahydro-2H-pyran-2'-yl)-2H-indazole (465)



General procedure A was applied to **465** (116 mg, 0.6 mmol) using Stock Solution A. *In-situ* ^1H NMR monitoring showed full conversion to **473** after 20 h.

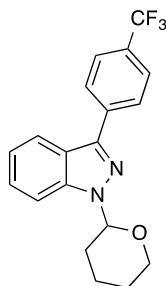
1-Methyl-3-phenyl-1H-indazole (481)



General procedure J was applied to **404** (121 mg, 0.9 mmol). The Suzuki-Miyaura step was run with iodobenzene in the presence of CuCl . Column eluent 5% EtOAc in hexanes. **481** (0.08 g, 43%) isolated as a pale yellow oil.

δ_{H} (700 MHz, CDCl_3) 8.03 (1H, d, $J = 8.0$, 4-*H*), 7.98 (2H, d, $J = 7.6$, 2', 6'-*H*), 7.51 (2H, t, $J = 7.6$, 3', 5'-*H*), 7.42 (3H, m, 6, 7, 4'-*H*), 7.22 (1H, ddd, $J = 8.0, 5.4, 2.2$, 5-*H*), 4.14 (3H, s, NCH_3); δ_{C} (176 MHz, CDCl_3) 143.9 (C-3), 141.6 (C-1a), 133.8 (C-1'), 128.9 (C-3', 5'), 127.9 (ArC), 127.5 (C-2', 6'), 126.4 (ArC), 121.8 (C-3a), 121.5 (C-4), 121.0 (C-5), 109.3 (ArC), 35.7 (NCH_3); GC/MS (EI) m/z 208 $[\text{M}]^+$, 131 $[\text{M}-\text{C}_6\text{H}_5]^+$, 77 $[\text{C}_6\text{H}_5]^+$; Accurate Mass (ASAP) m/z found $[\text{M}]^+$ 208.0995; $\text{C}_{14}\text{H}_{12}\text{N}_2$ requires M , 208.1000.

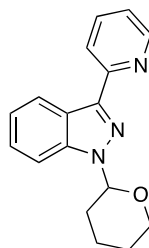
1-Tetrahydropyran-2'-yl-3-[4'-(trifluoromethyl)phenyl]-1H-indazole (**483**)



General procedure J was applied to **464** (263 mg, 1.3 mmol). The Suzuki-Miyaura step was run with 4-bromo-(trifluoromethyl)benzene in the presence of CuCl. Column eluent 0-3% Et₂O in hexanes. **483** (0.19 g, 42%) isolated as an off white amorphous solid.

δ_{H} (600 MHz, CDCl₃) 8.11 (2H, d, $J = 8.2$, 2'',6''-H), 7.99 (1H, d, $J = 8.0$, 4-H), 7.74 (2H, d, $J = 8.2$, 3'',5''-H), 7.67 (1H, d, $J = 8.0$, 7-H), 7.45 (1H, t, $J = 8.0$, 6-H), 7.28 (1H, t, $J = 8.0$, 5-H), 5.81 (1H, dd, $J = 9.3, 2.7$, 2'-H), 4.07 (1H, m, 6'-H), 3.79 (1H, m, 6'-H), 2.68 (1H, m, 3'-H), 2.21 (1H, m, 4'-H), 2.13 (1H, m, 3'-H), 1.79 (2H, m, 4', 5'-H), 1.69 (1H, m, 5'-H); δ_{C} (151 MHz, CDCl₃): 143.2 (C-3), 141.2 (C-1a), 137.4 (C-1''), 129.9 (q, $J = 31.7$, C-4''), 127.9 (C-2'', 6''), 126.9 (C-6), 125.8 (q, $J = 3.0$, C-3'', 5''), 124.3 (q, $J = 273.3$, CF₃), 122.5 (C-3a), 122.3 (C-5), 121.1 (C-4), 110.8 (C-7), 85.7 (C-2'), 67.7 (C-6'), 29.5 (C-3'), 25.3 (C-5'), 22.7 (C-4'); δ_{F} (376 MHz, CDCl₃): -62.5 (s); ν_{max} (ATR) 2948, 2866, 1615, 1332, 1066 cm⁻¹; Accurate Mass (ASAP) m/z found 347.1363; C₁₉H₁₈F₃N₂O requires M , 347.1371.

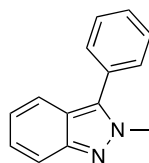
1-Tetrahydropyran-2'-yl-3-pyridin-2''-yl-1H-indazole (485)



General procedure J was applied to **464** (220 mg, 1.1 mmol). The Suzuki-Miyaura step was run with 2-bromopyridine in the presence of CuCl. Column eluent 0-10% EtOAc in hexanes. **485** (0.15 g, 48%) was isolated as a colourless oil.

δ_{H} (700 MHz, CDCl_3) 8.74 (1H, d, $J = 4.7$, 6''-H), 8.67 (1H, d, $J = 8.0$, 4-H), 8.23 (1H, d, $J = 7.9$, 3''-H), 7.76 (1H, m, 4''-H), 7.62 (1H, d, $J = 8.0$, 7-H), 7.43 (1H, t, $J = 8.0$, 6-H), 7.29 (1H, t, $J = 8.0$, 5-H), 7.24 (1H, m, 5''-H), 5.81 (1H, dd, $J = 9.2, 2.7$, 2'-H), 4.07 (1H, m, 6'-H), 3.78 (1H, m, 6'-H), 2.68 (1H, m, 3'-H), 2.21 (1H, m, 4'-H), 2.12 (1H, m, 3'-H), 1.79 (2H, m, 4', 5'-H), 1.69 (1H, m, 5'-H); δ_{C} (176 MHz, CDCl_3) 153.7 (C-2''), 149.3 (C-6''), 143.6 (C-3), 141.2 (C-1a), 136.4 (C-4''), 126.8 (C-6), 123.9 (C-4), 123.2 (C-3a), 122.4 (C-5''), 122.3 (C-5), 121.4 (C-3''), 110.1 (C-7), 85.7 (C-2'), 67.6 (C-6'), 29.5 (C-3'), 25.3 (C-5'), 22.7 (C-4'); ν_{max} (ATR) 1592, 1562, 1510, 1490, 1459, 1442, 1378, 1315, 1279, 1235, 1206, 1172, 1148, 1112, 1080, 1040, 1003, 906, cm^{-1} ; Accurate Mass (ASAP) m/z found $[\text{M}+\text{H}]^+$ 280.1441; $\text{C}_{17}\text{H}_{18}\text{N}_3\text{O}$ requires M , 280.1450.

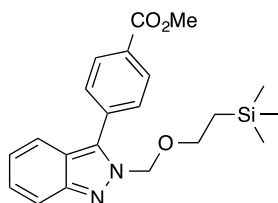
2-Methyl-3-phenyl-2H-indazole (487)



General procedure J was applied to **453** (92 mg, 0.7 mmol). The Suzuki-Miyaura step was run with iodobenzene. Column eluent 0-10% Et₂O in hexanes. **487** (64 mg, 44%) was isolated as a pale yellow oil.

δ_{H} (700 MHz, CDCl₃) 7.71 (1H, d, $J = 8.7$, 7-*H*), 7.59 (1H, d, $J = 8.4$, 4-*H*), 7.55 (4H, m, 2',3',5',6'-*H*), 7.50 (1H, m, 4'-*H*), 7.32 (1H, m, 6-*H*), 7.08 (1H, m, 5-*H*), 4.19 (3H, s, NCH₃); δ_{C} (176 MHz, CDCl₃): 148.3 (C-1a), 136.2 (C-3), 129.9 (C-1'), 129.8 (ArC), 129.2 (ArC), 128.9 (C-4'), 126.4 (C-6), 122.0 (C-5), 121.4 (C-3a), 120.3 (C-4), 117.2 (C-7), 38.7 (NCH₃); ν_{max} (ATR) 1500, 1361, 1287, 1009, 904 cm⁻¹; Accurate Mass (ASAP) m/z found [M+H]⁺ 209.1077; C₁₄H₁₃N₂ requires M , 209.1079.

2-([2-(Trimethylsilyl)ethoxy]methyl)-3-[4'-(methoxycarbonyl)phenyl]-2H-indazole (488)

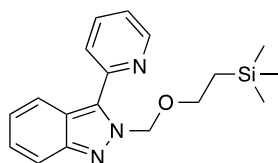


General procedure J was applied to **459** (273 mg, 1.1 mmol). The Suzuki-Miyaura step was run with methyl-4-iodobenzoate. Column eluent 0-10% EtOAc in hexanes. **488** (0.21 g, 51%) was isolated as an off-white amorphous solid.

δ_{H} (700 MHz, CDCl₃) 8.22 (2H, m, 3', 5'-*H*), 7.86 (2H, m, 2', 6'-*H*), 7.77 (1H, d, $J = 8.7$, 7-*H*), 7.68 (1H, d, $J = 8.5$, 4-*H*), 7.36 (1H, m, 6-*H*), 7.15 (1H, m, 5-*H*), 5.71 (2H, s, NCH₂O), 3.97 (3H, s, CO₂CH₃), 3.87 (2H, t, $J = 8.3$, OCH₂CH₂), 0.97 (2H, t, $J = 8.3$, CH₂Si(CH₃)₃), -0.01 (9H, s, Si(CH₃)₃); δ_{C} (176 MHz, CDCl₃) 166.7 (CO₂CH₃), 148.3 (C-

1a), 135.7 (C-3), 134.0 (ArC), 130.3, (C-3', 5'), 130.2 (ArC), 129.8 (C-2', 6'), 127.1 (C-6), 123.1 (C-5), 121.5 (C-3a), 120.5 (C-4), 118.2 (C-7), 79.6 (NCH₂O), 67.9 (OCH₂CH₂), 52.5 (CO₂CH₃), 18.1 (CH₂Si(CH₃)₃), -1.3 (Si(CH₃)₃); ν_{\max} (ATR) 1717, 1612, 1490, 1436, 1276, 1249, 1228, 1175, 1149, 1080, 1018, 906 cm⁻¹; Accurate Mass (ASAP) m/z found [M+H]⁺ 383.1803; C₂₁H₂₇N₂O₃Si requires M , 383.1791.

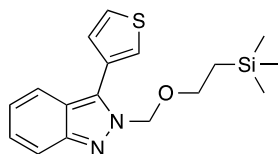
2-[[2-(Trimethylsilyl)ethoxy]methyl]-3-pyridin-2'-yl-2H-indazole (**489**)



General procedure J was applied to **459** (270 mg, 1.1 mmol). The Suzuki-Miyaura step was run with 2-bromopyridine. Column eluent 20% Et₂O in hexanes. **489** (0.16 g, 47%) was isolated as a colourless oil.

δ_{H} (700 MHz, CDCl₃) 8.80 (1H, m, 6'-H), 7.88 (3H, m, 4, 7, 4'-H), 7.79 (1H, d, J = 8.7, 3'-H), 7.34 (2H, m, 6, 5'-H), 7.18 (1H, m, 5-H), 6.15 (2H, s, NCH₂O), 3.68 (2H, t, J = 8.3, OCH₂CH₂), 0.86 (2H, t, J = 8.3, CH₂SiMe₃), -0.10 (9H, s, Si(CH₃)₃); δ_{C} (176 MHz, CDCl₃) 150.3 (C-6'), 149.5 (C-2'), 148.3 (C-1a), 137.0 (ArC), 134.4 (C-3), 126.8 (ArC), 124.4 (ArC), 123.4 (C-5), 122.7 (ArC), 121.7 (C-3a), 120.8 (ArC), 118.4 (C-3'), 80.3 (NCH₂O), 67.4 (OCH₂CH₂), 18.0 (CH₂Si(CH₃)₃), -1.4 (Si(CH₃)₃); ν_{\max} (ATR) 1586, 1490, 1459, 1364, 1306, 1249, 1152, 1088, 1021, 906 cm⁻¹; Accurate Mass (ASAP) m/z found [M+H]⁺ 326.1692; C₁₈H₂₄N₃O₂Si requires M , 326.1689.

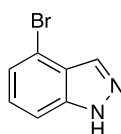
2-[[2-(Trimethylsilyl)ethoxy]methyl]-3-thiophen-3'-yl-2H-indazole (**490**)



General procedure J was applied to **459** (234 mg, 0.9 mmol). The Suzuki-Miyaura step was run with 3-bromothiophene. Column eluent 0-5% EtOAc in hexanes afforded **490** (0.13 g, 41%) as a pale yellow oil.

δ_{H} (700 MHz, CDCl_3) 7.85 (1H, m, 2'-H), 7.73 (2H, m, 4, 7-H), 7.58 (1H, m, 5'-H), 7.52 (1H, m, 4'-H), 7.33 (1H, m, 6-H), 7.12 (1H, m, 5-H), 5.73 (2H, s, NCH_2O), 3.82 (2H, t, $J = 8.3$, OCH_2CH_2), 0.96 (2H, t, $J = 8.3$, CH_2SiMe_3), -0.02 (9H, m, $\text{Si}(\text{CH}_3)_3$); δ_{C} (176 MHz, CDCl_3) 148.1 (C-1a), 132.4 (C-3), 129.8 (C-3'), 128.3 (C-5'), 127.0 (C-4'), 126.7 (C-6), 125.8 (C-2'), 122.4 (C-5), 121.2 (C-3a), 120.9 (ArC), 118.0 (ArC), 79.6 (NCH_2O), 67.6 (OCH_2CH_2), 18.2 ($\text{CH}_2\text{Si}(\text{CH}_3)_3$), -1.3 ($\text{Si}(\text{CH}_3)_3$); ν_{max} (ATR) 1627, 1478, 1408, 1293, 1267, 1249, 1080, 1021, 907 cm^{-1} ; Accurate Mass (ASAP) m/z found $[\text{M}+\text{H}]^+$ 331.1266; $\text{C}_{17}\text{H}_{23}\text{N}_2\text{OSSi}$ requires M , 331.1300.

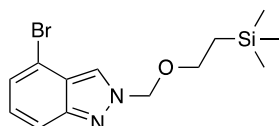
4-Bromo-1H-indazole (**497**)



General procedure K was applied to 2-bromo-6-fluorobenzaldehyde (**496**) (1.76 g, 8.7 mmol) to give **497** (1.20 g, 70%) as an orange amorphous solid.

δ_{H} (700 MHz, CDCl_3) 10.67 (1H, br, s, NH), 8.13 (1H, s, 3-H), 7.45 (1H, d, $J = 7.8$, ArH), 7.33 (1H, d, $J = 7.8$, ArH), 7.24 (1H, m, 6-H); δ_{C} (176 MHz, CDCl_3): 140.8 (C-1a), 135.3 (C-3), 128.0 (C-6), 124.7 (ArC), 124.1 (ArC), 114.8 (ArC), 109.0 (ArC); GC/MS (EI) m/z 199 ($[\text{M}]^+$, ^{81}Br), 198 $[\text{M}+\text{H}]^+$, 197 ($[\text{M}]^+$, ^{79}Br), 196, 117 $[\text{M}-\text{Br}]^+$.

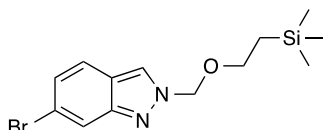
4-Bromo-2-[[2-(trimethylsilyl)ethoxy]methyl]indazole (**501**)



General procedure I was applied on to **497** (0.17 g, 0.9 mmol). Column eluent 0-10% Et₂O in hexanes. **501** (0.18 g, 64%) isolated as a colourless oil.

δ_{H} (700 MHz, CDCl₃) 8.13 (1H, s, 3-*H*), 7.68 (1H, d, *J* = 8.8, 7-*H*), 7.27 (1H, m, 5-*H*), 7.16 (1H, dd, *J* = 8.8, 7.1, 6-*H*), 5.72 (2H, s, NCH₂O), 3.64 (2H, m, OCH₂CH₂), 0.96 (2H, m, CH₂Si(CH₃)₃), -0.02 (9H, s, Si(CH₃)₃); δ_{C} (176 MHz, CDCl₃) 148.9 (C-1a), 127.2 (C-6), 124.9 (C-5), 124.5 (C-3a), 123.9 (C-3), 117.4 (C-7), 113.5 (C-4), 82.2 (NCH₂O), 67.9 (OCH₂CH₂), 17.8 (CH₂Si(CH₃)₃), -1.5 (Si(CH₃)₃); GC/MS (EI) *m/z* 329 ([M]⁺, ⁸¹Br), 327 ([M]⁺, ⁷⁹Br), 255 ([M-SiMe₃]⁺, ⁸¹Br), 253 ([M-SiMe₃]⁺, ⁷⁹Br), 228 ([M-CH₂CH₂SiMe₃]⁺, ⁸¹Br), 226 ([M-CH₂CH₂SiMe₃]⁺, ⁷⁹Br), 212 ([M-OCH₂CH₂SiMe₃]⁺, ⁸¹Br), 210 ([M-OCH₂CH₂SiMe₃]⁺, ⁷⁹Br), 73 [SiMe₃]⁺; *Accurate Mass* (ASAP) *m/z* found [M]⁺ 327.0537; C₁₃H₂₀⁷⁹BrN₂OSi requires *M*, 327.0528.

6-Bromo-2-[[2-(trimethylsilyl)ethoxy]methyl]indazole (**503**)

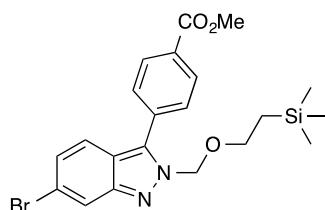


General procedure I was applied to 6-bromo-1H-indazole (**499**) (2.50 g, 12.7 mmol). Column eluent 5% EtOAc in hexanes. **503** (3.15 g, 76%) isolated as a pale orange oil.

δ_{H} (600 MHz, CDCl₃) 8.09 (1H, s, 3-*H*), 7.91 (1H, m, 7-*H*), 7.56 (1H, d, *J* = 8.9, 4-*H*), 7.18 (1H, dd, *J* = 8.9, 1.6, 5-*H*), 5.70 (2H, s, NCH₂O), 3.62 (2H, m, OCH₂CH₂), 0.94 (2H, m, CH₂Si(CH₃)₃), -0.03 (9H, s, Si(CH₃)₃); δ_{C} (151 MHz, CDCl₃) 149.6 (C-1a), 126.1 (C-5), 123.3 (C-3), 122.1 (C-4), 120.9 (C-3a), 120.6 (C-6), 120.5 (C-7), 82.1 (NCH₂O), 67.8

(OCH₂CH₂), 18.0 (CH₂Si(CH₃)₃), -1.3 (Si(CH₃)₃); GC/MS (EI) *m/z* 329 ([M]⁺, ⁸¹Br), 327 ([M]⁺, ⁷⁹Br), 255 ([M-SiMe₃]⁺, ⁸¹Br), 253 ([M-SiMe₃]⁺, ⁷⁹Br), 228 ([M-CH₂CH₂SiMe₃]⁺, ⁸¹Br), 226 ([M-CH₂CH₂SiMe₃]⁺, ⁷⁹Br), 212 ([M-OCH₂CH₂SiMe₃]⁺, ⁸¹Br), 210 ([M-OCH₂CH₂SiMe₃]⁺, ⁷⁹Br), 73 [SiMe₃]⁺; *Accurate Mass* (ASAP) *m/z* found [M]⁺ 327.0527; C₁₃H₂₀⁷⁹BrN₂OSi requires *M*, 327.0528.

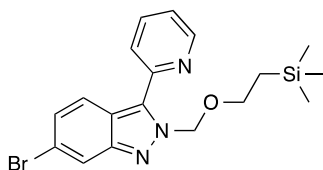
6-Bromo-2-([2-(trimethylsilyl)ethoxy]methyl)-3-[4'-(methoxycarbonyl)phenyl]-2H-indazole (508)



General Method L applied to **503** (200 mg, 0.61 mmol). The Suzuki-Miyaura step was run with methyl-4-iodobenzoate. Column eluent 0-10% EtOAc in hexanes. **508** (124 mg, 44%) isolated as a white amorphous solid.

δ_{H} (600 MHz, CDCl₃) 8.22 (2H, d, *J* = 8.2, 3',5'-*H*), 7.94 (1H, s, 7-*H*), 7.82 (2H, d, *J* = 8.2, 2', 6'-*H*), 7.54 (1H, d, *J* = 8.9, 4-*H*), 7.21 (1H, d, *J* = 8.9, 5-*H*), 5.67 (2H, s, NCH₂O), 3.98 (3H, s, CO₂CH₃), 3.85 (2H, t, *J* = 8.3, OCH₂CH₂), 0.96 (2H, t, *J* = 8.3, CH₂Si(CH₃)₃), -0.01 (9H, s, Si(CH₃)₃); δ_{C} (151 MHz, CDCl₃) 166.6 (CO₂CH₃), 148.9 (C-1a), 136.4 (C-3), 133.4 (C-1'), 130.6 (C-4'), 130.4 (C-3', 5'), 129.8 (C-2', 6'), 126.8 (C-5), 122.0 (C-4), 121.2 (ArC), 120.6 (C-7), 120.1 (ArC), 79.6 (NCH₂O), 68.0 (OCH₂CH₂), 52.5 (CO₂CH₃), 18.1 (CH₂Si(CH₃)₃), -1.2 (Si(CH₃)₃); ν_{max} (ATR) 1717, 1608, 1461, 1436, 1273, 1243, 1185, 1080, 996 cm⁻¹; *Accurate Mass* (ASAP) *m/z* found [M+H]⁺ 461.0882; C₂₁H₂₆⁷⁹BrN₂O₃Si requires *M*, 461.0896.

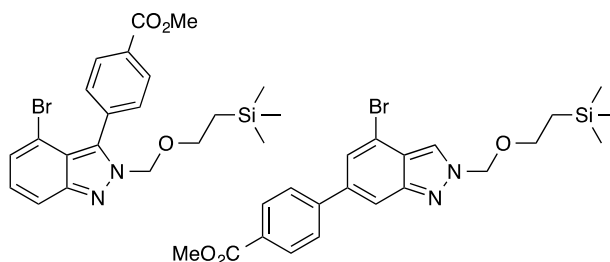
6-Bromo-2-[[2-(trimethylsilyl)ethoxy]methyl]-3-pyridin-2'-yl-2H-indazole (509)



General Method L was applied to **503** (280 mg, 0.85 mmol). The Suzuki-Miyaura step was run with 2-bromopyridine. Column eluent 15% EtOAc in hexanes. **509** (179 mg, 52%) isolated as a pale yellow oil.

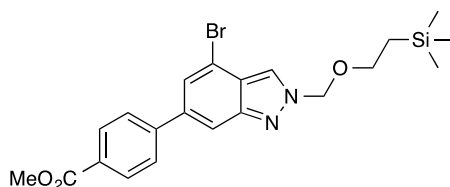
δ_{H} (700 MHz, CDCl_3) 8.80 (1H, d, $J = 5.4$, 6'-H), 7.95 (1H, s, 7-H), 7.87 (2H, m, 3', 4'-H), 7.79 (1H, d, $J = 8.9$, 4-H), 7.35 (1H, t, $J = 5.4$, 5'-H), 7.24 (1H, d, $J = 8.9$, 5-H), 6.08 (2H, s, NCH_2O) 3.68 (2H, t, $J = 8.3$, OCH_2CH_2), 0.87 (2H, t, $J = 8.3$, $\text{CH}_2\text{Si}(\text{CH}_3)_3$), -0.09 (9H, s, $\text{Si}(\text{CH}_3)_3$); δ_{C} (176 MHz, CDCl_3) 150.4 (C-6'), 148.9 (C-2'), 148.8 (C-1a), 137.2 (ArC), 135.1 (C-3), 127.1 (C-5), 124.4 (ArC), 123.1 (C-5'), 122.5 (C-4), 120.9 (ArC), 120.7 (C-7), 120.3 (ArC), 80.3 (NCH_2O), 67.6 (OCH_2CH_2), 18.0 ($\text{CH}_2\text{Si}(\text{CH}_3)_3$), -1.3 ($\text{Si}(\text{CH}_3)_3$); ν_{max} (ATR) 1584, 1470, 1244, 1092, 1014, 908 cm^{-1} ; Accurate Mass (ASAP) m/z found $[\text{M}+\text{H}]^+$ 404.0789; $\text{C}_{18}\text{H}_{23}^{79}\text{BrN}_3\text{OSi}$ requires M , 404.0794.

4-Bromo-2-[[2-(trimethylsilyl)ethoxy]methyl]-3-[4'-(methoxycarbonyl)phenyl]-2H-indazole (**505**) and 4-Bromo-2-[[2-(trimethylsilyl)ethoxy]methyl]-6-[4'-(methoxycarbonyl)phenyl]-2H-indazole (**511**)



General Method L was applied to **501** (328 mg, 1.0 mmol). The Suzuki-Miyaura step was run with methyl-4-iodobenzoate. Column eluent 0-25% Et₂O in hexanes. **505** and **511** (226 mg, 49%) isolated as a 31:69 mixture of isomers (¹H NMR).

4-Bromo-2-[[2-(trimethylsilyl)ethoxy]methyl]-6-[4'-(methoxycarbonyl)phenyl]-2H-indazole (**511**)

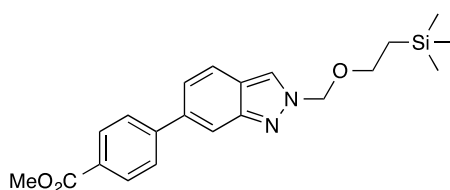


Borylation of **501** (310 mg, 0.95 mmol) was carried out with an aliquot of Stock Solution C at room temperature for 24 h. The reaction mixture was concentrated *in vacuo* and GC/MS analysis confirmed 69% conversion to 6-(Bpin) **513**. The Suzuki-Miyaura cross-coupling step was carried out as per General Method L for 3 h with methyl-4-iodobenzoate. Column eluent 0-25% Et₂O in hexanes. **511** (267 mg, 61%) isolated as an off white amorphous solid.

δ_H (700 MHz, CDCl₃) 8.16 (1H, s, 3-*H*), 8.13 (2H, m, 3', 5'-*H*), 7.89, (1H, s, Ar*H*), 7.71 (2H, m, 2', 6'-*H*), 7.57 (1H, d, *J* = 1.1, Ar*H*), 5.74 (2H, s, NCH₂O), 3.95 (3H, s, CO₂CH₃), 3.67, (2H, t, *J* = 8.3, OCH₂CH₂), 0.97 (2H, t, *J* = 8.3, CH₂Si(CH₃)₃), -0.01 (9H, s,

Si(CH₃)₃); δ_c (176 MHz, CDCl₃) 167.0 (CO₂CH₃), 149.1 (C-1a), 144.9 (C-1'), 139.6 (C-6), 130.4 (C-3', 5'), 129.5 (C-4'), 127.4 (C-2', 6'), 125.1 (ArC), 124.1 (C-3), 124.0 (ArC), 115.7 (ArC), 114.2 (ArC), 82.3 (NCH₂O), 68.0 (OCH₂CH₂), 52.3 (CO₂CH₃), 18.0 (CH₂Si(CH₃)₃), -1.3 (Si(CH₃)₃); ν_{max} (ATR) 1723, 1610, 1555, 1436, 1369, 1285, 1250, 1197, 1104, 1079, 1018, 930 cm⁻¹; *Accurate Mass* (ASAP) m/z found [M+H]⁺ 461.0893; C₂₁H₂₆⁷⁹BrN₂O₃Si requires *M*, 461.0896.

2-[[2-(Trimethylsilyl)ethoxy]methyl]-6-[4'-(methoxycarbonyl)phenyl]-2H-indazole (**514**)

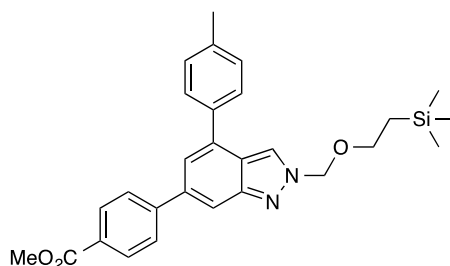


511 (130 mg, 0.28 mmol), was dissolved in ethanol (10 mL) and ammonium formate (353 mg, 5.6 mmol) was charged. The reaction vessel was evacuated and backfilled with nitrogen (x 3 cycles) before 10% Pd/C (15 mg, 0.014 mmol, 5 mol%) was slowly added under a positive pressure of nitrogen. The reaction was stirred at room temperature for 2 h then filtered through a plug of celite and dry-loaded onto silica for purification by flash column chromatography (15% ethyl acetate in hexane) giving **514** as a viscous clear oil (94 mg, 88%)

δ_H (700 MHz, CDCl₃) 8.13 (3H, m, 3, 3', 5'-H), 7.97 (1H, s, 7-H), 7.78 (1H, d, *J* = 8.7, 4-H), 7.74 (2H, m, 2', 6'-H), 7.40 (1H, dd, *J* = 8.7, 1.4, 5-H), 5.75 (2H, s, NCH₂O), 3.95 (3H, s, CO₂CH₃), 3.66 (2H, t, *J* = 8.3, OCH₂CH₂), 0.96 (2H, t, *J* = 8.3, CH₂Si(CH₃)₃), -0.02 (9H, s, Si(CH₃)₃); δ_c (176 MHz, CDCl₃) 167.2 (CO₂CH₃), 149.3 (C-1a), 146.2 (C-1'), 138.4 (C-6), 130.3 (C-3', 5'), 129.0 (C-4'), 127.4 (C-2', 6'), 122.9 (C-3), 122.6 (C-5), 122.0 (C-3a), 121.3 (C-4), 116.5 (C-7), 82.1 (NCH₂O), 67.8 (OCH₂CH₂), 52.3 (CO₂CH₃), 18.0

(CH₂Si(CH₃)₃), -1.3 (Si(CH₃)₃); ν_{\max} (ATR) 1720, 1607, 1435, 1281, 1108, 932 cm⁻¹;
Accurate Mass (ASAP) m/z found [M+H]⁺ 383.1787; C₂₁H₂₇N₂O₃Si requires *M*, 383.1791.

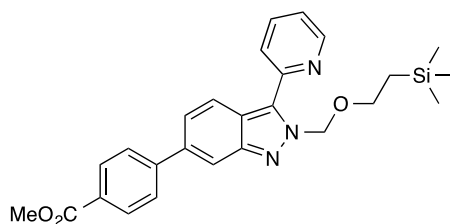
2-[[2-(Trimethylsilyl)ethoxy]methyl]-4-(4'-methylphenyl)-6-[4''-(methoxycarbonyl)phenyl]-2H-indazole (**518**)



General Method M was applied to **511** (115 mg, 0.25 mmol) with 4-tolylboronic acid (**105**). Column eluent 0-10% ethyl acetate in hexanes afforded **518** as a colourless oil (85 mg, 72%)

δ_{H} (700 MHz, CDCl₃) 8.27 (1H, s, 3-*H*), 8.14 (2H, d, $J = 8.3$, 3'', 5''-*H*), 7.93 (1H, s, 7-*H*), 7.79 (2H, d, $J = 8.3$, 2'', 6''-*H*), 7.64 (2H, d, $J = 8.0$, 2', 6'-*H*), 7.45 (1H, s, 5-*H*), 7.33 (2H, d, $J = 8.0$, 3', 5'-*H*), 5.75 (2H, s, NCH₂O), 3.95 (3H, s, CO₂CH₃), 3.67 (2H, t, $J = 8.3$, OCH₂CH₂), 2.45 (3H, s, PhCH₃) 0.96 (2H, t, $J = 8.3$, CH₂Si(CH₃)₃), -0.02 (9H, s, Si(CH₃)₃); δ_{C} (176 MHz, CDCl₃) 167.2 (CO₂CH₃), 150.0 (C-1a), 146.3 (C-1''), 138.9 (C-6), 138.0 (C-4'), 137.3 (C-1'), 135.6 (C-4), 130.3 (C-3'', 5''), 129.8 (C-3', 5'), 129.1 (C-4''), 128.1 (C-2', 6'), 127.5 (C-2'', 6''), 123.2 (C-3), 121.6 (C-3a), 121.2 (C-5), 115.3 (C-7), 82.2 (NCH₂O), 67.8 (OCH₂CH₂), 52.3 (CO₂CH₃), 21.4 (PhCH₃), 18.0 (CH₂Si(CH₃)₃), -1.3 (Si(CH₃)₃); ν_{\max} (ATR) 1719, 1612, 1511, 1435, 1278, 1102, 912 cm⁻¹; *Accurate Mass* (ASAP) m/z found [M+H]⁺ 473.2249; C₂₈H₃₃N₂O₃Si requires *M*, 473.2260.

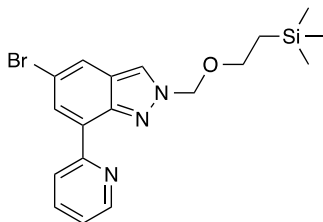
2-[[2-(Trimethylsilyl)ethoxy)methyl]-3-pyridin-2'-yl-6-[4''-(methoxycarbonyl)phenyl]-2H-indazole (**521**)



General Method M was applied to **509** (158 mg, 0.39 mmol) with 4-(methoxycarbonyl)phenylboronic acid. Column eluent 0-20% EtOAc in hexanes. **521** (137 mg, 76%) isolated as an off-white amorphous solid.

δ_{H} (700 MHz, CDCl_3) 8.82 (1H, d, $J = 4.5$, 6'-H), 8.14 (2H, d, $J = 8.3$, 3'', 5''-H), 8.02 (1H, s, 7-H), 7.99 (1H, d, $J = 8.3$, 4-H), 7.91 (2H, m, 3', 4'-H), 7.77 (2H, d, $J = 8.3$, 2'', 6''-H), 7.47 (1H, d, $J = 8.3$, 5-H), 7.35 (1H, ddd, $J = 6.6, 4.5, 1.4$, 5'-H), 6.16 (2H, s, NCH_2O), 3.95 (3H, s, CO_2CH_3), 3.71 (2H, t, $J = 8.3$, OCH_2CH_2), 0.88 (2H, t, $J = 8.3$, $\text{CH}_2\text{Si}(\text{CH}_3)_3$), -0.09 (9H, s, $\text{Si}(\text{CH}_3)_3$); δ_{C} (176 MHz, CDCl_3): 167.1 (CO_2CH_3), 150.4 (C-6'), 149.3 (C-2'), 148.6 (C-1a), 146.1 (C-1''), 138.7 (C-6), 137.1 (ArC), 134.6 (C-3), 130.3 (C-3'', 5''), 129.1 (C-4''), 127.4 (C-2'', 6''), 124.4 (ArC), 123.6 (C-5), 122.9 (C-5'), 121.6 (C-4), 121.4 (C-3a), 116.7 (C-7), 80.4 (NCH_2O), 67.5 (OCH_2CH_2), 52.3 (CO_2CH_3), 18.0 ($\text{CH}_2\text{Si}(\text{CH}_3)_3$), -1.3 ($\text{Si}(\text{CH}_3)_3$); ν_{max} (ATR) 1719, 1607, 1536, 1478, 1280, 1102 cm^{-1} ; Accurate Mass (ASAP) m/z found $[\text{M}+\text{H}]^+$ 460.2046; $\text{C}_{26}\text{H}_{30}\text{N}_3\text{O}_3\text{Si}$ requires M , 460.2056.

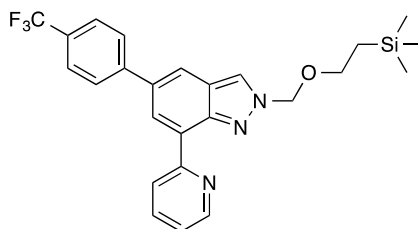
5-Bromo-2-[[2-(trimethylsilyl)ethoxy]methyl]-7-pyridin-2'-yl-2H-indazole (535)



General Method N applied to **502** (295 mg, 0.9 mmol). Borylation was carried out with Stock Solution C. The Suzuki-Miyaura step was run with 2-bromopyridine. Column eluent 0-20% EtOAc in hexanes. **535** (259 mg, 71%) isolated as a colourless oil.

δ_{H} (700 MHz, CDCl_3) 8.80 (1H, d, $J = 6.5$, 3'-H), 8.74 (1H, d, $J = 6.5$, 6'-H), 8.36 (1H, s, 6-H), 8.15 (1H, s, 3-H), 7.91 (1H, s, 4-H), 7.82 (1H, t, $J = 6.5$, 4'-H), 7.27 (1H, m, 5'-H), 5.77 (2H, s, NCH_2O), 3.70 (2H, t, $J = 8.2$, OCH_2CH_2), 0.97 (2H, t, $J = 8.2$, $\text{CH}_2\text{Si}(\text{CH}_3)_3$), -0.02 (9H, s, $\text{Si}(\text{CH}_3)_3$); δ_{C} (176 MHz, CDCl_3) 154.0 (C-2'), 149.7 (C-6'), 145.5 (C-1a), 136.6 (C-4'), 130.3 (C-7), 129.8 (C-6), 125.0 (C-3'), 124.9 (C-3a), 123.5 (C-4), 122.9 (C-5'), 122.5 (C-3), 116.4 (C-5), 82.1 (NCH_2O), 67.9 (OCH_2CH_2), 18.0 ($\text{CH}_2\text{Si}(\text{CH}_3)_3$), -1.3 ($\text{Si}(\text{CH}_3)_3$); ν_{max} (ATR) 1584, 1511, 1470, 1343, 1249, 1133, 1094, 1071 cm^{-1} ; Accurate Mass (ESI) m/z found $[\text{M}+\text{H}]^+$ 404.0788; $\text{C}_{18}\text{H}_{23}\text{N}_3\text{OSi}^{79}\text{Br}$ requires M , 404.0794.

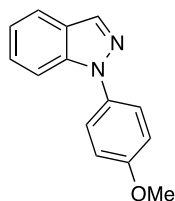
2-[[2-(Trimethylsilyl)ethoxy]methyl]-7-pyridin-2'-yl-5-[4''-(trifluoromethyl)phenyl]-2H-indazole (**537**)



General Method M was applied to **535** (120 mg, 0.30 mmol) with 4-(trifluoromethyl)benzeneboronic acid. Column eluent 15% EtOAc in hexanes. **537** (126 mg, 89%) isolated as a yellow amorphous solid.

δ_{H} (600 MHz, CDCl_3) 8.84 (1H, d, $J = 8.0$, 3'-H), 8.77 (1H, d, $J = 4.4$, 6'-H), 8.56 (1H, d, $J = 1.4$, 6-H), 8.29 (1H, s, 3-H), 7.97 (1H, d, $J = 1.4$, 3-H), 7.85 (3H, m, 4', 2'', 6''-H), 7.71 (2H, d, $J = 8.1$, 3'', 5''-H), 7.29 (1H, m, 5'-H), 5.82 (2H, s, NCH_2O), 3.74 (2H, t, $J = 8.3$, OCH_2CH_2), 1.00 (2H, t, $J = 8.3$, $\text{CH}_2\text{Si}(\text{CH}_3)_3$), 0.00 (9H, s, $\text{Si}(\text{CH}_3)_3$); δ_{C} (151 MHz, CDCl_3) 155.0 (C-2'), 149.6 (C-6'), 146.6 (C-1a), 145.1 (C-1''), 136.8 (C-4'), 134.4 (C-5), 129.2 (q, $J = 33.2$, C-4''), 129.2 (C-7), 127.7 (C-2'', 6''), 126.7 (C-7), 125.8 (C-3'', 5''), 125.0 (C-3'), 124.5 (q, $J = 271.8$, CF_3), 124.3 (C-3a), 124.0 (C-3), 122.7 (C-5'), 120.0 (C-4), 82.1 (NCH_2O), 67.9 (OCH_2CH_2), 18.0 ($\text{CH}_2\text{Si}(\text{CH}_3)_3$), -1.3 ($\text{Si}(\text{CH}_3)_3$); δ_{F} (328 MHz, CDCl_3) -62.3 (s); ν_{max} (ATR) 1616, 1586, 1435, 1325, 1251, 1165, 1112, 1070, 904 cm^{-1} ; Accurate Mass (ESI) m/z found $[\text{M}+\text{H}]^+$ 470.1879; $\text{C}_{25}\text{H}_{27}\text{F}_3\text{N}_3\text{OSi}$ requires M , 470.1876.

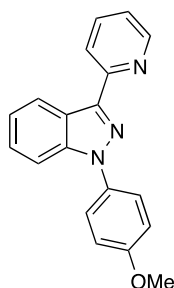
N-(4'-Methoxyphenyl)-1*H*-indazole (**540**)



A dry sealed microwave vial containing indazole (**402**) (400 mg, 3.40 mmol), CuI (65 mg, 0.34 mmol), K₃PO₄ (1.52 g, 7.10 mmol), 4-iodoanisole (950 mg, 4.10 mmol) and N,N-dimethyl-1,2-ethanediamine (60 mg, 0.68 mmol) was degassed with 3 evacuation/argon backfill cycles. Toluene (17 mL) was charged and the reaction heated to 110 °C for 24 h. The reaction mixture was cooled to room temperature, diluted with EtOAc (20 mL) and filtered through a silica plug. The liquors were dry loaded onto silica and the crude product purified by flash column chromatography (0-5% EtOAc in hexanes) to give **540** (674 mg, 88%) as a colourless oil.

δ_{H} (600 MHz, CDCl₃) 8.18 (1H, s, 3-*H*), 7.80 (1H, d, *J* = 8.0, 4-*H*), 7.65 (1H, d, *J* = 8.0, 7-*H*), 7.61 (2H, d, *J* = 8.8, 2', 6'-*H*), 7.41 (1H, t, *J* = 8.0, 6-*H*), 7.21 (1H, t, *J* = 8.0, 5-*H*), 7.06 (2H, d, *J* = 8.8, 3', 5'-*H*), 3.88 (3H, s, OCH₃); δ_{C} (151 MHz, CDCl₃) 158.5 (C-4'), 139.1 (C-1a), 134.9 (C-3), 133.5 (C-1'), 127.0 (C-6), 125.1 (C-3a), 124.6 (C-2', 6'), 121.4 (ArC), 121.3 (ArC), 114.7 (C-3', 5'), 110.3 (C-7), 55.7 (OCH₃); Accurate Mass (ESI) *m/z* found [M+H]⁺ 225.1028; C₁₄H₁₃N₂O requires *M*, 225.1030.

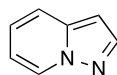
3-Pyridin-2'-yl-N-(4''-methoxyphenyl)-1H-indazole (541)



General procedure J was applied to **540** (207 mg, 0.92 mmol). The Suzuki-Miyaura step was run with 2-bromopyridine. Column eluent 0-7% EtOAc in hexanes. **541** (114 mg, 41%) isolated as a colourless oil.

δ_{H} (600 MHz, CDCl_3) 8.76 (2H, m, 4, 6'-H), 8.27 (1H, d, $J = 7.7$, 3'-H), 7.78 (1H, t, $J = 7.7$, 4'-H), 7.69 (2H, d, $J = 8.6$, 2'', 6''-H), 7.65 (1H, d, $J = 7.8$, 7-H), 7.44 (1H, t, $J = 7.8$, 6-H), 7.33 (1H, t, $J = 7.8$, 5-H), 7.26 (1H, m, 5'-H), 7.08 (2H, d, $J = 8.6$, 3'', 5''-H), 3.89 (3H, s, OCH_3); δ_{C} (151 MHz, CDCl_3) 158.8 (C-4''), 153.6 (C-2'), 149.5 (ArC), 144.5 (C-3), 140.9 (C-1a), 136.4 (C-4'), 133.3 (C-1''), 127.2 (C-6), 125.1 (C-2'', 6''), 124.1 (ArC), 123.4 (C-3a), 122.5 (C-5'), 122.4 (C-5), 121.3 (C-3'), 114.8 (C-3'', 5''), 110.3 (C-7), 55.8 (OCH_3); ν_{max} (ATR) 1590, 1519, 1504, 1458, 1442, 1248, 1180, 1115, 1018, 905 cm^{-1} ; *Accurate Mass* (ESI) m/z found $[\text{M}+\text{H}]^+$ 302.1293; $\text{C}_{19}\text{H}_{16}\text{N}_3\text{O}$ requires M , 302.1285.

Pyrazolo[1,5-a]pyridine (543)

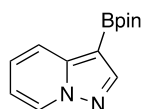


A mixture of ethyl pyrazolo[1,5-a]pyridine-3-carboxylate (**542**) (250 mg, 1.32 mmol) in sulphuric acid (50% v/v in water)(5 mL) was heated to reflux for 2 h. The reaction was cooled to room temperature and NaOH (50% w/w solution) was added until basic whilst maintaining the temperature below 10 °C. The resulting suspension was stirred until everything dissolved. The aqueous mixture was extracted with Et_2O (2 x 20 mL) and the

combined organics were washed with water (15 mL) then brine (15 mL) before being dried over magnesium sulphate, filtered and concentrated *in vacuo* to yield the crude product as an orange oil. The crude was plugged through silica and washed copiously with Et₂O. The liquors were concentrated *in vacuo* to give **543** (110 mg, 71%) as a yellow oil.

δ_{H} (700 MHz, CDCl₃) 8.47 (1H, dd, $J = 6.8, 1.1$, 7-*H*), 7.94 (1H, d, $J = 1.8$, 2-*H*), 7.52 (1H, dd, $J = 8.9, 1.1$, 4-*H*), 7.08 (1H, ddd, $J = 8.9, 6.8, 1.1$, 5-*H*), 6.72 (1H, ddd, $J = 6.8, 6.8, 1.1$, 6-*H*), 6.50 (1H, d, $J = 1.8$, 3-*H*); δ_{C} (176 MHz, CDCl₃) 141.9 (C-2), 140.2 (C-3a), 128.7 (C-7), 123.3 (C-5), 118.2 (C-4), 117.1 (C-6), 96.8 (C-3); ν_{max} (ATR) 1634, 1516, 1434, 1372, 1338, 1252, 1226 cm⁻¹; Accurate Mass (ESI) m/z found [M+H]⁺ 119.0589; C₇H₇N₂ requires M , 119.0609.

3-(Bpin)-Pyrazolo[1,5-*a*]pyridine (**544**)

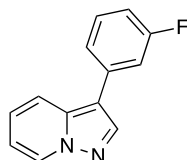


General Method B was applied to pyrazolo[1,5-*a*]pyridine (**543**) (95 mg, 0.81 mmol). The reaction was stirred at room temperature for 16 h at which point the observed precipitate was filtered by vacuum filtration. The filtered solid was recrystallised from hot MTBE (5 mL) and washed with cold MTBE (3 x 3 mL) to give **544** (48 mg, 24%) as a deep red amorphous solid.

δ_{H} (700 MHz, CDCl₃) 8.51 (1H, d, $J = 7.5$ Hz, 7-*H*), 8.23 (1H, s, 2-*H*), 7.96 (1H, d, $J = 7.5$, 4-*H*), 7.21 (1H, t, $J = 7.5$, 5-*H*), 6.81 (1H, t, $J = 7.5$, 6-*H*), 1.36 (12H, s, pinCH₃); 148.9 (C-2), 145.7 (C-3a), 128.9 (C-7), 124.9 (C-5), 120.2 (C-4), 112.6 (C-6), 83.2 (C(CH₃)₂), 25.1 (pinCH₃); δ_{B} (128 MHz, CDCl₃) 29.7 (s(br)); ν_{max} (ATR) 1517, 1473, 1456, 1373,

1338, 1146, 983 cm^{-1} ; Accurate Mass (ASAP) m/z found $[\text{M}]^+$ 243.1424; $\text{C}_{13}\text{H}_{17}^{10}\text{BN}_2\text{O}_2$ requires M , 243.1419.

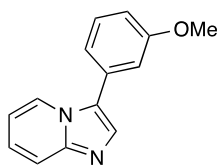
3-(3'-Fluorophenyl)pyrazolo[1,5-a]pyridine (**545**)



General Method B was applied to pyrazolo[1,5-a]pyridine (**543**) (110 mg, 0.93 mmol). The reaction was stirred for 16 h at room temperature before being concentrated *in vacuo*. A tandem Suzuki-Miyaura cross-coupling reaction was then carried out as per General Method E; Pd(Amphos) Cl_2 (40 mg, 0.056 mmol), $\text{Na}_2\text{CO}_{3(\text{aq})}$ (2M, 197 mg, 1.86 mmol), 3-iodo-fluorobenzene (248, 1.12 mmol) in DME (3 mL) at 80 °C for 3 h. Purification by reverse phase column chromatography. **545** (61 mg, 31%) isolated as a pale yellow oil.

δ_{H} (600 MHz, CDCl_3) 8.38 (1H, d, $J = 7.7$, 7-*H*), 8.03 (1H, s, 2-*H*), 7.69 (1H, d, $J = 7.7$, 4-*H*), 7.35 (2H, m, 2', 6'-*H*), 7.24 (1H, m, 4'-*H*), 7.16 (1H, t, $J = 7.7$, 5-*H*), 6.95 (1H, m, 5'-*H*), 6.77 (1H, t, $J = 7.7$, 6-*H*); δ_{C} (151 MHz, CDCl_3) 163.4 (d, $J = 246.0$, C-3'), 140.6 (C-2), 137.1 (C-3a), 135.5 (d, $J = 8.4$, C-3), 130.6 (d, $J = 8.7$, ArC), 129.3 (C-7), 124.5 (C-5), 122.7 (d, $J = 2.7$, ArC), 117.4 (C-4), 113.7 (d, $J = 22.0$, C-4'), 113.0 (d, $J = 21.1$, C-5'), 112.3 (C-6), 111.9 (d, $J = 2.3$, C-1'); δ_{F} (376 MHz, CDCl_3): -112.8 (m); ν_{max} (ATR) 1634, 1613, 1584, 1546, 1531, 1453, 1366, 1260, 1217, 1178, 1017, 904 cm^{-1} ; Accurate Mass (ESI) m/z found $[\text{M}+\text{H}]^+$ 213.0814; $\text{C}_{13}\text{H}_{10}\text{N}_2\text{F}$ requires M , 213.0828.

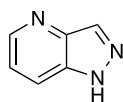
3-(3'-Methoxyphenyl)pyrazolo[1,2-a]pyridine (**552**)



General Method E applied to pyrazolo[1,2-a]pyridine (**546**) (118 mg, 1 mmol); Borylation with Stock Solution B for 24 h at room temperature gave ca. 85% conversion (¹H NMR) to the 3-(Bpin) product (**547**). The Suzuki-Miyaura step was carried out for 2 h with PdXPhos G2 (39 mg, 0.05 mmol), K₃PO₄ (425 mg, 2 mmol), 3-iodoanisole (257 mg, 1.1 mmol) in DMAc:H₂O (10:1) (2.5 mL) at 50 °C. Column eluent 0-50% EtOAc in hexanes. **552** (92 mg, 41%) isolated as a grey amorphous solid.

δ_{H} (700 MHz, CDCl₃) 8.37 (1H, d, $J = 7.6$, 4-*H*), 7.70 (1H, s, 2-*H*), 7.67 (1H, d, $J = 7.6$, 7-*H*), 7.43 (1H, t, $J = 7.9$, 5'-*H*), 7.20 (1H, m, 6-*H*), 7.15 (1H, d, $J = 7.9$, 6'-*H*), 7.09 (1H, m, 2'-*H*), 6.96 (1H, dd, $J = 7.9, 1.9$, 4'-*H*), 6.81 (1H, t, $J = 7.6$, 5-*H*), 3.87 (3H, s, OCH₃); δ_{C} (176 MHz, CDCl₃) 160.2 (C-3'), 146.2 (C-1a), 132.6 (C-2), 130.6 (C-1'), 130.2 (C-5'), 125.6 (C-3), 124.2 (C-6), 123.5 (C-4), 120.2 (C-6'), 118.3 (C-7), 113.7 (C-2'), 113.5 (C-4'), 112.5 (C-5), 55.4 (OCH₃); ν_{max} (ATR) 1602, 1580, 1501, 1299, 1283, 1237, 1165, 1047 cm⁻¹; Accurate Mass (ESI) m/z found [M+H]⁺ 225.1019; C₁₄H₁₃N₂O requires M , 225.1030.

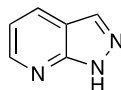
4-Aza-1H-indazole (**555**)¹⁹⁵



General Method K was applied to 3-fluoropyridine-2-carboxaldehyde (**553**) (1.03 g, 8.24 mmol) to give crude **555** (522 mg, 53%) as a yellow amorphous solid.

δ_{H} (700 MHz, CDCl_3) 8.62 (1H, dd, $J = 4.3, 1.1$ Hz, 5-*H*), 8.36 (1H, d, $J = 1.1$ Hz, 3-*H*), 7.88, (1H, ddd, $J = 8.5, 1.1, 1.1$, 7-*H*), 7.31 (1H, dd, $J = 8.5, 4.3$, 6-*H*); δ_{C} (176 MHz, CDCl_3) 145.8 (C-5), 141.1 (C-3), 135.1 (C-3a), 133.1 (C-1a), 121.3 (C-6), 118.5 (C-7); ν_{max} (ATR) 3141, 1577, 1507, 1409, 1387, 1344, 1310, 1185, 1127, 935 cm^{-1} .

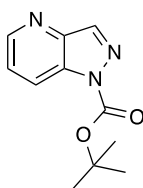
7-Aza-1H-indazole (**556**)¹⁹⁶



General Method K was applied to 2-fluoropyridine-3-carboxaldehyde (**554**) (1.12 g, 8.96 mmol) to give crude **556** (971 mg, 91%) as an orange amorphous solid.

δ_{H} (700 MHz, CDCl_3) 8.68 (1H, dd, $J = 4.6, 1.5$, 6-*H*), 8.18 (1H, dd, $J = 8.0, 1.5$, 4-*H*), 8.14, (1H, s, 3-*H*), 7.21 (1H, dd, $J = 8.0, 4.6$, 5-*H*); δ_{C} (176 MHz, CDCl_3) 151.6 (C-1a), 148.7 (C-6), 134.1 (C-3), 130.9 (C-4), 117.2 (C-5), 115.6 (C-3a); ν_{max} (ATR) 3147, 1606, 1590, 1430, 1315, 1291, 938 cm^{-1} .

4-Aza-1-(tert-butoxycarbonyl)-1H-indazole (**557**)

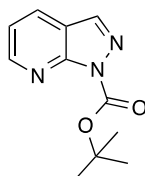


General Method G was applied to **555** (500 mg, 4.2 mmol). Column eluent 0-40% EtOAc in hexanes. **557** (832 g, 90%) isolated as a yellow oil.

δ_{H} (600 MHz, CDCl_3) 8.67 (1H, d, $J = 4.5$, 5-*H*), 8.46 (1H, d, $J = 8.5$, 7-*H*), 8.40 (1H, s, 3-*H*), 7.44 (1H, dd, $J = 8.5, 4.5$, 6-*H*), 1.72 (9H, s, $\text{C}(\text{CH}_3)_3$); δ_{C} (151 MHz, CDCl_3) 148.8 (CO_2^tBu) 147.8 (C-5), 143.7 (C-3a), 140.3 (C-3), 133.3 (C-1a), 123.0 (C-6), 122.6 (C-7)

85.9 (C(CH₃)₃), 28.3 (C(CH₃)₃); ν_{\max} (ATR) 1739, 1411, 1368, 1340, 1285, 1140, 1023, 912 cm⁻¹; *Accurate Mass* (ESI) m/z found [M+H]⁺ 220.1113; C₁₁H₁₄N₃O₂ requires M , 220.1086.

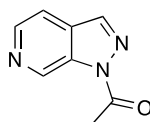
7-Aza-1-(tert-butoxycarbonyl)-1H-indazole (558)



General Method G was applied to **556** (920 mg, 7.7 mmol). Column eluent 30% EtOAc in hexanes. **558** (1.53 g, 91%) isolated as a yellow oil.

δ_{H} (700 MHz, CDCl₃) 8.76 (1H, dd, $J = 4.6, 1.6$, 6-*H*), 8.17 (1H, s, 3-*H*), 8.09 (1H, dd, $J = 7.9, 1.6$, 4-*H*), 7.30 (1H, dd, $J = 7.9, 4.6$, 5-*H*), 1.72 (9H, s, C(CH₃)₃); δ_{C} (176 MHz, CDCl₃) 152.0 (C-1a), 150.8 (C-6), 148.0 (CO₂C(CH₃)₃), 137.5 (C-3), 130.4 (C-4), 119.4 (C-5), 117.9 (C-3a), 85.5 (C(CH₃)₃), 28.2 (C(CH₃)₃); ν_{\max} (ATR) 1751, 1601, 1579, 1457, 1394, 1369, 1256, 1157, 1145, 1057 cm⁻¹; *Accurate Mass* (ESI) m/z found [M+H]⁺ 220.1112; C₁₁H₁₄N₃O₂ requires M , 220.1086.

6-Aza-1-acetyl-1H-indazole (560)

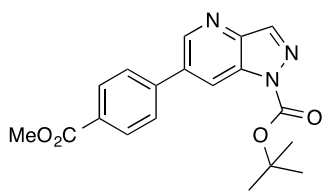


Pyridine (3.9 mL, 3.86 g, 48.8 mmol) then Ac₂O (2.8 mL, 2.99 g, 29.3 mmol) were added dropwise to a solution of 3-amino-4-methylpyridine (2.63 g, 24.4 mmol) in DCM (20 mL). The reaction was stirred at room temperature for 16 h then concentrated *in vacuo*. The crude solid was taken into EtOAc (20 mL) then washed with sat. NaHCO₃ solution (10

mL) then brine (10 mL). The organic layer was then dried over MgSO₄, filtered through celite and concentrated in vacuo to yield the crude product. *Tert*-butylnitrite (2.8 mL, 2.45 g, 23.8 mmol), Ac₂O (4.2 mL, 4.6 g, 44.7 mmol) and KOAc (1.76 g, 17.9 mmol) were added sequentially to a suspension of the crude solid (2.23 g, 14.9 mmol) in toluene (15 mL). The mixture was heated at 80 °C for 16 h, before being cooled to room temperature and diluted with EtOAc (20 mL). The organic mixture was washed sequentially with sat. NaHCO₃ solution (15 mL), water (15 mL) and brine (15 mL) before being dried over MgSO₄, filtered and concentrated *in vacuo*. The crude product was purified by flash column chromatography (10-60% EtOAc in hexanes) to give **560** (841 mg, 35%) as a white amorphous solid.

δ_{H} (700 MHz, CDCl₃) 9.83 (1H, s, 7-*H*), 8.58 (1H, d, *J* = 5.5, 5-*H*), 8.20 (1H, s, 3-*H*), 7.67 (1H, dd, *J* = 5.5, 1.2, 4-*H*), 2.82 (3H, s, COCH₃); δ_{C} (176 MHz, CDCl₃) 170.6 (COCH₃), 143.3 (C-5), 139.0 (C-7), 138.8 (C-3), 135.6 (C-1a), 130.9 (C-3a), 114.8 (C-4), 22.8 (COCH₃); GC/MS (EI) *m/z* 161 [M]⁺, 119 [M-COCH₃]⁺, 92; Accurate Mass (ASAP) found [M]⁺ 161.0587; C₈H₇N₃O requires *M*, 161.0589.

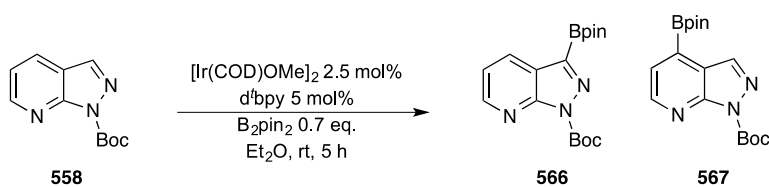
4-Aza-6-[4'-(methoxycarbonyl)phenyl]-1-(tert-butoxycarbonyl)-1H-indazole (565)



General Method N applied to **557** (204 mg, 0.93 mmol). Borylation was carried out using Stock Solution B to give full conversion (¹H NMR) to 3,6-bis(Bpin) (**562**) product. The Suzuki-Miyaura step was run with methyl-4-iodobenzoate. Column eluent 0-35% EtOAc in hexanes. **565** (151 mg, 46%) isolated as an off white amorphous solid.

δ_{H} (700 MHz, CDCl_3) 8.91 (1H, d, $J = 1.8$, 5-*H*), 8.58 (1H, d, $J = 1.8$, 7-*H*), 8.16 (2H, m, 3', 5'-*H*), 7.71 (2H, m, 2', 6'-*H*), 7.15 (1H, s, 3-*H*), 3.96 (3H, s, CO_2CH_3), 1.56 (9H, s, $\text{C}(\text{CH}_3)_3$); δ_{C} (176 MHz, CDCl_3) 166.6 (CO_2CH_3), 151.9 (ArC), 143.4 (C-7), 140.4 (C-1'), 139.9 (ArC), 139.8 (ArC), 131.1 (C-4'), 130.6 (C-3', 5'), 127.7 (C-2', 6'), 124.6 (C-5), 120.5 (C-6), 115.1 (C-3), 83.2 ($\text{C}(\text{CH}_3)_3$), 52.5 (CO_2CH_3), 28.3 ($\text{C}(\text{CH}_3)_3$); ν_{max} (ATR) 1725, 1562, 1505, 1444, 1369, 1280, 1238, 1151, 1113 cm^{-1} ; Accurate Mass (ESI) found $[\text{M}+\text{H}]^+$ 354.1447; $\text{C}_{19}\text{H}_{20}\text{N}_3\text{O}_4$ requires M , 354.1454.

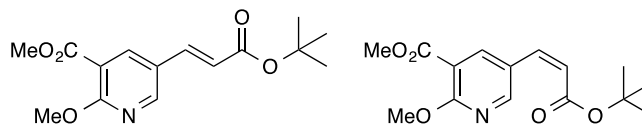
Borylation of 7-aza-1-(tert-butoxycarbonyl)-1H-indazole (558)



General Method B was applied to **558** (354 mg, 1.62 mmol) with additional B_2pin_2 (82 mg, 0.32 mmol) using Et_2O as solvent. The reaction was stirred at room temperature for 5 h giving an 88% conversion (^1H NMR) to **566** and **567** in a 57:43 ratio.

Tandem 'one-pot' C-H Borylation/Oxidative Heck Couplings

Methyl 5-[(1*E*)-3'-*tert*-butoxy-3'-oxoprop-1'-en-1'-yl]-2-nicotinate (**578**) and Methyl 5-[(1*Z*)-3'-*tert*-butoxy-3'-oxoprop-1'-en-1'-yl]-2-methoxynicotinate (**579**)

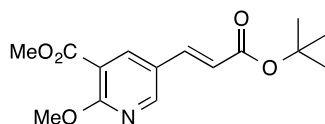


General procedure O was applied to methyl-2-methoxynicotinate (**304**) (122 mg, 0.73 mmol). Borylation was carried out with Stock Solution A over 24 h to give full conversion to **306:307** in a 93:7 ratio. The oxidative Heck step was carried out at room temperature for 16 h with Na₂CO₃ and *tert*-butylacrylate. Column eluent 0-10% EtOAc in hexanes. **578:579** (83 mg, 39%) isolated as a 5:1 mixture of isomers.

578: Data given below

579: δ_{H} (700 MHz, CDCl₃) 8.12 (1H, d, $J = 3.0$, 6-*H*), 7.90 (1H, d, $J = 3.0$, 4-*H*), 7.59 (1H, d, $J = 12.2$, 1'-*H*), 5.39 (1H, d, $J = 12.2$, 2'-*H*), 4.03 (3H, s, OCH₃), 3.90 (3H, s, CO₂CH₃), 1.47 (9H, s, C(CH₃)₃); δ_{C} (176 MHz, CDCl₃) 166.1 (CO₂^tBu), 164.6 (CO₂CH₃), 159.7 (C-2), 158.6 (C-1'), 146.5 (ArC), 141.5 (C-6), 132.0 (C-4), 114.3 (ArC), 104.5 (C-2'), 80.7 (C(CH₃)₃), 54.7 (OCH₃), 52.7 (CO₂CH₃), 28.4 (C(CH₃)₃).

Methyl 5-[(1*E*)-3'-*tert*-butoxy-3'-oxoprop-1'-en-1'-yl]-2-methoxynicotinate(**578**)

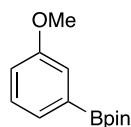


General procedure O was applied to methyl-2-methoxynicotinate (**304**) (105 mg, 0.63 mmol). Borylation was carried out with Stock Solution A over 24 h to give full conversion to **306:307** in a 93:7 ratio. The oxidative Heck step was carried out at 50 °C for 6 h with

Cs₂CO₃ and *tert*-butyl acrylate. Column eluent 0-10% EtOAc in hexanes gave **578** (140 mg, 76%) as a colourless oil.

δ_{H} (700 MHz, CDCl₃) 8.38 (1H, d, $J = 2.4$, 6-*H*), 8.31 (1H, d, $J = 2.4$, 4-*H*), 7.52 (1H, d, $J = 16.0$, 1'-*H*), 6.34 (1H, d, $J = 16.0$, 2'-*H*), 4.06 (3H, s, OCH₃), 3.90 (3H, s, CO₂CH₃), 1.52 (9H, s, C(CH₃)₃); δ_{C} (176 MHz, CDCl₃) 165.9 (CO₂^{*t*}Bu), 165.0 (CO₂CH₃), 163.1 (C-2), 151.0 (C-6), 139.2 (C-4), 138.8 (C-1'), 124.0 (C-5), 120.7 (C-2'), 114.3 (C-3), 80.9 (C(CH₃)₃), 54.7 (OCH₃), 52.6 (CO₂CH₃), 28.3 (C(CH₃)₃); ν_{max} (ATR) 1735, 1706, 1478, 1399, 1328, 1278, 1251, 1207, 1149, 1086, 907 cm⁻¹; Accurate Mass (ESI) found [M+H]⁺ 294.1346; C₁₅H₂₀NO₅ requires *M*, 294.1341.

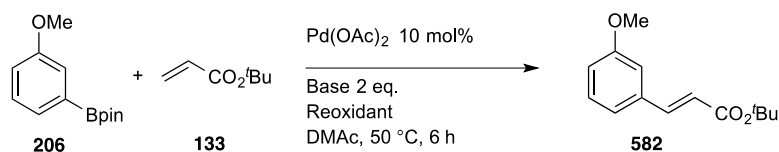
3-(*Bpin*)-Anisole (**206**)



Anisole-3-boronic acid (1 g, 6.6 mmol), pinacol (780 mg, 6.6 mmol) and MgSO₄ (3.97 g, 33 mmol) were stirred in Et₂O at room temperature for 16 h under an argon atmosphere. The reaction mixture was filtered through a pad of celite before being dry loaded onto silica and purified by flash column chromatography (2% Et₂O in hexanes) to give **206** (1.09 g, 74%) as a colourless oil.

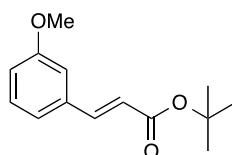
δ_{H} (700 MHz, CDCl₃) 7.41 (1H, d, $J = 7.1$, 4-*H*), 7.34 (1H, s, 2-*H*), 7.30 (1H, t, $J = 7.1$, 5-*H*), 7.02 (1H, d, $J = 7.1$, 6-*H*), 3.84 (3H, s, OCH₃), 1.35 (12H, s, pinCH₃); δ_{C} (176 MHz, CDCl₃) 159.2 (C-1), 129.1 (C-5), 127.3 (C-4), 118.4 (C-2), 118.0 (C-6), 84.0 (C(CH₃)₂), 55.4 (OCH₃), 25.0 (pinCH₃); δ_{B} (128 MHz, CDCl₃) 30.9 (s(br)); ν_{max} (ATR) 1421, 1352, 1312, 1240, 1226, 1143, 1045, 964 cm⁻¹; Accurate Mass (ASAP) *m/z* found [M+H]⁺ 234.1523; C₁₃H₂₀¹⁰BO₃ requires *M*, 234.1542.

Oxidative Heck screening experiments using **206**



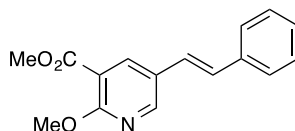
On a 1 mmol scale **206** (234 mg, 1 mmol) was reacted with *tert*-butyl acrylate (**133**) (256 mg, 2 mmol) in DMAc (3 mL), catalysed by Pd(OAc)₂ (22 mg, 0.1 mmol) in the presence of base (2 mmol), under oxidative conditions. The reactions were heated at 50 °C for 6 h then dry loaded onto silica and purified by flash column chromatography (0-5% Et₂O in hexanes). Product **582** was obtained as a colourless oil.

3-[(1*E*)-3'-*tert*-Butoxy-3'-oxoprop-1'-en-1'-yl]anisole (**582**)



δ_{H} (700 MHz, CDCl₃) 7.55 (1H, d, $J = 16.0$, 1'-*H*), 7.28 (1H, t, $J = 7.9$, 5-*H*), 7.10 (1H, d, $J = 7.9$, 4-*H*), 7.03 (1H, s, 2-*H*), 6.91 (1H, dd, $J = 7.9, 2.0$, 6-*H*), 6.35 (1H, d, $J = 16.0$, 2'-*H*), 3.83 (3H, s, OCH₃), 1.54 (9H, s, C(CH₃)₃); δ_{C} (176 MHz, CDCl₃) 166.4 (CO₂^tBu), 160.0 (C-1), 143.6 (C-1'), 136.2 (C-3), 129.9 (C-5), 120.8 (C-4), 120.6 (C-2'), 116.0 (C-6), 112.9 (C-2), 80.7 (C(CH₃)₃), 55.4 (OCH₃), 28.4 (C(CH₃)₃); ν_{max} (ATR) 1703, 1637, 1368, 1294, 1250, 1147, 1042, 980 cm⁻¹; Accurate Mass (ESI) found [M+H]⁺ 235.1341; C₁₄H₁₉O₃ requires M , 235.1334.

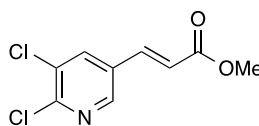
Methyl 2-methoxy-5-[(1E)-2'-phenylethenyl]nicotinate (583)



General procedure O was applied to methyl-2-methoxynicotinate (**304**) (50 mg, 0.30 mmol). Borylation was carried out with Stock Solution A over 24 h to give full conversion to **306:307** in a 93:7 ratio. The oxidative Heck step was carried out at 50 °C for 6 h with Cs₂CO₃ and styrene. Column eluent 0-5% EtOAc in hexanes. **583** (56 mg, 70%) isolated as a colourless oil.

δ_{H} (700 MHz, CDCl₃) 8.37 (1H, d, $J = 2.5$, 6-*H*), 8.36 (1H, d, $J = 2.5$, 4-*H*), 7.50 (2H, d, $J = 7.5$, 2'', 6''-*H*), 7.37 (2H, t, $J = 7.5$, 3'', 5''-*H*), 7.28 (1H, t, $J = 7.5$, 4''-*H*), 7.03 (2H, m, 1', 2'-*H*), 4.07 (3H, s, OCH₃), 3.94 (3H, s, CO₂CH₃); δ_{C} (176 MHz, CDCl₃) 165.6 (CO₂CH₃), 161.8 (C-2), 149.3 (C-6), 138.1 (C-4), 136.9 (C-1''), 129.4 (ArC), 128.9 (C-3'', 5''), 128.1 (C-4''), 126.6 (C-5), 126.6 (C-2'', 6''), 123.7 (ArC), 114.0 (C-3), 54.5 (OCH₃), 52.5 (CO₂CH₃); ν_{max} (ATR) 1733, 1477, 1400, 1309, 1286, 1240, 1087, 1012, 960 cm⁻¹; Accurate Mass (ESI) found [M+H]⁺ 270.1133; C₁₆H₁₆NO₃ requires *M*, 270.1130.

Methyl (2E)-3-(5',6'-dichloropyridin-3'-yl)-prop-2-enoate (585)



2,3-Dichloropyridine (**316**) (148 mg, 1 mmol) was borylated as per General Procedure A using a diglyme Stock Solution B. The reaction was heated at 80 °C for 2 h at which point GC/MS confirmed full conversion to 5-(Bpin) product **317**. To the reaction mixture were added Pd(OAc)₂ (22 mg, 0.10 mmol), cesium fluoride (304 mg, 2 mmol), methyl acrylate (172 mg, 2 mmol). The oxidative Heck step was carried out at 50 °C for 6 h. Reaction

worked up as per General Method O. Flash column chromatography (column eluent 0-10% Et₂O in hexanes) gave **585** (155 mg, 67%) as a white amorphous solid.

δ_{H} (600 MHz, CDCl₃) 8.41 (1H, s, 2'-H), 7.91 (1H, s, 4'-H), 7.60 (1H, d, $J = 16.1$, 3-H), 6.50 (1H, d, $J = 16.1$, 2-H), 3.83 (3H, s, CO₂CH₃); δ_{C} (151 MHz, CDCl₃) 166.3 (C-1), 150.4 (C-6'), 146.8 (C-2'), 138.4 (C-3), 136.5 (C-4'), 131.2 (C-5'), 130.7 (C-3'), 122.0 (C-2), 52.3 (CO₂CH₃); ν_{max} (ATR) 1704, 1608, 1456, 1402, 1255, 1184 cm⁻¹; Accurate Mass (ESI) found [M+H]⁺ 231.9937; C₉H₈NO₂³⁵Cl₂ requires M , 231.9932.

6 Bibliography

- (1) Hall, D. G. *Boronic acids : preparation and applications in organic synthesis and medicine / edited by Dennis G. Hall*; Wiley-VCH: Weinheim :, 2005.
- (2) Sana, M.; Leroy, G.; Wilante, C. *Organometallics* **1991**, *10*, 264.
- (3) Kuivila, H. G.; Nahabedian, K. V. *J. Am. Chem. Soc.* **1961**, *83*, 2159.
- (4) Kuivila, H. G.; Reuwer Jr, J. F.; Mangravite, J. A. *Can. J. Chem.* **1963**, *41*, 3081.
- (5) Kuivila, H. G.; Reuwer, J. F.; Mangravite, J. A. *J. Am. Chem. Soc.* **1964**, *86*, 2666.
- (6) Miyaura, N.; Yanagi, T.; Suzuki, A. *Synth. Commun.* **1981**, *11*, 513.
- (7) Lennox, A. J. J.; Lloyd-Jones, G. C. *Chem. Soc. Rev.* **2014**, *43*, 412.
- (8) Frankland, E. *J. Chem. Soc.* **1862**, *15*, 363.
- (9) Garg, N. K.; Sarpong, R.; Stoltz, B. M. *J. Am. Chem. Soc.* **2002**, *124*, 13179.
- (10) Clary, J. W.; Rettenmaier, T. J.; Snelling, R.; Bryks, W.; Banwell, J.; Wipke, W. T.; Singaram, B. *J. Org. Chem.* **2011**, *76*, 9602.
- (11) Sharp, M. J.; Cheng, W.; Snieckus, V. *Tetrahedron Lett.* **1987**, *28*, 5093.
- (12) Wong, K.-T.; Chien, Y.-Y.; Liao, Y.-L.; Lin, C.-C.; Chou, M.-Y.; Leung, M.-k. *J. Org. Chem.* **2002**, *67*, 1041.
- (13) Kristensen, J.; Lysén, M.; Vedsø, P.; Begtrup, M. *Org. Lett.* **2001**, *3*, 1435.
- (14) Gilman, H.; Moore, L. O. *J. Am. Chem. Soc.* **1958**, *80*, 3609.
- (15) James, C. A.; Coelho, A. L.; Gevaert, M.; Forgione, P.; Snieckus, V. *J. Org. Chem.* **2009**, *74*, 4094.
- (16) Caron, S.; Hawkins, J. M. *J. Org. Chem.* **1998**, *63*, 2054.
- (17) Sharp, M. J.; Snieckus, V. *Tetrahedron Lett.* **1985**, *26*, 5997.
- (18) Larsen, R. D.; King, A. O.; Chen, C. Y.; Corley, E. G.; Foster, B. S.; Roberts, F. E.; Yang, C.; Lieberman, D. R.; Reamer, R. A. *J. Org. Chem.* **1994**, *59*, 6391.
- (19) Lin, S.; Danishefsky, S. J. *Angew. Chem. Int. Ed.* **2001**, *40*, 1967.
- (20) Ishiyama, T.; Murata, M.; Miyaura, N. *J. Org. Chem.* **1995**, *60*, 7508.
- (21) Murata, M.; Oyama, T.; Watanabe, S.; Masuda, Y. *J. Org. Chem.* **2000**, *65*, 164.
- (22) Molander, G. A.; Trice, S. L. J.; Dreher, S. D. *J. Am. Chem. Soc.* **2010**, *132*, 17701.
- (23) Molander, G. A.; Trice, S. L. J.; Kennedy, S. M.; Dreher, S. D.; Tudge, M. T. *J. Am. Chem. Soc.* **2012**, *134*, 11667.
- (24) Jung, M. E.; Lazarova, T. I. *J. Org. Chem.* **1999**, *64*, 2976.
- (25) Nakamura, H.; Fujiwara, M.; Yamamoto, Y. *J. Org. Chem.* **1998**, *63*, 7529.
- (26) Yang, W.; He, H.; Drueckhammer, D. G. *Angew. Chem. Int. Ed.* **2001**, *40*, 1714.
- (27) Zhu, W.; Ma, D. *Org. Lett.* **2006**, *8*, 261.
- (28) Kleeberg, C.; Dang, L.; Lin, Z.; Marder, T. B. *Angew. Chem. Int. Ed.* **2009**, *48*, 5350.

- (29) Marciasini, L. D.; Richy, N.; Vaultier, M.; Pucheault, M. *Adv. Synth. Catal.* **2013**, *355*, 1083.
- (30) Mo, F.; Jiang, Y.; Qiu, D.; Zhang, Y.; Wang, J. *Angew. Chem. Int. Ed.* **2010**, *49*, 1846.
- (31) Erb, W.; Hellal, A.; Albin, M.; Rouden, J.; Blanchet, J. *Chemistry – A European Journal* **2014**, *20*, 6608.
- (32) Del Grosso, A.; Pritchard, R. G.; Muryn, C. A.; Ingleson, M. J. *Organometallics* **2010**, *29*, 241.
- (33) Prokofjevs, A.; Kampf, J. W.; Vedejs, E. *Angew. Chem. Int. Ed.* **2011**, *50*, 2098.
- (34) Grosso, A. D.; Helm, M. D.; Solomon, S. A.; Caras-Quintero, D.; Ingleson, M. J. *Chem. Commun.* **2011**, *47*, 12459.
- (35) Del Grosso, A.; Singleton, P. J.; Muryn, C. A.; Ingleson, M. J. *Angew. Chem. Int. Ed.* **2011**, *50*, 2102.
- (36) Obligacion, J. V.; Semproni, S. P.; Chirik, P. J. *J. Am. Chem. Soc.* **2014**, *136*, 4133.
- (37) Dombray, T.; Werncke, C. G.; Jiang, S.; Grellier, M.; Vendier, L.; Bontemps, S.; Sortais, J.-B.; Sabo-Etienne, S.; Darcel, C. *J. Am. Chem. Soc.* **2015**, *137*, 4062.
- (38) Vedejs, E.; Chapman, R. W.; Fields, S. C.; Lin, S.; Schrimpf, M. R. *J. Org. Chem.* **1995**, *60*, 3020.
- (39) Lennox, A. J. J.; Lloyd-Jones, G. C. *Angew. Chem. Int. Ed.* **2012**, *51*, 9385.
- (40) Bagutski, V.; Ros, A.; Aggarwal, V. K. *Tetrahedron* **2009**, *65*, 9956.
- (41) Noguchi, H.; Hojo, K.; Suginome, M. *J. Am. Chem. Soc.* **2007**, *129*, 758.
- (42) Fagnou, K.; Lautens, M. *Chem. Rev.* **2003**, *103*, 169.
- (43) Hayashi, T.; Yamasaki, K. *Chem. Rev.* **2003**, *103*, 2829.
- (44) Chan, D. M. T.; Monaco, K. L.; Wang, R.-P.; Winters, M. P. *Tetrahedron Lett.* **1998**, *39*, 2933.
- (45) Lam, P. Y. S.; Clark, C. G.; Saubern, S.; Adams, J.; Winters, M. P.; Chan, D. M. T.; Combs, A. *Tetrahedron Lett.* **1998**, *39*, 2941.
- (46) Evans, D. A.; Katz, J. L.; West, T. R. *Tetrahedron Lett.* **1998**, *39*, 2937.
- (47) Chan, D. M. T.; Monaco, K. L.; Li, R.; Bonne, D.; Clark, C. G.; Lam, P. Y. S. *Tetrahedron Lett.* **2003**, *44*, 3863.
- (48) Ainley, A. D.; Challenger, F. *Journal of the Chemical Society (Resumed)* **1930**, 2171.
- (49) Thiebes, C.; Thiebes, C.; Prakash, G. K. S.; Petasis, N. A.; Olah, G. A. *Synlett* **1998**, *1998*, 141.
- (50) Thompson, A. L. S.; Kabalka, G. W.; Akula, M. R.; Huffman, J. W. *Synthesis* **2005**, *2005*, 547.
- (51) Murphy, J. M.; Liao, X.; Hartwig, J. F. *J. Am. Chem. Soc.* **2007**, *129*, 15434.
- (52) Furuya, T.; Ritter, T. *Org. Lett.* **2009**, *11*, 2860.
- (53) Fier, P. S.; Luo, J.; Hartwig, J. F. *J. Am. Chem. Soc.* **2013**, *135*, 2552.
- (54) Partridge, B. M.; Hartwig, J. F. *Org. Lett.* **2013**, *15*, 140.

- (55) Webb, K. S.; Levy, D. *Tetrahedron Lett.* **1995**, *36*, 5117.
- (56) Maleczka, R. E.; Shi, F.; Holmes, D.; Smith, M. R. *J. Am. Chem. Soc.* **2003**, *125*, 7792.
- (57) Matteson, D. S.; Ray, R. *J. Am. Chem. Soc.* **1980**, *102*, 7590.
- (58) Kianmehr, E.; Yahyaei, M.; Tabatabai, K. *Tetrahedron Lett.* **2007**, *48*, 2713.
- (59) Watson, C. G.; Aggarwal, V. K. *Org. Lett.* **2013**, *15*, 1346.
- (60) Chu, L.; Qing, F.-L. *Org. Lett.* **2010**, *12*, 5060.
- (61) Jiang, X.; Chu, L.; Qing, F.-L. *J. Org. Chem.* **2012**, *77*, 1251.
- (62) Senecal, T. D.; Parsons, A. T.; Buchwald, S. L. *J. Org. Chem.* **2011**, *76*, 1174.
- (63) Novák, P.; Lishchynskiy, A.; Grushin, V. V. *Angew. Chem. Int. Ed.* **2012**, *51*, 7767.
- (64) Litvinas, N. D.; Fier, P. S.; Hartwig, J. F. *Angew. Chem. Int. Ed.* **2012**, *51*, 536.
- (65) Xu, J.; Luo, D.-F.; Xiao, B.; Liu, Z.-J.; Gong, T.-J.; Fu, Y.; Liu, L. *Chem. Commun.* **2011**, *47*, 4300.
- (66) Ye, Y.; Sanford, M. S. *J. Am. Chem. Soc.* **2012**, *134*, 9034.
- (67) Huber, M.-L.; Pinhey, J. T. *J. Chem. Soc., Perkin Trans. 1* **1990**, 721.
- (68) Tao, C.-Z.; Cui, X.; Li, J.; Liu, A.-X.; Liu, L.; Guo, Q.-X. *Tetrahedron Lett.* **2007**, *48*, 3525.
- (69) Grimes, K. D.; Gupte, A.; Aldrich, C. C. *Synthesis* **2010**, *2010*, 1441.
- (70) Salzbrunn, S.; Simon, J.; Surya Prakash, G. K.; Petasis, N. A.; Olah, G. A. *Synlett* **2000**, *2000*, 1485.
- (71) Prakash, G. K. S.; Panja, C.; Mathew, T.; Surampudi, V.; Petasis, N. A.; Olah, G. A. *Org. Lett.* **2004**, *6*, 2205.
- (72) Zhang, Z.; Liebeskind, L. S. *Org. Lett.* **2006**, *8*, 4331.
- (73) Liskey, C. W.; Liao, X.; Hartwig, J. F. *J. Am. Chem. Soc.* **2010**, *132*, 11389.
- (74) Kim, J.; Choi, J.; Shin, K.; Chang, S. *J. Am. Chem. Soc.* **2012**, *134*, 2528.
- (75) Zhang, G.; Zhang, L.; Hu, M.; Cheng, J. *Adv. Synth. Catal.* **2011**, *353*, 291.
- (76) Akrawi, O. A.; Hussain, M.; Langer, P. *Tetrahedron Lett.* **2011**, *52*, 1093.
- (77) Nguyen, H. N.; Huang, X.; Buchwald, S. L. *J. Am. Chem. Soc.* **2003**, *125*, 11818.
- (78) Suzuki, A. *J. Organomet. Chem.* **1999**, *576*, 147.
- (79) Sengupta, S.; Bhattacharyya, S. *J. Org. Chem.* **1997**, *62*, 3405.
- (80) Antoft-Finch, A.; Blackburn, T.; Snieckus, V. *J. Am. Chem. Soc.* **2009**, *131*, 17750.
- (81) Quasdorf, K. W.; Tian, X.; Garg, N. K. *J. Am. Chem. Soc.* **2008**, *130*, 14422.
- (82) Liebeskind, L. S.; Srogl, J. *J. Am. Chem. Soc.* **2000**, *122*, 11260.
- (83) Kusturin, C.; Liebeskind, L. S.; Rahman, H.; Sample, K.; Schweitzer, B.; Srogl, J.; Neumann, W. L. *Org. Lett.* **2003**, *5*, 4349.
- (84) Yokozawa, T.; Kohno, H.; Ohta, Y.; Yokoyama, A. *Macromolecules* **2010**, *43*, 7095.

- (85) Elmalem, E.; Biedermann, F.; Johnson, K.; Friend, R. H.; Huck, W. T. S. *J. Am. Chem. Soc.* **2012**, *134*, 17769.
- (86) Kitney, S. P.; Cheng, F.; Khan, S.; Hope, C. N.; McNab, W.; Kelly, S. M. *Liq. Cryst.* **2011**, *38*, 1027.
- (87) Li, J.; Ballmer, S. G.; Gillis, E. P.; Fujii, S.; Schmidt, M. J.; Palazzolo, A. M. E.; Lehmann, J. W.; Morehouse, G. F.; Burke, M. D. *Science* **2015**, *347*, 1221.
- (88) Glasnov, T. N.; Kappe, C. O. *Adv. Synth. Catal.* **2010**, *352*, 3089.
- (89) Lennox, A. J. J.; Lloyd-Jones, G. C. *Isr. J. Chem.* **2010**, *50*, 664.
- (90) Deng, J. Z.; Paone, D. V.; Ginnetti, A. T.; Kurihara, H.; Dreher, S. D.; Weissman, S. A.; Stauffer, S. R.; Burgey, C. S. *Org. Lett.* **2008**, *11*, 345.
- (91) Molander, G. A.; Petrillo, D. E. *J. Am. Chem. Soc.* **2006**, *128*, 9634.
- (92) Molander, G. A.; Cooper, D. J. *J. Org. Chem.* **2007**, *72*, 3558.
- (93) Molander, G. A.; Figueroa, R. *J. Org. Chem.* **2006**, *71*, 6135.
- (94) Molander, G. A.; Sandrock, D. L. *J. Am. Chem. Soc.* **2008**, *130*, 15792.
- (95) Darses, S.; Genêt, J.-P.; Brayer, J.-L.; Demoute, J.-P. *Tetrahedron Lett.* **1997**, *38*, 4393.
- (96) Gillis, E. P.; Burke, M. D. *J. Am. Chem. Soc.* **2008**, *130*, 14084.
- (97) Gillis, E. P.; Burke, M. D. *J. Am. Chem. Soc.* **2007**, *129*, 6716.
- (98) Dick, G. R.; Woerly, E. M.; Burke, M. D. *Angew. Chem. Int. Ed.* **2012**, *51*, 2667.
- (99) Cho, J.-Y.; Tse, M. K.; Holmes, D.; Maleczka, R. E.; Smith, M. R. *Science* **2002**, *295*, 305.
- (100) Ishiyama, T.; Nobuta, Y.; Hartwig, J. F.; Miyaura, N. *Chem. Commun.* **2003**, 2924.
- (101) Kikuchi, T.; Nobuta, Y.; Umeda, J.; Yamamoto, Y.; Ishiyama, T.; Miyaura, N. *Tetrahedron* **2008**, *64*, 4967.
- (102) Robbins, D. W.; Hartwig, J. F. *Angew. Chem. Int. Ed.* **2013**, *52*, 933.
- (103) Mizoroki, T.; Mori, K.; Ozaki, A. *Bull. Chem. Soc. Jpn.* **1971**, *44*, 581.
- (104) Heck, R. F.; Nolley, J. P. *J. Org. Chem.* **1972**, *37*, 2320.
- (105) Dieck, H. A.; Heck, R. F. *J. Org. Chem.* **1975**, *40*, 1083.
- (106) Jung, Y. C.; Mishra, R. K.; Yoon, C. H.; Jung, K. W. *Org. Lett.* **2003**, *5*, 2231.
- (107) Yoo, K. S.; Yoon, C. H.; Jung, K. W. *J. Am. Chem. Soc.* **2006**, *128*, 16384.
- (108) O'Neill, J.; Yoo, K. S.; Jung, K. W. *Tetrahedron Lett.* **2008**, *49*, 7307.
- (109) Du, X.; Suguro, M.; Hirabayashi, K.; Mori, A.; Nishikata, T.; Hagiwara, N.; Kawata, K.; Okeda, T.; Wang, H. F.; Fugami, K.; Kosugi, M. *Org. Lett.* **2001**, *3*, 3313.
- (110) Parrish, J. P.; Jung, Y. C.; Shin, S. I.; Jung, K. W. *J. Org. Chem.* **2002**, *67*, 7127.
- (111) Delcamp, J. H.; Brucks, A. P.; White, M. C. *J. Am. Chem. Soc.* **2008**, *130*, 11270.
- (112) Enquist, P.-A.; Lindh, J.; Nilsson, P.; Larhed, M. *Green Chemistry* **2006**, *8*, 338.
- (113) Ruan, J.; Li, X.; Saidi, O.; Xiao, J. *J. Am. Chem. Soc.* **2008**, *130*, 2424.
- (114) Andappan, M. M. S.; Nilsson, P.; Larhed, M. *Chem. Commun.* **2004**, 218.

- (115) Andappan, M. M. S.; Nilsson, P.; von Schenck, H.; Larhed, M. *J. Org. Chem.* **2004**, *69*, 5212.
- (116) Nguyen, P.; Blom, H. P.; Westcott, S. A.; Taylor, N. J.; Marder, T. B. *J. Am. Chem. Soc.* **1993**, *115*, 9329.
- (117) Waltz, K. M.; He, X.; Muhoro, C.; Hartwig, J. F. *J. Am. Chem. Soc.* **1995**, *117*, 11357.
- (118) Iverson, C. N.; Smith, M. R. *J. Am. Chem. Soc.* **1999**, *121*, 7696.
- (119) Shimada, S.; Batsanov, A. S.; Howard, J. A. K.; Marder, T. B. *Angew. Chem. Int. Ed.* **2001**, *40*, 2168.
- (120) Ishiyama, T.; Takagi, J.; Ishida, K.; Miyaura, N.; Anastasi, N. R.; Hartwig, J. F. *J. Am. Chem. Soc.* **2002**, *124*, 390.
- (121) Ishiyama, T.; Takagi, J.; Hartwig, J. F.; Miyaura, N. *Angew. Chem. Int. Ed.* **2002**, *41*, 3056.
- (122) Larsen, M. A.; Hartwig, J. F. *J. Am. Chem. Soc.* **2014**, *136*, 4287.
- (123) Preshlock, S. M.; Ghaffari, B.; Maligres, P. E.; Krska, S. W.; Maleczka, R. E.; Smith, M. R. *J. Am. Chem. Soc.* **2013**, *135*, 7572.
- (124) Tamura, H.; Yamazaki, H.; Sato, H.; Sakaki, S. *J. Am. Chem. Soc.* **2003**, *125*, 16114.
- (125) Boller, T. M.; Murphy, J. M.; Hapke, M.; Ishiyama, T.; Miyaura, N.; Hartwig, J. F. *J. Am. Chem. Soc.* **2005**, *127*, 14263.
- (126) Chotana, G. A.; Rak, M. A.; Smith, M. R. *J. Am. Chem. Soc.* **2005**, *127*, 10539.
- (127) Tajuddin, H.; Harrisson, P.; Bitterlich, B.; Collings, J. C.; Sim, N.; Batsanov, A. S.; Cheung, M. S.; Kawamorita, S.; Maxwell, A. C.; Shukla, L.; Morris, J.; Lin, Z.; Marder, T. B.; Steel, P. G. *Chemical Science* **2012**, *3*, 3505.
- (128) Vanchura, I. I. B. A.; Preshlock, S. M.; Roosen, P. C.; Kallepalli, V. A.; Staples, R. J.; Maleczka, J. R. E.; Singleton, D. A.; Smith, I. I. I. M. R. *Chem. Commun.* **2010**, *46*, 7724.
- (129) Tajuddin, H. *New strategies for synthesis with boronate esters [electronic resource] / Hazmi Tajuddin* [Durham], 2013.
- (130) Takagi, J.; Sato, K.; Hartwig, J. F.; Ishiyama, T.; Miyaura, N. *Tetrahedron Lett.* **2002**, *43*, 5649.
- (131) Ishiyama, T.; Miyaura, N. *J. Organomet. Chem.* **2003**, *680*, 3.
- (132) Nguyen, P.; Dai, C.; Taylor, N. J.; Power, W. P.; Marder, T. B.; Pickett, N. L.; Norman, N. C. *Inorg. Chem.* **1995**, *34*, 4290.
- (133) Mkhaldid, I. A. I. *Transition metal catalysed borylation of C-H bonds* [Durham], 2006.
- (134) Robbins, D. W.; Hartwig, J. F. *Org. Lett.* **2012**, *14*, 4266.
- (135) Fuller, A. A.; Hester, H. R.; Salo, E. V.; Stevens, E. P. *Tetrahedron Lett.* **2003**, *44*, 2935.
- (136) Noonan, G.; Leach, A. G. *Org. Biomol. Chem.* **2015**, *13*, 2555.
- (137) Billingsley, K. L.; Buchwald, S. L. *Angew. Chem. Int. Ed.* **2008**, *47*, 4695.

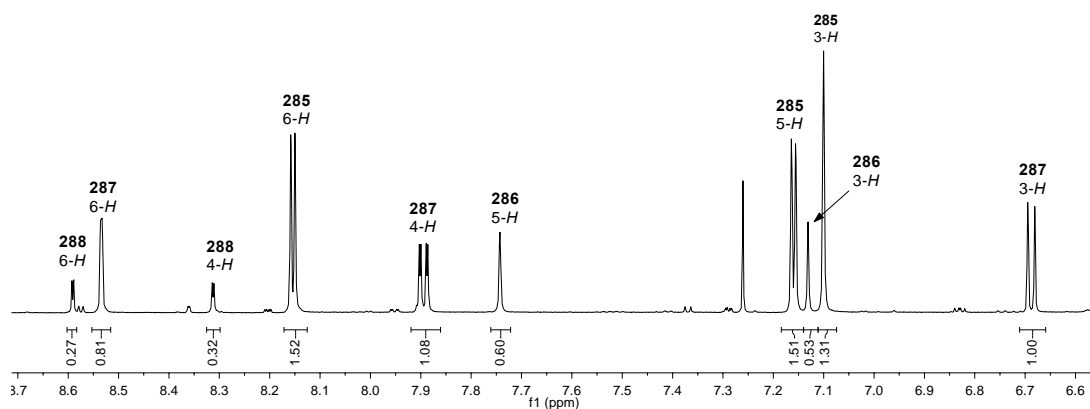
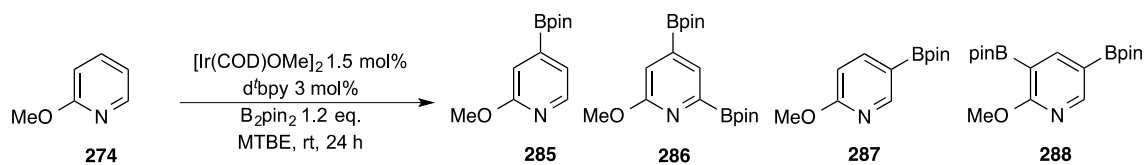
- (138) Mkhaliid, I. A. I.; Coventry, D. N.; Albesa-Jove, D.; Batsanov, A. S.; Howard, J. A. K.; Perutz, R. N.; Marder, T. B. *Angew. Chem. Int. Ed.* **2006**, *45*, 489.
- (139) Brown, H. C.; McDaniel, D. H. *J. Am. Chem. Soc.* **1955**, *77*, 3752.
- (140) Bouillon, A.; Lancelot, J.-C.; Sopkova de Oliveira Santos, J.; Collot, V.; Bovy, P. R.; Rault, S. *Tetrahedron* **2003**, *59*, 10043.
- (141) Jayasundara, C. R. K.; Unold, J. M.; Oppenheimer, J.; Smith, M. R.; Maleczka, R. E. *Org. Lett.* **2014**, *16*, 6072.
- (142) Ram, S.; Ehrenkauser, R. E. *Synthesis* **1988**, 1988, 91.
- (143) Anwer, M. K.; Sherman, D.; Roney, J. G.; Spatola, A. F. *J. Org. Chem.* **1989**, *54*, 1284.
- (144) Brieger, G.; Nestrick, T. J. *Chem. Rev.* **1974**, *74*, 567.
- (145) Narayan, S.; Seelhammer, T.; Gawley, R. E. *Tetrahedron Lett.* **2004**, *45*, 757.
- (146) Liu, M.; Mao, X.-a.; Ye, C.; Huang, H.; Nicholson, J. K.; Lindon, J. C. *Journal of Magnetic Resonance* **1998**, *132*, 125.
- (147) Xiong, F.; Qian, C.; Lin, D.; Zeng, W.; Lu, X. *Org. Lett.* **2013**, *15*, 5444.
- (148) Welsch, M. E.; Snyder, S. A.; Stockwell, B. R. *Curr. Opin. Chem. Biol.* **2010**, *14*, 347.
- (149) Zhichkin, P.; Beer, C. M. C.; Rennells, W. M.; Fairfax, D. J. *Synlett* **2006**, 2006, 0379.
- (150) Sakai, N.; Tamura, K.; Shimamura, K.; Ikeda, R.; Konakahara, T. *Org. Lett.* **2012**, *14*, 836.
- (151) Shafakat Ali, N. A.; Ahmad Dar, B.; Pradhan, V.; Farooqui, M. *Mini Reviews in Medicinal Chemistry* **2013**, *13*, 1792.
- (152) Baiocchi, L.; Corsi, G.; Palazzo, G. *Synthesis* **1978**, 1978, 633.
- (153) Szmant, H. H.; Harmuth, C. M. *J. Am. Chem. Soc.* **1959**, *81*, 962.
- (154) Halley, F.; Sava, X. *Synth. Commun.* **1997**, *27*, 1199.
- (155) Walser, A.; Flynn, T.; Mason, C. *J. Heterocycl. Chem.* **1991**, *28*, 1121.
- (156) In *Chem. Heterocycl. Compd.*; John Wiley & Sons, Inc.: 2008, p 289.
- (157) Preshlock, S. M.; Plattner, D. L.; Maligres, P. E.; Krska, S. W.; Maleczka, R. E.; Smith, M. R. *Angew. Chem. Int. Ed.* **2013**, *52*, 12915.
- (158) Gorelsky, S. I. *Organometallics* **2012**, *31*, 794.
- (159) Slade, D. J.; Pelz, N. F.; Bodnar, W.; Lampe, J. W.; Watson, P. S. *J. Org. Chem.* **2009**, *74*, 6331.
- (160) Luo, G.; Chen, L.; Dubowchik, G. *J. Org. Chem.* **2006**, *71*, 5392.
- (161) Unsinn, A.; Knochel, P. *Chem. Commun.* **2012**, *48*, 2680.
- (162) Counciller, C. M.; Eichman, C. C.; Wray, B. C.; Stambuli, J. P. *Org. Lett.* **2008**, *10*, 1021.
- (163) Robbins, D. W.; Boebel, T. A.; Hartwig, J. F. *J. Am. Chem. Soc.* **2010**, *132*, 4068.
- (164) Konishi, S.; Kawamorita, S.; Iwai, T.; Steel, P. G.; Marder, T. B.; Sawamura, M. *Chemistry – An Asian Journal* **2014**, *9*, 434.
- (165) Siddle, J. S.; Batsanov, A. S.; Bryce, M. R. *Eur. J. Org. Chem.* **2008**, 2008, 2746.

- (166) Antilla, J. C.; Baskin, J. M.; Barder, T. E.; Buchwald, S. L. *J. Org. Chem.* **2004**, *69*, 5578.
- (167) Hansch, C.; Sammes, P. G.; Taylor, J. B., - *Comprehensive medicinal chemistry : the rational design, mechanistic study & therapeutic application of chemical compounds*; Pergamon P.: Oxford :, 1990.
- (168) Bagdi, A. K.; Santra, S.; Monir, K.; Hajra, A. *Chem. Commun.* **2015**, *51*, 1555.
- (169) Bethel, P. A.; Campbell, A. D.; Goldberg, F. W.; Kemmitt, P. D.; Lamont, G. M.; Suleman, A. *Tetrahedron* **2012**, *68*, 5434.
- (170) Lukasik, P. M.; Elabar, S.; Lam, F.; Shao, H.; Liu, X.; Abbas, A. Y.; Wang, S. *Eur. J. Med. Chem.* **2012**, *57*, 311.
- (171) Egan, B. A.; Burton, P. M. *RSC Advances* **2014**, *4*, 27726.
- (172) Dehmlow, H.; Aebi, J. D.; Jolidon, S.; Ji, Y.-H.; von der Mark, E. M.; Himber, J.; Morand, O. H. *J. Med. Chem.* **2003**, *46*, 3354.
- (173) Steffan, R. J.; Matelan, E.; Ashwell, M. A.; Moore, W. J.; Solvibile, W. R.; Trybulski, E.; Chadwick, C. C.; Chippari, S.; Kenney, T.; Eckert, A.; Borges-Marcucci, L.; Keith, J. C.; Xu, Z.; Mosyak, L.; Harnish, D. C. *J. Med. Chem.* **2004**, *47*, 6435.
- (174) Spiteri, C.; Keeling, S.; Moses, J. E. *Org. Lett.* **2010**, *12*, 3368.
- (175) Li, P.; Zhao, J.; Wu, C.; Larock, R. C.; Shi, F. *Org. Lett.* **2011**, *13*, 3340.
- (176) Bunnell, A.; O'Yang, C.; Petrica, A.; Soth, M. J. *Synth. Commun.* **2006**, *36*, 285.
- (177) Welch, W. M.; Hanau, C. E.; Whalen, W. M. *Synthesis* **1992**, *1992*, 937.
- (178) Hattori, K.; Yamaguchi, K.; Yamaguchi, J.; Itami, K. *Tetrahedron* **2012**, *68*, 7605.
- (179) Yi, C.-L.; Liu, T.-J.; Cheng, J.-H.; Lee, C.-F. *Eur. J. Org. Chem.* **2013**, *2013*, 3910.
- (180) Ben-Yahia, A.; Naas, M.; El Kazzouli, S.; Essassi, E. M.; Guillaumet, G. *Eur. J. Org. Chem.* **2012**, *2012*, 7075.
- (181) Tajuddin, H.; Shukla, L.; Maxwell, A. C.; Marder, T. B.; Steel, P. G. *Org. Lett.* **2010**, *12*, 5700.
- (182) Boebel, T. A.; Hartwig, J. F. *Tetrahedron* **2008**, *64*, 6824.
- (183) Cheng, J.-H.; Yi, C.-L.; Liu, T.-J.; Lee, C.-F. *Chem. Commun.* **2012**, *48*, 8440.
- (184) Murphy, J. M.; Tzschucke, C. C.; Hartwig, J. F. *Org. Lett.* **2007**, *9*, 757.
- (185) Shi, F.; Smith, M. R.; Maleczka, R. E. *Org. Lett.* **2006**, *8*, 1411.
- (186) Tzschucke, C. C.; Murphy, J. M.; Hartwig, J. F. *Org. Lett.* **2007**, *9*, 761.
- (187) Gottumukkala, A. L.; Teichert, J. F.; Heijnen, D.; Eisink, N.; van Dijk, S.; Ferrer, C.; van den Hoogenband, A.; Minnaard, A. J. *J. Org. Chem.* **2011**, *76*, 3498.
- (188) Lima, C. F. R. A. C.; Rodrigues, A. S. M. C.; Silva, V. L. M.; Silva, A. M. S.; Santos, L. M. N. B. F. *ChemCatChem* **2014**, *6*, 1291.
- (189) Matos, K.; Soderquist, J. A. *J. Org. Chem.* **1998**, *63*, 461.
- (190) Amatore, C.; Jutand, A.; Le Duc, G. *Angew. Chem. Int. Ed.* **2012**, *51*, 1379.
- (191) Gurung, S. K.; Thapa, S.; Kafle, A.; Dickie, D. A.; Giri, R. *Org. Lett.* **2014**, *16*, 1264.
- (192) Uson, R.; Oro, L. A.; Cabeza, J. A.; Bryndza, H. E.; Stepro, M. P. In *Inorg. Synth.*; John Wiley & Sons, Inc.: 2007, p 126.

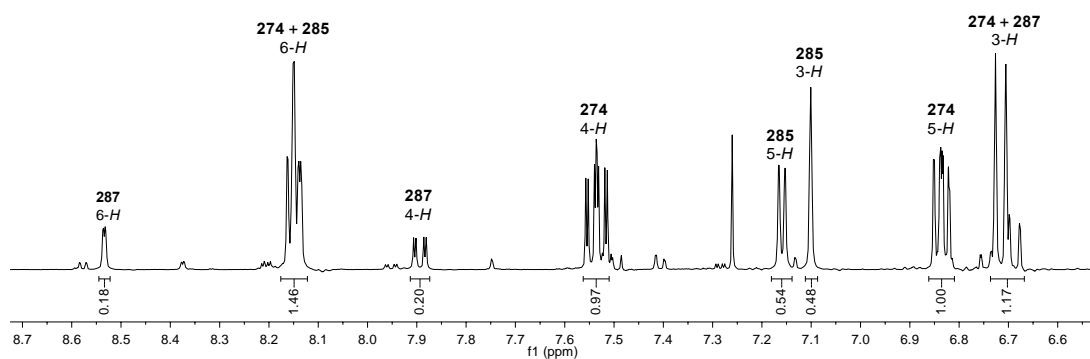
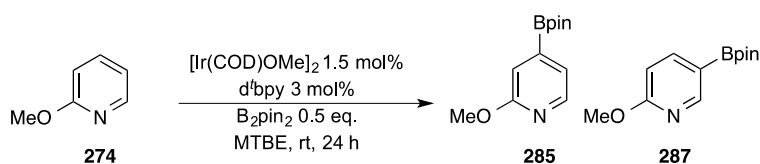
- (193) Bernhammer, J. C.; Singh, H.; Huynh, H. V. *Organometallics* **2014**, *33*, 4295.
- (194) Baddam, S. R.; Uday Kumar, N.; Panasa Reddy, A.; Bandichhor, R. *Tetrahedron Lett.* **2013**, *54*, 1661.
- (195) Herdemann, M.; Heit, I.; Bosch, F.-U.; Quintini, G.; Scheipers, C.; Weber, A. *Bioorg. Med. Chem. Lett.* **2010**, *20*, 6998.
- (196) Ye, Q.; Shen, Y.; Zhou, Y.; Lv, D.; Gao, J.; Li, J.; Hu, Y. *Eur. J. Med. Chem.* **2013**, *68*, 361.

7 Appendix

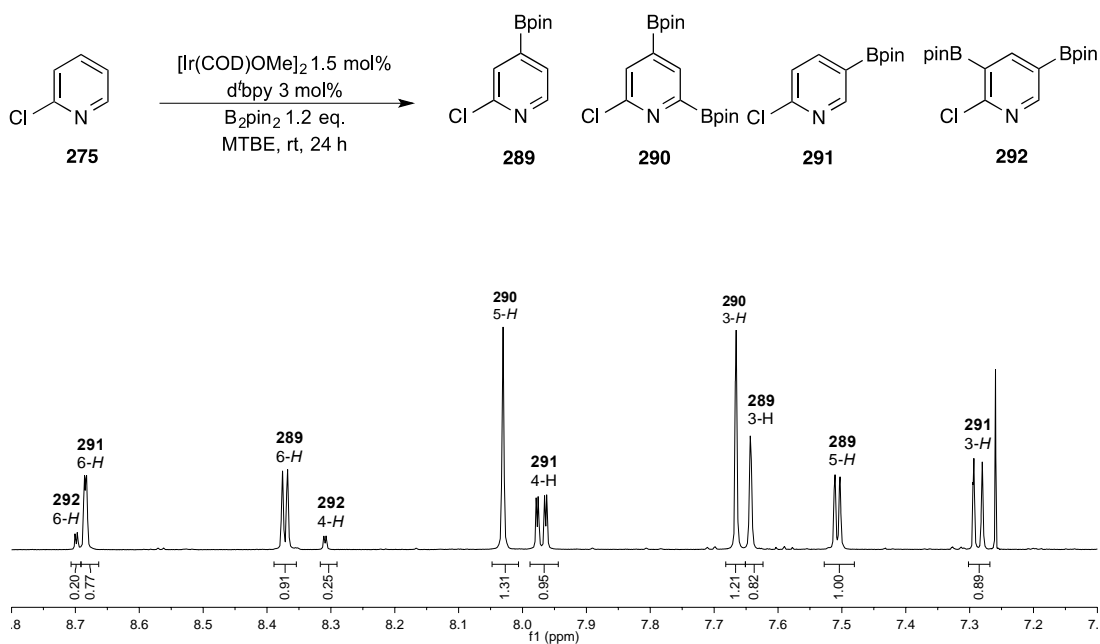
Borylation of 2-methoxypyridine (**274**) (400 MHz, CDCl₃)



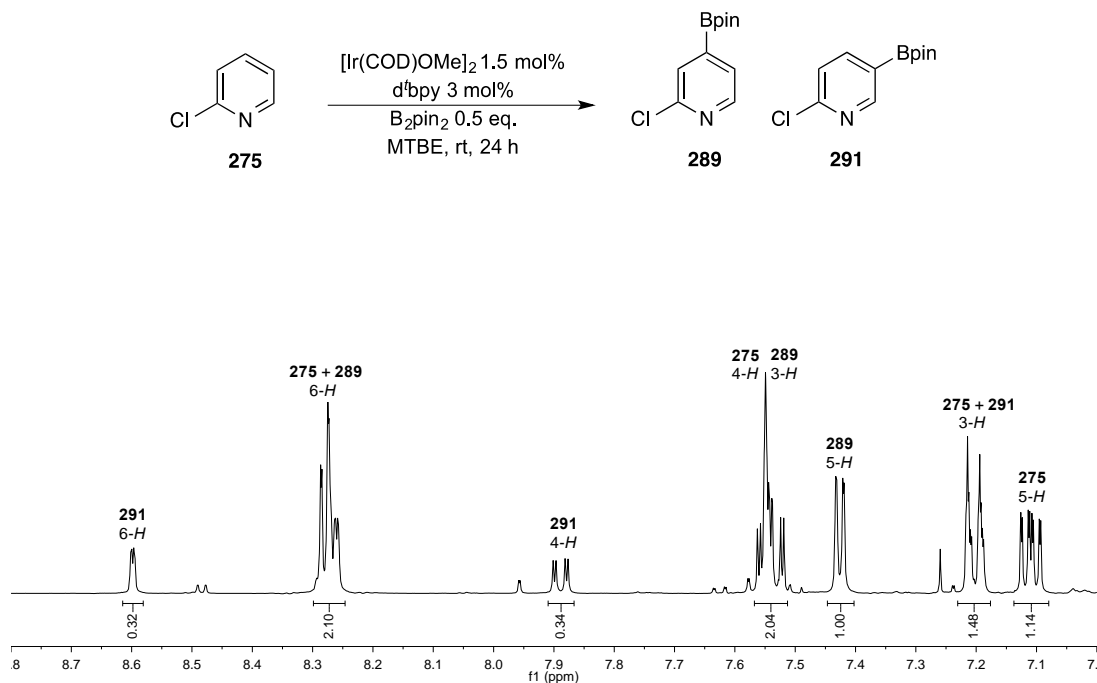
Borylation of 2-methoxypyridine (**274**) under boron-limiting conditions (400 MHz, CDCl₃)



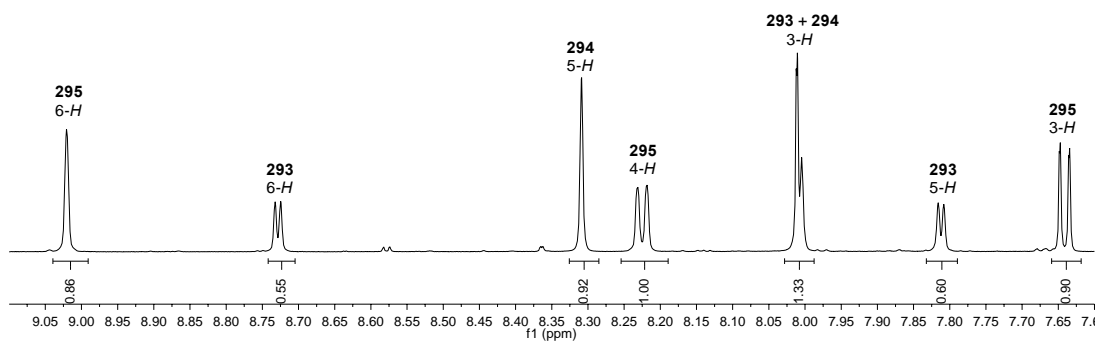
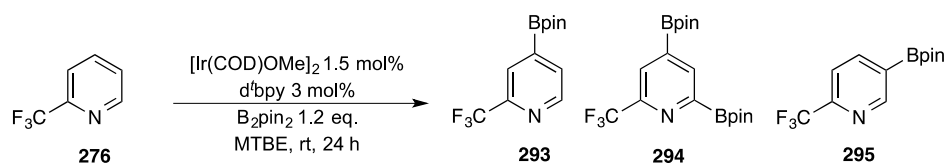
Borylation of 2-chloropyridine (275) (400 MHz, CDCl₃)



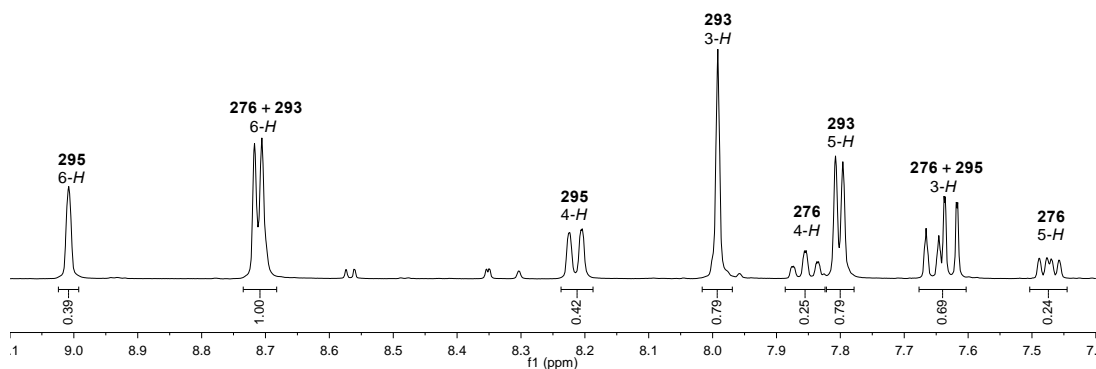
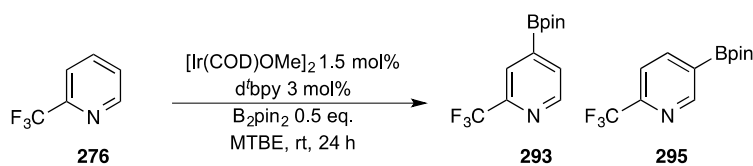
Borylation of 2-chloropyridine (275) under boron-limiting conditions (400 MHz, CDCl₃)



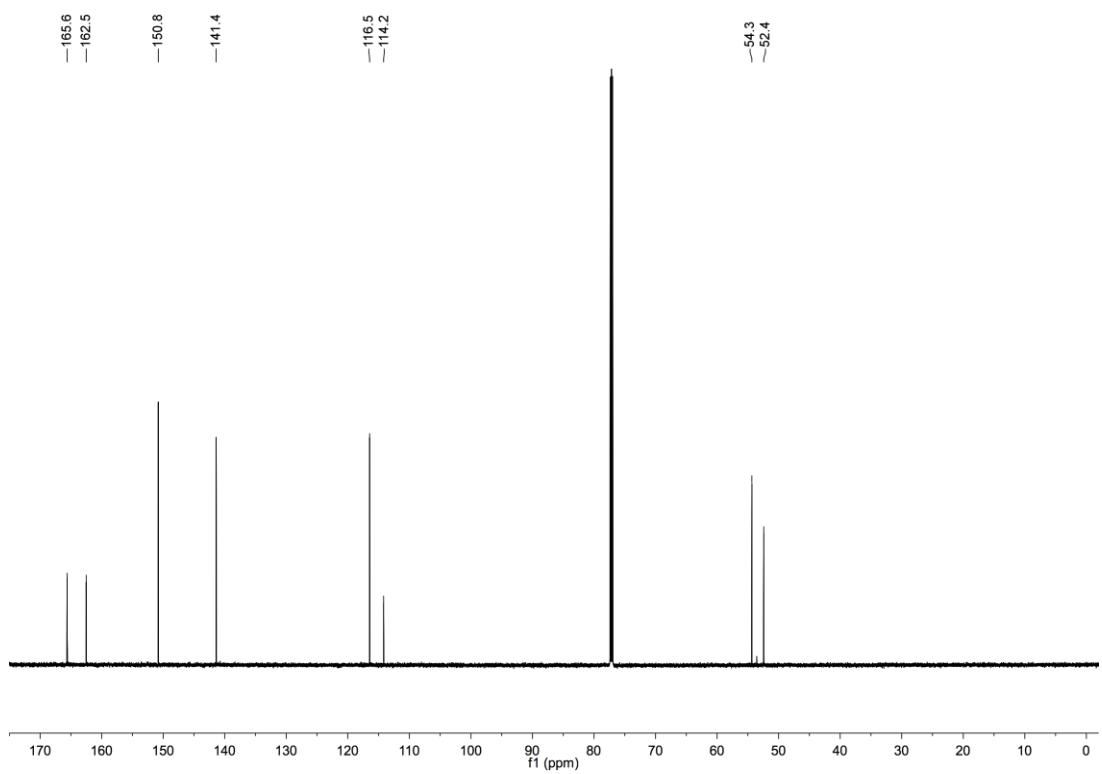
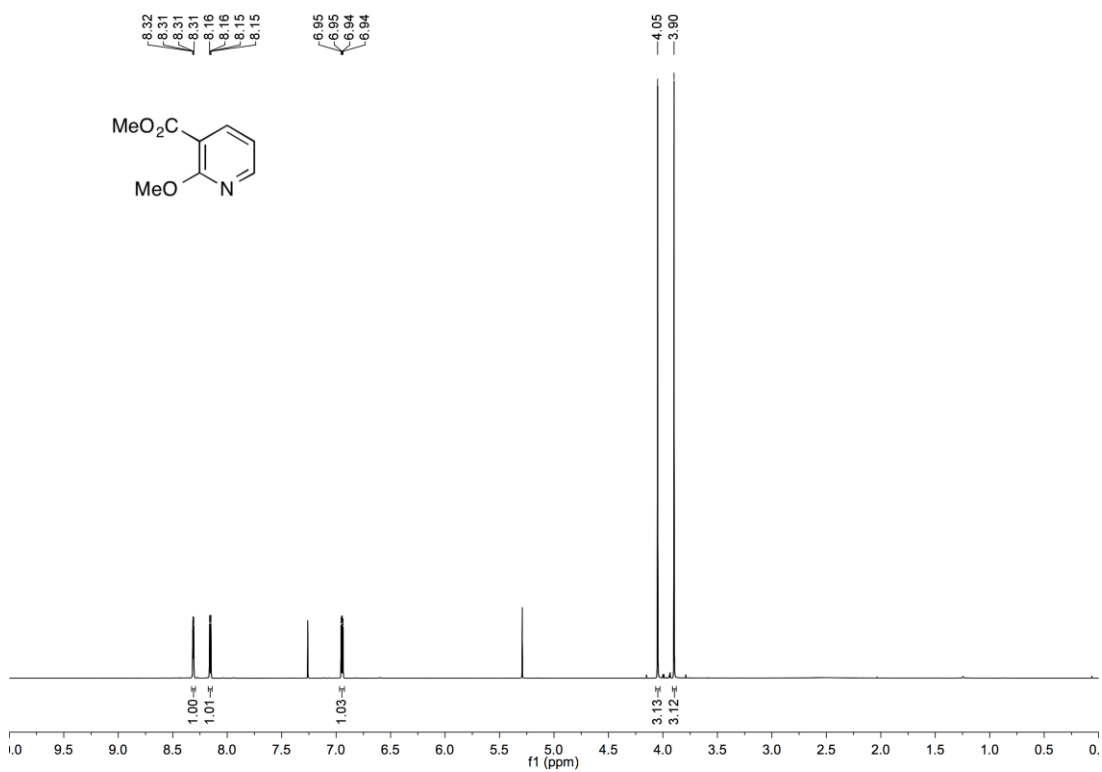
Borylation of 2-(trifluoromethyl)pyridine (276) (400 MHz, CDCl₃)



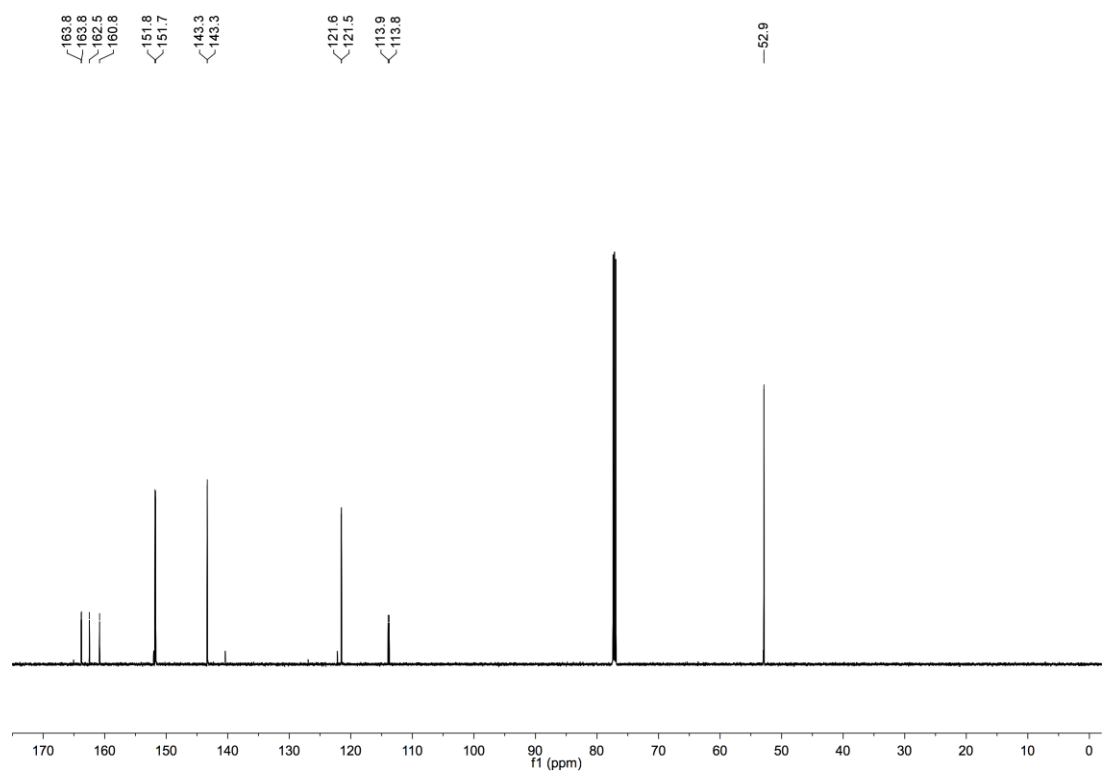
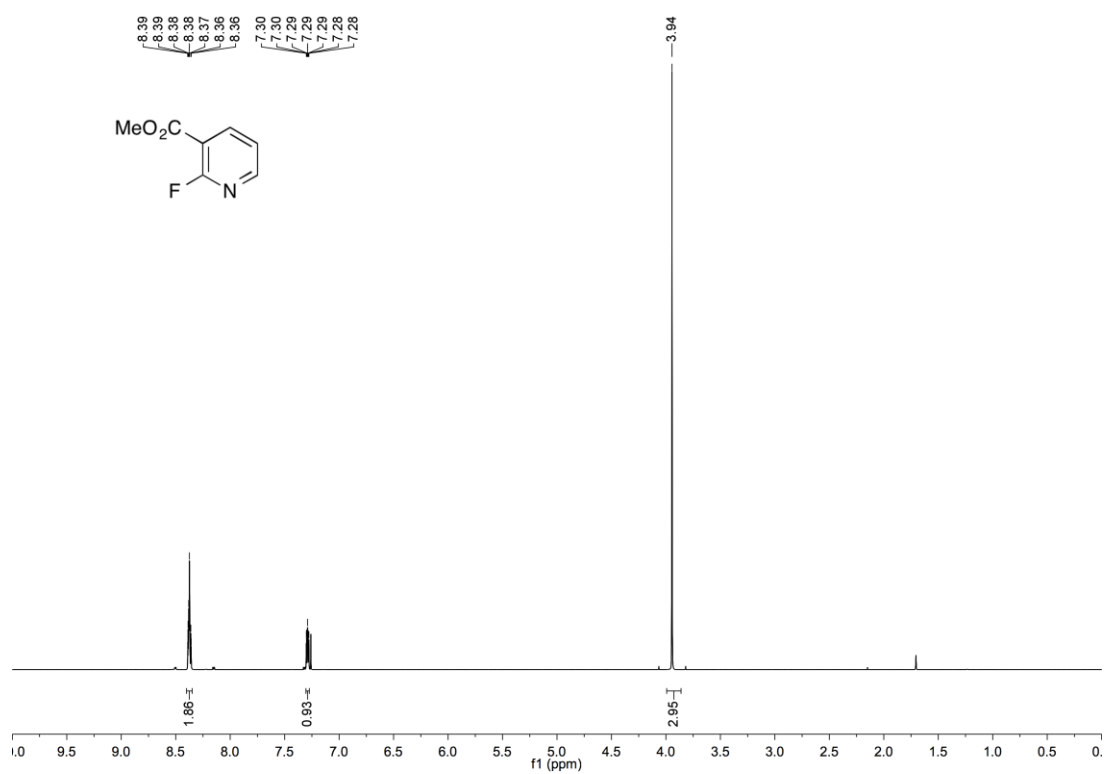
Borylation of 2-(trifluoromethyl)pyridine (276) under boron-limiting conditions (400 MHz, CDCl₃)

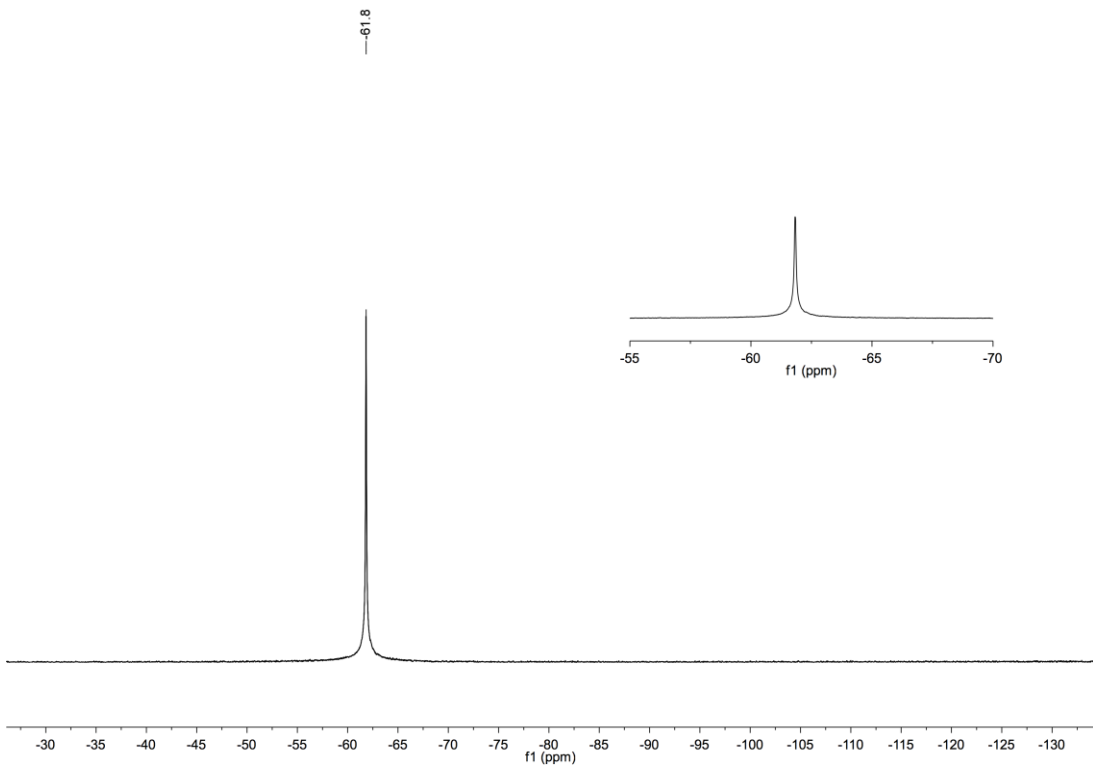


Methyl-2-methoxynicotinate (304)

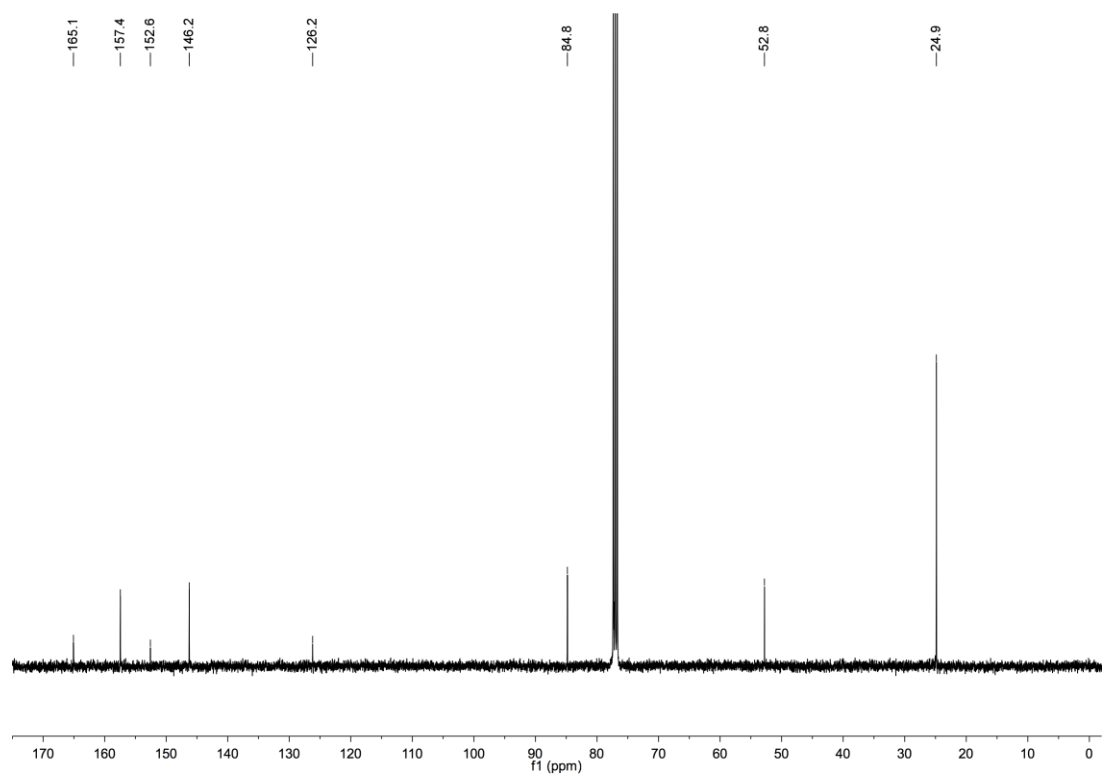
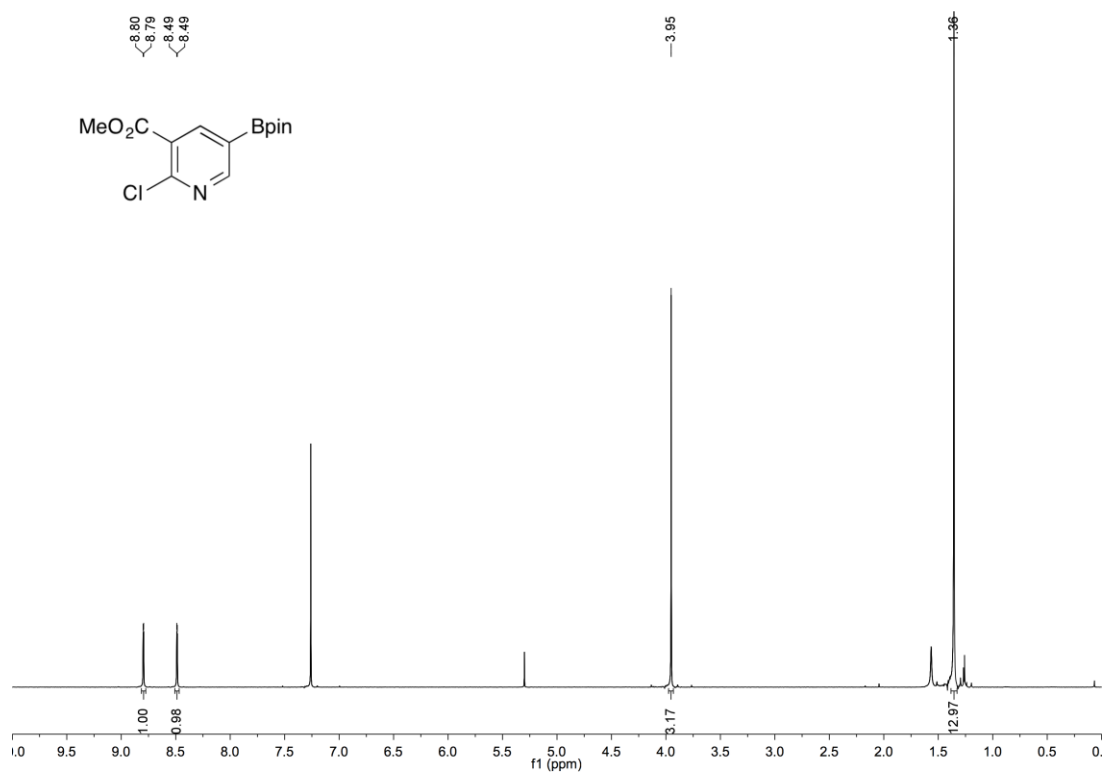


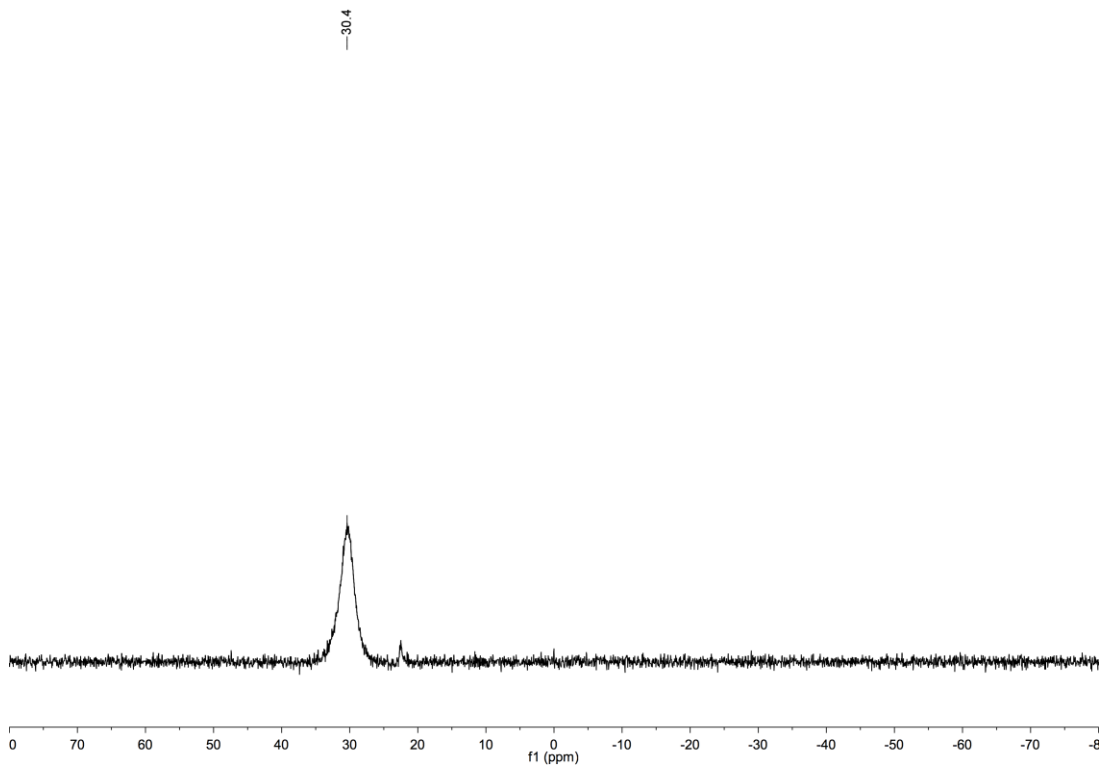
Methyl-2-fluoronicotinate (305)



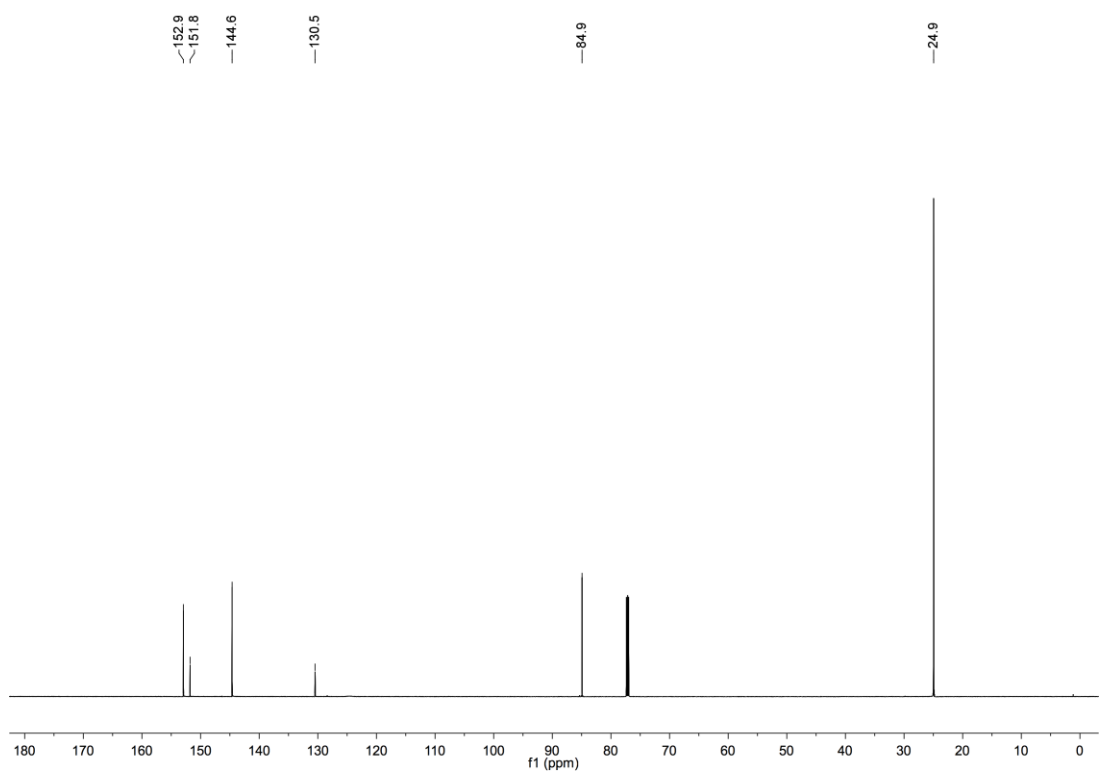
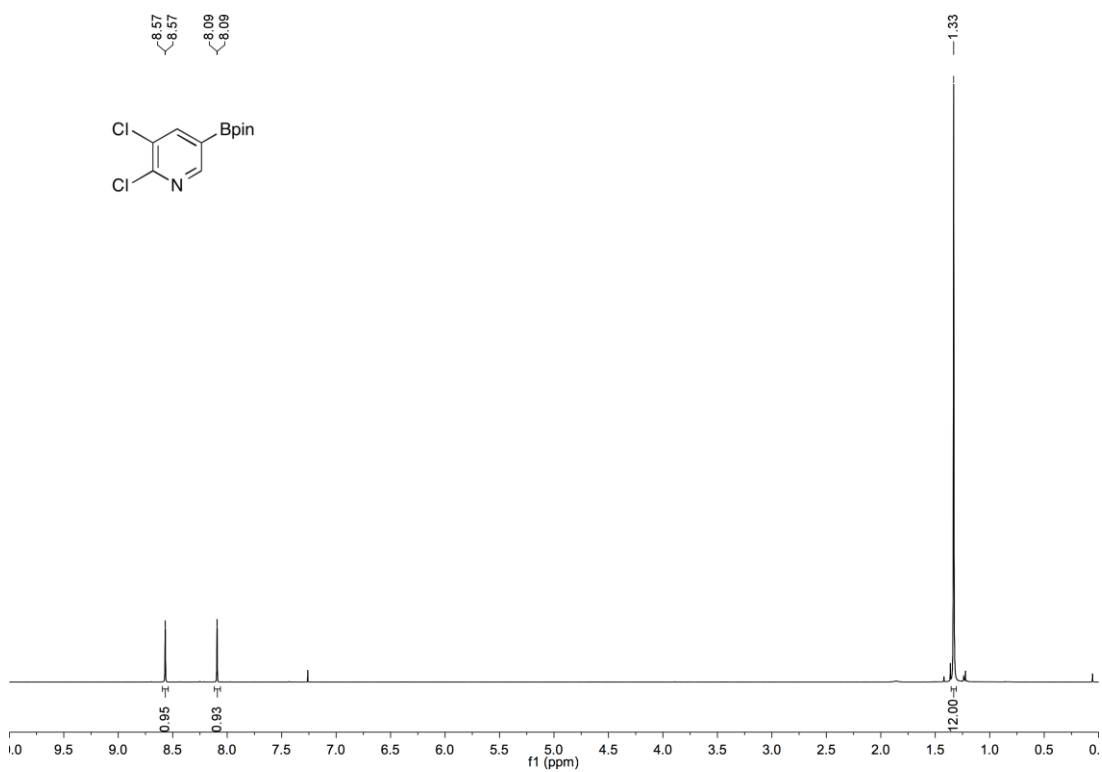


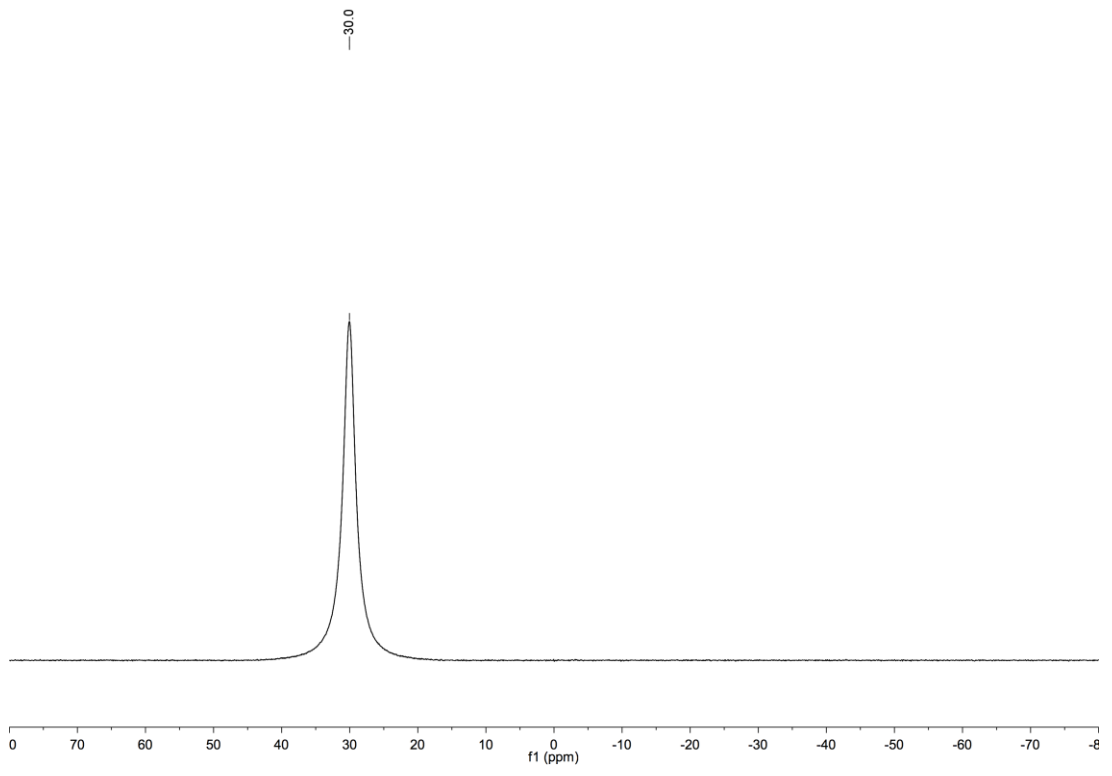
Methyl-2-chloro-5-(Bpin)nicotinate (**311**)



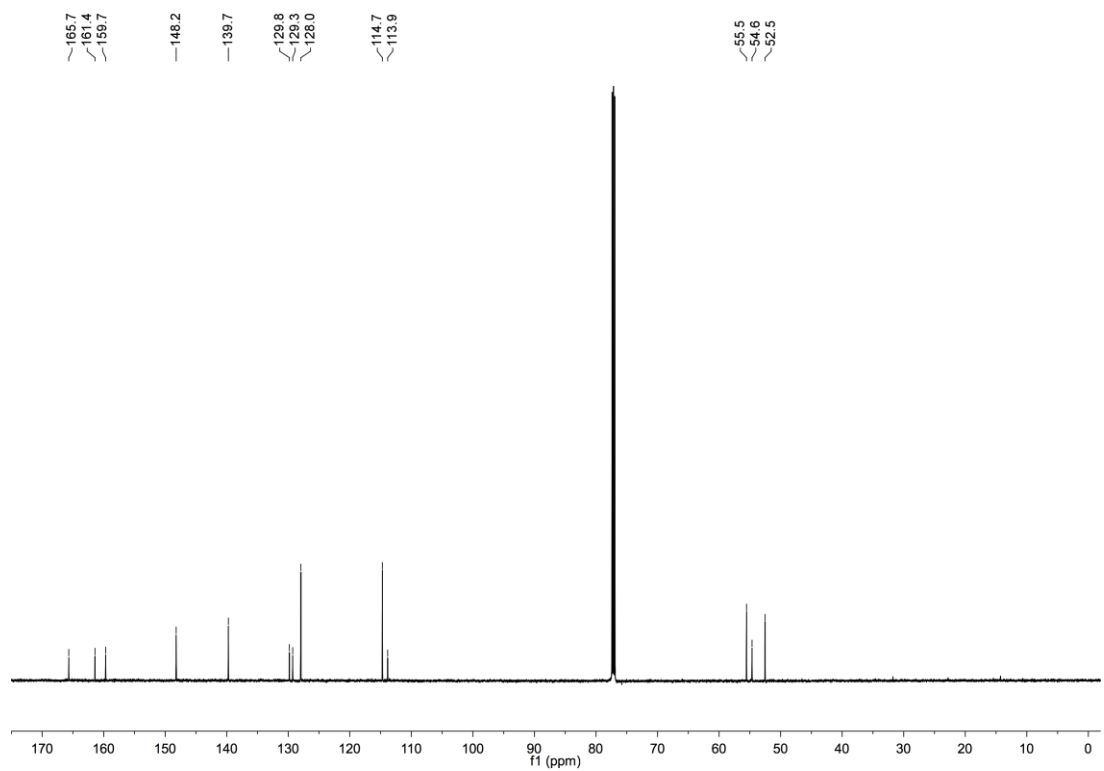
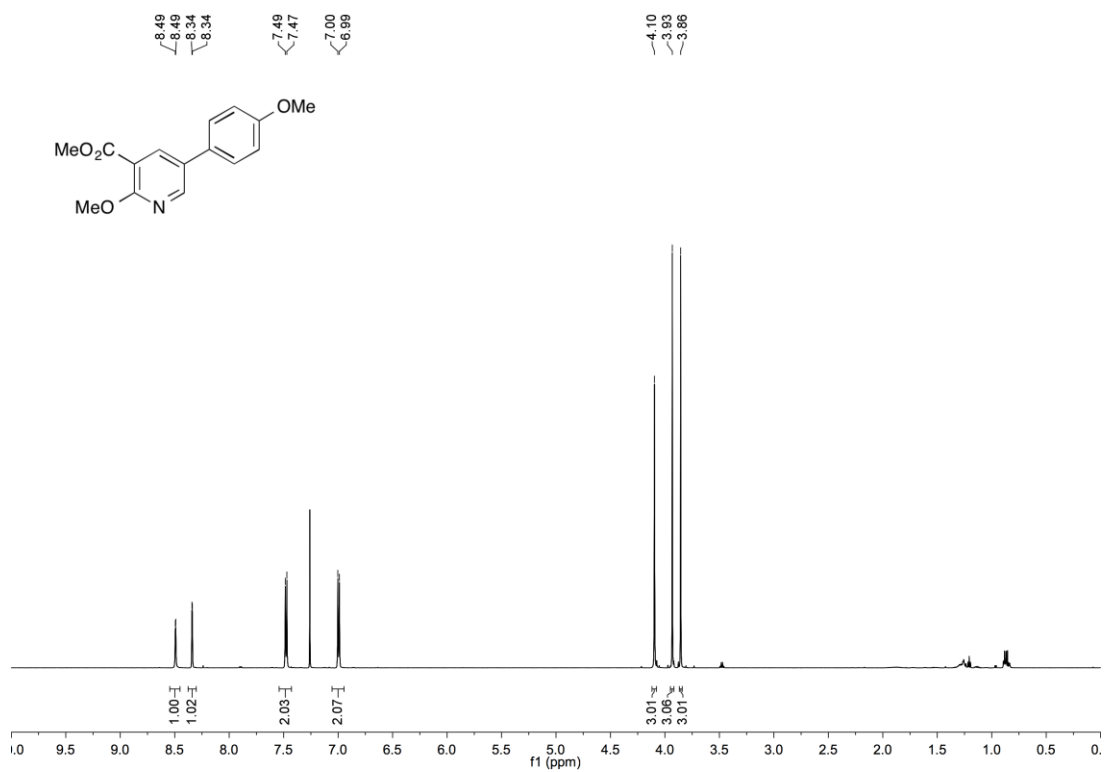


2,3-Dichloro-5-(Bpin)-pyridine (317)

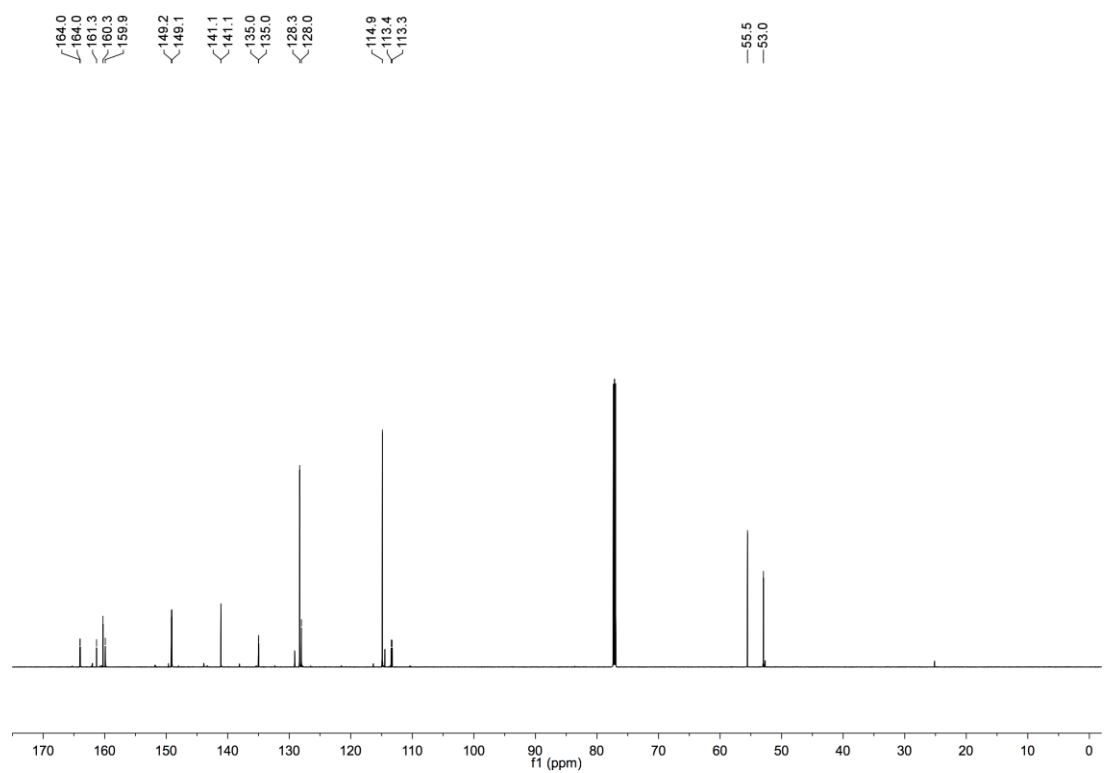
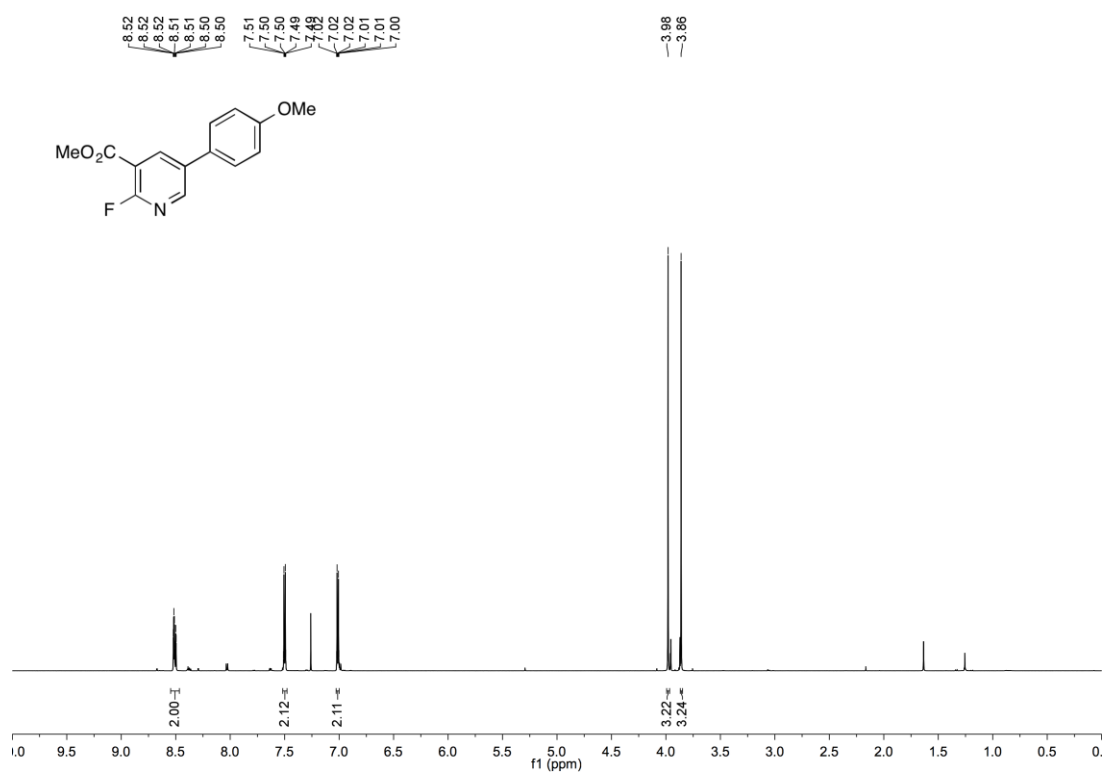




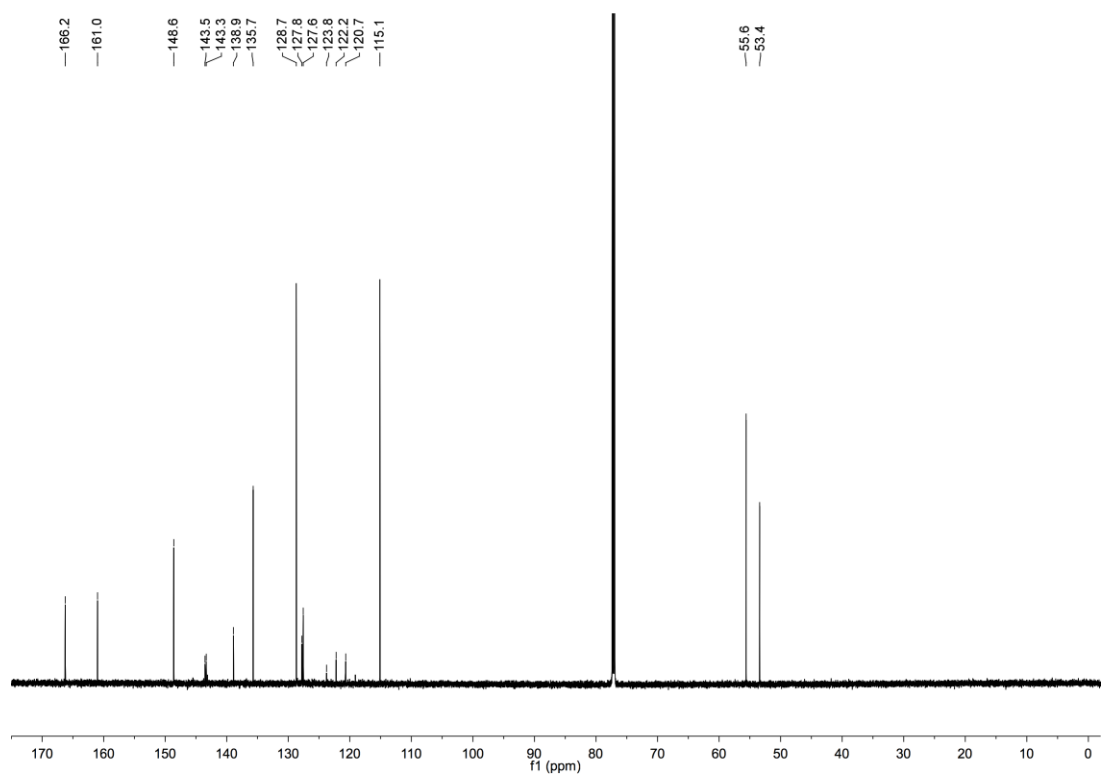
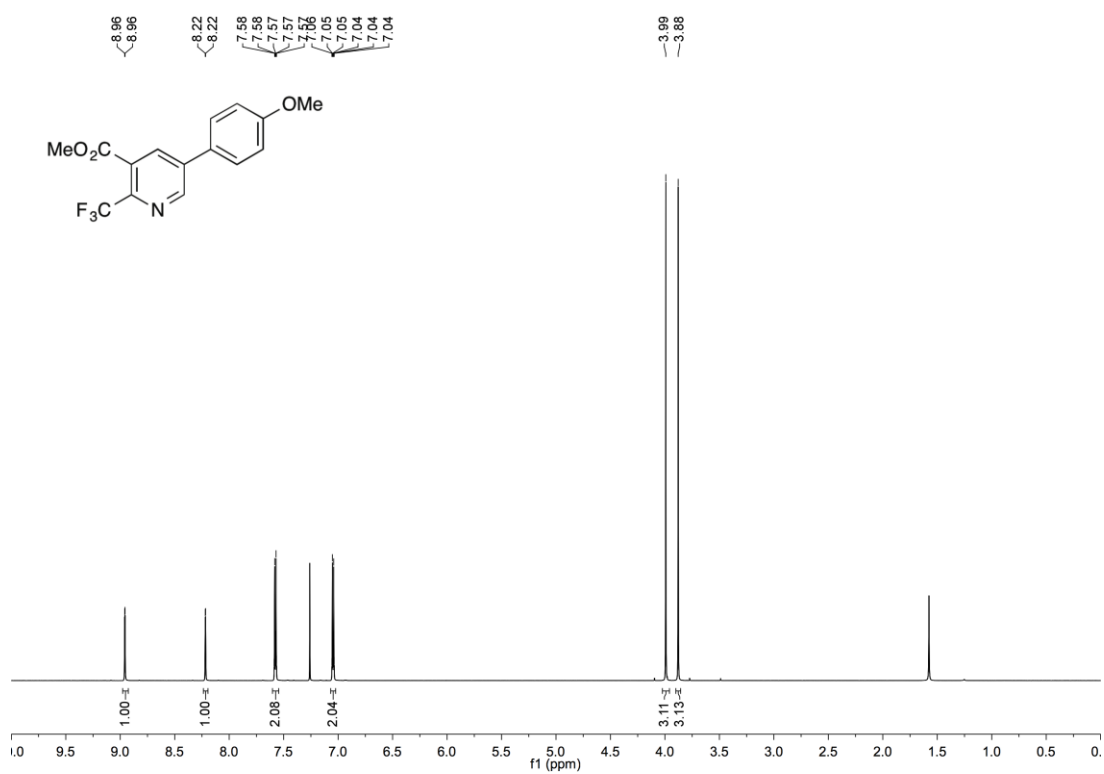
Methyl-2-methoxy-5-(4'-methoxyphenyl)nicotinate (319)

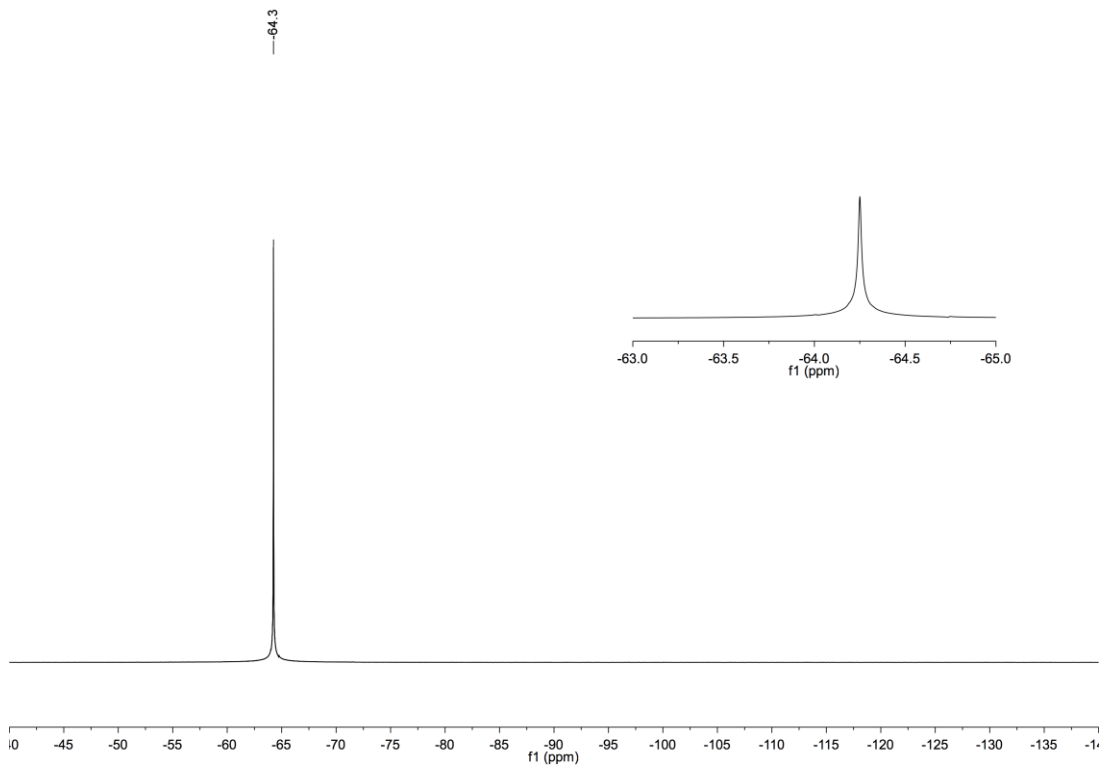


Methyl-2-fluoro-5-(4'-methoxyphenyl)nicotinate (320)

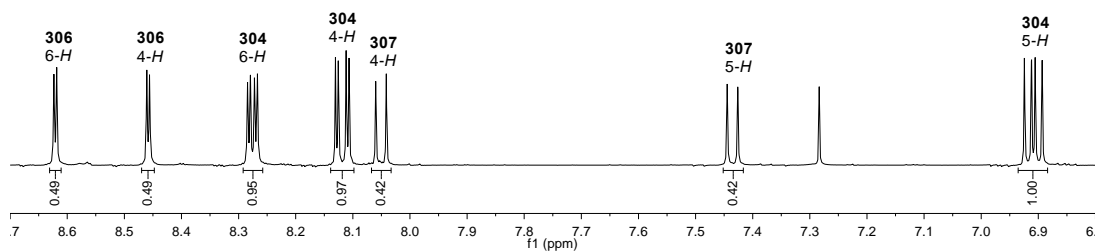
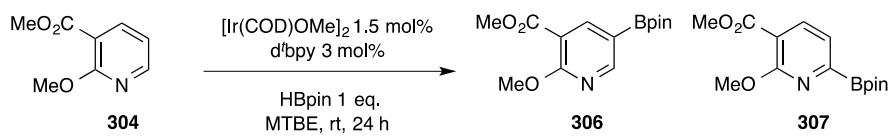


Methyl-2-(trifluoromethyl)-5-(4'-methoxyphenyl)nicotinate (321)

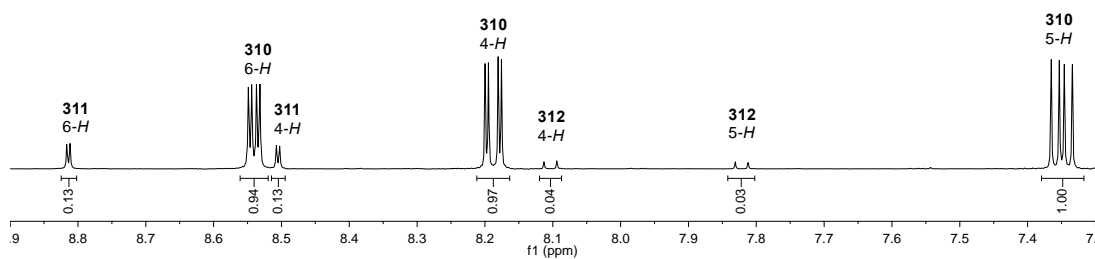
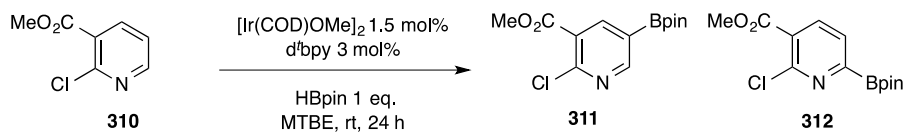




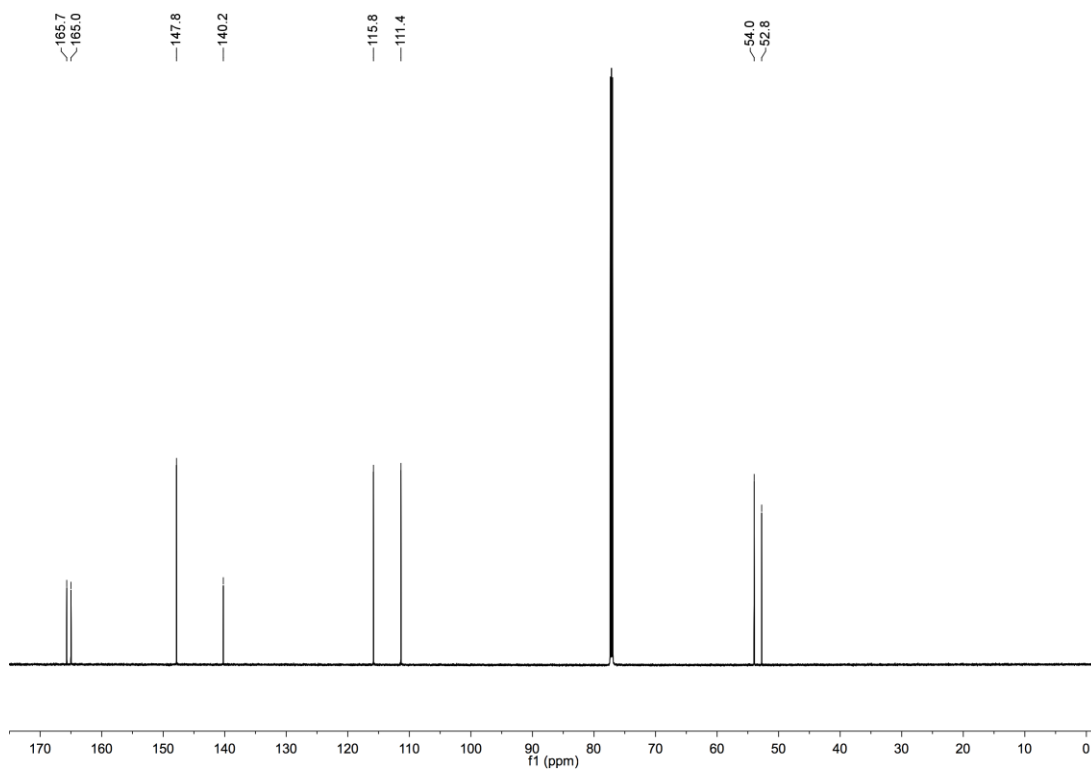
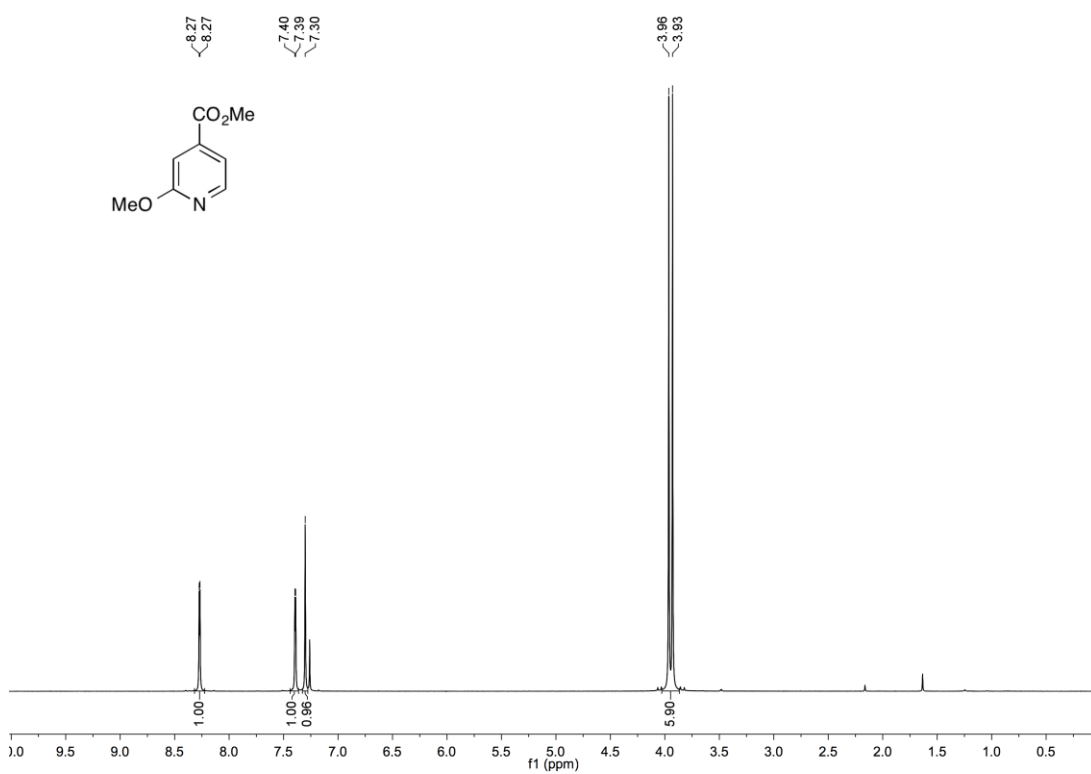
Borylation of methyl-2-methoxynicotinate (304) with HBpin (400 MHz, CDCl₃)



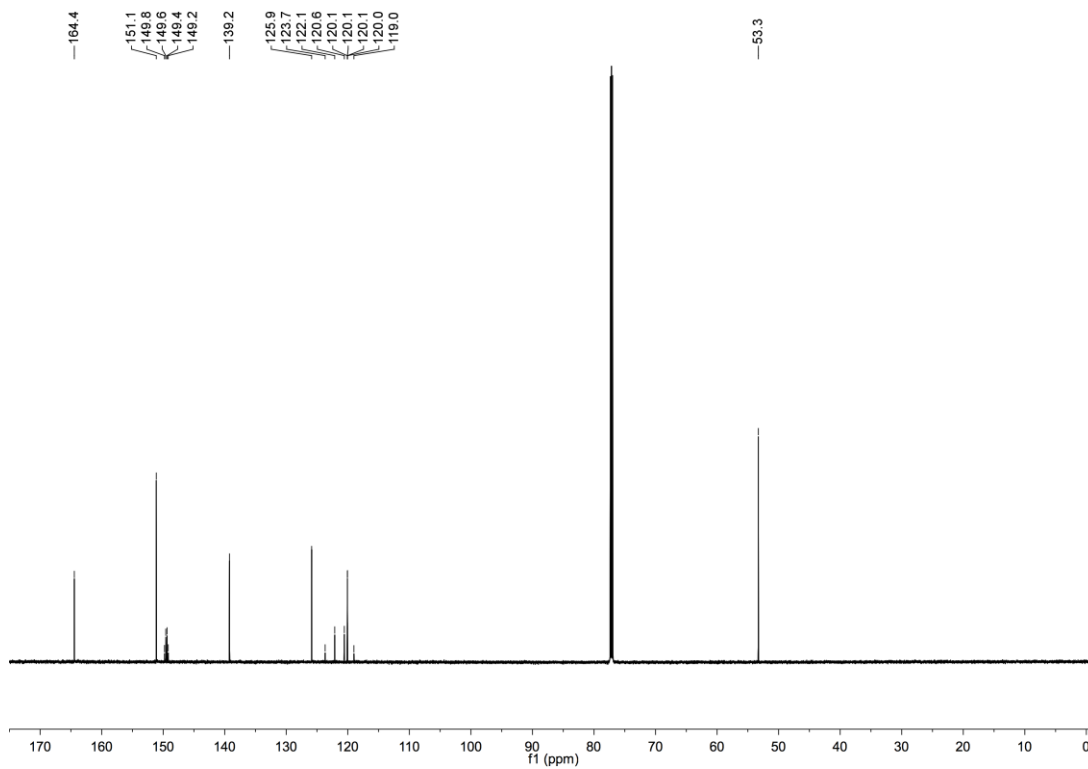
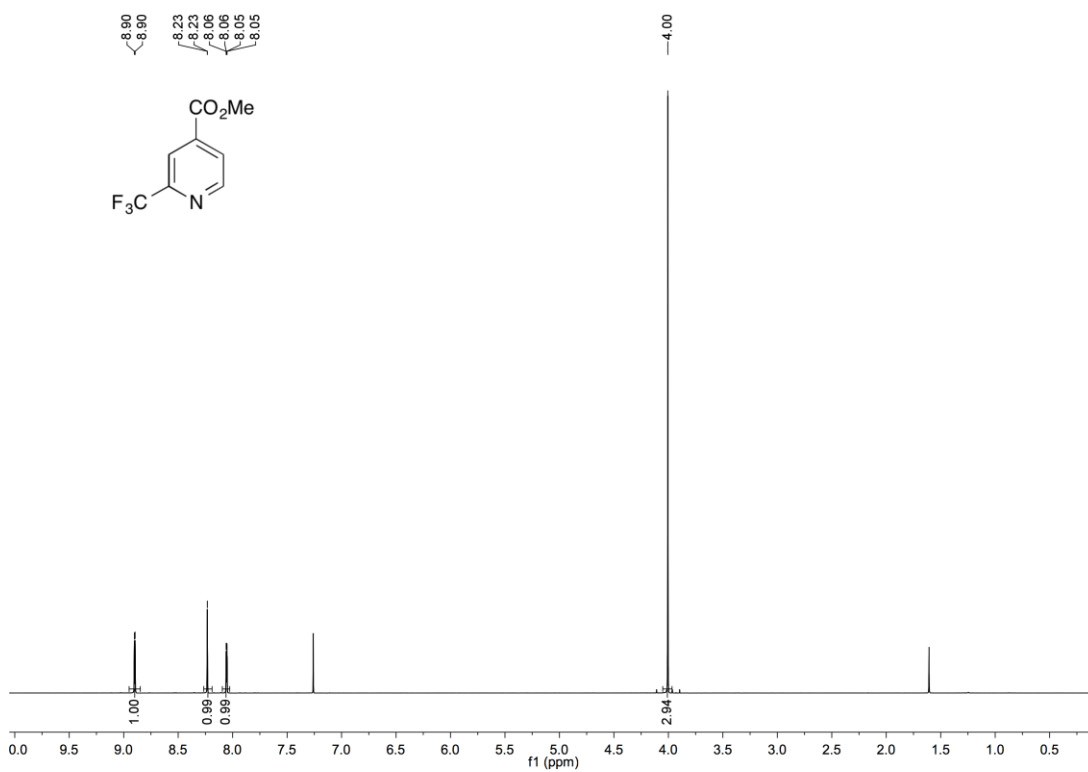
Borylation of methyl-2-chloronicotinate (310) with HBpin (400 MHz, CDCl₃)

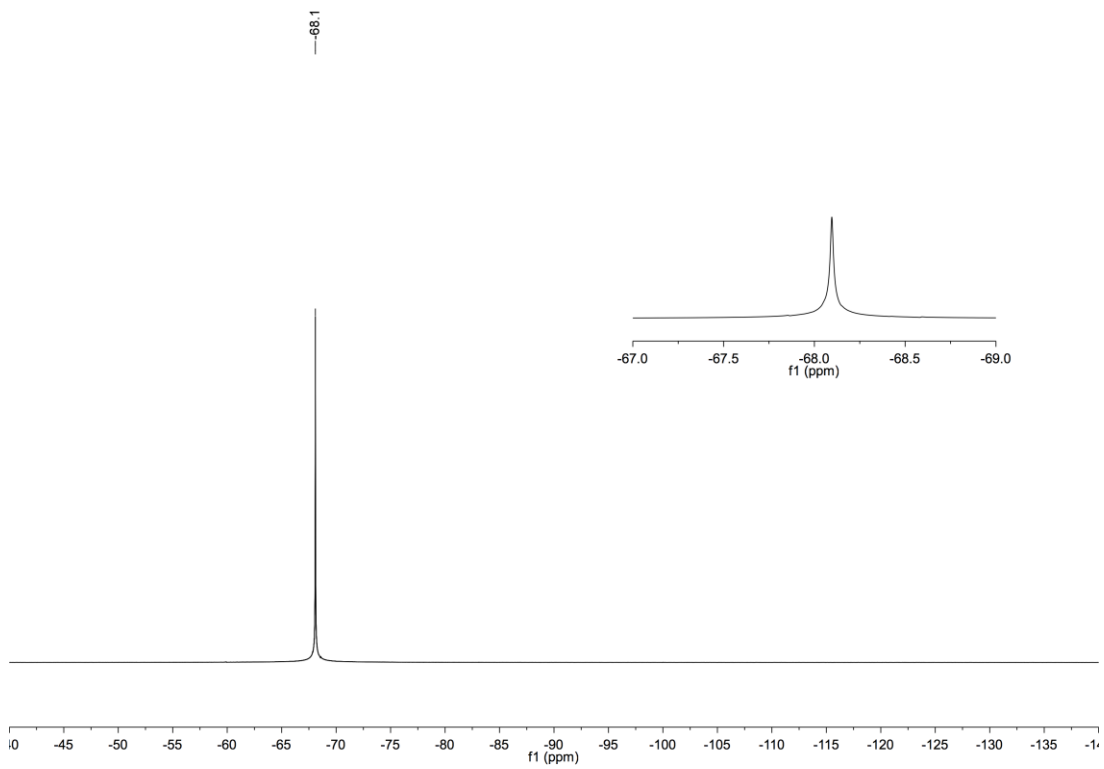


Methyl-2-methoxyisonicotinate (**325**)

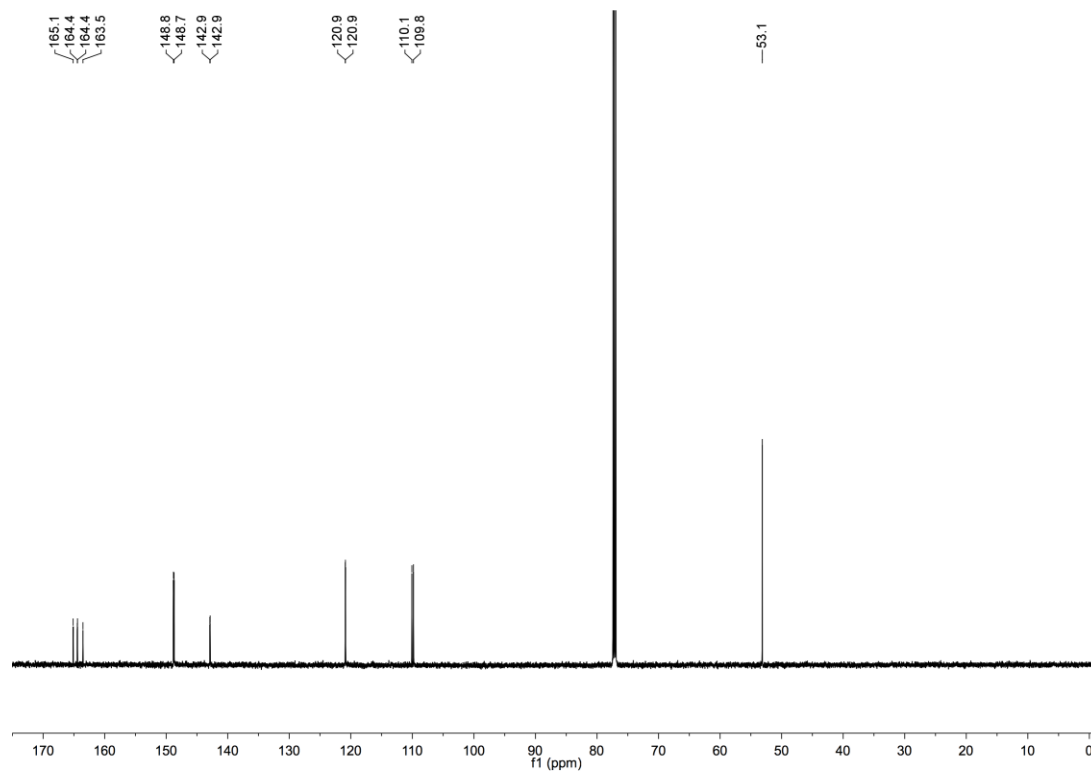
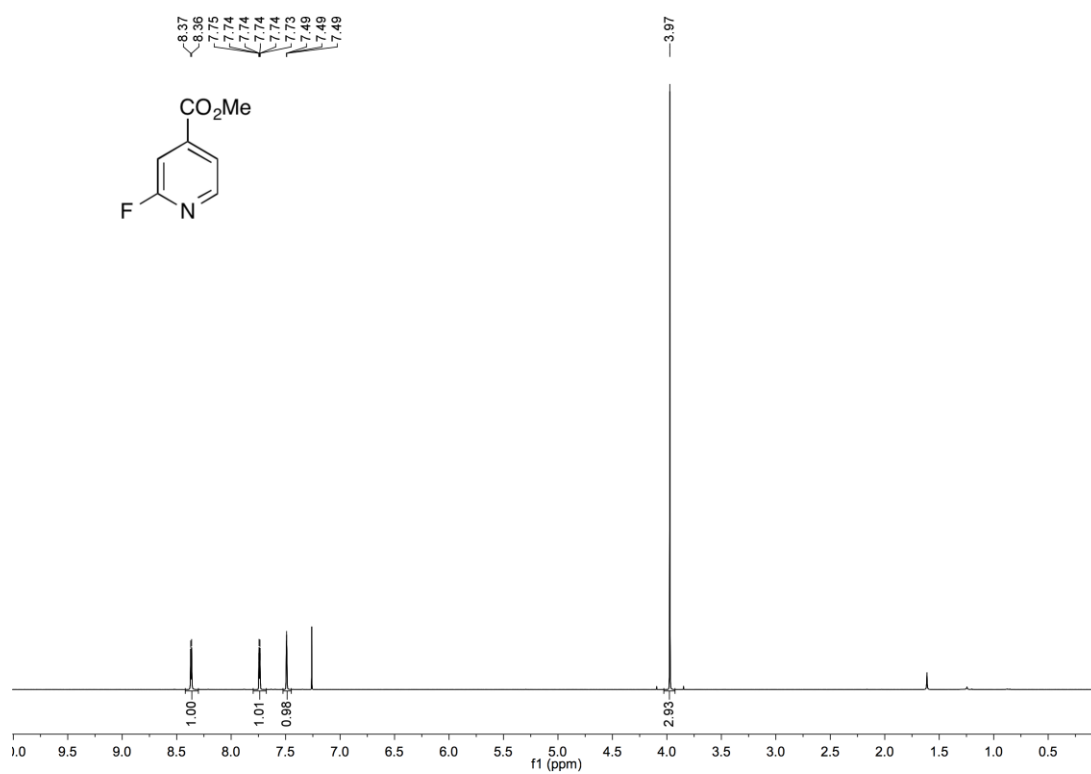


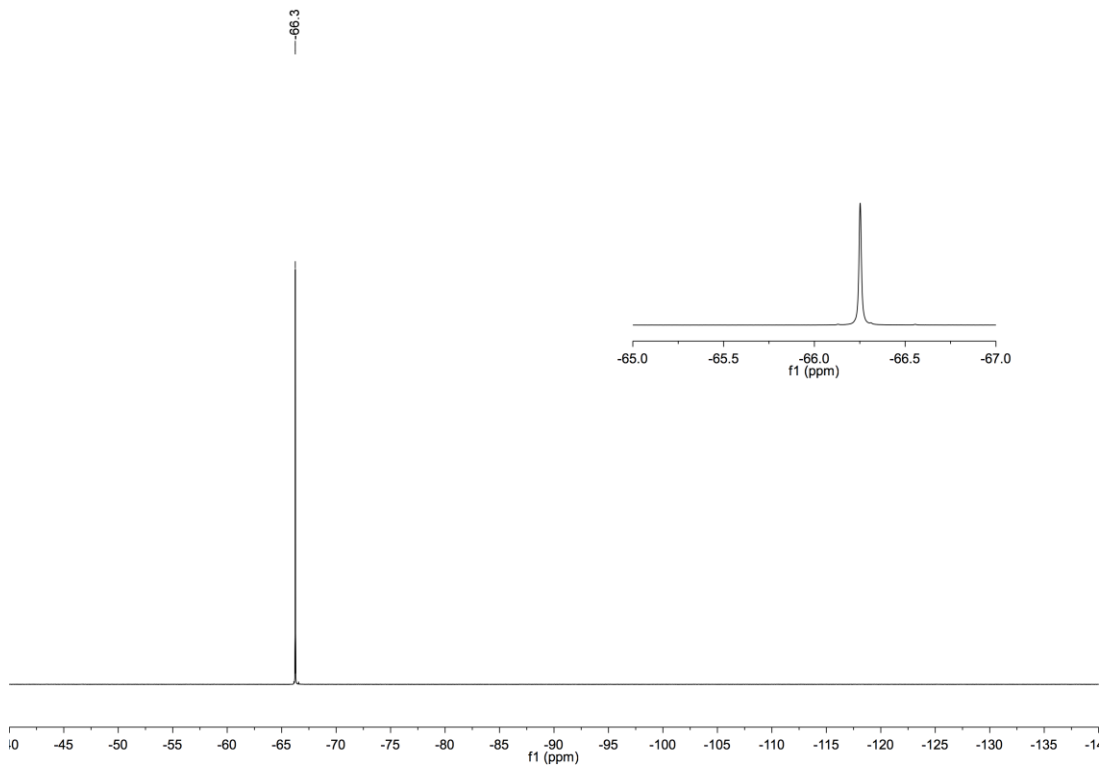
Methyl-2-(trifluoromethyl)isonicotinate (326)



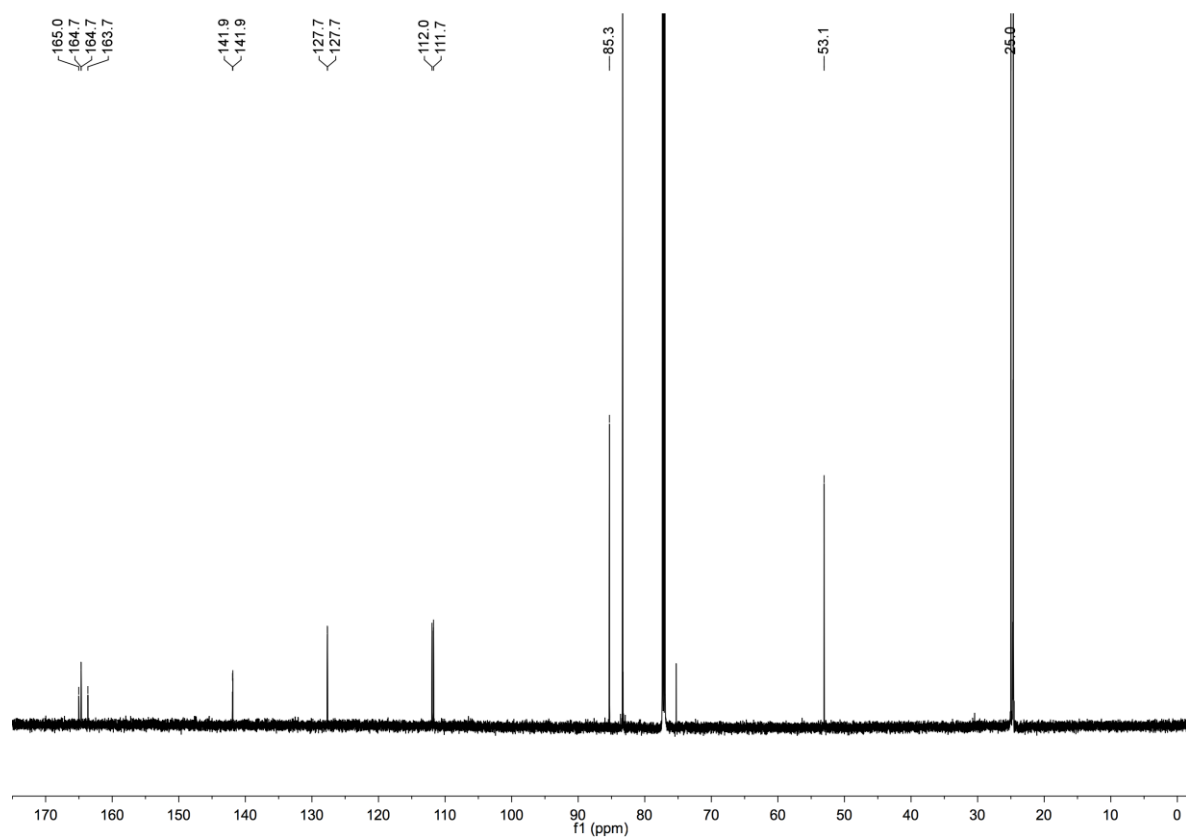
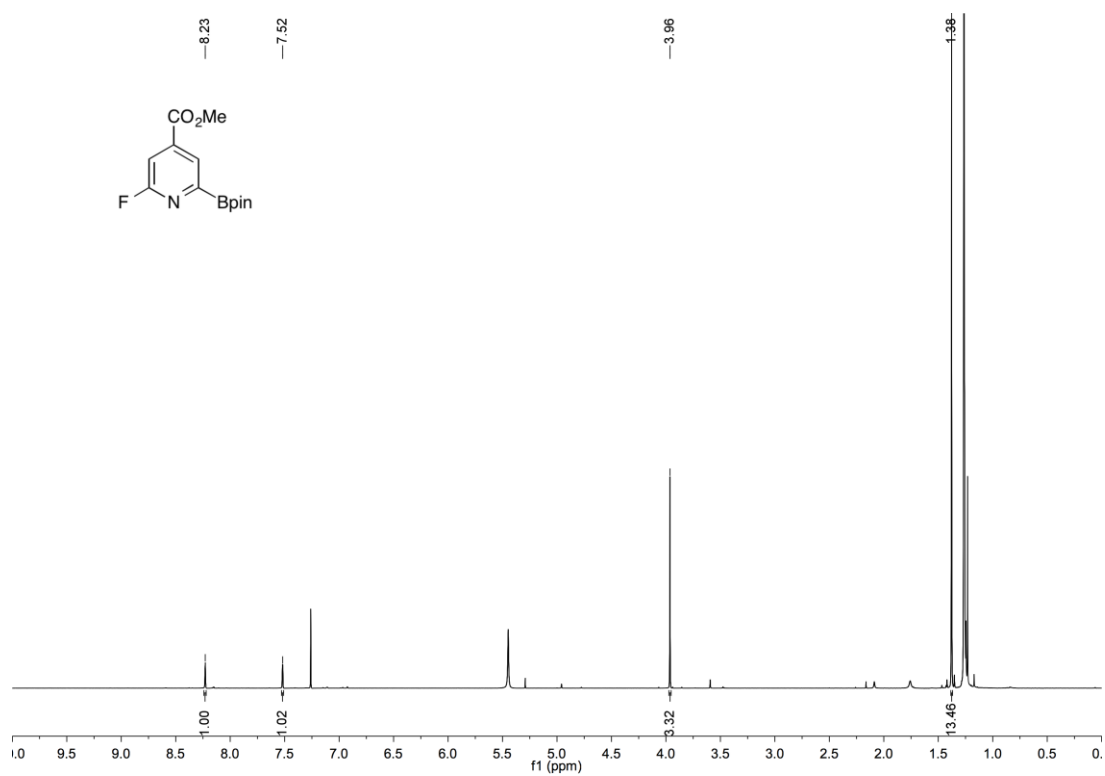


Methyl-2-fluoroisonicotinate (327)

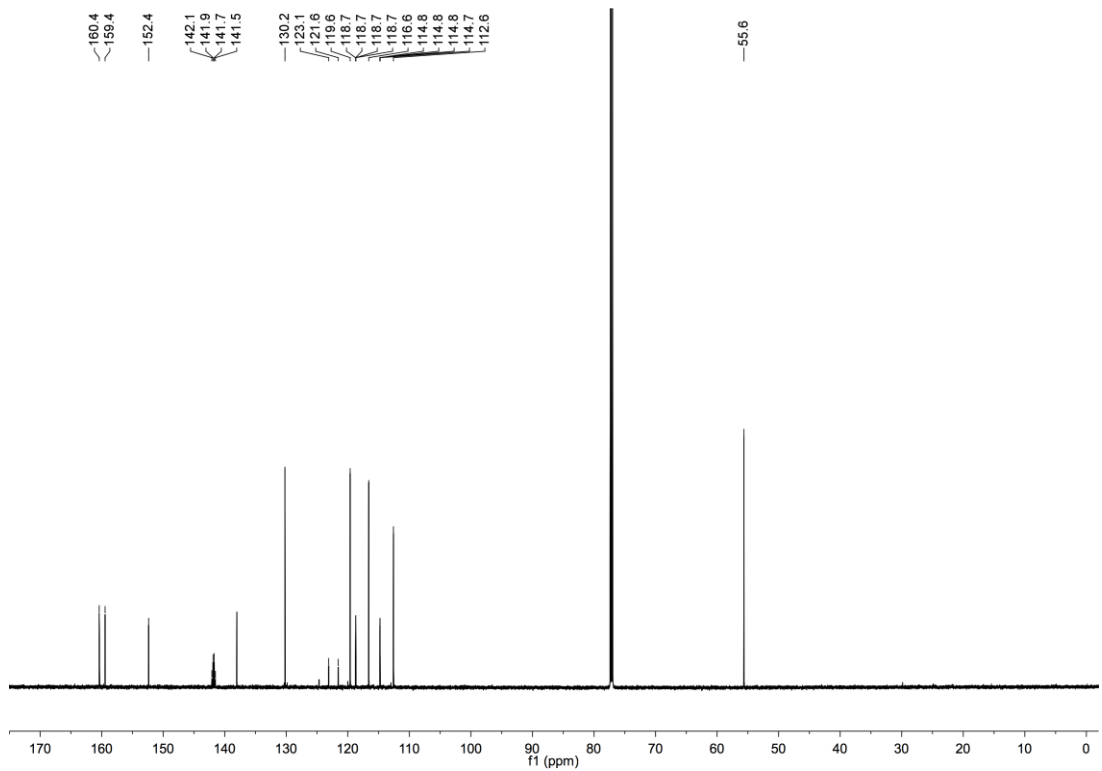
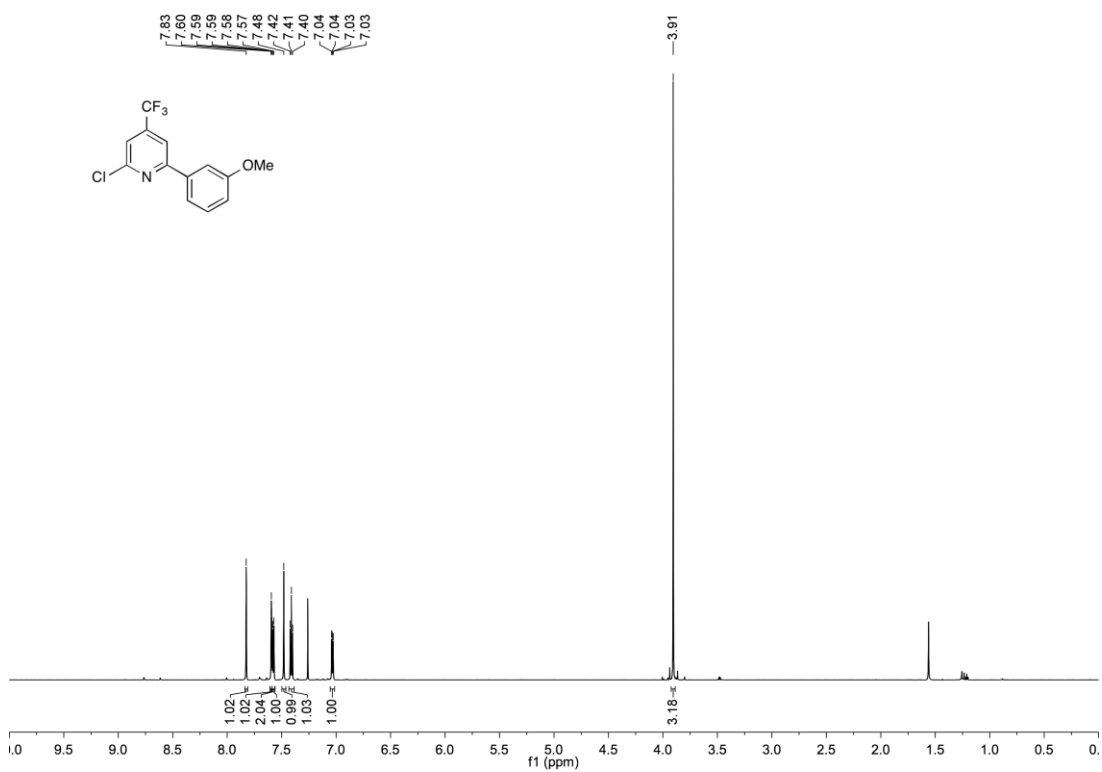


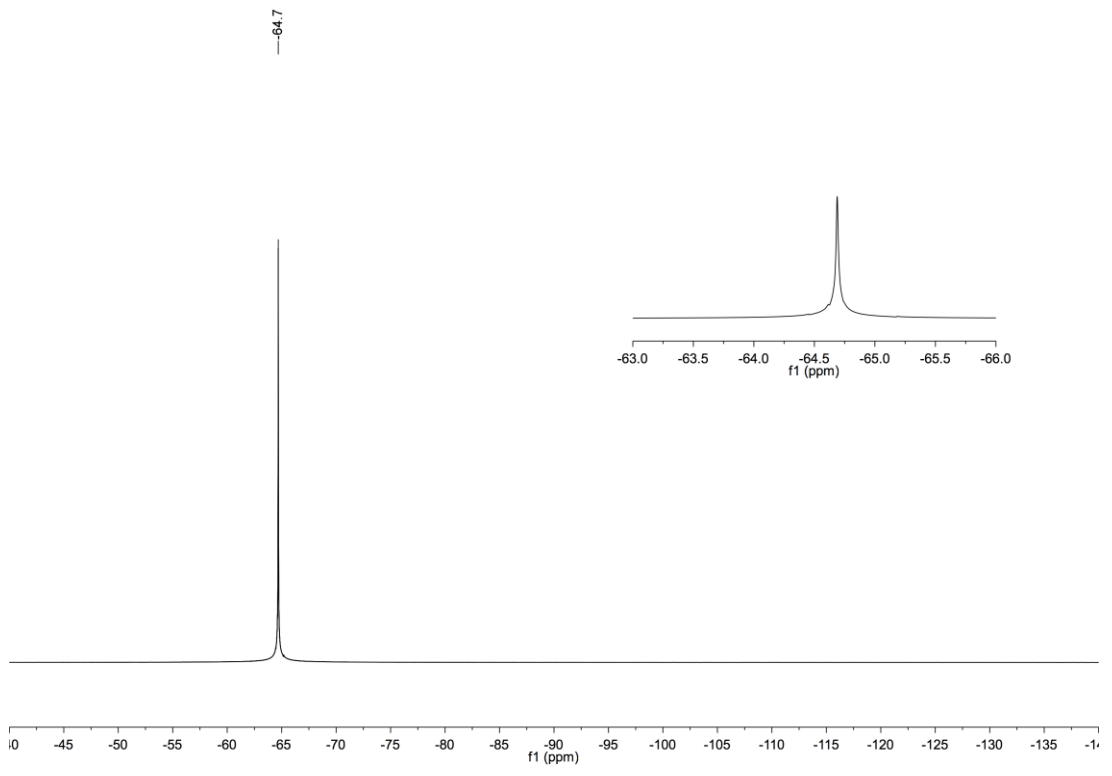


Methyl-2-fluoro-6-(Bpin)isonicotinate (**339**)

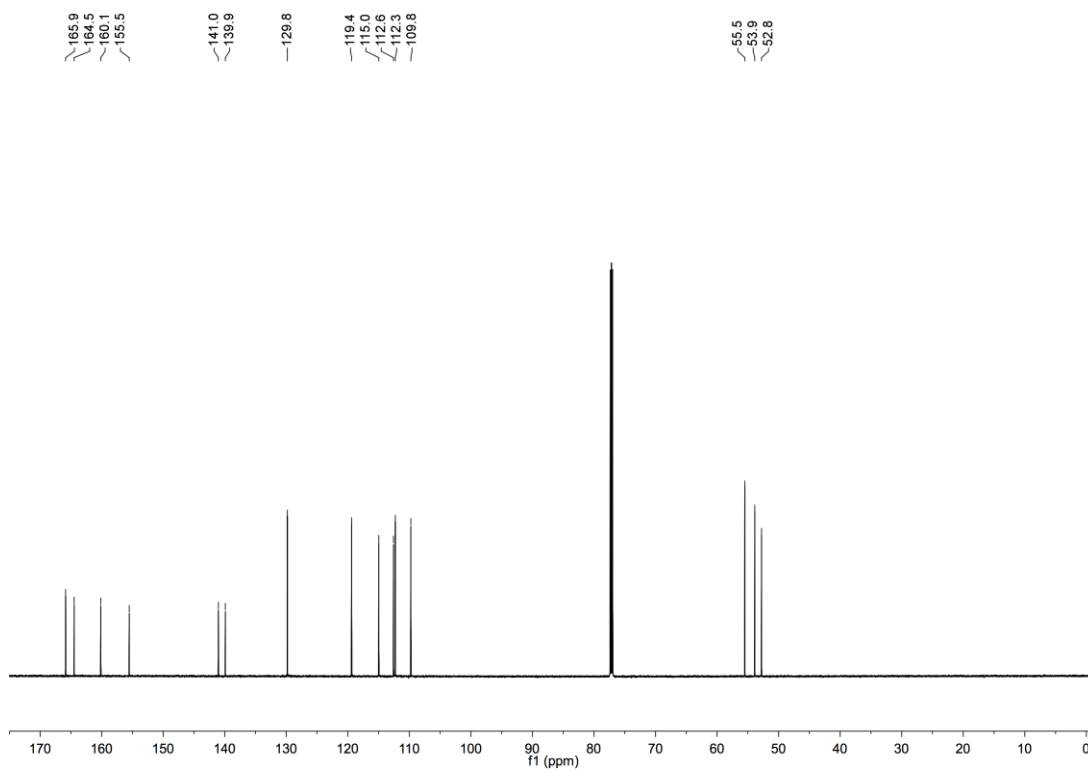
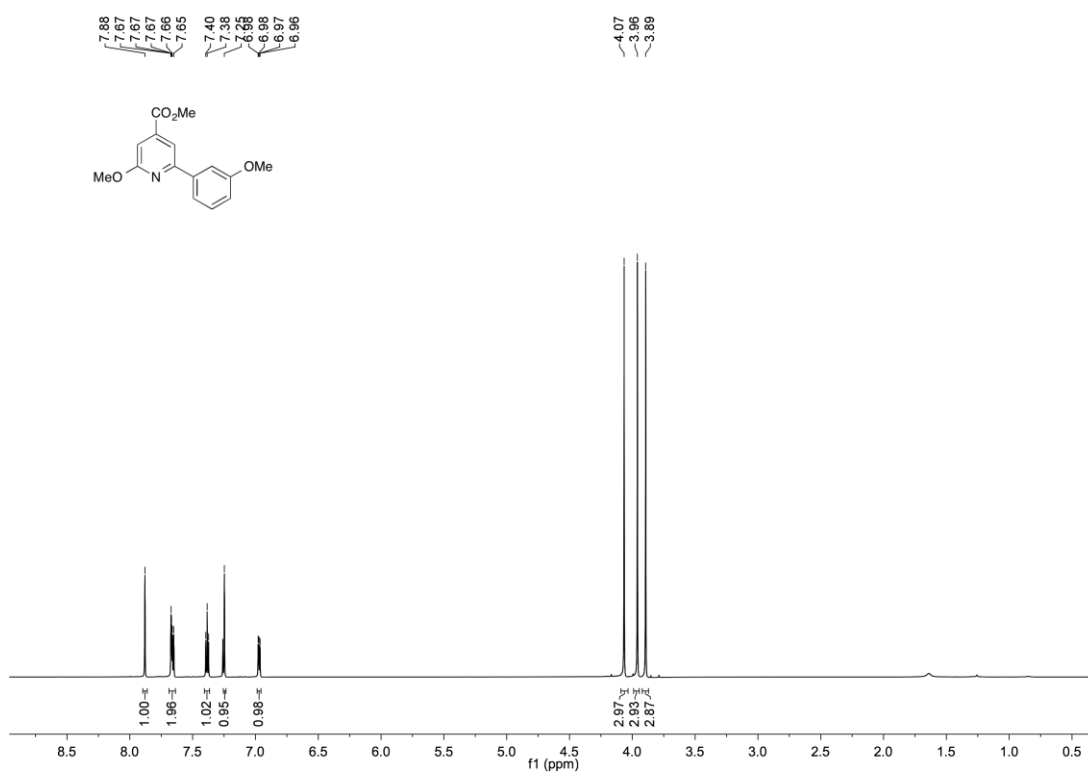


2-Chloro-4-(trifluoromethyl)-6-(3'-methoxyphenyl)pyridine (341)

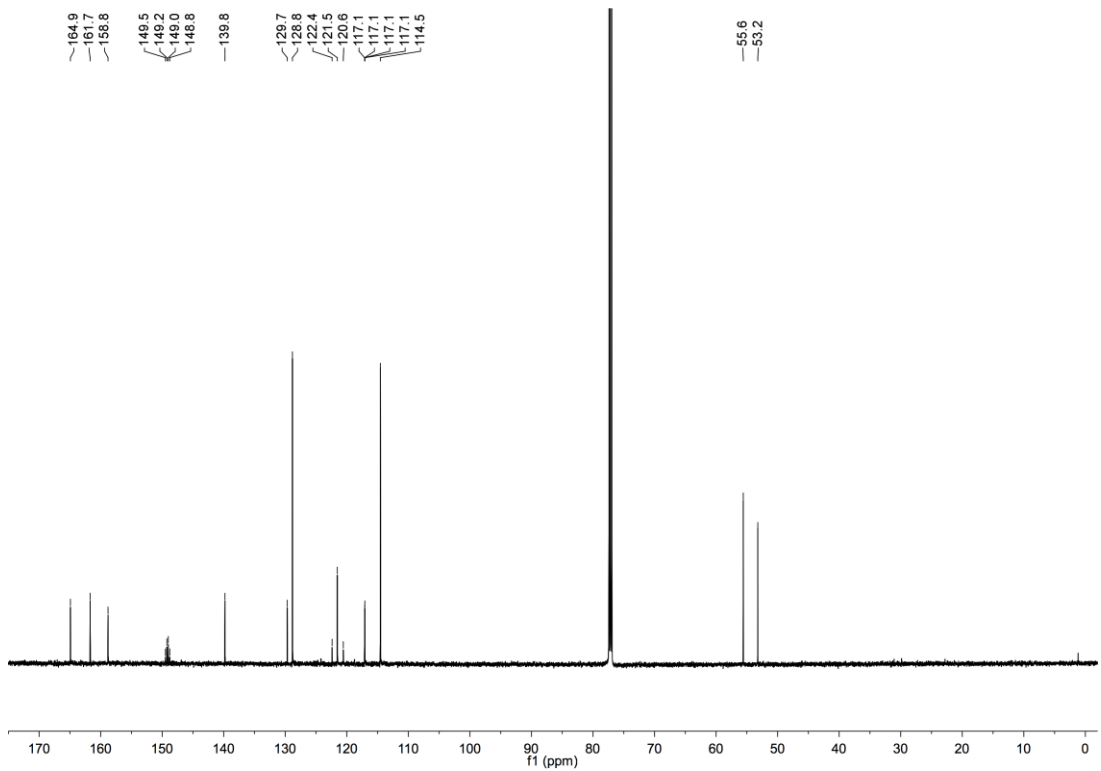


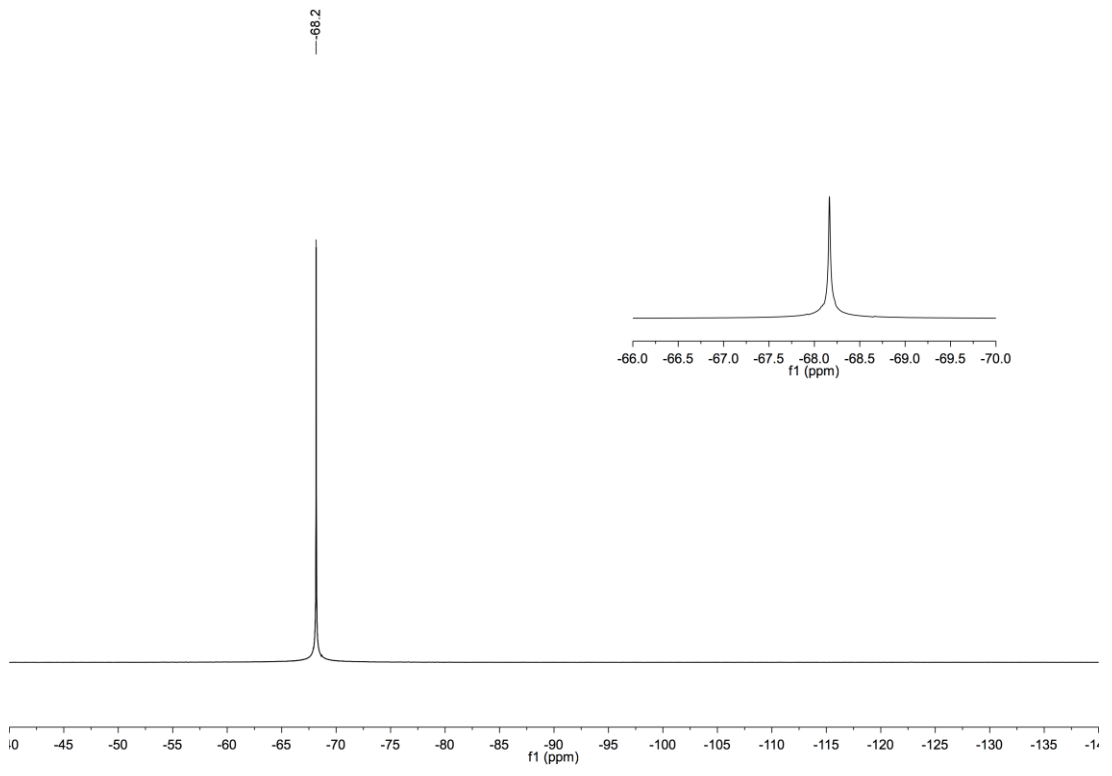


Methyl-2-methoxy-6-(3'-methoxyphenyl)isonicotinate (**342**)

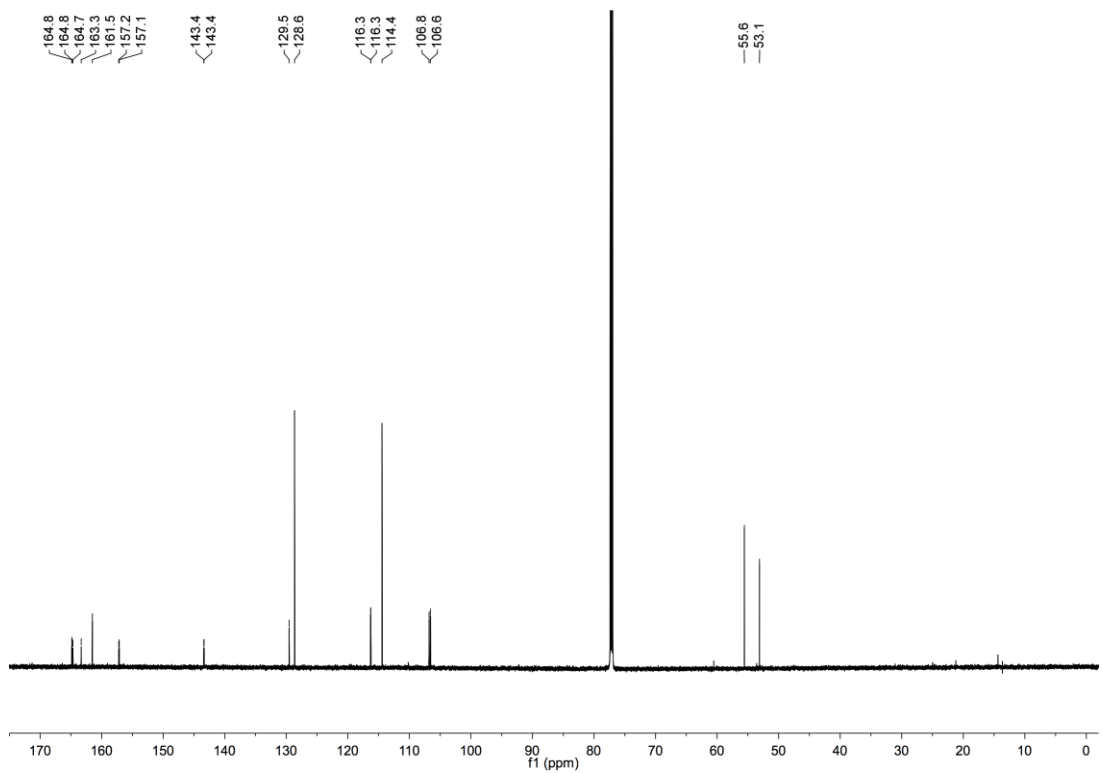
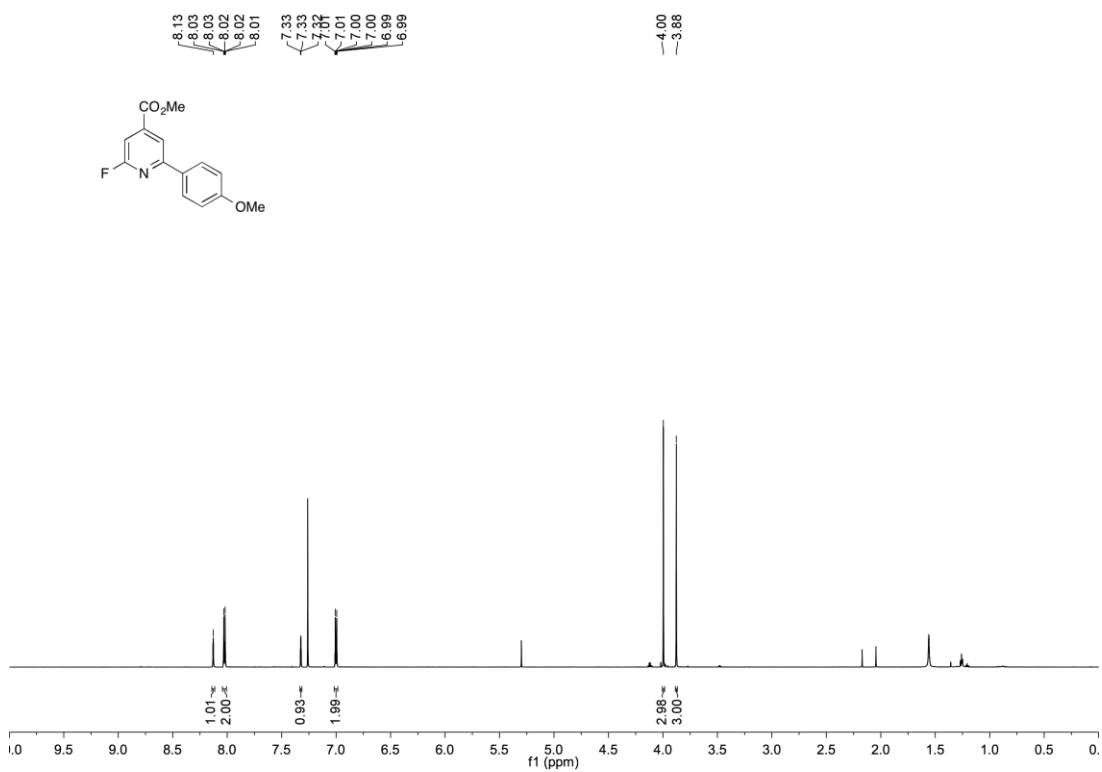


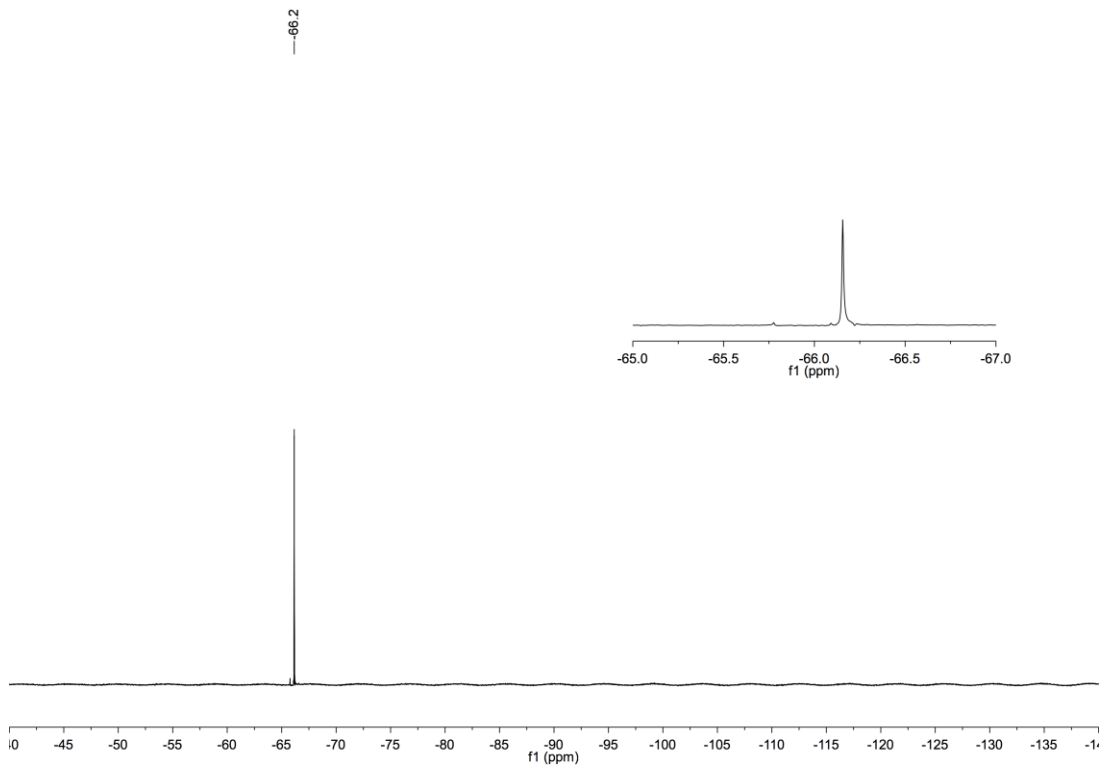
Methyl-2-(trifluoromethyl)-6-(4'-methoxyphenyl)isonicotinate (**343**)



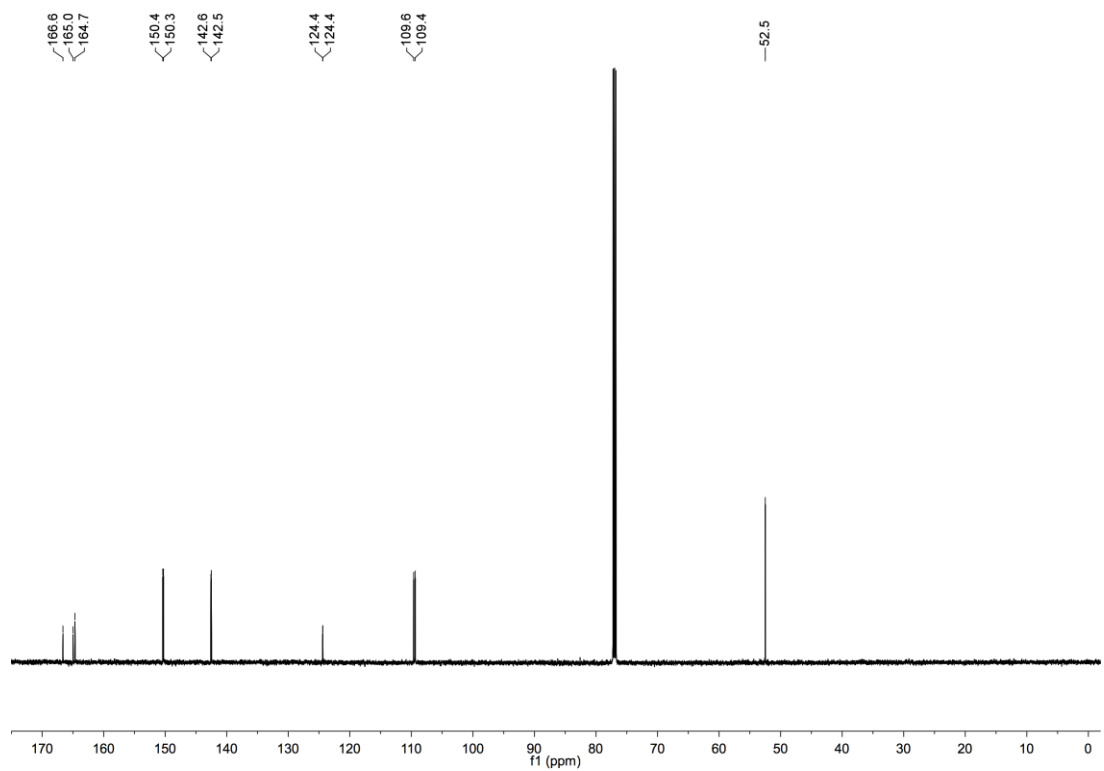
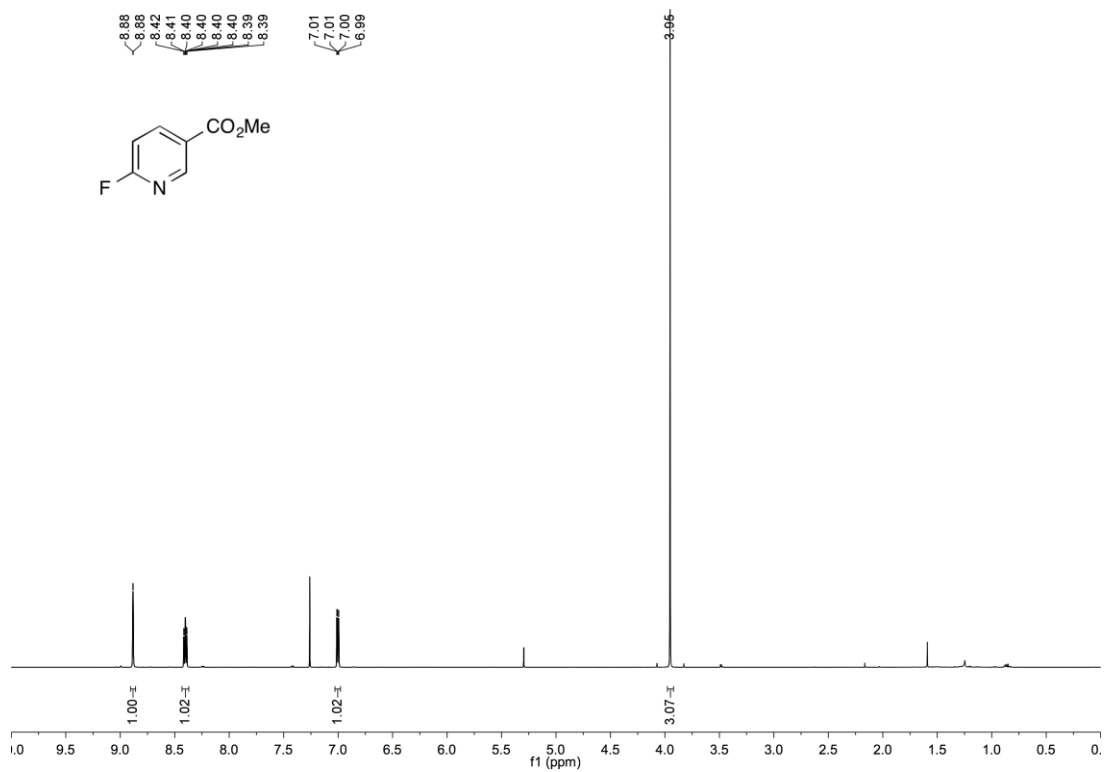


Methyl-2-fluoro-6-(4'-(methoxycarbonyl)phenyl)isonicotinate (**344**)

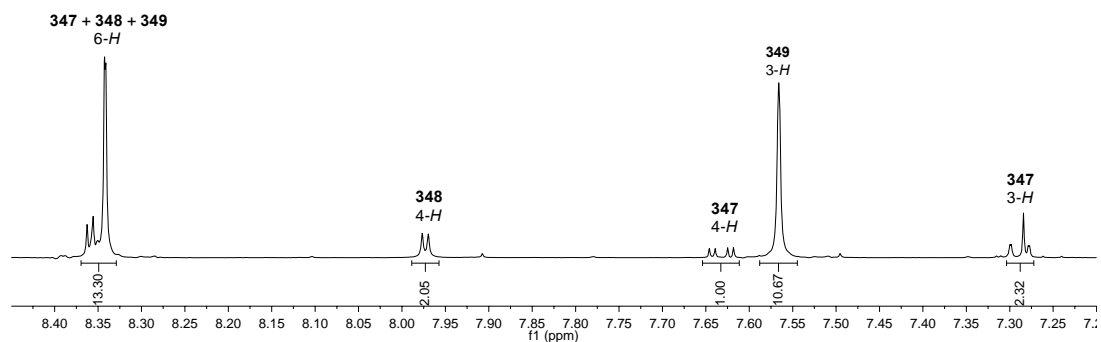
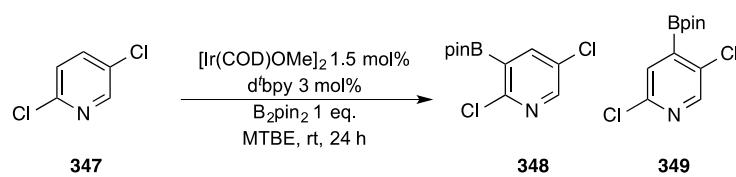




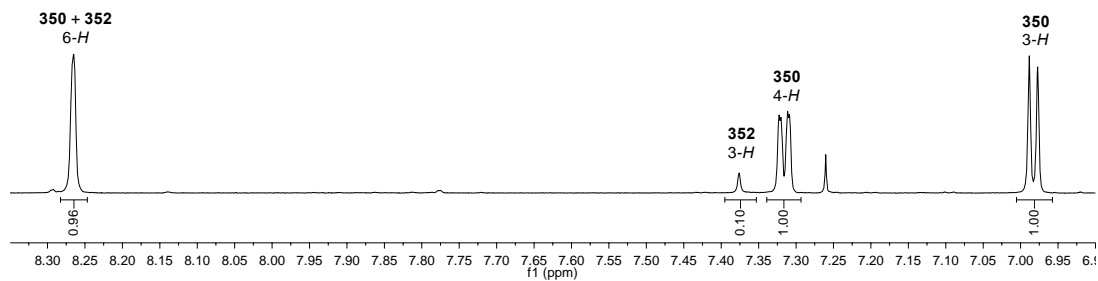
Methyl-6-fluoronicotinate (346)



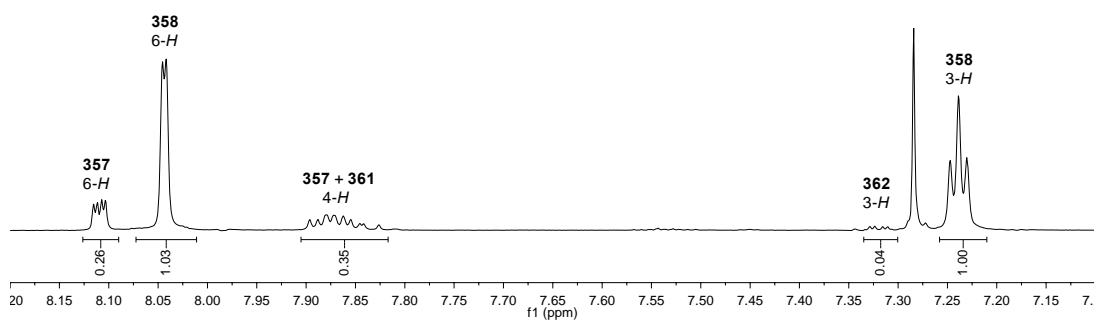
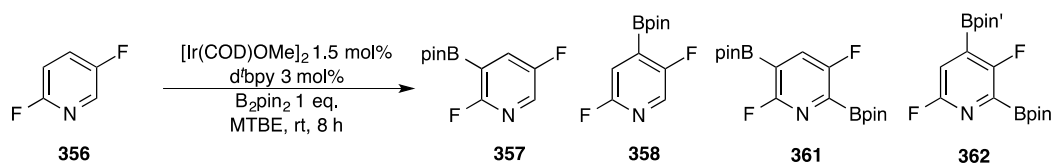
Borylation of 2,5-dichloropyridine (347) (400 MHz, CDCl₃)



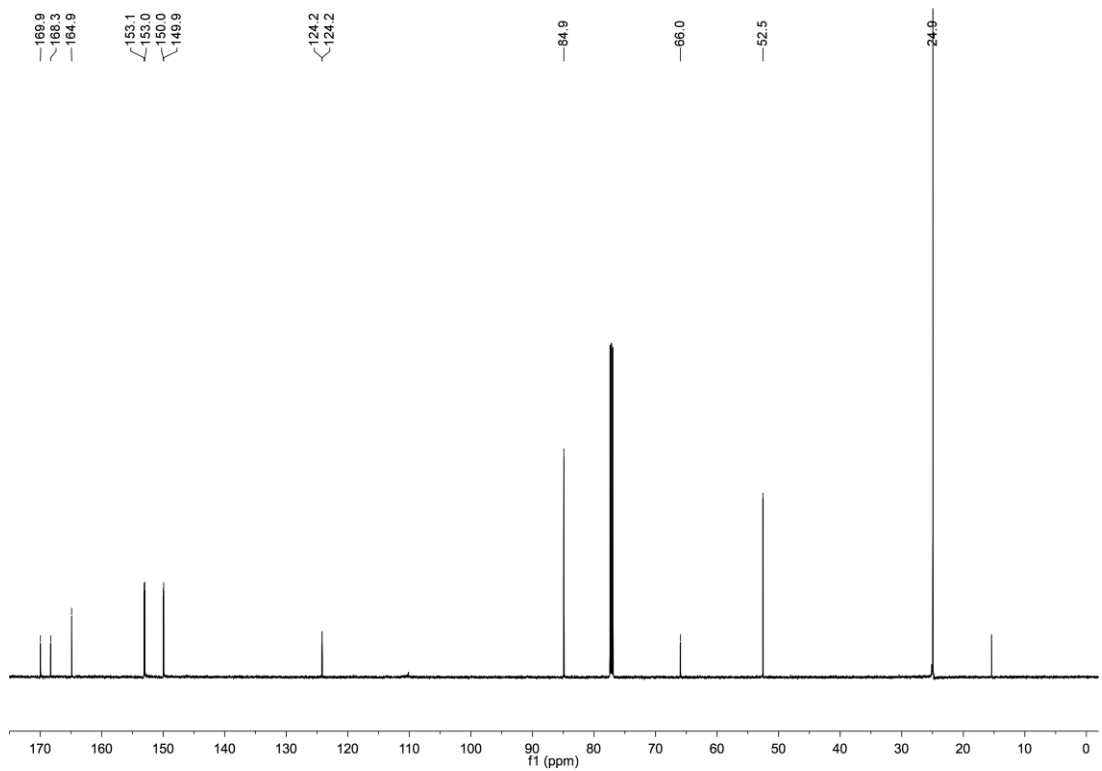
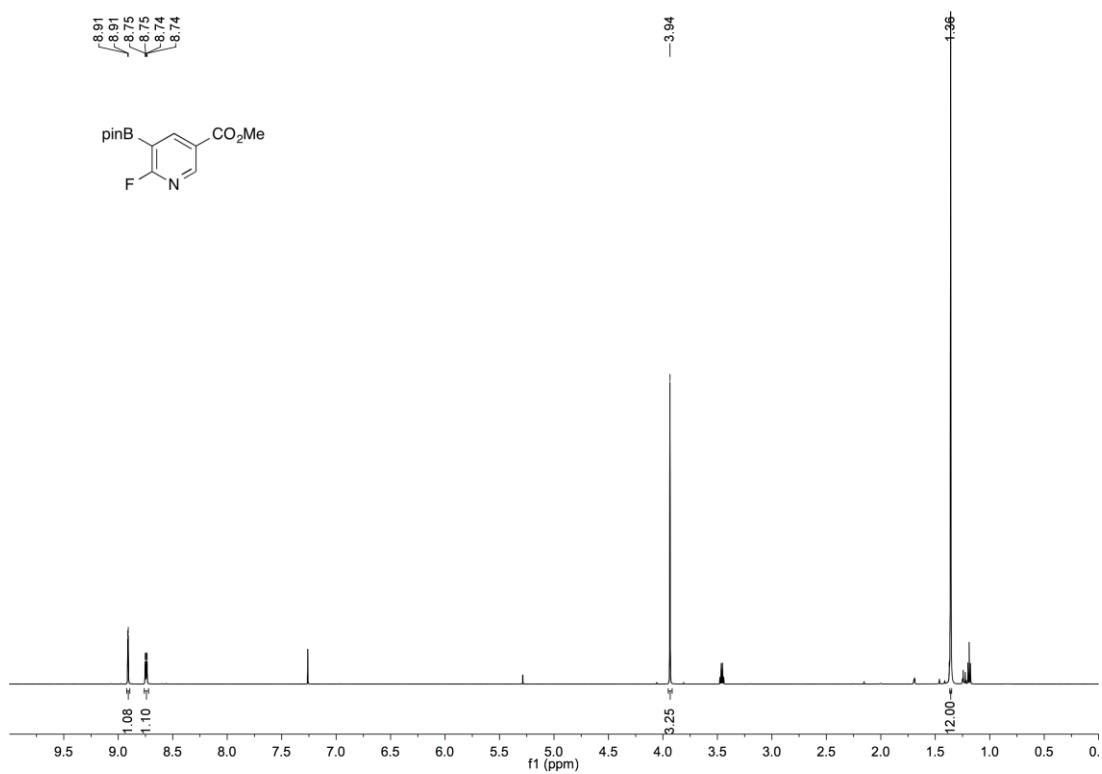
Borylation of 2,5-lutidine (350) (400 MHz, CDCl₃)

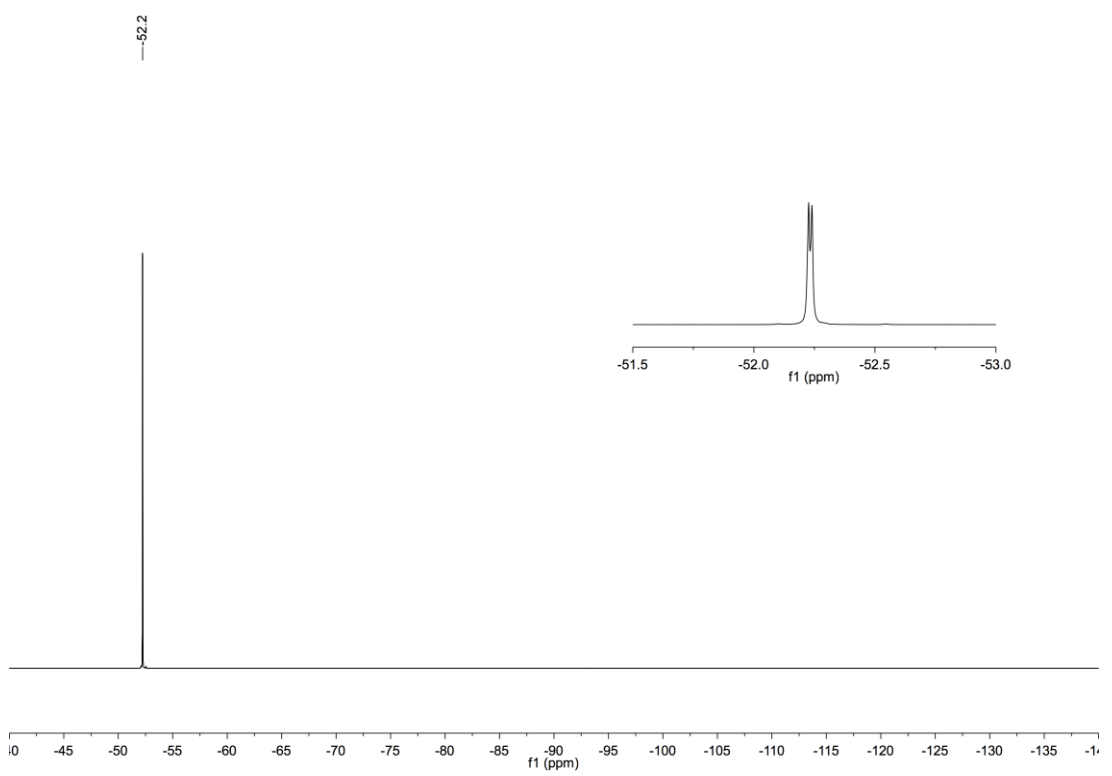
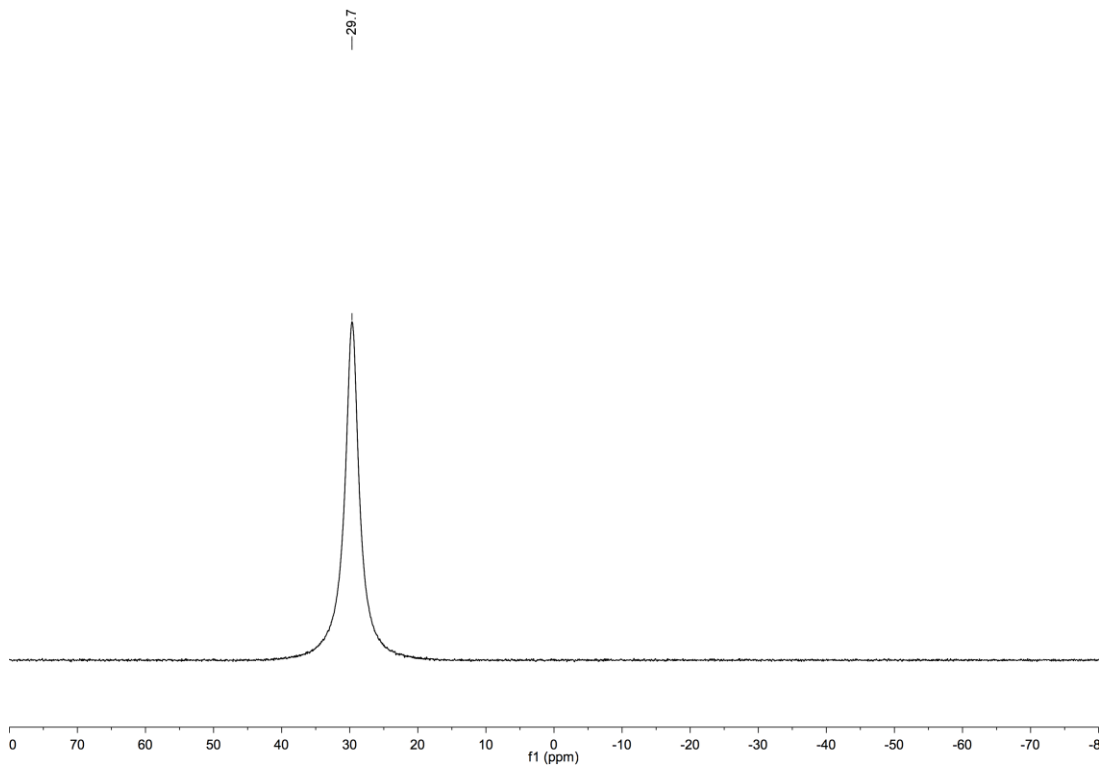


Borylation of 2,5-difluoropyridine (**356**) (400 MHz, CDCl₃)

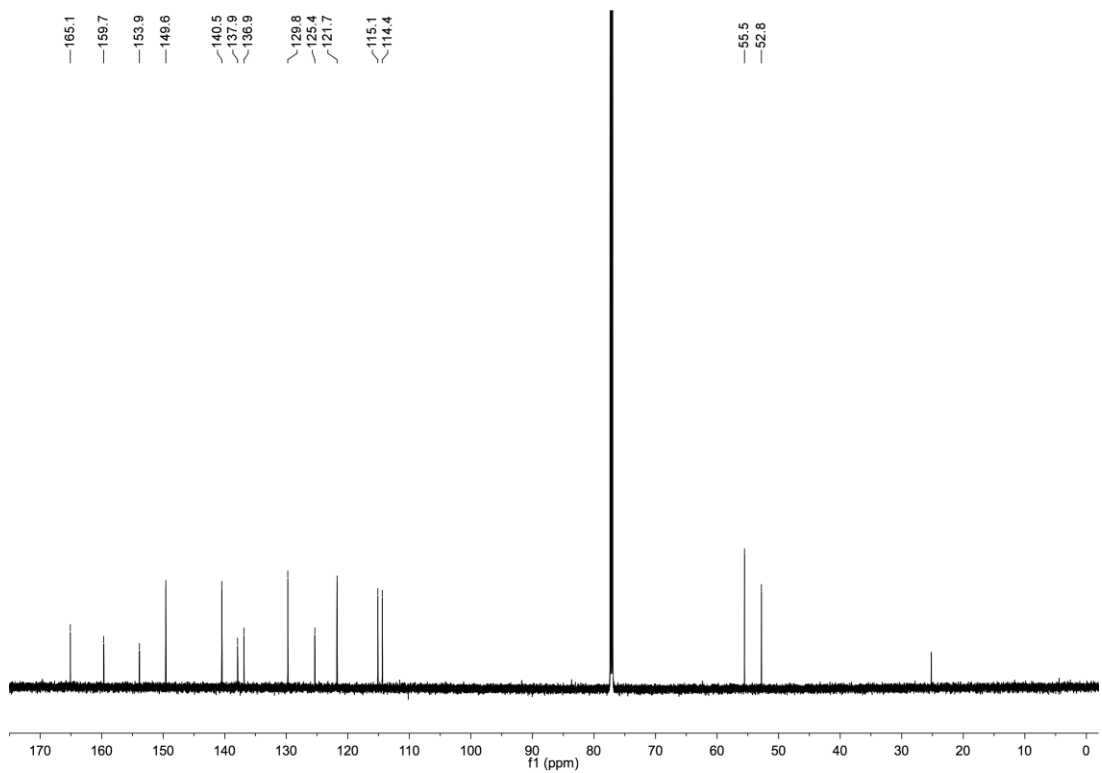
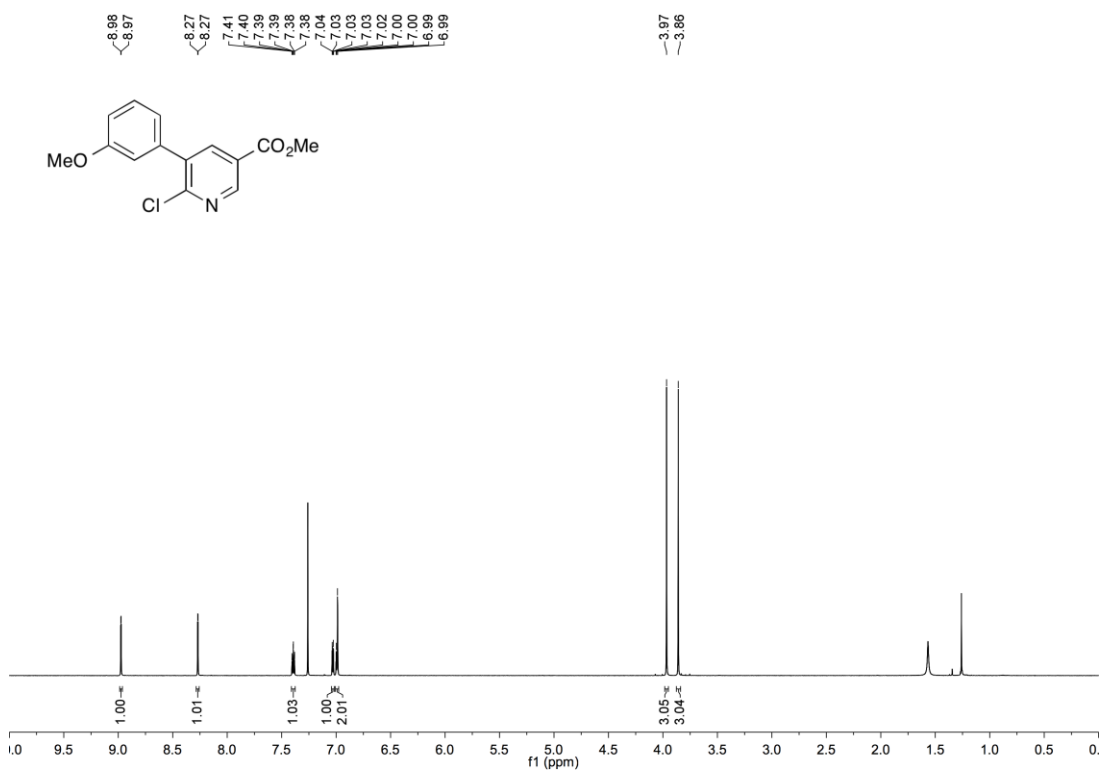


Methyl-6-fluoro-5-(Bpin)nicotinate (**359**)

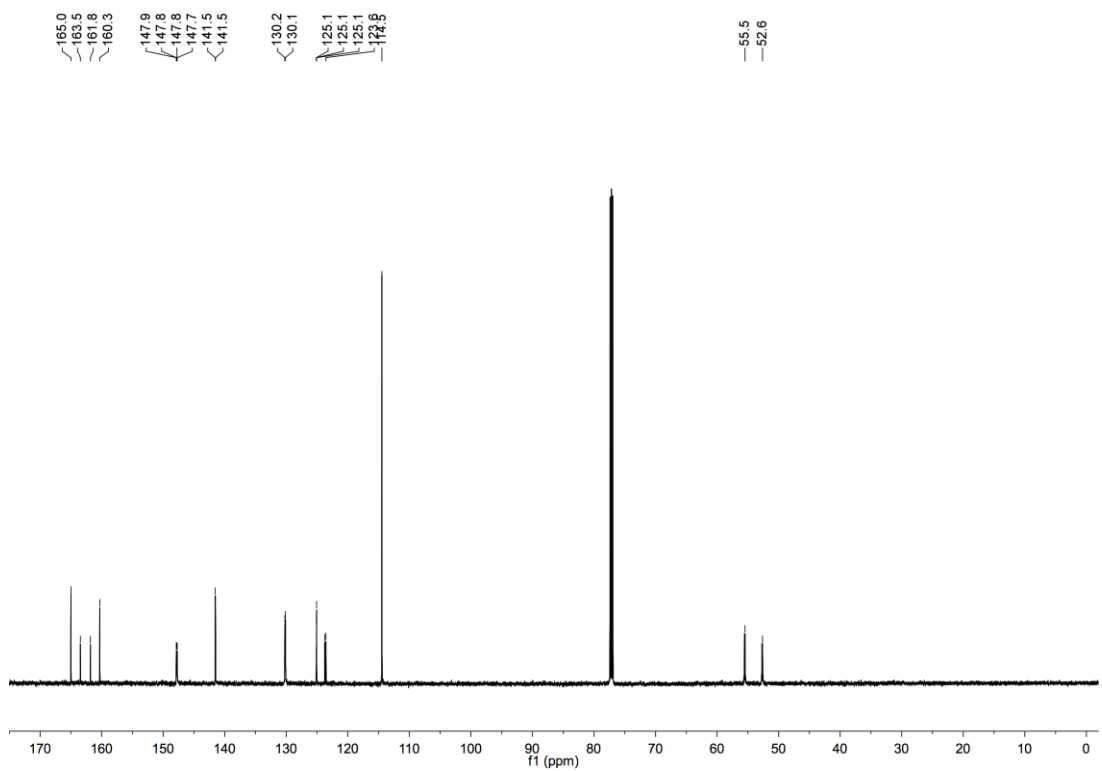
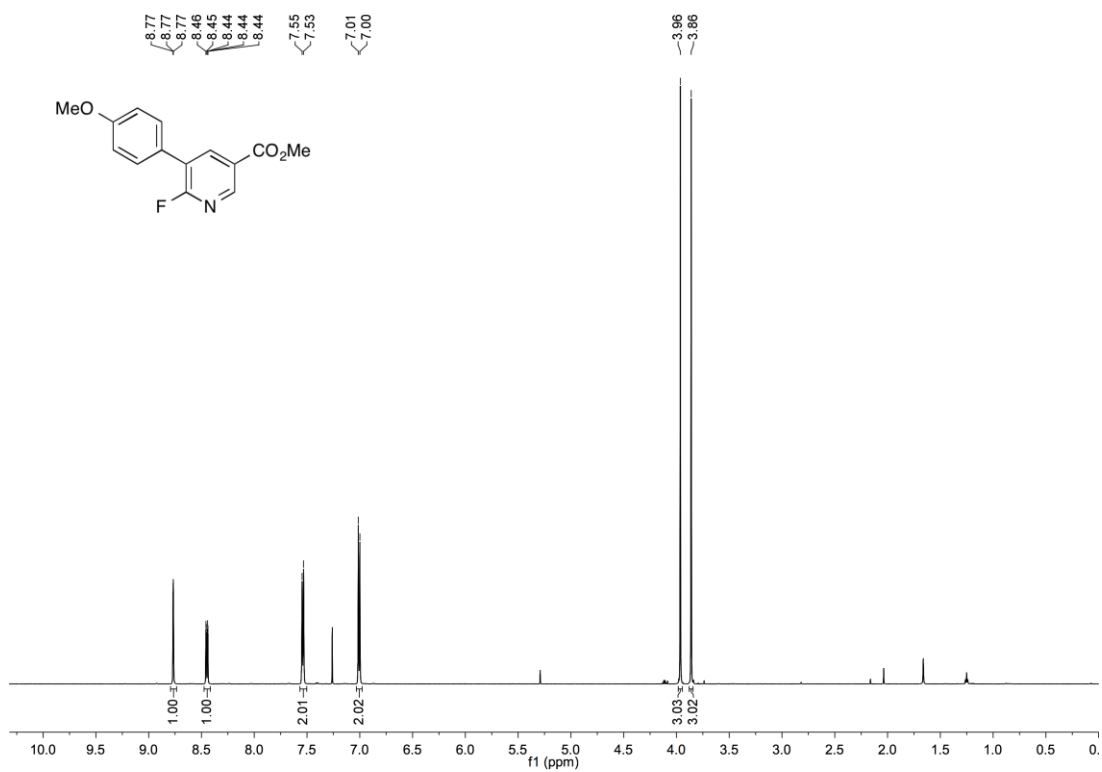


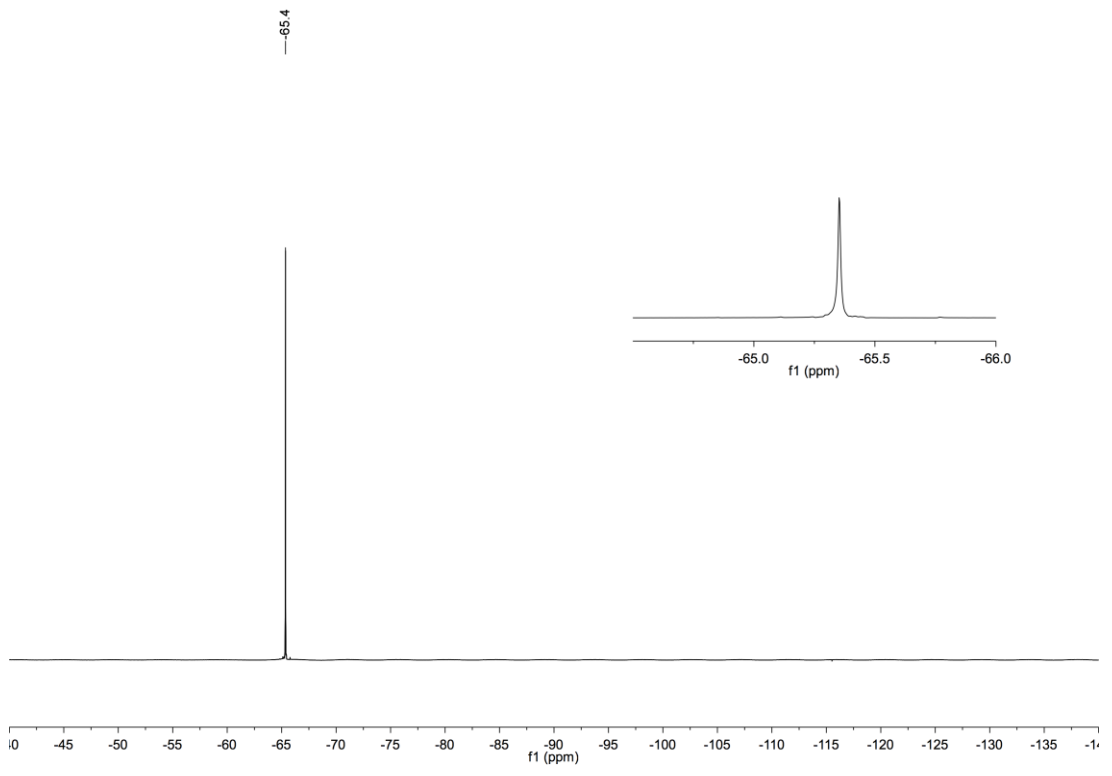


Methyl-6-chloro-5-(3'-methoxyphenyl)nicotinate (363)

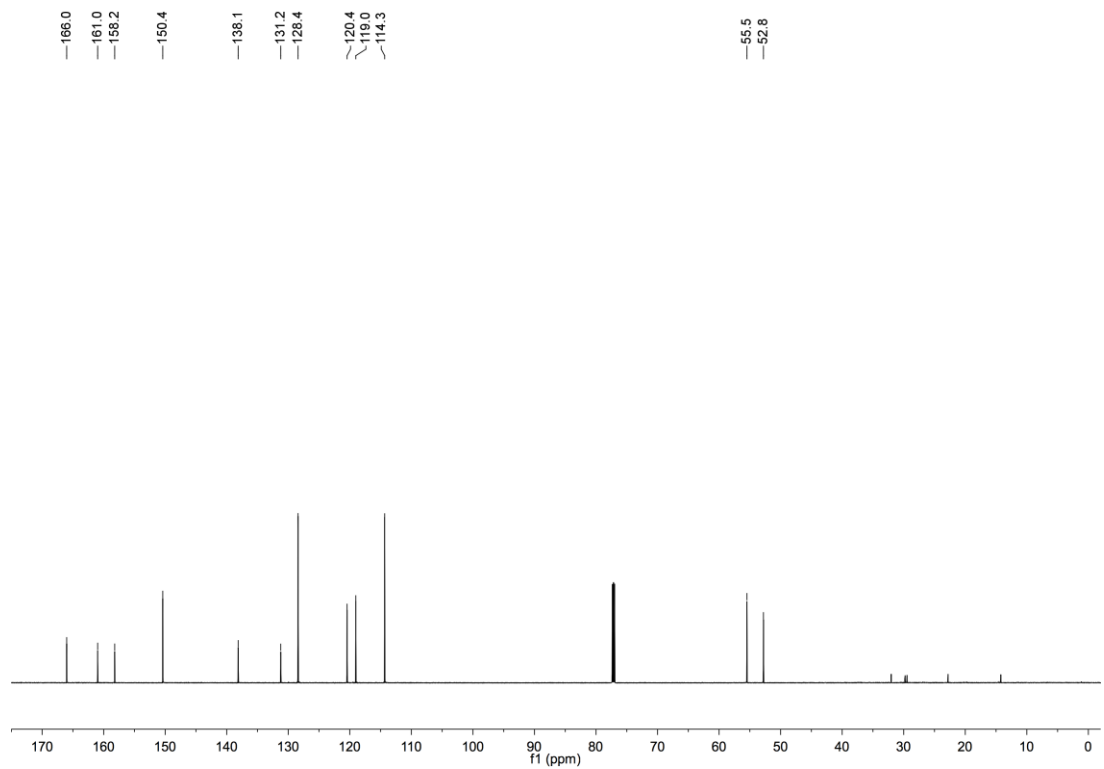
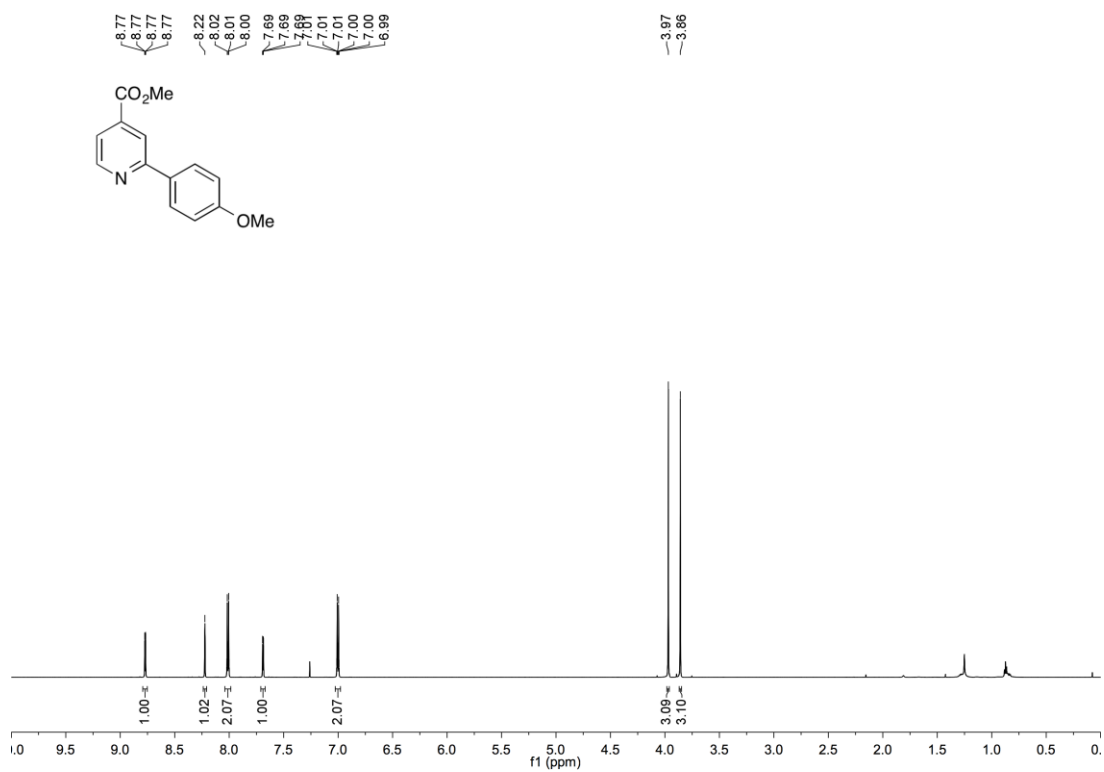


Methyl-6-fluoro-5-(4'-methoxyphenyl)nicotinate (364)

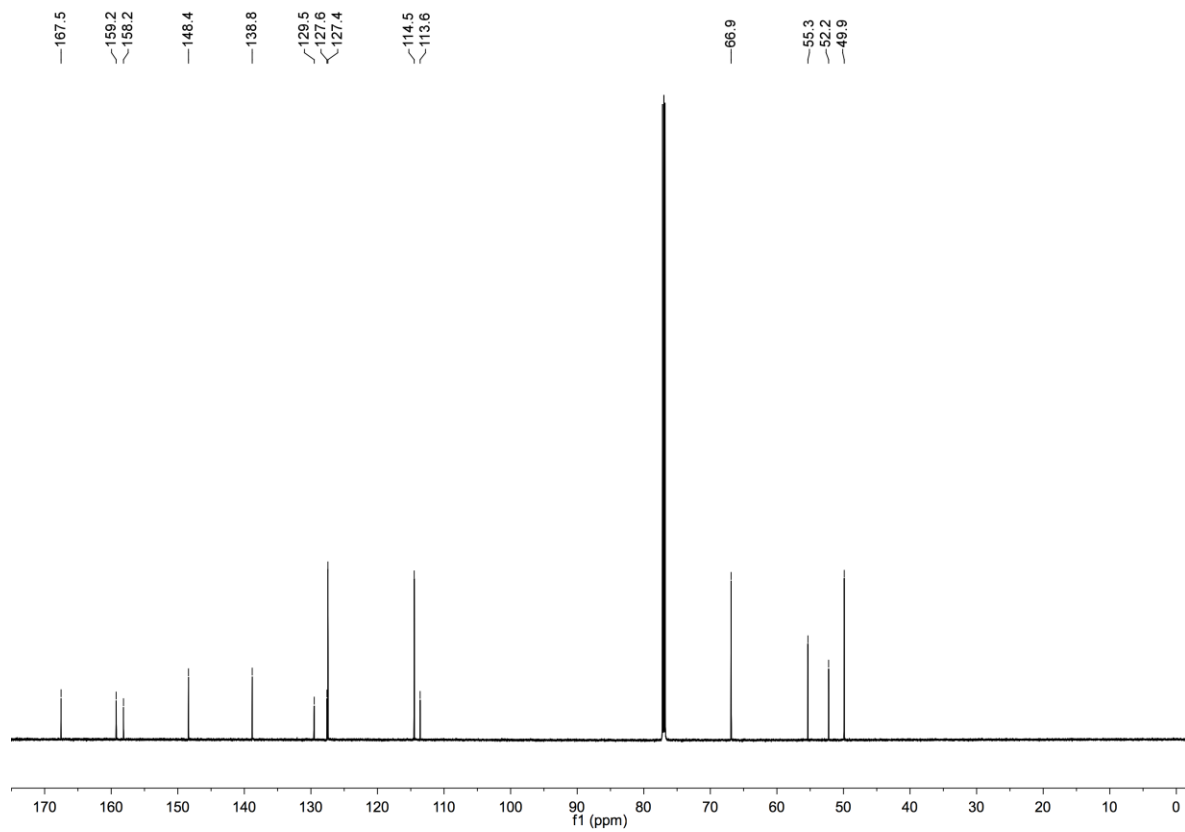
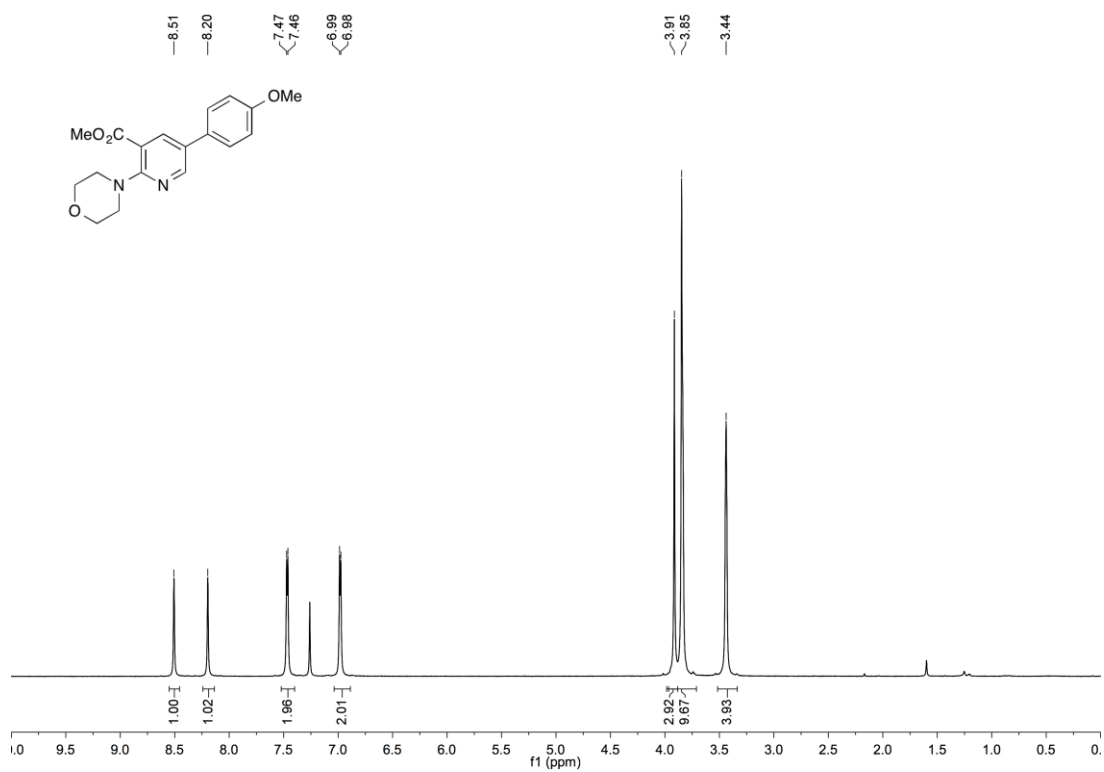




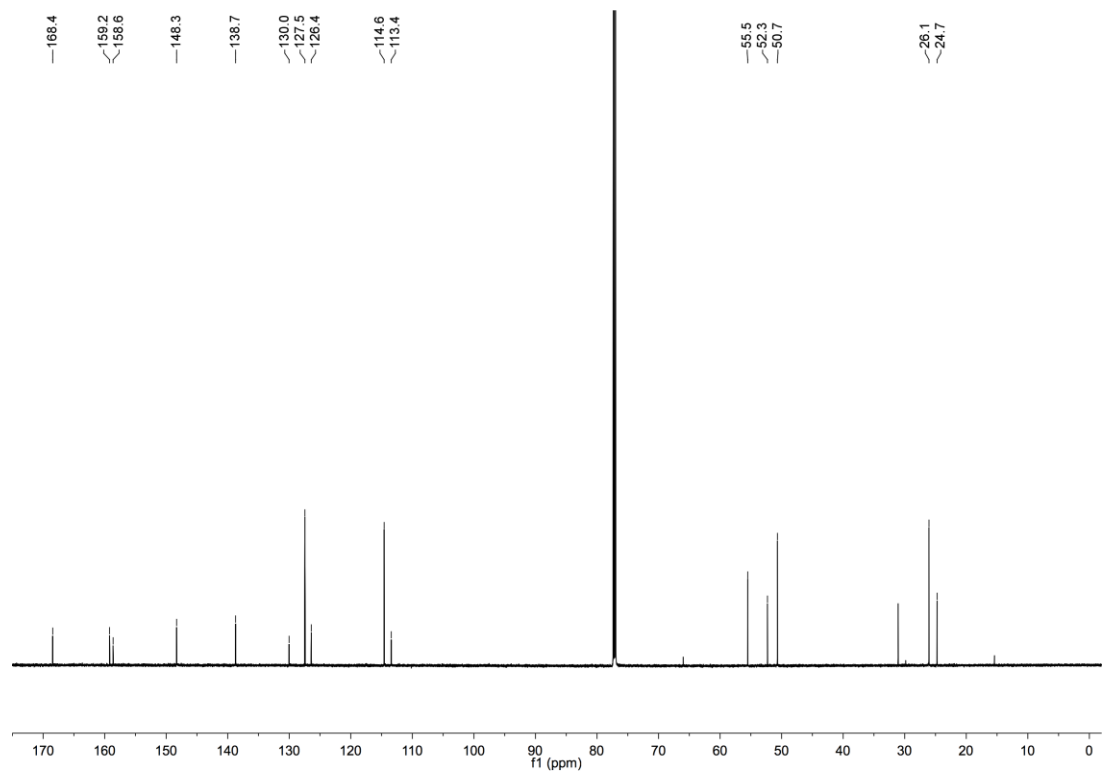
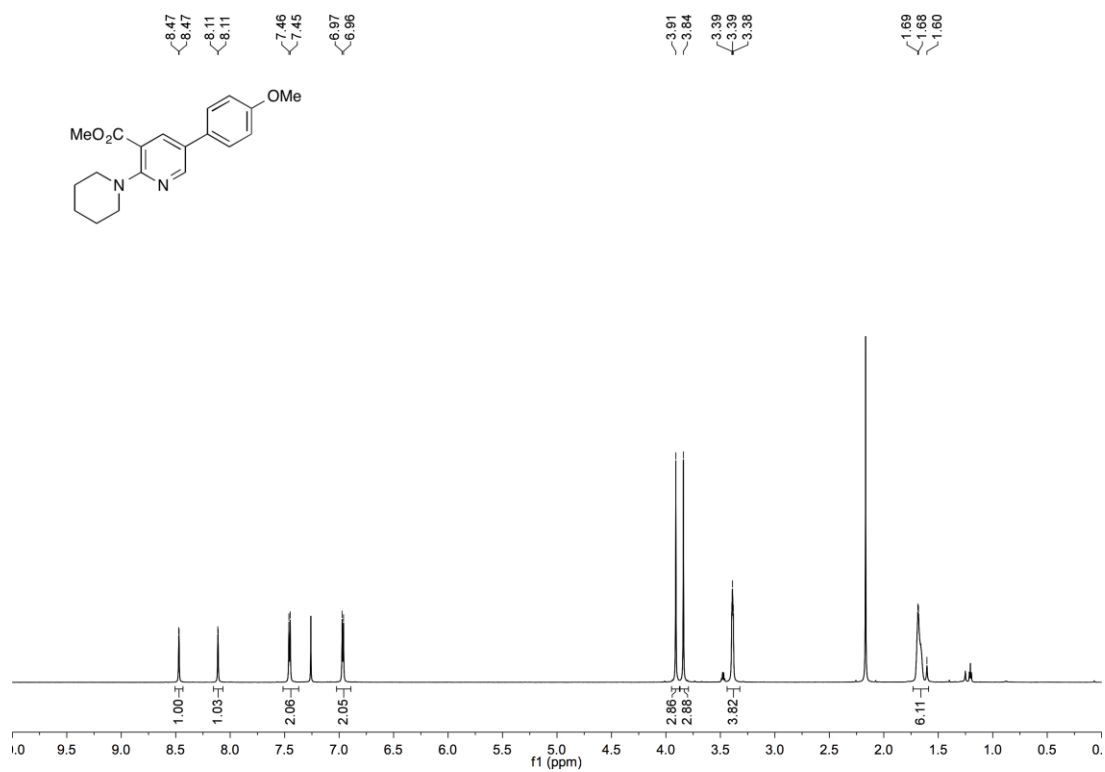
Methyl 2-(4'-methoxyphenyl)isonicotinate (**366**)



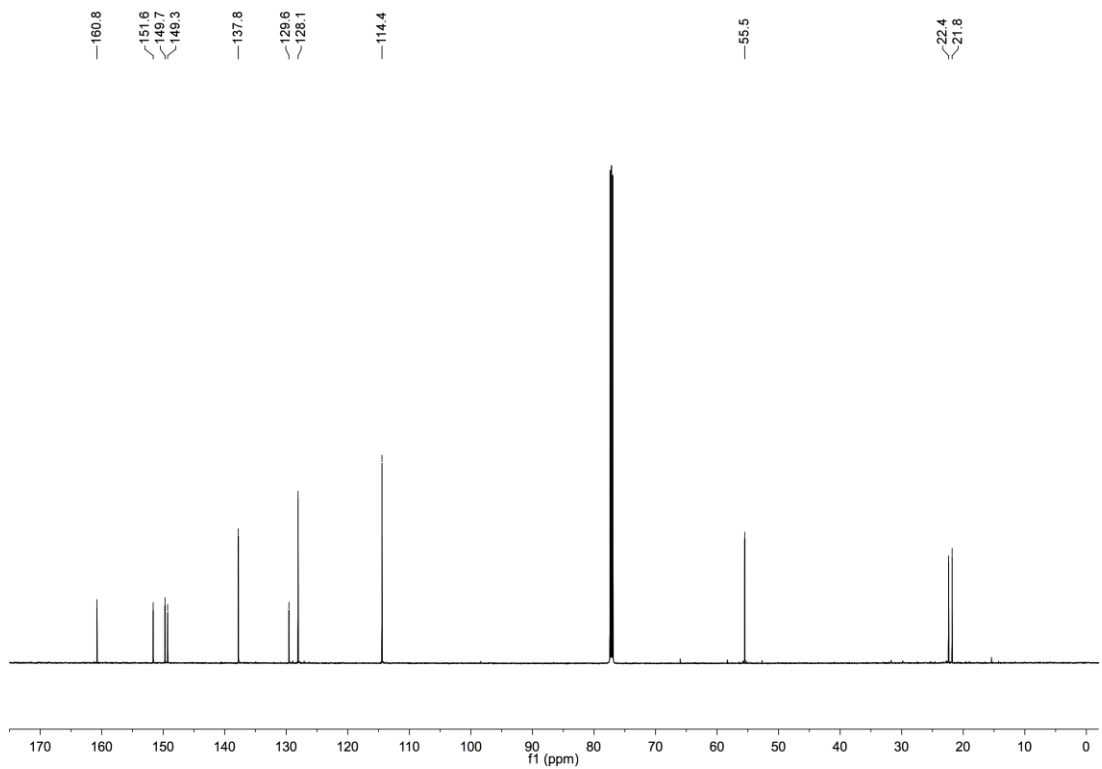
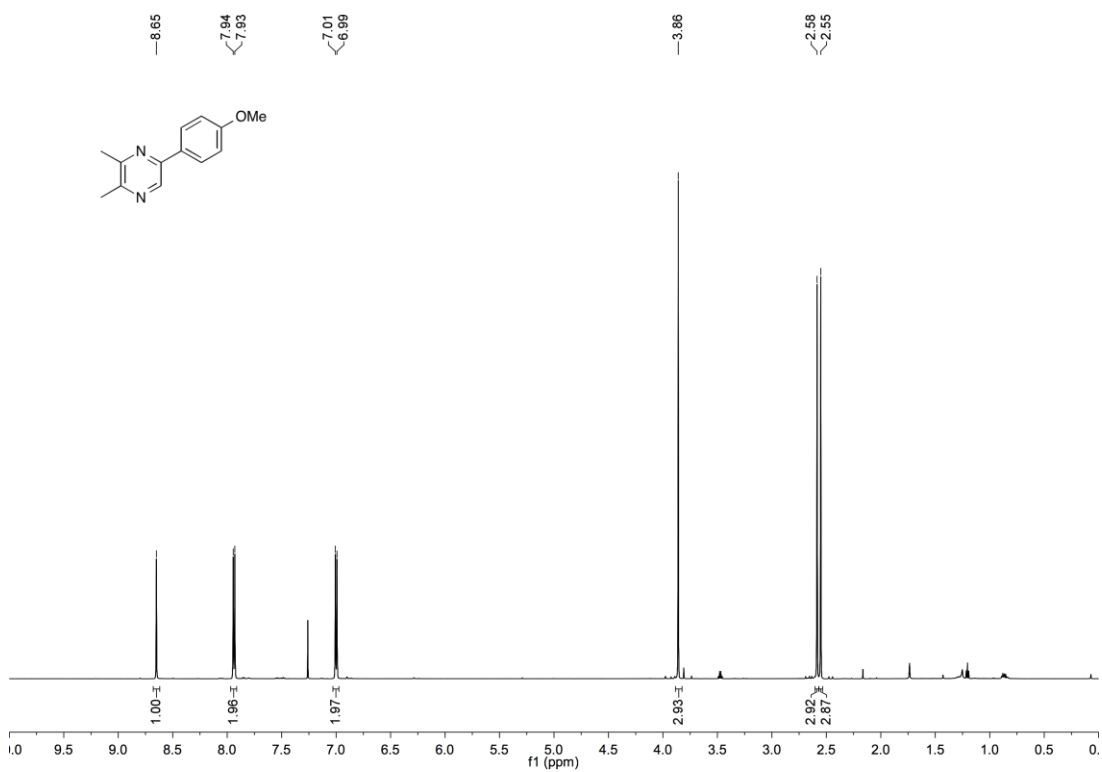
Methyl-2-(N-morpholinyl)-5-(4''-methoxyphenyl)nicotinate (369)



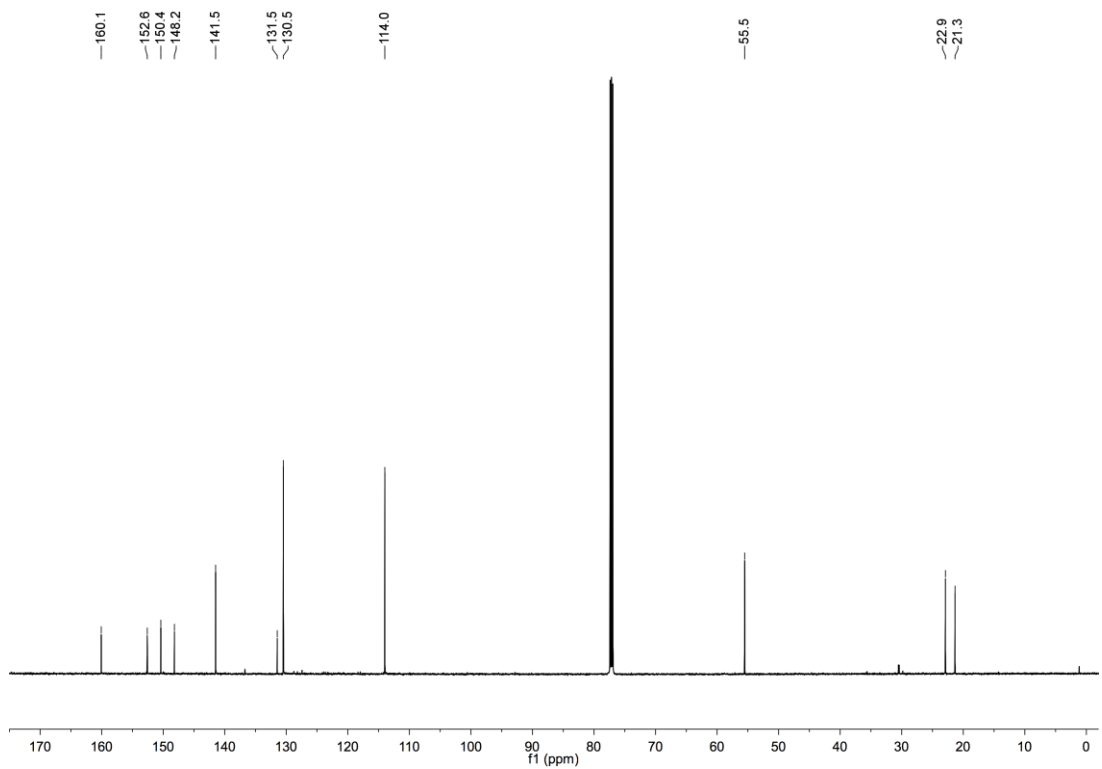
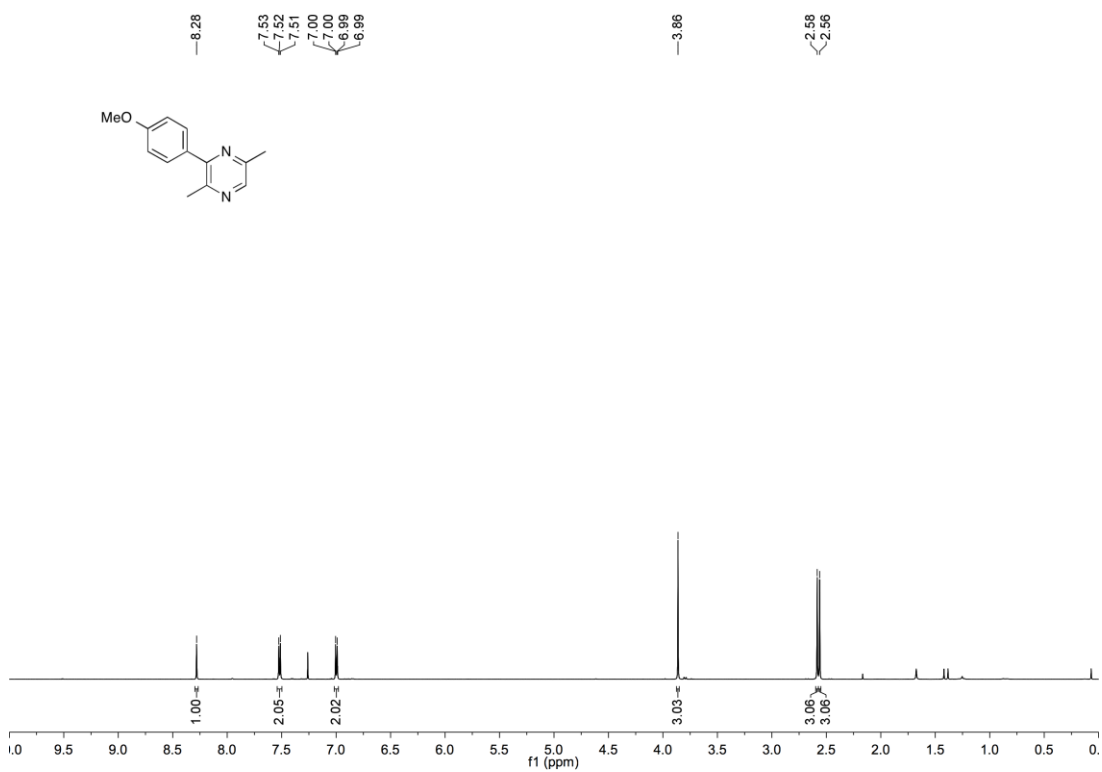
Methyl-2-(N-piperazinyl)-5-(4''-methoxyphenyl)nicotinate (**371**)



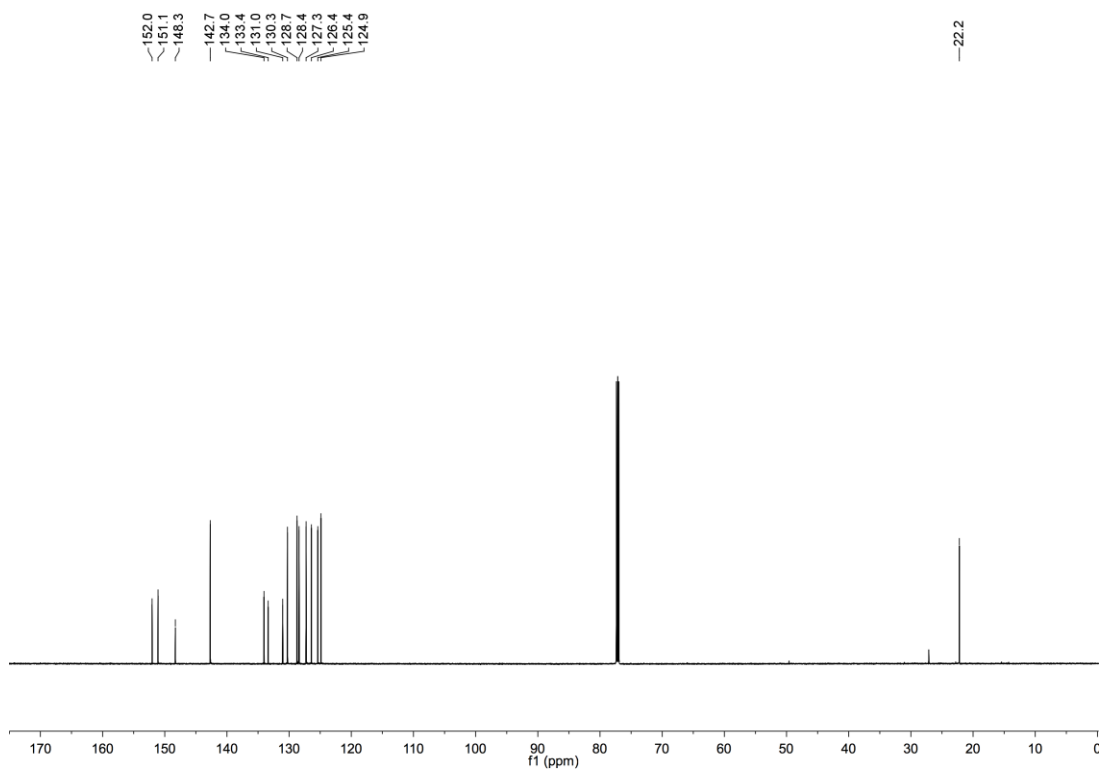
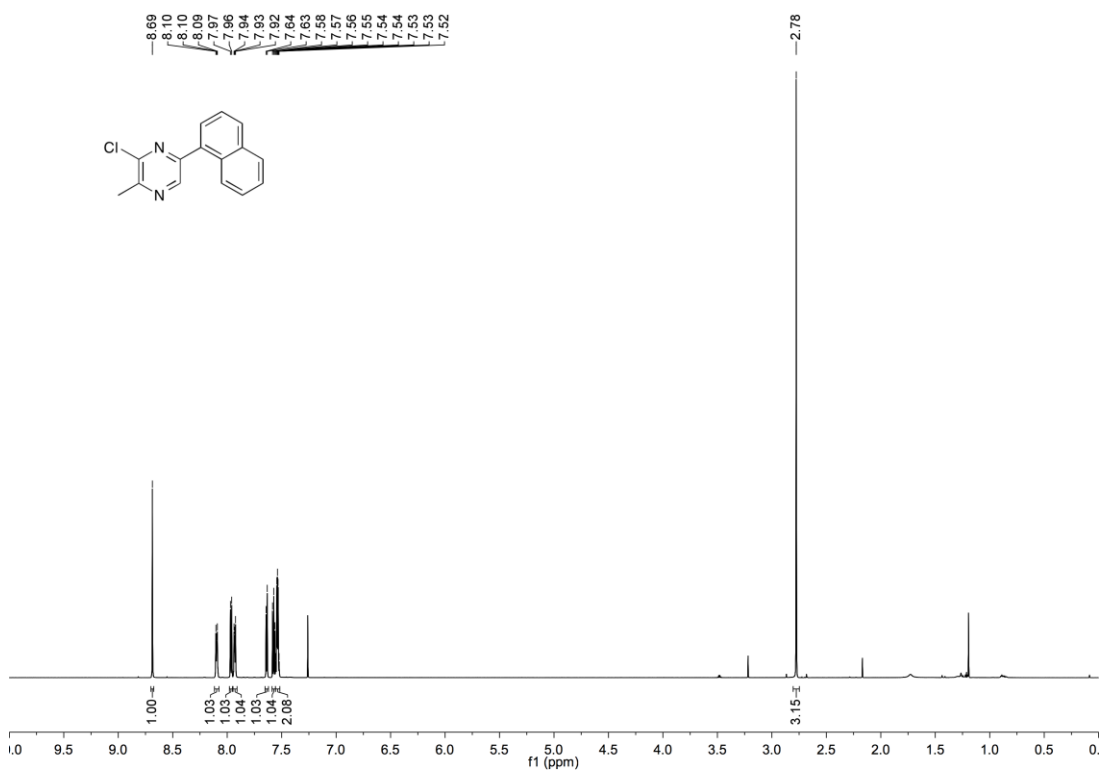
2,3-Dimethyl-5-(4'-methoxyphenyl)pyrazine (391)



2,5-Dimethyl-3-(4'-methoxyphenyl)pyrazine (392)

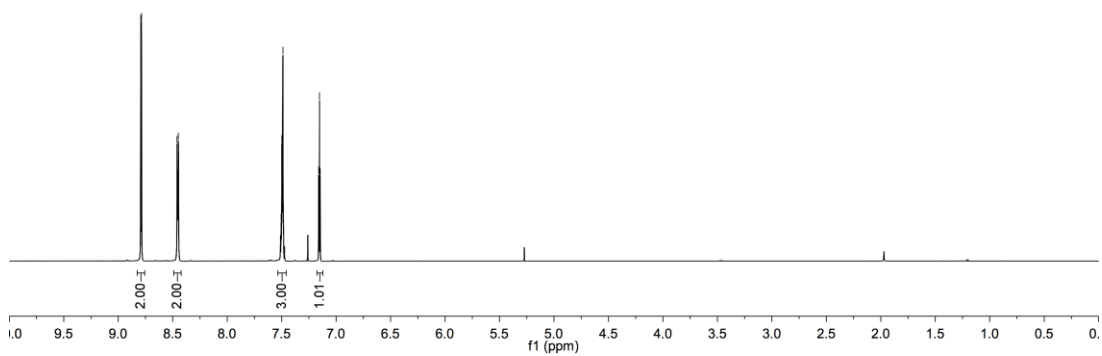
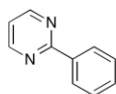


2-Chloro-3-methyl-6-naphthalen-1'-yl-pyrazine (393)

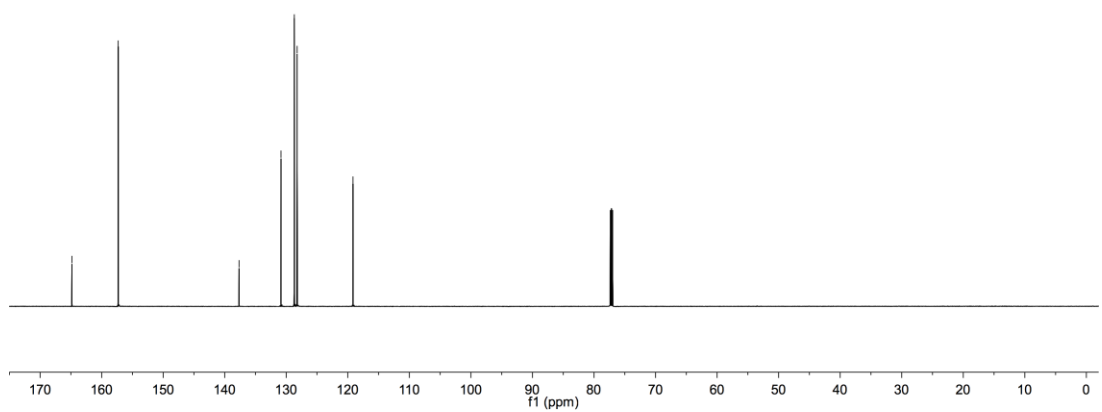


2-Phenylpyrimidine (398)

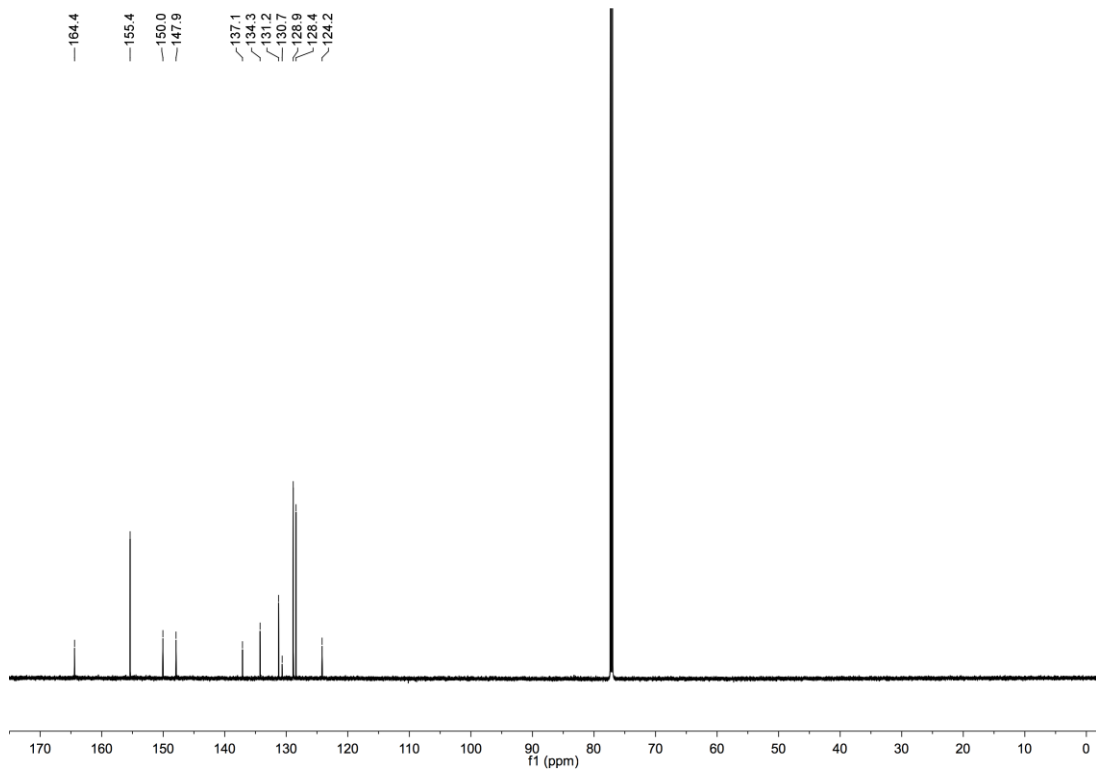
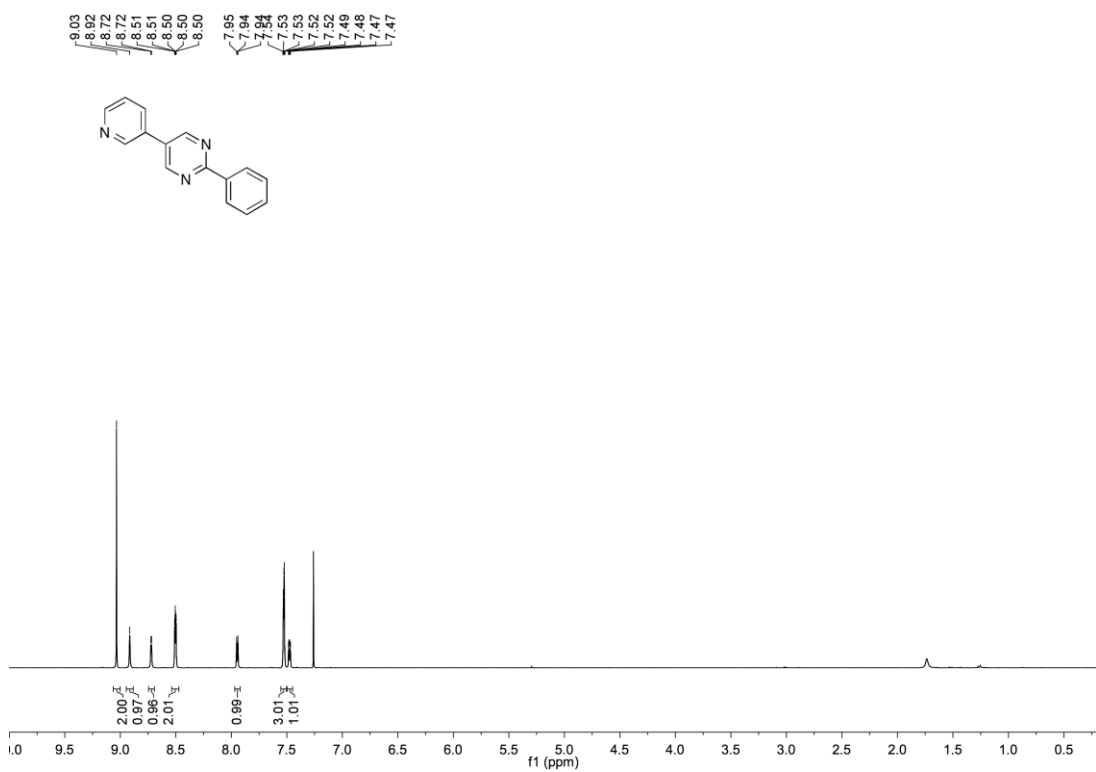
8.79
8.79
8.46
8.46
8.45
8.45
7.50
7.49
7.49
7.48
7.15
7.15



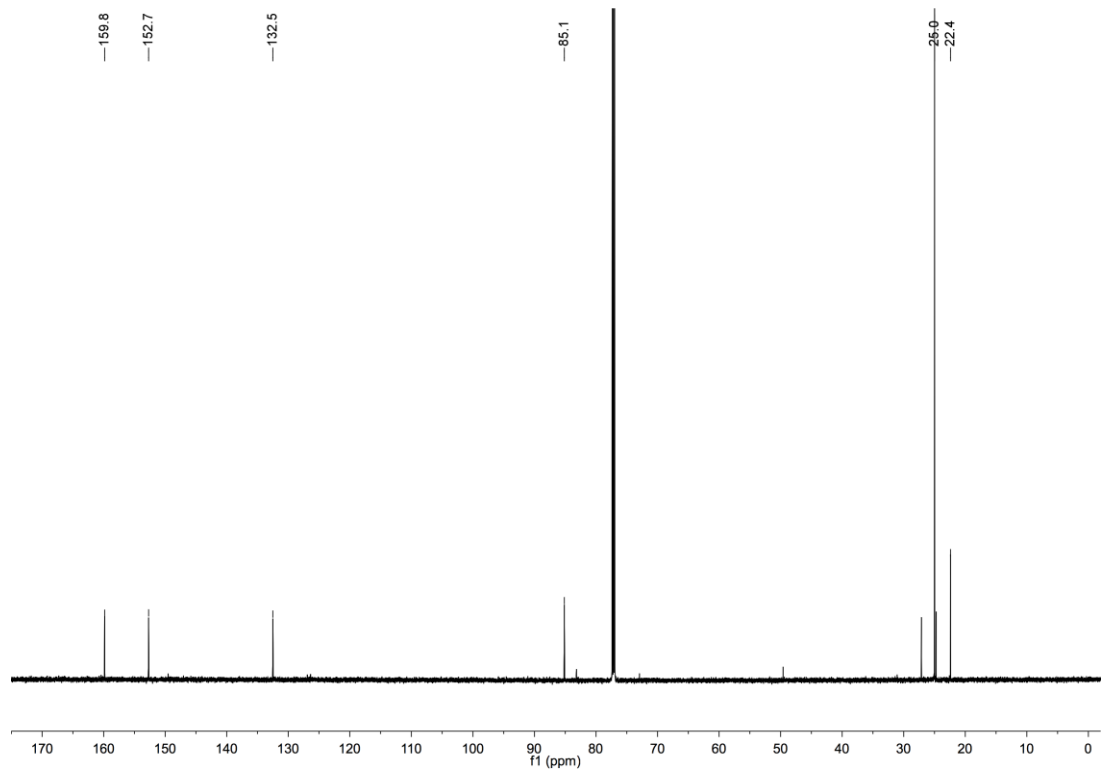
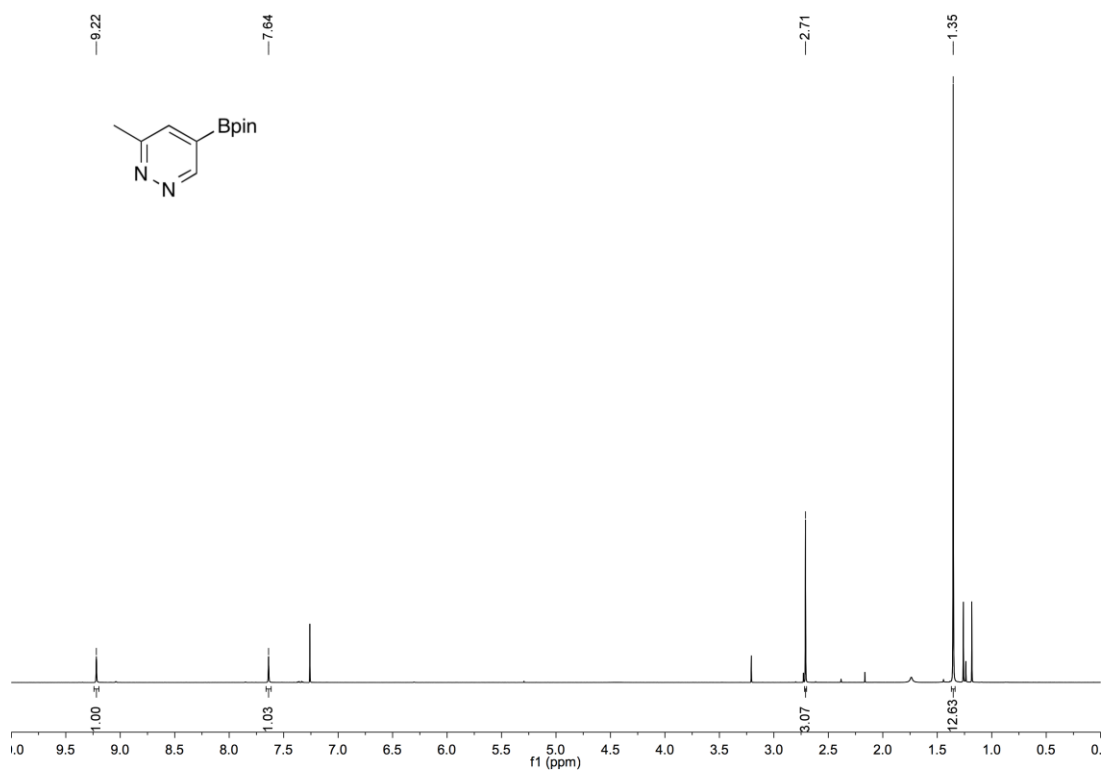
164.8
157.3
137.7
130.9
128.7
128.2
119.2

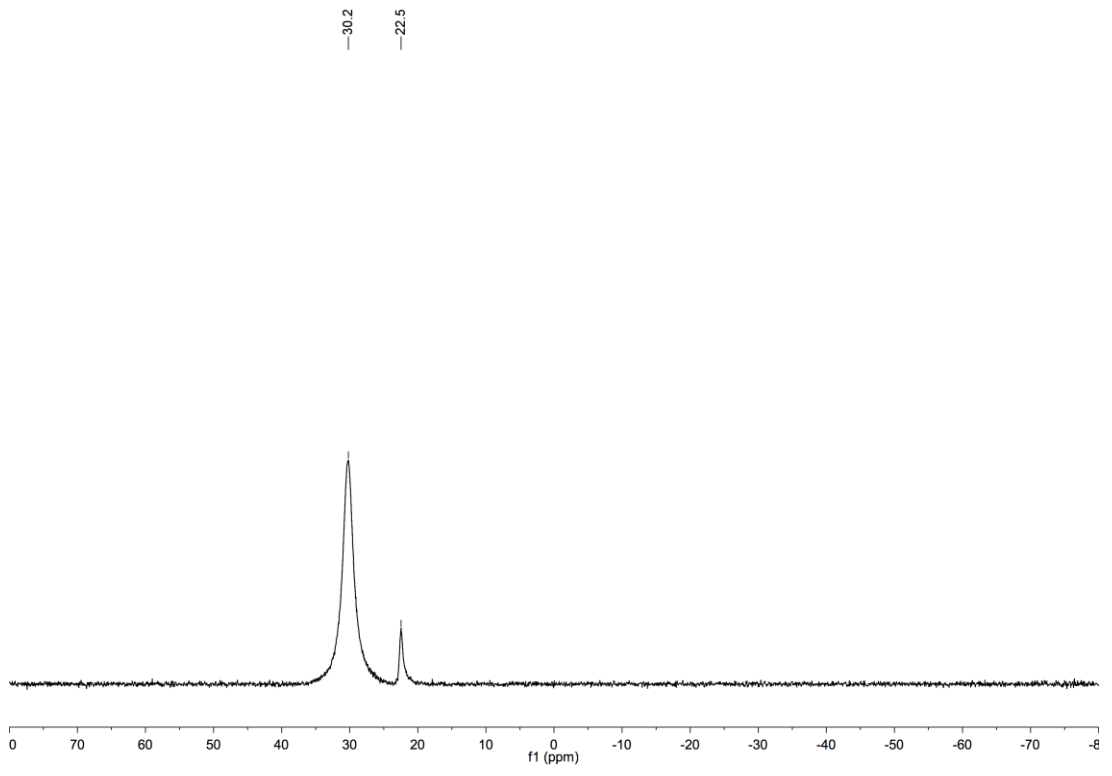


2-Phenyl-5-pyridin-3''-yl-pyrimidine (401)

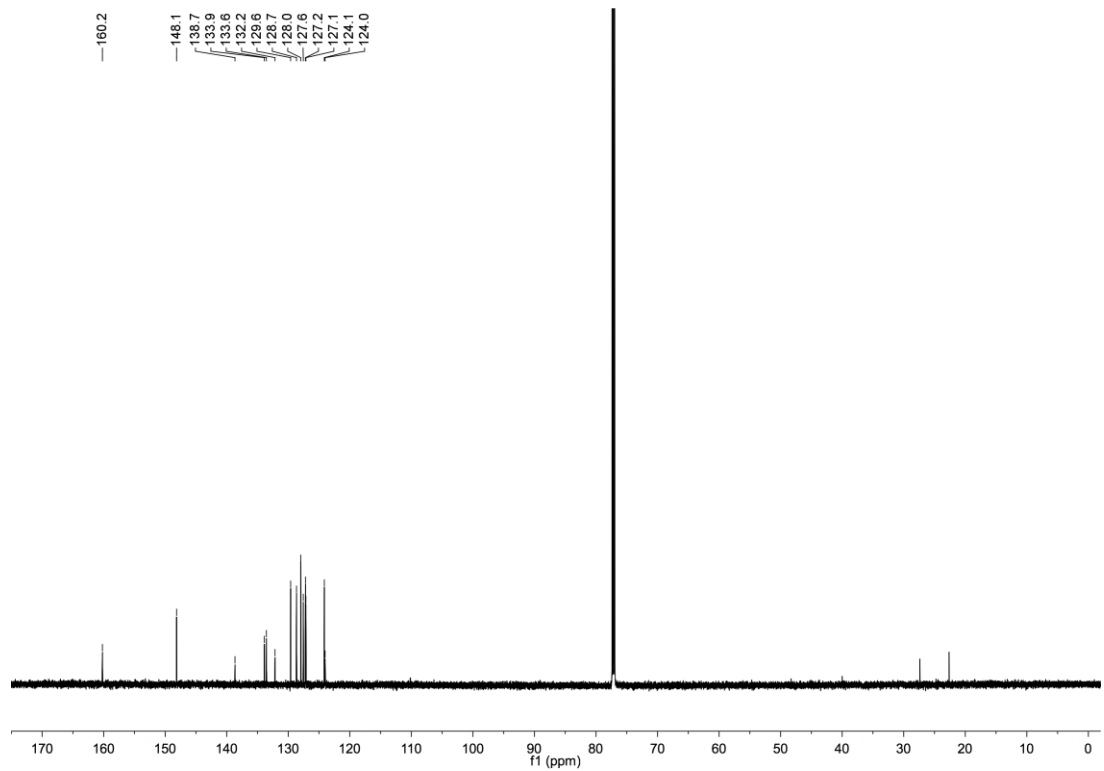
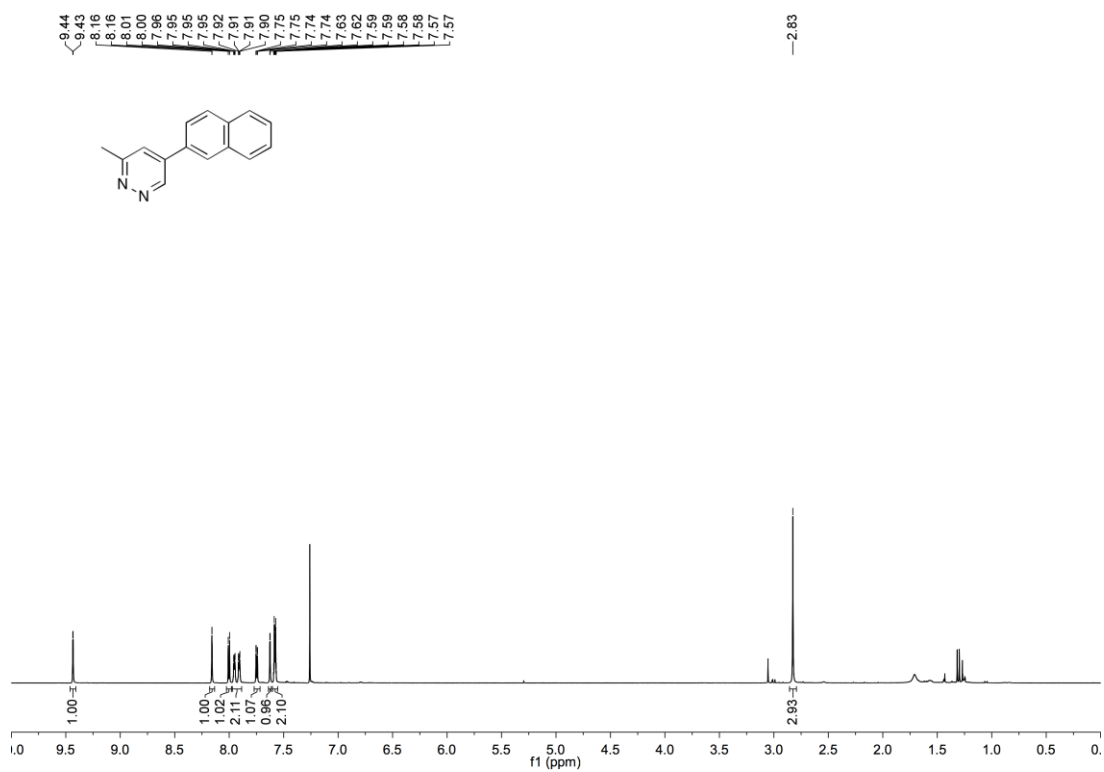


3-Methyl-5-(Bpin)-pyridazine (410)

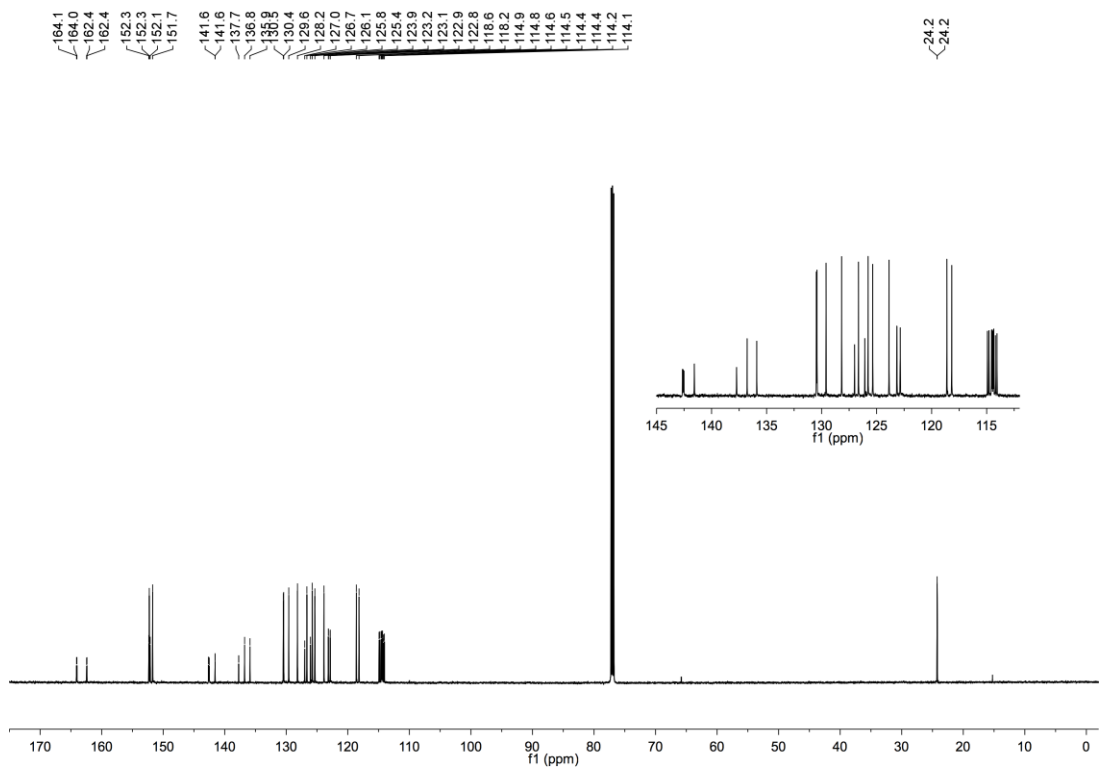
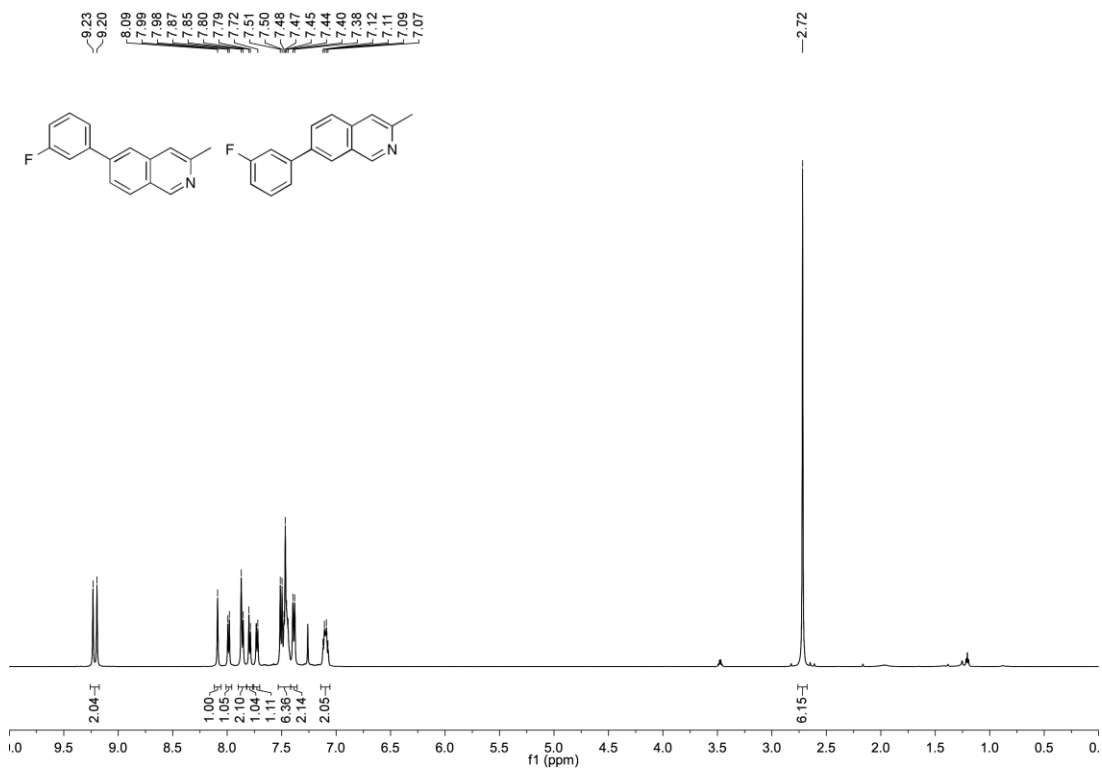


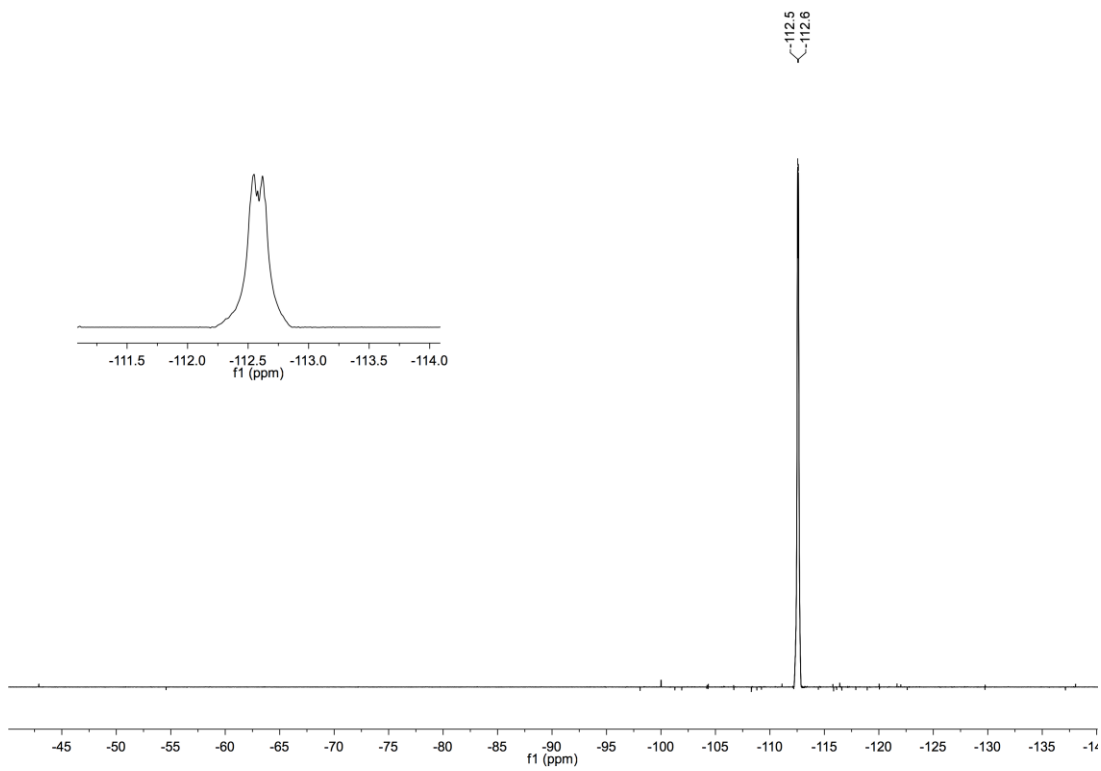


3-Methyl-5-naphthalen-2'-ylpyridazine (413)

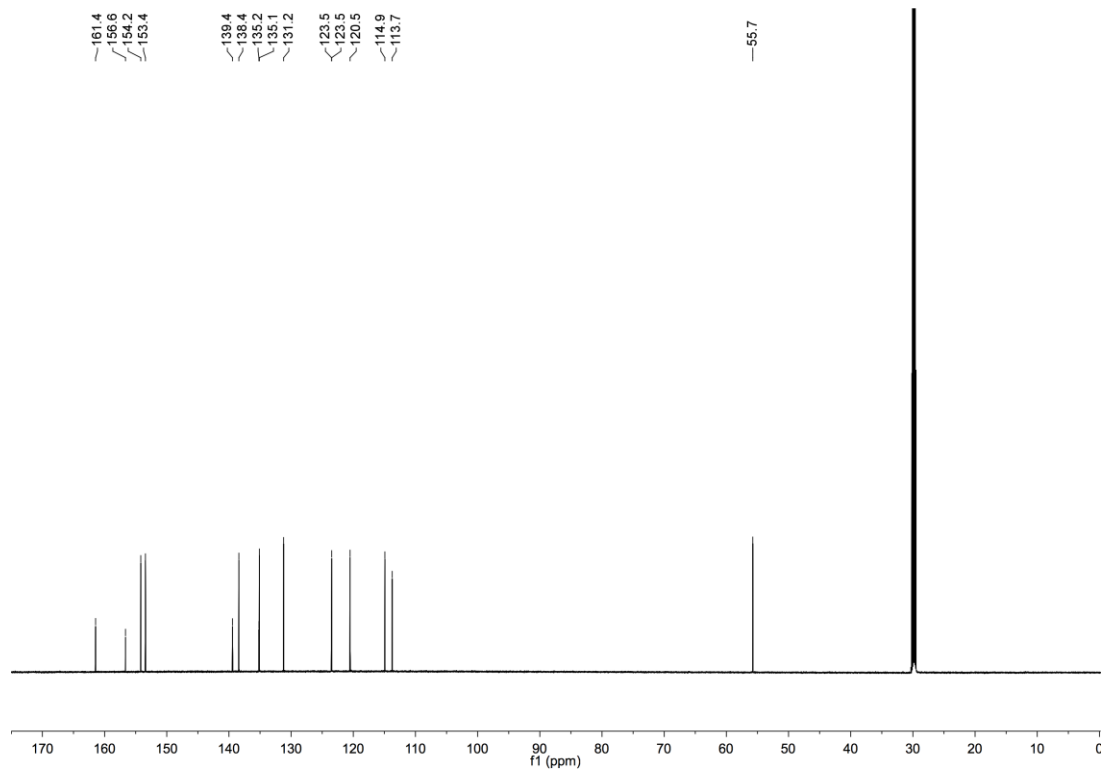
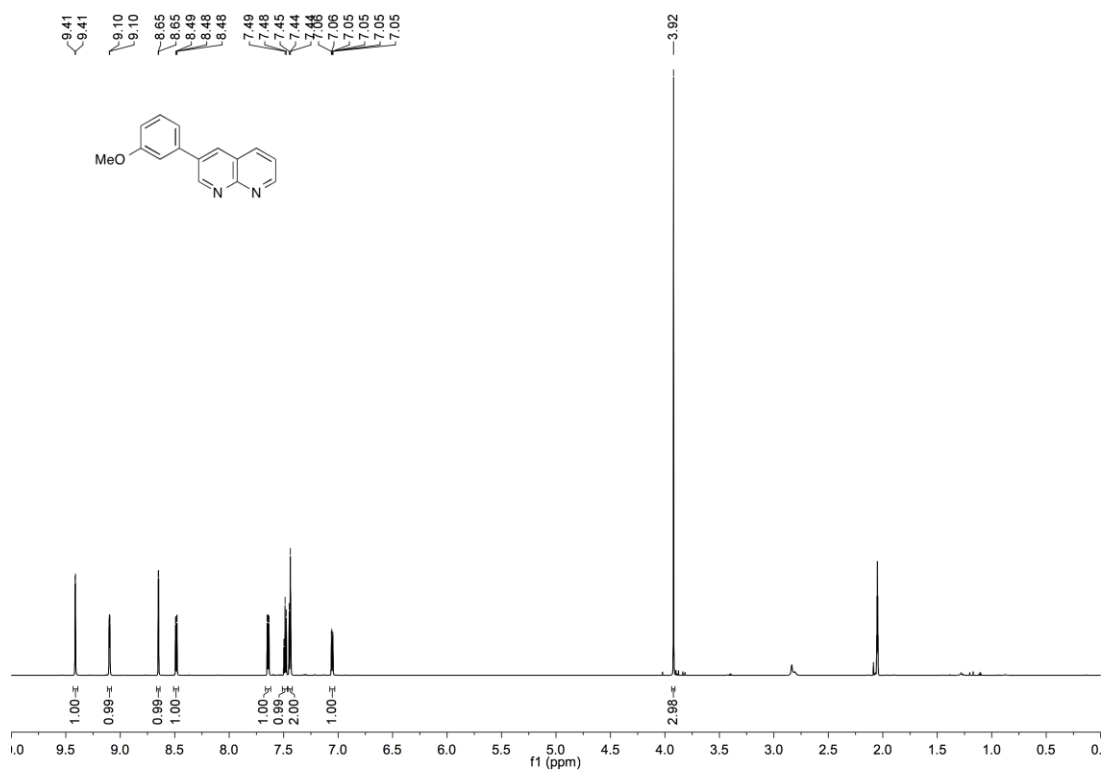


3-Methyl-6-(3'-fluorophenyl)isoquinoline (423) and 3-Methyl-7-(3'-fluorophenyl)isoquinoline (424)

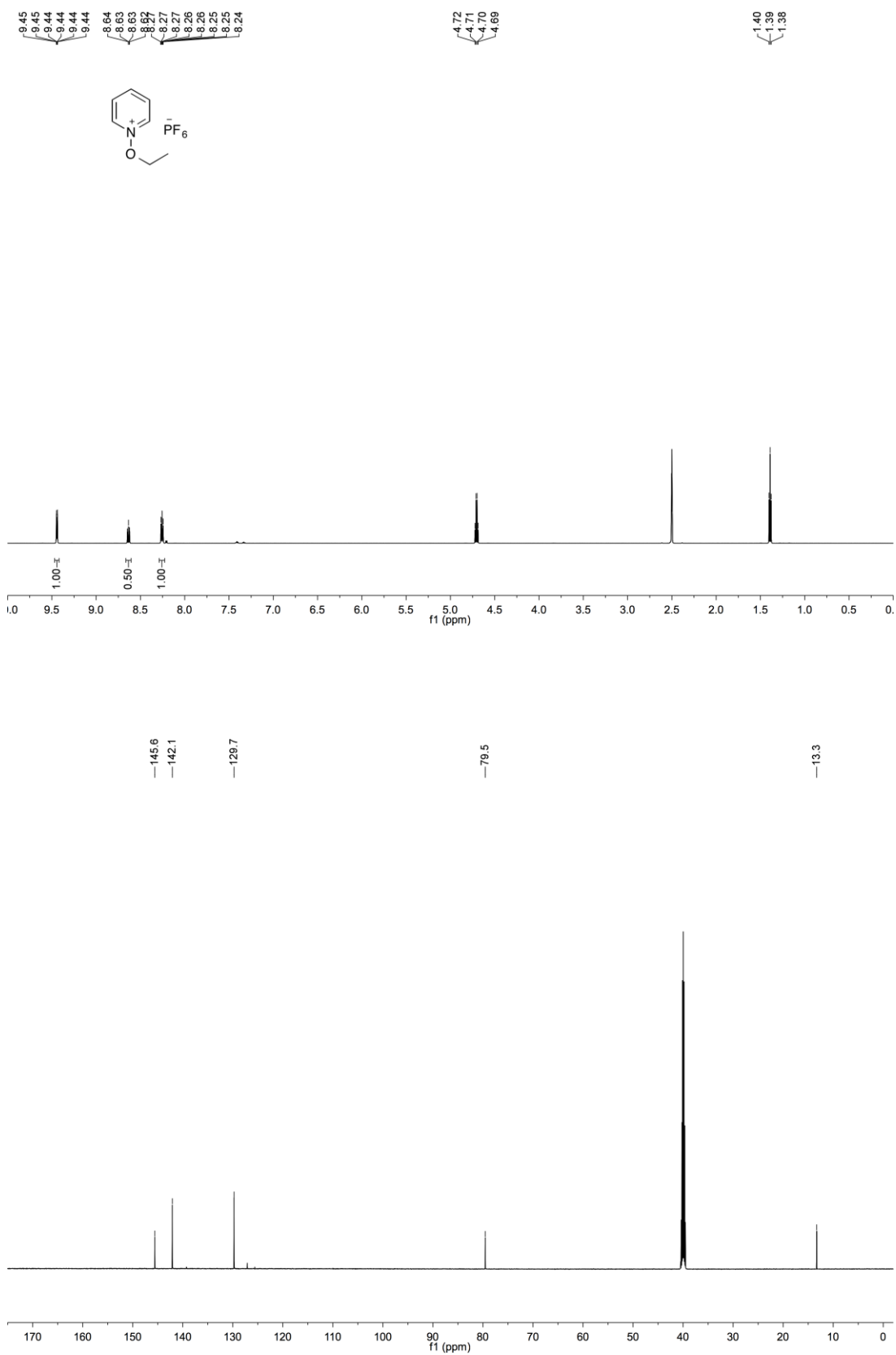


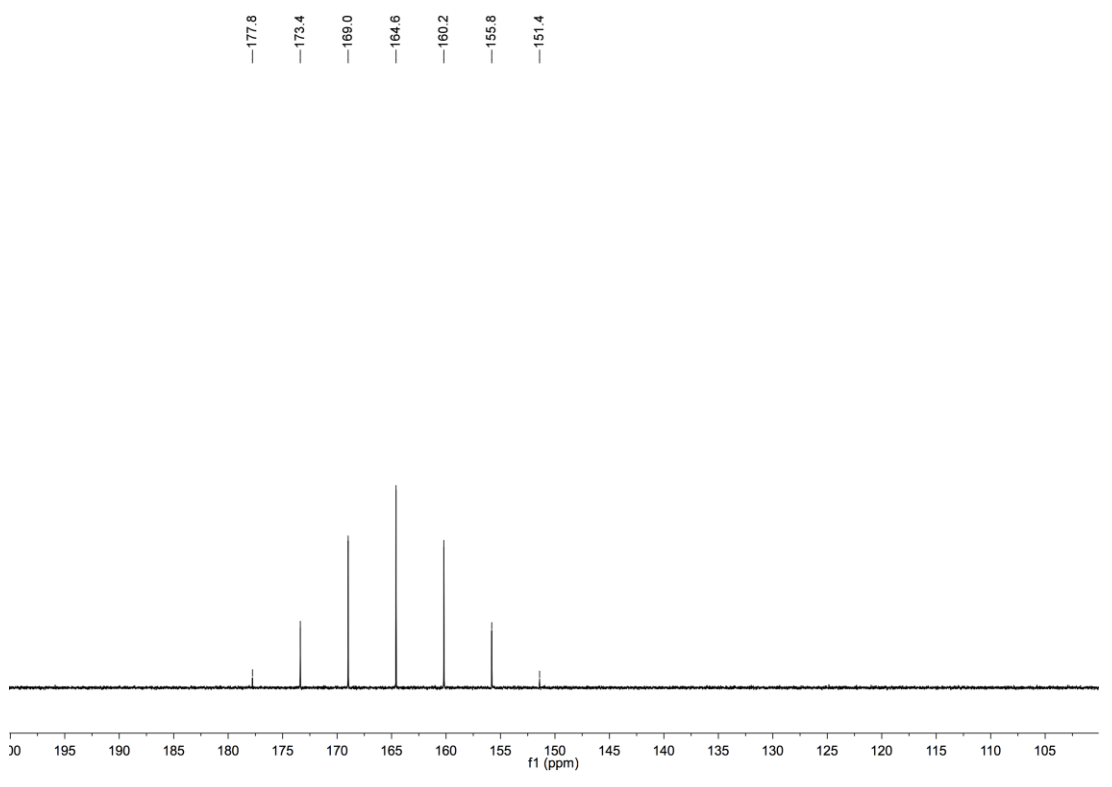
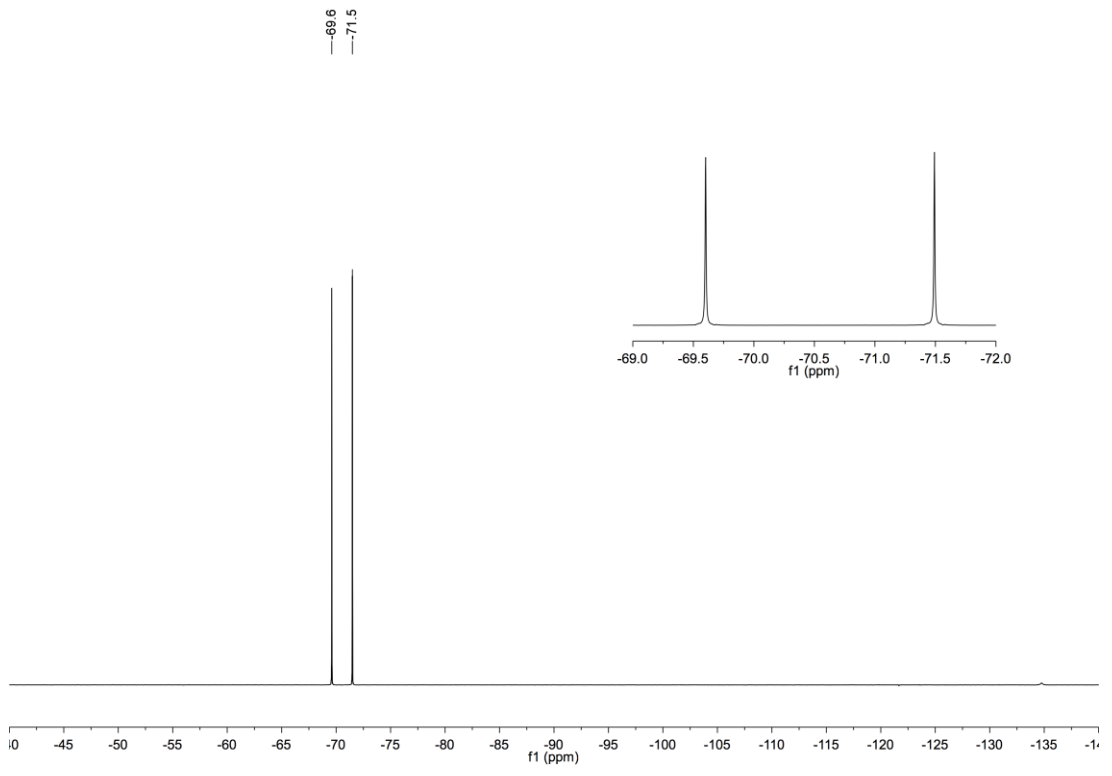


3-(3'-Methoxyphenyl)-1,8-naphthyridine (427)

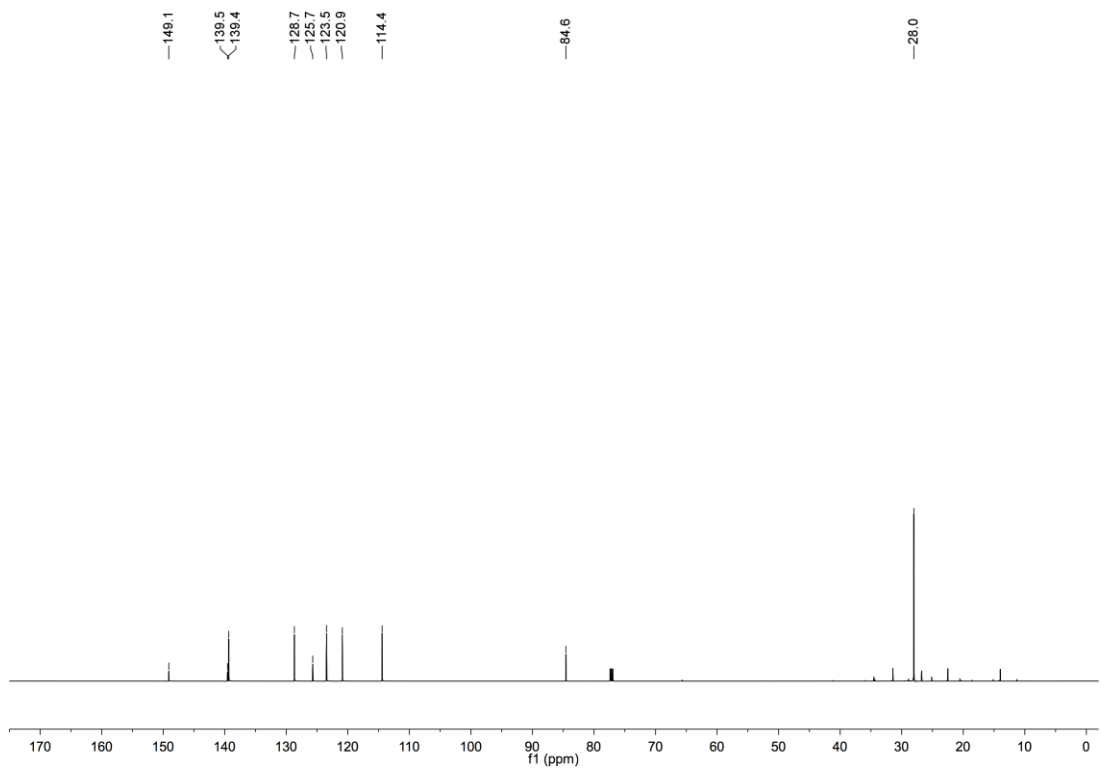
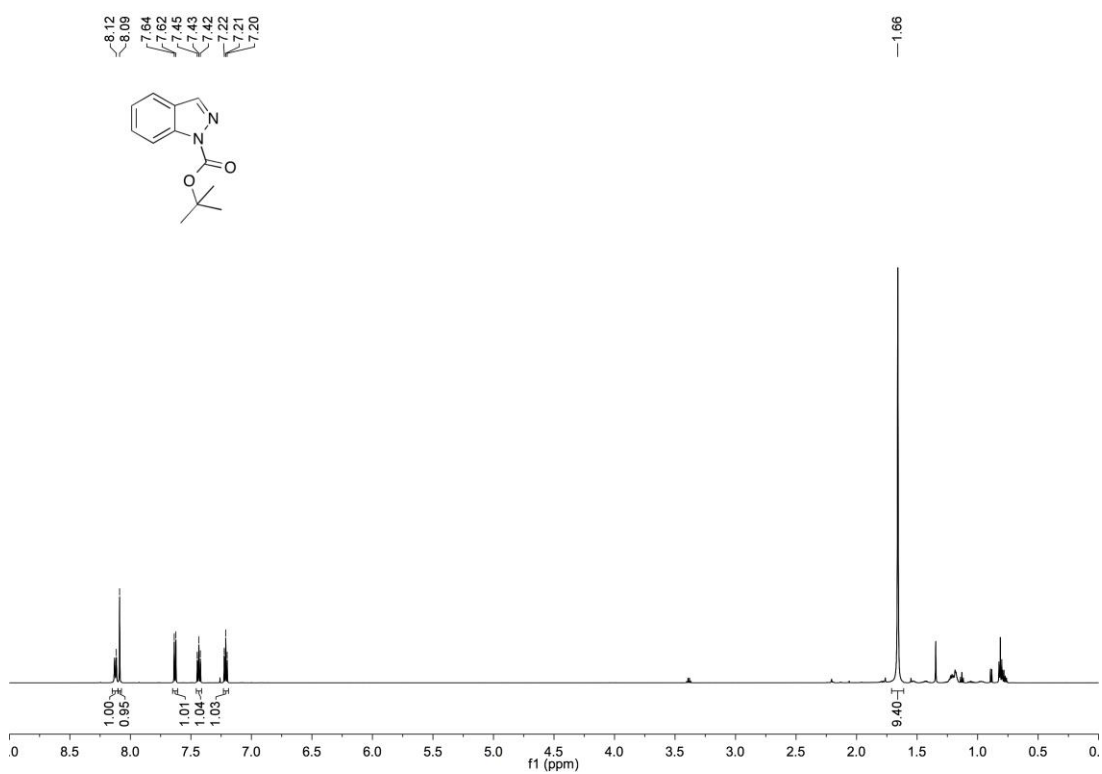


N-Ethoxy-pyridinium hexafluorophosphate (431)

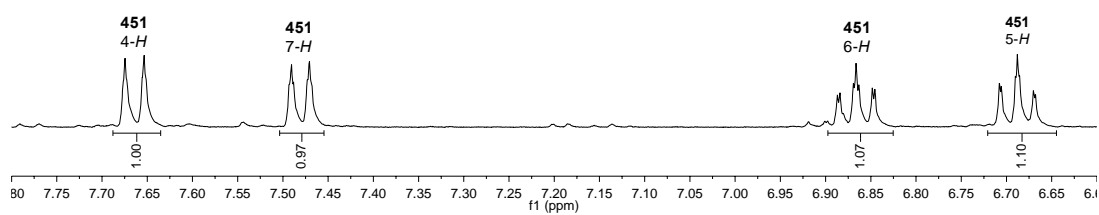




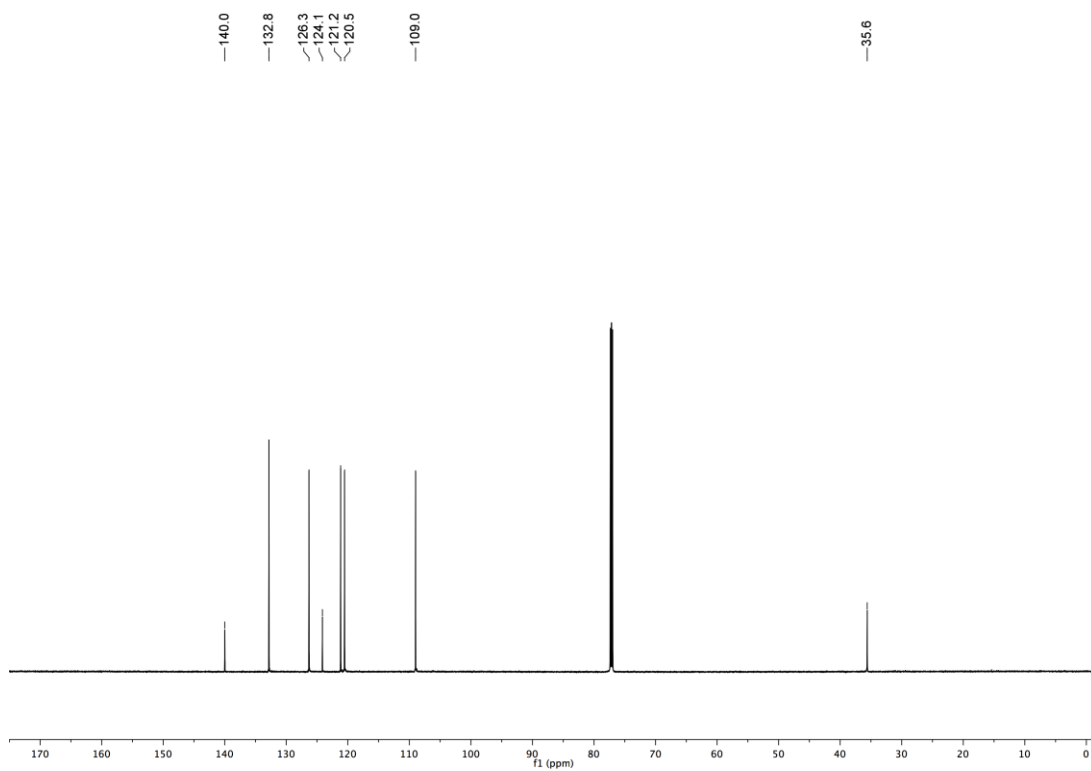
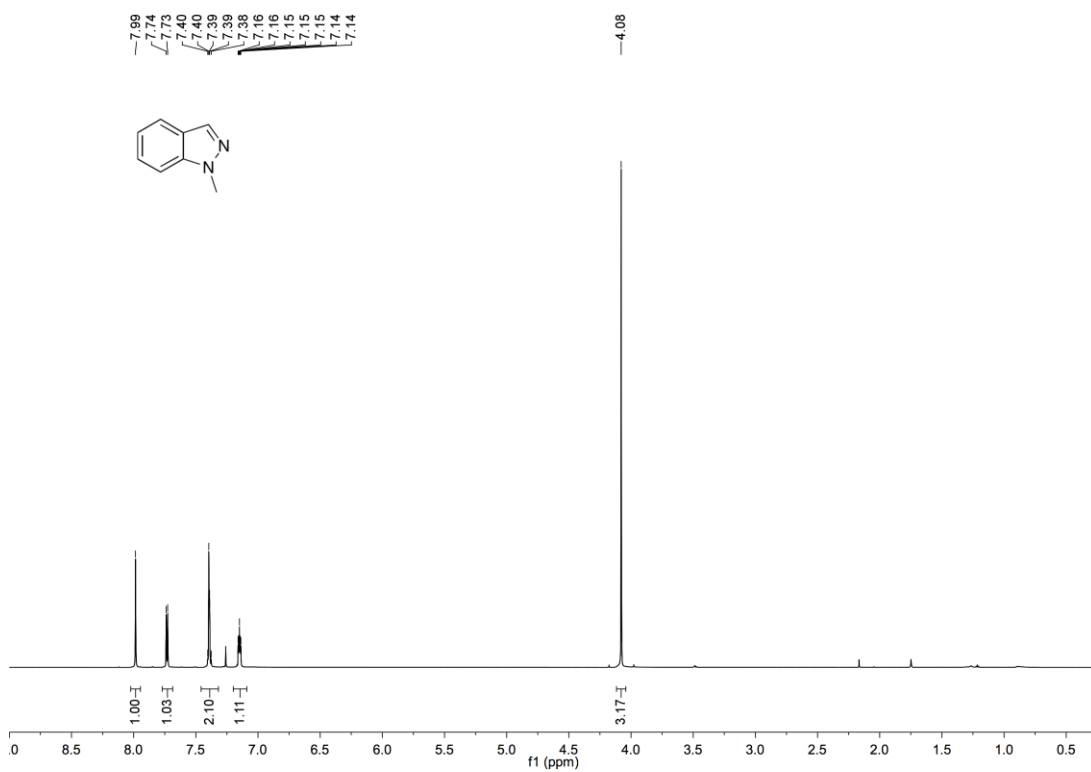
*t*Butyl-1H-indazole-1-carboxylate (450)



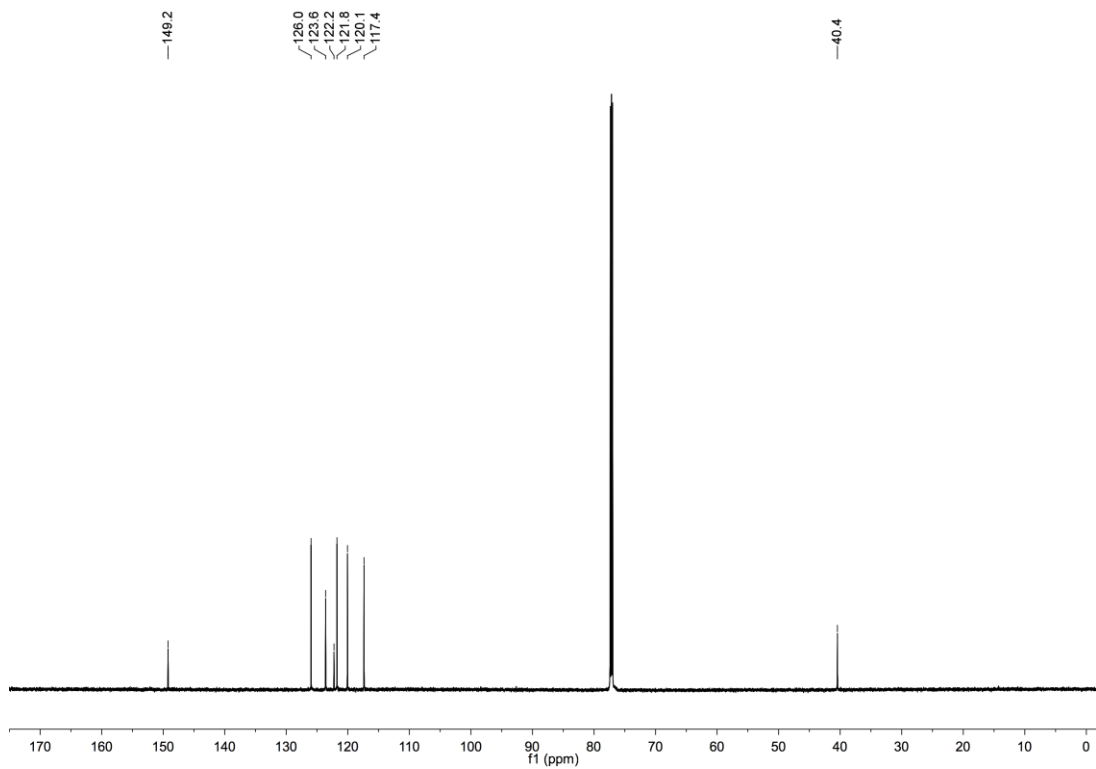
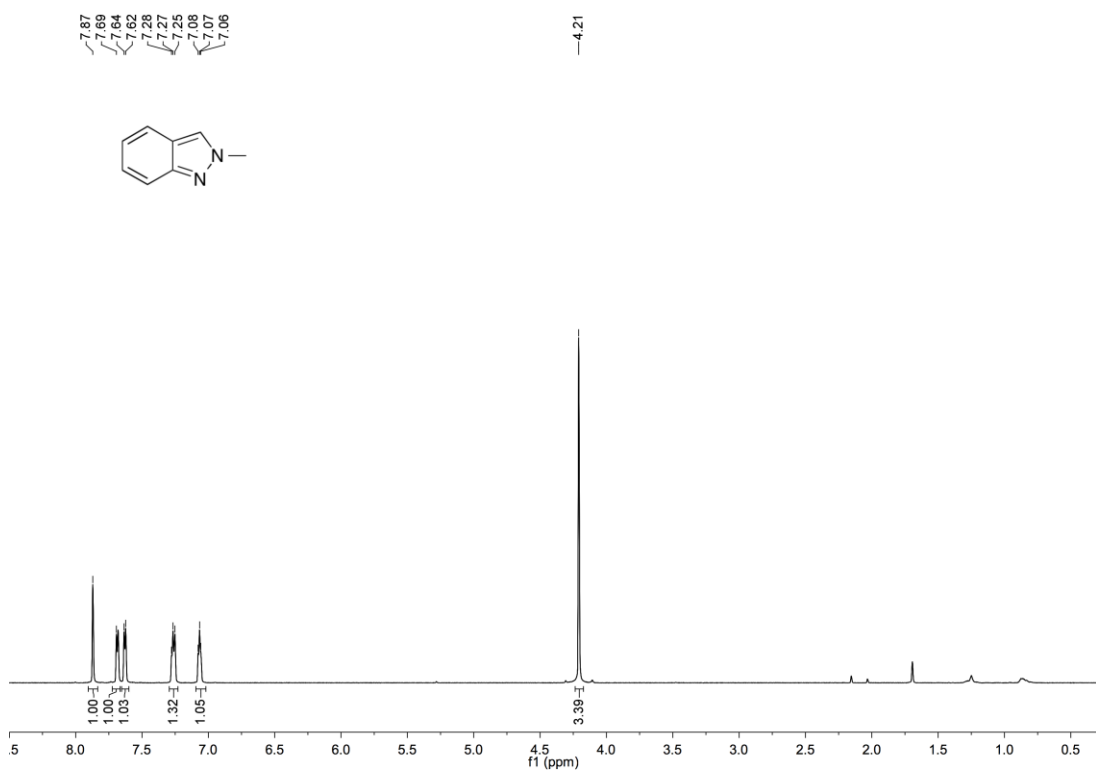
Borylation of *t*-butyl-1*H*-indazole-1-carboxylate (**450**) (*in-situ*, 400 MHz, (CD₃)₂CO)



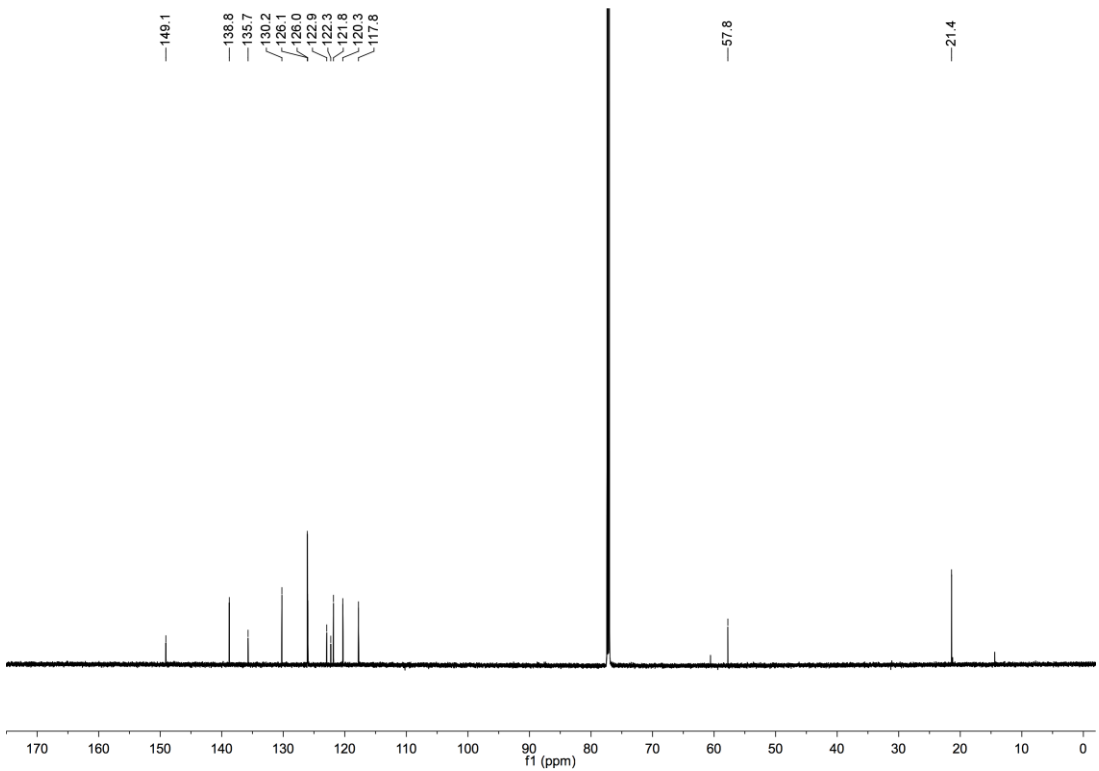
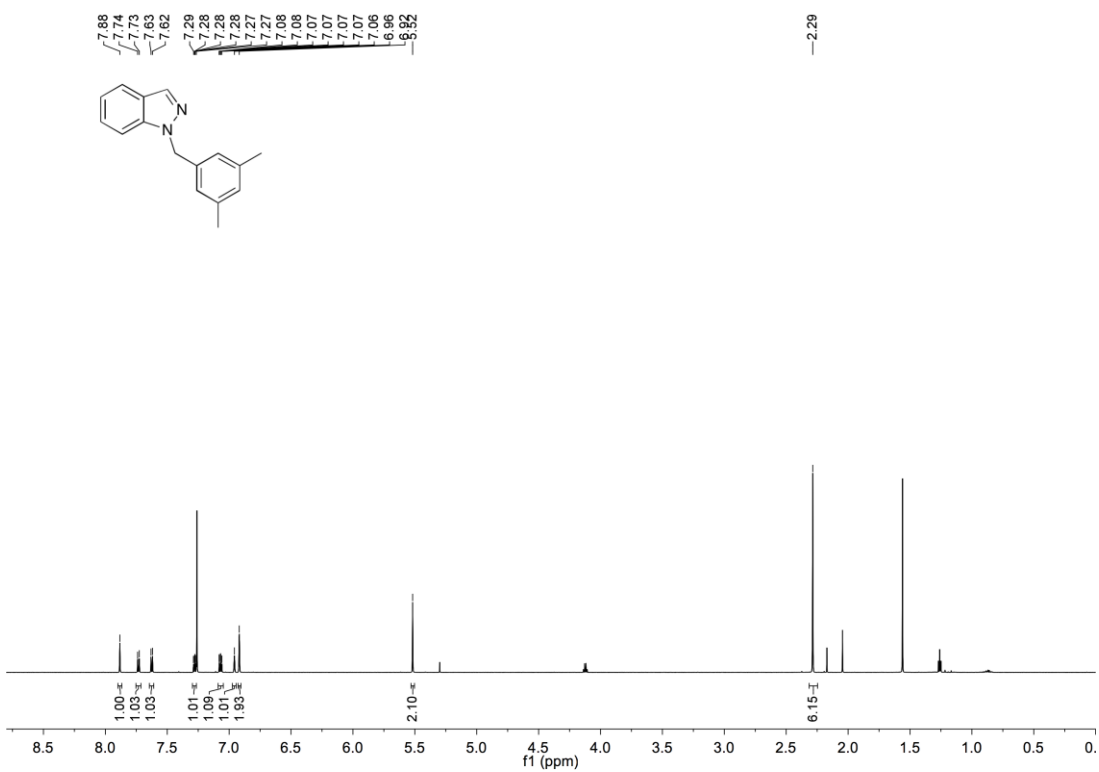
1-Methyl-1H-indazole (404)



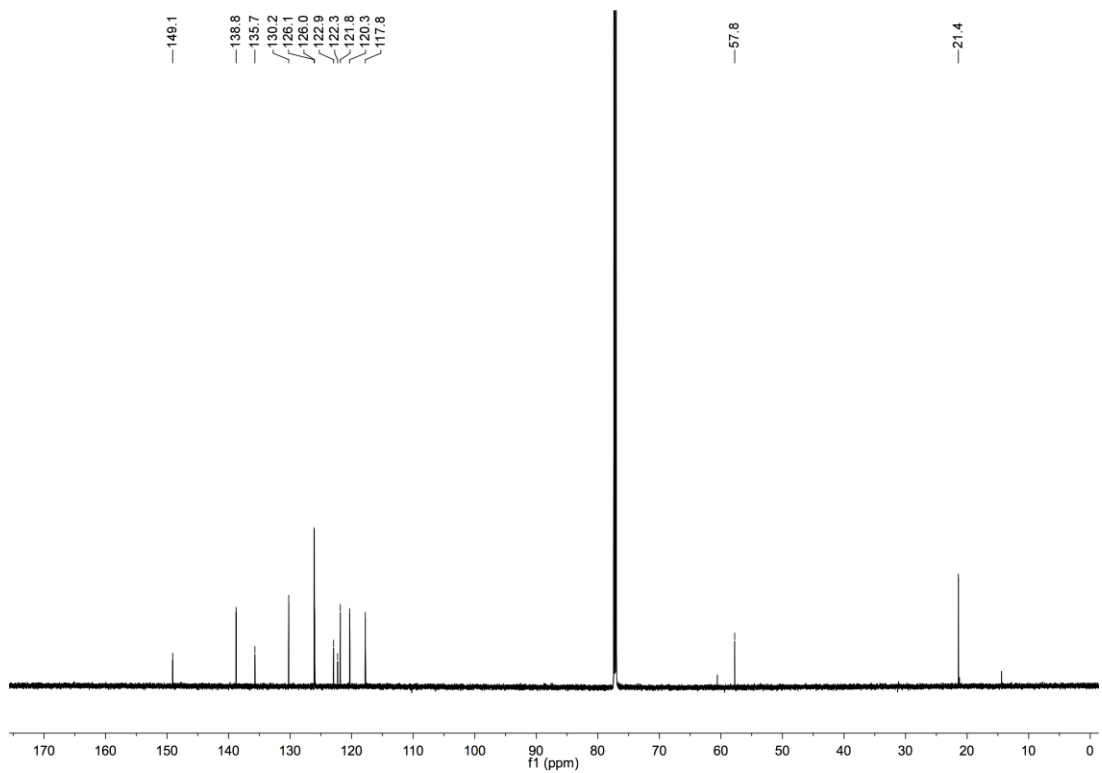
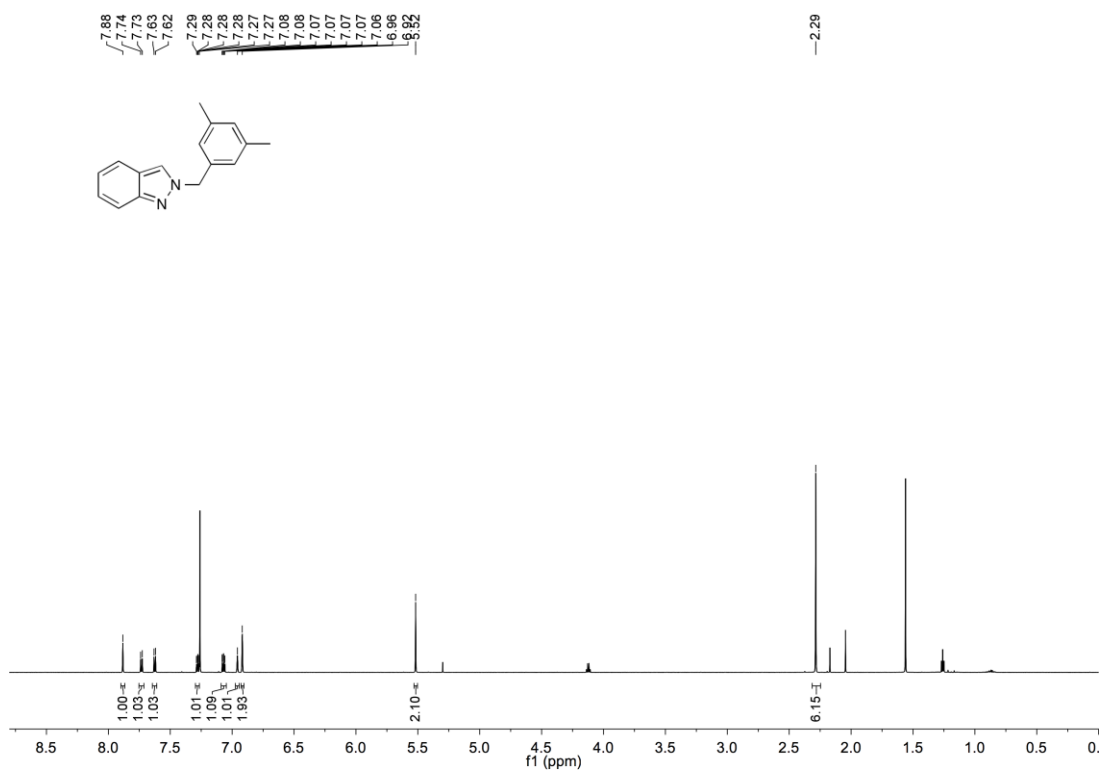
2-Methyl-2H-indazole (453)



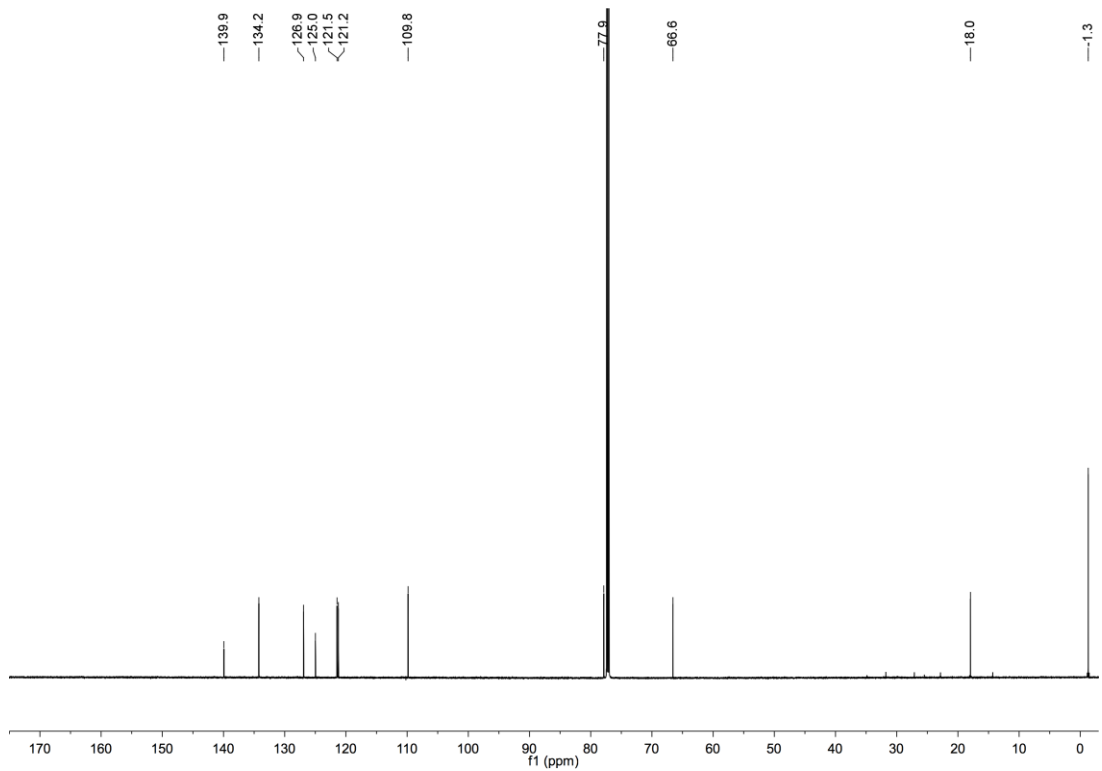
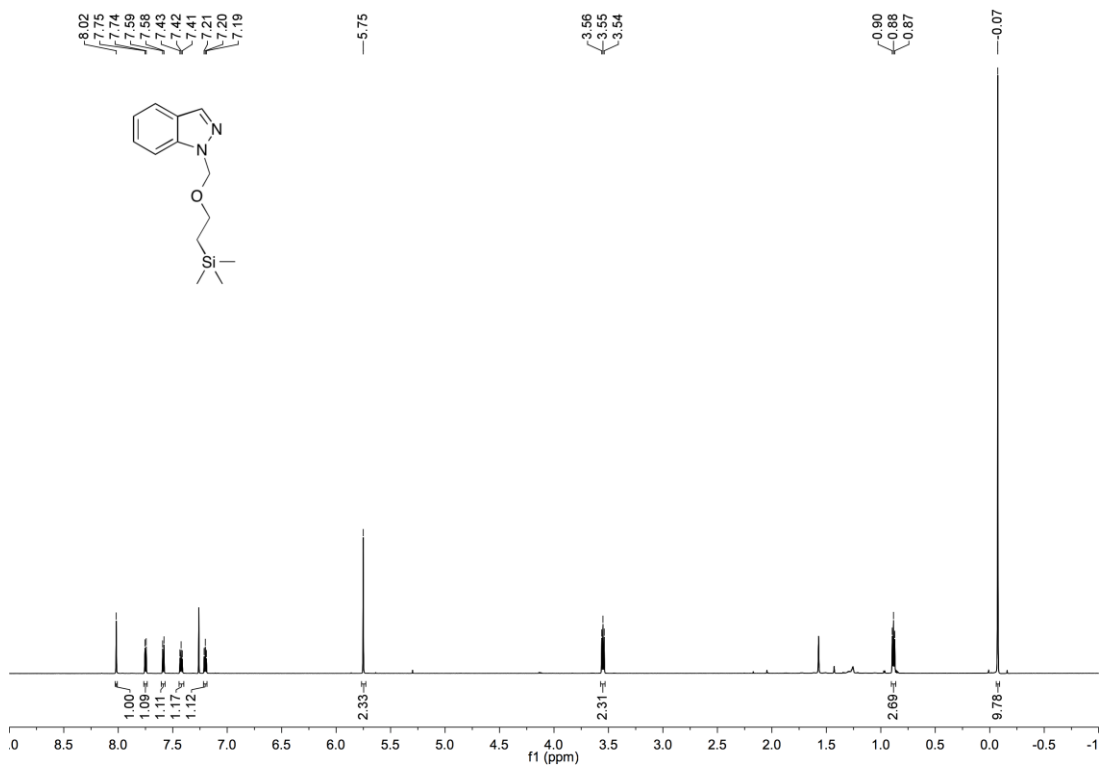
1-(3', 5'-Dimethylbenzyl)-1H-indazole (455)



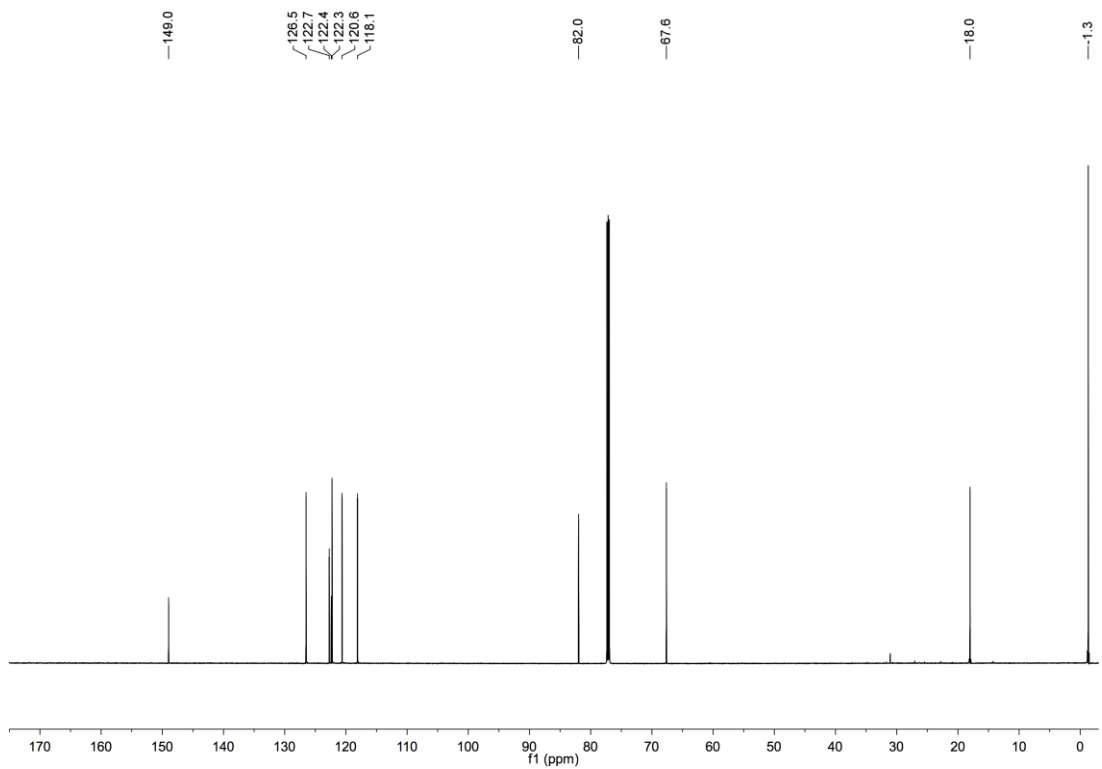
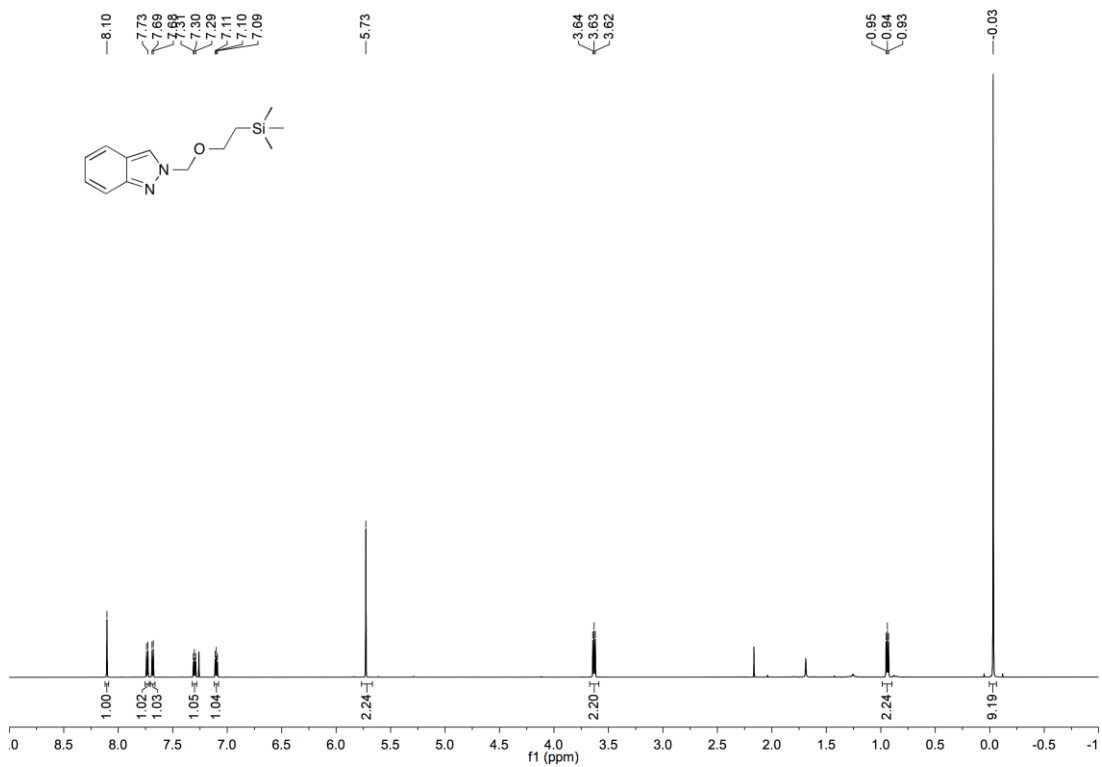
2-(3', 5'-Dimethylbenzyl)-2H-indazole (456)



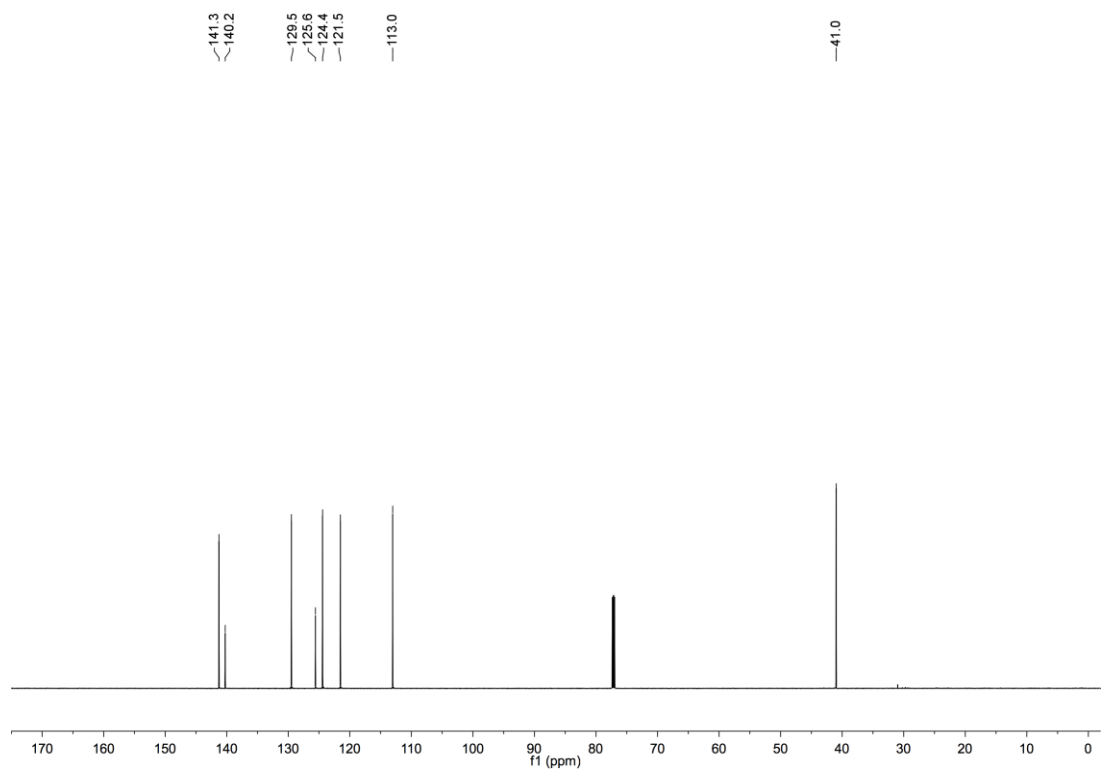
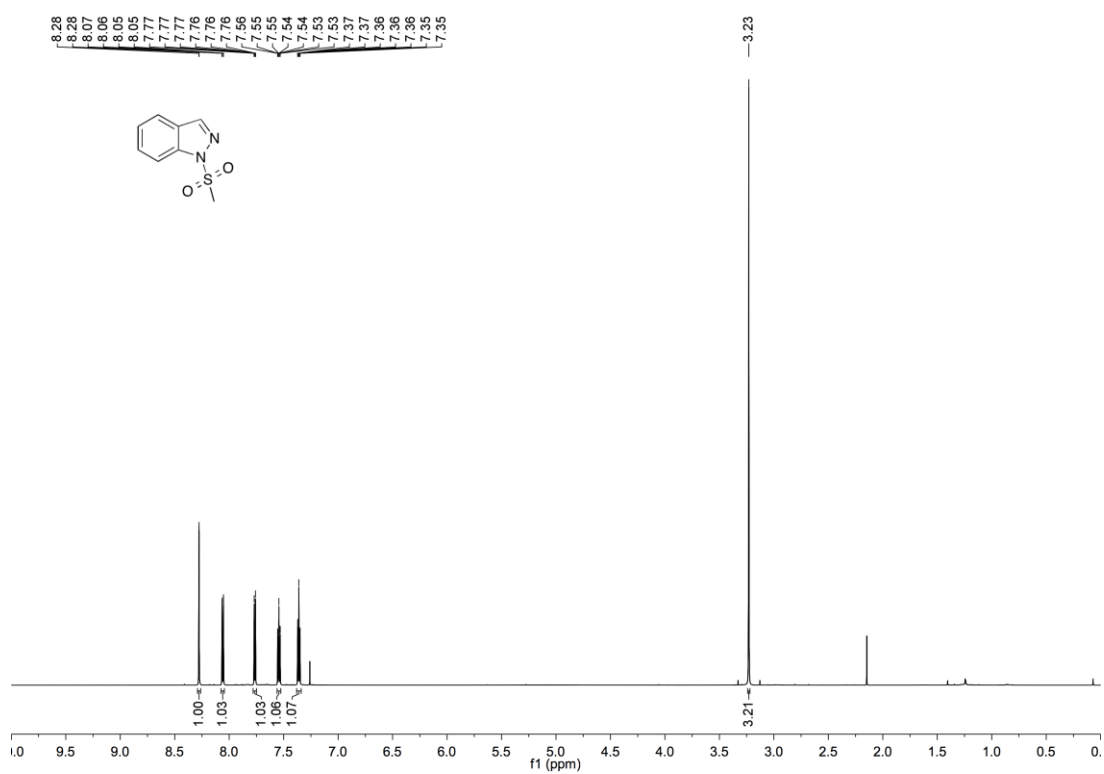
1-([2-(Trimethylsilyl)ethoxy]methyl)-1H-indazole (458)



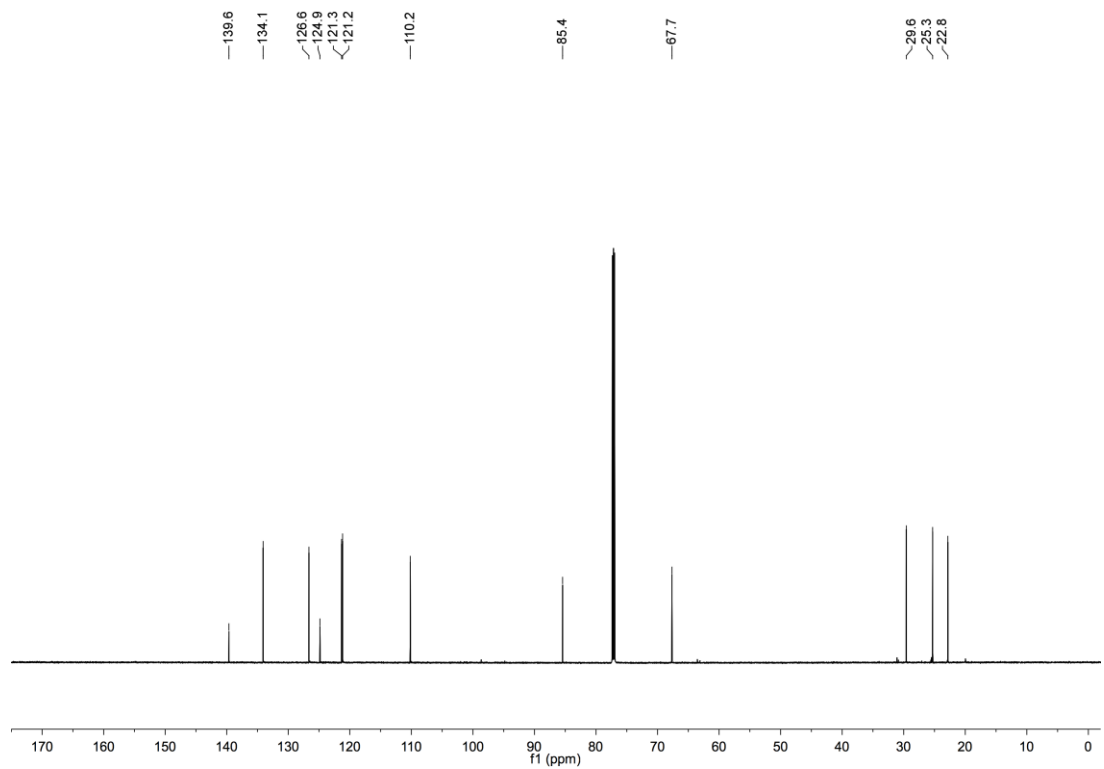
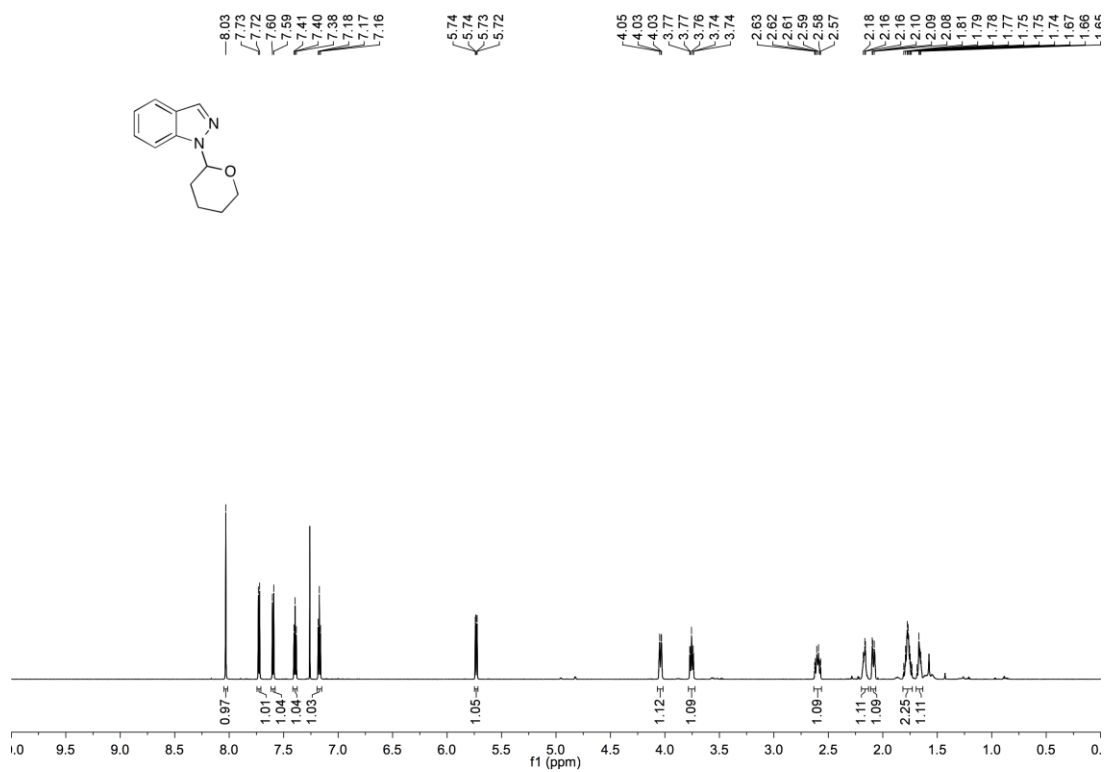
2-([2-(Trimethylsilyl)ethoxy]methyl)-2H-indazole (459)



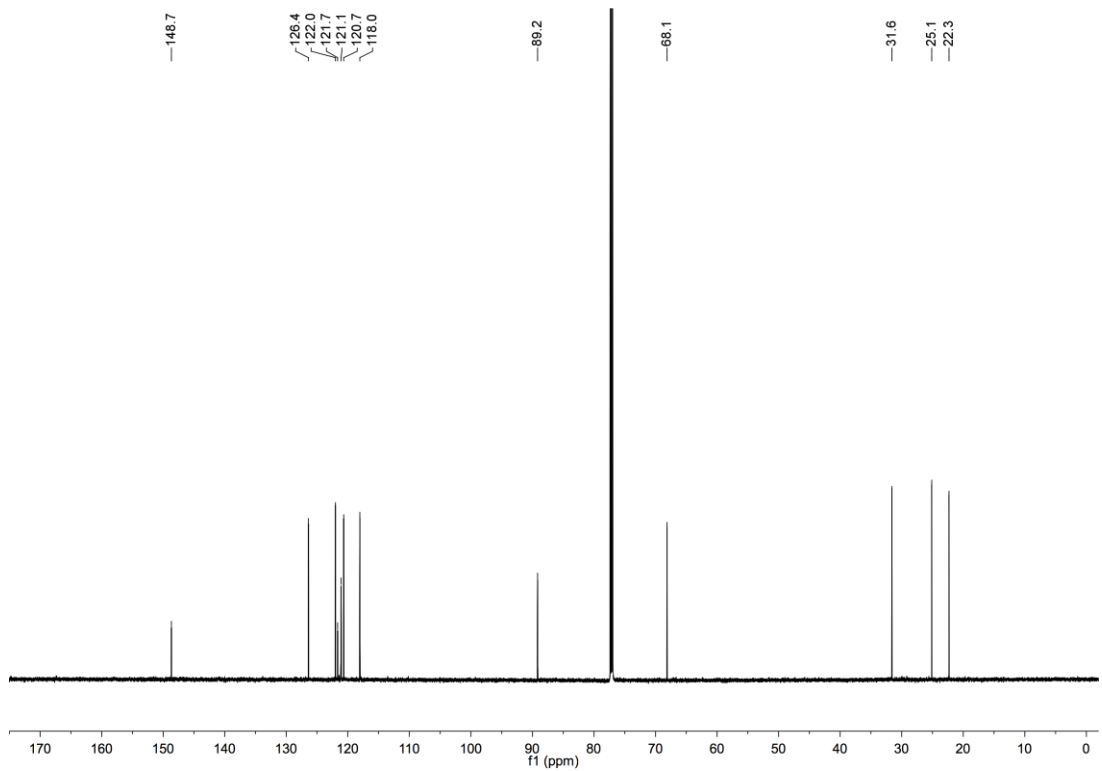
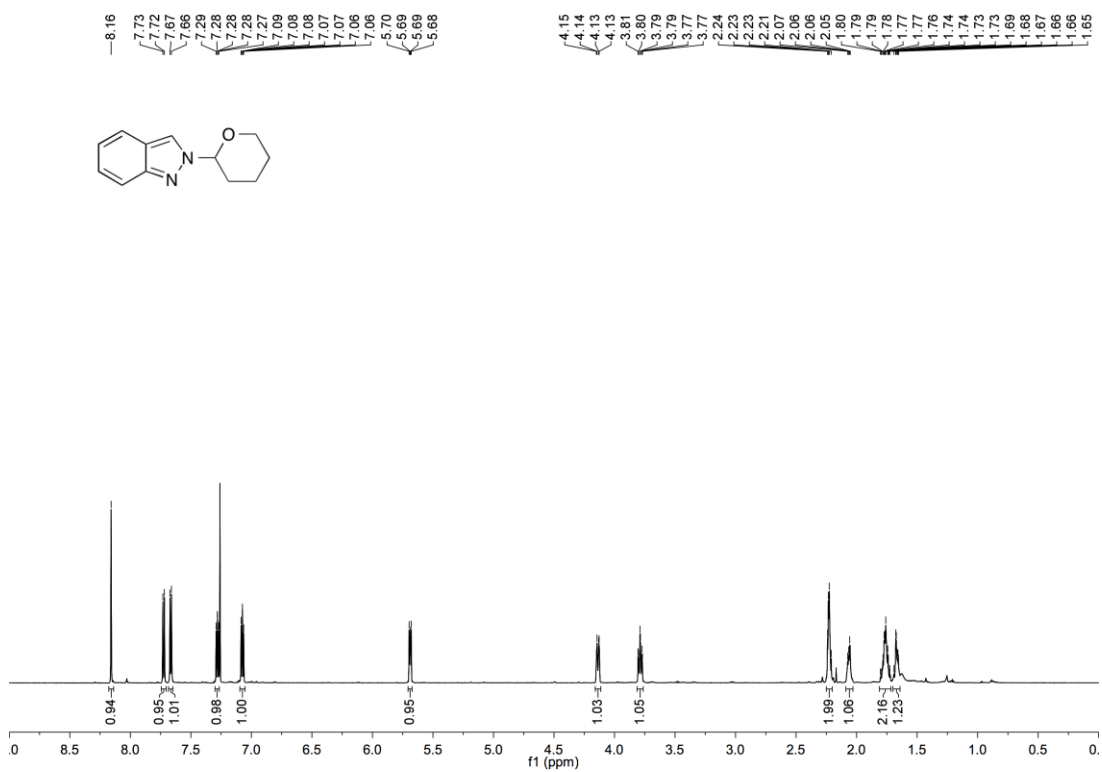
1-(Methanesulfonyl)-1H-indazole (461)



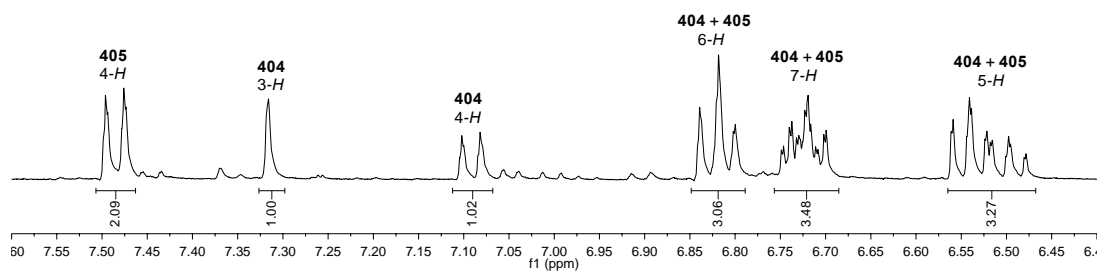
1-(Tetrahydro-2H-pyran-2'-yl)-1H-indazole (464)



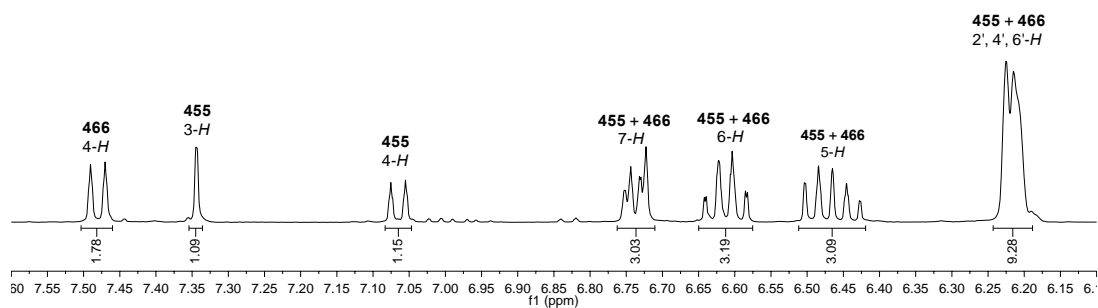
2-(Tetrahydro-2H-pyran-2'-yl)-2H-indazole (465)



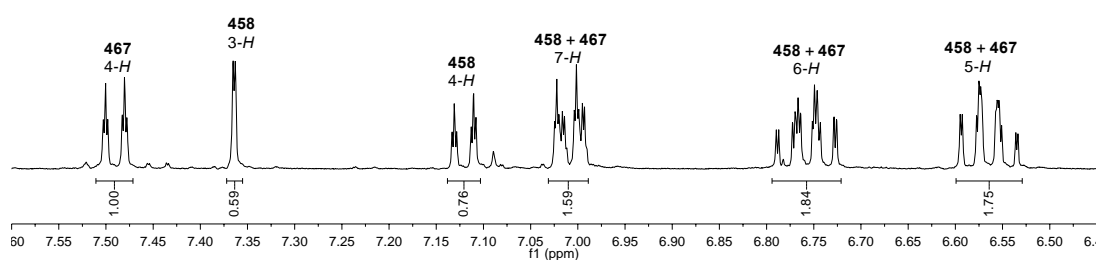
Borylation of 1-methyl-1H-indazole (**404**) (*in-situ*, 400 MHz, (CD₃)₂CO)



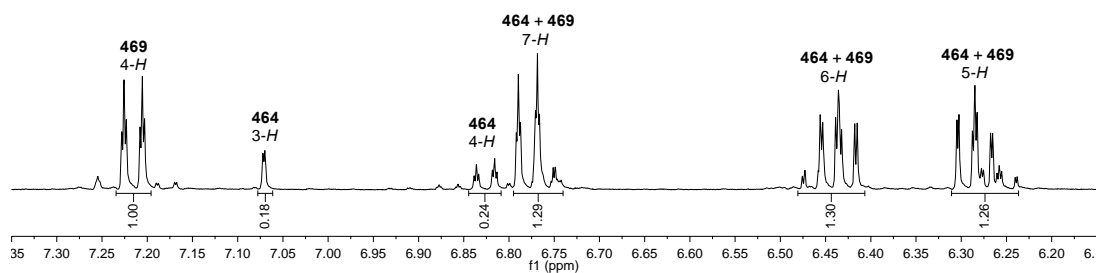
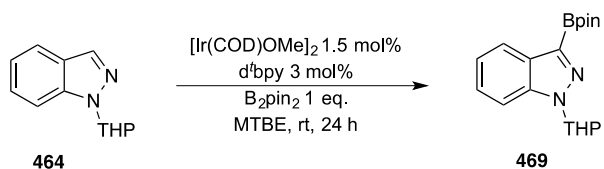
Borylation of 1-(3', 5'-dimethylbenzyl)-1H-indazole (**455**) (*in-situ*, 400 MHz, (CD₃)₂CO)



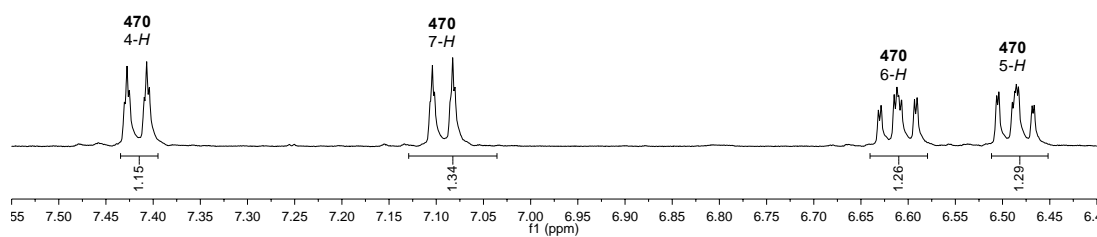
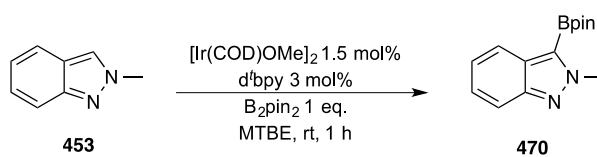
Borylation of 1-[[2-(trimethylsilyl)ethoxy]methyl]-1H-indazole (**458**) (*in-situ*, 400 MHz, (CD₃)₂CO)



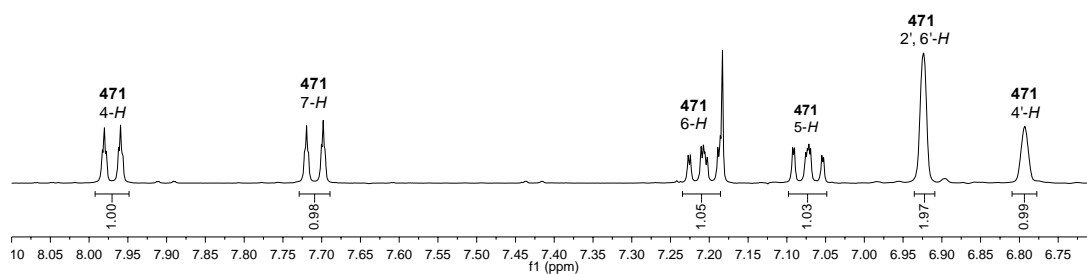
Borylation of 1-(tetrahydro-2H-pyran-2'-yl)-1H-indazole (**464**) (*in-situ*, 400 MHz, (CD₃)₂CO)



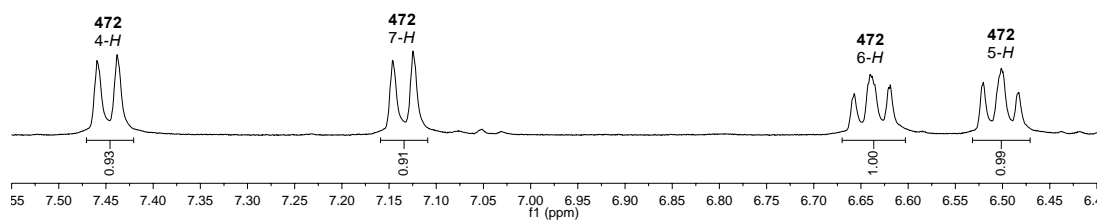
Borylation of 2-(methyl)-2H-indazole (453) (in-situ, 400 MHz, (CD₃)₂CO)



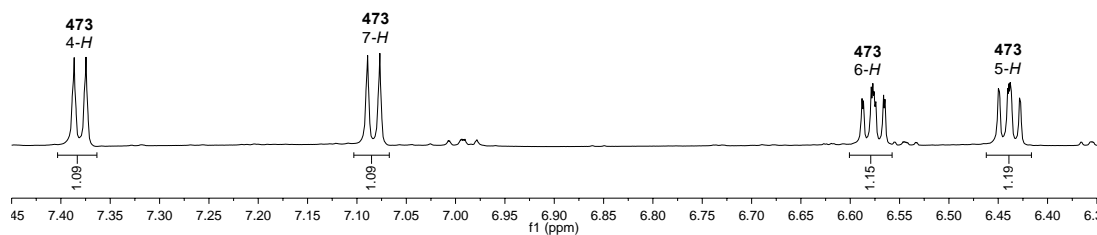
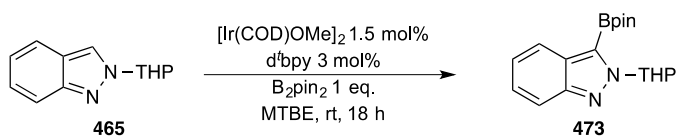
Borylation of 2-(3', 5'-dimethylbenzyl)-2H-indazole (456) (in-situ, 400 MHz, (CD₃)₂CO)



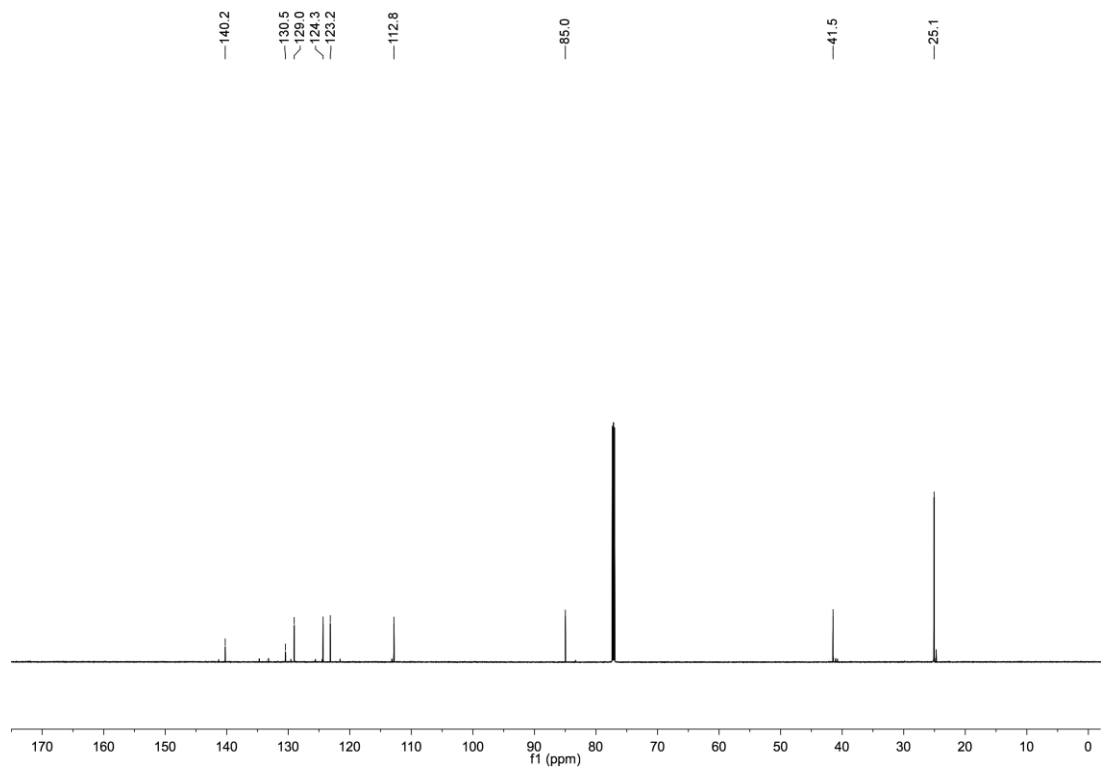
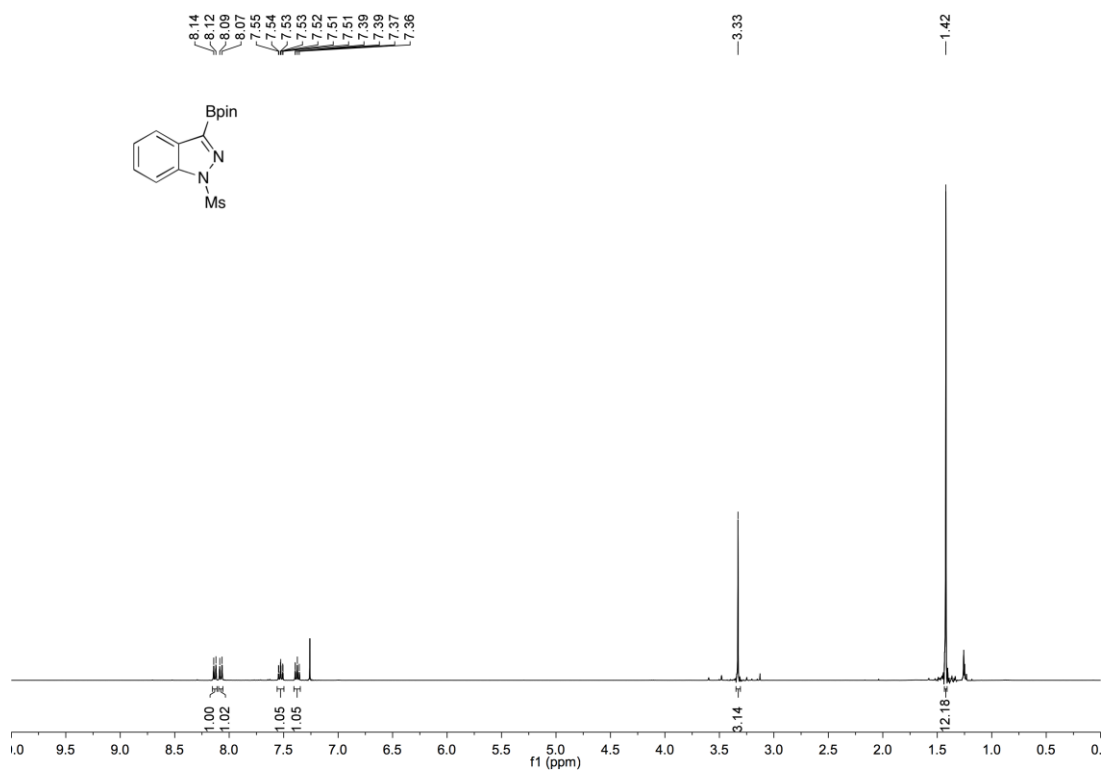
Borylation of 2-[[2-(trimethylsilyl)ethoxy]methyl]-2H-indazole (**459**) (*in-situ*, 400 MHz, (CD₃)₂CO)

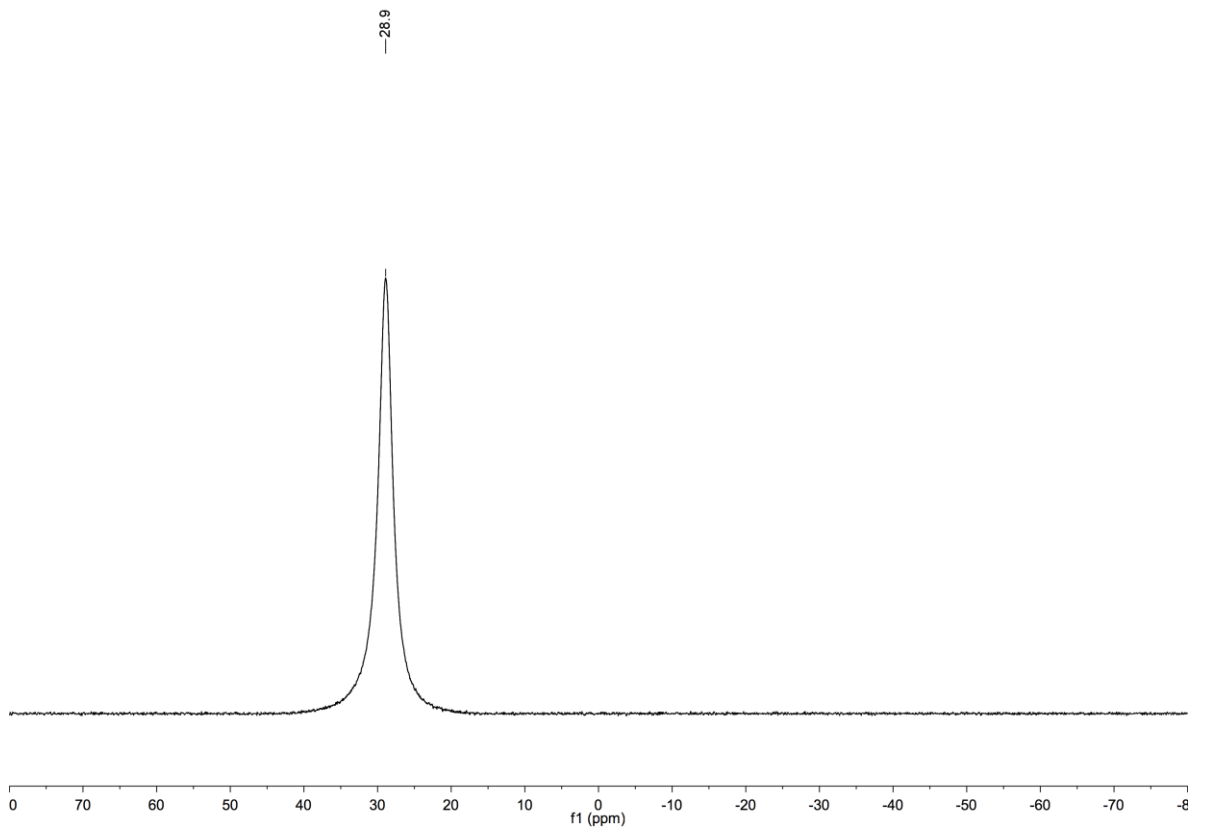


Borylation of 2-(tetrahydro-2H-pyran-2'-yl)-2H-indazole (**465**) (*in-situ*, 400 MHz, (CD₃)₂CO)

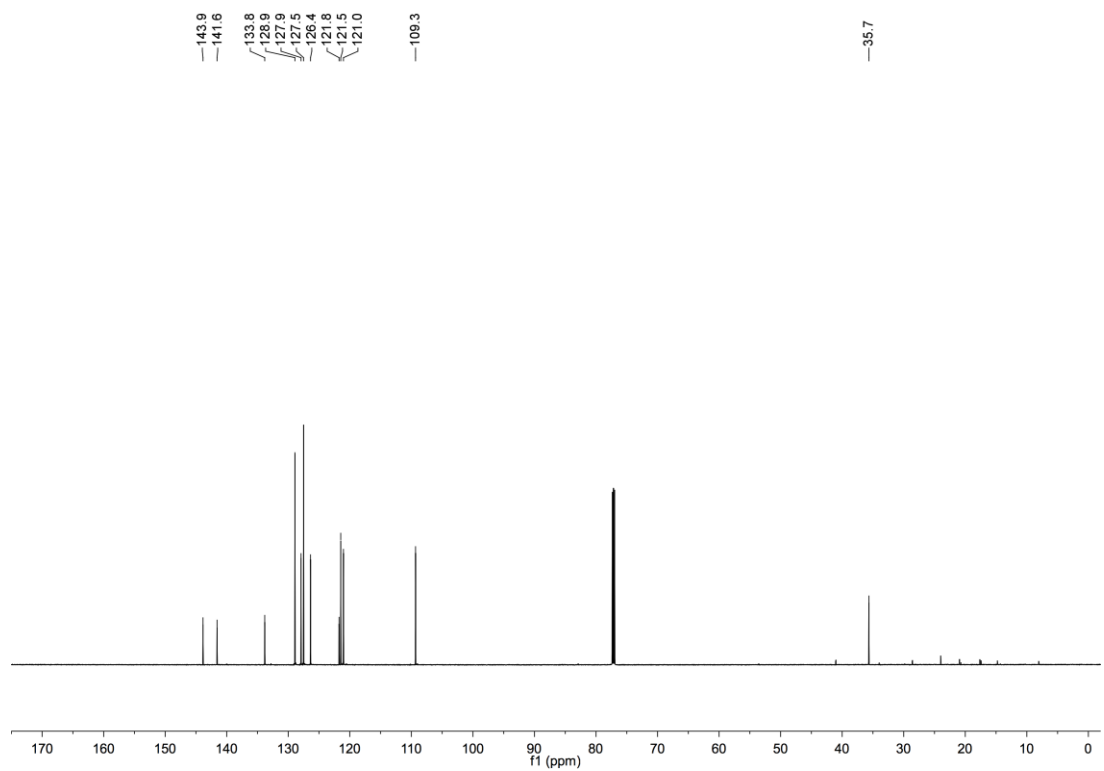
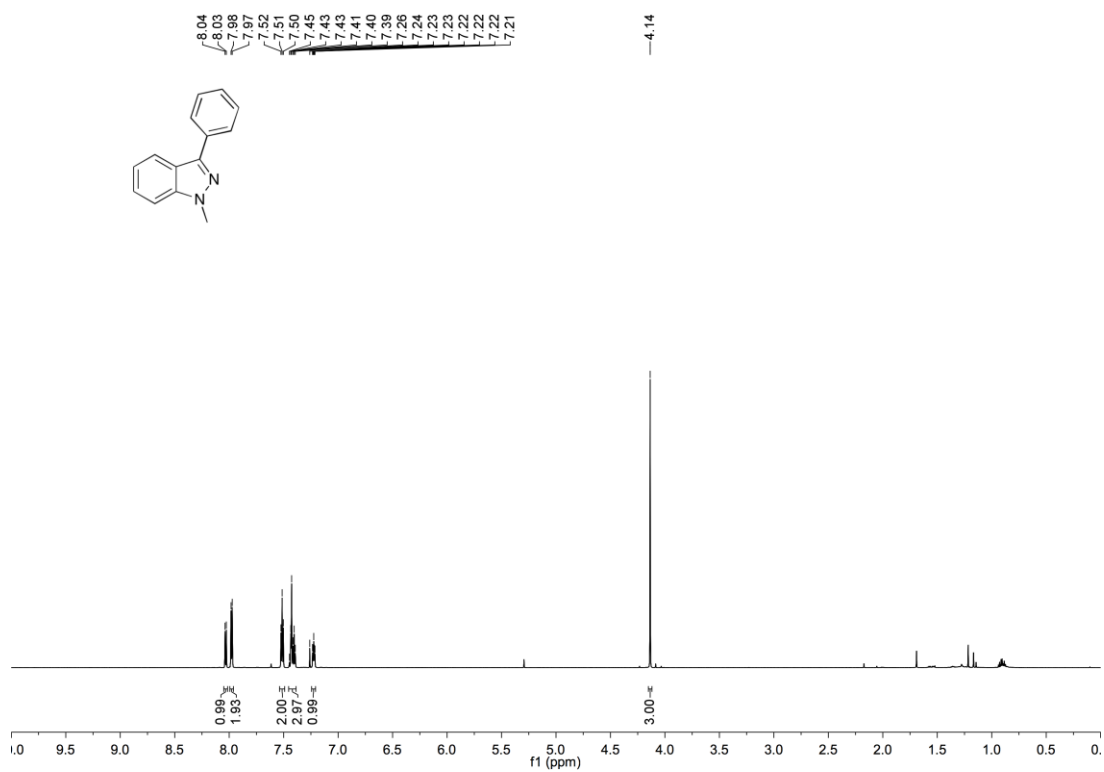


1-(Methanesulfonyl)-3-(Bpin)-1H-indazole (468)

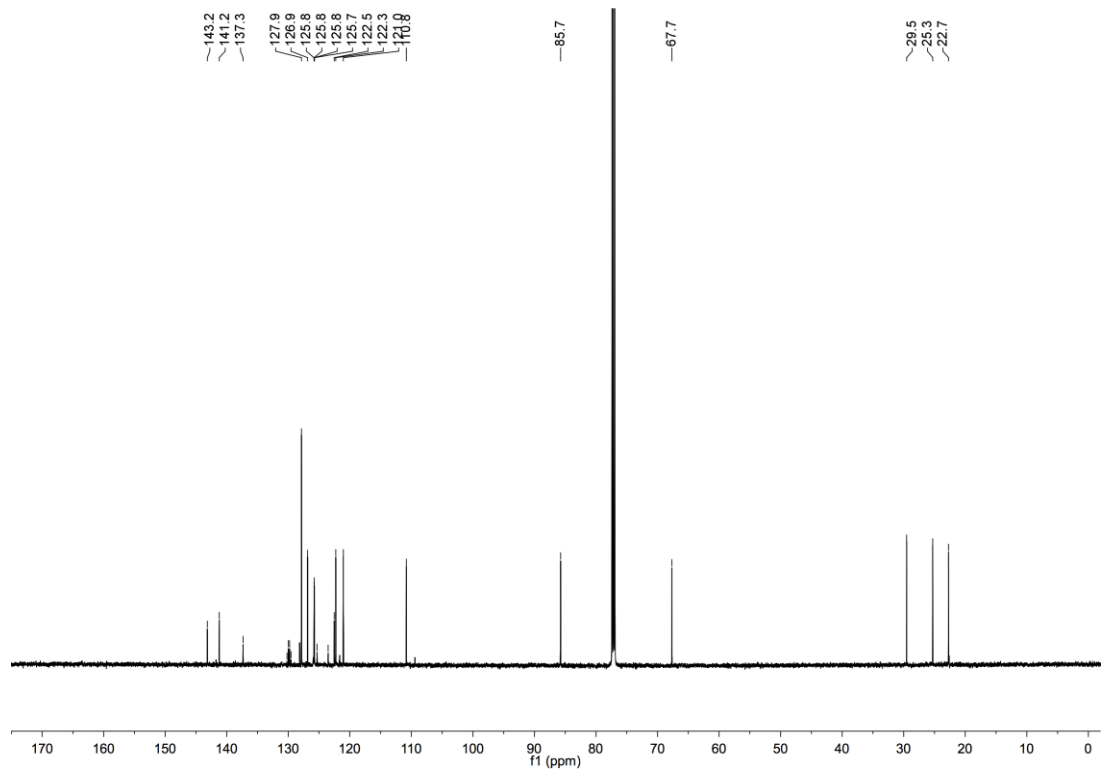
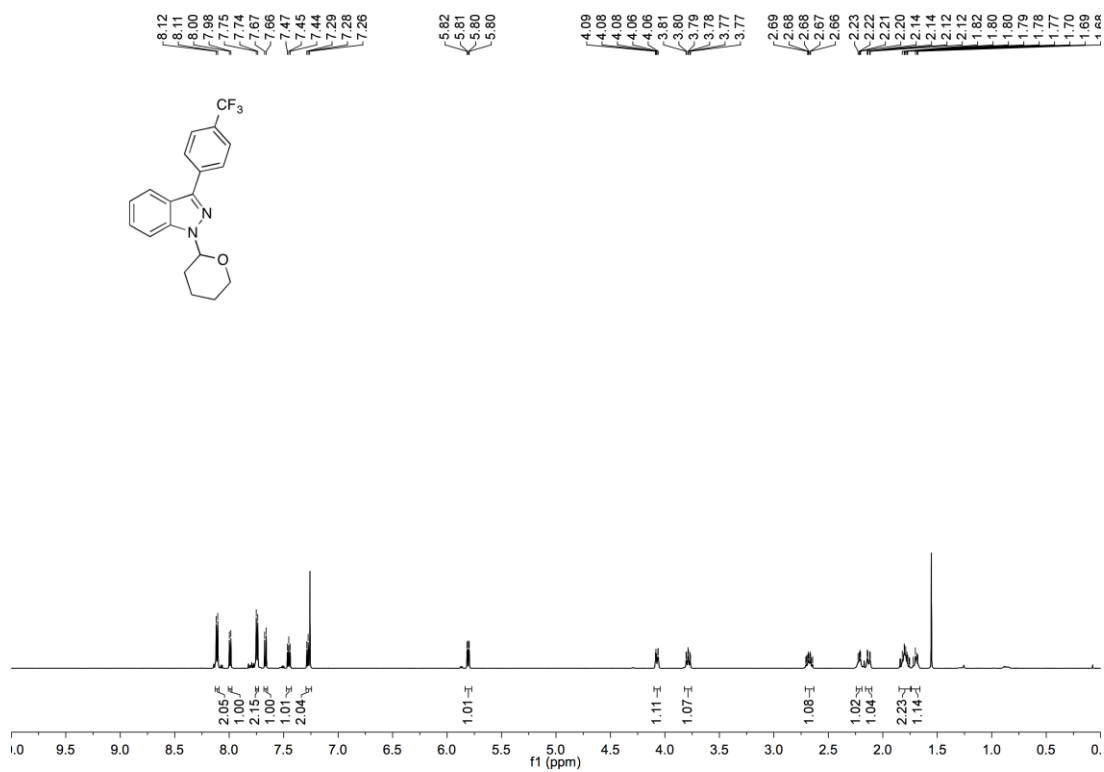


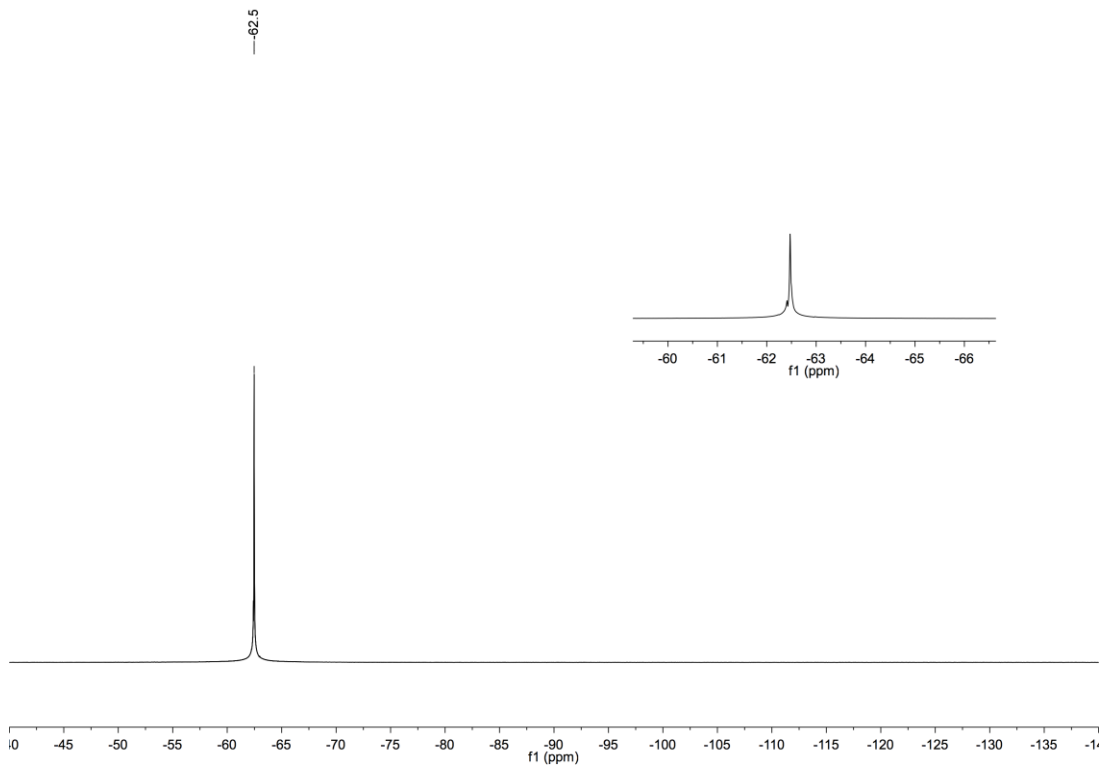


1-Methyl-3-phenyl-1H-indazole (481)

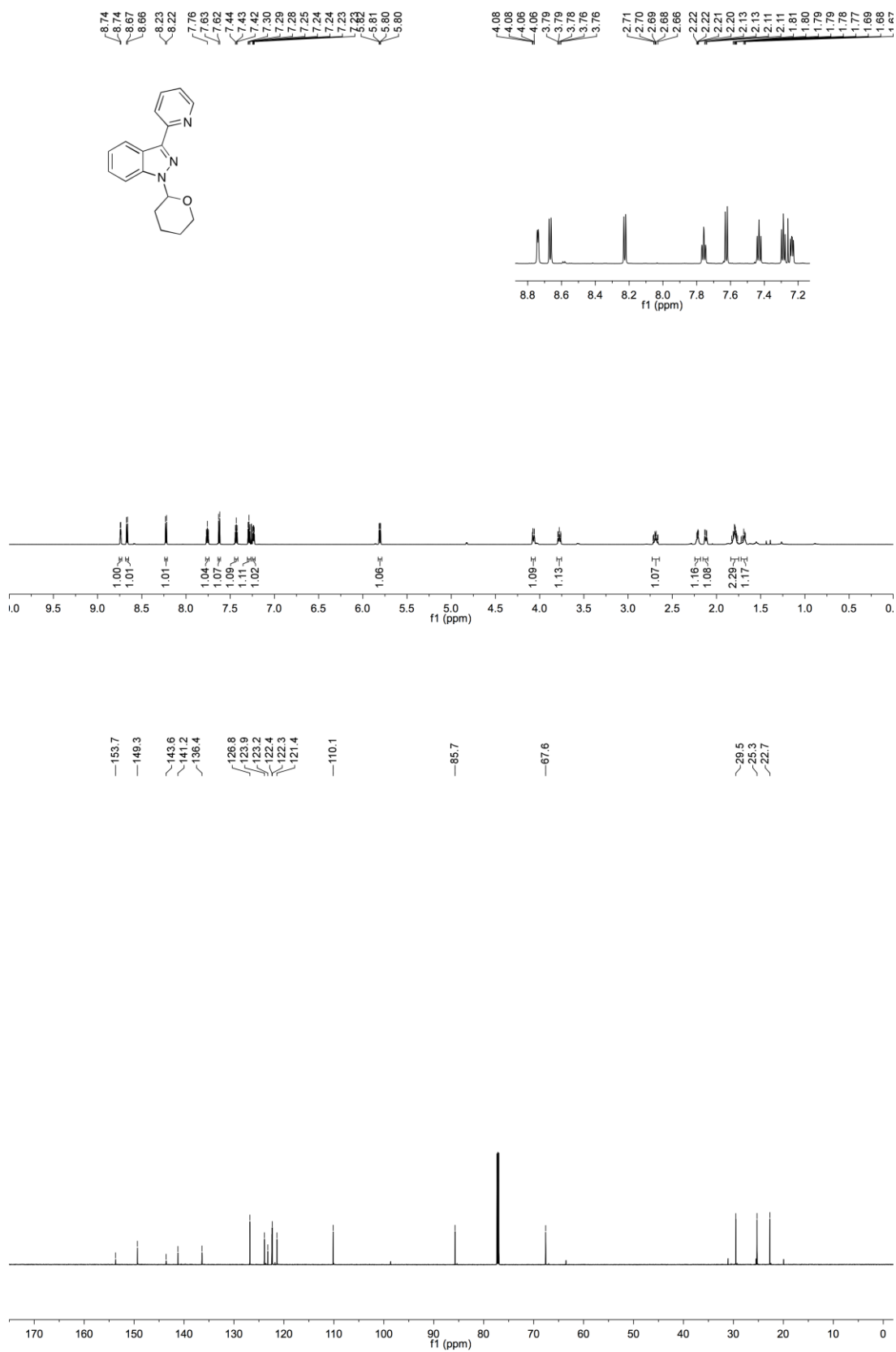


1-Tetrahydropyran-2'-yl-3-(4'-(trifluoromethyl)phenyl)-1H-indazole (483)

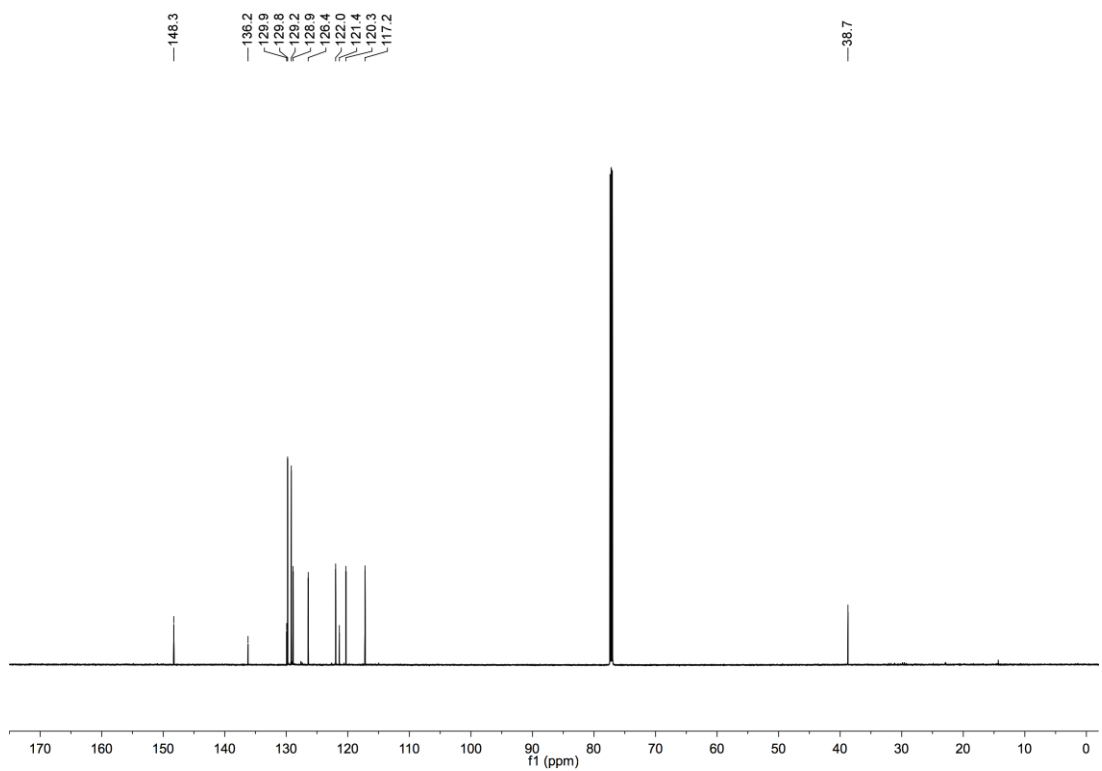
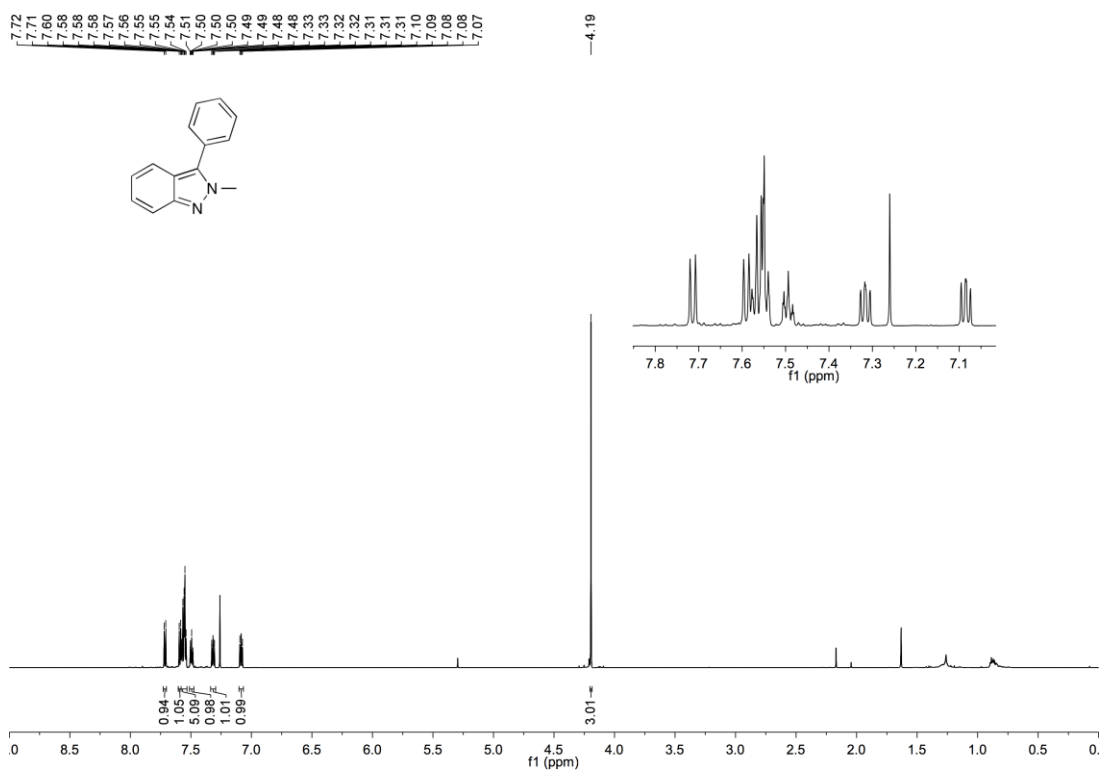




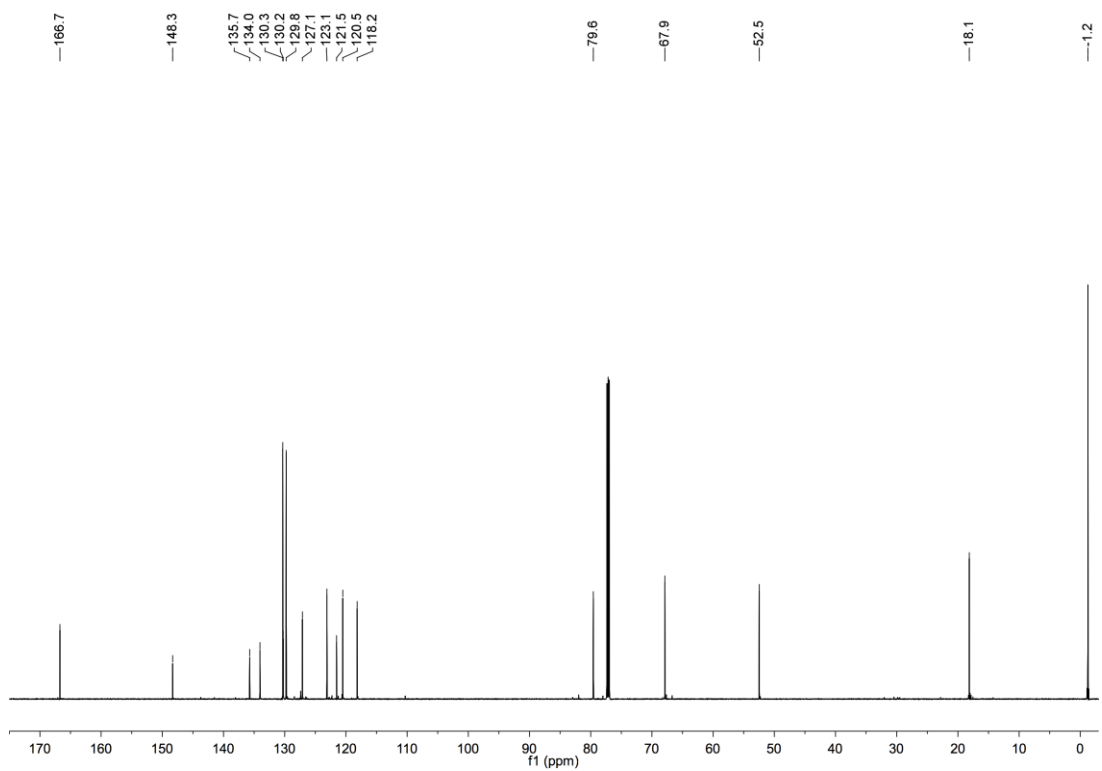
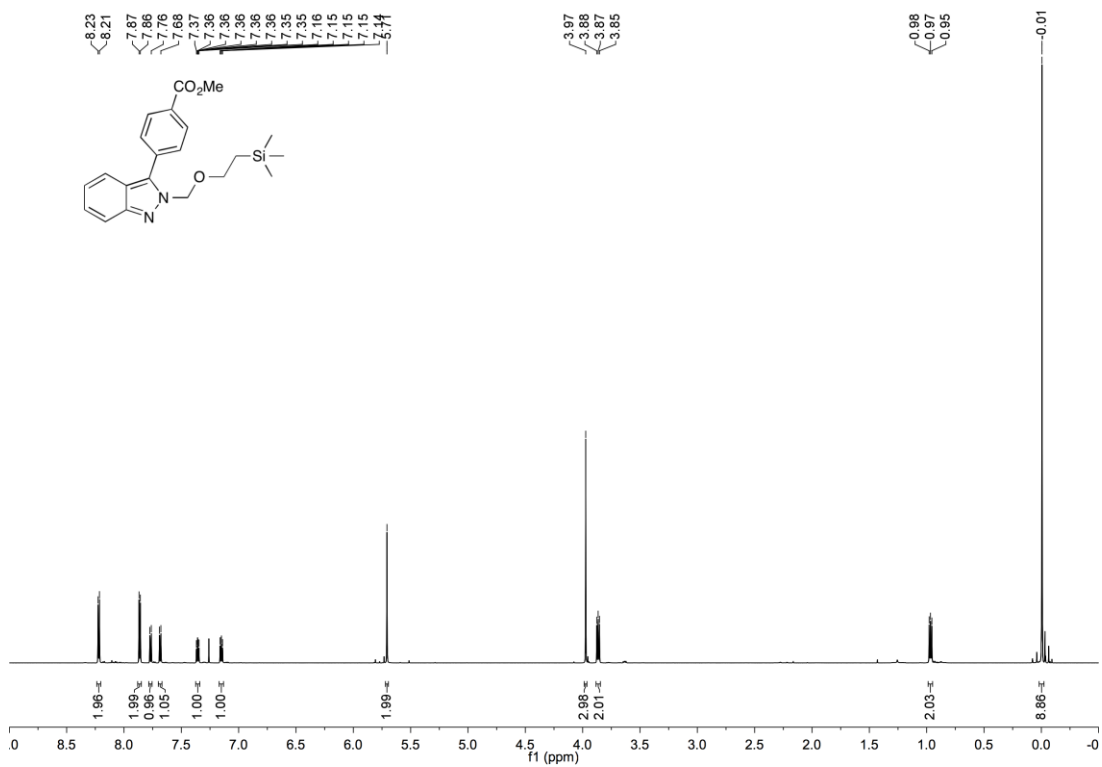
1-Tetrahydropyran-2'-yl-3-pyridin-2''-yl-1H-indazole (485)



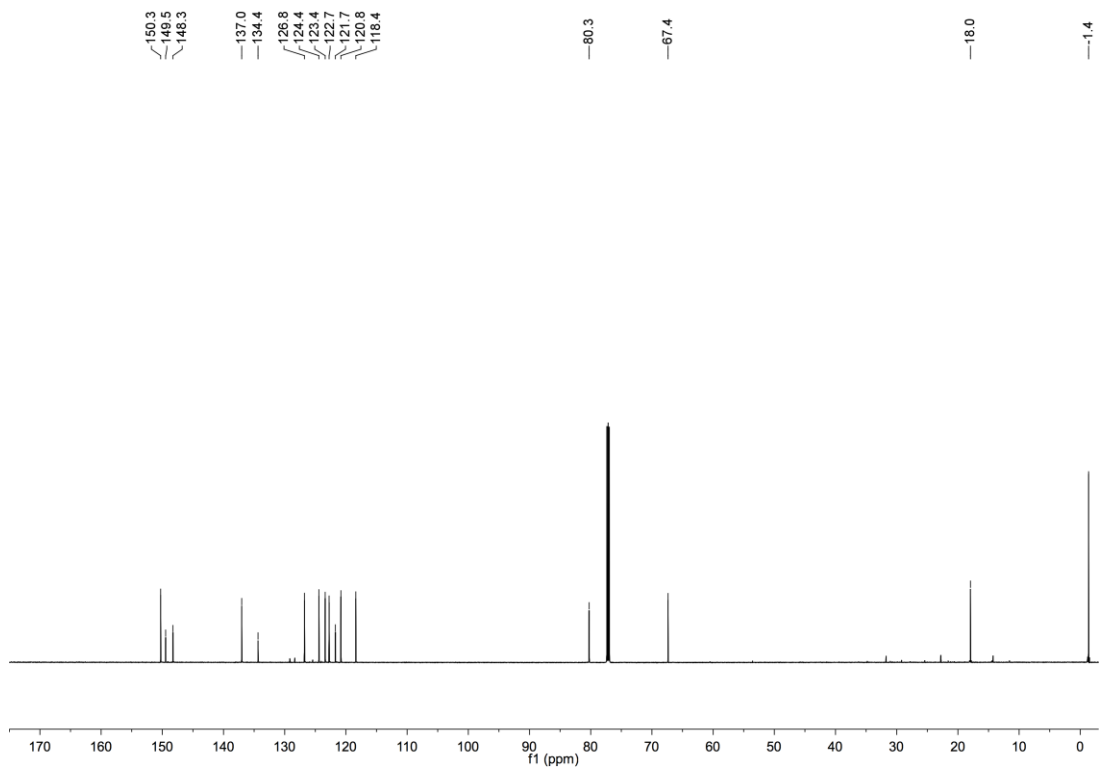
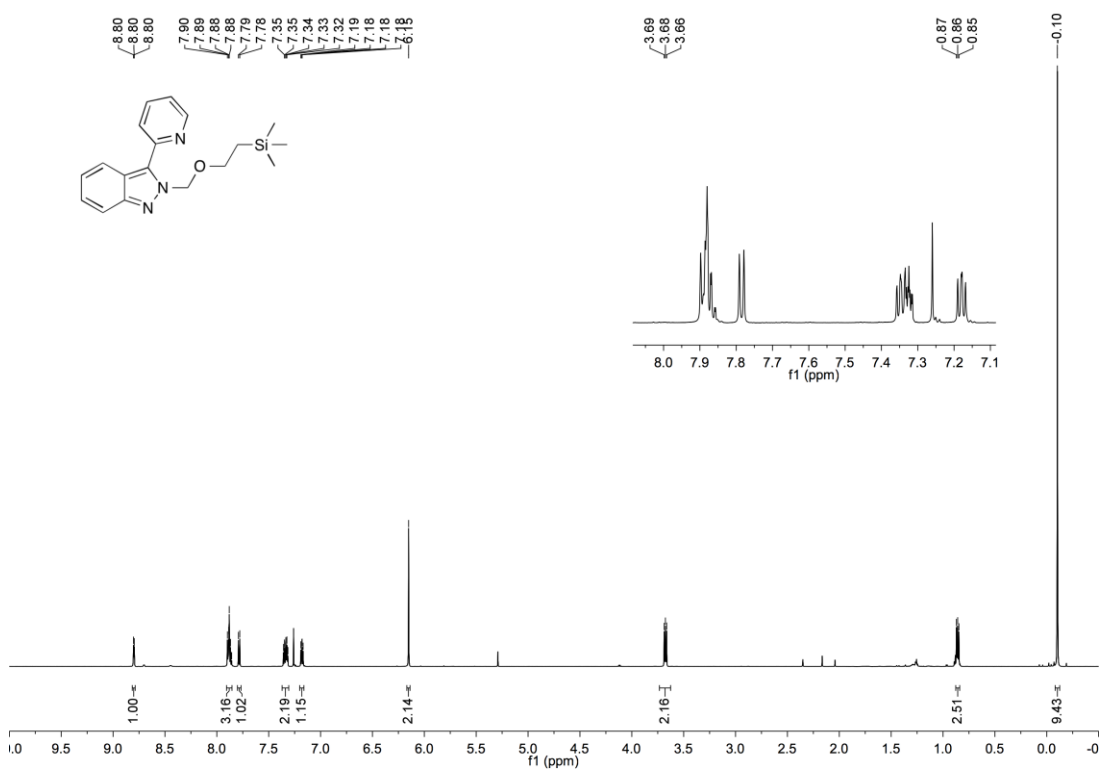
2-Methyl-3-phenyl-2H-indazole (487)



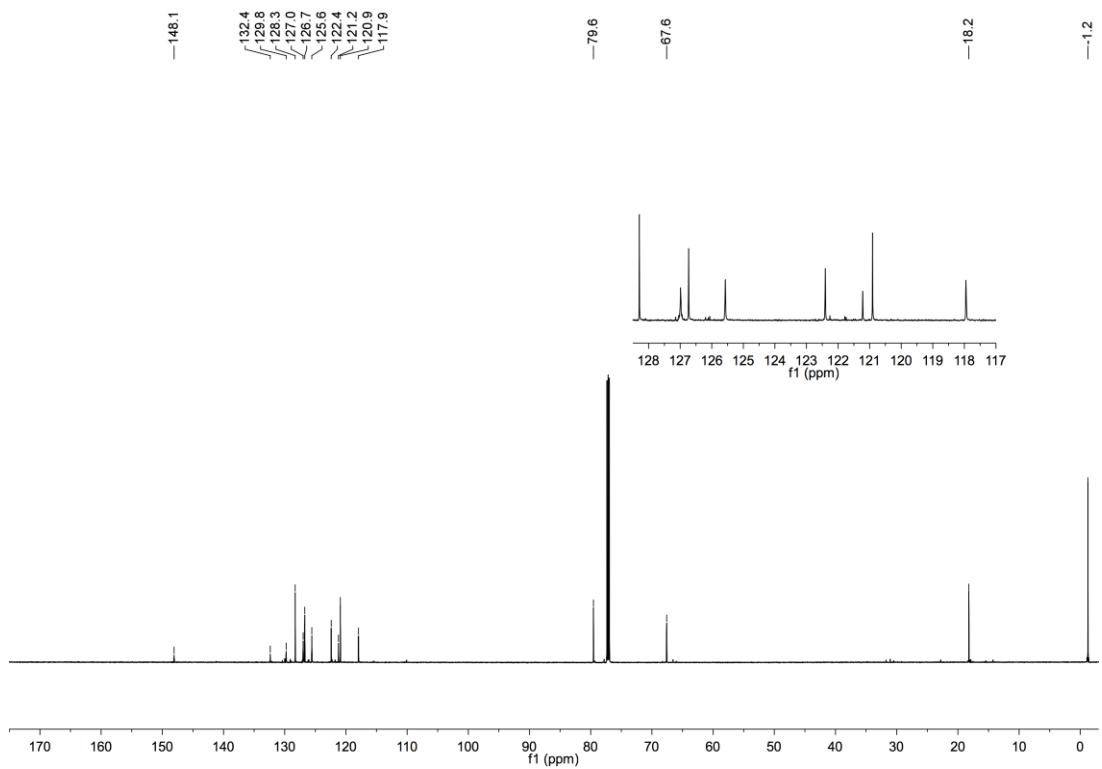
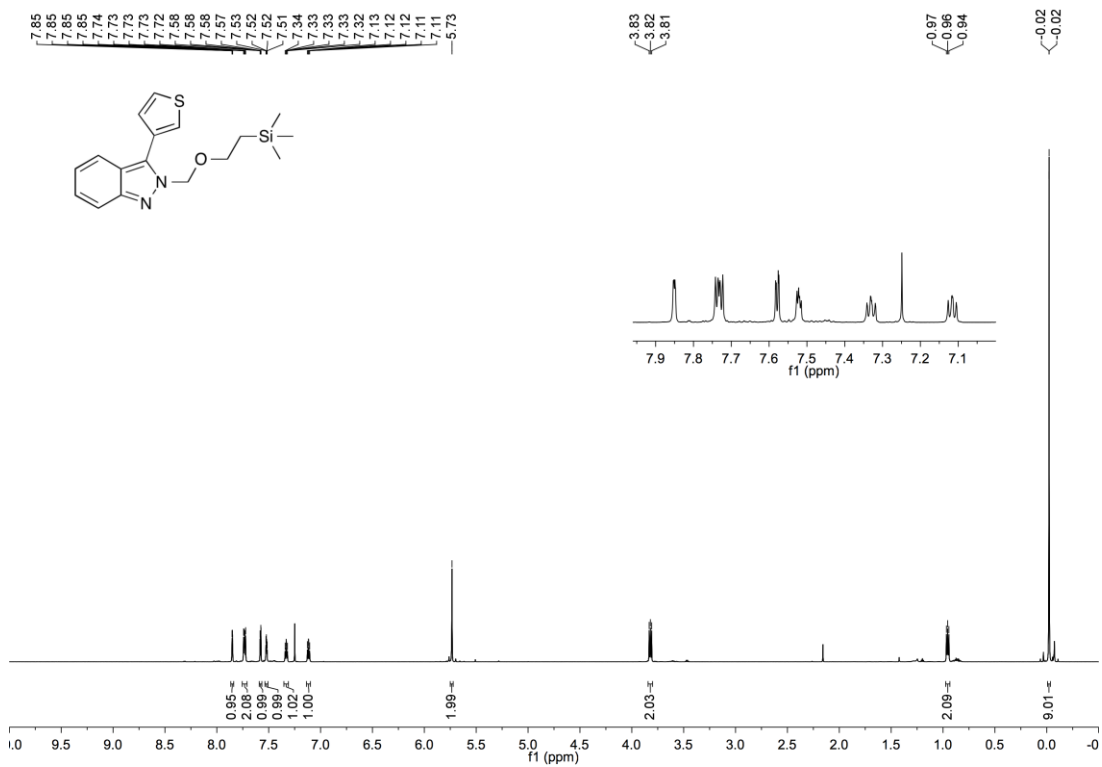
2-[[2-(Trimethylsilyl)ethoxy]methyl]-3-[4'-(methoxycarbonyl)phenyl]-2H-indazole (488)



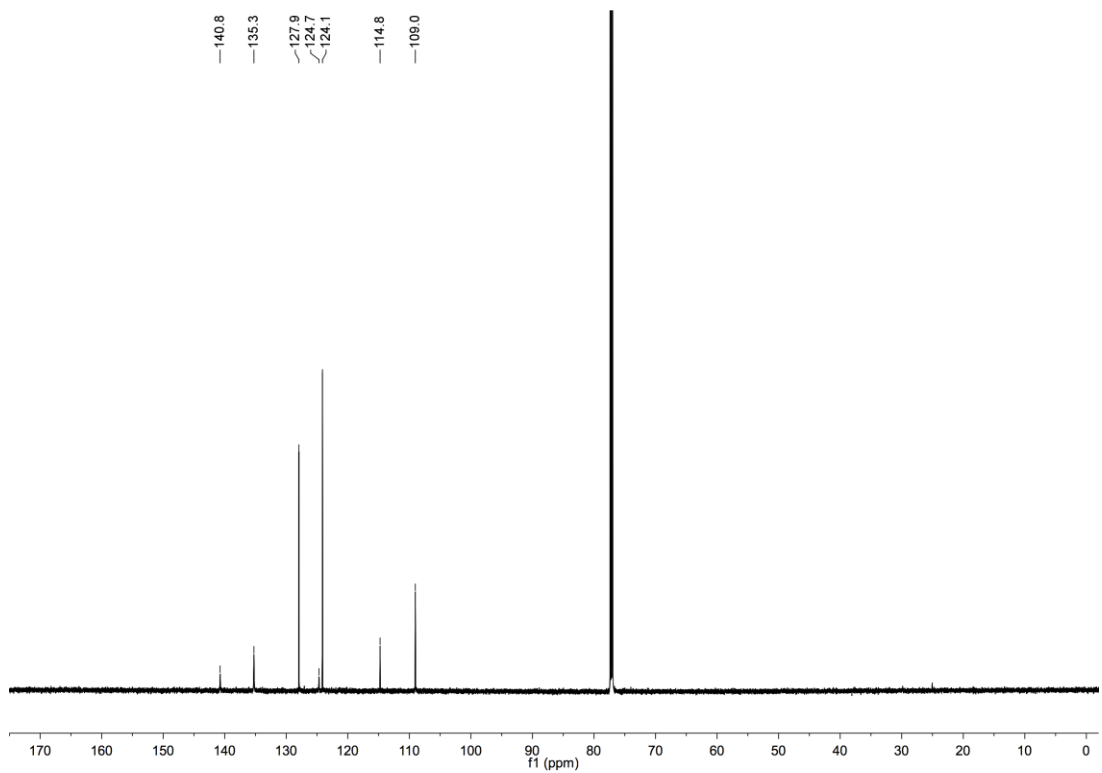
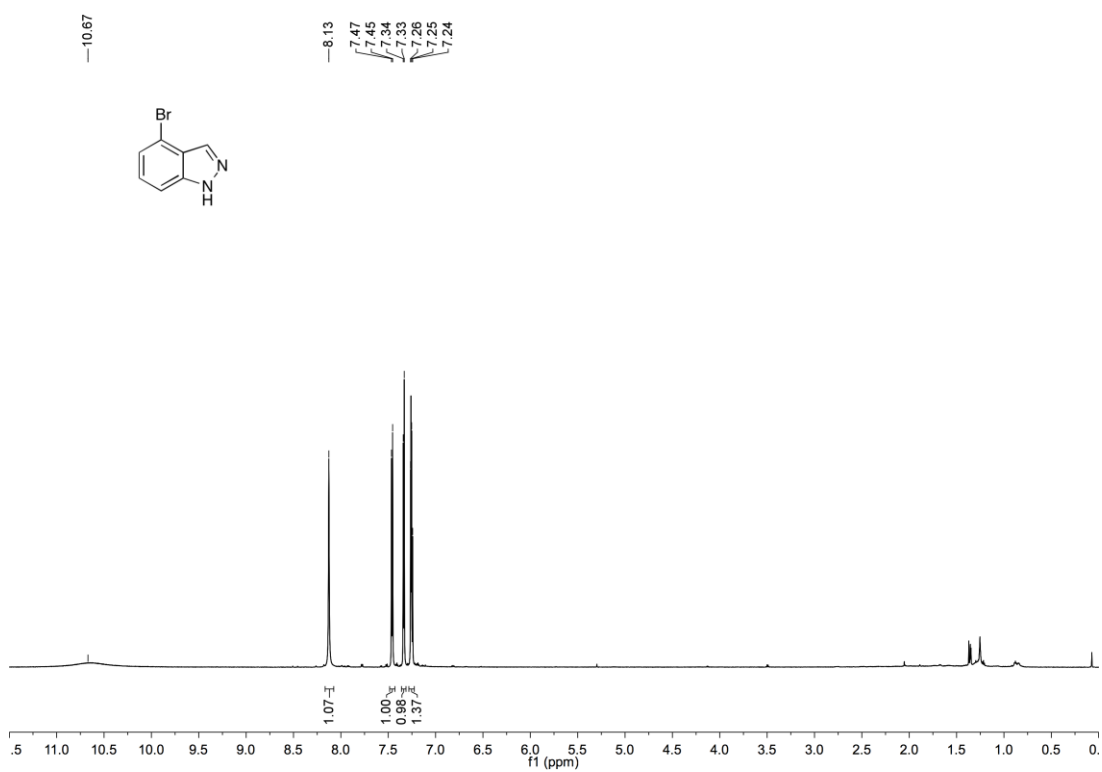
2-[[2-(Trimethylsilyl)ethoxy]methyl]-3-pyridin-2'-yl-2H-indazole (489)



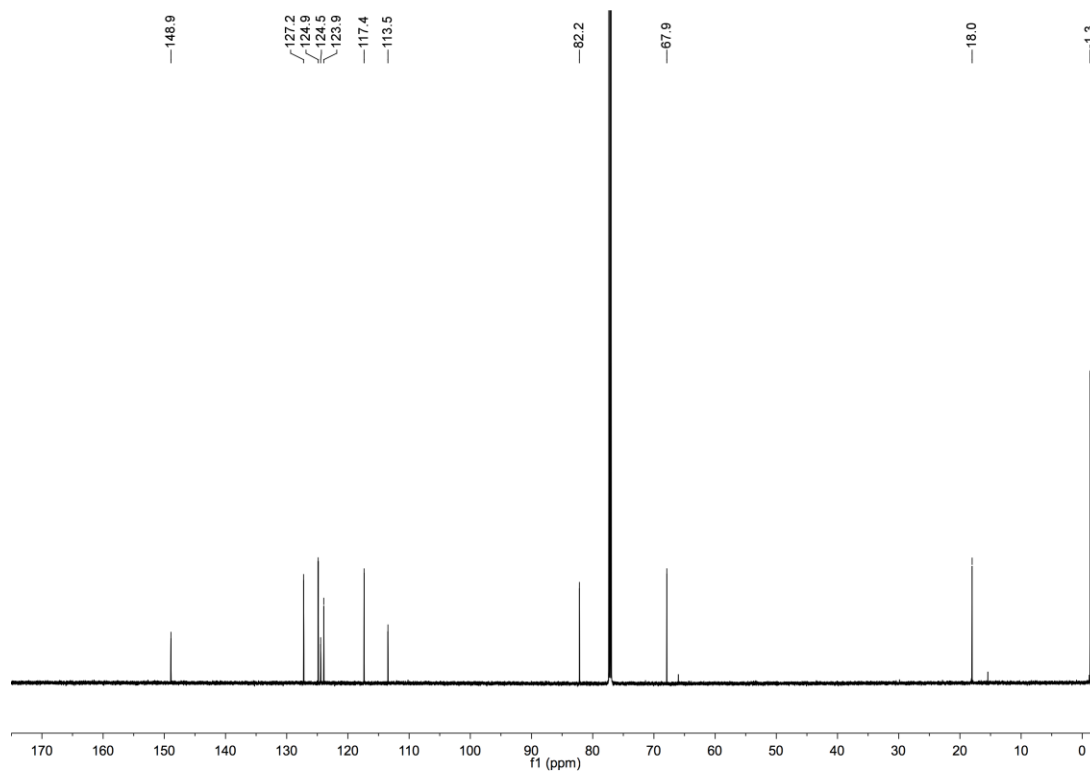
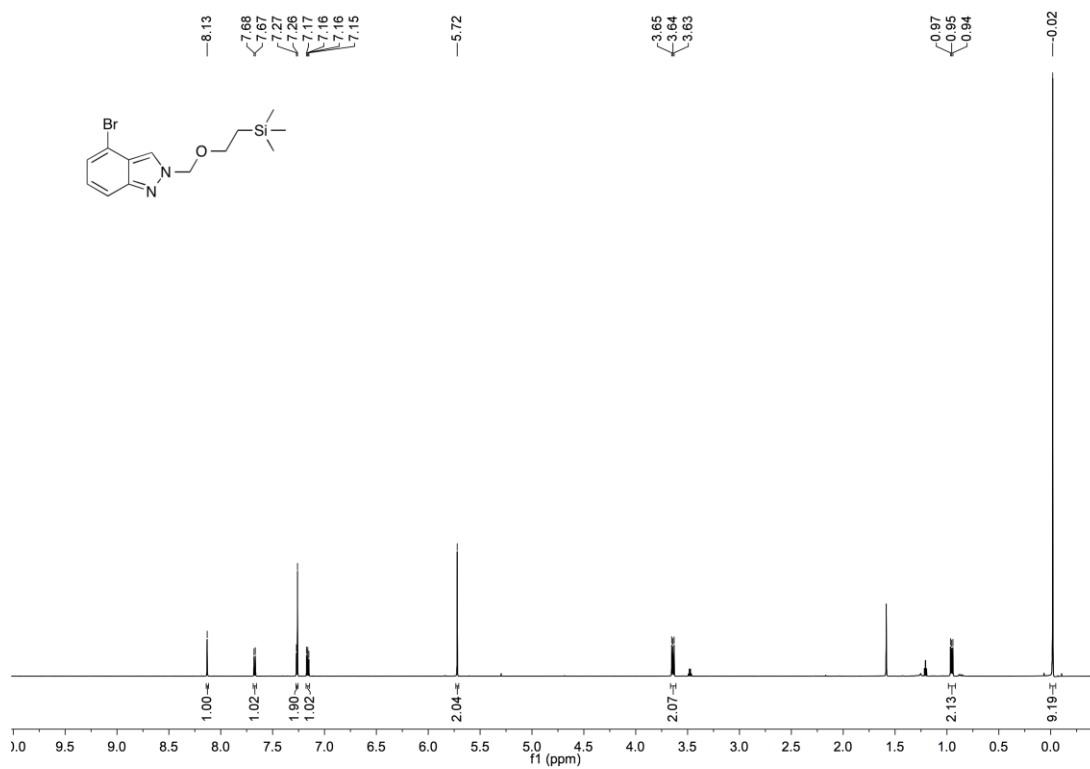
2-[[2-(Trimethylsilyl)ethoxy]methyl]3-thiophen-3'-yl-2H-indazole (490)



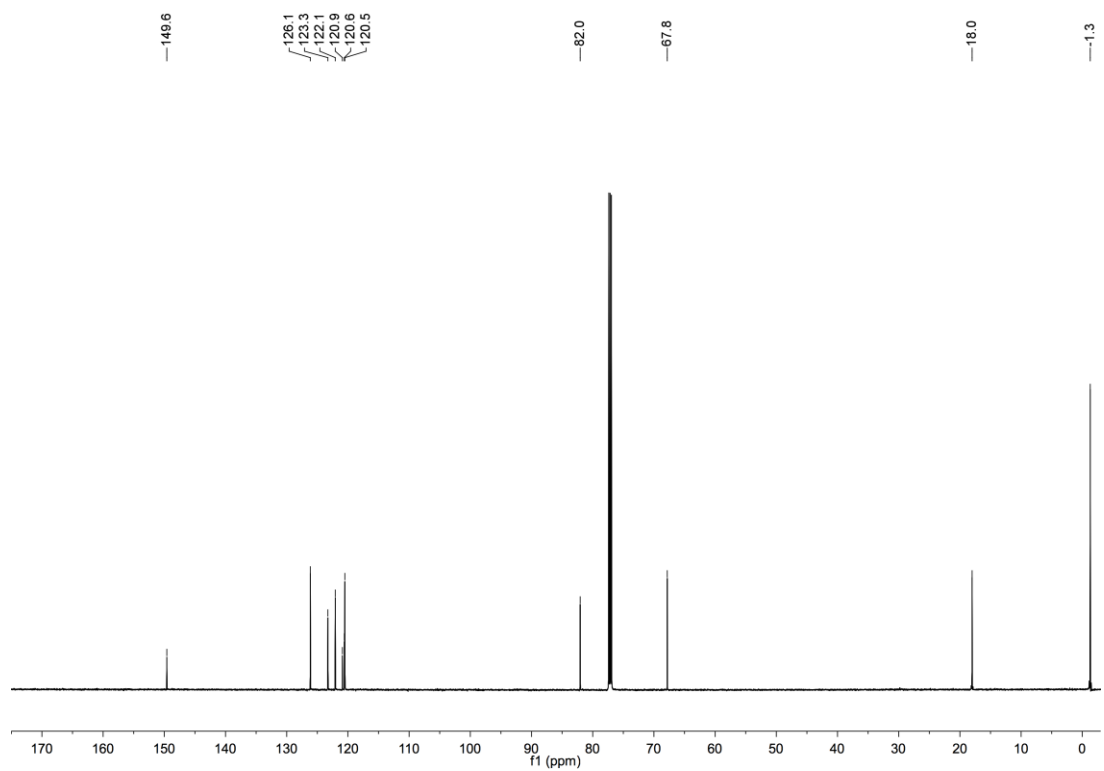
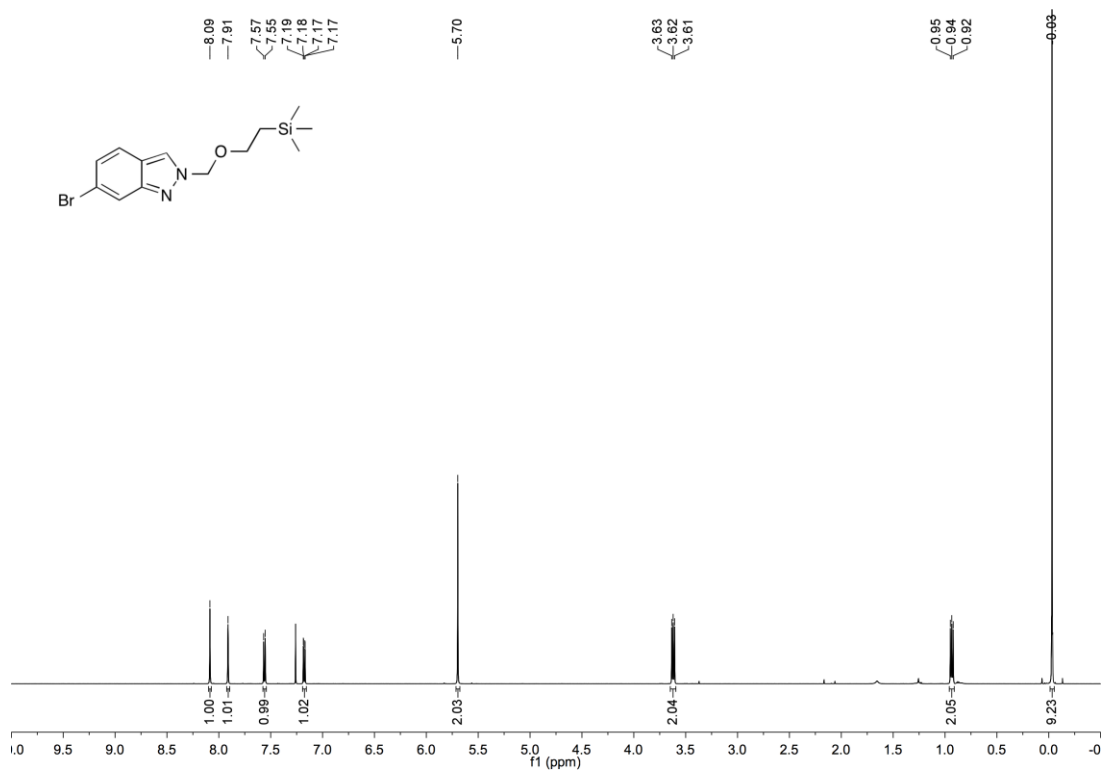
4-Bromo-1H-indazole (497)



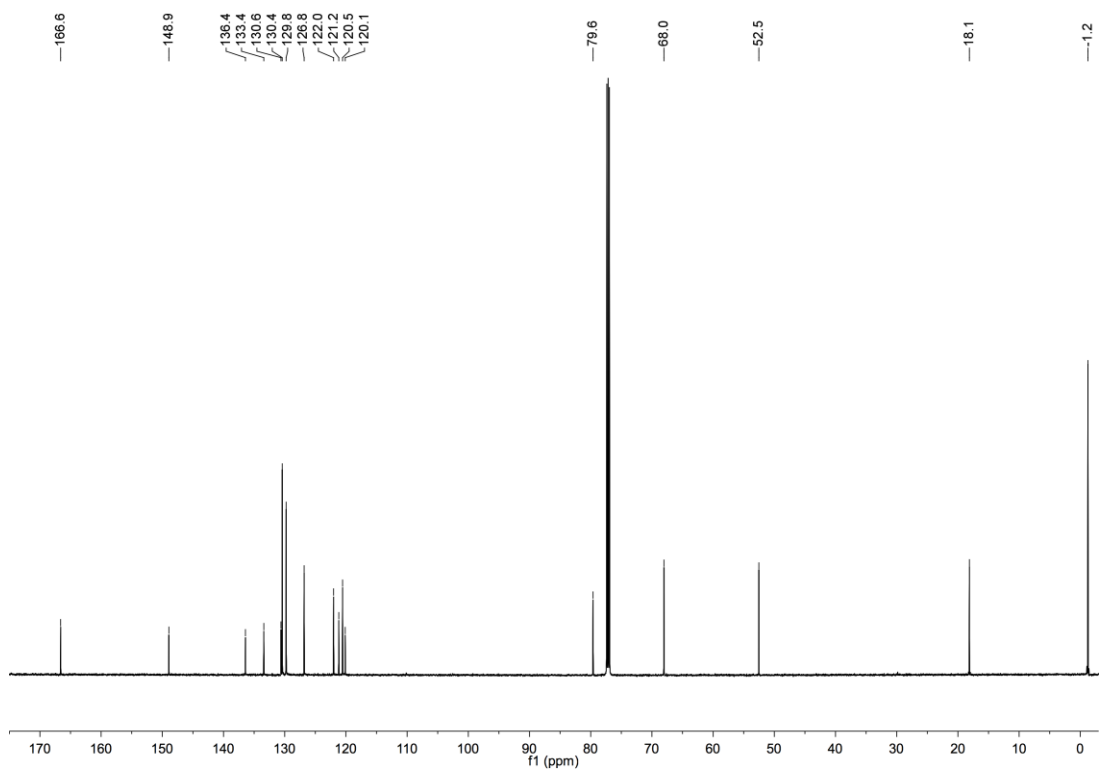
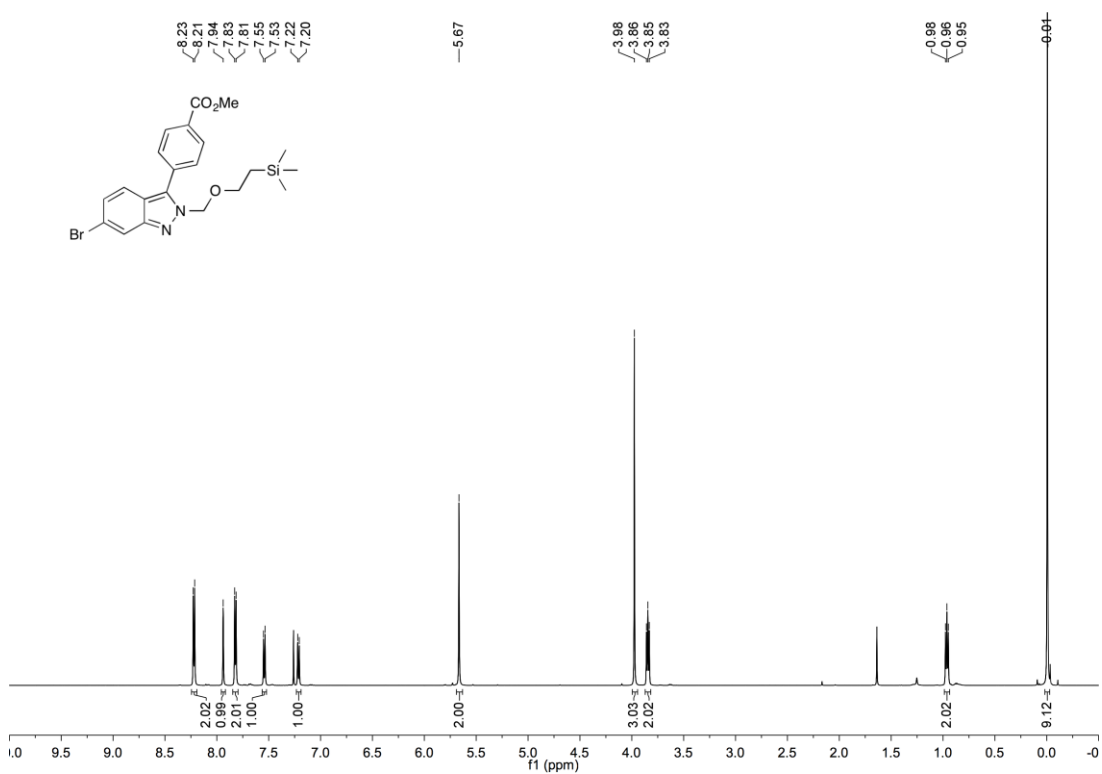
4-Bromo-2-[[2-(trimethylsilyl)ethoxy]methyl]indazole (501)



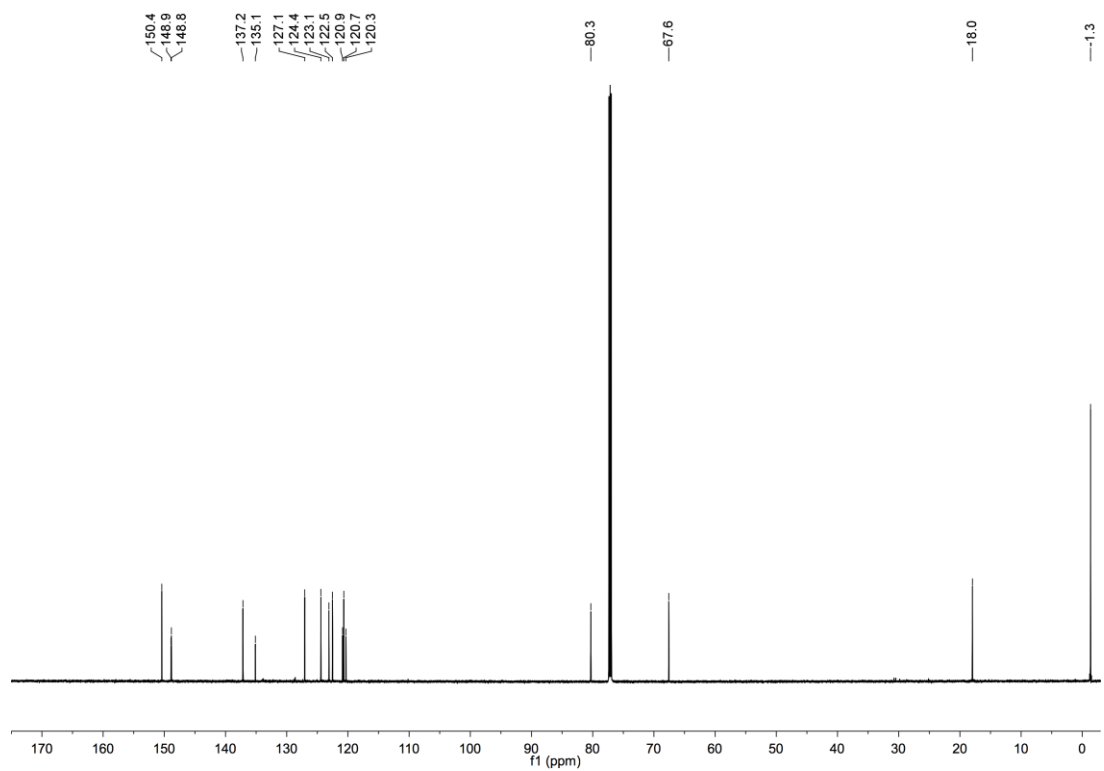
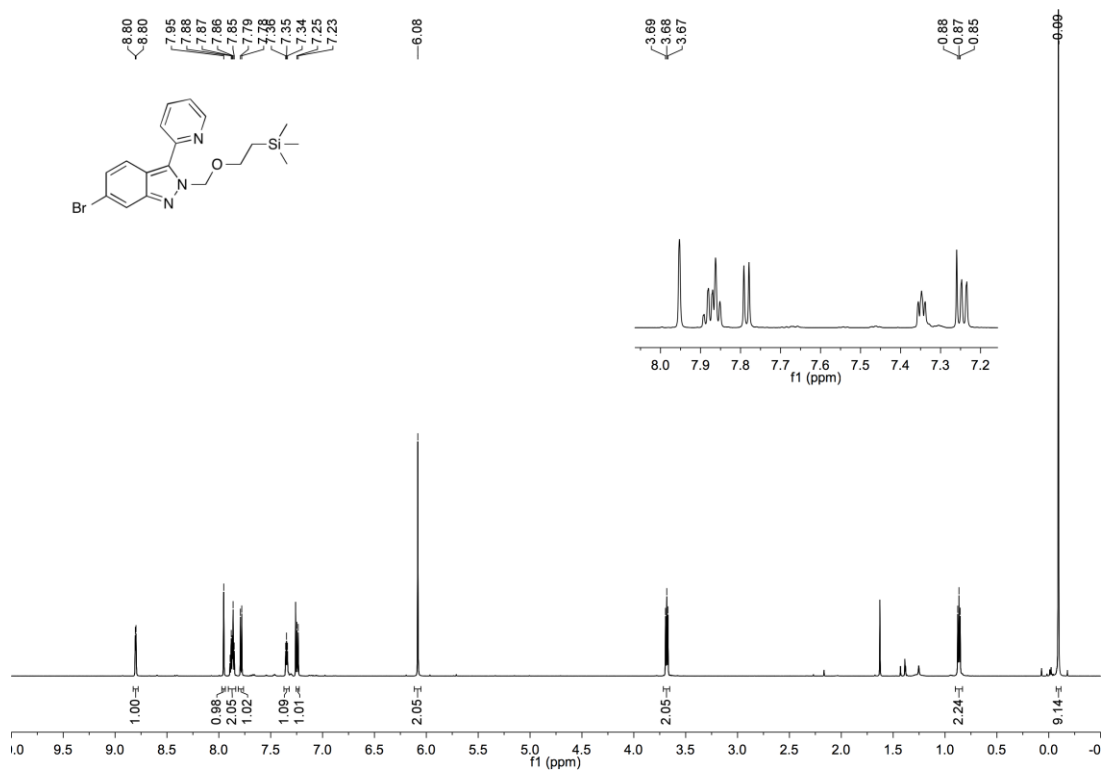
6-Bromo-2-[[2-(trimethylsilyl)ethoxy]methyl]indazole (503)



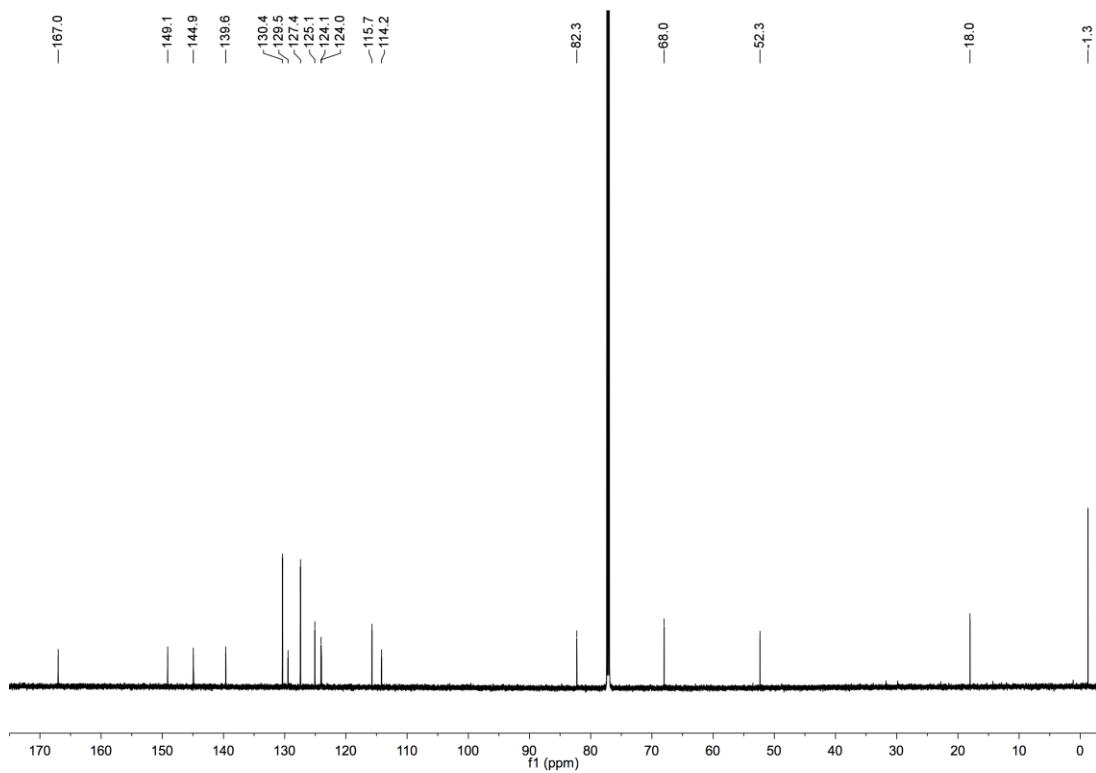
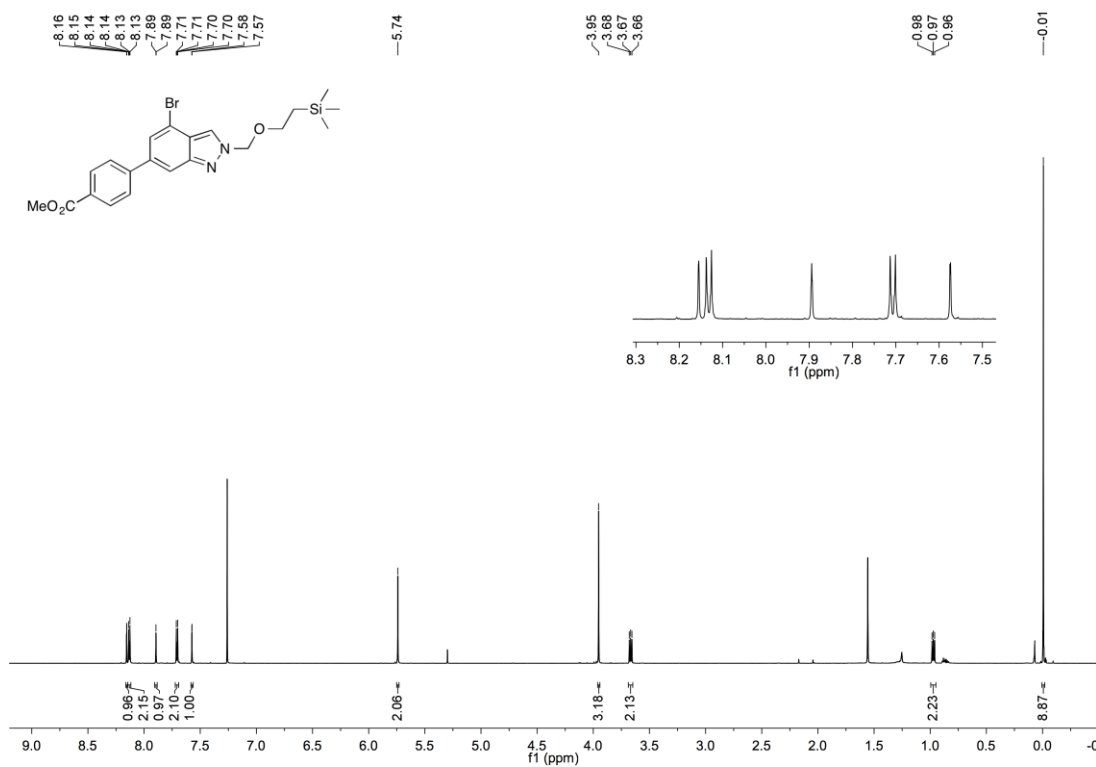
6-Bromo-2-[[2-(trimethylsilyl)ethoxy]methyl]-3-[4'-(methoxycarbonyl)phenyl]-2H-indazole (508)



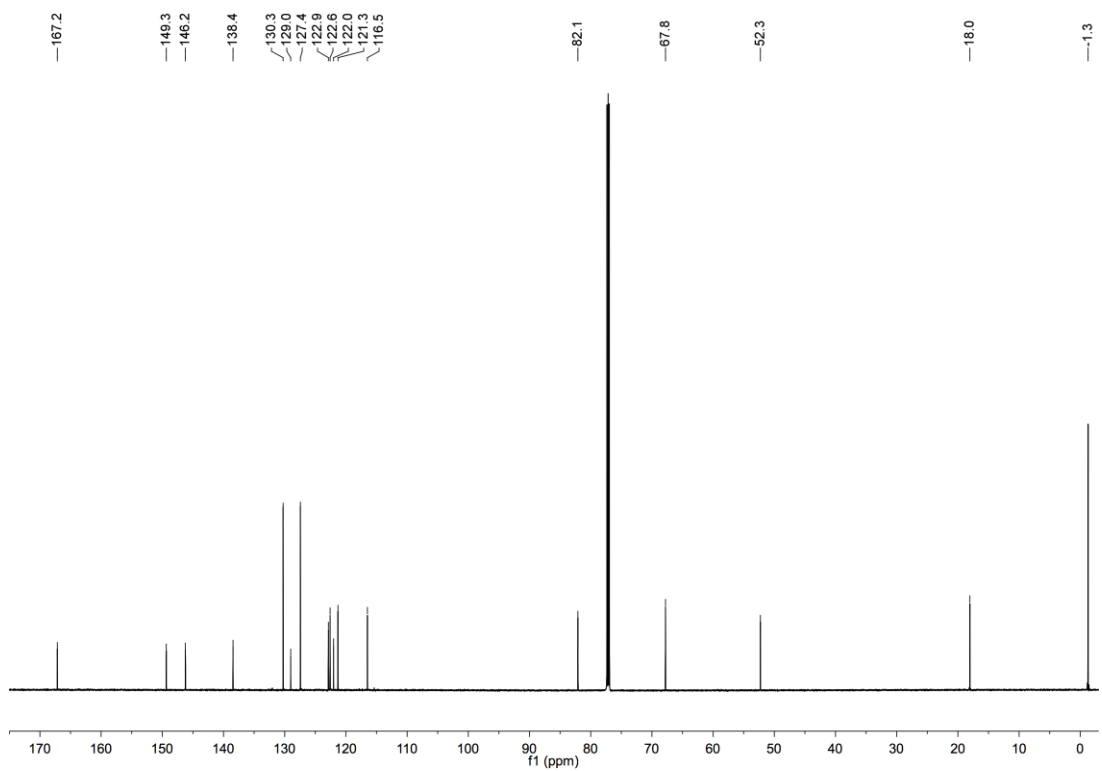
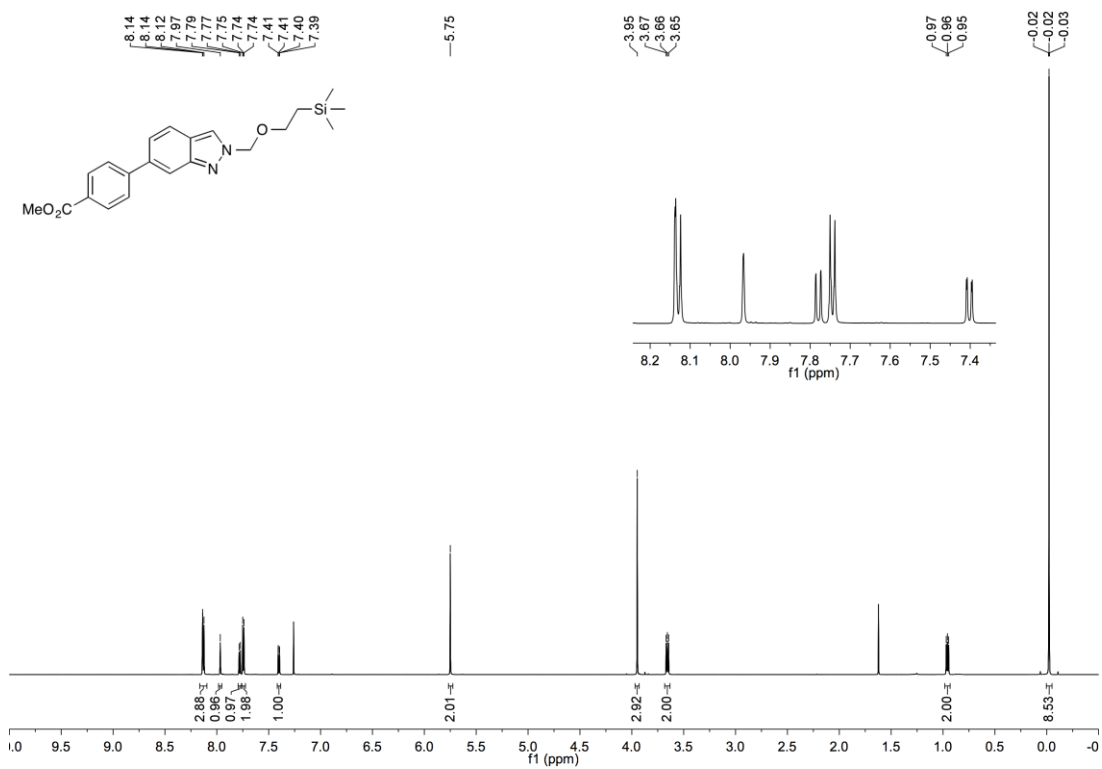
6-Bromo-2-[[2-(trimethylsilyl)ethoxy]methyl]-3-pyridin-2'-yl-2H-indazole (509)



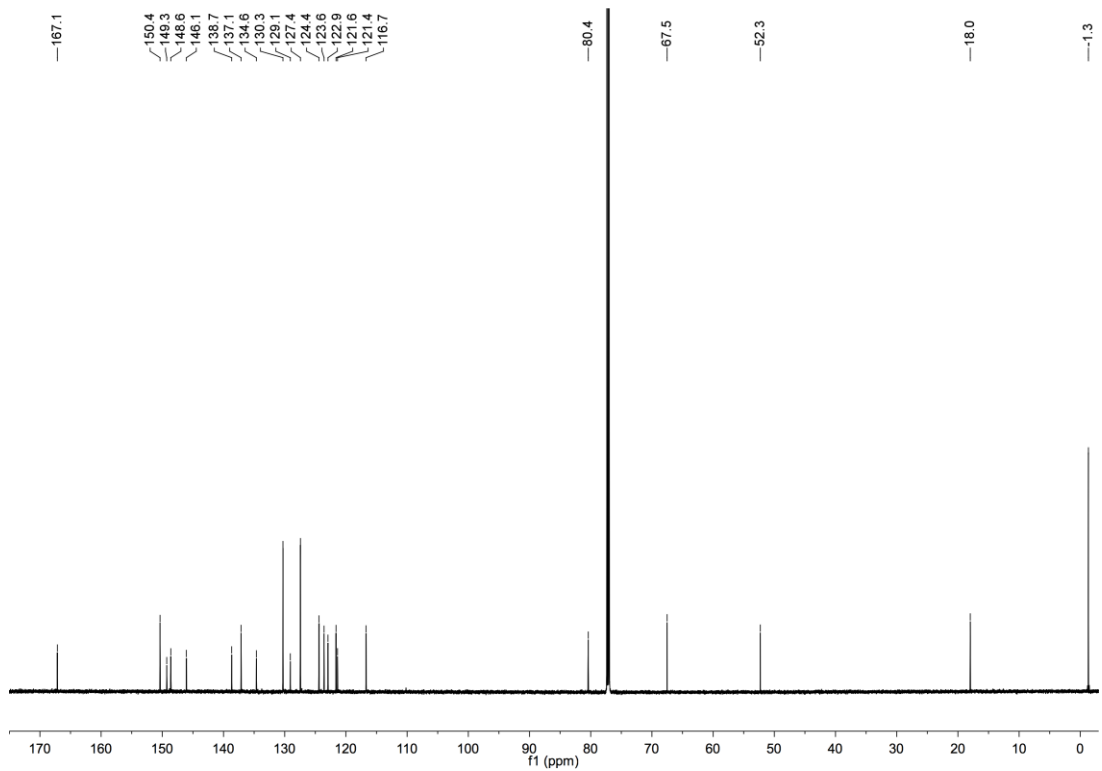
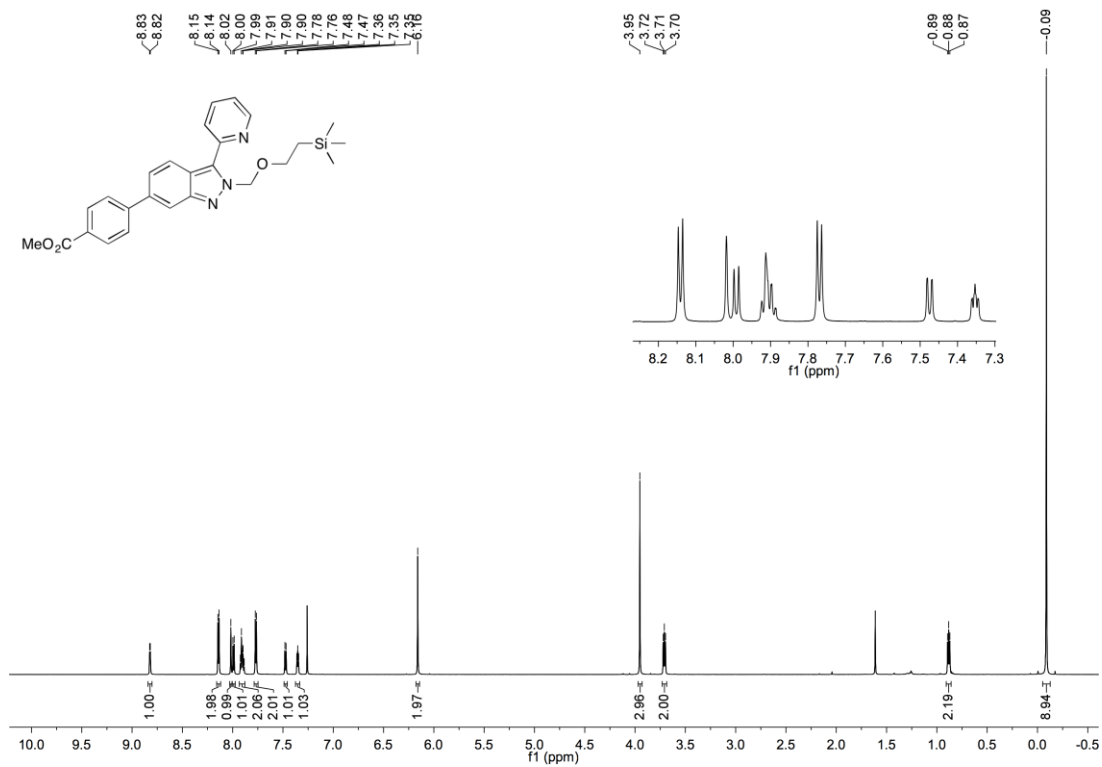
4-Bromo-2-[[2-(trimethylsilyl)ethoxy]methyl]-6-[4'-(methoxycarbonyl)phenyl]-2H-indazole (511)



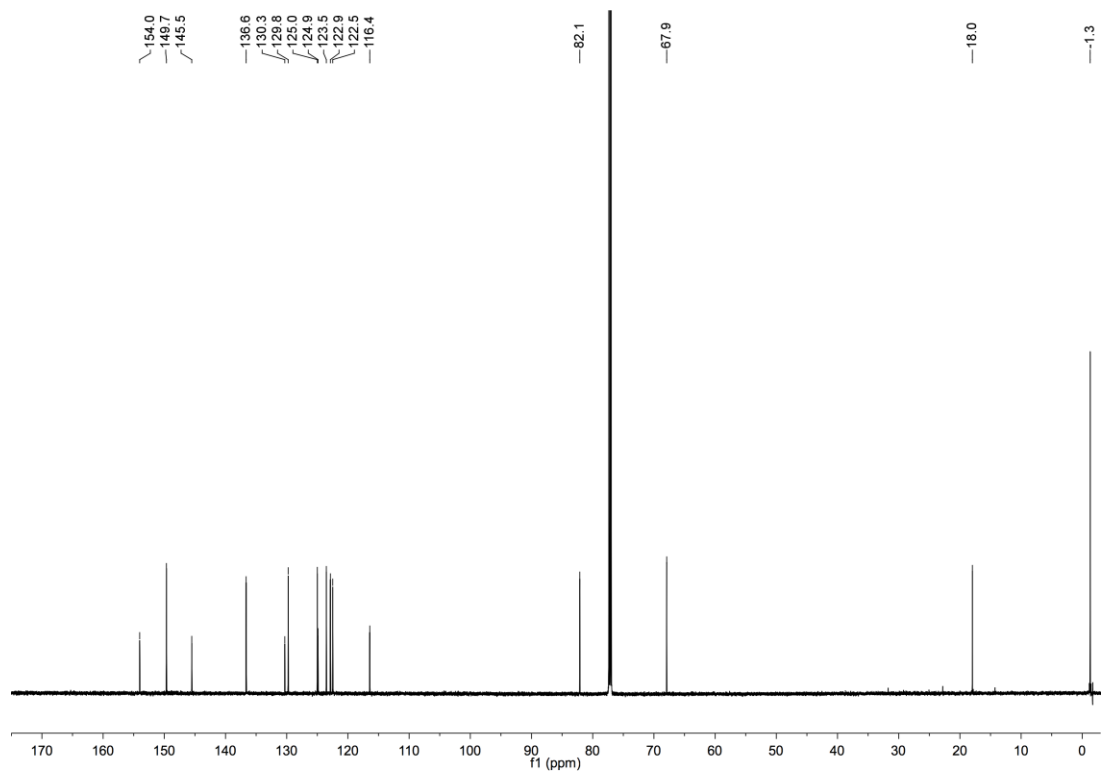
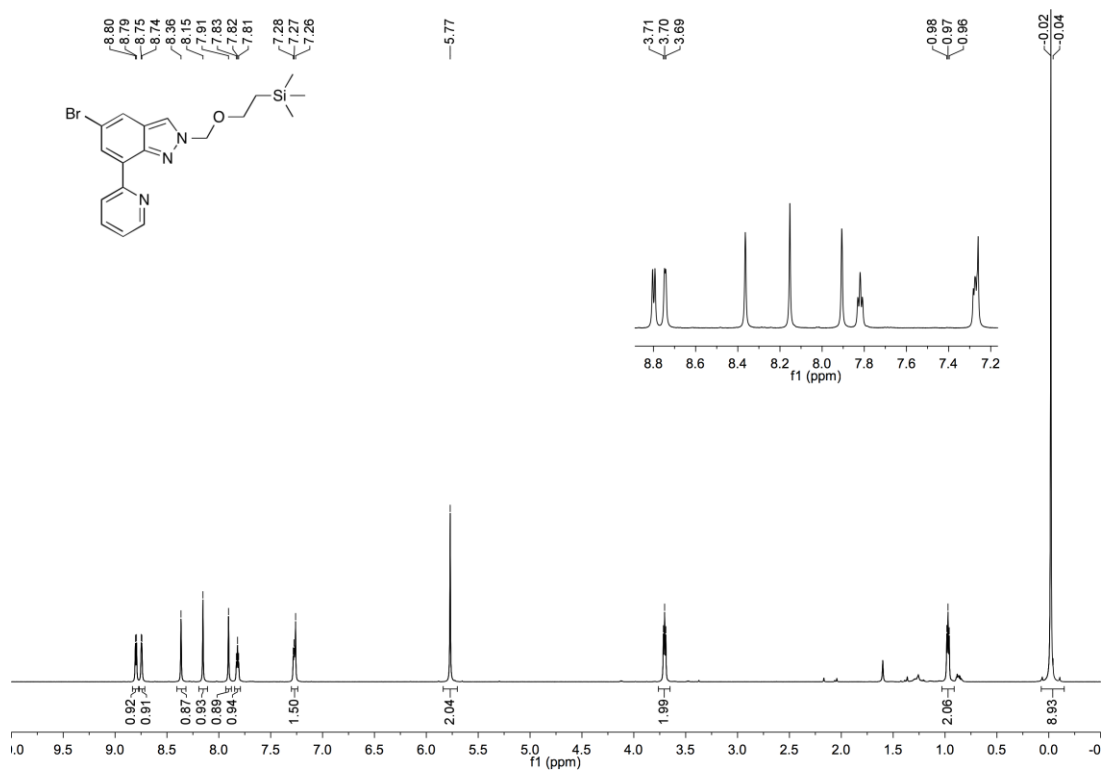
2-[[2-(Trimethylsilyl)ethoxy]methyl]-6-[4'-(methoxycarbonyl)phenyl]-2H-indazole (514)



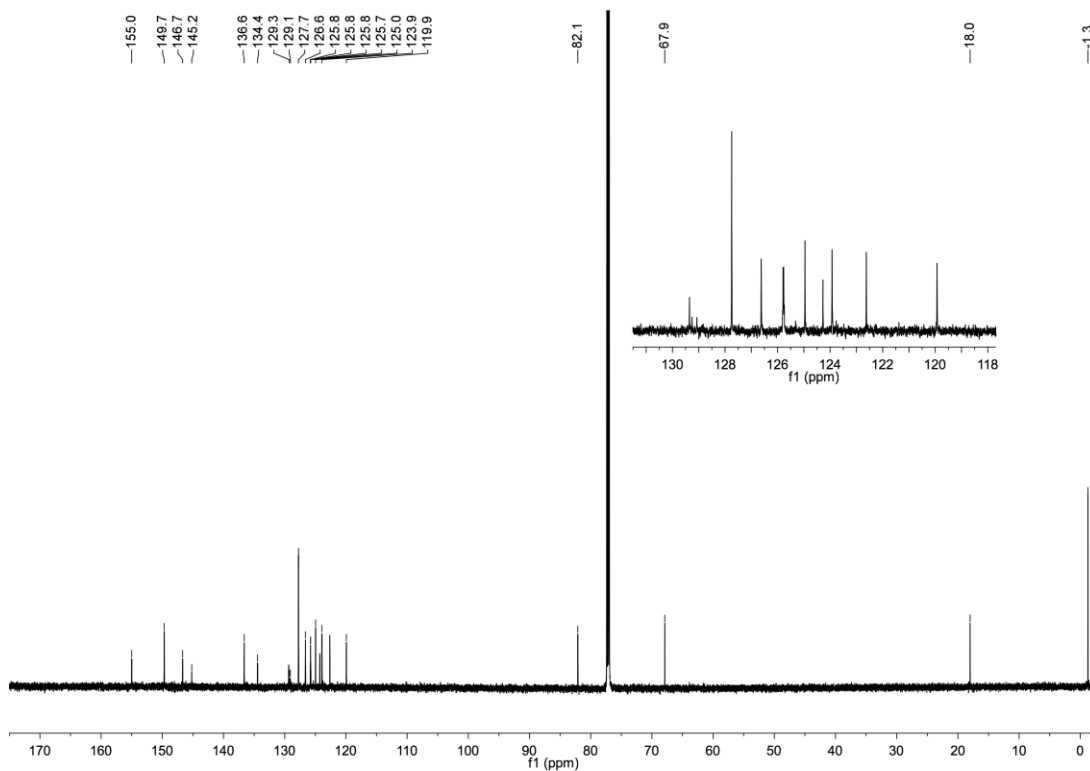
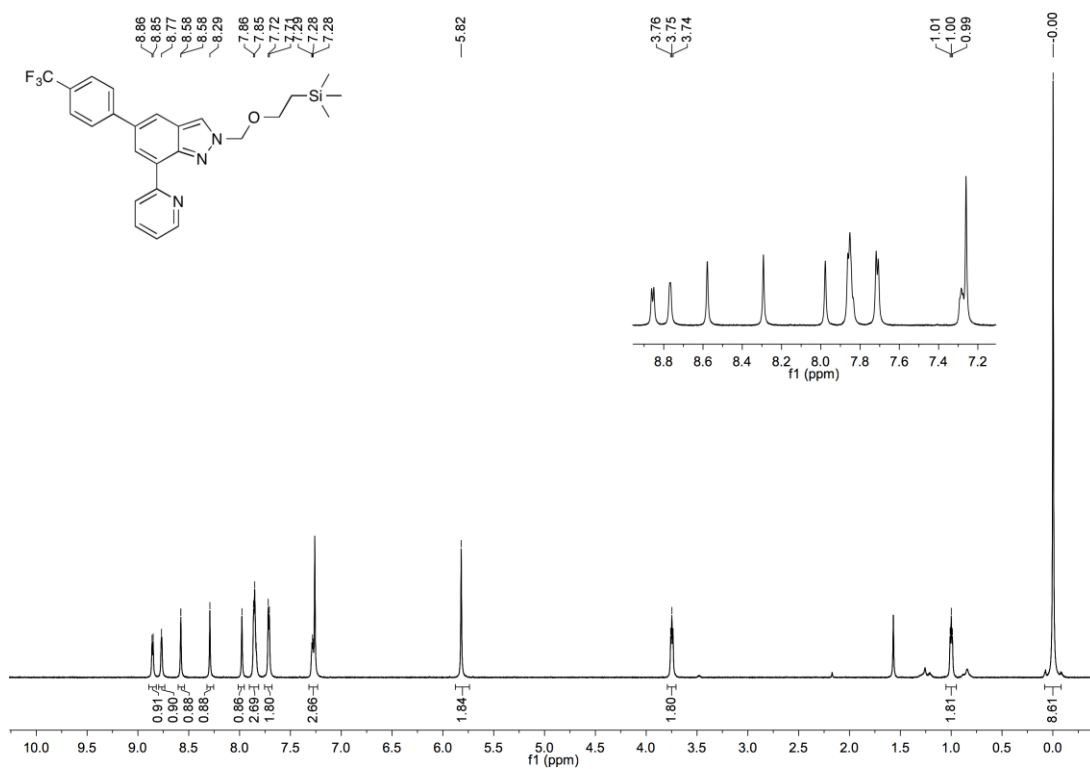
2-[[2-(Trimethylsilyl)ethoxy]methyl]-3-pyridin-2'-yl-6-[4''-(methoxycarbonyl)phenyl]-2H-indazole (521)

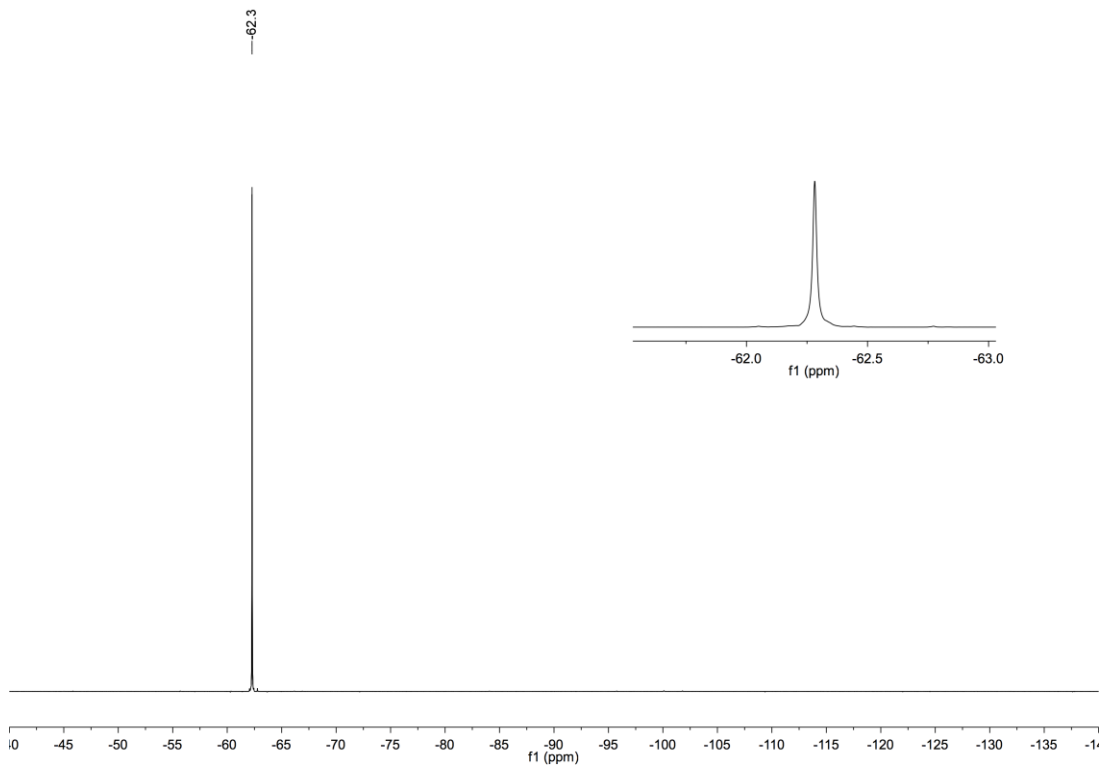


5-Bromo-2-[[2-(trimethylsilyl)ethoxy]methyl]-7-pyridin-2'-yl-2H-indazole (535)

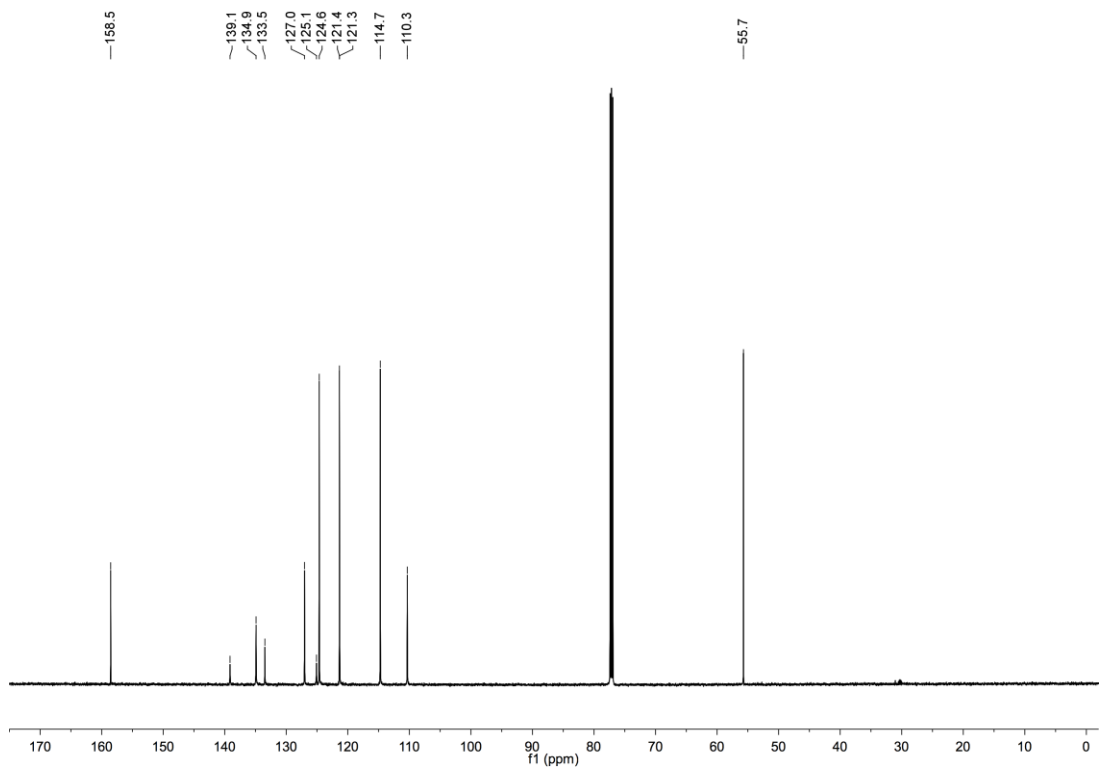
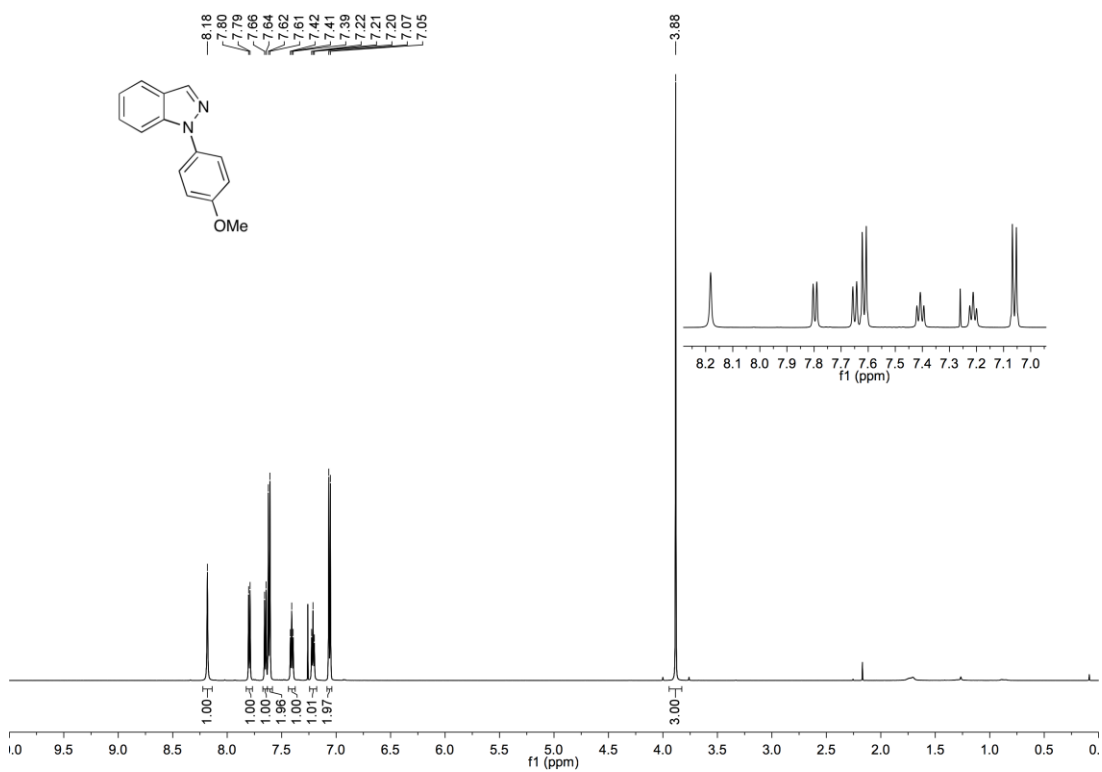


2-([2-(Trimethylsilyl)ethoxy]methyl)-7-pyridin-2'-yl-5-[4''-(trifluoromethyl)phenyl]-2H-indazole (537)

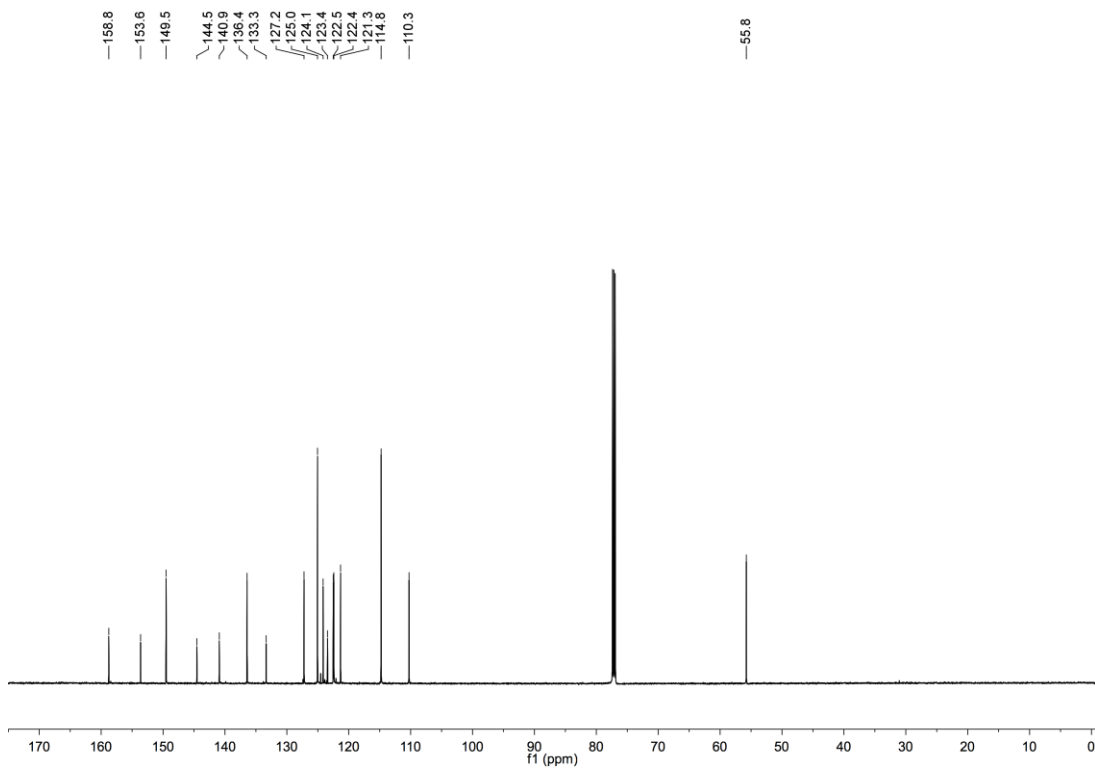
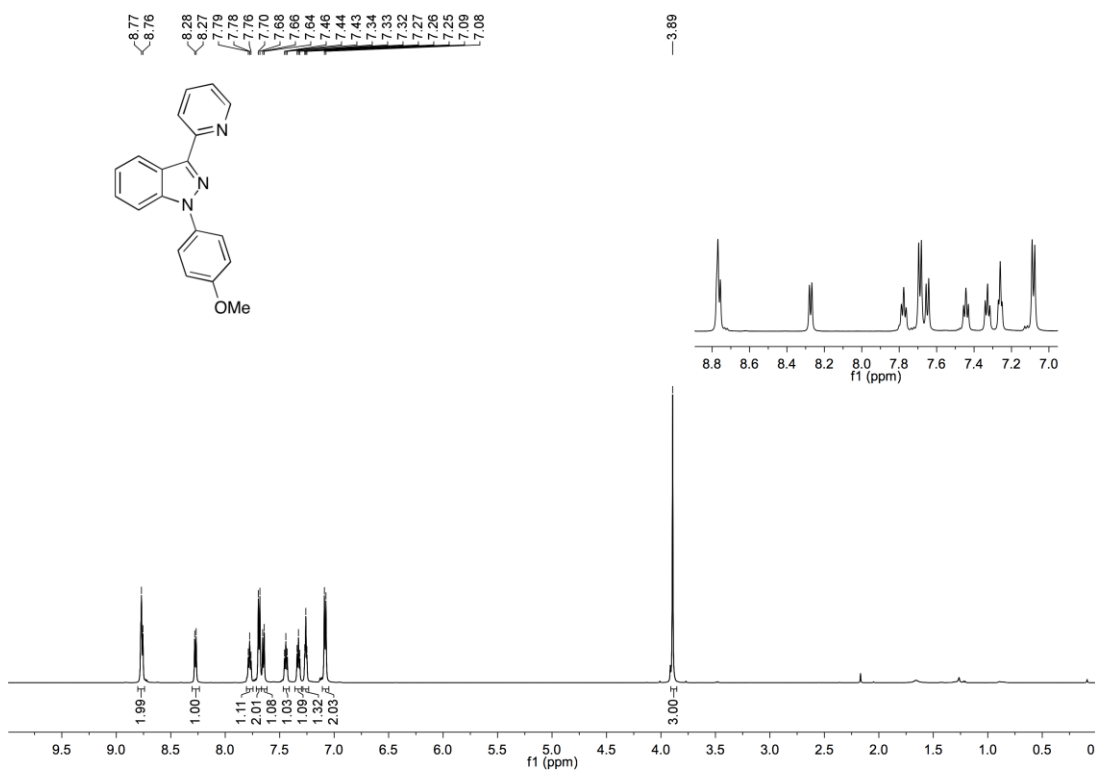




N-(4'-Methoxyphenyl)-1*H*-indazole (540)

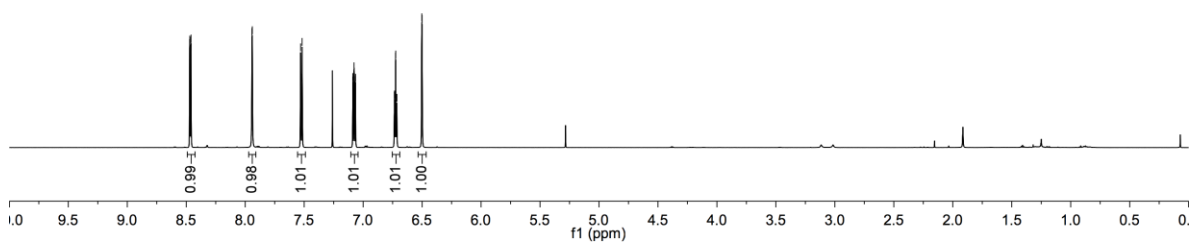
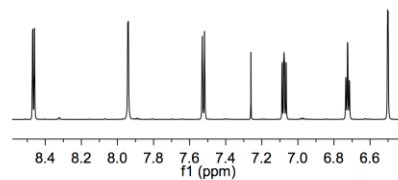
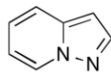


3-Pyridin-2'-yl-N-(4''-methoxyphenyl)-1H-indazole (541)

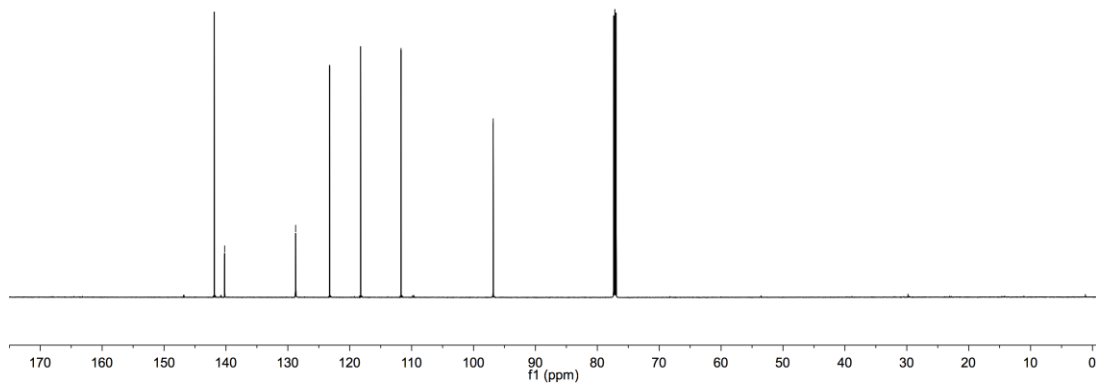


Pyrazolo[1,5-a]pyridine (543)

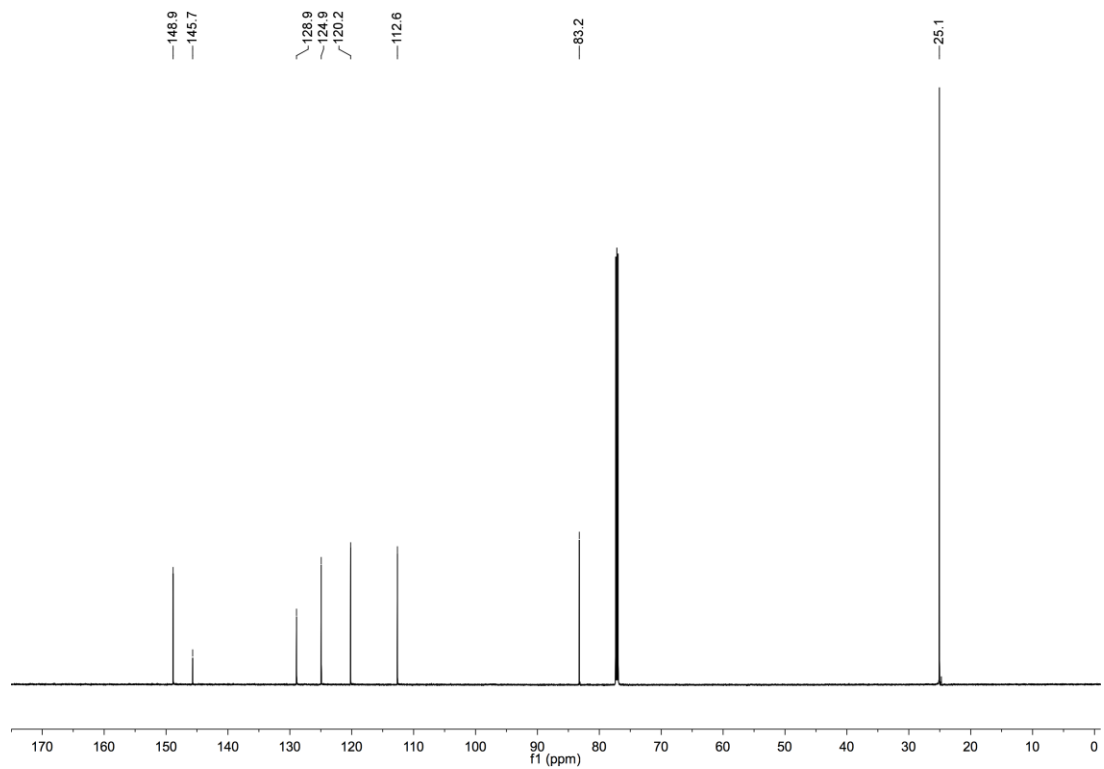
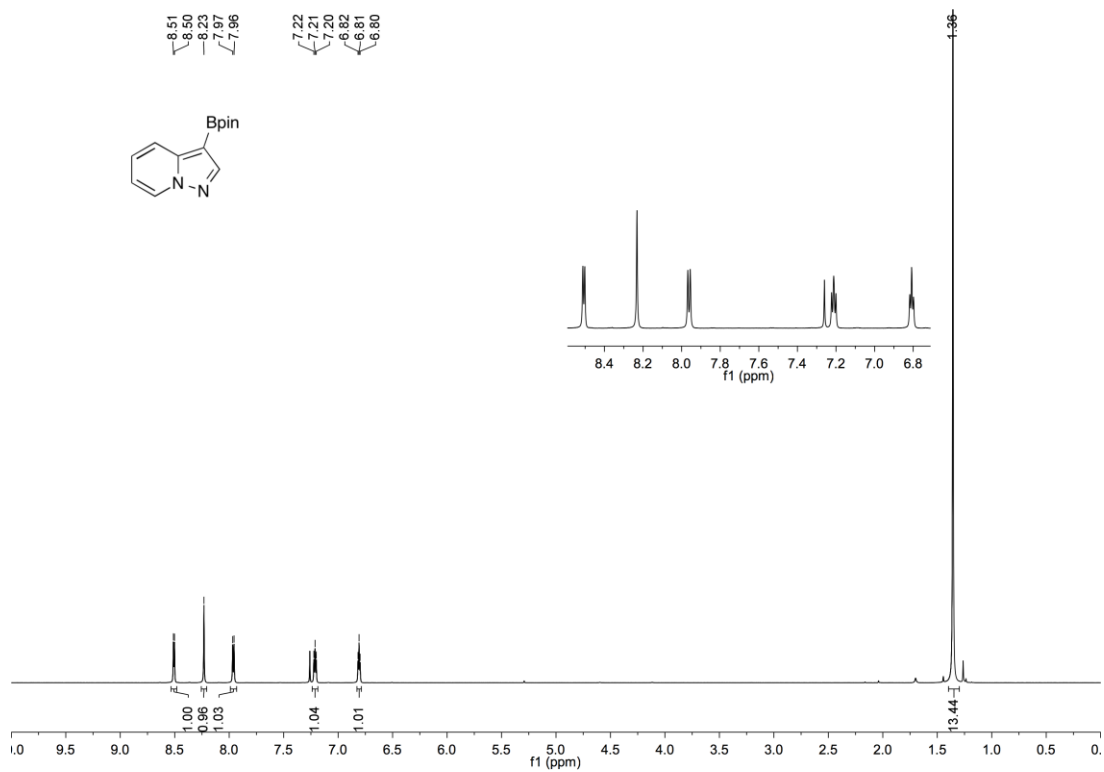
8.47
8.47
8.46
8.46
7.94
7.94
7.53
7.52
7.52
7.08
7.08
6.73
6.72
6.72
6.71
6.50
6.50

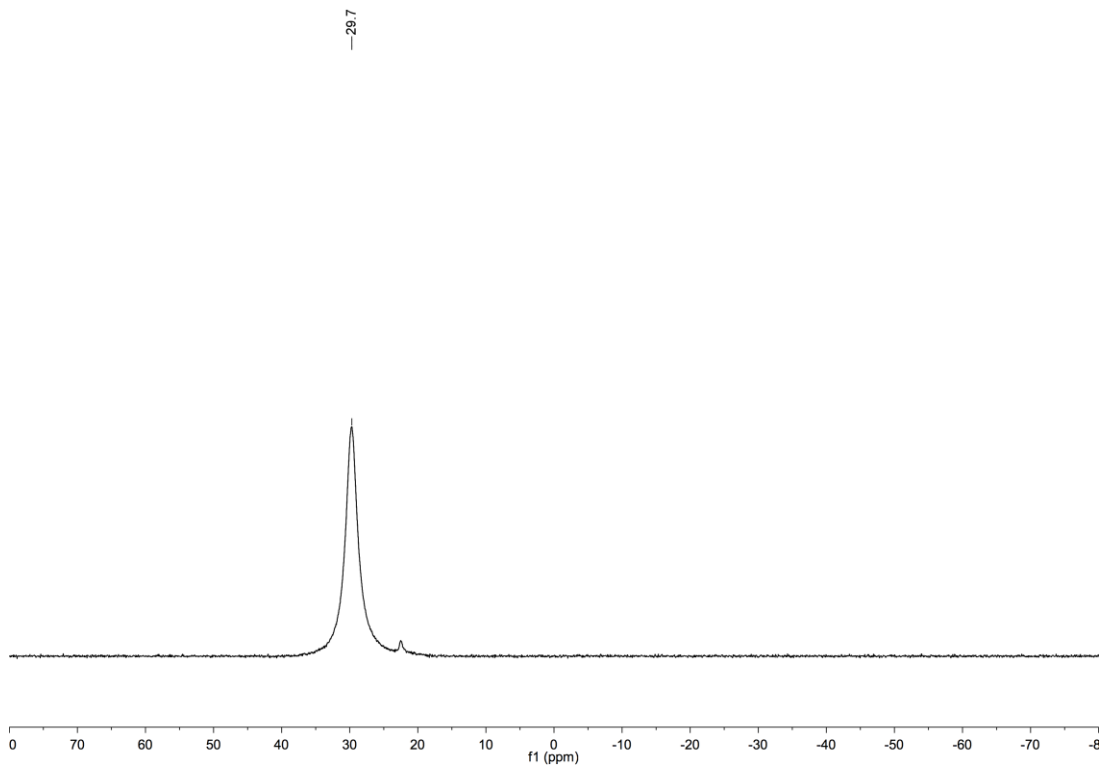


141.9
140.2
128.7
123.3
118.2
111.7
96.8

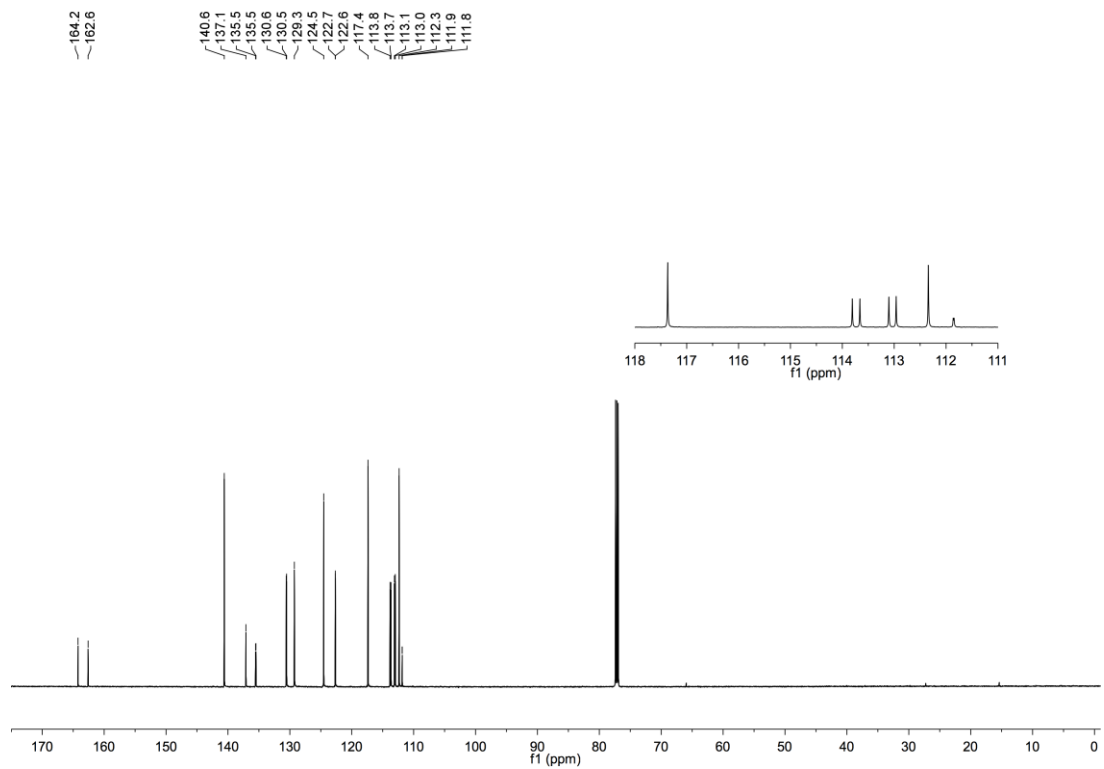
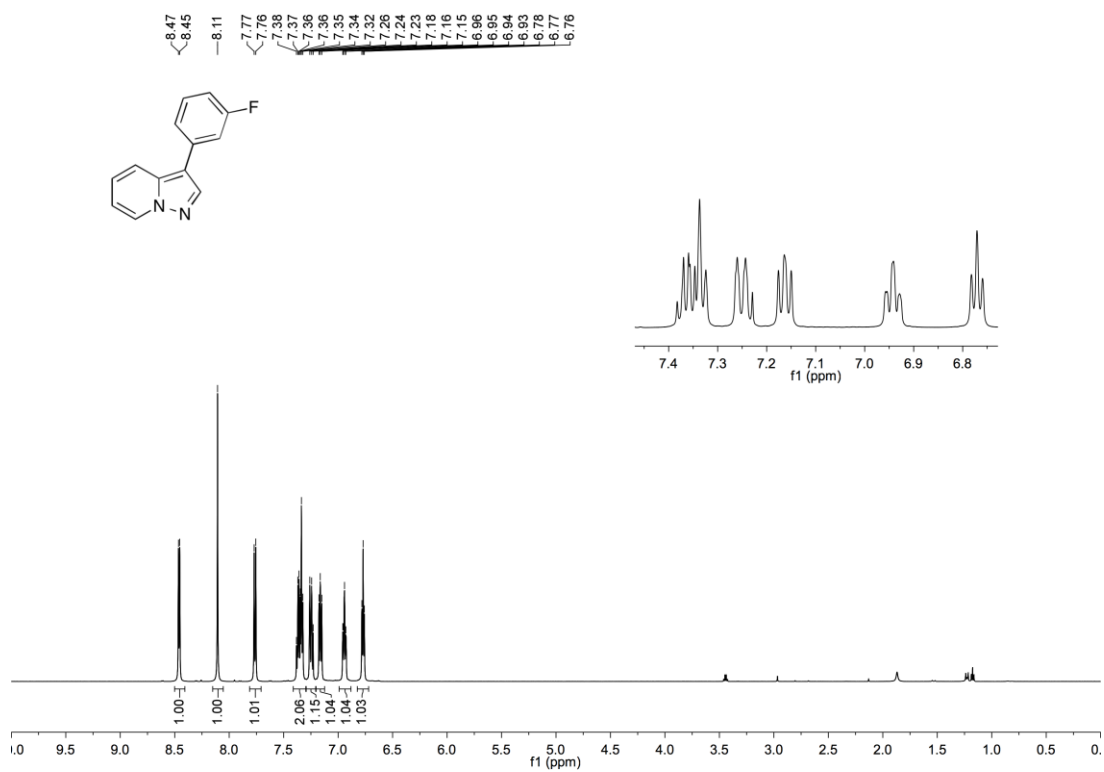


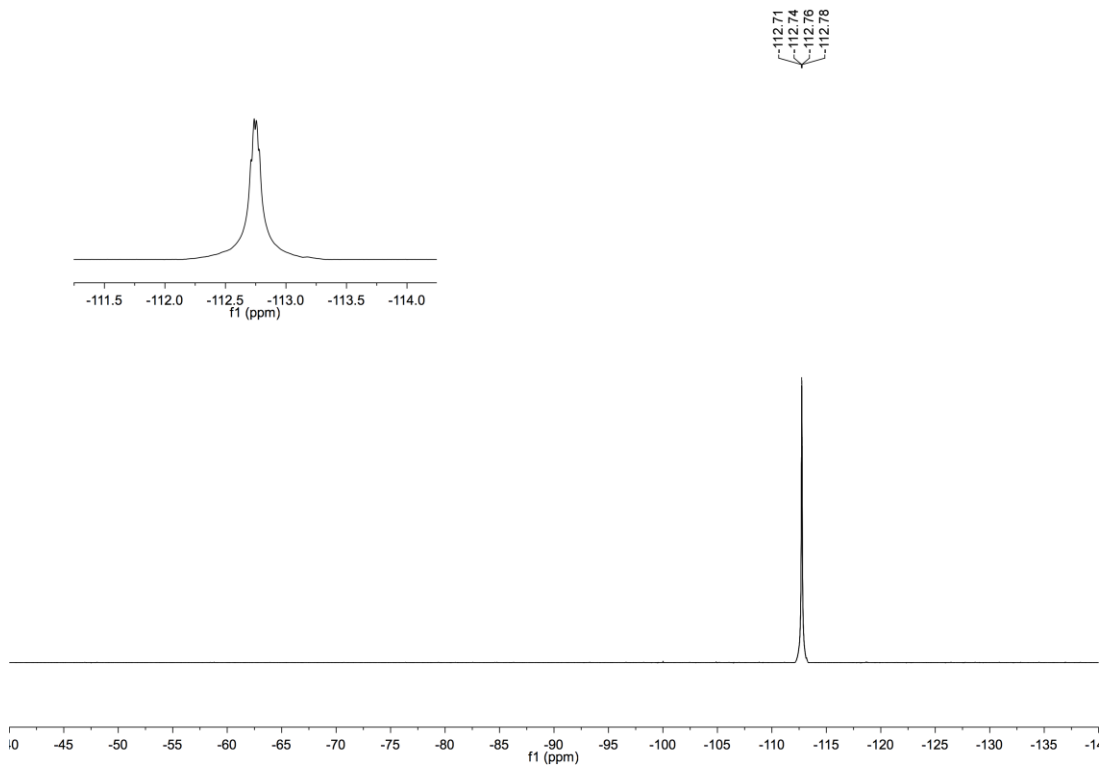
3-(Bpin)-Pyrazolo[1,5-a]pyridine (544)



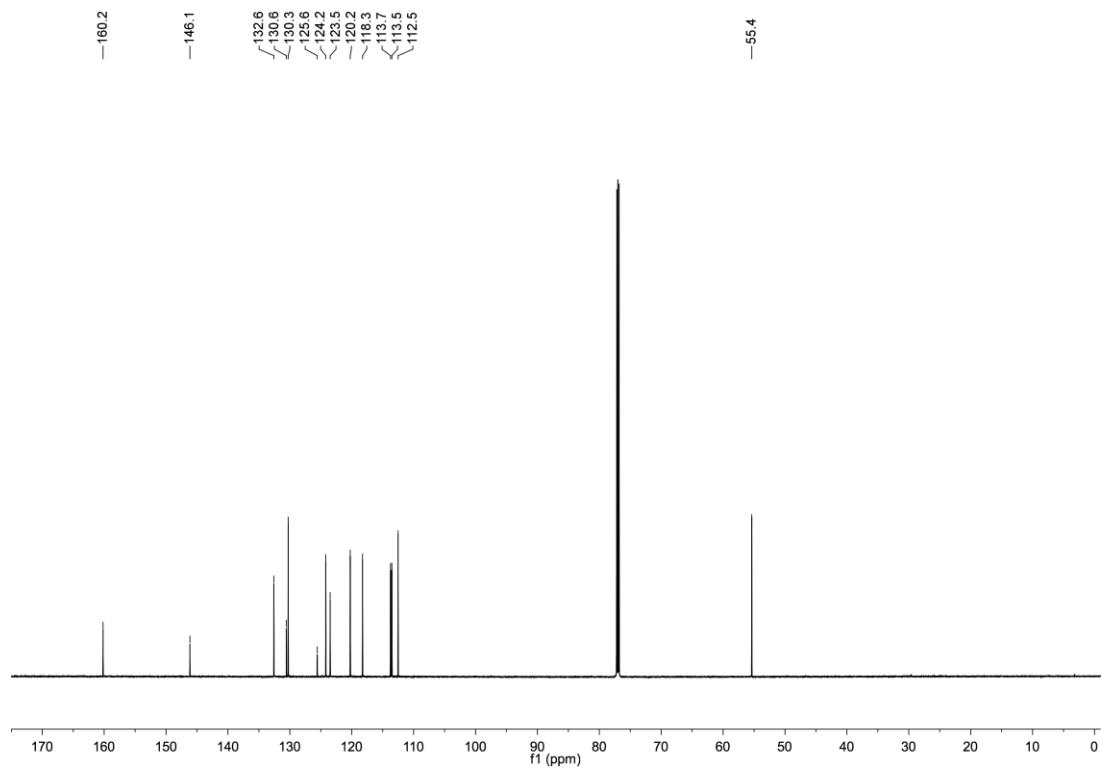
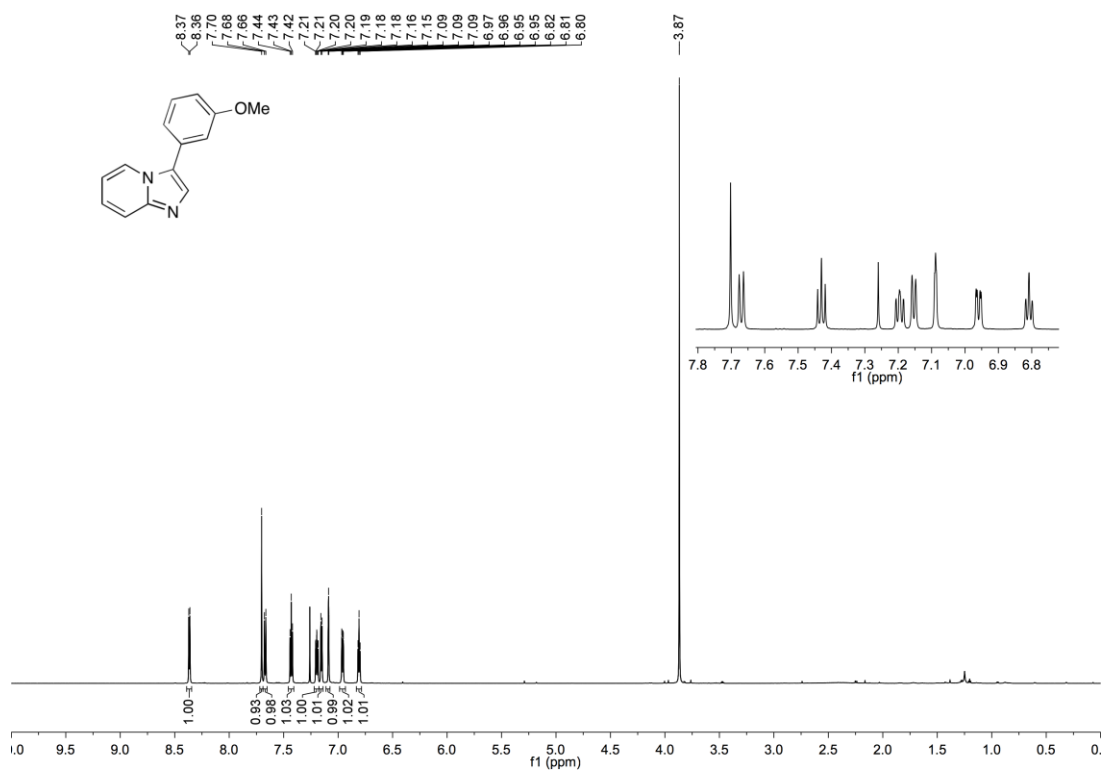


3-(3'-Fluorophenyl)pyrazolo[1,5-a]pyridine (545)



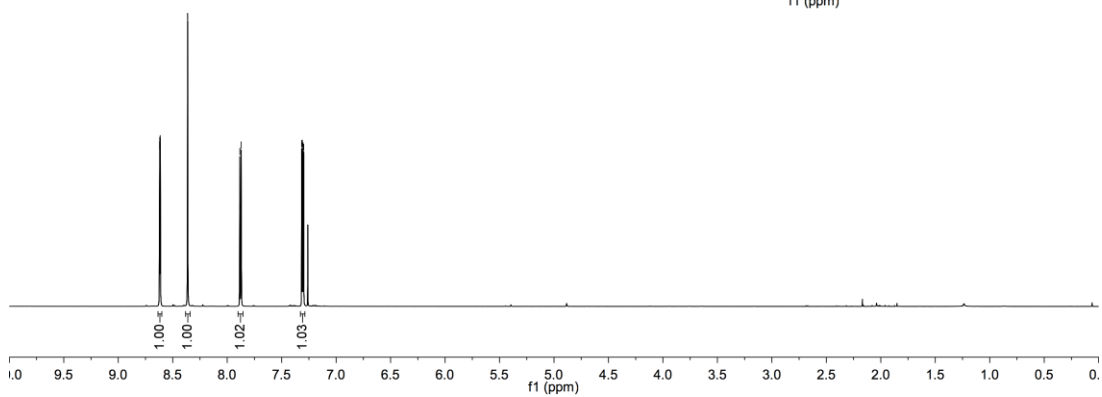
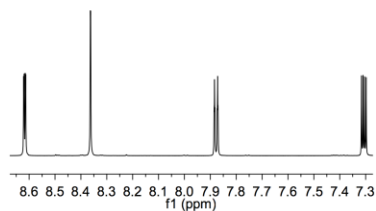
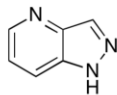


3-(3'-Methoxyphenyl)pyrazolo[1,2-a]pyridine (552)

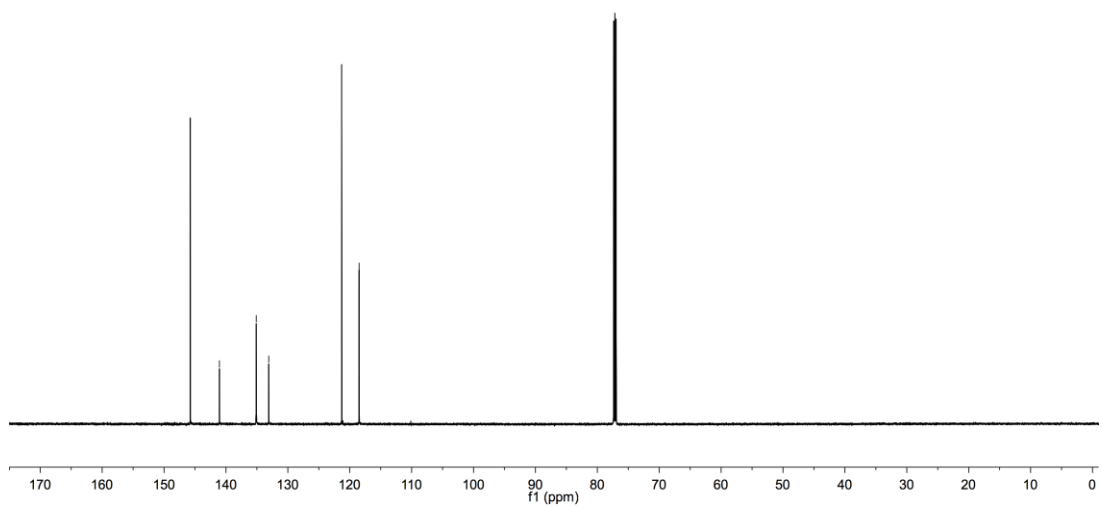


4-Aza-1H-indazole (555)

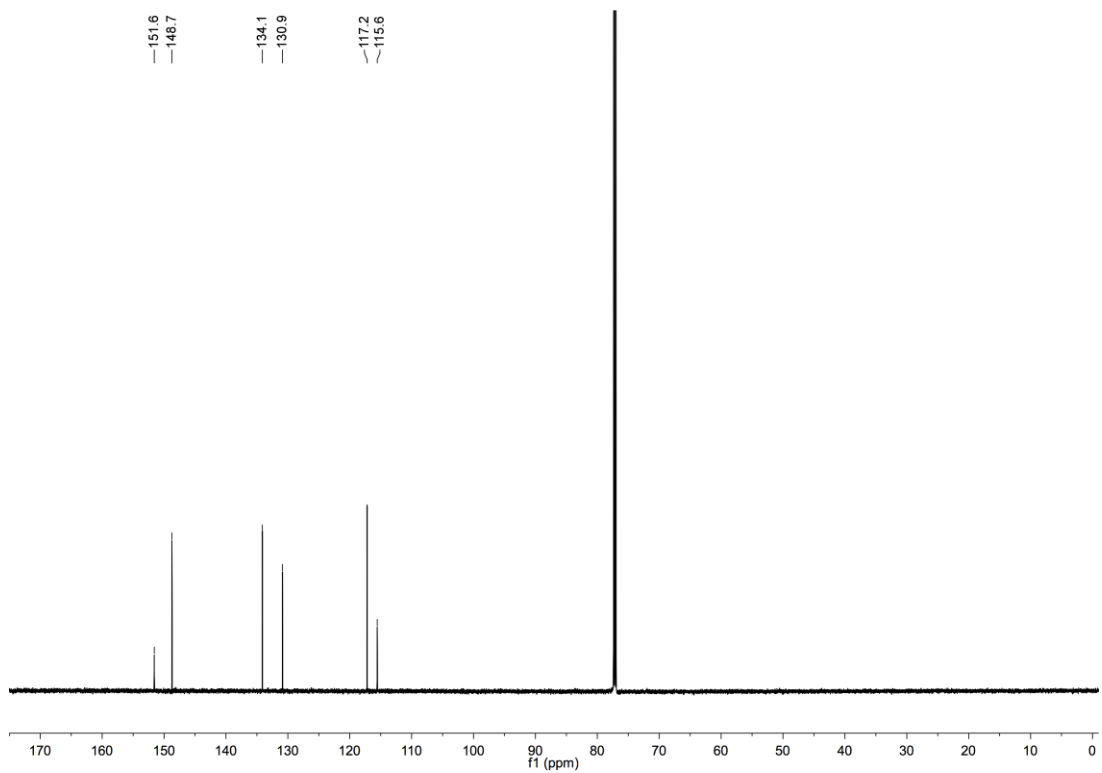
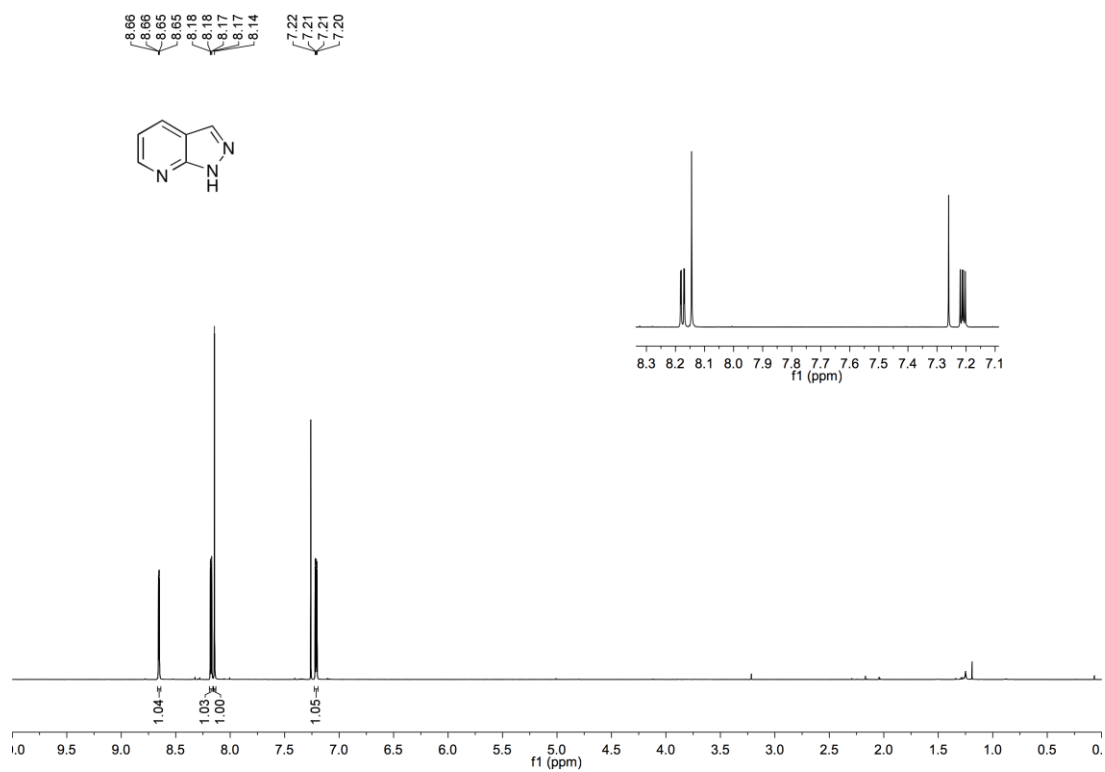
8.62
8.62
8.61
8.36
7.88
7.87
7.82
7.31
7.30
7.30



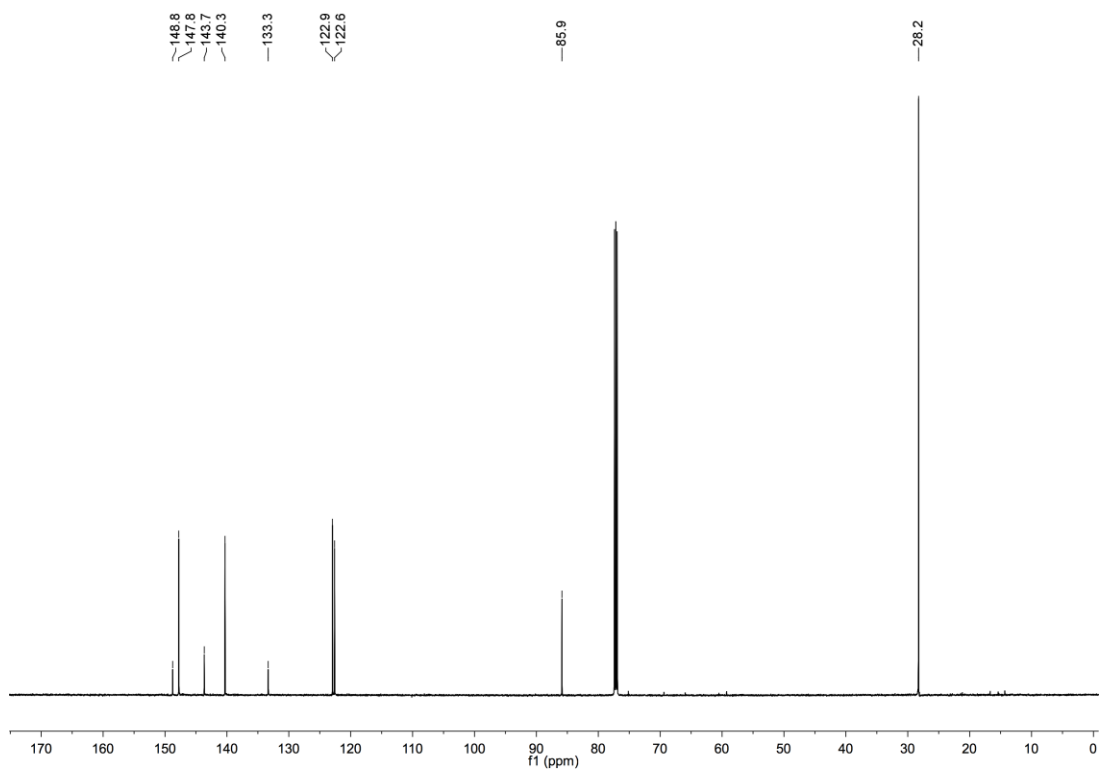
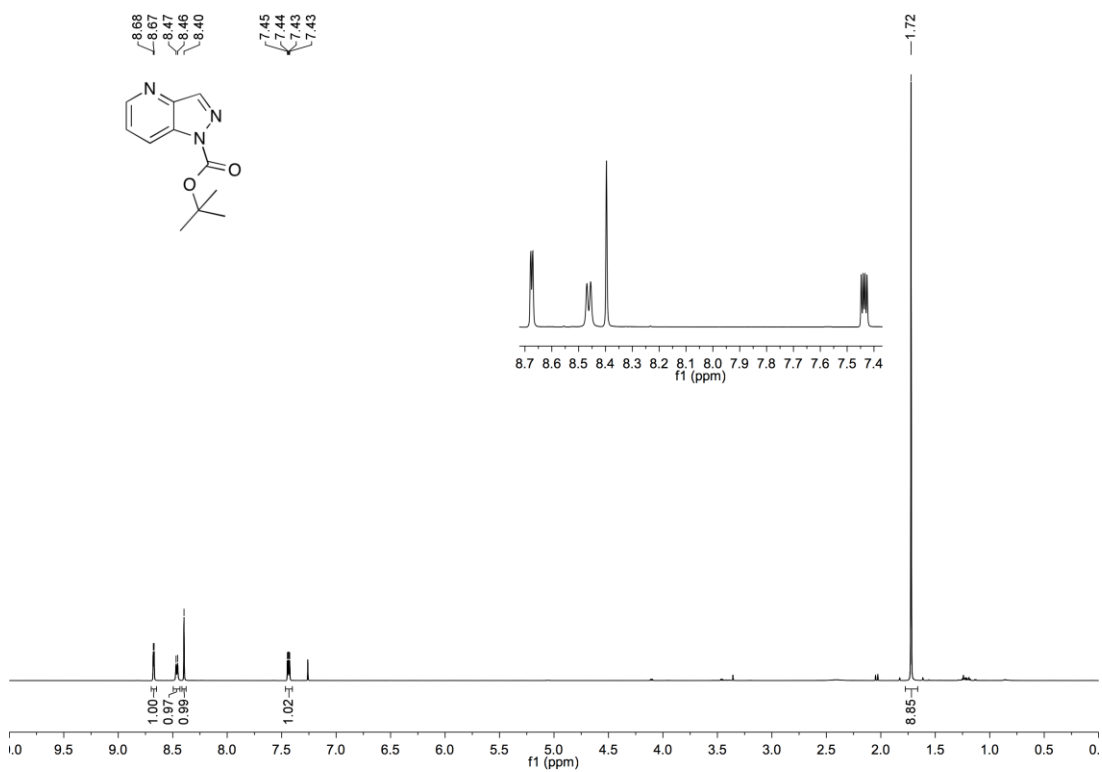
145.8
141.1
135.1
133.1
121.3
118.5



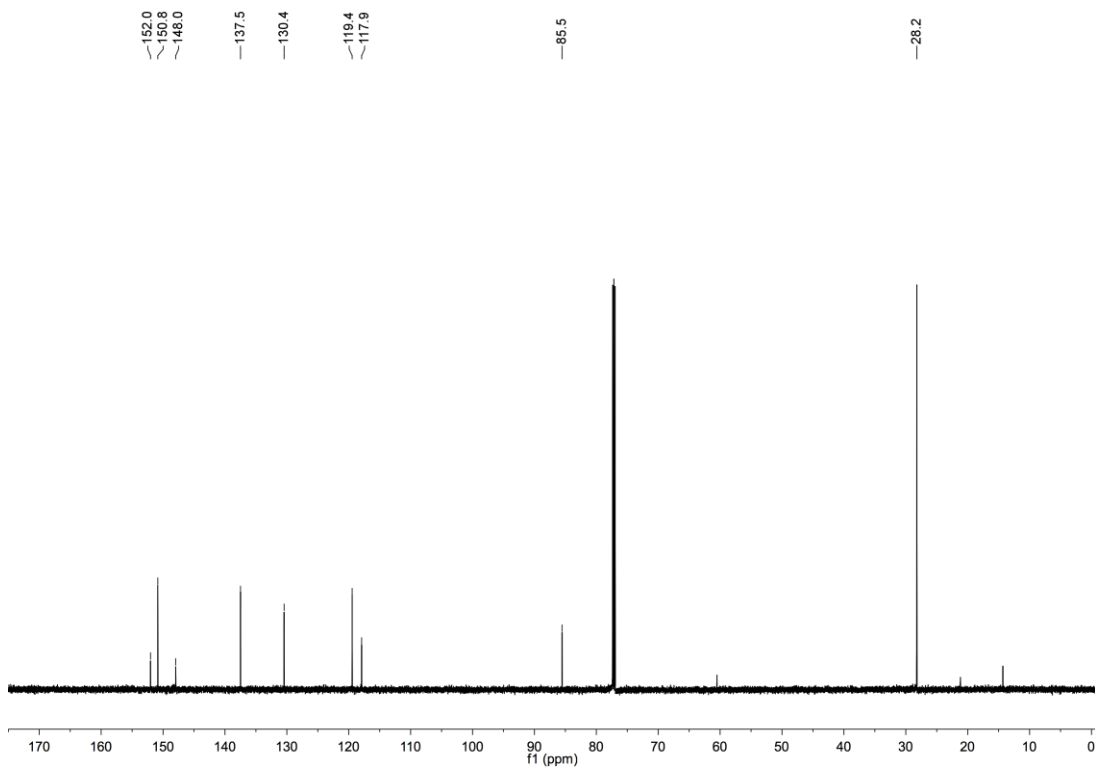
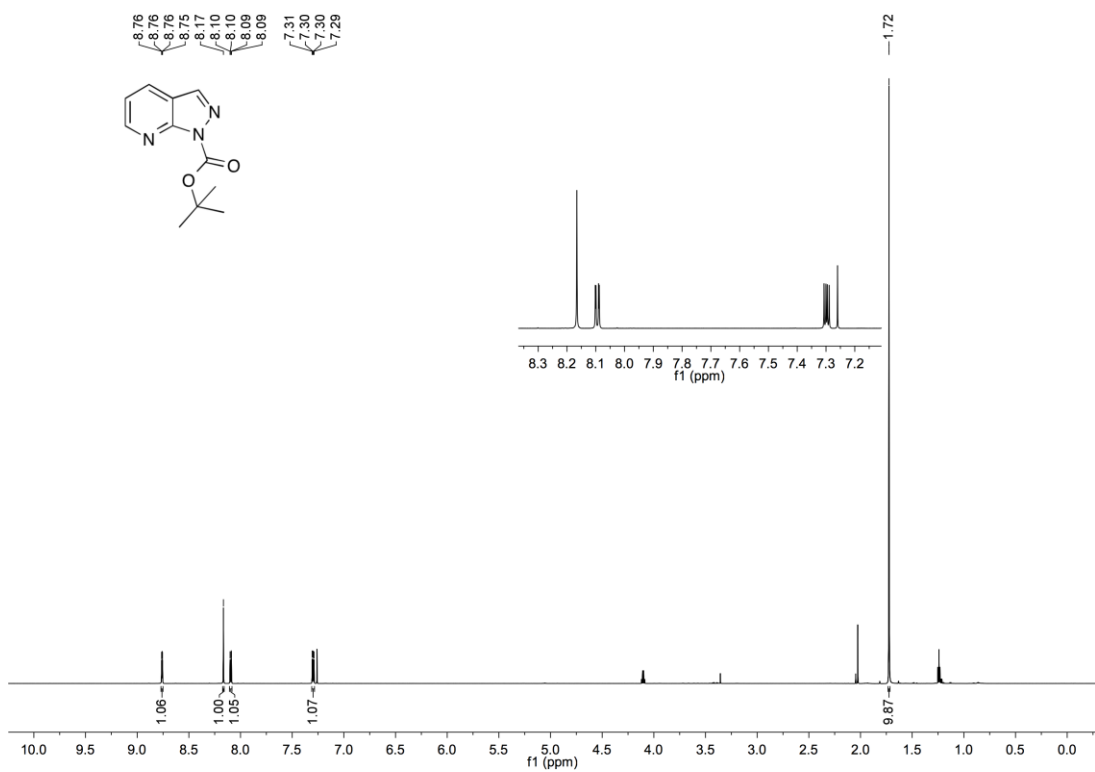
7-Aza-1H-indazole (556)



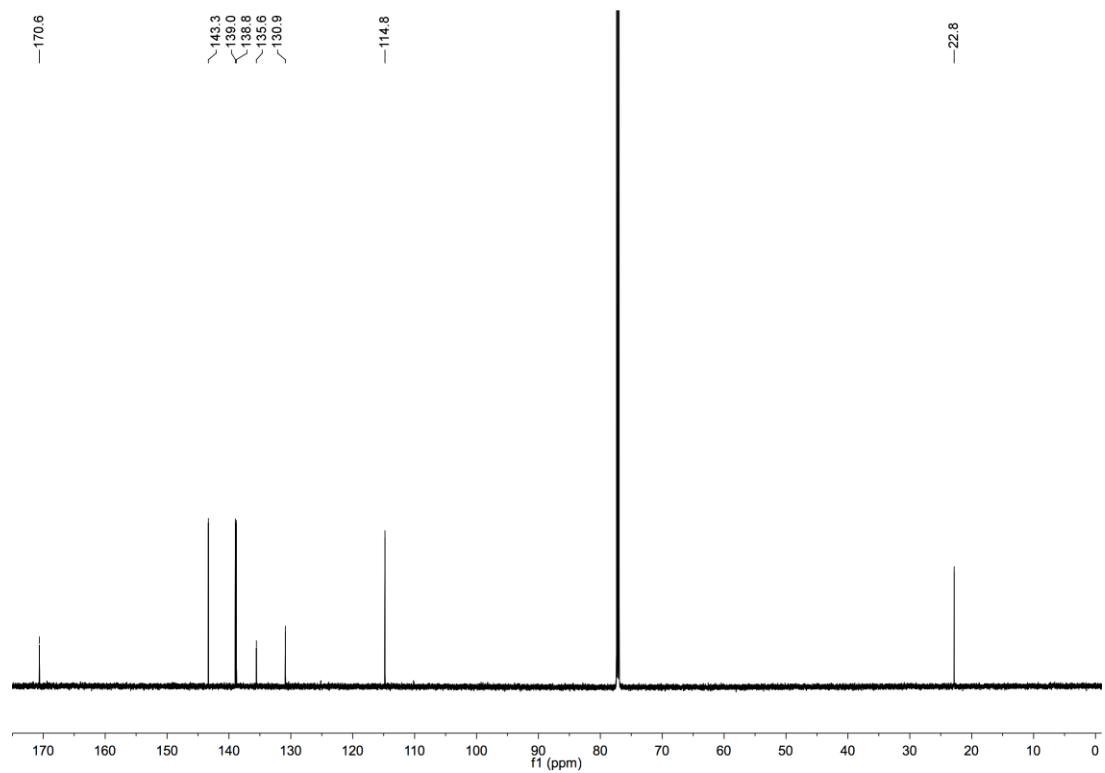
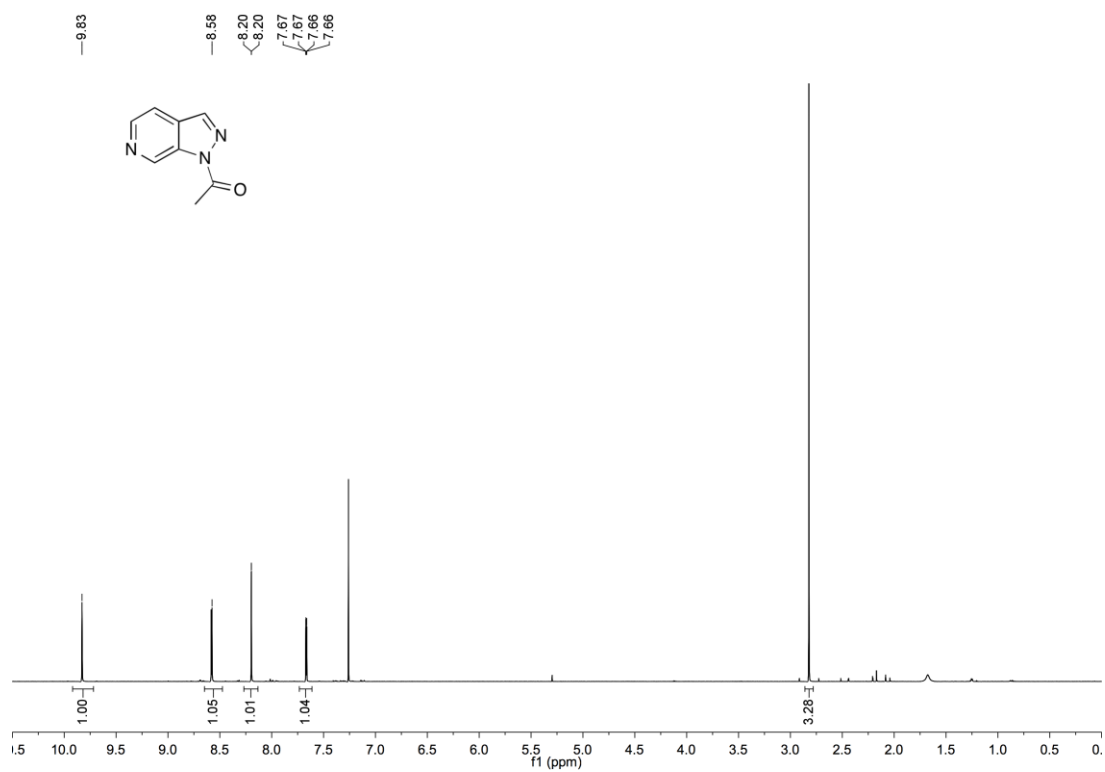
4-Aza-1-(tert-butoxycarbonyl)-1H-indazole (557)



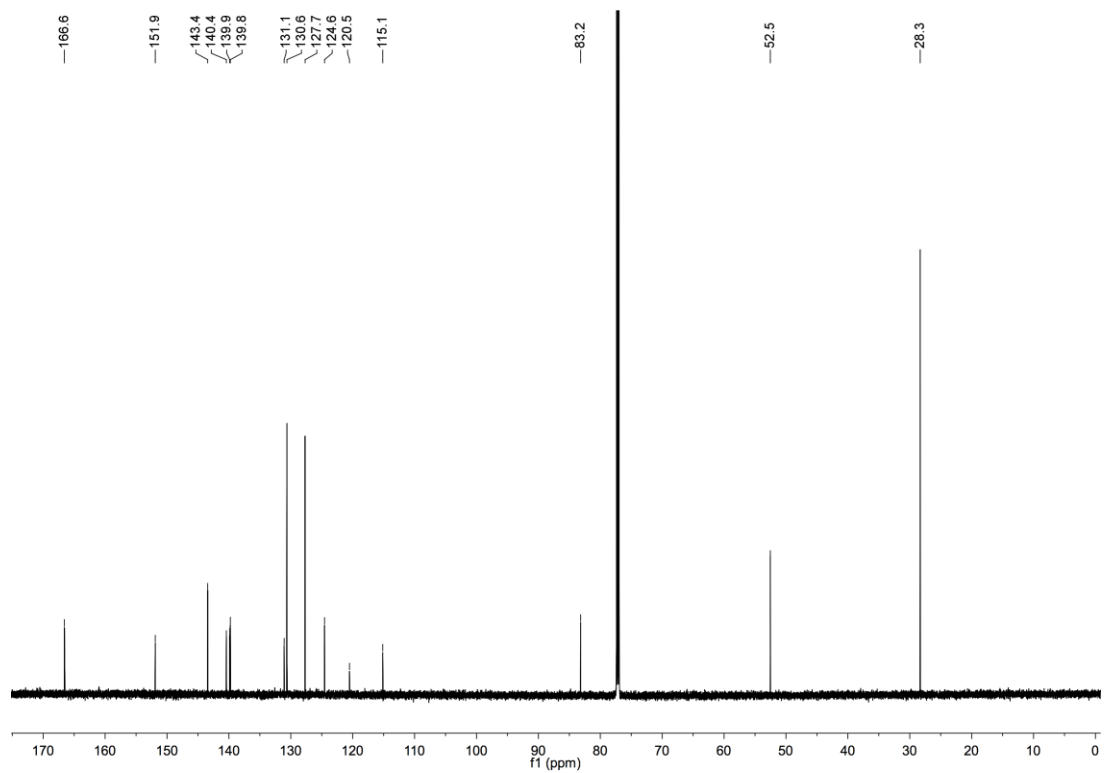
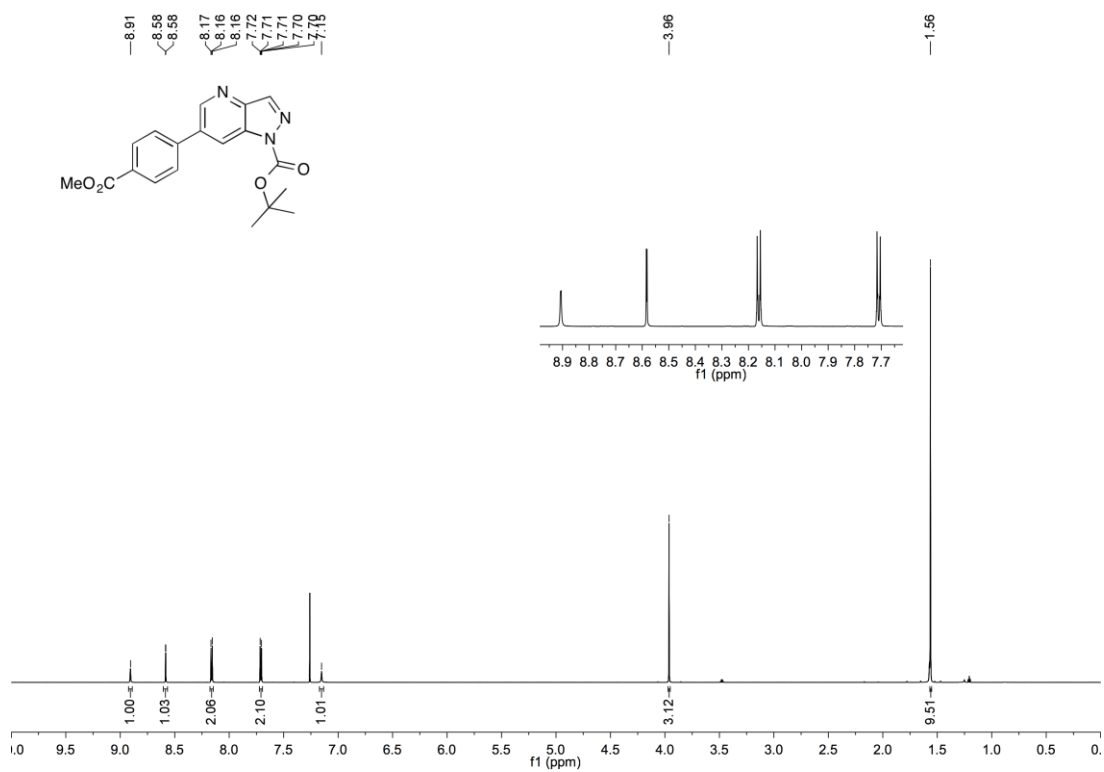
7-Aza-1-(tert-butoxycarbonyl)-1H-indazole (558)



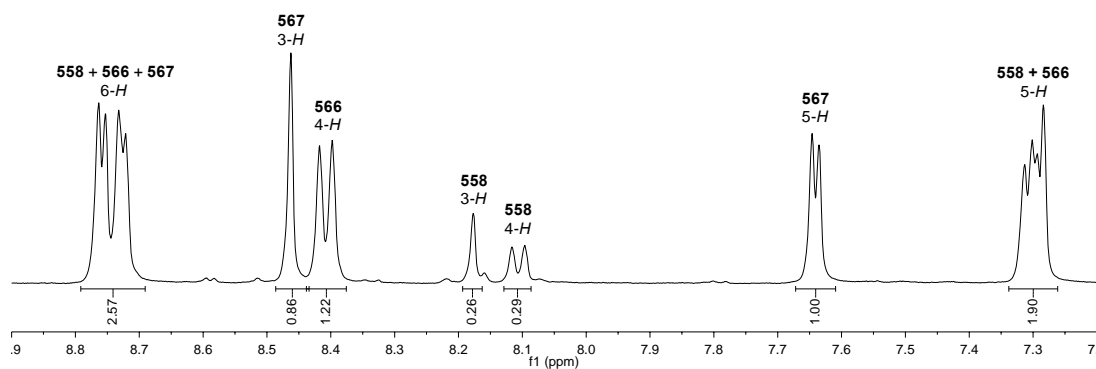
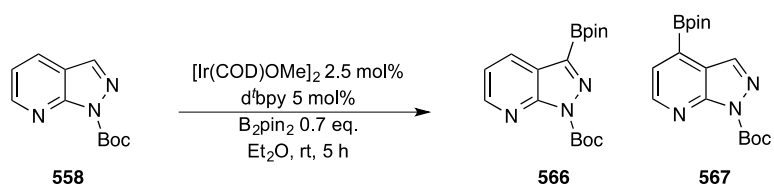
6-Aza-1-acetyl-1H-indazole (560)



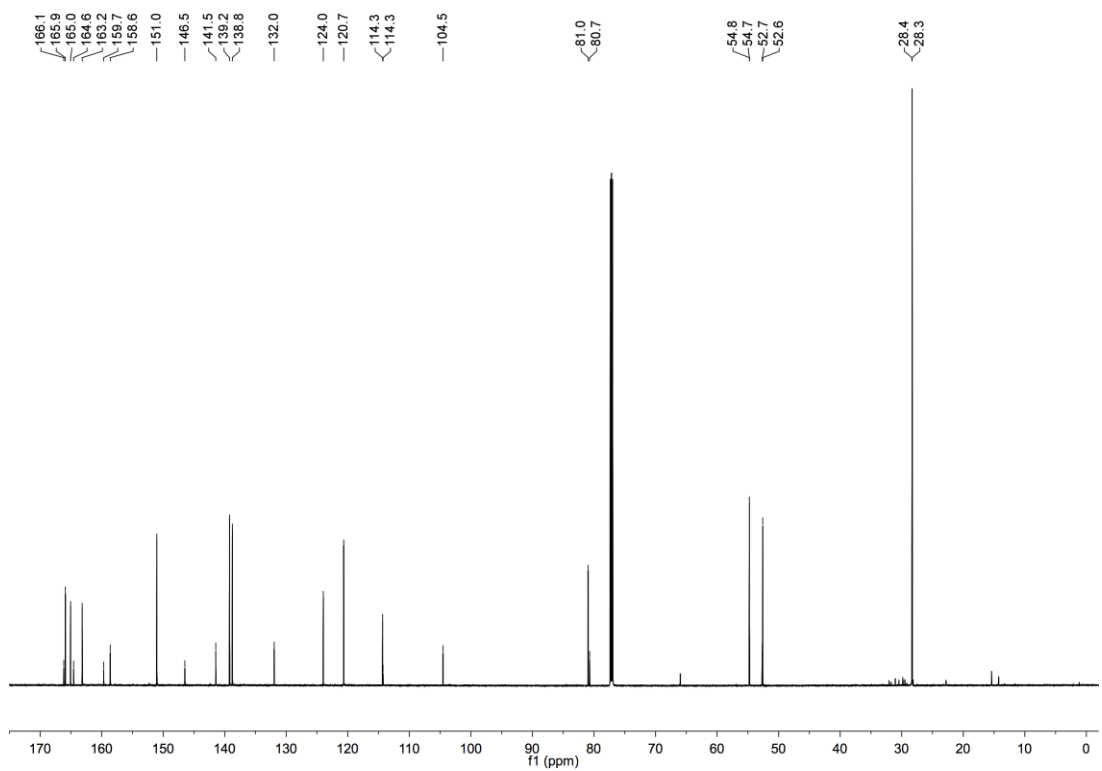
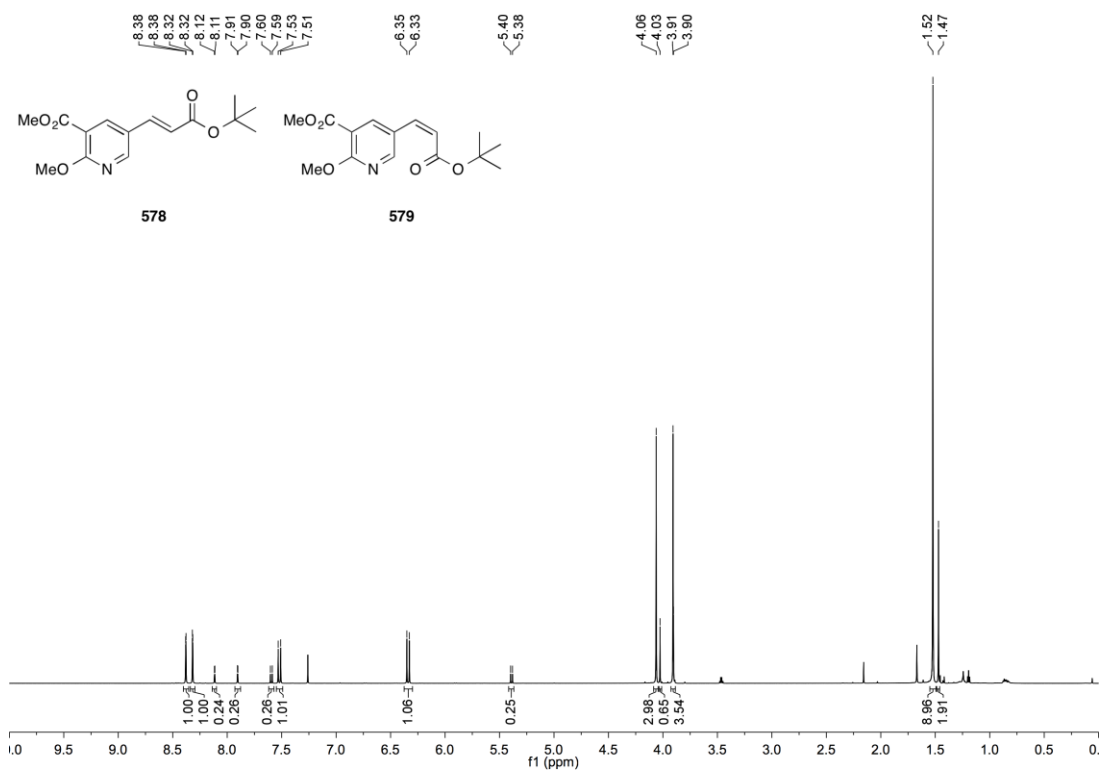
4-Aza-6-[4'-(methoxycarbonyl)phenyl]-1-(tert-butoxycarbonyl)-1H-indazole (565)



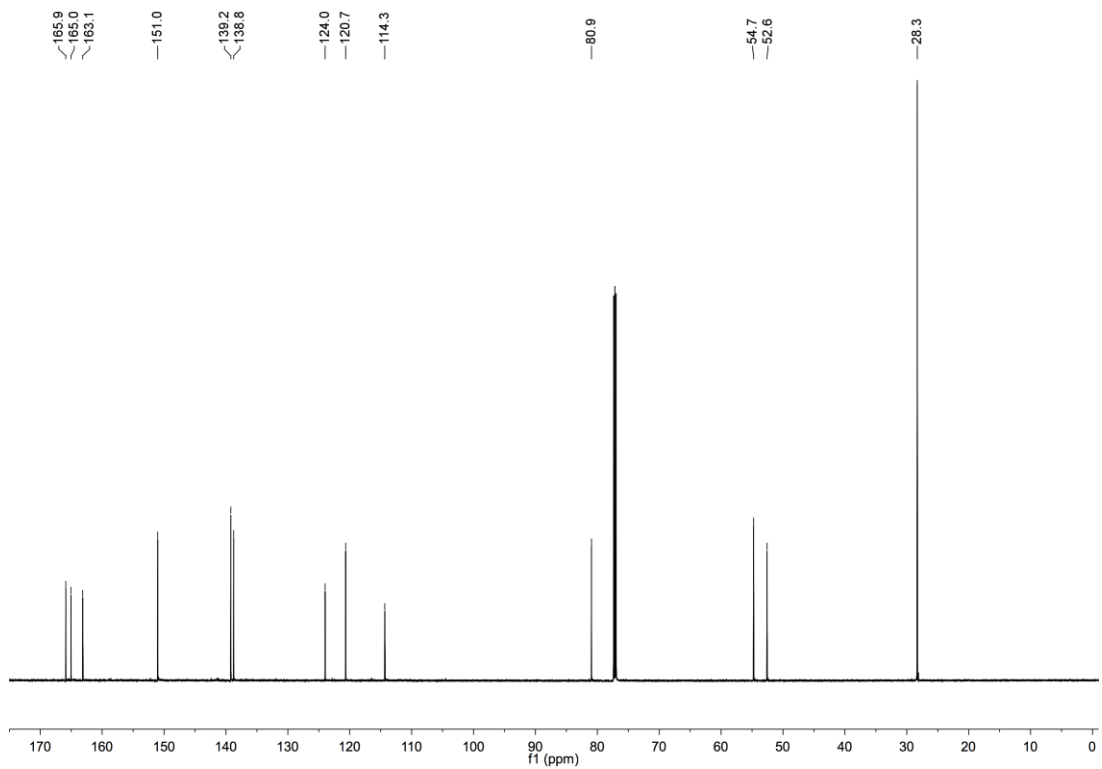
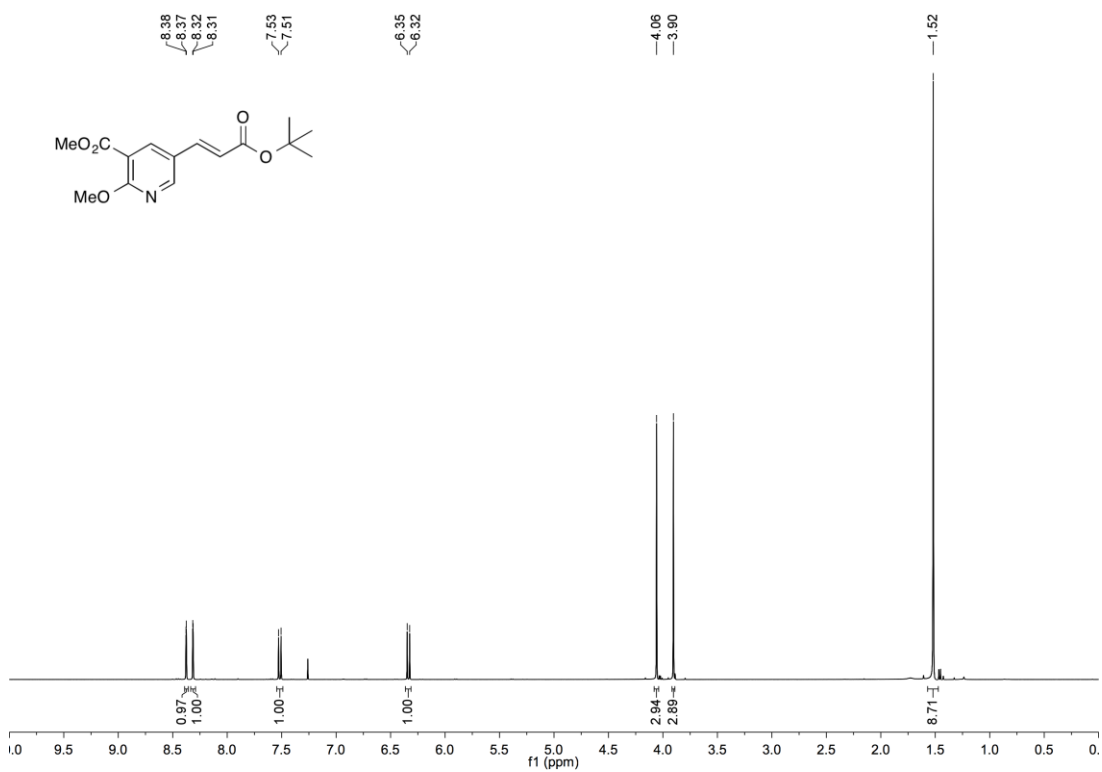
Borylation of 7-aza-1-(tert-butoxycarbonyl)-1H-indazole (**558**) (400 MHz, CDCl₃)



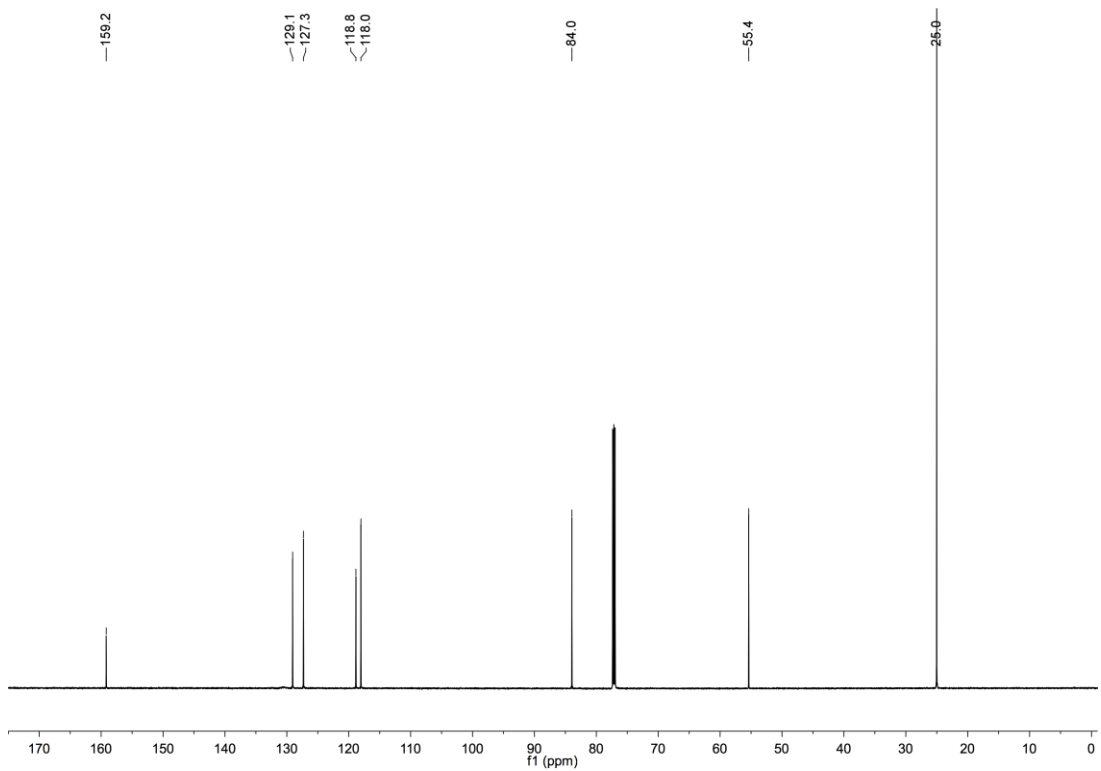
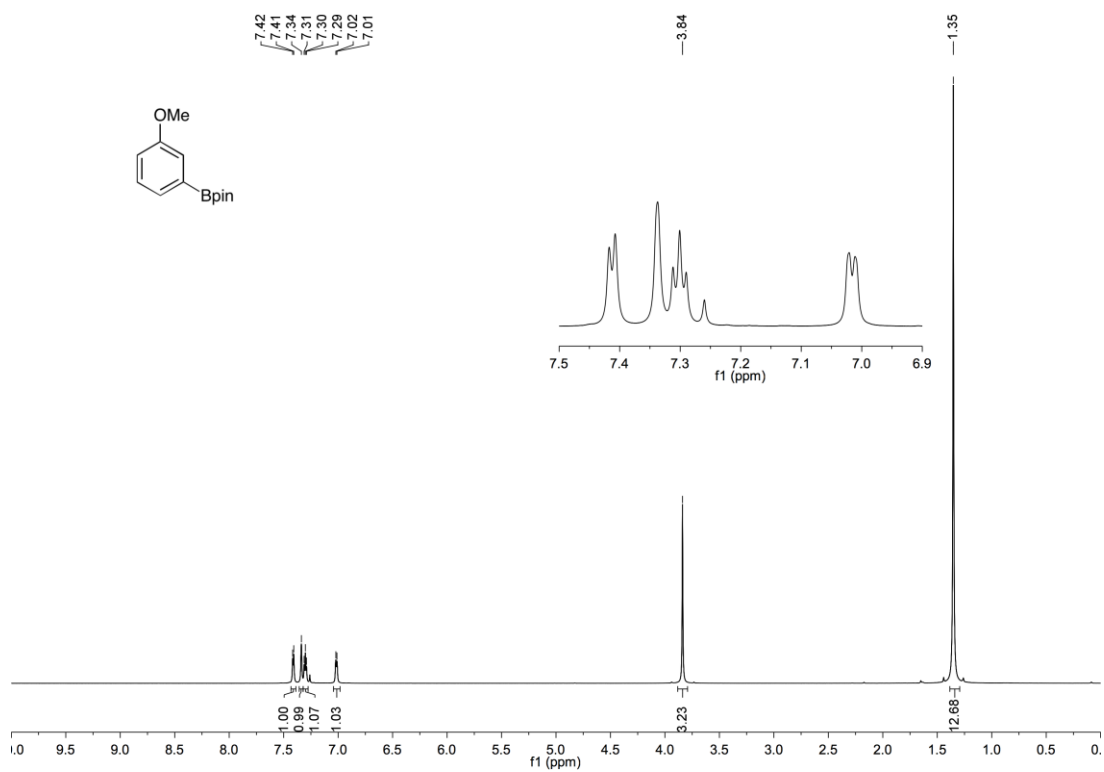
Methyl 5-[(1E)-3'-tert-butoxy-3'-oxoprop-1'-en-1'-yl]-2-nicotinate (**578**) and Methyl 5-[(1Z)-3'-tert-butoxy-3'-oxoprop-1'-en-1'-yl]-2-methoxynicotinate (**579**)

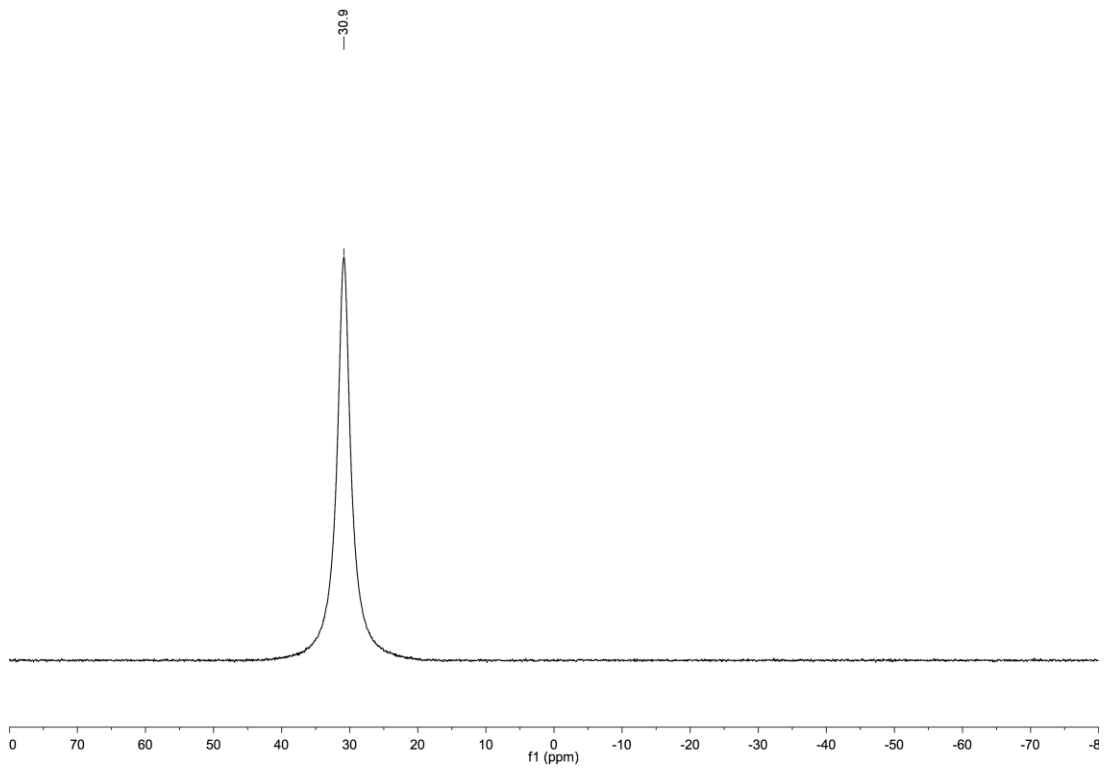


Methyl 5-[(1E)-3'-tert-butoxy-3'-oxoprop-1'-en-1'-yl]-2-methoxynicotinate(578)

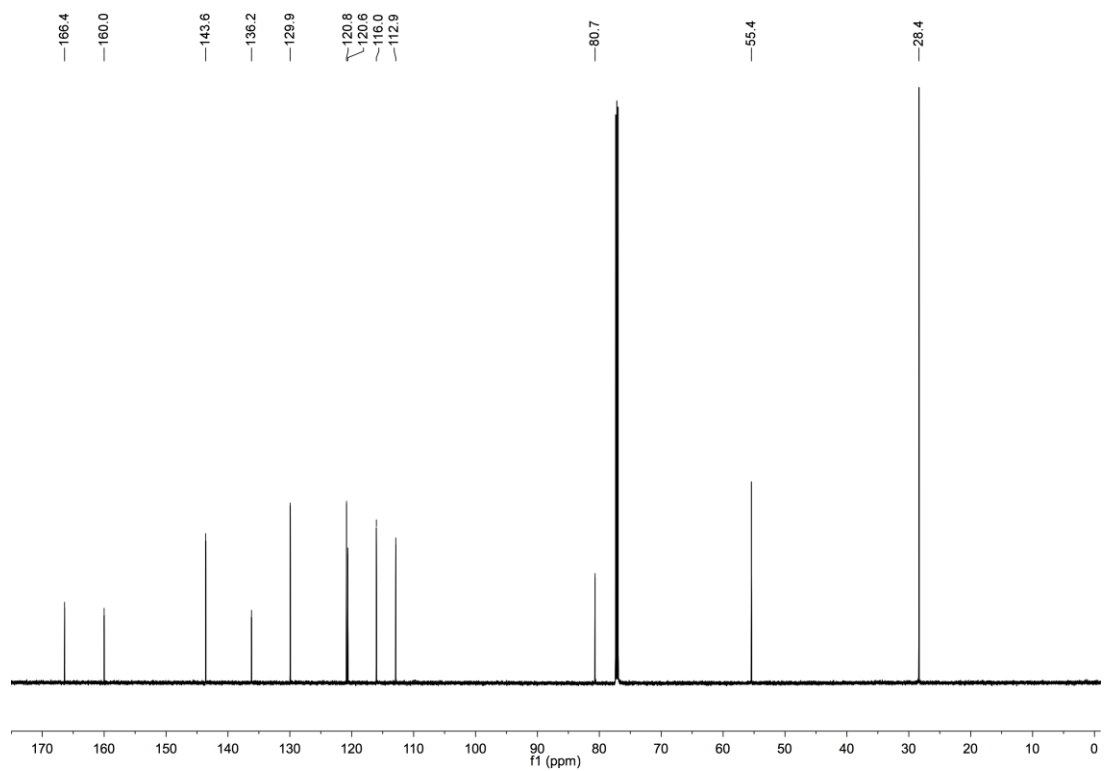
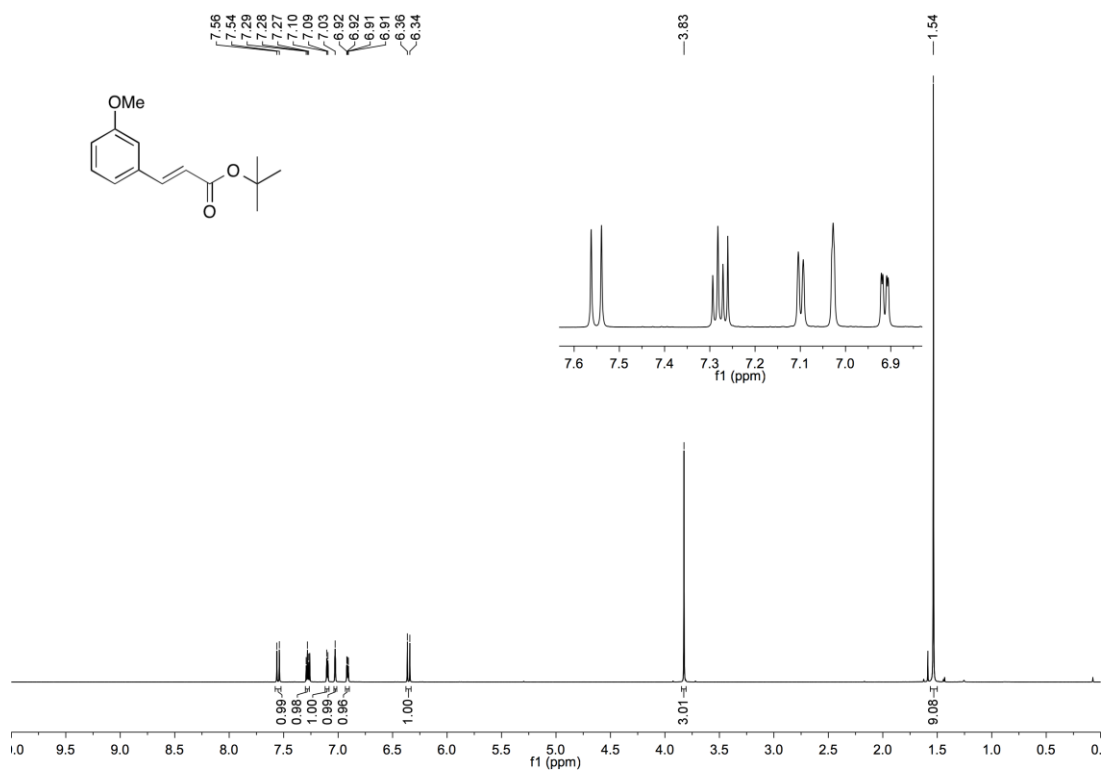


3-(Bpin)-Anisole (206)

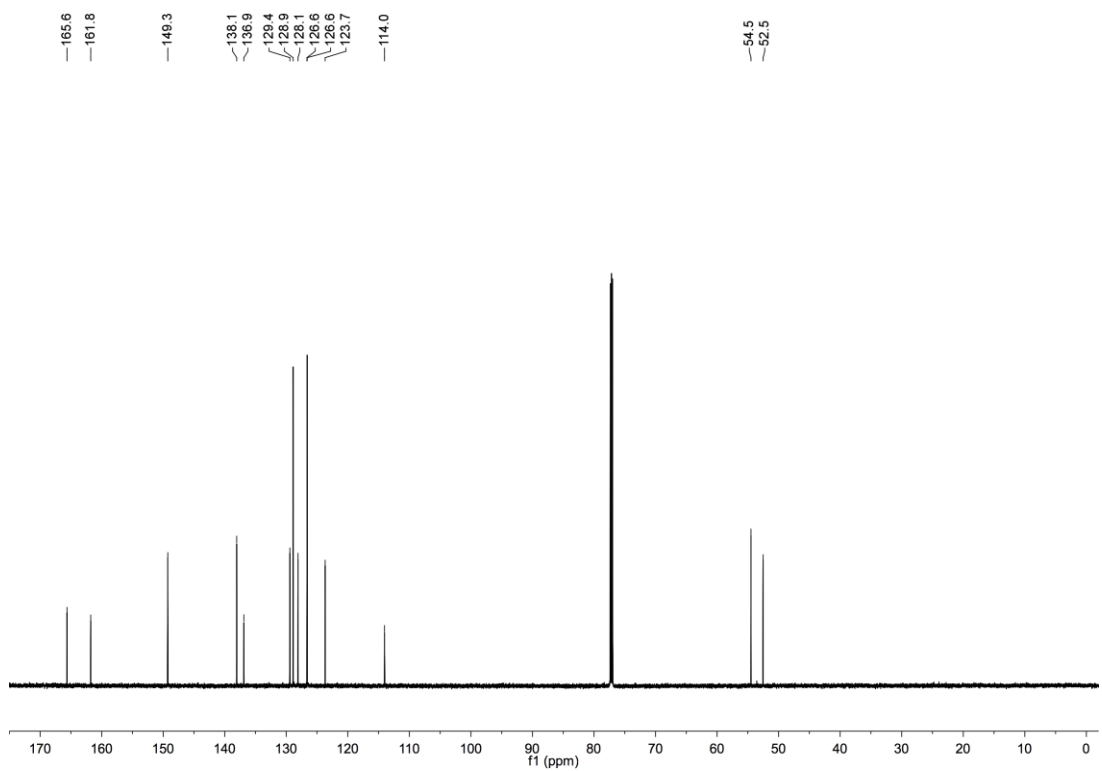
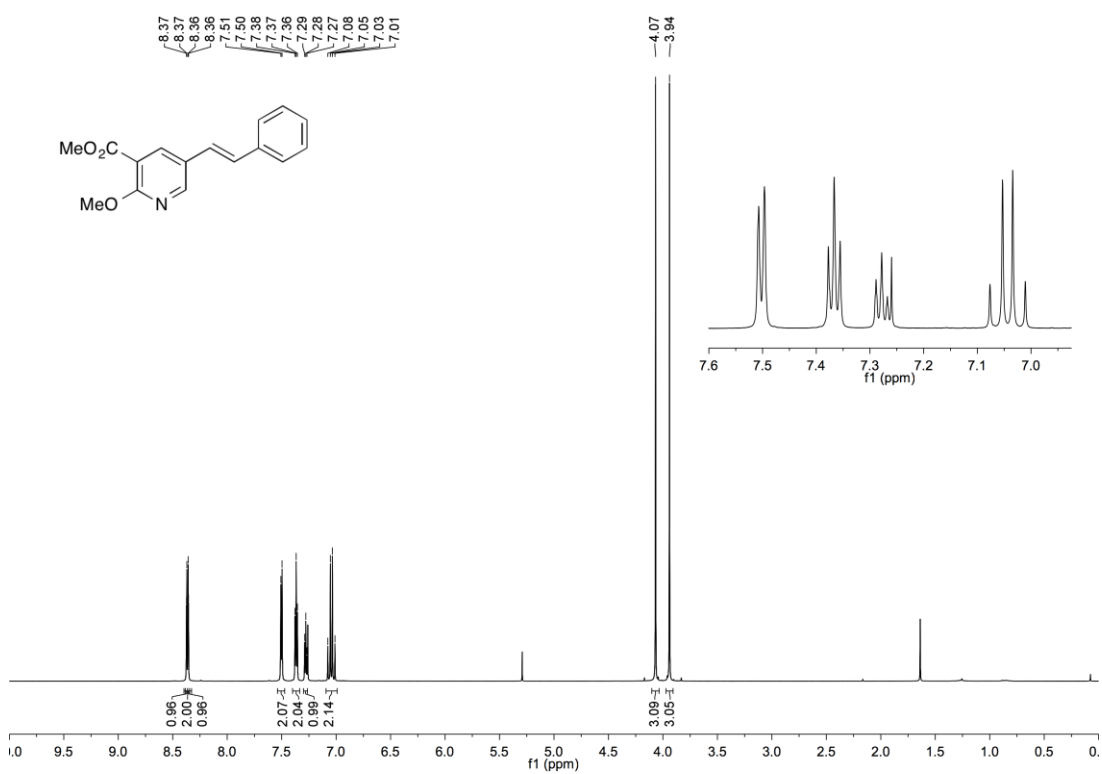




3-[(1E)-3'-tert-Butoxy-3'-oxoprop-1'-en-1'-yl]anisole (582)



Methyl 2-methoxy-5-[(1E)-2'-phenylethenyl]nicotinate (**583**)



Methyl (2E)-3-(5,6'-dichloropyridin-3'-yl)-prop-2-enoate (585)

